

Role of Plant Protease in Manure Protein Hydrolysis and Biohydrogen Production during Dark Fermentation

By

Tasnia Hassan Nazifa

A thesis submitted to the School of Graduate Studies in partial
fulfillment of the requirements for the degree of

MASTER OF ENGINEERING

Department of Civil Engineering

Faculty of Engineering and Applied Science

Memorial University of Newfoundland

October 2024

St. John's, Newfoundland and Labrador, Canada

CO-AUTHORSHIP STATEMENT

I hereby declare that this thesis incorporates material that is the result of research conducted by myself (the author) under the supervision of Dr. Noori Saady. For the research work described in chapters 2, 3, 4, 5, and 6, Dr. Saady suggested the area of the research, and the author developed the research proposal. In consultation with Dr. Noori Saady, the author designed and conducted the experiments. The engineering laboratory work, data analysis and interpretation, were performed by the author under the guidance of Dr. Noori Saady.

The draft of all manuscripts presented in chapters 2, 3, 4, 5, and 6 have been prepared by the author. Dr. Saady, reviewed, corrected, and edited the manuscripts.

I am aware of the Memorial University Policy on Authorship, and I certify that I have properly acknowledged the contribution of other researchers to my thesis, if any.

Previous Publication: I hereby declare that no portion of this thesis has been previously published or submitted for publication elsewhere.

ABSTRACT

Protein-rich waste dark fermentation is challenging because protein degradation produces ammonia that inhibits anaerobic microorganisms. This thesis presents a study of the plant proteases role in manure protein degradation and hydrogen production in dark fermentation. The study used kiwi peel waste (KPW) and pineapple peel waste (PPW) as sources of protease enzymes (actinidin and bromelain, respectively) and Box-Behnken Design (BBD) and Response Surface Methodology (RSM) to evaluate the effects of multiple variables and identify optimal conditions. KPW and PPW reduced ammonia nitrogen by $64\pm 0.65\%$ and $72\pm 0.48\%$, respectively, and increased protein degradation by $39\pm 0.54\%$ and $36\pm 0.25\%$, respectively. Further investigations used BBD and RSM to optimize hydrogen production under inhibited methanogenesis. The maximum hydrogen yields were 510 ± 7 and 385 ± 7 mL g^{-1} VS with KPW and PPW, respectively. In addition, the study includes a comparative analysis of biohydrogen production from protein-rich manure with pure proteins (albumin and casein), unveiling optimal conditions that resulted in high biohydrogen yields, up to 554 ± 3 and 247 ± 6 mL H_2 g^{-1} VS_{albumin} with KPW and PPW, respectively, and 400 ± 4 and 312 ± 3 mL H_2 g^{-1} VS_{casein} with KPW and PPW, respectively.

The thesis also explores the protease-induced structural and functional transformations by Scanning electron microscopy (SEM) and Fourier transform infrared Spectroscopy (FTIR) analyses, providing insights into the profound changes in the protein morphological and molecular composition, highlighting the effectiveness of KPW and PPW in disrupting manure protein structures to facilitate enhanced degradation and hydrogen production. The current study highlights the potential of using protein-rich waste for improving hydrogen yield in dark fermentation outcomes and establishes a foundation for future research into waste-to-energy conversion strategies.

Keywords: Manure protein hydrolysis, Response surface methodology, Manure, Protease enzyme, Hydrogen.

ACKNOWLEDGEMENT

I express my deep gratitude to my supervisor, Dr. Noori Saady, for his guidance and support throughout my M.Eng program, which has been invaluable to my growth as a researcher. His encouragement and expertise have been pivotal to my success.

I am thankful for the funding provided by the Natural Sciences and Engineering Research Council of Canada (NSERC), Memorial University of Newfoundland, and the Department of Fisheries, Forestry, and Agriculture, Government of Newfoundland and Labrador, through the Canadian Agriculture Partnership Program.

Gratitude is also due to my colleagues for their support and to the faculty, students, and staff of Memorial University of Newfoundland for creating a nurturing academic environment. A special thank you to my husband, parents, and siblings, whose unwavering support and belief in me have been my constant source of motivation and strength.

Table of Contents

<i>CO-AUTHORSHIP STATEMENT</i>	<i>ii</i>
<i>ABSTRACT</i>	<i>iii</i>
<i>ACKNOWLEDGEMENT</i>	<i>v</i>
<i>LIST OF ABBREVIATIONS AND SYMBOLS</i>	<i>xxvii</i>
<i>CHAPTER ONE</i>	<i>1</i>
<i>INTRODUCTION</i>	<i>1</i>
1.1 Background	1
1.2 Problem Statement	2
1.3 Objectives	5
<i>CHAPTER TWO</i>	<i>13</i>
<i>LITERATURE REVIEW</i>	<i>13</i>
2.1 Introduction	13
2.2 Biohydrogen and Biomethane as Energy Sources	13
2.3 Anaerobic Digestion Process	17
2.3.1 Hydrolysis	17
2.3.2 Acidogenesis	18
2.3.3 Acetogenesis	19
2.3.4 Methanogenesis.....	20
2.4 Biomethane and Biohydrogen Production	21
2.5 Biohydrogen and Biomethane Production Process Parameters	22
2.5.1 Hydraulic retention time.....	22

2.5.2	Temperature.....	25
2.5.3	Effects of volatile fatty acids.....	28
2.5.4	Hydrogen partial pressure	29
2.5.5	Total solids content.....	30
2.6	Feedstock Sources for Anaerobic Digestion	31
2.6.1	Feedstocks for biohydrogen production.....	31
2.6.2	Feedstocks for biomethane.....	33
2.6.3	Manure	35
2.6.4	Carbohydrates-rich substrates	36
2.6.5	Protein-rich substrates	37
2.7	Codigestion.....	39
2.8	Protein Anaerobic Digestion	41
2.8.1	Mechanism of protein degradation by proteinase.....	43
2.8.2	Amino acid metabolism (Stickland reaction).....	46
2.9	Challenges of Nitrogen-Rich Sources in Anaerobic Digestion.....	53
2.9.1	Ammonia accumulation	53
2.9.2	Volatile fatty acids accumulation.....	57
2.10	Microbiology of Biohydrogen Production	60
2.11	Kinetics of Protein Substrate in Anaerobic Digestion	64
2.12	Modeling of Protein Anaerobic Digestion.....	68
2.13	Proteinase Enzyme.....	72
2.13.1	Plant sources of proteinase enzymes	73
2.13.2	Microbial sources of proteinase enzyme	76
CHAPTER THREE	136

***ENHANCING MANURE PROTEIN DEGRADATION BY KIWI PEEL WASTE:
STATISTICAL OPTIMIZATION USING BOX-BEHNKEN DESIGN AND RESPONSE
SURFACE METHODOLOGY 136***

Abstract..... 136

3.1 Introduction 137

3.2 Materials and Methods 145

 3.2.1 Chemicals and reagents 145

 3.2.2 Feedstock..... 146

3.3 Hydrolysis Tests 146

3.4 Box-Behnken Design 147

3.5 Analytical Methods..... 149

 3.5.1 Protein quantity measurement 150

 3.5.2 NH₃-N and NH₄-N measurement 151

 3.5.3 Volatile solids measurement 152

 3.5.4 Fourier transform infrared spectroscopy (FTIR) 153

 3.5.5 Scanning electron microscope (SEM) 153

3.6 Statistical Analysis of Experimental Results 154

3.7 Results and Discussion 154

 3.7.1 Overall experiment..... 155

 3.7.2 ANOVA and response model..... 156

 3.7.3 Interactive effects of parameters 159

 3.7.4 Effect on ammonium reduction 165

 3.7.5 Effect on volatile solids reduction..... 170

3.8 Optimization and Model Validation..... 172

3.9 Chemical and Morphological Analysis	174
3.9.1 FTIR	175
3.9.2 SEM	177
3.10 Conclusions.....	180
CHAPTER FOUR.....	200
<i>ENHANCING MANURE PROTEIN DEGRADATION BY PINEAPPLE PEEL WASTE: STATISTICAL OPTIMIZATION USING BOX-BEHNKEN DESIGN AND RESPONSE SURFACE METHODOLOGY</i>	
<i>Abstract.....</i>	<i>200</i>
4.1 Introduction	201
4.2 Materials and Method.....	205
4.2.1 Chemicals and reagent	206
4.2.2 Feedstock.....	206
4.3 Hydrolysis Tests	207
4.4 Box-Behnken Design	208
4.5 Analytical Methods.....	211
4.5.1 Protein quantity measurement	211
4.5.2 NH ₃ -N and NH ₄ -N measurement	212
4.5.3 Volatile solids measurement	213
4.5.4 Fourier transform infrared spectroscopy (FTIR)	214
4.5.5 Scanning electron microscope (SEM)	214
4.6 Statistical Analysis of Experimental Data	214
4.7 Results and Discussion	215

4.7.1	Overall experiment.....	215
4.7.2	ANOVA and response model.....	216
4.7.3	Interactive effects of parameters	220
4.7.4	Effects on ammonium reduction	226
4.7.5	Effects on volatile solids reduction	229
4.8	Optimization and Model Validation.....	231
4.9	Chemical and Morphological Analysis	232
4.9.1	Fourier Transform Infrared (FTIR) spectroscopy.....	232
4.9.2	Scanning Electron Microscopy	235
4.10	Conclusions.....	237
CHAPTER FIVE		251
<i>ENHANCING BIOHYDROGEN PRODUCTION FROM MANURE AND KIWI PEEL</i>		
<i>WASTE: BOX-BEHNKEN DESIGN AND RESPONSE SURFACE METHODOLOGY</i>		
<i>OPTIMIZATION</i>		<i>251</i>
<i>Abstract.....</i>		<i>251</i>
5.1	Introduction	252
5.2	Materials and Methods	256
5.2.1	Chemicals and reagents.....	256
5.2.2	Inoculum	256
5.2.3	Feedstock.....	257
5.3	Batch Anaerobic Digestion Tests	257
5.4	Overall Experimental Design	258
5.5	Box-Behnken Design	260

5.6 Analytical Methods.....	263
5.6.1 Biohydrogen and biomethane measurement.....	263
5.6.2 Gas composition analysis	264
5.6.3 Volatile fatty acids (VFAs) measurement	264
5.6.4 Fourier transform infrared (FTIR).....	265
5.6.5 Scanning electron microscope (SEM)	265
5.7 Results and Discussion	265
5.7.1 Hydrogen yield.....	266
5.7.2 COD removal	277
5.7.3 Volatile solids reduction	279
5.7.4 Volatile fatty acids	281
5.7.5 Model validation	287
5.8 Biohydrogen from Pure Proteins.....	288
5.8.1 Biohydrogen and biomethane yield.....	288
5.8.2 Protein quantity	294
5.8.3 Fourier transform infrared (FTIR).....	297
5.8.4 Scanning Electron Microscopy (SEM).....	300
5.8.5 Volatile fatty acids	305
5.9 Conclusions	311
<i>CHAPTER SIX</i>	<i>334</i>
<i>ENHANCING BIOHYDROGEN PRODUCTION FROM MANURE AND PINEAPPLE</i>	
<i>PEEL WASTE: BOX-BEHNKEN DESIGN AND RESPONSE SURFACE METHODOLOGY</i>	
<i>.....</i>	<i>334</i>
<i>Abstract.....</i>	<i>334</i>
6.1 Introduction	335

6.2 Materials and Methods	340
6.2.1 Chemicals and reagents	340
6.2.2 Inoculum	340
6.2.3 Feedstock.....	341
6.3 Batch Anaerobic Digestion Tests	341
6.4 Overall Experimental Design	342
6.5 Box-Behnken Design	345
6.6 Analytical Methods.....	347
6.7 Results and Discussion	347
6.7.1 Hydrogen yield.....	348
6.7.2 Volatile solids reduction	359
6.7.3 Volatile fatty acids	361
6.7.4 Model validation	368
6.8 Biohydrogen from Albumin and Casein	368
6.8.1 Biohydrogen and biomethane yield.....	369
6.8.2 Protein quantity measurement	374
6.8.3 Fourier Transform Infrared (FTIR)	378
6.8.4 Scanning Electron Microscopy (SEM).....	381
6.8.5 Volatile fatty acids	385
6.9 Conclusions	393
<i>CHAPTER SEVEN.....</i>	<i>414</i>
<i>CONCLUSIONS AND RECOMMENDATION</i>	<i>414</i>
7.1 Summary	414
7.2 Conclusions	417

7.3 Recommendations for Future Studies.....	423
--	------------

List of Figures

Figure 1- 1. Thesis organization.	7
Figure 2- 1. Degradation of organic wastes in anaerobic digestion process. Modified from (Cheng and Brewer, 2021).	18
Figure 2- 2. Schematic of a typical AD process with solids recycling.	24
Figure 2- 3. Primary, secondary, tertiary, and quaternary structure of proteins.	44
Figure 2- 4. Proposed metabolic pathway for anaerobic bio-hydrogen production from protein- rich wastewater. Adopted from Xiao et al. (2014).	45
Figure 2- 5. Standard amino acids at pH 7. Adopted from Roberts et al. (1965).	48
Figure 2- 6. Schematic representation of ammonia toxicity during anaerobic digestion (AD) of protein-rich biowastes. Modified from Ling et al. (2022) with copyright permission.	56
Figure 2- 7. Different plant proteases with their enzyme number (Madhusankha and Thilakarathna, 2021; Mohd Azmi et al., 2023).	73
Figure 3- 1. Schematic of the experimental setup and responses of the hydrolysis process optimization test.	150
Figure 3- 2. Ammonia and ammonium measurement using (a) ammonia (b) and ammonium probes.	152
Figure 3- 3. (a) Samples for total solids (TS) or volatile solids (VS) determination in the oven and (b) measuring the weight of the aluminum pans for TS or VS reduction determination.	152
Figure 3- 4. Contour response surface and 3D plots of the interactive effect of (a) and (b) manure with kiwi peel waste (KPW) dosage, (c) and (d) manure dosage with hydrolysis time, and (e) and (f) KPW dosage with time on protein reduction.	160

Figure 3- 5. 3D plots and contour response surface of the interactive effect of each variable on NH ₃ -N reduction; (a) and (d) manure with kiwi peel waste (KPW) loading, (b) and (e) manure with hydrolysis time, and (c) and (f) KPW with time on NH ₃ -N reduction.	162
Figure 3- 6. NH ₄ -N concentration of control and after 3 to 48 h in the test samples.	165
Figure 3- 7. NH ₃ and NH ₄ -N reduction efficiency of kiwi peel waste and manure hydrolysis as per statistical design.	166
Figure 3- 8. Schematic drawing of hydrolysis of glycine.	168
Figure 3- 9. Volatile solids (VS) reduction in 15 experimental sets for manure protein hydrolysis by KPW.	171
Figure 3- 10. FTIR spectrum of manure and kiwi peel waste at 0 h (control) and 48 h.	175
Figure 3- 11. Scanning electron microscope (SEM) images of (a) and (b) manure-kiwi peel waste (KPW) substrate control, and after hydrolysis at (c) and (d) 6 h, (e) and (f) 12 h, (g) and (h) 24 h, and (i) and (j) 48 h.	178
Figure 4- 1. Clean pineapple peel cuts ready for blending using a blender.	207
Figure 4- 2. Illustration of the experimental arrangement and outcomes of the optimization tests for the manure and pineapple peel waste hydrolysis.	211
Figure 4- 3. A mixture of Coomassie dye and samples ready for protein quantity measurement.	212
Figure 4- 4. Ammonium measurement using Cole Parmer ammonium probe meter connected with a pH-ORP monitor.	213
Figure 4- 5. Contour response surface and 3D plots of the interactive effect of (a) and (b) manure with pineapple peel waste (PPW) dosage, (c) and (d) manure dosage with hydrolysis time, and (e) and (f) PPW dosage with time on protein reduction.	221

Figure 4- 6. Contour response surface and 3D plots of the interactive effect of (a) and (b) manure with pineapple peel waste (PPW) dosage, (c) and (d) manure dosage with hydrolysis time, and (e) and (f) PPW dosage with time on $\text{NH}_3\text{-N}$ reduction.....	224
Figure 4- 7. Ammonium nitrogen ($\text{NH}_4\text{-N}$) concentration of control and in the test samples....	227
Figure 4- 8. Ammonia nitrogen ($\text{NH}_3\text{-N}$) and ammonium nitrogen ($\text{NH}_4\text{-N}$) reduction efficiency of pineapple peel waste and manure hydrolysis as per statistical design.	228
Figure 4- 9. Volatile solids (VS) reduction in the experimental sets for manure protein hydrolysis by pineapple peel waste.	230
Figure 4- 10. FTIR spectrum of manure and pineapple peel waste at 0 h (control) and 48 h. ...	233
Figure 4- 11. Scanning electron microscope (SEM) images of (a) and (b) manure-pineapple peel waste (PPW) substrate control, and after hydrolysis at (c) and (d) 6 h, (e) and (f) 12 h, (g) and (h) 24 h, and (i) and (j) 48 h.....	236
Figure 5- 1. Nitrogen gas is purged through the culture and substrate, ensuring the maintenance of anaerobic conditions in each digester.	258
Figure 5- 2. Flowchart of the experimental works conducted in (a) Part I with manure and KPW and (b) Part II with pure proteins and KPW.....	259
Figure 5- 3. Experimental design and the measured responses for optimizing the anaerobic digestion of manure using kiwi peel waste.	262
Figure 5- 4. Accumulative hydrogen yield during anaerobic digestion of manure and kiwi peel waste as per statistical design.	266
Figure 5- 5. Accumulative methane yield during anaerobic digestion of manure and kiwi peel waste as per statistical design.	267

Figure 5- 6. 3D surface plots and contour response surface of the interactive effect of (a) and (b) manure:KPW ratio and pH, (c) and (d) manure:KPW ratio and inoculum, and (e) and (f) pH and inoculum on biohydrogen yield.	274
Figure 5- 7. Chemical Oxygen Demand (COD) reduction (%) in each run on days 6 and 12. ..	277
Figure 5- 8. Volatile solids (VS) profile of fifteen experimental sets.	280
Figure 5- 9. Total volatile fatty acids (TVFAs) production over the digestion time.....	281
Figure 5- 10. Volatile fatty acid produced measured on days 6 and 12 (a) acetic acid (b) butyric acid (c) propionic acid (d) isovaleric acid and (e) valeric acid.	284
Figure 5- 11. Biohydrogen profile using albumin and casein as substrates for 12 days.....	289
Figure 5- 12. Protein quantity of (a) albumin set A1 (albumin:KPW ratio of 0.5, pH 6, inoculum 5.5 g VS L ⁻¹), set A2 (albumin:KPW ratio of 0.5, pH 5, inoculum 4 g VS L ⁻¹), set A3 (albumin: KPW ratio of 0.5, pH 4, inoculum 5.5 g VS L ⁻¹) on day 6 and day 12 (b) casein set C1 (casein:KPW ratio of 0.5, pH 6, inoculum 5.5 g VS L ⁻¹), set C2 (casein:KPW ratio of 0.5, pH 5, inoculum 4 g VS L ⁻¹), set C3 (casein:KPW ratio of 0.5, pH 4, inoculum 5.5 g VS L ⁻¹) on day 6 and 12.	294
Figure 5- 13. Fourier Transform Infrared (FTIR) spectrum of (a) albumin and (b) casein on day 0 and day 12.	298
Figure 5- 14. Scanning Electron Microscopy (SEM) images of (a) and (b) albumin-KPW substrate on day 0, and after AD at (c) and (d) day 6, (e) and (f) day 12.	302
Figure 5- 15. SEM images of (a) and (b) casein -KPW substrate on day 0, and after AD at (c) and (d) day 6, (e) and (f) day 12.	304
Figure 5- 16. Total volatile fatty acids (TVFAs) production by albumin and casein samples....	305

Figure 5- 17. Single volatile fatty acids (VFAs) measured on day 6 and 12 (a) acetic acid (b) butyric acid (c) propionic acid (d) isovaleric acid and (e) valeric acid.	309
Figure 6- 1. Nitrogen gas is flushed in each digester to sustain an anaerobic environment.	342
Figure 6- 2. Flowchart of the experiment's details of pineapple peel waste (PPW) with (a) Part I: manure and (b) Part II: pure proteins.	344
Figure 6- 3. Layout of the experimental setup and outcomes for the anaerobic digestion optimization.	346
Figure 6- 4. Cumulative hydrogen yield in the anaerobic digestion of manure and pineapple peel waste.	348
Figure 6- 5. Cumulative methane yield in the anaerobic digestion of manure and pineapple peel waste.	349
Figure 6- 6. 3D and contour plots illustrating the effects on biohydrogen yield from (a) and (b) manure:PPW ratio and pH, (c) and (d) manure:PPW ratio and inoculum, and (e) and (f) pH and inoculum.	357
Figure 6- 7. Profile of volatile solids (VS) across fifteen experiments.	360
Figure 6- 8. Profile of total volatile acids (TVFAs) generated by 15 experimental sets measured on day 12.	362
Figure 6- 9. Volatile fatty acid profile measured on days 6 and 12 (a) acetic acid, (b) butyric acid, (c) propionic acid, (d) isovaleric acid, and (e) valeric acid.	364
Figure 6- 10. Profile of biohydrogen yield using pineapple waste with albumin or casein as a substrate for 12 days.	369
Figure 6- 11. Protein quantity of (a) albumin set A1 (albumin:PPW ratio of 0.9, pH 5, inoculum 7 g VS L ⁻¹), set A2 (albumin:PPW ratio of 0.9, pH 4, inoculum 5.5 g VS L ⁻¹), set A3	

(albumin:PPW ratio of 0.9, pH 6, inoculum 5.5 g VS L ⁻¹) on days 6 and 12 (b) casein set C1 (casein:PPW ratio of 0.9, pH 5, inoculum 7 g VS L ⁻¹), set C2 (casein:PPW ratio of 0.9, pH 4, inoculum 5.5 g VS L ⁻¹), set C3 (casein:PPW ratio of 0.9, pH 6, inoculum 5.5 g VS L ⁻¹) on days 6 and 12.	375
Figure 6- 12. Comparative FTIR Spectra for (a) albumin and (b) casein on days 0 and 12.....	379
Figure 6- 13. Scanning Electron Microscopy (SEM) micrographs of albumin-PPW substrates on day 0 (a, b), on day 6 (c, d), and on day 12 (e, f) of anaerobic digestion.	383
Figure 6- 14. Scanning Electron Microscopy (SEM) micrographs of casein-PPW substrates on day 0 (a, b), on day 6 (c, d), and on day 12 (e, f) of anaerobic digestion.	384
Figure 6- 15. Total volatile fatty acids (TVFAs) production by albumin-PPW and casein-PPW substrates.....	386
Figure 6- 16. Individual volatile fatty acids (VFAs) observed on days 6 and 12 (a) acetic acid (b) butyric acid (c) propionic acid (d) isovaleric acid and (e) valeric acid.	389
Figure 7- 1. Flowchart of the research conducted in this thesis using complex protein-rich (manure) as substrate with kiwi peel waste (KPW) and pineapple peel waste (PPW).	415
Figure 7- 2. Flowchart of the anaerobic digestion section of the thesis based on pure protein substrate (albumin and casein).	416

List of Tables:

Table 2- 1. Comparison of the production of energy from different feedstocks utilized for biogas generation (Abanades et al., 2021; Achinas et al., 2017; Ramos-Suárez et al., 2019; Yaqoob et al., 2021).	15
Table 2- 2. Bio-hydrogen production at psychrophilic and mesophilic temperatures from the mixed culture.	27
Table 2- 3. Carbohydrate and protein proportions of various wastes utilised in AD.....	32
Table 2- 4. Comparison of hydrogen production potential from carbohydrate and protein-based substrates.....	33
Table 2- 5. Feedstocks having different substrate compositions used for CH ₄ generation.....	34
Table 2- 6. Biogas and methane yield from different livestock manures.	36
Table 2- 7. Protein, lipid, and carbohydrate content of different substrates derived from various animal and plant sources are available for AD.	38
Table 2- 8. Selected studies on co-digestion of dairy manure with various fruits and vegetables. Wastes.	41
Table 2- 9. Molecular and linear formulas of 20 amino acids (Ahern et al., 2018).....	49
Table 2- 10. Amino acid-degrading anaerobic bacteria and produced enzymes. Adopted from Ramsay and Pullammanappallil (2001).....	51
Table 2- 11. Examples of the physicochemical characteristics of different nitrogen-rich wastes and their impact on the inhibition of AD.	54
Table 2- 12. Microbial communities involved in protein-rich substrate digestion.	62
Table 2- 13. Kinetic coefficients of the first-order rate of hydrolysis of different substrates.....	67

Table 2- 14. Kinetic models and description.	71
Table 2- 15. Plant protease enzyme effect on biohydrogen production using different substrates.	75
Table 2- 16. pH, temperature and strength of hydrolysis of myofibrillar proteins and collagen by various plant and microbial proteases.	76
Table 2- 17. Protease-producing microorganism and enzyme characteristics.	79
Table 3- 1. Plant proteases with source and industrial uses.	142
Table 3- 2. pH, Temperature, and strength of hydrolysis of myofibrillar proteins and collagen by various enzymes.	144
Table 3- 3. Physiochemical characteristics of the substrates	146
Table 3- 4. Levels of different variables for Box-Behnken Design for manure and kiwi peel waste.	148
Table 3- 5. Matrix transformation of Box-Behnken Design for manure and kiwi peel waste (KPW) hydrolysis.	149
Table 3- 6. Box-Behnken Design with predicted and experimental responses for manure and kiwi peel waste.	155
Table 3- 7. ANOVA table for a quadratic model of protein reduction with three-factor Box- Behnken Design for manure and kiwi peel waste (KPW).	156
Table 3- 8. ANOVA table for a quadratic model of NH ₃ -N reduction with three factors Box- Behnken Design for manure and kiwi peel waste (KPW).	157
Table 3- 9. A comprehensive comparison of ammonia and/or protein reduction from manure across various variables.	170
Table 3- 10. Volatile solids reduction of various substrates.	172

Table 3- 11. Ammonia nitrogen and protein reduction under optimum conditions.	174
Table 4- 1. Application of bromelain in various studies.	204
Table 4- 2. Physiochemical characteristics of the substrates.	207
Table 4- 3. Variations in levels for different parameters in the Box-Behnken Design applied to manure and pineapple peel waste.	209
Table 4- 4. Transformation of the matrix in the Box-Behnken Design applied to the hydrolysis of manure and pineapple peel waste (PPW).....	210
Table 4- 5. Box-Behnken Design with predicted and experimental responses for manure and pineapple peel waste.	216
Table 4- 6. ANOVA table for a quadratic model of protein reduction with three-factor Box- Behnken Design for manure and pineapple peel waste (PPW).	218
Table 4- 7. ANOVA table for a quadratic model of NH ₃ -N reduction with three-factor Box- Behnken Design for manure and pineapple peel waste (PPW).	218
Table 4- 8. Ammonia nitrogen, ammonium nitrogen, and protein reduction under optimum conditions.....	232
Table 5- 1. Physiochemical characteristics of the substrates.	257
Table 5- 2. Three experimental sets of albumin and casein used in Part II of the study.....	260
Table 5- 3. Levels of different variables for Box-Behnken Design (BBD) for biohydrogen production using manure (M) and kiwi peel waste (KPW).	261
Table 5- 4. Matrix transformation of Box-Behnken Design for manure (M) and kiwi peel waste (KPW) anaerobic digestion.....	261

Table 5- 5. Cumulative hydrogen yield during anaerobic digestion of manure and kiwi peel waste as per statistical design.....	269
Table 5- 6. Cumulative methane yield during anaerobic digestion of manure and kiwi peel waste as per statistical design.....	270
Table 5- 7. Analysis of variance (ANOVA) for a quadratic model of hydrogen yield with three factors: BBD for manure and KPW for anaerobic digestion.	272
Table 5- 8. Chemical Oxygen Demand (COD) removal efficiency of different substrates	279
Table 5- 9. Comparison of biohydrogen yield from manure and pure proteins under similar experimental conditions.....	290
Table 5- 10. An overview of biohydrogen production from manure and organic wastes.....	292
Table 6- 1. Physiochemical characteristics of the substrates.	341
Table 6- 2. Three distinct experimental sets of albumin and casein for part II of the research. .	343
Table 6- 3. Different variables for Box-Behnken Design (BBD) for biohydrogen yield using manure (M) and pineapple peel waste (PPW).	345
Table 6- 4. Box-Behnken Design matrix for the anaerobic digestion using manure (M) and pineapple peel waste (PPW).	346
Table 6- 5. Cumulative hydrogen yield in the anaerobic digestion of manure and pineapple peel waste.	350
Table 6- 6. Cumulative methane yield in the anaerobic digestion of manure and pineapple peel waste.	351
Table 6- 7. Analysis of variance (ANOVA) for the quadratic model assessing hydrogen production, comprising three variables: Box Behnken Design (BBD) applied to manure and pineapple peel waste (KPW).....	355

Table 6- 8. Evaluating hydrogen production from pineapple peel waste with manure and pure proteins under similar experimental settings. 371

LIST OF ABBREVIATIONS AND SYMBOLS

Acronym

AD	Anaerobic digestion
ANOVA	Analysis of variance
AP	Aspartic protease
BBD	Box Behnken Design
BSA	Bovine serum albumin
C/N	Carbon to Nitrogen
CCD	Central composite design
CHO	Carbohydrates
COD	Chemical oxygen demand
CSTR	Continuous stirred tank reactor
FAN	Free ammonia nitrogen
FID	Flame ionization detector
FTIR	Fourier Transform Infrared spectroscopy
GC	Gas chromatograph
GHG	Greenhouse gas
h	Hour
HRT	Hydraulic retention time
ISA	Ionic standard adjuster
KPW	Kiwi peel waste
kWh	Kilowatt hour
LCFA	Long chain fatty acid

M	Manure
NL	Newfoundland and Labrador
OLR	Organic loading rate
OLR	Organic loading rate
P _{H2}	Hydrogen partial pressure
PPW	Pineapple peel waste
Pro	Proteins
Q	Influent flow rate
RSM	Response Surface Methodology
SEM	Scanning Electron Microscope
SRT	Solid retention time
STP	Standard temperature and pressure
STR	Stirred tank reactor
TAN	Total ammonia nitrogen
TCD	Thermal conductivity detector
TCOD	Total chemical oxygen demand
TS	Total solids
UV	Ultraviolet
V	Volume
VFA	Volatile fatty acids
VSS	Volatile suspended solids

Symbols

C_2H_5OH	Ethanol
$C_6H_{12}O_6$	Glucose
$CH_3CH_2CH_2COOH$	Butyric acid
CH_3CH_2COOH	Propionic acid
CH_3COOH	Acetic acid
CH_4	Methane
CO_2	Carbon dioxide
$COOH$	Carboxyl group
H_2	Hydrogen
N_2	Nitrogen
NH_2	Amine
NH_3	Ammonia
NH_4^+	Ammonium ion
OH	Hydroxyl
SH	Sulfhydryl

Greek Letters

E	Enzyme concentrations
k	Maximum hydrolysis rate constant
K_c	Growth coefficient of the Contois function,
K_m	Half-saturation rate coefficient
k_{SBK}	Surface based hydrolysis constant
N_0	Initial cell density

N_t	Cell density at time t
S	Substrate concentration
S	Substrate concentrations
X	Microbial concentration
ϵ	Biohydrogen or methane content in the biogas as a percentage
λ	Lag time
μ	Specific growth rate
μ_{\max}	Maximum specific growth rate

CHAPTER ONE

INTRODUCTION

1.1 Background

The consumption of fossil fuels has led to the diminishing of natural resources, significant alterations in the global climate, and extensive environmental pollution, threatening humanity's survival. Energy utilization varies globally, with countries like Canada using a mix of oil, natural gas, hydroelectric power, and nuclear energy (Barrington-Leigh & Ouliaris, 2017). The global population is expected to grow by approximately two billion in the next 20 years, leading to a projected 50% surge in electricity usage from 2021 to 2040 (International Energy Agency 2022). Fossil fuels account for 66% of energy demand. Energy demand is projected to rise by 21% by 2040, with natural gas demand up by 28% and oil by 17% by 2050 (International Energy Agency 2022).

In response to the growing need for energy and the adverse effects of fossil fuel consumption, there is a shift towards developing clean, renewable energy sources. Canada's demand for renewable energy is expected to grow significantly, from 878 Petajoules (PJ) in 2018 to 1,643 PJ by 2050, shifting the energy mix towards more natural gas and renewable sources (Canada Energy Regulator 2020). Renewable energy in Canada encompasses hydroelectric, wind, tidal, solar, geothermal, biomass, and organic waste sources. The consumption of biofuels is projected to double by 2050, and hydrogen demand is expected to reach a demand of 112 PJ by 2050 (Canada Energy Regulator 2020).

The prospect of generating hydrogen from renewable resources, including the vast amounts of organic waste produced annually, is gaining attention as a way to mitigate GHG emissions and

address energy needs. Annually, between 7 to 9 billion tons of organic waste are generated (Chen et al., 2020). A significant portion ends up in landfills or dumping areas. Only about 19% of this waste is recycled, and a mere 11% is converted into energy (Ashokkumar et al., 2022). Hydrogen has a higher energy content (MJ kg^{-1}) (lower heating value of 120) compared to other fuels like liquefied natural gas (54.4), ethanol (29.6), and methane (50.0) (Dincer, 2012; Dutta, 2014). However, over 90% of global hydrogen production currently comes from fossil fuels, contributing significantly to GHG emissions (Hanley et al., 2018). Given that fossil fuels are limited and their costs continue to rise, it becomes necessary to explore affordable alternative materials and technologies for hydrogen production in the future.

The transformation of organic waste into biofuels through anaerobic digestion (AD) offers a sustainable solution to meet energy needs and manage waste effectively. Due to its numerous benefits, AD stands out among various waste management methods, such as composting, landfills, fermentation, gasification, and incineration. It significantly reduces environmental impact and converts waste into valuable products, including energy sources like hydrogen, methane, and ethanol, as well as organic fertilizers and other useful products (Tayibi et al., 2021). Research indicates that the digestate resulting from AD has reduced odor, fewer pathogens, and a higher nutrient content compared to untreated waste (Linville et al., 2015). Choosing organic waste as feedstock for AD not only supports eco-friendliness and cost efficiency but also helps reduce landfill waste and sustainably address the scarcity of resources.

1.2 Problem Statement

Livestock wastes (manure, offal, and mortalities) significantly contribute to agricultural organic waste in Canada (Statistics Canada, 2017). For example, Canadian livestock produces

around 180 million tonnes of manure annually, and dairy cows produce 38% of the total (He et al., 2020). In Newfoundland, the combined manure production from dairy, poultry, and mink farms amounts to $536.26 \text{ m}^3 \text{ day}^{-1}$. This total comes from 23 animal producers in the Avalon region, eight in the Eastern region, five in the Central region, and 21 in the Western region (Dillon Consulting, 2014). Animal manure can account for as much as 37% of global GHG emissions if not properly managed (Shakoor et al., 2021).

Manure, a protein-rich waste (contains 12 to 48 wt.% proteins), presents two key challenges during AD. The first key challenge in the AD of manure, specifically with high protein content, revolves around the issue of protein hydrolysis. Protein hydrolysis is the process of breaking down complex protein molecules into simpler, smaller compounds, such as amino acids and peptides, and can be a rate-limiting step in AD due to the complex structure of proteins (Tavano, 2013). This means the overall process can be slowed down if proteins are not adequately broken down. This process is crucial in AD because proteins are not readily biodegradable due to their complex and sturdy molecular structure (Alberts et al., 2002). This slow rate of protein hydrolysis can significantly hinder the overall efficiency of the AD process, as it delays the subsequent stages of digestion and biogas production. The challenge intensifies when manure's high protein content leads to ammonia accumulation during digestion, inhibiting microbial activity and reducing the efficiency of the AD process (Abid et al., 2021; Tasaki, 2021). Notably, when the total ammonia nitrogen (sum of NH_3 and NH_4^+) concentration reaches around 7 gN L^{-1} , the dominant methanogenic pathway shifts to hydrogenotrophic, which consumes H_2 and CO_2 , and total ammonia nitrogen exceeding 8 to 9 gN L^{-1} results in a failure of the AD system (Cheng & Brewer, 2021).

In the context of protein-rich wastes, where protein content can be substantial, enhancing protein hydrolysis becomes a critical research problem. The use of specific enzymes, particularly proteases, in AD is a promising approach to address this issue. Protease enzymes act as biological catalysts, accelerating the breakdown of proteins (Tavano, 2013). This can potentially lead to a more efficient release of substrates for anaerobic bacteria and archaea, which in turn can increase the rate and volume of biogas production (Parawira et al., 2005). However, the application of proteases enzymes in AD must be carefully tailored. Factors such as enzyme type, dosage, and the specific characteristics of the substrates, such as pH, temperature, digestion time, and the existing microbial population, play crucial roles in the effectiveness of enzymatic treatment (Yu et al., 2013). Addressing the mentioned bottlenecks can significantly improve the conversion efficiency of organic waste into valuable biogas, thereby providing a dual benefit: reducing the environmental impact of organic waste disposal and increasing the production of renewable energy.

Despite recognizing the potential of AD to convert organic waste into renewable energy sources, challenges persist due to the rate-limiting step of protein hydrolysis and the subsequent accumulation of ammonia, which can inhibit the AD process. Additionally, while organic waste, including livestock manure, presents a significant opportunity for renewable energy production, the specific application of protease enzymes to enhance protein hydrolysis in AD and its impact on biohydrogen yield has not been extensively explored. These gaps signify a critical need for research to improve biohydrogen production efficiency from high-protein organic wastes through targeted enzymatic treatment.

1.3 Objectives

This research aims to assess the potential of biohydrogen and biomethane production from dairy manure with kiwi peel waste and pineapple peel waste in wet AD at a psychrophilic temperature (20 ± 1 °C) in a batch reactor. It aims to examine the degradation of the protein structure of manure at the earlier stage of AD and consequently convert the waste into biohydrogen and biomethane in a laboratory-based experiment following a statistically designed model. To obtain the research output successfully, the following objectives were set:

- 1) Identify three key factors for optimizing AD hydrolysis of protein-rich manure with kiwi peel waste (KPW) and pineapple peel wastes (PPW) (as a source of protease enzymes actinidin and bromelain) through extensive literature review and parameters pre-screening through statistical models.
- 2) Investigating the effects of KPW and PPW on the hydrolysis of manure, focusing on optimizing the hydrolysis process through reducing manure protein and ammonia accumulation during the early stage of AD. This also includes understanding the substrate complex's functional group and morphological changes during pre and post-hydrolysis and digestion.
- 3) Identifying and optimizing key operational parameters via statistical modeling for maximizing biohydrogen production from protein-rich manure using KPW and PPW.
- 4) Investigating the effects of KPW (actinidin source) and PPW (bromelain source) on the conversion of pure protein substrates like albumin and casein into biohydrogen and biomethane in AD and comparing the outcomes with manure-KPW and manure-PPW digestion. This includes assessing the functional group and morphological changes in albumin and casein during biohydrogen and biomethane production in AD.

1.4 Thesis Structure

This thesis is composed of seven chapters. Chapter 1 presents an overview of the research context, articulates the problem statement, delineates the primary objectives, and describes the organizational structure of the thesis. Chapter 2 is a literature review focused on biohydrogen and biomethane as energy sources, covering their production from various feedstocks and the steps of anaerobic digestion. It addresses challenges in production, the role of proteinase enzymes, and key process parameters. Chapter 3 explores the enhancement of manure protein degradation using kiwi peel waste, applying Box-Behnken Design and Response Surface Methodology for optimization. Chapter 4 explores the enhancement of manure protein degradation using pineapple peel waste, employing the Box-Behnken Design and Response Surface Methodology for optimal results. Chapters 5 and 6 describe the optimization of biohydrogen and biomethane production, detailing methods like Box-Behnken Design and Response Surface Methodology and various analytical techniques for gas yield and VFA analysis, emphasizing model validation. There is a special focus on biohydrogen and biomethane production from pure proteins (albumin and casein) using KPW (Chapter 5) and PPW (Chapter 6). Finally, chapter 7 presents the conclusions and recommendations. Figure 1-1 presents the structure of the thesis.

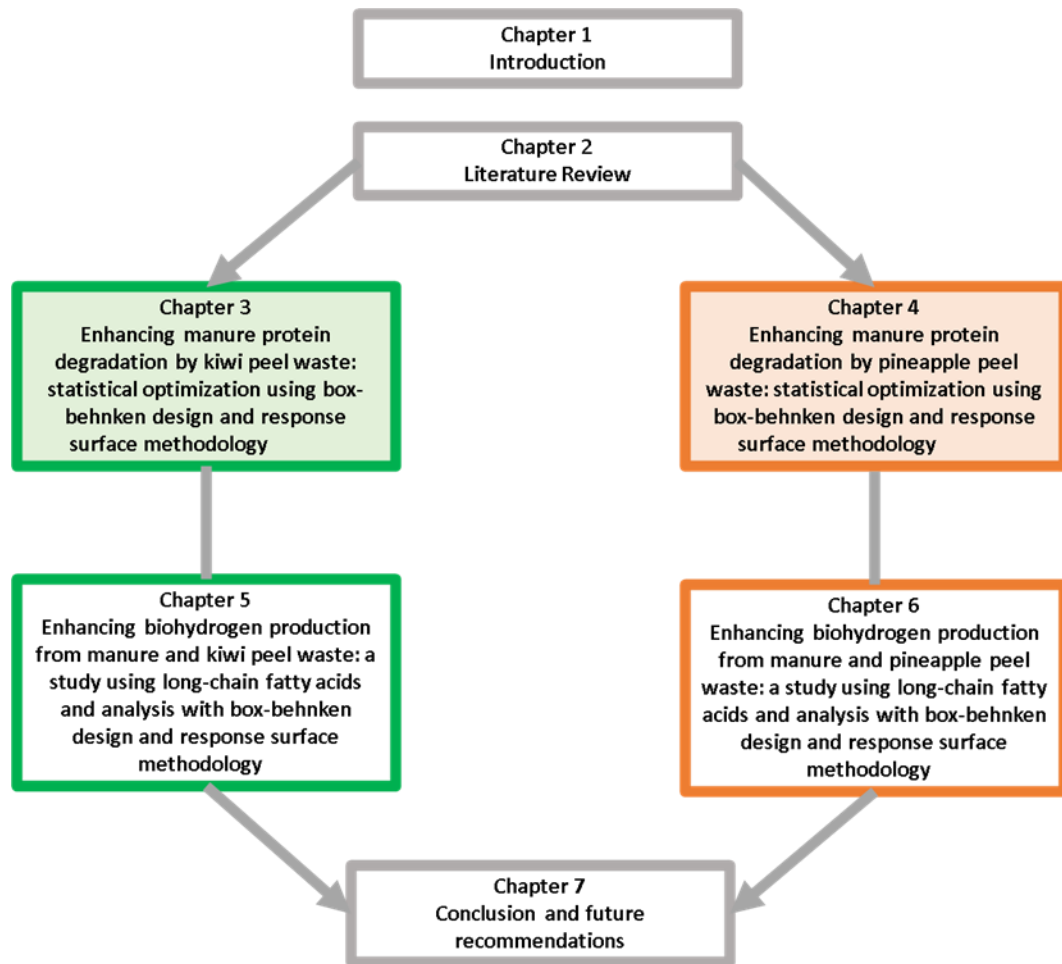


Figure 1-1. Thesis organization.

References

- Abid, M., Wu, J., Seyedsalehi, M., Hu, Y.-y., & Tian, G. (2021). Novel insights of impacts of solid content on high solid anaerobic digestion of cow manure: Kinetics and microbial community dynamics. *Bioresource Technology*, 333, 125205.
<https://doi.org/10.1016/j.biortech.2021.125205>.
- Alberts, B., Johnson, A., Lewis, J., Raff, M., Roberts, K., & Walter, P. The shape and structure of proteins. In Alberts, B., Johnson, A., Lewis, J., (ED). *Molecular Biology of the Cell (4th edition)*, Garland Science, New York, USA;2002.
<https://www.ncbi.nlm.nih.gov/books/NBK26830/>.
- Amores, E., Sánchez, M., Rojas, N., & Sánchez-Molina, M. Renewable hydrogen production by water electrolysis (pp. 271-313). In Dutta, S. and Hussain, C. M. (ED). *Sustainable fuel technologies handbook*, Elsevier, USA; 2021; ISBN 978-0-12-822989-7.
<https://doi.org/10.1016/B978-0-12-822989-7.00010-X>.
- Ashokkumar, V., Flora, G., Venkatkarthick, R., SenthilKannan, K., Kuppam, C., Stephy, G. M., Kamyab, H., Chen, W.-H., Thomas, J., & Ngamcharussrivichai, C. (2022). Advanced technologies on the sustainable approaches for conversion of organic waste to valuable bioproducts: Emerging circular bioeconomy perspective. *Fuel*, 324, 124313.
<https://doi.org/10.1016/j.fuel.2022.124313>.
- Barrington-Leigh, C., & Ouliaris, M. (2017). The renewable energy landscape in Canada: a spatial analysis. *Renewable and Sustainable Energy Reviews*, 75, 809-819.
<https://doi.org/10.1016/j.rser.2016.11.061>.
- Butler, L., Altdorff, D., Young, E., Galagedara, L., Hawboldt, K., Helleur, R. J., & Unc, A. (2017). Organic Waste in Newfoundland and Labrador: A Review of Available

Agriculture, Fishery, Forestry and Municipal Waste Literature. Research Report. The Harris Centre, Memorial University of Newfoundland, St. John's, Newfoundland and Labrador.

https://www.mun.ca/harriscentre/media/production/memorial/administrative/the-harris-centre/media-library/reports/UNC_WASTE_15-16.pdf.

Canada energy regulator, 2020. World Energy Needs. Stated Policies Scenario.

<https://www.capp.ca/energy/world-energy-needs/>. Accessed on January 15th, 2024.

Chen, D. M.-C., Bodirsky, B. L., Krueger, T., Mishra, A., & Popp, A. (2020). The world's growing municipal solid waste: trends and impacts. *Environmental Research Letters*, 15(7), 074021. 10.1088/1748-9326/ab8659.

Cheng, F., & Brewer, C. (2021). Conversion of protein-rich lignocellulosic wastes to bio-energy: Review and recommendations for hydrolysis+ fermentation and anaerobic digestion. *Renewable and Sustainable Energy Reviews*, 146, 111167.

<https://doi.org/10.1016/j.rser.2021.111167>.

Dillon Consulting (2014). Study of Organic Waste Processing Options for Newfoundland

Dincer, I. (2012). Green methods for hydrogen production. *International journal of hydrogen energy*, 37(2), 1954-1971. <https://doi.org/10.1016/j.ijhydene.2011.03.173>.

Dutta, S. (2014). A review on production, storage of hydrogen and its utilization as an energy resource. *Journal of Industrial and Engineering Chemistry*, 20(4), 1148-1156.

<https://doi.org/10.1016/j.jiec.2013.07.037>.

Hanley, E. S., Deane, J., & Gallachóir, B. Ó. (2018). The role of hydrogen in low carbon energy futures—A review of existing perspectives. *Renewable and Sustainable Energy Reviews*, 82, 3027-3045. <https://doi.org/10.1016/j.rser.2017.10.034>.

- He, W., Dutta, B., Grant, B. B., Chantigny, M. H., Hunt, D., Bittman, S., & Smith, W. N. (2020). Assessing the effects of manure application rate and timing on nitrous oxide emissions from managed grasslands under contrasting climate in Canada. *Science of the Total Environment*, Vol. 716, 135374. <https://doi.org/10.1016/j.scitotenv.2019.135374>.
- International Energy Agency, 2022. Potential Energy Demand. IEA World Energy Outlook. <https://www.capp.ca/energy/world-energy-needs/>. Accessed on January 20th, 2024.
- Körner, A., Tam, C., Bennett, S., & Gagné, J. (2015). Technology roadmap-hydrogen and fuel cells. *International Energy Agency (IEA)*, 1-29. Paris, France.
- Linville, J. L., Shen, Y., Wu, M. M., & Urgun-Demirtas, M. (2015). Current state of anaerobic digestion of organic wastes in North America. *Current Sustainable/Renewable Energy Reports*, 2, 136-144. <https://doi.org/10.1007/s40518-015-0039-4>.
- Parawira, W., Murto, M., Read, J., & Mattiasson, B. (2005). Profile of hydrolases and biogas production during two-stage mesophilic anaerobic digestion of solid potato waste. *Process Biochemistry*, 40(9), 2945-2952. <https://doi.org/10.1016/j.procbio.2005.01.010>.
- Statistics Canada, 2017, _Census of Agriculture: Farm and Farm Operator Data. Census of Agriculture. <https://www150.statcan.gc.ca/n1/pub/95-640-x/2016001/article/14800-eng.htm>. Accessed on January 16th, 2024.
- Shakoor, A., Shakoor, S., Rehman, A., Ashraf, F., Abdullah, M., Shahzad, S. M., & Altaf, M. A. (2021). Effect of animal manure, crop type, climate zone, and soil attributes on greenhouse gas emissions from agricultural soils-A global meta-analysis. *Journal of Cleaner Production*, Vol. 278, 124019. <https://doi.org/10.1016/j.jclepro.2020.124019>.

Tasaki, K. (2021). Chemical-free recovery of protein from cow manure digestate solid and antioxidant activity of recovered protein. *Environmental Challenges*, 4, 100132.

<https://doi.org/10.1016/j.envc.2021.100132>.

Tavano, O. L. (2013). Protein hydrolysis using proteases: An important tool for food biotechnology. *Journal of Molecular Catalysis B: Enzymatic*, 90, 1-11.

<https://doi.org/10.1016/j.molcatb.2013.01.011>.

Tian, H., Li, J., Yan, M., Tong, Y. W., Wang, C.-H., & Wang, X. (2019). Organic waste to biohydrogen: A critical review from technological development and environmental impact analysis perspective. *Applied Energy*, 256, 113961.

<https://doi.org/10.1016/j.apenergy.2019.113961>.

Yu, S., Zhang, G., Li, J., Zhao, Z., & Kang, X. (2013). Effect of endogenous hydrolytic enzymes pretreatment on the anaerobic digestion of sludge. *Bioresource Technology*, 146, 758-761.

<https://doi.org/10.1016/j.biortech.2013.07.087>.

CHAPTER TWO

LITERATURE REVIEW

2.1 Introduction

It reviews the background and basics of biohydrogen and biomethane production through anaerobic digestion, various types of wastes, particularly protein or nitrogen-rich wastes, the mechanism of protein-rich substrate degradation, and the challenges associated with these wastes in anaerobic digestion.

2.2 Biohydrogen and Biomethane as Energy Sources

The steady rise of the world population and economic and social progress are increasing global energy consumption. Currently, fossil fuels contribute 33% to energy consumption, and it is not sustainable in the long-term (Bilandzija et al., 2018). According to the British Petroleum statistical review of world energy 2021 report, 83% of the world's total energy consumption in 2018 came from fossil fuels, while 12.6% and 6.3% came from renewable (primarily hydro, wind, and solar) and nuclear energy sources, respectively. To achieve zero fossil fuel use by 2050, renewable energy production will need to be increased up to 6- or 8-fold, assuming energy demand remains constant or increases by 50% from the 2020 energy demand level. If the 2050 world energy demand is limited to a 25% increase over the 2020 level, the probability of achieving independence from fossil fuels improves. The acceleration of improvements in energy efficiency beyond the current rate of ~1.5% per year is also necessary (Holechek et al., 2022). To achieve the required energy sector decarbonization, the share of renewables in power generation would need to increase from around one-quarter in 2015 to around 60% by 2030 and 85% by 2050. However, this would require

a substantial annual growth rate of renewables in total generation, which was 0.7% over the past five years, to more than double (Gielen et al., 2019).

As a result, one of the sustainable development goals (SDG 7) declared by the United Nations is to ensure access to cheap, dependable, sustainable, and modern energy (Mutezo & Mulopo, 2021). Therefore, alternative energy sources other than fossil fuels are required to accomplish SDG 7. Recently, there has been a significant focus on anaerobic digestion (AD), a highly effective biological process for transforming various organic wastes into valuable resources like biogas and biohydrogen. This process has garnered considerable attention due to its numerous benefits (Harirchi et al., 2022). Biomass is the world's largest and most frequently used renewable energy source (Lim et al., 2012), and its application is steadily increasing (Amjith and Bavanish, 2022). The worldwide biomass potential for 2050 is anticipated to be 1500 EJ, of which around 200-500 EJ might be used sustainably, accounting for 40-50% of the estimated primary energy demand (Gutiérrez et al., 2020).

Biohydrogen and biomethane are two potential energy carriers that have gained increasing attention as alternatives to fossil fuels due to their environmental friendliness and sustainability. Unlike the hydrogen produced from fossil fuels, biohydrogen is a clean and carbon-free fuel, which makes it an ideal alternative to traditional energy sources (Sindhu et al., 2020). The energy content of 25 kg of gasoline is equivalent to 9.5 kg of hydrogen (Kirli and Karapinar, 2018). Biomethane, also known as "renewable natural gas," can provide a way to integrate rural communities and industries into the energy sector transformation. Biomethane can be either upgraded biogas from anaerobic digestion or cleaned syngas from biomass gasification; thus, it is 100% renewable. In the latter case, CO₂ is removed from the biogas to produce biomethane, later compressed as a

transportation or heating fuel (Holm-Nielsen et al., 2009); Ardolino and Arena (2019). Table 2-1 compares biogas yields and the energy produced from various substrates.

Table 2-1. Comparison of the production of energy from different feedstocks utilized for biogas generation (Abanades et al., 2021; Achinas et al., 2017; Ramos-Suárez et al., 2019; Yaqoob et al., 2021).

Types of waste	Biogas yield (m ³ tonne ⁻¹ fresh waste)	Electricity (kWh) produced ton ⁻¹ fresh waste
Pig slurry	11 to 25	23.5
Sewage sludge	47	96
Cattle dung	55 to 68	122.5
Poultry litter	126	257
Fat	826 to 1200	1687
Horse manure	56	114
Fruit waste	74	151
Swine manure	2.74 Mm ³ year ⁻¹	721.2 KW year ⁻¹
Cow manure	6.75 Mm ³ year ⁻¹	1631.1 KW year ⁻¹
Buffalo dung	4,196,055 m ³ d ⁻¹	1101 GWh y ⁻¹
Sheep dung	119 m ³ d ⁻¹	0.03 GWh y ⁻¹

According to Wu et al. (2016), AD is a promising and attractive technology to treat organic waste, produce bioenergy, recover nutrients, and reduce pathogens. The AD process can be used to extract energy from domestic, industrial, and agricultural waste as methane or hydrogen with some operational control (Kopasz et al., 2022; Li et al., 2011). Hydrogen is more energetic than methane and does not produce CO₂ when combusted, making it advantageous and allowing for more efficient CO₂ capture and sequestration at the fermentation site. Hence, it is preferred over methane as an end product of AD (Moscoviz et al., 2018; Patel et al., 2021). Recovering hydrogen instead of methane can increase the energy yield of anaerobic digestion. To be sustainable, all components of the hydrogen production process, including the feedstock, biocatalyst (inoculum), and any other input material, should be obtained from renewable and sustainable sources. A McKinsey and Company report suggests that the hydrogen economy could generate \$140 billion

in annual revenue by 2030 and support 700,000 jobs (Kopasz et al., 2022). In the U.S.A., 22.7×10^9 kWh of biomethane was produced from slaughterhouse waste, equivalent to 0.8% of the natural gas used for electricity generation in 2016 (Wang et al., 2018).

Biomass is materials that come from plants, animals, humans, and their waste products, as well as from industrial and food processing waste. These waste materials also contain metabolically active, cultivatable, and non-cultivatable microbial populations (cells). Depending on the waste properties, it can be transformed into energy or fuel through various methods such as combustion, gasification, co-firing, and anaerobic digestion (Neshat et al., 2017). AD can greatly impact renewable energy supplies by converting organic waste into methane and hydrogen. This waste can come from various sources, such as agriculture, livestock, food-processing industries, municipalities, and human activities. Animal manures are suitable sources for biogas production due to the significant roles of rumen microorganisms in AD (Jin et al., 2018). Animal manures are frequently co-digested with energy crops (Agostini et al., 2015) and fruit and vegetable wastes (Wang et al., 2018). Co-digestion involves the simultaneous AD of multiple organic wastes in one digester, which enhances methane yield by establishing positive synergisms in the digestion medium, diversifying bacterial species, and supplying missing nutrients with co-substrates (Shen et al., 2019; Wang et al., 2018).

Ammonium nitrogen plays a crucial role in AD, supporting bacterial growth. However, high concentrations of ammonium nitrogen, particularly free ammonium (NH_3), can be toxic to anaerobic microorganisms. Studies suggest that manure has a higher nitrogen content (low C/N ratio) due to the presence of uric acid and undigested protein, which are decomposed and contained in the form of total ammonium nitrogen (TAN) and NH_3 (Muske and Venkateswara Rao, 2019). Lignin content and complex cell wall structure make it difficult to use crop residues as feedstock

for biogas production (Cu et al., 2015). On the other hand, because of high moisture and organic content, fruit wastes are easily biodegradable, making AD an appropriate approach for fruit waste disposal. However, flavor chemicals' chemical composition and presence in fruit wastes can influence methane generation during AD (Sanjaya et al., 2016).

2.3 Anaerobic Digestion Process

Anaerobic digestion (AD) or degradation involves biomass breakdown by a rigorous action of microorganisms in an oxygen-deficit environment. AD is a suitable treatment compared to aerobic digestion because it requires less energy and produces smaller volumes of sludge. Therefore, AD has been increasingly applied in treating complex wastes, including recalcitrant nitrogen-rich wastes (Cheng and Brewer, 2021; Kovács et al., 2013).

AD decomposes organic matter into biogas with different groups of microorganisms following four stages (Figure 2-1): hydrolysis, acidogenesis, acetogenesis, and methanogenesis. Each group of microorganisms performs their respective role in the whole degradation process.

As an end product, biogas is formed during the AD process and used directly to generate electricity and heat energy. Biogas contains approximately 60% CH₄, 40% CO₂, and a few other trace gases such as N₂, H₂, NH₃, and H₂S (Perman et al., 2022).

2.3.1 Hydrolysis

The first step of AD is Hydrolysis; it initiates the physical conversion of organic substrates (polymers) like proteins, lipids, and carbohydrates into small components and monomers (Shanmugam et al., 2021). Therefore, carbohydrate wastes are disintegrated into simple sugars,

proteins into amino acids, and long-chain fatty acids (LCFAs) are formed from lipids hydrolysis (Abdelgadir et al., 2014).

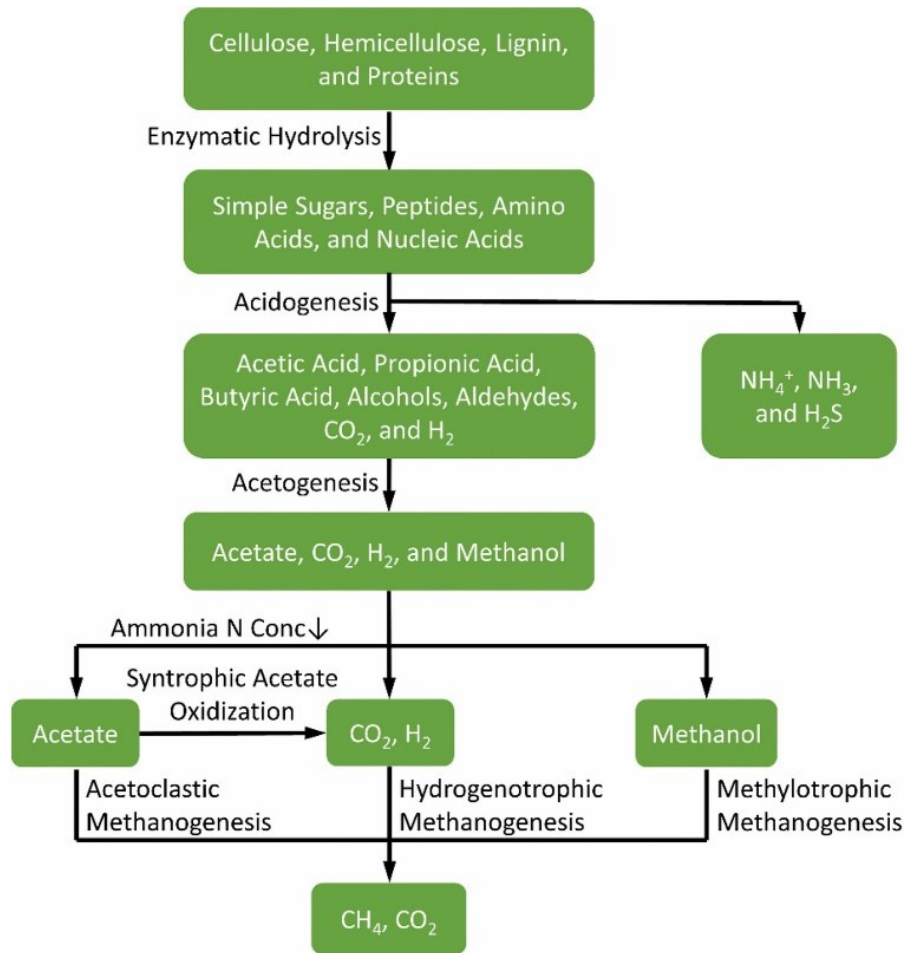


Figure 2-1. Degradation of organic wastes in anaerobic digestion process. Modified from (Cheng and Brewer, 2021).

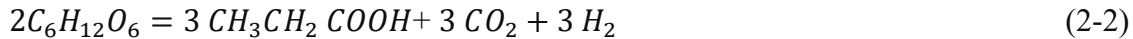
2.3.2 Acidogenesis

Acidogenesis is the second stage of anaerobic digestion. It involves the fermentation of soluble organic compounds to produce alcohols, aldehydes, volatile fatty acids (VFAs), and H₂ and CO₂ (Sarkar et al., 2018). During acidogenesis, acidogenic bacteria transform the products of the first

stage, such as sugars and amino acids, into carbon dioxide, hydrogen, ammonia, and organic acids. The principal acidogenesis stage products are acetic acid (CH₃COOH), propionic acid (CH₃CH₂COOH), butyric acid (CH₃CH₂CH₂COOH), and ethanol (C₂H₅OH) (Habib et al., 2015).

Most organic matter in an equilibrated system is transformed into substrates that are easily available to methanogenic microorganisms, including hydrogen, acetate, and carbon dioxide (Abdelgadir et al., 2014). Nonetheless, roughly 30% of organic matter is converted into short-chain fatty acids or alcohols (Kangle et al., 2012). Hydrogen, carbon dioxide, and acetic acid obtained from these products can bypass the third stage (acetogenesis) and be directly utilized by methanogenic bacteria in the final stage (methanogenesis) (Abdelgadir et al., 2014).

Equations (2-1) to (2-3) represent typical acidogenesis reactions where glucose (C₆H₁₂O₆) is converted to ethanol, propionate, and acetic acid, respectively.

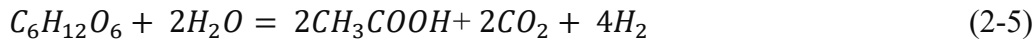
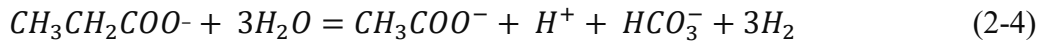


2.3.3 Acetogenesis

Acetogenic bacteria use the energy generated from electrons produced by the oxidation of organic acids and alcohols to reduce carbon dioxide to acetate through the Wood-Ljungdahl pathway (Jin et al., 2021; Sravan et al., 2021). These bacteria can also utilize inorganic materials, such as photoresponsive semiconductors, as a source of redox energy for acetogenesis (Jin et al., 2021). Some acetogens are capable of extracellular electron transfer, enabling electron exchange between cells and their environment, which allows them to produce acetate from CO₂ with high

energy efficiency and have been investigated as biocatalysts of CO₂ conversion into valuable chemicals (Igarashi and Kato, 2017). During the fermentation step, acetogens oxidize organic acids and alcohols (e.g., propionate, butyrate, and ethanol) to acetate while generating electrons that are transferred to protons to produce hydrogen or bicarbonate to produce formate (Liu et al., 2021).

The following are reaction equations (Eqs. (2-4) to (2-5)) of acetogenesis of anaerobic digestion:



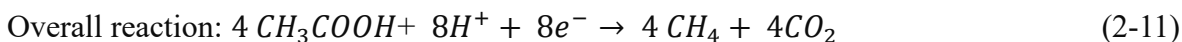
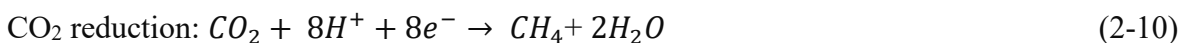
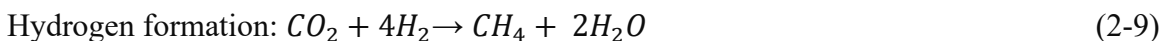
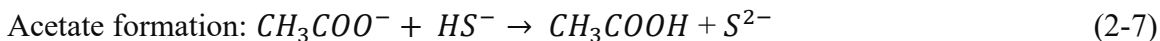
The produced acetic acid can be further converted to methane by methanogenic archaea in the third stage of AD.

2.3.4 Methanogenesis

Methanogenesis is a unique and critical stage of anaerobic digestion in which organic matter is further broken down into methane and carbon dioxide. This process is carried out by methanogenic archaea (MA), which are strictly anaerobic and are found in various environments, including soil, sediments, and the digestive tracts of animals, including humans (Söllinger and Urich, 2019). Methanogenesis occurs via two main pathways: CO₂ reduction and methane formation from methylated compounds via the acetyl-CoA pathway (Berghuis et al., 2019). The overall reaction for methanogenesis can be expressed as (Eq. (2-6)):



This reaction is carried out in four steps: acetate formation, acetate oxidation, hydrogen formation, and CO₂ reduction (He et al., 2002). The biochemical equations (Eqs (2-7) to (2-11)) for these steps are as follows:



These complex reactions are catalyzed by various enzymes produced by methanogenic archaea.

2.4 Biomethane and Biohydrogen Production

Biogas is a renewable energy source produced through AD of organic matter, which is then further processed to produce biomethane and biohydrogen. Organic wastes such as agricultural and food, manure, slaughterhouse, and sewage sludge are anaerobically (oxygen-free environment) digested in the digester to generate biomethane and biohydrogen. Biogas primarily comprises methane gas, carbon dioxide, and trace amounts of nitrogen, hydrogen, and carbon monoxide. Methane is the main component of biogas and is produced during the AD process by two main pathways: acetoclastic methanogenesis and hydrogenotrophic methanogenesis. Acetoclastic methanogenesis accounts for up to 72% of methane production, while up to 28% of

methane is generated through hydrogenotrophic methanogenesis (Harirchi et al., 2022). However, the exact percentage of methane production from each pathway may vary depending on the type of feedstock and the production pathway used (Schnürer, 2016). The bio-hydrogen production process shares similarities with the biogas production process in that they both use AD with organic compounds, and the digester used is identical for both processes. However, there are some differences between the two processes, such as removing hydrogen before it can convert into methane gas (Liu et al., 2020). Additionally, the product extraction and various pre-treatment methods also differ between the biomethane and biohydrogen processes. Both of these production are being developed to help combat environmental pollution and reduce our dependence on non-renewable fossil fuels (Wang et al., 2021). Biomethane and biohydrogen can be converted into energy through combustion, fuel cells, or heat engines.

2.5 Biohydrogen and Biomethane Production Process Parameters

Optimizing the biohydrogen and biomethane production process parameters in AD of recalcitrant nitrogen-rich wastes such as manure, slaughterhouses, and other biomass wastes requires careful consideration of various parameters. These parameters include hydraulic retention time, temperature, VFA, and hydrogen partial pressure. Optimizing these parameters makes it possible to maximize the production of biogas.

2.5.1 Hydraulic retention time

Hydraulic retention time (HRT) is one of the most significant parameters influencing microbial activities and the AD process. HRT is the average duration a soluble component remains in a digester (Eq. (2-12)). Besides HRT, another relevant parameter is the solid retention time (SRT)

(Eq. (2-13), the average time microorganisms (solids) remain in the digester. The HRT and SRT are considered the same in the case of anaerobic digesters without recycling.

$$HRT = \frac{V}{Q} \quad (2-12)$$

Where V is the digester volume in cubic meters (m^3) or liters (L), and Q is the influent flow rate in cubic meters per day ($m^3 \text{ day}^{-1}$) or liters per day ($L \text{ day}^{-1}$).

$$SRT = \frac{VSS}{QR} \quad (2-13)$$

where VSS is the volatile suspended solids concentration in the reactor ($kg \text{ m}^{-3}$), Q is the influent flow rate ($m^3 \text{ day}^{-1}$), and R is the mass ratio of VSS to total suspended solids (TSS).

When solids recycling is incorporated, the HRT and SRT may vary due to the change in solids concentration in the reactor (Gerardi, 2003). The schematic below (Figure 2-2) shows a typical anaerobic digestion process with solids recycling. The solids separator separates a portion of the solids from the influent and recirculates it to the digester using a pump. This can increase the reactor's solids concentration, affecting the HRT and SRT.

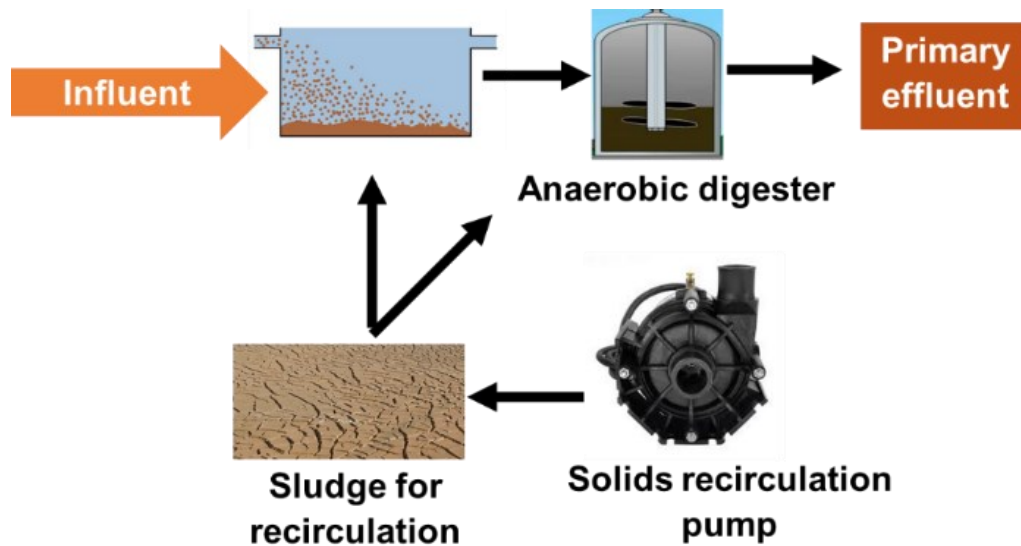


Figure 2-2. Schematic of a typical AD process with solids recycling.

Optimal HRT should not be too short nor too long but adequate for the microorganisms to degrade substrates and reproduce. Both too short and too long HRT negatively impact the process; shorter than the optimum HRT may accumulate volatile fatty acids (VFA) and thus may inhibit methanogenic activities (the ability of methanogens to produce methane), and longer HRT increases the digester operation cost (Pera et al., 2021). A suitable HRT can inhibit hydrogen consumption by hydrogen-consuming bacteria or methanogens (Zhang et al., 2006). The reported HRTs for biohydrogen production from bean wastewater, potato, and sucrose are 12, 18, and 24 h, producing 80, 150, and 320 mL H₂ VS g⁻¹ (Salem et al., 2018). Alexandropoulou et al. (2018) found that the best HRT is between 6 and 12 h, with hydrogen yields of 96.27 (at 12 h) and 101.75 L H₂ kg⁻¹ food waste (at 6 h), respectively. Biohydrogen production increased from 1.18 L H₂ L⁻¹ d⁻¹ to 40.41 mL H₂ g⁻¹ VS when HRT was decreased from 10 to 5 days (Sillero et al., 2022).

2.5.2 Temperature

Temperature is a crucial parameter in AD affecting microbial growth rate and substrate conversion efficiency into biohydrogen. Thermophilic AD has a faster hydrolysis rate than mesophilic AD; however, thermophilic AD promotes high VFA production (Xiao et al., 2018).

A wide range of temperatures can be applied for biohydrogen production, from extreme thermophilic (>70 °C) (Aboudi et al., 2021) to psychrophilic (<25 °C) (McHugh et al., 2006; Vasiliadou et al., 2023; Zhang et al., 2012). Mesophilic and thermophilic AD generate a good hydrogen production rate than psychrophilic AD; however, higher temperature reduces the overall system efficiency due to the energy requirements (Das and Veziroglu, 2008; Dasgupta et al., 2010).

Fermentative microorganisms are usually inactive at low-temperature (Scherer and Neuhaus, 2006). However, few are found to be cold-tolerant and produce specific enzymes providing optimum activities at low or moderate temperatures. Considering cold regions, these microorganisms and their enzymes could be potentially applied in producing various commercial bio-products (Feller and Gerday, 2003). For example, Kundu et al. (2012) and Lu et al. (2011) have noticed that biohydrogen could be produced at 4 and 9 °C. Because of such microbial properties, this process shows a promising technology for biohydrogen generation (Lu et al., 2012).

Psychrotolerant bacteria grow well at low temperatures close to the freezing point of water; however, the fastest growth rates are observed above 20 °C, whereas strict psychrophilic organisms grow faster under 15 °C or lower temperature but are unable to survive above 20 °C (Cavicchioli et al., 2002). At psychrophilic temperature, microorganisms show low metabolism rates but greater

catalytic efficiencies compared to mesophilic microorganisms (Margesin and Schinner, 1994); therefore, psychrophilic microorganisms offer economic benefit by saving energy in commercial

operations that would not need the costly heating of digesters (Feller and Gerday, 2003). Moreover, the psychrophilic temperature reduces the risk of microorganism contamination (Margesin and Schinner, 1994). Such advantages promote the psychrophilic temperature as an economically suitable approach for biohydrogen production.

Zieliński et al. (2017) found biohydrogen production ranged from 20 to 58 mL H₂ g⁻¹ COD_{fed} from cheese whey digestion and 16 to 52 mL H₂ g⁻¹ COD fed from glucose digestion at 20 °C for 20 days. Similarly, Alvarado-Cuevas et al. (2015) found 2.5 times higher biohydrogen production at 25 °C and pH 5.5 when glucose was used as a carbohydrate source compared to other experimental screening conditions. Table 2-2 presents a summary of hydrogen yield at different temperatures, and it suggests that the type of inoculum and substrate fed for the biohydrogen production process impact the overall yield.

Table 2-2. Bio-hydrogen production at psychrophilic and mesophilic temperatures from the mixed culture.

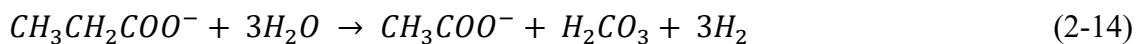
Feed	Digester configuration	Inoculum	pH	Temp. (°C)	H ₂ yield or rate	Reference
Intestinal waste	Batch	WWTP AnS		35	74.23±6.11 dm ³ kg VS ⁻¹	Cieciura-Włoch and Borowski (2019)
Meat tissue	Batch	WWTP AnS		35	30.36±1.57 dm ³ kg VS ⁻¹	Cieciura-Włoch and Borowski (2019)
Protein (Peptone)	Batch	Heat-treated AnS	7	35	0.034 mL H ₂ mg protein ⁻¹	Xiao et al. (2010)
Protein (Peptone)	Batch	-		55	0.26 mmol mg protein ⁻¹	Cheng et al. (2002)
Protein (Peptone)	Batch	Heat-treated AnS	6.9 ± 0.1	37	0.08 mmol H ₂ mg protein ⁻¹	Xiao et al. 2010)
Cattle manure	Semi- CSTR	Sludge	3.62–5.28	35	30.22 mL H ₂ g ⁻¹ VS	Liu et al. (2020)
Buffalo dung	CSTR	-	5.5	30±2	165 ± 25.16 mL H ₂ g ⁻¹ COD _{added}	Wadjeam et al. (2019)
Cow manure	Semi-CSTR	Digester cultures	6.9	60	10.25 ± 4.96 mL H ₂ g ⁻¹ VS	Wang et al. (2013)
Pig manure	Batch	Sewage sludge	7	20	11.15 mL H ₂ g ⁻¹ VS	Chen et al. (2021)
Carbohydrate (glucose)	Batch	Heat-treated AnS	6.9±0.1	37	0.14 mL H ₂ mg ⁻¹ glucose	Xiao et al. (2010)
Carbohydrate Glucose)	Batch	Heat-treated AnS	6.2	25	0.968 mol mol ⁻¹	Oh et al. (2003)
Carbohydrate (Sucrose)	Batch	Heat-treated AnS	5.5	34.8	34.8±3.4 mol mol ⁻¹	Mu et al. (2006)

AnS = anaerobic sludge; CSTR = Continuously Stirred Tank Reactors; WWTP = Wastewater Treatment Plant.

2.5.3 Effects of volatile fatty acids

The composition of by-products depends on the substrate used and the environmental conditions of the experiment. Cheng et al. (2002) found acetate and butyrate as the major volatile fatty acids (VFAs) produced from carbohydrate-rich substrates, whereas acetate, butyrate, and propionate are produced from protein-rich substrates. Butyric, acetic, and propionic acids were the three main VFAs for glucose, peptone, and glycerol, respectively (Mu et al., 2006). The higher concentration of butyrate and acetate can significantly increase biohydrogen production. Zhang et al. (2012) observed the highest biohydrogen yield at 0 g L⁻¹ VFA. The biohydrogen yield decreased with the increasing butyrate and acetate concentrations. Also, the inhibitory impact of acetate on fermentative biohydrogen yield was less compared to butyrate.

With the increase of acetate, from 0 to 300 mM, 70-90% glucose was degraded compared to 52% when 400 mM acetate was added (Fotidis et al., 2013). High concentrations of VFAs can lower the digester's pH, consequently inhibiting hydrolysis, acidogenesis, and methanogenesis. Moreover, high VFAs concentrations can inhibit methanogenesis directly (Fotidis et al., 2013). Dogan et al. (2005) showed that acetate, butyrate, and propionate concentration of more than 13, 15, and 3.5 g L⁻¹ reduced methane yield by 50% in AD using granular sludge. Moreover, acetoclastic methanogenic activity (acetate-degrading bacteria) was decreased when acetate concentrations were above 4 g L⁻¹ in the same experiment. Metabolism of propionic acid is the most sensitive to hydrogen partial pressure (Kopasz et al., 2022; Moletta et al., 1985), which should be less than 9×10^{-5} atm to allow its degradation according to the following equation (Eq. (2-14)):



Cytoplasmic membranes of microorganisms prevent ionized components from diffusing into the microbial cell. Hence, only the unionized propionic acid ($\text{CH}_3\text{CH}_2\text{COOH}$) can enter the cell and impact bacterial metabolism by free diffusion. However, the ionized form ($\text{CH}_3\text{CH}_2\text{COO}^-$) remains outside the microorganism cell. Both outside and inside the cell, the balance between the unionized and ionized forms depends on the environment pH, according to Eq. (2-15) (Gourdon & Vermande, 1987):

$$pH = pKa + \log \frac{\text{CH}_3\text{CH}_2\text{COO}^-}{\text{CH}_3\text{CH}_2\text{COOH}} \quad (pKa = 4.88 \text{ at } 25 \text{ }^\circ\text{C}) \quad (2-15)$$

2.5.4 Hydrogen partial pressure

Hydrogen partial pressure (P_{H_2}) affects the production of H_2 . When the P_{H_2} is high, VFAs production increases, lowering the pH value ($\text{pH} < 6$). Such a change in pH may impact substrate hydrolysis, acetogenesis, and methanogenesis steps (Cazier et al., 2019). Moreover, Cazier et al. (2015) found that high initial P_{H_2} in the headspace was the main inhibitory factor of the hydrolysis of wheat straw in dry AD. Indeed, hydrolysis inhibition was not detected when CO_2 was present with H_2 initially in the reactor's headspace. In this case, H_2 was quickly consumed by methanogens and homoacetogens.

Gas sparging impacts the H_2 yield compared to un-sparged conditions in mixed cultures. Kraemer Bagley (2007) found sparging increased H_2 yield by 20 to 70% (N_2), 80 to 120% (CO_2), 88% (CH_4), and 0 to 12% (H_2/CO_2 ; biogas). Similarly, Mizuno et al. (2000) noticed that the addition of nitrogen gas to the liquid phase caused a decrease in dissolved hydrogen concentration, increasing the hydrogen yield by 68% compared to control.

According to Cazier et al. (2019), the performance of methanogenic microorganisms depends on the time of exposure to high P_{H_2} , which has a persistent impact on AD kinetics. They also suggest injecting CO_2 may improve solid-state AD at high TS content (25% TS) by avoiding local inhibition of H_2 while using wheat straw as substrate and inoculating with anaerobic granular sludge for 11 and 18 days. As soon as CO_2 was purged, the methanogenic activity increased from 0.41 to 3.77 within three days, following hydrogenotrophic and acetoclastic pathways. In AD, fatty acids are decomposed to hydrogen and acetates by syntrophic bacteria at a very low hydrogen partial pressure, which can only be provided by the activity of hydrogen-consuming methanogens (Cieciura-Włoch and Borowski, 2019).

2.5.5 Total solids content

Studies have shown that substrates' total solids (TS) content plays a crucial role in biohydrogen and biomethane production in the AD process. The TS content and the initial pH significantly influence batch biohydrogen production in solid substrate fermentation of agroindustrial wastes. For example, hydrogen production decreased as the initial total solids content increased from 6.65 to 18%, with hydrogen production of approximately $3 \text{ mmol } H_2 \text{ g}^{-1} \text{ dry solids}$ (Robledo-Narváez et al., 2013). Total solids content was found to influence the biohydrogen and biomethane potential of palm oil mill effluent in a two-stage AD system. Ghimire et al. (2018) found that biohydrogen and biomethane production increased with an increase in the TS content of food waste and wheat straw up to a certain point (from 10 to 15%). A higher TS content (> 15% to 30%) decreased the biogas production potential.

2.6 Feedstock Sources for Anaerobic Digestion

Hydrogen and methane have been among the most extensively researched renewable energy carriers in recent decades. AD, one of the renewable energy-producing technologies for both heat and power, has the potential to become cost-effective since it can use recalcitrant nitrogen-rich wastes and low-value wastes as feedstock, e.g., manure and slaughterhouse waste (Khamtib et al., 2021), agricultural, organic municipal waste and wastewater (Kotay and Das, 2008), fruit wastes (Krishna et al., 2023; Nguyen et al., 2021) to produce biogas (Khawer et al., 2022), biomethane and biohydrogen (Shen et al., 2022b; Stamatelatou et al., 2014). Proteins and carbohydrates in account for over two-thirds of the total organic matter in most organics (Bharathiraja et al., 2016).

2.6.1 Feedstocks for biohydrogen production

Various organic wastes have been used for H₂ production. Organic wastes from industrial processes such as slaughterhouses, breweries, wineries, fruit residues, food processing, bakery, etc., are ideal substrates for H₂ production (Hajizadeh et al., 2021). Moreover, the biohydrogen production potential of many organic wastes, including waste molasses, plant wastes, dairy wastewater, sewage sludge, and macroalgae, has recently gained popularity (Badawi et al., 2023; L. Guo et al., 2008; Mohan et al., 2008; Sambusiti et al., 2015).

The hydrogen yield from these wastes varies due to their differences in organic composition, and the primary components in such organic wastes are generally carbohydrates and proteins. Table 2-3 provides the fraction of carbohydrates and protein in wastes used for biohydrogen production.

However, carbohydrate-rich substrates may produce around 20 times more H₂ than protein-rich or fat-content substrates (Rafieenia et al., 2017). Similarly, Jarunglumlert et al. (2018) found

the production of hydrogen gas through dark fermentation using carbohydrate-rich waste significantly more efficient than that from fat-rich or protein-rich waste, with approximately 16 and 20 times greater yields. This could be due to carbohydrates' faster hydrolysis rate than proteins (Lay et al., 2003). Table 2-4 presents the biohydrogen production from various carbohydrate- and protein-rich compounds.

Table 2-3. Carbohydrate and protein proportions of various wastes utilised in AD.

Wastes	Carbohydrate (CHO) and protein (Pro) constituents	Reference
Animal manure	1.8% N, 0.38% P, and 0.41% K (Weight %, dry basis)	Qaramaleki et al. (2020)
Poultry blood	13-15% Pro, <1% fat, and <1% CHO	Cuetos et al. (2017)
Dairy wastewater	CHO (26.0% of DM), Pro (25.4% of DM)	Vidal et al. (2000)
Wheat straw	CHO (848.5 g kg ⁻¹ DM)	Bauer et al. (2009)
sewage sludge	Pro (1.04 g L ⁻¹) and CHO (0.27 g L ⁻¹)	Cai et al. (2004)
Waste sludge	Pro (25.41 mg L ⁻¹) and CHO (18.72 mg L ⁻¹)	Guo et al. (2008)
Waste molasses	CHO (48%–58% of DM)	Guo et al. (2008)
Macroalgae	Pro (7–15% dry wt.) and CHO (25–60%) (dry weight)	Sambusiti et al. (2015)
Waste activated sludge	total CHO, 2315.6 mg L ⁻¹ ; total Pro, 5180 mg L ⁻¹	Yang and Wang (2019)

CHO = carbohydrates; Pro = Proteins

AD of starch produced a maximum hydrogen yield of 138 mL g⁻¹ volatile solids with 60.4% hydrogen content in biogas, and the minimum was obtained from fats (4.9 mL g⁻¹ VS) and proteins (4.1 mL g⁻¹ VS) (Litti et al., 2021). Wang et al. (2017) found 1.72 mol H₂ mol⁻¹ obtained from 10 g L⁻¹ cassava starch. The AD of the protein sample (peptone) in a batch study achieved a hydrogen yield of 0.16 mmol g⁻¹ COD_{added} at neutral pH (Cheng et al., 2002). Akutsu et al. (2009) investigated different substrates, including starch as a carbohydrate and peptone as a protein source. Considerable hydrogen yields were observed from starch (20.4 to 175.5 mL H₂ g⁻¹ COD_{starch}), and for peptone, there was almost no hydrogen production (Akutsu et al., 2009).

Table 2-4. Comparison of hydrogen production potential from carbohydrate and protein-based substrates.

Substrates	Carbohydrate	Protein	H ₂ production (mL H ₂ g ⁻¹ VS)	References
Organic fraction of municipal solid waste	100%	-	152	Alibardi and Cossu (2015)
	-	100%	5	
Rice	100%	-	134	Dong et al. (2009)
Potato	100%	-	106	
Meat	-	100%	100	
Rice	100%	-	167	Alibardi and Cossu (2016)
Rice	100%	-	96	Okamoto et al. (2000)
Peptone	-	-	< 5	Litti et al. (2021)
Starch	-	-	138	

2.6.2 Feedstocks for biomethane

As for protein or nitrogen-rich wastes for biogas or biomethane production in anaerobic digestion, a wide range of substrates, such as animal manure, food waste, and agricultural residues, can be used (Table 2.5). For instance, meat processing residues have been shown to increase methane production in AD. Meat processing wastes generated 707±46 and 756±56 L CH₄ (at standard temperature and pressure) kg⁻¹ VS. Similarly, poultry manure and urea have also been shown to enhance methane production (100 to 850 mL g⁻¹ VS) (Cai et al., 2021).

Slaughterhouse wastes are a significant source of nitrogen-rich organic matter and are increasingly used as a feedstock for AD to generate bio methane, a renewable energy source. Slaughterhouse wastes include blood, bones, carcasses, offals, skin, and feet. This kind of waste is composed of a huge amount of proteins, COD, lipids, total solids (TS), volatile solids (VS), and less carbohydrates with low pH (Rawoof et al., 2021). Blood is a proteinaceous organic matter; 94 to 96% of blood is protein. This highly degradable protein of blood plus its lipid/fat content (3% of the volatile solids (VS)) contribute to its high potential methane yield (500 L kg⁻¹ VS) (Nazifa et al., 2021). Because blood is very rich in protein, and its nitrogenous content is high, it should be

co-digested with other substrates of high carbon content to adjust the carbon: nitrogen ratio (C:N) within the optimum range for AD. Feedstock such as manure, wheat straw, and paunch could be co-digested with blood. Blood provides powerful and nutritive components to anaerobic microbial cultures (Cuetos et al., 2017; Nazifa et al., 2021). The co-digestion of fruit and vegetable waste, spent coffee residue, and swine manure yielded 198.1 mL CH₄ g⁻¹ VS (de Quadros et al., 2022).

Table 2-5. Feedstocks having different substrate compositions used for CH₄ generation.

Feedstocks	Substrate composition	CH ₄ yield (mL g ⁻¹ VS)	References
Canteen waste	TS = 15.01 ± 0.98% VS = 14.18 ± 0.52% Proteins = 3.58 ± 0.15%	724	Li et al. (2018)
Passion fruit peel	-	78-115	dos Santos et al. (2020)
Canteen waste	TS = 24.7% VS = 95.2%TS Carbohydrate = 34.3% Protein = 22.4% Lipid = 43.3%	626	Li et al. (2018)
Cow dung	TS = 34.66% VS = 19.52% Fibers = 18.7%TS Proteins = 0.6%TS Lipids = 12.3%TS	238	Qiao et al. (2011)
Pig slurry	TS = 3.93% VS = 73.62% COD = 28000 mg L ⁻¹	740	Ozbayram et al. (2018)
Cow manure	TS = 15.1 ± 0.08% VS = 13.1 ± 0.08% sCOD = 13250 ± 315 mg L ⁻¹	138	Dhiman et al. (2018)
Swine slaughterhouse waste	TS= 91% VS= 91.5%	851	Ning et al. (2016)
Cattle manure	TS = 6.60 ± 0.01% VS = 4.98 ± 0.09% Lignocellulose = 37.70 ± 1.32%	124	Neshat et al. (2017)
Grass silage	TS = 27%, VS= 91%	238	Dooms et al. (2018)

2.6.3 Manure

Manure is an organic waste generated by animals, most often in cattle production. Manure includes organic molecules such as nitrogen, phosphorus, carbon, and other nutrients. Manure qualities might vary based on the animal species, the type of feed ingested, and the management practices employed. Because of its high organic content and nutritional value, manure is a significant feedstock for AD. Manure's nitrogen and carbon components offer an important energy source for the microorganisms driving the AD process, creating biogas (Mutungwazi et al., 2022). Aside from generating electricity, AD can also assist in minimizing the volume of manure and other organic wastes.

Manure contains considerable protein (12 to 48 wt.%), depending on the animal and the growth stage (Tasaki, 2021). Poultry breeding industries produce massive amounts of manure waste. The global production of manure is about 20,708 million tonnes, with Asia and Europe generating 11,514 and 2039 million tonnes of chicken manure per year, respectively (Konkol et al., 2023). However, only 30-40% of this manure is converted into biogas by AD (Bayrakdar et al., 2017). The technological difficulties lower the broader use of manure for renewable energy generation. The reason is that poultry manure is hard to disintegrate and biodegrade into biogas efficiently (Molaey et al., 2019). In China, approximately 155 million tonnes of poultry manure are produced annually, which can produce 3×10^{14} KJ energy (Bi et al., 2020). In Canada, 1.61×10^7 oven-dried tonnes of agriculture livestock manure is produced annually, generating 7.10×10^6 tonnes total carbon (Levin et al., 2007) and 2.415×10^{14} Btu (Lory, 2019). Table 2-6 comprehensively outlines the contribution of different animal manures to biogas production, providing a detailed breakdown of biogas components to the overall yield.

Table 2-6. Biogas and methane yield from different livestock manures.

Type of manure	Biogas produced (m ³ kg ⁻¹)	CH ₄ content (%)	CO ₂ content (%)	CH ₄ yield (m ³ kg ⁻¹)	References
Chicken	0.4–0.6	5–72	30–50	0.27	Jain et al. (1981); Noorollahi et al. (2015); Taiganides and Stroschine (1971);
Cow	0.26–0.28	50–60	34–38	0.14	Jain et al. (1981); Noorollahi et al. (2015)
Cow	4.00	54.50	44.25	2.18	Obileke et al. (2020)
Sheep	0.22–0.24	40–50	37.6	0.1	Babae et al. (2013); Jain et al. (1981)
Sheep	0.258	65	35		Halim et al. (2017)
Goat	0.58	29.5	-	0.172	Halim et al. (2017)
Chicken	0.466	30.2	-	0.14	Halim et al. (2017)
Goat	0.120-0.130	-	-	-	Ndubuisi-Nnaji et al. (2020)
Pig	-	-	-	0.316	Zhang et al. (2014)
Buffallo	8.98	52.27	42.8	-	Chuanchai and Ramaraj (2018)
Horse	-	-	-	0.17	Mönch-Tegeger et al. (2013)
Swine	0.320 (of TS)	58.8–69.5	-	-	Xiao et al. (2019)
Pig	0.444±0.011	-	-	-	Feng et al. (2017)
Mink		-	-	0.239–0.428	Bulak et al. (2020)
Mink		-	-	0.368–0.591	Zarkadas et al. (2016)
Horse		-	-	0.245	Carabeo-Pérez et al. (2021)
Rabbit		-	-	0.326	Carabeo-Pérez et al. (2021)
Goat		-	-	0.112	Carabeo-Pérez et al. (2021)
Pig	-	-	-	0.41	Li et al. (2015)
Chicken		-	-	0.377	Li et al. (2015)
Rabbit		-	-	0.323	Li et al. (2015)
Elephant		-	-	0.275	Sawatdeenarunat et al. (2021)
Donkey	0.0023	-	-		Harrison et al. (2020)

2.6.4 Carbohydrates-rich substrates

Carbohydrate-rich feedstocks or wastes can produce higher yields of biohydrogen and biomethane compared to protein- and lipid-rich substrates. Carbohydrate-rich organic wastes include food waste, agricultural residues, and municipal solid waste (Lin et al., 2016). Studies have shown that these wastes contain a larger amount of carbohydrates, which can result in 20 times more hydrogen production than fat-rich organic waste (Lay et al., 2003). The fermentation process

of carbohydrates leads to higher hydrogen yields than lipids and proteins, which produce glycerol and long-chain fatty acids and ammonia, respectively (Okamoto et al., 2000).

For instance, Cai et al. (2004) noticed 3.47 mL H₂ g⁻¹ dry solid from protein-rich waste (alkali pre-treated sludge), while Guo et al. (2008) observed 16.6 mol H₂ mol⁻¹ sucrose from carbohydrate-rich wastewater (molasses). The experiment conducted by Xiao et al. (2010) showed that the highest hydrogen yields obtained were 0.077 mL H₂ mg⁻¹ protein and 0.14 mL H₂ mg⁻¹ glucose at neutral initial pH. While high levels of carbohydrates in substrates can encourage the proliferation of acid-forming bacteria, it can adversely impact the growth of methane-producing bacteria (Gelegenis et al., 2007).

2.6.5 Protein-rich substrates

According to Ling et al. (2022), around 100 million tonnes (Mt) of protein-rich waste is generated annually, mainly from municipal solid waste, which is inadequately treated. In the United States, 18.4 Mt of slaughterhouse waste was generated in 2016 (Loganath and Senophiyah-Mary, 2020) and globally, 19.71 Mt of poultry meat was produced in 2019, with 20% (i.e., 3.94 Mt) of it was wasted, causing greenhouse gas emissions (Ghosh et al., 2019; Loganath and Senophiyah-Mary, 2020). The poultry industry generates several byproducts, such as viscera, bones, blood, heads, feet, and feathers, which form 28–30% of the total weight. Specifically, the intestines represent 20–30% of these processing byproducts and are a rich source of proteins and lipids (Jamdar & Harikumar, 2005). Poultry waste components, including feathers (85–99% pure keratin protein), blood meal (60–80% of crude protein), bones (23–24% of crude protein), heads and feet (16% of crude protein), viscera (11–12% of soluble protein), and intestines (53–60% protein content), exhibit high protein percentages, indicating their substantial protein content

(Lasekan et al., 2013). The fishing industry generates 75.24 Mt of fish waste annually worldwide, accounting for 30-70% of the raw material by weight (Shanthi et al., 2021). The composition of carbohydrates, protein, and lipids of various feedstocks is provided in Table 2-7.

Table 2-7. Protein, lipid, and carbohydrate content of different substrates derived from various animal and plant sources are available for AD.

Feedstocks (% VS) unless indicated otherwise	Carbohydrate	Protein	Lipid	References
Blood	5.3	94	0.3	Hallaji et al. (2019)
Meat extract	3	68	< 1	Kovács et al. (2015)
Waste activated sludge (g COD L ⁻¹)	2.23	9.01	4.01	Kovács et al. (2015)
Slaughterhouse waste	2.1	70	27	Handous et al. (2019)
Fish waste (g ⁻¹ TS)	0.85	0.15	-	Wu and Song (2021)
Animal kitchen waste	10	54	35	Kobayashi et al. (2012)
Bovine blood serum water	26	73	1	Langone et al. (2019)

Many studies have been performed to improve the biohydrogen production potential from protein-rich wastes. The hydrogen yield from protein-rich food waste with *S. cerevisiae* produced 186.1 mL H₂ g⁻¹ TVS, whereas 171.9 mL H₂ g⁻¹ TVS was produced from the same substrate when mixed with hydrogen-producing bacteria derived from activated sludge (Song et al., 2010). The authors justified the findings by stating that *S. cerevisiae* produced some proteinase enzymes that facilitated protein degradation besides providing a conducive anaerobic environment for hydrogen-producing bacteria (Song et al., 2010).

Some previous studies have demonstrated that sufficient protein content in the complex substrates improves biohydrogen production. For example, Xia et al. (2012) found that adding chicken feathers (37% w/w protein) to swine manure increased methane yield from 452 to 496 L kg⁻¹ VS fed, indicating a potential improvement in CH₄ production. In the same study of anaerobic digestion of slaughterhouse sludge, total gas volume was increased by 183%, rising from 104 L in controls (sludge only) to 294 L when mixed with feather (23% w/w protein). In another study,

using a mixed substrate containing 40% protein (85% slaughterhouse waste, 4% food industry residues, 6% hydrolyzing yeast, and 5% manure) yielded 466.8 mL H₂ day⁻¹, significantly outperforming the control, which produced less than 100 mL H₂ day⁻¹ (Karlsson et al., 2008). The efficiency improved when the fruit and vegetable waste was supplemented with crude cheese whey (739.46 ± 4.6 µg protein mL⁻¹) to produce 10.68 mmol H₂ L⁻¹ h⁻¹ and biohydrogen yield of 450 mL H₂ g⁻¹ COD. On the other hand, when only fruit and vegetable waste was used as a single substrate (C/N ratio = 46) the biohydrogen production was initiated many days after that obtained when these two feedstocks were combined and produced 330 mL H₂ g⁻¹ COD. This fact suggests a lack of proteinaceous nutrients in fruit and vegetable waste, essential for biohydrogen production (Gomez-Romero et al., 2014).

2.7 Codigestion

Even if carbohydrates have higher biohydrogen potentials than proteins, carbohydrates are needed in AD to balance the carbon-to-nitrogen (C/N) ratio for hydrogen-producing bacteria growth. Numerous studies have examined the appropriate nitrogen levels for enhancing hydrogen production, but an optimal C/N ratio cannot be universally defined because of variations in the fermentation processes. For example, digesting manure as a single substrate (mono-digestion) has some drawbacks (Li et al., 2013) since AD depends on substrate characteristics. For example, substrates with high nitrogen content produce ammonia during degradation, and high ammonia concentration prevents microorganisms from growing. This issue could be solved by co-digesting another substrate with low nitrogen content. Ammonia nitrogen is less inhibitory in its ionic form (NH₄⁺) than as free ammonia (NH₃), but the partitioning between these forms is dependent on temperature and pH. For this reason, ammonia inhibition has been reported in a wide range of total

ammonia nitrogen (TAN) concentrations between 1500 and 7000 mg N L⁻¹ (Sun et al., 2016). Lin and Lay (2004) determined that a high concentration of nitrogen (C/N ratio of 47) was necessary for improving hydrogen production to a yield of 4.8 mol H₂ mol⁻¹ sucrose, while Cheong and Hansen (2007) found maximum hydrogen rates of 25 mL H₂ h⁻¹ g⁻¹ at lower C/N ratio (30). However, the best hydrogen yield of 281 mL H₂ g⁻¹ starch was obtained by Argun et al. (2008) at a C/N ratio of 200 and a C/P ratio of 1000, namely, for lower concentrations of nutrients.

Bai et al. (2004) conducted batch experiments using a mixture of 40% protein (peptone) and 60% carbohydrate (glucose). They noticed that mixed substrates improved the biohydrogen yield (3.5 to 3.65 mmol H₂ COD g⁻¹) compared to mono-substrate (0.4-0.5 mmol H₂ COD g⁻¹ peptone). Dairy manure is usually codigested with another substrate to enhance digestion and increase biohydrogen or biogas yield. Generally, the biogas yield of feedstocks with a higher proportion of fats and lipids is maintained equal to or more than that of feedstocks containing more nitrogen or proteins (Neves et al., 2009). Moreover, feeding poultry manure as the main substrate in co-digestion helps mitigate GHG emissions and energy production. Nguyen et al. (2021) showed that the two-stage co-digestion process involving manure and pineapple waste increased the COD removal efficiency, hydrogen production rate, and net energy gains, produced high-quality biogas, and significantly reduced fermentation time. The maximum hydrogen and methane production rates were 1488.62 and 991.57 mL L⁻¹ d⁻¹, respectively, reaching optimal HRTs of 4.5 h for hydrogen and 9 days for methane production. Table 2-8 provides the results of studies on the co-digestion of dairy manure and other substrates.

Ruiz and Flotats (2016) found that the mean upper potential for methane production was 356 NmL CH₄ g⁻¹ VS when using orange peel with bovine manure under mesophilic conditions. Martín

et al. (2010) obtained a lower potential of 230 NmL CH₄ g⁻¹ VS using sludge with orange peel under mesophilic conditions.

Table 2-8. Selected studies on co-digestion of dairy manure with various fruits and vegetables. Wastes.

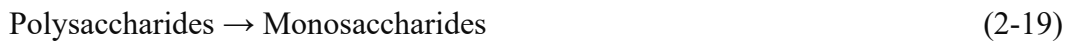
Co-substrate	Reactor type	Mixing ratio (manure: co-substrate)	Temp (°C)	Methane or Hydrogen yield	References
Aloe peel waste	Batch	3:1 wt. basis	36	195.1 mL g ⁻¹ VS	Huang et al., 2016)
Meat and bone meal	Batch	90:10 VS basis	38	0.25 m ³ CH ₄ kg ⁻¹ VS	Andriamanohiarisoamanana et al. (2017)
Pineapple waste	CSTR	1:1 and 1:1.5 COD based	37	1488.62 mL H ₂ L ⁻¹ d ⁻¹ and 991.57 mL CH ₄ L ⁻¹ d ⁻¹	Nguyen et al. (2021)
Corn silage and olive pomace	Batch	Cattle manure 45%, corn silage 25%, chicken manure 15%, and olive pomace 15% w based	40	50.4 mL H ₂ g ⁻¹ VS	Shen et al. (2022a)
Fruit-vegetable	Batch	35: 65 w based	55	126 ± 22 mL H ₂ g ⁻¹ VS	Tenca et al. (2011)
Sorghum stem	Batch	36 C:N based	37	478 mL biogas g ⁻¹ VS	Zhang et al. (2016)
Coffee mucilage	Batch	1: 3 w based	35–55	7.6 NL H ₂ L ⁻¹ d ⁻¹	Hernández et al. (2014)

2.8 Protein Anaerobic Digestion

The first stage of AD (hydrolysis) is the most important step for methane and hydrogen production from protein-rich waste (Xiao et al., 2014). This step dramatically affects methane and hydrogen production (Xue et al., 2015). Unlike carbohydrates, proteins possess a unique three-dimensional structure. Generally, hydrolysis (stage-I) is slow since the protein remains unsusceptible to protease enzyme cleavage in its native folded conformation (Carbonaro et al., 2012). Therefore, hydrolysis is a rate-limiting step in AD of solid and particulate substrates such as dairy manure (12 to 24% total solids). The hydrolysis rate is inversely proportional to the solids content. Therefore, hydrolysis of dairy manure's cellulosic or lignocellulosic fraction improves its

biomethane yield, requiring lower retention time (Saady et al., 2021). Besides cellulosic or lignocellulosic fractions, fiber and crude protein are the two major animal manure components (Shang, 2007; Wen et al., 2007). In protein hydrolysis, complex proteins in animal manure are broken down into simpler compounds. This process helps recover protein from manure for animal feed or other applications (Zubair et al., 2020). Manure contains organic nitrogen, a mixture of proteinaceous compounds, purines, nucleic acids, uric acid, urea, and other compounds containing nitrogen. Through enzymatic hydrolysis, these compounds are transformed into ammonium (NH_4^+) and become available for use by crops (Whalen et al., 2019).

The hydrolysis step is mostly catalyzed by enzymes. Other than proteases, enzymes such as cellulase, amylase, and lipase also break down large molecules of complex substrates into small molecules secreted by microbes or plant-based, making them available for other bacteria (Abdelgadir et al., 2014). Equations (2-16) to (2-20) show an example of a hydrolysis reaction where a protein (Nazifa et al., 2021) and polysaccharide molecule (Abdelgadir et al., 2014) are broken down into amino acids and monosaccharides:



Some challenges may appear during the hydrolysis of nitrogen-rich cellulosic material like manure. These challenges include (i) higher protein content ($\pm 20\%$ of the dry matter), (ii) large

particulate size (75% of the dairy manure has size >0.125 mm), and (iii) low fiber degradability (Saady et al., 2021).

In the presence of protease-producing microorganisms, protein is hydrolyzed to amino acids and peptides by the extracellular enzymes (stage I). Then, amino acid units are degraded into organic short-chain and branched-chain organic acids, consequently metabolized into hydrogen and methane through acetogenesis and methanogenesis (stage II). In anaerobic fermentation, the acidogens (responsible for acetogenesis) and methanogens (responsible for methanogenesis) differ in their physiology, nutritional needs, growth kinetics, and sensitivity to environmental conditions (Kayhanian, 1994).

2.8.1 Mechanism of protein degradation by proteinase

Protein structure can be categorized into four classes: primary, secondary, tertiary, and quaternary (Figure 2-3). In primary structure, amino acid units are connected with covalent peptide bonds. The common secondary protein structures observed are the alpha (α) helix, the beta (β) sheet, loops, turns, etc. Tertiary and quaternary structures describe how various secondary structures in polypeptide chains assemble to form a three-dimensional architecture (Kuhar et al., 2021).

Protein is hydrolyzed in stage I of AD to amino acids and peptides by extracellular enzymes. The amino acid units are degraded to organic short-chain and branched-chain organic acids, which are metabolized into hydrogen and methane through acetogenesis and methanogenesis (stage II).

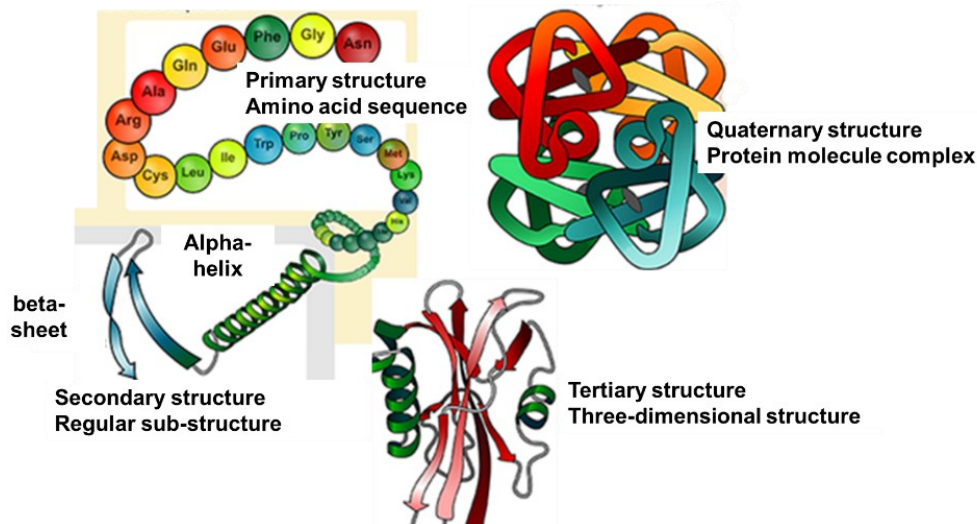


Figure 2-3. Primary, secondary, tertiary, and quaternary structure of proteins.

Bovine serum albumin (BSA), a model protein, is dominated by α -helix (65% α -helix, 25% β -strand, 6% β -turn, and 2% unordered structures) (Wang & Lee, 2006; Xiao et al., 2014). The decrease of the α -helix unit refers to the rupture of hydrogen bonding networks, consequently initiating protein degradation during anaerobic digestion for biomethane production (Xiao et al., 2014).

Protein hydrolysis by rumen in animals significantly differs from the protein degradation in anaerobic digesters. According to Xiao et al. (2014), their proposed metabolic pathway of protein degradation for biohydrogen formation shows it can be seen that the hydrogen production from protein wastewater comes from the conversion of amino acids to volatile fatty acids (Figure 2-4).

Metabolic pathways are a series of interconnected chemical reactions that convert one or more starting molecules into products through intermediates (Agapakis et al., 2012). The proposed metabolic pathway converts protein into hydrogen through a series of enzymatic reactions in anaerobic fermentation. NADH-Fd reductase and hydrogenase are the key metalloenzymes responsible for hydrogen formation in this metabolic pathway.

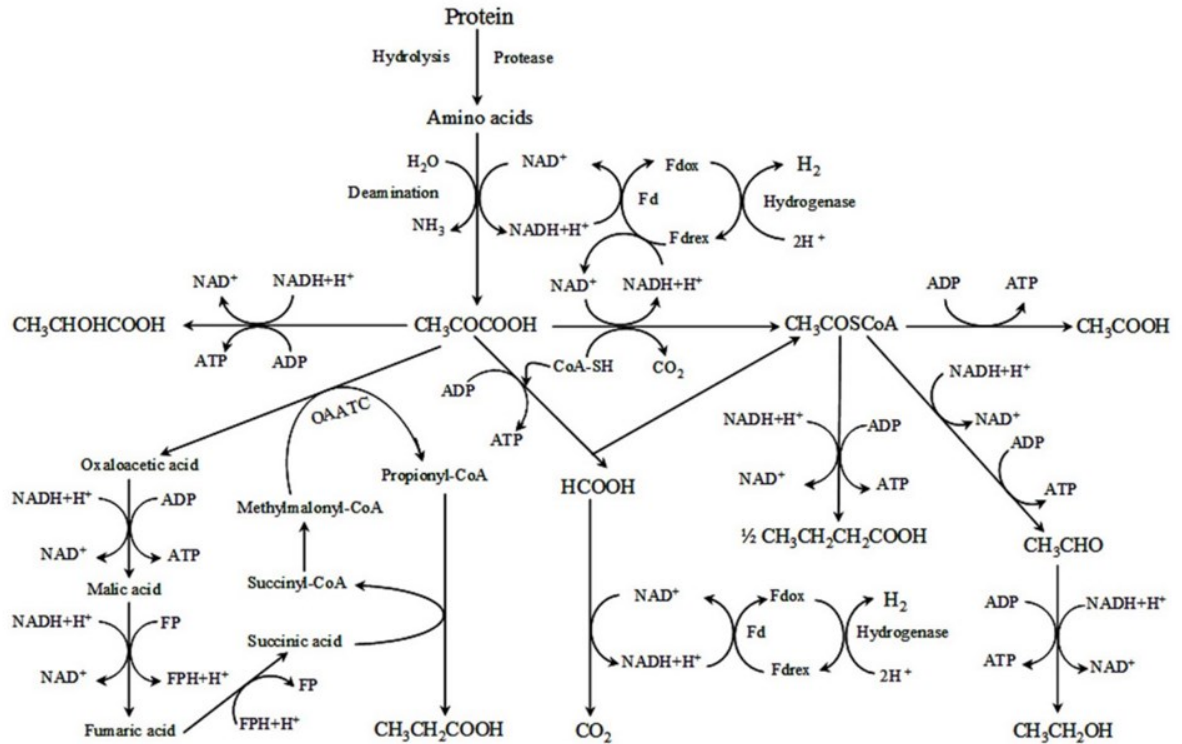


Figure 2-4. Proposed metabolic pathway for anaerobic bio-hydrogen production from protein-rich wastewater. Adopted from Xiao et al. (2014).

NADH is oxidized by NADH-Fd reductase to recycle NAD⁺, while hydrogenase oxidizes reduced ferredoxin to produce molecular hydrogen (Vignais et al., 2001). Furthermore, oxaloacetate transcarboxylase (OAATC) is a key enzyme involved in the propionic acid synthesis and NADH consumption (Xiao et al., 2014).

In rumen, carbohydrate-fermenting microorganisms degrade proteins, and fermentation of amino acids can not yield sufficient energy for microorganism growth. Whereas protein degradation in AD is mediated by proteolytic bacteria with energy yield (Karasov and Douglas, 2013). For instance, methane production rate from protein substrates added to digestate from a single reactor was 96.2 mL CH₄ g⁻¹ VS day⁻¹. Abundance of the potentially proteolytic genera *Proteiniphilum*, *Fastidiosipila*, and *Acetomicrobium* was observed in the

digester (Perman et al., 2022). *Proteiniphilum* has been described to degrade peptides, complex carbohydrates, and *Fastidiosipila* has previously been coupled to proteolytic activity in pure cultures and AD systems (Hahnke et al., 2016). *Proteobacteria* degraded $47.42 \pm 5.62\%$ protein of sewage sludge, and methane and biogas yield were 270 ± 33 and 438 ± 53 mL g⁻¹ VS_{added}. Moreover, the biogas production rate was observed at 0.49 ± 0.06 L day⁻¹ (Zhu et al., 2021). Proteolytic bacteria in the anaerobic digesters are gram-positive bacteria from the *Clostridia* genus, which ferment amino acids dominantly (Ramsay and Pullammanappallil, 2001).

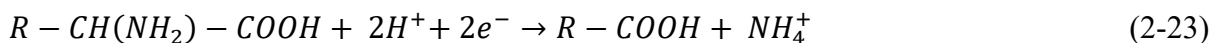
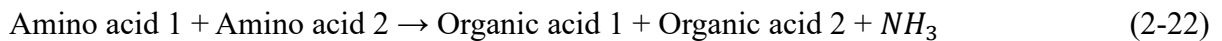
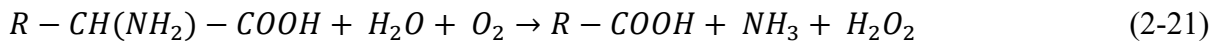
For microbial growth in anaerobic digester, nitrogen is one of the important factors in nutritional requirements (Abomohra et al., 2022). In an anaerobic digester, proteins, and amino acids usually act as a nitrogen source for microorganisms. Various microorganisms and enzymes (extracellular proteases) degrade the protein unit of substrates and convert them into amino acids through purine and pyrimidine bases (Fonknechten et al., 2010; Yokoyama et al., 2007). Microorganisms use the produced amino acids as a nitrogen source; however, the fermentation process forms free ammonia or ammonium ions as the final product (Fonknechten et al., 2010; Sharma and Melkania, 2018). Free ammonia is considered a main inhibitor; these molecules reduce the specific enzyme activity, alter intracellular pH levels, and may cause proton imbalance after diffusing through microbial cells (Wang et al., 2016).

2.8.2 Amino acid metabolism (Stickland reaction)

Amino acid's structure comprises a central carbon atom linked to a hydrogen atom, an acidic carboxyl group (—COOH), and an amino group (—NH₂). Additionally, each amino acid also has an organic side chain or R group, which is unique among the 20 amino acids. The structure of amino acids is provided in Figure 2-5.

This R group distinguishes one amino acid from the other, while the α carbon, carboxyl, and amino groups remain common to all amino acids. Proline is a minor exception to this structure since its R group is linked to the α -amine, which forms a ring-like structure. The general linear formula of an amino acid is $R-CH(NH_2)-COOH$. The amino acids are grouped in classes according to their side chains (Table 2-9). The approximate molecular weight of a protein is found by the number of amino acids multiplied by 110 Da.

Proteins are hydrolyzed by extracellular enzymes (proteases) into amino acids and polypeptides. Then, amino acids are fermented through various pathways and produce different products depending on the concentration and type of the amino acids present (Ramsay and Pullammanappallil, 2001). Under anaerobic conditions, amino acids follow three pathways: 1) oxidative deamination of a single unit of amino acid utilizing hydrogen utilizing bacteria; 2) pairs of amino acids can be degraded following the Stickland reaction; 3) reductive deamination of a single unit of amino acid (Yin et al., 2016). The general equation for these three pathways (Eqs (2-21) to (2-23)) of amino acids are as follows (Shen and Sergi, 2022).



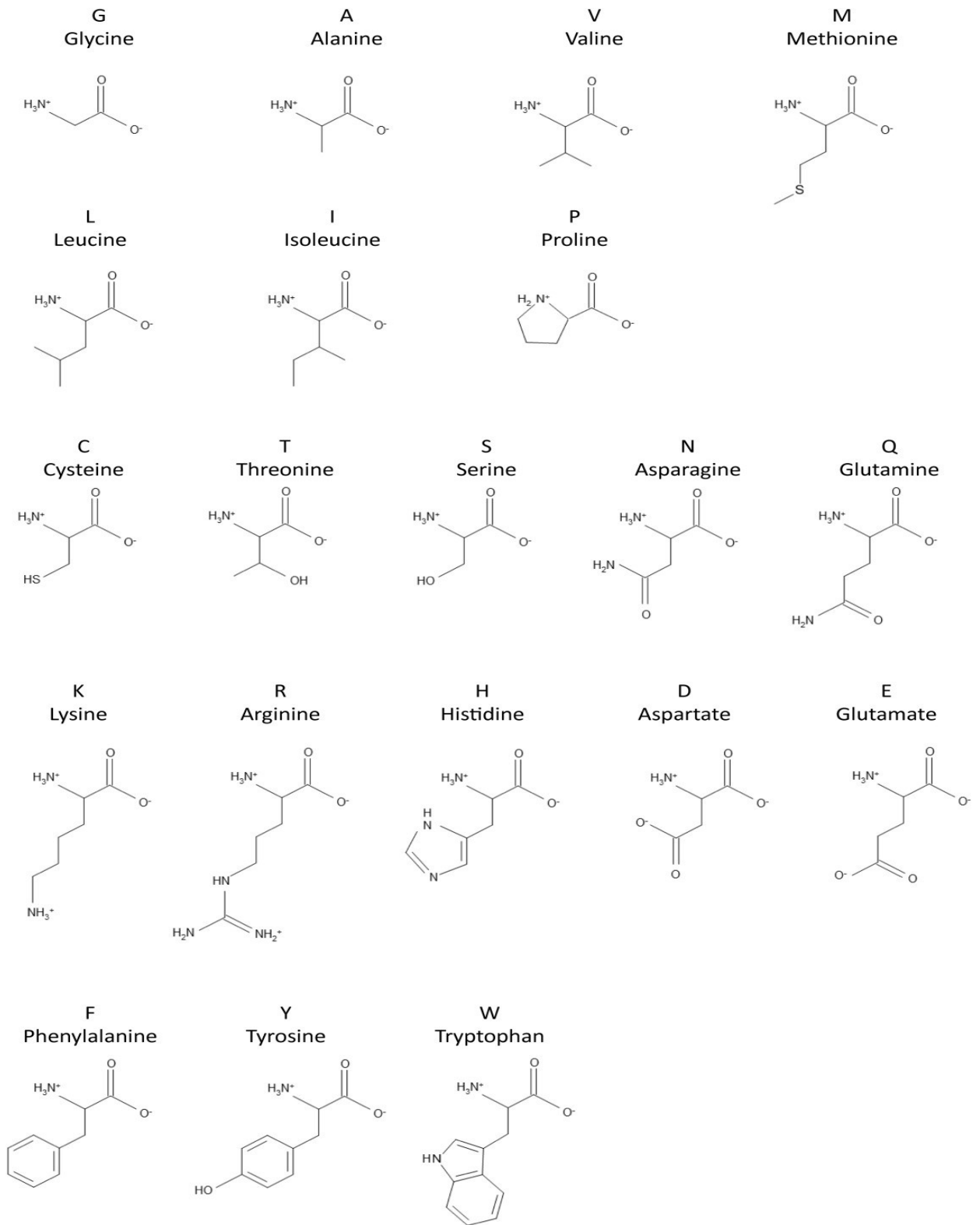
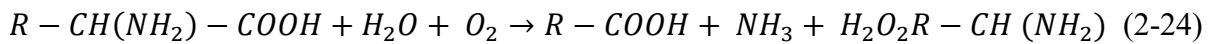


Figure 2-5. Standard amino acids at pH 7. Adopted from Roberts et al. (1965).

Table 2-9. Molecular and linear formulas of 20 amino acids (Ahern et al., 2018).

Amino acid	Abbreviations		Molecular formula	Molecular weight
Alanine	Ala	A	C ₃ H ₇ NO ₂	89.1
Arginine	Arg	R	C ₆ H ₁₄ N ₄ O ₂	174.2
Asparagine	Asn	N	C ₄ H ₈ N ₂ O ₃	132.1
Aspartic acid	Asp	D	C ₄ H ₇ NO ₄	133.1
Cysteine	Cys	C	C ₃ H ₇ NO ₂ S	121.2
Glutamine	Gln	Q	C ₅ H ₁₀ N ₂ O ₃	146.2
Glutamic acid	Glu	E	C ₅ H ₉ NO ₄	-
Glycine	Gly	G	C ₂ H ₅ NO ₂	75.1
Histidine	His	H	C ₆ H ₉ N ₃ O ₂	155.2
Isoleucine	Ile	I	C ₆ H ₁₃ NO ₂	131.2
Leucine	Leu	L	C ₆ H ₁₃ NO ₂	131.2
Lysine	Lys	K	C ₆ H ₁₄ N ₂ O ₂	146.2
Methionine	Met	M	C ₅ H ₁₁ NO ₂ S	149.2
Phenylalanine	Phe	F	C ₉ H ₁₁ NO ₂	165.2
Proline	Pro	P	C ₅ H ₉ NO ₂	115.1
Serine	Ser	S	C ₃ H ₇ NO ₃	105.1
Threonine	Thr	T	C ₄ H ₉ NO ₃	119.1
Tryptophan	Trp	W	C ₁₁ H ₁₂ N ₂ O ₂	204.2
Tyrosine	Tyr	Y	C ₉ H ₁₁ NO ₃	181.2
Valine	Val	V	C ₅ H ₁₁ NO ₂	117.1



During paired amino acids degradation through Stickland reaction, one amino acid having a shortage of one carbon atom than the parent amino acid acts as an electron donor, whereas an amino acid having the same carbon atoms as the parent amino acid acts as an electron acceptor (Eqs (2-24) and (2-25)) (Chen et al., 2021). Amino acid Leucine can act as an electron donor and acceptor (Sangavai et al., 2019). Stickland reaction controls around 90% of the amino acid

degradation. The Stickland reaction is the simplest way of amino acids fermentation, which provides the bacterial cell with approximately $0.5 \text{ mol ATP mol}^{-1}$ amino acid (Sangavai et al., 2019). In Stickland reactions, paired amino acids decomposition occurs faster than uncoupled amino acids decomposition (Sangavai et al., 2019).

Amino acids like alanine, histidine, methionine, lysine and cysteine were used by Sharma and Melkania (2018) in AD of organic fraction of solid waste for biohydrogen production. Butyrate, acetate, propionate, and lactate were the major VFA produced in all samples. Microorganisms utilize amino acids and produce acetate and pyruvate, and subsequently, from pyruvate results, hydrogen, carbon dioxide, butyrate, and acetate. According to Elbeshbishy et al. (2011), acetic acid and butyrate type metabolism is favorable for hydrogen; butyrate is produced with 2 mol hydrogen as end products, and acetic acid is produced with 4 mol hydrogen from one-mole glucose fermentation (Elbeshbishy et al., 2011). Table 2-10 presents group 1 bacteria, which typically utilize the listed amino acids, the type of enzyme production of each bacteria, and the characteristics of group 1-V bacteria.

Table 2-10. Amino acid-degrading anaerobic bacteria and produced enzymes. Adopted from Ramsay and Pullammanappallil (2001).

Group Species	Enzyme production by each bacteria	Utilized Amino acids by all bacteria of group 1	Characteristics of all group 1 bacteria
Group I bacteria			
<i>C. sordellii</i>	proteo/saccharolytic	proline, serine,	organism that
<i>C. botulinum types A, B, F</i>	proteo/saccharolytic	arginine,	carry out
<i>C. caloritolerans</i>	proteo/saccharolytic	glycine, leucine,	Stickland
<i>C. sporogenes</i>	-	isoleucine,	reaction;
<i>C. cochlearium – one strain.</i>	proteo/saccharolytic	valine,	proline utilized
<i>C. difficile</i>	specialist	ornithine, lysine,	by all species;
<i>C. putrificum</i>	saccharolytic	alanine,	δ -
<i>C. sticklandii</i>	proteo/saccharolytic	cysteine,	aminovalerate,
<i>C. ghoni</i>	specialist proteolytic	methionine,	α -
<i>C. manganotii</i>	proteolytic	aspartate,	aminobutyrate
<i>C. scatologenes</i>	saccharolytic	threonine,	and
<i>C. lituseburens</i>	proteo/saccharolytic	phenylalanine,	γ -
<i>C. aerofoetidum</i>	-	tyrosine,	aminobutyrate
<i>C. butyricum</i>	saccharolytic	tryptophan, and	produced.
<i>C. caproicum</i>	-	glutamate	
<i>C. carnofoetidum</i>	-		
<i>C. indolicum</i>	-		
<i>C. mitelmanii</i>	-		
<i>C. saprotoxicum</i>	-		
<i>C. valerianicum</i>	-		
Group II bacteria			
<i>C. botulinum types C</i>	proteo/saccharolytic	glycine, arginine,	glycine used by
<i>C. histolyticum</i>	proteolytic specialist	histidine and	all species;
<i>C. cochlearium – one strain</i>	proteolytic	lysine	δ -aminovalerate
<i>C. subterminale</i>	-		not produced,
<i>C. botulinum types G</i>	-		
<i>P. anaerobius</i>	-		
<i>P. variabilis</i>	-		
<i>P. micros</i>	-		

Table 2-10. Continued.

Group Species	Enzyme production by each bacteria	Utilised Amino acids by all bacteria of group 1	Characteristics of all group 1 bacteria
Group III			
<i>C. cochlearium</i> – one strain.	Specialist Proteolytic Saccharolytic	glutamate, serine, histidine, arginine,	δ -aminovalerate not produced;
<i>C. tetani</i>	-	aspartate,	histidine, serine and glutamate used by all species.
<i>C. tetanomorphum</i>	proteolytic specialist	threonine,	
<i>C. lentoputrescens</i>	-	tyrosine,	
<i>C. limosum</i>	proteo/saccharolytic	tryptophan and	
<i>C. malenomenatum</i>	saccharolytic	cysteine	
<i>C. microsporum</i>	-		
<i>C. perfringens</i>	-		
<i>C. butyricum</i>	-		
<i>P. asaccharolyticus</i>	-		
<i>P. prevotii</i>	-		
<i>P. activus</i>			
Group IV			
<i>C. putrefaciens</i>	proteolytic	serine and threonine	δ -aminovalerate not produced
Group V			
<i>C. propionicum</i>	specialist	alanine, serine, threonine, cysteine and methionine	δ -aminovalerate not produced

These microorganisms utilize proline and produce δ -aminovalerate, α -aminobutyrate or γ -aminobutyrate as intermediates in the fermentation process. This type of reaction has only been reported with *Clostridial* species. Amino acids known to be commonly involved in Stickland reactions include proline, serine, arginine, ornithine, glycine, leucine, isoleucine, valine, serine, lysine, alanine, cysteine, methionine, aspartate, threonine, phenylalanine, tyrosine, and tryptophan (Ramsay and Pullammanappallil, 2001).

2.9 Challenges of Nitrogen-Rich Sources in Anaerobic Digestion

Biohydrogen and biomethane production from nitrogen-rich sources in AD can face several challenges. The high protein contents in nitrogen-rich waste easily lead to inhibitory levels of ammonia, hydrogen sulfide, and long-chain fatty acids or cause foam formation in the digester (Xu et al., 2018). Accumulation of ammonia in AD can inhibit the activity of methanogens and reduce the overall methane yield. Moreover, the accumulation of volatile fatty acids (VFAs) is another common problem in the AD of manure, which can also negatively impact the methane yield.

2.9.1 Ammonia accumulation

According to Chen et al. (2008), ammonia is one of the primary factors responsible for reactor upsets because it is present almost everywhere in the digester and is often generated in high concentrations in waste materials. The principal components of animal waste are manure, urine, flushing water, and animal dead bodies, known for their high nitrogen content due to the decomposition of urea and proteins (Möller and Müller, 2012). Although ammonia can stimulate microbial growth at low concentrations, it can be highly inhibitory when its concentration surpasses a certain threshold. Research has identified various inhibitory thresholds of total ammonia nitrogen (TAN) concentrations ranging from 3.4 to 5.77 g L⁻¹. These high concentrations can significantly reduce methane yield during the AD process, ranging from 20% to 100% (Climenhaga & Banks, 2008; Yang et al., 2018). The variations in the results can be attributed to the variations in temperature, modes and configuration of the reactor operations, and microbial communities unique to different systems (Alsouleman, 2019). Examples of various nitrogen-rich wastes and their inhibition of AD is presented in Table 2-11.

Table 2-11. Examples of the physicochemical characteristics of different nitrogen-rich wastes and their impact on the inhibition of AD.

Type of waste	VS (%)	TS (%)	Total NH ₄ ⁺ Nitrogen (mg L ⁻¹)	Total Nitrogen (mg L ⁻¹)	TCOD (g L ⁻¹)	Reduction in methane or biogas yield (%)	References
Pig manure	4.6	5.9	4000	6700	-	11 g L ⁻¹ TAN –50% CH ₄ yield 0.3 g L ⁻¹ FAN –53% CH ₄ yield	Nakakubo et al. (2008)
Chicken manure	8.27	11.5	-	6450	104	10 g L ⁻¹ TAN –20% biogas yield 16 g L ⁻¹ TAN –100% biogas yield	Niu et al. (2015)
Food waste	23.5	25.3	335	6000	181	4.69 g L ⁻¹ TAN –100% CH ₄	Chen et al. (2016)
Chicken manure	71.87	90.98	-	4.91	-	8 g L ⁻¹ NH ₄ ⁺ –43% biogas yield	Wu et al. (2016)
Municipal waste	-	-	190 –224	-	2.714–3.289	2 g L ⁻¹ TAN –50% CH ₄ Yield	Gao et al. (2019)
Dairy manure	6.24	7.3	2100	3.8	-	3.2 g L ⁻¹ –29% CH ₄ yield	Sutaryo et al. (2014)

TAN = total ammonium nitrogen (i.e., the sum of free ammonia and ionized ammonia); TCOD = total chemical oxygen demand; TS

= total solids; VS = volatile solids.

Excess ammonia's impact on thermophilic AD performance was explored by Alsouleman (2019). A 25% and 50% nitrogen-rich poultry manure were added to cattle slurry. The long-term (81 to 162 days) experiments revealed that adding 25% manure led to restoring the reactor's normal functioning by reorganizing the microbial community structure. However, when 50% manure was added, despite the microbial community shift after long-term (day 177- 341) acclimation, the process was disrupted and eventually failed after a short, steady operation period (between days 250 and 270).

2.9.1.1 Mechanism of ammonia inhibition

Free ammonia nitrogen (FAN) is of primary importance to ammonia inhibition in AD (Capson-Tojo et al., 2017). The accumulation of metabolites such as ammonia and free ammonia in high concentrations can impede methanogenesis during AD of protein-rich substrates. These metabolites can inhibit microbial activity (Yenigün and Demirel, 2013) by diffusing across the cell membrane and leading to cellular content leakage, ultimately affecting microbial cell growth (Fagbohunge et al., 2017). The diffusion of free ammonia into filamentous bacteria cells is faster than into non-filamentous cells (Demirel and Scherer, 2008). The normal toxic concentrations of free ammonia and total ammonia nitrogen (TAN) are reported to be 600 mg L⁻¹ and 5700 mg L⁻¹, respectively (Kovács et al., 2015). Figure 2-6 depicts the indirect effect of free ammonia on the methane-producing machinery in bacterial cells.

During the digestion of protein-rich waste, ammonia is produced as free ammonia and ammonium ions (NH₄⁺) in an aqueous solution. The toxic effect of free ammonia and NH₄⁺ on methanogens involves different inhibitory mechanisms (Wang et al., 2015).

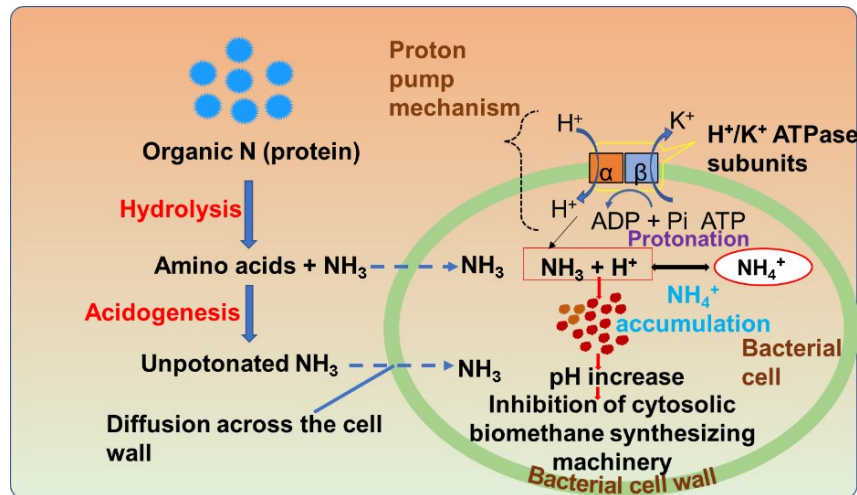


Figure 2- 6. Schematic representation of ammonia toxicity during anaerobic digestion (AD) of protein-rich biowastes. Modified from Ling et al. (2022) with copyright permission.

Free ammonia can passively diffuse into bacterial cells through cell pores, depending on the concentration gradient, and once inside the cells, it can absorb intracellular protons and partially convert to NH_4^+ . This conversion of free ammonia to NH_4^+ increases the energy requirement for the cell's potassium (K^+) efflux to balance the number of protons, which potentially causes inhibition of specific enzyme reactions. Moreover, when the K^+ pump cannot work efficiently due to higher ammonia exposure, the accumulated NH_4^+ inside the cells destabilizes the intracellular pH, leading to cytotoxicity. Other essential cytosolic cations, such as Mg^{2+} and Na^+ have also been reported to be affected by ammonia through a similar mechanism. High ammonia can also disturb the uptake of essential trace elements required for cell function and cause micronutrient deficiency. NH_4^+ also affects the biomethane-synthesizing machinery, inhibiting specific enzymatic reactions (Faisal et al., 2021). The methanogen inhibition by ammonia is attributed to changes in pH, NH_4^+ ion concentration, and interference with biomethane-synthesizing enzymatic reactions. Methanogens can acclimatize to high-ammonia stress during long-term AD or induce an inhibited

steady state in which free NH_3 is limited by VFAs accumulation. The microbial communities showed changes from acetoclastic to hydrogenotrophic methanogenesis during acclimatization to ammonia, accompanied by syntrophic acetate-oxidizing bacteria (Yan et al., 2019).

The intracellular NH_4^+ accumulation is stopped when FAN is found between intracellular pH and extracellular pH (7.0 to 8.5 for most methanogens). Lowering the extracellular pH can reverse the intracellular accumulation and alleviate ammonia inhibition. Protein, which is a substrate of anaerobic digestion, is a common source of both acid and ammonia. Eq. (2-26) shows that pH substantially influences the balance between FAN and NH_4^+ .

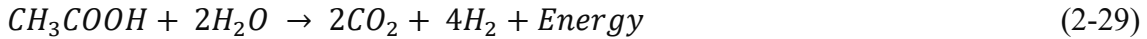
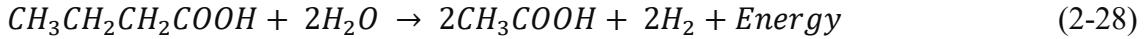
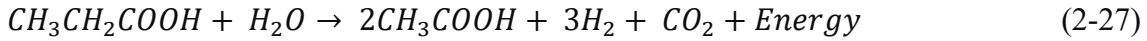
$$\text{NH}_3 \text{ (Free ammonia Nitrogen or FAN)} = \frac{[\text{TAN}]}{(1+10^{\text{pKa}-\text{pH}})} \quad (2-26)$$

With a given TAN content, a higher pH increases FAN concentration. When two systems have the same TAN content and are operated at 37 °C, for instance, the FAN concentration is around 44 times greater in a solution with a pH of 9 than a pH of 7, which might lead to a more severe inhibitory impact. Moreover, most orders of methanogens develop best in a pH range between 6 to 8 (Harirchi et al., 2022), highlighting the need to maintain a nearly neutral pH during the AD process.

2.9.2 Volatile fatty acids accumulation

High TAN amounts can cause secondary inhibition in AD reactors due to the buildup of intermediate compounds, including volatile fatty acids (VFAs) (Yuan and Zhu, 2016). In AD, VFAs such as acetic (C_2), propionic (C_3), butyric (C_4), valeric (C_5), and caproic (C_6) are produced

from organic wastes during acidogenesis and acetogenesis steps, and they are converted to methane in methanogenesis step (Harirchi et al., 2022). According to Eqs (2-27) to (2-29), hydrogen is a typical by-product of the breakdown of different VFAs.



According to Siegert and Banks (2005), souring or over-acidification due to the buildup of excessive volatile fatty acids (VFAs) by acidogenic and acetogenic bacteria during AD is the most common upset. This reflects a prominent imbalance between acid production and consumption rates. This imbalance typically drops the pH sharply, causing the reactor's buffering ability to fail.

An interesting phenomenon related to VFA and daily methane yield was observed by Zheng et al. (2015). The author studied the effect of VFA on manure-switchgrass AD. The VFA concentration was more than 6 g L⁻¹ on day 3 and 4, which inhibited methane production and delayed the peak of methane production in the 2:2 (manure: switchgrass) digesters until day 6. On the other hand, digesters with ratios of 1:3 and 0:4 (manure: switchgrass) stopped producing methane when the pH decreased below 6.0, and the VFA was above 7.0 g L⁻¹. In addition, the peak in daily methane yield did not appear until the VFA content began to decrease and the pH began to recover. The high total VFAs concentration (10 g L⁻¹) in digesters was responsible for the longest delay in biogas production from two nitrogen-rich substrates (pig manure and kitchen waste), propionic and butyric acid were the major composition of the total VFAs (Tian et al., 2015). Butyric acid accounted for a large proportion, and acetic acid and propionic acid accounted for

small proportions in AD of manure, rice straw, and pig manure. $1035.30 \pm 48.37 \text{ mg L}^{-1}$ was obtained at 5:1 (rice straw: pig manure), confirming that butyric acid accumulation was positively associated with biohydrogen production (Chen et al., 2021).

Changes in pH can significantly affect the microorganism's development and metabolic pathways. Excessive VFAs concentration can cause the pH to fall below the ideal range, leading to lower biogas output and monetary losses (Theuerl et al., 2019). Acidogenic bacteria may operate in a wider range of pH (4.0 to 8.5), but methane-forming archaea are particularly sensitive to pH fluctuations and can only withstand a small range (6.5 to 7.2) (Xu et al., 2020). Nevertheless, acidification in AD reactors can interfere with the hydrolysis and acidogenesis stages and inhibit methanogenesis, such as slowing down or reducing the efficiency of hydrolysis and methanogenesis steps (Li et al., 2009).

The AD performance can be adversely affected by over-acidification in full-scale installations, according to laboratory tests carried out in precisely controlled environments by Moeller and Zehnsdorf (2016). A full-scale AD reactor fed with animal manure and energy crops encountered excessive acidification for just two days, as Moeller and Zehnsdorf's research demonstrated, which dramatically declined biogas and power production from 13.5 to 6.9 MWh day^{-1} . Their investigation detected the highest acidity as 9196 mg L^{-1} of VFA. It is crucial to remember that, while uncommon, these instances happen and significantly influence the performance.

VFAs produced in AD may have different effects on the process. This has led to differing opinions on which type of short-chain fatty acid is the key indicator of reactor acidification and potential process failure. However, studies like Srisowmeya et al. (2020), Wang et al. (2006), and Wang et al. (2009) have reported that propionic acid has a greater inhibitory effect on biogas production compared to other VFAs. This is due to the slower degradation process and higher

sensitivity associated with this VFA. The maximum inhibitory levels of propionic acid in various experiments are found from 0.8 g L⁻¹ (Ma et al., 2009) to 21.6 g L⁻¹ (Capson-Tojo et al., 2017), depending on factors such as the substrate and inoculant used, reactor configuration, and operating conditions.

2.10 Microbiology of Biohydrogen Production

Microorganisms, specifically hydrogen-producing microorganisms (HPMs), play a vital role in the biohydrogen production process of organic matter through AD. AD involves using enzymes, such as hydrogenase and ferredoxin (Fd), to produce gaseous hydrogen (Kim and Kim, 2011). Hydrogenases are key enzymes many microorganisms use to expel excess reducing power or to oxidize molecular hydrogen as an energy and electron source (Yu and Takahashi, 2007). These enzymes are usually located at accessible positions from outside by electron shuttles in the periplasm of HPMs, which are specialized microbial compartments (Schuchmann et al., 2018). The Fd, an iron-sulfur protein, acts as an electron carrier at low redox potential and plays an important role in this process. Moreover, hydrogen production is essential in maintaining the balanced redox potential of microorganisms. More reduced compounds will form with the prohibited hydrogen production (Harirchi et al., 2022).

Mixed culture fermentation is widely used for biohydrogen and biomethane production in AD of nitrogen-rich waste. The process involves the synergistic action of different groups of microorganisms, particularly bacteria and archaea (Bharathiraja et al., 2016). The dominant communities of HPMs, which can grow faster and have a broader pH range compared to hydrogen-consuming microorganisms (HCMs), are usually responsible for favorable conditions for hydrogen production. HPMs are also more resistant to harsh conditions than methanogens.

Several bacterial species are known to play a crucial role in the hydrolysis and fermentation of nitrogen-rich waste in AD. These include *Clostridium*, *Bacillus*, *Enterobacter*, and *Proteus* species, among others. Among HPMs, *clostridium* is considered one of the most effective nitrogen-rich waste degraders, with some species capable of producing biohydrogen, biomethane, and other value-added products (Rawoof et al., 2021). Other bacterial species, such as *Bacillus coagulans* and *Enterobacter aerogenes*, have also been reported to produce biohydrogen from nitrogen-rich waste in mixed culture fermentation (Laxman Pachapur et al., 2015). A list of microbial communities involved in protein-rich substrate degradation is provided in Table 2-12.

Anaerobic digestion of organic waste involves a complex microbial community where different bacterial species work synergistically to break down the organic matter into simpler compounds, which are further metabolized to produce biogas (Harirchi et al., 2022). The primary factor responsible for the changes in the microbiome composition during the digestion of protein-rich substrates is the formation and accumulation of ammonia. Temperature, solution pH, and substrate feeding also contribute to changes in the microbiome composition. In the mono-digestion of pig blood and casein, pronounced changes in bacterial communities have been observed, including an abundance of *Firmicutes*, *Proteobacteria*, and *Bacteroidetes*. Pig blood (94% protein) digestion resulted in an abundance of *Dethiosulfovibrio peptidovorans*, a strict amino acid-using bacterium. Casein (82 % protein) digestion was associated with an increase in *Clostridium sticklandii*, *Alkaliphilus oremlandii*, and *Alkaliphilus metalliredigens* (Kovács et al., 2013).

Similarly, fish waste AD was abundantly associated with *Clostridium* (in acetogenesis step), *Cryptanaerobacter* (aromatic amino acid biodegrader), *Proteiniclasticum* (anaerobic proteolytic bacteria), and *A. colombiense* (protein degrader) (Bücker et al., 2020).

Table 2-12. Microbial communities involved in protein-rich substrate digestion.

Waste source	Major bacteria involved	Experiment summary	References
Meat extract	<i>Cloacamonas acidaminovorans</i> , <i>Bacillus coagulans</i> , <i>Bacillus subtilis</i> , <i>Candidatus Pseudomonas fluorescens</i> ,	Limiting factors were NH ₃ and H ₂ S accumulation	Kovács et al. (2015)
Pig blood protein and casein	<i>Alkaliphilus metalliredigens</i> , <i>Alkaliphilus oremlandii</i> , <i>Dethiosulfovibrio peptidovorans</i>	Essential to have proper process control and allow the microbial community to adjust to the uncommon substrate.	Treu et al. (2019)
Slaughterhouse waste	<i>Syntrophomonas</i> sp., <i>Coprothermobacter</i> sp., <i>Anaerobaculum</i> sp.	Limiting factors were the substrate's lipid content and the microbial community's structure.	Palatsi et al. (2011)
Meat extract and kitchen waste	<i>Clostridia</i> , <i>Thermotogae</i> , <i>P. fluorescens</i> , <i>B. coagulans</i> , <i>B. subtilis</i>	Acclimation at low substrate levels is necessary for the microbial community to adapt sufficiently.	Kovács et al. (2015)
Fish waste, silage, and cow manure	<i>Clostridium</i> sp., <i>Syntrophomonas</i> , <i>Candidatus Cloacimonas acidaminovorans</i>	As microbial communities break down the same substrate over time, they become less diverse and specialized. This process is often observed in the presence of high concentrations of ammonium and VFAs, where syntrophic prokaryotes are commonly found.	Solli et al. (2014)
Shrimp chaff and cornstraw	<i>Proteiniphilum</i> , <i>Ercella</i>	Due to optimum C/N, co-digestion of protein waste with carbonaceous wastes significantly improves biomethane yield.	Ali et al. (2021)
Cow manure, food and vegetable waste, corn straw	Bacteroidetes, Proteobacteria, Firmicutes, Fibrobacteres, Spirochaetes	AD increased hydrolysis rates and bacterial community diversity through differential carbon release rates of substrates.	Wang et al. (2018)
Fish waste and garden grass	Clostridiales, Bacteroidales, Cloacimonadales	Found dependency of archaea and bacterial population abundance on the substrate composition.	Puig-Castellví et al. (2020)

Treu et al. (2019) utilized cheese whey in their mono-digestion experiment and observed a significant increase in the prevalence of specific microorganisms, including *Cloacimonetes* (amino

acid fermenter and propionate and butyrate oxidizer), *Clostridiales* spp. (contributed in butyrate production), and *Aminobacterium colombiense* (acetate and propionate producer from amino acid).

Some previous studies have demonstrated that sufficient protein content balances C:N (20:1 to 30:1) in the complex substrates, leading to an improvement in biohydrogen production (Chowdhury et al., 2022; Łukajtis et al., 2018). Moreover, many studies have been performed to improve the biohydrogen production potential using protein-rich wastes. The hydrogen yield from protein-rich food waste with *S. cerevisiae* produced 186.1 mL H₂ g⁻¹ TVS, whereas 171.9 mL H₂ g⁻¹ TVS was produced from the same substrate when mixed with hydrogen-producing bacteria derived from activated sludge (Song et al., 2010). The authors justified the findings by stating that *S. cerevisiae* produced some proteinase enzymes that facilitated protein degradation besides providing a conducive anaerobic environment for hydrogen-producing bacteria (Song et al., 2010).

While there are different bacterial species involved in the anaerobic digestion process, some of the key species responsible for manure hydrolysis are listed below:

Hydrolytic bacteria: These bacteria are responsible for the initial step in the anaerobic digestion process, which involves the hydrolysis of complex organic compounds into simpler compounds. Some of the key hydrolytic bacteria involved in manure hydrolysis are *Clostridium thermocellum*, *Clostridium cellulolyticum*, and *Ruminococcus albus* (Basak et al., 2022).

Acidogenic bacteria: These bacteria utilize the simple compounds produced by hydrolytic bacteria and produce short-chain fatty acids, hydrogen, and carbon dioxide as end products. Some of the key acidogenic bacteria involved in manure hydrolysis are *Acetobacterium woodii*, *Clostridium kluyveri*, and *Bacteroides thetaiotaomicron* (Liu et al., 2018).

Methanogenic microorganisms (Archea): These bacteria convert the simple compounds produced by acidogenic bacteria into biogas, which is composed primarily of methane (CH₄) and

carbon dioxide (CO₂). Some key methanogenic archaea involved in manure hydrolysis are *Methanosarcina barkeri*, *Methanobacterium formicicum*, and *Methanococcus jannaschii* (Czatzkowska et al., 2020).

2.11 Kinetics of Protein Substrate in Anaerobic Digestion

The kinetics of the anaerobic process are crucial in developing and operating treatment systems. Kinetics are based on the biochemistry and microbiology of the process and offer a logical foundation for process analysis, control, and design. These kinetics provide a quantitative understanding of waste utilization rates, including carbohydrates, proteins, and lipid wastes, and they consider operational and environmental factors that can impact these rates. Therefore, a sound understanding of process kinetics is essential for optimizing performance, achieving more stable operation, and better controlling the AD process (Gavala et al., 2003; Morais et al., 2021).

In a process consisting of multiple reactions, the rate of the entire process is determined by the slowest reaction, called the rate-limiting step. This step typically involves the hydrolysis of solids for AD involving suspended organic matter. In most cases discussed in the literature, disintegration, solubilization, and enzymatic hydrolysis are expressed using the term 'hydrolysis' (Candido et al., 2019; Wouters et al., 2016). The Michaelis–Menten kinetics (Eq. (2-30)) may be applied for the hydrolysis of a soluble substrate and is expressed as:

$$dS/dt = \frac{(k.E.S)}{(K_m+S)} = Vm/(K_m + S) \quad (2-30)$$

Where E and S are the enzyme and substrate concentrations, k is the maximum hydrolysis rate constant, and K_m is the half-saturation rate coefficient (Vavilin et al., 2008).

Kinetics of the degradation of protein-rich wastes in AD refers to studying the rate and mechanism of the breakdown of protein waste materials by microorganisms in anaerobic conditions, such as those found in biogas reactors. The rate of protein hydrolysis is affected by the accessibility of the protein to the hydrolytic enzymes, which can be influenced by the protein structure and properties, such as molecular weight, solubility, and amino acid composition. The rate of protein hydrolysis also depends on the microbial community present in the digester, pH, and temperature, as different microorganisms produce different types of enzymes that can break down proteins at different rates.

According to Jovanović et al. (2016), the rate of protein hydrolysis generally increases with temperature, with the optimum temperature range for protein hydrolysis being around 50-60 °C. However, at temperatures above 70 °C, the rate of protein hydrolysis may decrease due to enzyme denaturation. pH can also affect the rate of protein breakdown, with the optimum pH range for protein hydrolysis is between 6.5 and 8.0. Retention time can influence the protein breakdown rate in AD. Longer retention times can lead to higher protein breakdown rates, as more time is allowed for the microorganisms to break down the proteins into amino acids (Pilli et al., 2015). A study conducted by Duong et al. (2021) found gelatine hydrolysis at pH 5 was 12-fold slower than at pH 7. Hydrolysis is the rate-limiting step in gelatine degradation at pH 5. Even after long-term exposure of the substrate to pH 5 (480 days), the hydrolysis rate constant for protein ($0.05 \text{ L g}^{-1} \text{ VSS day}^{-1}$) was still much lower than at pH 7 ($0.62 \text{ L g}^{-1} \text{ VSS day}^{-1}$).

The traditional model used for the hydrolysis of particulate material, such as cow manure, is a first-order kinetics model for the substrate. This model was developed empirically to encompass the combined effects of a series of microscopic processes. It assumes that the rate of hydrolysis is not dependent on the concentration of microorganisms involved (López et al., 2021).

The differential equation (Eq. (2-31)), addressing hydrolysis as the first-order reaction not directly associated with bacterial growth, is:

$$dS/dt = -kS \rightarrow \frac{dP}{dt} = \alpha k S \quad (2-31)$$

where S is the volatile solids (VS) concentration, P is the product concentration, k is the first-order rate coefficient, and α is the conversion coefficient of VS to product (Vavilin et al., 2008). This does not imply that microbial growth does not exist, but because the biomass is in excess, its concentration is approximately constant and does not influence the rates of substrate consumption and methane production (López et al., 2021). Table 2-13 summarizes the typical values of rate coefficients for different substrates that can be found in the literature.

When discussing hydrolysis, several different kinetic equations have been reported in the literature, including surface-based and Contois kinetics (Lawrance et al., 2022; Ramírez Calderón, 2020). While some models assume hydrolysis to be a first-order reaction, it is important to note that these kinetics are typically only apparent first-order and that the kinetic constants can vary greatly depending on a variety of factors, such as the specific type of microorganisms present or changes in particle size distribution (Gaibor-Chávez et al., 2019; Lauwers et al., 2013).

Sanders et al. (2000) proposed a kinetic expression based on surface coverage, which describes the presence of hydrolytic exo-enzymes on bacterial-covered particles. This allows for a constant hydrolysis constant per unit area, accounting for fluctuations in enzyme concentration. The corresponding equation represents this concept (Eq. (2-32)).

Table 2-13. Kinetic coefficients of the first-order rate of hydrolysis of different substrates.

Substrate	k (day ⁻¹)	References
Primary sludge	0.99	Ristow et al. (2006)
Slaughterhouse waste	0.35	Lokshina et al. (2003)
Crushed manure	0.091 to 0.137	Momoh and Saroj (2016)
Cow manure	0.347	Yaldız (2015)
Flushed manure	0.43	Ma et al. (2013)
Swine manure and food waste	0.28	Dennehy et al. (2016)
Fruit residue	0.12	Zhao et al. (2016)
Sieved manure	0.3 to 0.8	Jabłoński et al. (2015)
Blood water	0.29	Bauer (2011); Hejnfelt and Angelidaki (2009)
Milk protein	0.096	Ho et al. (2019)
Protein	0.02 to 0.03	Gujer and Zehnder (1983)
Protein	0.65	Flotats et al. (2006)
Albumin	0.57	Nagase and Matsuo (1982)

$$\mu = k_{SBK}A \quad (2-32)$$

where k_{SBK} (g m⁻² d⁻¹) is the surface-based hydrolysis constant and A (m²) is the surface area (of substrate) available for hydrolysis.

In the initial stage, bacteria colonize the particulate matter, secreting hydrolytic enzymes, which subsequently cause the degradation of the substrate (carbohydrates, lipids, proteins) surface at a constant rate. This phenomenon can be effectively modeled by employing Contois-kinetics, as described by Eq. (2-33) while accounting for the enzyme's variable concentrations.

$$\mu = \frac{\mu_{max}S}{(K_c X) + S} \quad (2-33)$$

Here, μ is the specific growth rate, μ_{max} is the maximum specific growth rate, S is the substrate concentration, K_c is the growth coefficient of the Contois function, and X is the microbial

concentration. This equation is used to model microbial growth on soluble substrates but has also been accepted for kinetic modeling of insoluble substrate degradation (Xu et al., 2012). The Contois kinetics equation has also been used to associate and investigate the effect of the degradation kinetics of substrates in compost matrix (Nelson and Holder, 2009; Nikolaeva et al., 2009).

2.12 Modeling of Protein Anaerobic Digestion

Optimizing the AD parameters can considerably improve biogas production. Hence, optimizing and stabilizing process parameters is essential for biogas production from organic wastes (Menon et al., 2017). However, traditional methods are inappropriate because they require numerous tests and consume a long time and a lot of materials. Statistical models are widely used to overcome these limitations. Response Surface Methodology (RSM) is a statistical and mathematical tool that can evaluate the influence of significant independent parameters, design experiments, and optimize and model the desired responses. The RSM approach has many advantages, such as reducing the number of experiments, simultaneously understanding the interactions of all parameters, and requiring less time and materials. This analysis technique was successfully used for optimizing and modeling manure and other organic wastes AD (Cai et al., 2021; Jacob and Banerjee, 2016; Yılmaz and Şahan, 2020). The statistical technique is beneficial because it involves fewer tests and less time than a full-factorial design (Khoobakht et al., 2016).

The optimization of several factors (such as pH, temperature, OLR, HRT, substrate concentration, and inoculum concentration) is necessary to improve the response variable, which could be biogas production or methane yield in AD. While a single-factor optimization is commonly used, it is not sufficient to explain the interactions between different factors. To address

this, studies have used response surface methodology (RSM) with Box-Behnken design (BBD) (Rai et al., 2019) or with a Central Composite design (CCD) (Yılmaz and Şahan, 2020) to investigate the interactions between various factors. These designs are especially useful in sequential experiments, allowing the researcher to build on previous factorial experiments by adding axial and center points. CCD is a response surface methodology that is used to model the response of a system or process to multiple factors. At the same time, BBD is a type of CCD that is particularly useful for three-factor models offering some advantage in requiring fewer runs. This advantage disappears for four or more factors (Glyk et al., 2015). Both designs involve a combination of factorial and axial points that are used to create a model of the system under study, and the system's response is then analyzed using statistical techniques.

The minimum and maximum values of the independent variables (OLR, time, concentration, pH, etc.) need to be extracted from previous literature of similar studies, and the center point (0) is determined from this range. Finally, the dependent variables, such as gas yield, substrate degradation, etc., are investigated depending on the experiment's objectives. To optimize cattle manure and food waste in AD, Liu et al. (2020) examined hydrogen yield using BBD, assuming independent variables such as the substrate (manure) mixing ratio, the substrate concentration, and HRT having 15 trials, comprising 12 factorial points and 3 center points, were run. In another study, Yılmaz and Şahan (2020) studied the influences of independent parameters (manure TS%, inoculum ratio, the amount of additive, and particle size of additive) with 30 sets of experiments with six replications of the center points. Each independent parameter in CCD was coded at three levels (-1 (lowest)), 0 (central), and +1 (highest)). Design Expert software was used to optimize and predict the results of the experiments. Finally, a second-order polynomial model function was used to describe system behavior.

In AD research, linear regression analysis can be used to understand the relationship between a dependent variable and one or more independent variables. The simple linear regression equation is used to predict the value of the dependent variable based on the value of a single independent variable. The formula for simple linear regression (Eq. (2-34)) is:

$$y = B_0 + B_1 * x \quad (2-34)$$

where y is the predicted value of the dependent variable (i.e., the outcome variable), x is the independent variable (i.e., the predictor variable), B_0 is the intercept (i.e., the predicted value of y when x is equal to 0), and B_1 is the regression coefficient (i.e., the change in y for a unit change in x).

On the other hand, multiple variable linear regression equations are used to predict the value of the dependent variable based on the values of two or more independent variables. The equation (Eq. (2-35)) takes the form:

$$y = B_0 + B_1x_1 + B_2x_2 + \dots + B_nx_n \quad (2-35)$$

where x_1, x_2, \dots, x_n are the independent variables, B_0 is the intercept, and B_1, B_2, \dots, B_n are the regression coefficients associated with each independent variable (Tangwe et al., 2022).

Various kinetic models such as the first-order kinetic model, modified Gompertz model, Chen and Hashimoto, and logistic function model are used to closely analyze the microbial kinetics involved during the AD process of protein-rich wastes such as cow manure and chicken waste (Kafle and Chen, 2016; Siddique and Wahid, 2018). Most studies also aimed to find the most suitable kinetic model (i.e., more statistically relative to the experimental values). All these kinetic

models (Table 2-14) have different added benefits determining the parameters such as cumulative biogas production potential, hydrolysis kinetics, lag phase duration, and maximum methane production (Pramanik et al., 2019).

Table 2-14. Kinetic models and description.

Kinetic model	Equation	Description
First-order kinetic model	$G(t) = G_o * (1 - e^{-kt})$	Where, $G(t)$ = cumulative methane yield at digestion time t (mLg^{-1} VS), G_o = methane potential of the substrate (mLg^{-1} VS), K = methane production rate constant (first order disintegration rate constant) (day^{-1}) (Kafle and Chen, 2016).
Modified Gompertz model	$P(t) = A * \exp \left\{ -\exp \left[\frac{\mu}{A} (\lambda - t) + 1 \right] \right\}$	Where $P(t)$ is the cumulative biogas production at time t , A is the potential biogas production, λ is the lag time, μ is the maximum biogas production rate, and \exp is the base of the natural logarithm (Kafle & Chen, 2016).
Logistic function model	$N_t = N_o / (1 + \exp^{-(\mu_{\max} * (t - t_{\text{lag}}))})$	Where N_t is the cell density at time t , N_o is the initial cell density, μ_{\max} is the maximum specific growth rate, and t_{lag} is the time lag (Kafle and Chen, 2016).

The first-order kinetic model describes the rate of a reaction as being proportional to the concentration of a reactant. In the case of methane production, the production rate is proportional to the concentration of the substrate being digested. The first-order kinetic model equation relates the rate of methane production to the substrate concentration, the substrate's methane potential,

and the methane production rate constant. It is commonly used to model the kinetics of methane production in AD processes. The modified Gompertz model is commonly used to describe the cumulative biogas production in AD processes. The logistic function model is usually used to describe the growth of microorganisms in batch culture.

2.13 Proteinase Enzyme

Decomposition of proteins to amino acids is a critical step, and one of the most important preconditions to using the protein-rich substrate is protease activity level in the system. Proteases are enzymes found in almost all living organisms at some point during their lifetimes (Hamza, 2017). These enzymes have been broadly grouped into three primary classes based on the sources from which they are obtained: animal proteases, plant proteases, and microbial proteases (Hasan et al., 2022). Commonly studied plant proteases include papain from papaya latex, bromelain from pineapple stem, ficin from fig fruit, actinidin from kiwifruit, and zingibain from ginger rhizome (Gagaoua et al., 2021). Plant proteases are categorized based on their catalytic mechanism. Most of the plant proteases are thiol proteases (CP); serine (SP), metallo (MP), and aspartic (AP) proteases are represented among the other plant proteases (Gonzalez-Rabade et al., 2011).

Proteolytic enzymes are a group of enzymes capable of breaking down long protein chains into shorter fragments, such as peptides, and subsequently into their amino acids. They cleave peptide bonds, which can lead to the degradation of protein substrates into amino acids or can be specific, leading to selective protein cleavage for processing post-translational modification (Callis, 1995). Proteases are present in microorganisms like bacteria, archaea, algae, viruses, and plants (Dhagat and Jujjavarapu, 2022). In animals, proteolytic enzymes are particularly abundant in the digestive tract, aiding in the breakdown of dietary proteins. Pepsin is a gastric endopeptidase, i.e., it breaks

peptide bonds within the interior of protein molecules. It is one of the proteolytic enzymes present in the stomach, and it is responsible for breaking down proteins into smaller peptides and amino acids, which the body can absorb and utilize (Bond, 2019).

2.13.1 Plant sources of proteinase enzymes

Proteinase enzymes are used in various applications, including food processing, pharmaceuticals, and industrial processes. Plant sources for proteinase enzymes have gained attention due to their advantages over animal-based sources, such as cost-effectiveness and environmental sustainability. A literature review on five plant sources (Figure 2-7) of proteinase enzymes: papain, bromelain, ficin, actinidin, and zingibain are discussed in the following section:

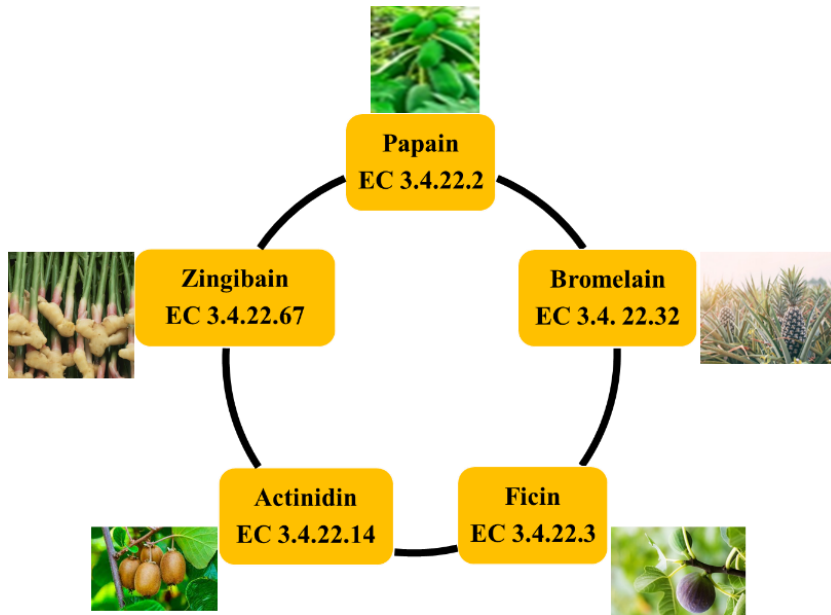


Figure 2- 7. Different plant proteases with their enzyme number (Madhusankha and Thilakarathna, 2021; Mohd Azmi et al., 2023).

2.13.1.1 *Papain*

Papain is a proteolytic enzyme found in the latex of papaya (*Carica papaya*) fruit. It has a wide range of applications in the food and pharmaceutical industries, including meat tenderization, clarification of beer, and anti-inflammatory activity (Silva-López and Gonçalves, 2019). Papain has been reported to have broad substrate specificity, making it useful for hydrolyzing proteins of various origins (Arvanitoyannis and Varzakas, 2008).

2.13.1.2 *Bromelain*

Bromelain is a mixture of proteolytic enzymes found in the stem and fruit of pineapple (*Ananas comosus*). Bromelain shows anti-inflammatory, anti-cancer, and anti-thrombotic activities and is used in various applications, such as meat tenderization, cosmetic products, and digestive aids (Nelson et al., 2022). Bromelain has a wide range of substrate specificity and can hydrolyze proteins, peptides, and amino acids (Tavano, 2013). A list of studies on biohydrogen production using plant proteolytic enzymes is presented in Table 2-15.

2.13.1.3 *Ficin*

Ficin is a proteolytic enzyme extracted from the latex of fig (*Ficus carica*) trees. Ficin has a broad substrate specificity and is used in the food and pharmaceutical industries for meat protein tenderization, digestive aids, and anti-inflammatory agents (Ramezani et al., 2003).

2.13.1.4 *Actinidin*

Actinidin is a proteolytic enzyme found in kiwifruit that aids in protein hydrolysis. It is the predominant soluble protein in green kiwifruit, accounting for 40% of soluble protein, and belongs to the peptidase C1 family of papain-like proteases (Mills et al., 2004). Actinidin can be called Actinidia anionic protease, actinidain, and Act d1 (Boland, 2013).

Table 2-15. Plant protease enzyme effect on biohydrogen production using different substrates.

Enzyme	Substrate	Effect on Biohydrogen	References
Papain	Glucose	HY increased from 69.5 ± 3.7 to 244.4 ± 19.4 mLg ⁻¹ glucose	Elsamadony et al. (2015)
Papain	Protein	HY increased from 52.2 ± 7.5 to 130.6 ± 8.5 mLg ⁻¹ protein,	Elsamadony et al. (2015)
Papain	Lipids	Hydrogen yield increased from 43.0 ± 5.3 to 64.8 ± 3.1 mL g ⁻¹ lipid	Elsamadony et al. (2015)
Bromelain	Residual sludge of cows dung biogas plant	The higher the concentration of bromelain, the higher quantity of hydrogen. Cumulative hydrogen yield increased from 2.3 to 3.7 mL g ⁻¹ VS for substrate concentration of 8.8 gVS L ⁻¹ and 26.4 gVS L ⁻¹ .	Cahyari et al. (2018)
Bromelain	Swine manure	At HRT 6 h, hydrogen and methane production rate of 1240 and 812 mL L ⁻¹ d ⁻¹ were obtained.	Nguyen et al. (2022)
Bromelain	Swine manure	Hydrogen and methane yield were 26.2 and 8.6 mL g ⁻¹ COD	Nguyen et al. (2022)
Bromelain	Cow dung	Improved process stability in terms of C/N ratio, total ammonia nitrogen, VS removal and pH. highest biogas production rate was observed at 12.80 mL g ⁻¹ VS day.	Hamzah et al. (2022)
Ficin	Anaerobic sludge	The highest yielded obtained was 79 mL H ₂ g ⁻¹ total sugar without any pre-treatment	Özmişçi et al. (2022)

Hy = hydrogen yield;

2.13.1.5 Zingibain

Zingibain is a proteolytic enzyme found in the rhizomes of ginger (*Zingiber officinale*). It has a broad substrate specificity and is used in the food industry for myofibrillar protein tenderization, and in the pharmaceutical industry for anti-inflammatory activity and digestive aids (Abdeldaiem

et al., 2014). Table 2-16 concisely presents the ideal conditions for plant proteases to effectively hydrolyze protein and collagen, including temperature, pH, and time. It also compares hydrolysis rates, offering insights to optimize enzymatic breakdown for these molecules.

Table 2-16. pH, temperature and strength of hydrolysis of myofibrillar proteins and collagen by various plant and microbial proteases.

Protease	pH		Temp. (°C)		Hydrolysis of myofibrillar proteins	Hydrolysis of collagen	References
	Optimal	Active range	Optimal	Active range			
Papain	4.0-6.0	4.0 - 9.0	65-75	50-80	Excellent	Moderate	Arshad et al. (2016)
Actinidin	4.5-6.0		58-62		Mild	Mild	Tantamacharik et al. (2018)
Bromelain	5.0-6.0	4.0 - 7.0	65-75	50-80	Moderate	Excellent	Madhusankha & Thilakarathna (2021)
Ficin	7	5.0 - 9.0	60-70	45-75	Moderate	Moderate	Mohd Azmi et al. (2023); Madhusankha & Thilakarathna (2021)
Aspergillus	7	5.0 - 9.0	55-60	50-65	Moderate	Poor	Calkins and Sullivan (2007)
Bacillus	< 6.5	2.5 - 7.0	55-60	40-60	Poor	Excellent	Arshad et al. (2016)

2.13.2 Microbial sources of proteinase enzyme

Microbial proteases, enzymes produced by microorganisms, have been widely used in various industries due to their ability to catalyze the hydrolysis of proteins. In the context of AD,

microbial proteinases initiate the breakdown of complex substrates like animal manure, food waste, and sewage sludge through a process known as proteolysis, which is the enzymatic cleavage of peptide bonds within proteins (Kim et al., 2002). This process is crucial for the AD of protein-rich organic wastes, serving as the first step in converting these substrates into biogas. Theoretically, these enzymes operate by recognizing specific sites on the protein substrate where they can bind and exert their catalytic action, cleaving the peptide bonds and leading to protein decomposition (López-Otín & Bond, 2008). The specificity and efficiency of microbial proteinases

towards different protein substrates are influenced by the enzyme's active site geometry and the physicochemical environment, including pH and temperature (Goswami et al., 2016). Then, by breaking down complex proteins into smaller, more soluble molecules, proteinases increase the availability of these substrates for other microorganisms in the AD process. Smaller peptides and amino acids are more easily transported across microbial cell membranes, facilitating their uptake by a wide range of bacteria and archaea involved in AD (Christensen et al., 2022). Protein breakdown products are used in further metabolism, providing nutrients and energy for microorganisms' growth, notably within AD systems. This process supports a diverse microbial community, including acidogenic bacteria that convert these products into volatile fatty acids, hydrogen, and carbon dioxide (Wang et al., 2022). By initiating the breakdown of proteins, proteinases contribute to the degradation of waste and enhance the overall efficiency and stability of the AD process.

Many studies investigated the use of microbial proteases in AD, particularly for treating protein-rich waste materials. For example, Sellami-Kamoun et al. (2011) evaluated using microbial proteases from *Bacillus cereus* to hydrolyze fish waste. They found that the protease treatment significantly increased biogas production compared to the untreated control. Another study by Yong et al. (2020) investigated using microbial proteases from *Bacillus* sp. for the hydrolysis of chicken feather waste and found that the protease treatment improved the solubilization and biodegradability of the feather waste.

Microbial proteases produced by fungi, bacteria, and other microorganisms have different characteristics and properties that make them suitable for various applications (dos Santos Aguilar and Sato, 2018). For instance, some microbial proteases have broad substrate specificity and can

hydrolyze various protein types. In contrast, others have specific substrate preferences and are more selective in their activity (Solanki et al., 2021).

Microbial proteases are hydrolytic enzymes that have been extensively studied and are considered one of the most important types of enzymes. Over the past decade, proteases produced by microorganisms have gained considerable attention due to their potential use in various industrial biotechnological processes, including detergent, textile, dairy, pharmaceutical, and leather processing. Proteolytic enzymes from microorganisms are preferred in many industrial applications due to their economic and technical advantages (Razzaq et al., 2019; Singh et al., 2016). This protease group represents approximately 60% of the total enzyme sales worldwide (Razzaq et al., 2019).

In meat industries, proteolytic enzymes, both endogenous in meat and exogenously added from plant or microbial sources, play a key role in the tenderization process of meat or meat products during aging (Bhat et al., 2018). Bacterial proteases can denature meat proteins due to their low inactivation temperature and high specific activity. *B. subtilis* produces two major proteases, subtilisin and neutral protease, approved by the US Food and Drug Administration as Generally Recognized As Safe (GRAS) strains for use in the meat industry (Contesini et al., 2018). Plant proteases such as bromelain and papain have higher hydrolytic activity in myofibrillar proteins than bacterial proteases and are widely used for tenderization (Arshad et al., 2016). However, bacterial proteases have been found to have intermediate hydrolytic activity for mediating the degradation of collagen, which is comparable to the activity of plant enzymes like papain and bromelain (Singh et al., 2019). Table 2-17 shows the properties of some proteases from different microbial sources.

Naveena et al. (2004) found elastase produced by *Bacillus* sp. can degrade elastin, collagen, and myofibrillar protein when tenderizing meat. The optimal pH range for elastase activity was 5.5 to 6, while the optimal temperature range was between 10 and 50 °C.

Hsiao et al. (2014) found that Aspartic proteases, which are commercial proteases derived from *A. oryzae*, remain stable when the temperature is below 70 °C and have a broad pH range. These proteases display optimal activity between pH 2.5 and 6, but their activity decreases to almost 20% when the temperature rises to 75 °C (Ha et al., 2013).

Table 2-17. Protease-producing microorganism and enzyme characteristics.

Microorganism	Optimum pH	Optimum Temperature (°C)	Molecular weight (KDa)	References
<i>pseudoalteromonas</i> sp. 129-1	8	50	35	Wu et al. (2015)
<i>Alcaligenes faecalis</i> APCMST-MKW6	9	60	49	Maruthiah et al. (2016)
<i>Bacillus cereus</i> VITSN04	8	30	32	Sundararajan et al. (2011)
<i>Pseudoalteromonas arctica</i> PAMC 21717	9	40	74	Park et al. (2018)
<i>Bacillus circulans</i> BM15	7	40	30	Venugopal and Saramma (2007)
<i>Bacillus</i> sp.	8	65	68	Srinivasan et al. (2009)
<i>Xenorhabdus nematophila</i>	8	30	39	Mohamed and Hussein (2007)
<i>Streptomyces nogalator</i> AC 80	7.5 to 8.5	28	66	Mitra and Chakrabartty (2005)
<i>Bacillus subtilis</i> PE 11	10	60	15	dos Santos Aguilar and Sato (2018)
<i>Bacillus</i> sp	7	70	-	Karikalan and Mohankumar (2016)

References

- Abanades, S., Abbaspour, H., Ahmadi, A., Das, B., Ehyaei, M., Esmacilion, F., El Haj Assad, M., Hajilounezhad, T., Jamali, D., & Hmida, A. (2021). A critical review of biogas production and usage with legislations framework across the globe. *International Journal of Environmental Science and Technology*, 19, 3377–3400. <https://doi.org/10.1007/s13762-021-03301-6>
- Abdeldaiem, M., Hoda, G. A., & Ali, G. (2014). Tenderization of camel meat by using fresh ginger (*Zingiber officinale*) extract. *Food Science and Quality Management*, 21, 25-38.
- Abdelgadir, A., Chen, X., Liu, J., Xie, X., Zhang, J., Zhang, K., Wang, H., & Liu, N. (2014). Characteristics, process parameters, and inner components of anaerobic bioreactors. *BioMed Research International*, vol. 2014, 1-10. <https://doi.org/10.1155/2014/841573>.
- Abomohra, A., Faisal, S., Ebaid, R., Huang, J., Wang, Q., & Elsayed, M. (2022). Recent advances in anaerobic digestion of lipid-rich waste: challenges and potential of seaweeds to mitigate the inhibitory effect. *Chemical Engineering Journal*, Vol. . 449, 137829. <https://doi.org/10.1016/j.cej.2022.137829>.
- Aboudi, K.; Fernández, L.; Álvarez, C.; Romero, L. (2021) Biogas, biohydrogen, and polyhydroxyalkanoates production from organic waste in the circular economy context. In *Sustainable Biofuels*; Ray, R., (ED); Academic Press: Cambridge, MA, USA; pp. 305–343. <https://doi.org/10.1016/B978-0-12-820297-5.00002-5>.
- Achinas, S., Achinas, V., & Euverink, G. J. W. (2017). A technological overview of biogas production from biowaste. *Engineering*, 3(3), 299-307. <https://doi.org/10.1016/J.ENG.2017.03.002>.

- Agapakis, C. M., Boyle, P. M., & Silver, P. A. (2012). Natural strategies for the spatial optimization of metabolism in synthetic biology. *Nature Chemical Biology*, 8(6), 527-535. <https://doi.org/10.1038/nchembio.975>.
- Agostini, A., Battini, F., Giuntoli, J., Tabaglio, V., Padella, M., Baxter, D., Marelli, L., & Amaducci, S. (2015). Environmentally sustainable biogas? The key role of manure co-digestion with energy crops. *Energies*, 8(6), 5234-5265. <https://doi.org/10.3390/en8065234>.
- Ahern, K., Rajagopal, I., & Tan, T. (2018). *Biochemistry free for all*. Oregon State University. <https://openlibrary-repo.ecampusontario.ca/jspui/handle/123456789/836>.
- Akutsu, Y., Lee, D.-Y., Li, Y.-Y., & Noike, T. (2009). Hydrogen production potentials and fermentative characteristics of various substrates with different heat-pretreated natural microflora. *International Journal of Hydrogen Energy*, 34(13), 5365-5372. <https://doi.org/10.1016/j.ijhydene.2009.04.052>.
- Alexandropoulou, M., Antonopoulou, G., Trably, E., Carrere, H., & Lyberatos, G. (2018). Continuous biohydrogen production from a food industry waste: influence of operational parameters and microbial community analysis. *Journal of Cleaner Production*, 174, 1054-1063. <https://doi.org/10.1016/j.jclepro.2017.11.078>.
- Ali, G., Ling, Z., Saif, I., Usman, M., Jalalah, M., Harraz, F. A., Al-Assiri, M., Salama, E.-S., & Li, X. (2021). Biomethanation and microbial community response during agricultural biomass and shrimp chaff digestion. *Environmental Pollution*, 278, 116801. <https://doi.org/10.1016/j.envpol.2021.116801>.

- Alibardi, L., & Cossu, R. (2015). Composition variability of the organic fraction of municipal solid waste and effects on hydrogen and methane production potentials. *Waste Management, 36*, 147-155. <https://doi.org/10.1016/j.wasman.2014.11.019>.
- Alibardi, L., & Cossu, R. (2016). Effects of carbohydrate, protein and lipid content of organic waste on hydrogen production and fermentation products. *Waste Management, 47*, 69-77. <https://doi.org/10.1016/j.wasman.2015.07.049>.
- Alsouleman, K. (2019). Effect of Increasing Amounts of Ammonium Nitrogen Induced by Consecutive Mixture of Poultry Manure and Cattle Slurry on the Microbial Community during Thermophilic Anaerobic Digestion. *Journal of Microbiology and Biotechnology, 29*(12), 1993-2005. <https://doi.org/10.4014/jmb.1909.09023>.
- Alvarado-Cuevas, Z. D., López-Hidalgo, A. M., Ordoñez, L. G., Ocegüera-Contreras, E., Ornelas-Salas, J. T., & De León-Rodríguez, A. (2015). Biohydrogen production using psychrophilic bacteria isolated from Antarctica. *International Journal of Hydrogen Energy, 40*(24), 7586-7592. <https://doi.org/10.1016/j.ijhydene.2014.10.063>.
- Amjith, L., & Bavanish, B. (2022). A review on biomass and wind as renewable energy for sustainable environment. *Chemosphere, 293*, 133579. <https://doi.org/10.1016/j.chemosphere.2022.133579>.
- Andriamanohiarisoamanana, F. J., Saikawa, A., Tarukawa, K., Qi, G., Pan, Z., Yamashiro, T., Iwasaki, M., Ihara, I., Nishida, T., & Umetsu, K. (2017). Anaerobic co-digestion of dairy manure, meat and bone meal, and crude glycerol under mesophilic conditions: Synergistic effect and kinetic studies. *Energy for Sustainable Development, 40*, 11-18. <https://doi.org/10.1016/j.esd.2017.05.008>.

- Ardolino, F., & Arena, U. (2019). Biowaste-to-Biomethane: An LCA study on biogas and syngas roads. *Waste Management*, 87, 441-453. <https://doi.org/10.1016/j.wasman.2019.02.030>.
- Argun, H., Kargi, F., Kapdan, I. K., & Oztekin, R. (2008). Biohydrogen production by dark fermentation of wheat powder solution: effects of C/N and C/P ratio on hydrogen yield and formation rate. *International Journal of Hydrogen Energy*, 33(7), 1813-1819. <https://doi.org/10.1016/j.ijhydene.2008.01.038>.
- Arshad, M. S., Kwon, J.-H., Imran, M., Sohaib, M., Aslam, A., Nawaz, I., Amjad, Z., Khan, U., & Javed, M. (2016). Plant and bacterial proteases: A key towards improving meat tenderization, a mini review. *Cogent Food & Agriculture*, 2(1), 1261780. <https://doi.org/10.1080/23311932.2016.1261780>.
- Arvanitoyannis, I. S., & Varzakas, T. H. (2008). Fruit/fruit juice waste management: Treatment methods and potential uses of treated waste. *Waste Management for the food industries*, 2, 569-628, Elsevier, Newyork, USA. ISBN: 9780123736543.
- Babae, A., Shayegan, J., & Roshani, A. (2013). Anaerobic slurry co-digestion of poultry manure and straw: effect of organic loading and temperature. *Journal of Environmental Health Science and Engineering*, 11(1), 1-6. <https://doi.org/10.1186/2052-336X-11-15>.
- Badawi, E. Y., Elkharsa, R. A., & Abdelfattah, E. A. (2023). Value proposition of bio-hydrogen production from different biomass sources. *Energy Nexus*, Vol. 10, 100194. <https://doi.org/10.1016/j.nexus.2023.100194>.
- Bai, M.-D., Cheng, S.-S., & Chao, Y.-C. (2004). Effects of substrate components on hydrogen fermentation of multiple substrates. *Water Science and Technology*, 50(8), 209-216. <https://doi.org/10.2166/wst.2004.0517>.

- Basak, B., Ahn, Y., Kumar, R., Hwang, J.-H., Kim, K.-H., & Jeon, B.-H. (2022). Lignocellulolytic microbiomes for augmenting lignocellulose degradation in anaerobic digestion. *Trends in Microbiology*, *30*(1), 6-9. <https://doi.org/10.1016/j.tim.2021.09.006>.
- Bauer, A. (2011). Investigation into the biochemical methane potential of abattoir wastewater. <https://sear.unisq.edu.au/id/eprint/21885>.
- Bauer, A., Bösch, P., Friedl, A., & Amon, T. (2009). Analysis of methane potentials of steam-exploded wheat straw and estimation of energy yields of combined ethanol and methane production. *Journal of Biotechnology*, *142*(1), 50-55. <https://doi.org/10.1016/j.jbiotec.2009.01.017>.
- Bayrakdar, A., Molaey, R., Sürmeli, R. Ö., Sahinkaya, E., & Çalli, B. (2017). Biogas production from chicken manure: Co-digestion with spent poppy straw. *International Biodeterioration & Biodegradation*, *119*, 205-210. <https://doi.org/10.1016/j.ibiod.2016.10.058>.
- Berghuis, B. A., Yu, F. B., Schulz, F., Blainey, P. C., Woyke, T., & Quake, S. R. (2019). Hydrogenotrophic methanogenesis in archaeal phylum Verstraetearchaeota reveals the shared ancestry of all methanogens. *Proceedings of the National Academy of Sciences*, *116*(11), 5037-5044. <https://doi.org/10.1073/pnas.1815631116>.
- Bharathiraja, B., Sudharsanaa, T., Bharghavi, A., Jayamuthunagai, J., & Praveenkumar, R. (2016). Biohydrogen and Biogas—An overview on feedstocks and enhancement process. *Fuel*, *185*, 810-828. <https://doi.org/10.1016/j.fuel.2016.08.030>.
- Bhat, Z. F., Morton, J. D., Mason, S. L., & Bekhit, A. E. D. A. (2018). Applied and emerging methods for meat tenderization: A comparative perspective. *Comprehensive Reviews in Food Science and Food Safety*, *17*(4), 841-859. <https://doi.org/10.1111/1541-4337.12356>.

- Bi, S., Westerholm, M., Qiao, W., Xiong, L., Mahdy, A., Yin, D., Song, Y., & Dong, R. (2020). Metabolic performance of anaerobic digestion of chicken manure under wet, high solid, and dry conditions. *Bioresource Technology*, 296, 122342. <https://doi.org/10.1016/j.biortech.2019.122342>.
- Bilandzija, N., Voca, N., Jelcic, B., Jurisic, V., Matin, A., Grubor, M., & Kricka, T. (2018). Evaluation of Croatian agricultural solid biomass energy potential. *Renewable and Sustainable Energy Reviews*, 93, 225-230. <https://doi.org/10.1016/j.rser.2018.05.040>.
- Boland, M. (2013). Kiwifruit proteins and enzymes: actinidin and other significant proteins. *Advances in Food and Nutrition Research*, 68, 59-80. <https://doi.org/10.1016/B978-0-12-394294-4.00004-3>.
- Bond, J. S. (2019). Proteases: History, discovery, and roles in health and disease. *Journal of Biological Chemistry*, 294(5), 1643-1651. <https://doi.org/10.1074/jbc.TM118.004156>.
- Bücker, F., Marder, M., Peiter, M. R., Lehn, D. N., Esquerdo, V. M., de Almeida Pinto, L. A., & Konrad, O. (2020). Fish waste: An efficient alternative to biogas and methane production in an anaerobic mono-digestion system. *Renewable Energy*, 147, 798-805. <https://doi.org/10.1016/j.renene.2019.08.140>.
- Bulak, P., Proc, K., Pawłowska, M., Kasprzycka, A., Berus, W., & Bieganski, A. (2020). Biogas generation from insects breeding post production wastes. *Journal of Cleaner Production*, 244, 118777. <https://doi.org/10.1016/j.jclepro.2019.118777>.
- Cahyari, K., Putri, A., Oktaviani, E., Hidayat, M., & Norajsha, J. (2018). Biohydrogen production from pineapple waste: effect of substrate concentration and acid pretreatment. *IOP Conference Series: Materials Science and Engineering*, (358) 012001, Putrajaya, Malaysia. 10.1088/1757-899X/358/1/012001.

- Cai, M., Liu, J., & Wei, Y. (2004). Enhanced biohydrogen production from sewage sludge with alkaline pretreatment. *Environmental Science & Technology*, 38(11), 3195-3202.
<https://doi.org/10.1021/es0349204>.
- Cai, Y., Gallegos, D., Zheng, Z., Stinner, W., Wang, X., Pröter, J., & Schäfer, F. (2021). Exploring the combined effect of total ammonia nitrogen, pH and temperature on anaerobic digestion of chicken manure using response surface methodology and two kinetic models. *Bioresource Technology*, 337, 125328.
<https://doi.org/10.1016/j.biortech.2021.125328>.
- Calkins, C. R., & Sullivan, G. (2007). Adding enzymes to improve beef tenderness. Beef facts: Product enhancement, University of Nebraska, Cattlemen's Beef Board, Centennial Colorado, Lincoln, NE .
- Callis, J. (1995). Regulation of protein degradation. *The Plant Cell*, 7(7), 845.
<https://doi.org/10.1105%2Ftpc.7.7.845>.
- Candido, R., Mori, N., & Gonçalves, A. (2019). Sugarcane straw as feedstock for 2G ethanol: evaluation of pretreatments and enzymatic hydrolysis. *Industrial Crops and Products*, 142, 111845. <https://doi.org/10.1016/j.indcrop.2019.111845>.
- Capson-Tojo, G., Ruiz, D., Rouez, M., Crest, M., Steyer, J.-P., Bernet, N., Delgenès, J.-P., & Escudé, R. (2017). Accumulation of propionic acid during consecutive batch anaerobic digestion of commercial food waste. *Bioresource Technology*, 245, 724-733.
<https://doi.org/10.1016/j.biortech.2017.08.149> .
- Carabeo-Pérez, A., Odales-Bernal, L., López-Dávila, E., & Jiménez, J. (2021). Biomethane potential from herbivorous animal's manures: Cuban case study. *Journal of Material*

- Cycles and Waste Management*, 23(4), 1404-1411. <https://doi.org/10.1007/s10163-021-01220-9>.
- Carbonaro, M., Maselli, P., & Nucara, A. (2012). Relationship between digestibility and secondary structure of raw and thermally treated legume proteins: a Fourier transform infrared (FT-IR) spectroscopic study. *Amino Acids*, 43(2), 911-921. <https://doi.org/10.1007/s00726-011-1151-4>.
- Cavicchioli, R., Siddiqui, K. S., Andrews, D., & Sowers, K. R. (2002). Low-temperature extremophiles and their applications. *Current Opinion in Biotechnology*, 13(3), 253-261. [https://doi.org/10.1016/S0958-1669\(02\)00317-8](https://doi.org/10.1016/S0958-1669(02)00317-8).
- Cazier, E., Trably, E., Steyer, J.-P., & Escudié, R. (2015). Biomass hydrolysis inhibition at high hydrogen partial pressure in solid-state anaerobic digestion. *Bioresource Technology*, 190, 106-113. <https://doi.org/10.1016/j.biortech.2015.04.055>.
- Cazier, E. A., Trably, E., Steyer, J.-P., & Escudie, R. (2019). Reversibility of hydrolysis inhibition at high hydrogen partial pressure in dry anaerobic digestion processes fed with wheat straw and inoculated with anaerobic granular sludge. *Waste Management*, 85, 498-505. <https://doi.org/10.1016/j.wasman.2019.01.019>.
- Chen, H., Wang, W., Xue, L., Chen, C., Liu, G., & Zhang, R. (2016). Effects of ammonia on anaerobic digestion of food waste: process performance and microbial community. *Energy & Fuels*, 30(7), 5749-5757. <https://doi.org/10.1021/acs.energyfuels.6b00715>.
- Chen, H., Wu, J., Wang, H., Zhou, Y., Xiao, B., Zhou, L., Yu, G., Yang, M., Xiong, Y., & Wu, S. (2021). Dark co-fermentation of rice straw and pig manure for biohydrogen production: effects of different inoculum pretreatments and substrate mixing ratio. *Environmental Technology*, 42(28), 4539-4549. <https://doi.org/10.1080/09593330.2020.1770340>.

- Chen, S., Gao, J., & Dong, B. (2021). Bottlenecks of anaerobic degradation of proteins in sewage sludge and the potential targeted enhancing strategies. *Science of the Total Environment*, 759, 143573. <https://doi.org/10.1016/j.scitotenv.2020.143573>.
- Chen, Y., Cheng, J. J., & Creamer, K. S. (2008). Inhibition of anaerobic digestion process: a review. *Bioresource Technology*, 99(10), 4044-4064. <https://doi.org/10.1016/j.biortech.2007.01.057>.
- Cheng, F., & Brewer, C. (2021). Conversion of protein-rich lignocellulosic wastes to bio-energy: Review and recommendations for hydrolysis+ fermentation and anaerobic digestion. *Renewable and Sustainable Energy Reviews*, 146, 111167. <https://doi.org/10.1016/j.rser.2021.111167>.
- Cheng, S.-S., Chang, S.-M., & Chen, S.-T. (2002). Effects of volatile fatty acids on a thermophilic anaerobic hydrogen fermentation process degrading peptone. *Water Science and Technology*, 46(4-5), 209-214. <https://doi.org/10.2166/wst.2002.0589>.
- Cheong, D.-Y., & Hansen, C. L. (2007). Feasibility of hydrogen production in thermophilic mixed fermentation by natural anaerobes. *Bioresource Technology*, 98(11), 2229-2239. <https://doi.org/10.1016/j.biortech.2006.09.039>.
- Chowdhury, M. W., Nabi, M. N., Arefin, M. A., Rashid, F., Islam, M. T., Gudimetla, P., & Muyeen, S. (2022). Recycling slaughterhouse wastes into potential energy and hydrogen sources: An approach for the future sustainable energy. *Bioresource Technology Reports*, 19, 101133. <https://doi.org/10.1016/j.biteb.2022.101133>.
- Christensen, L. F., García-Béjar, B., Bang-Berthelsen, C. H., & Hansen, E. B. (2022). Extracellular microbial proteases with specificity for plant proteins in food fermentation.

- International Journal of Food Microbiology*, 381, 109889.
<https://doi.org/10.1016/j.ijfoodmicro.2022.109889>.
- Chuanchai, A., & Ramaraj, R. (2018). Sustainability assessment of biogas production from buffalo grass and dung: biogas purification and bio-fertilizer. *3 Biotech*, 8(3), 151.
<https://doi.org/10.1007/s13205-018-1170-x>.
- Cieciura-Włoch, W., & Borowski, S. (2019). Biohydrogen production from wastes of plant and animal origin via dark fermentation. *Journal of Environmental Engineering and Landscape Management*, 27(2), 101-113. <https://doi.org/10.3846/jeelm.2019.9806>.
- Climenhaga, M., & Banks, C. (2008). Anaerobic digestion of catering wastes: effect of micronutrients and retention time. *Water Science and Technology*, 57(5), 687-692.
<https://doi.org/10.2166/wst.2008.092>.
- Contesini, F. J., Melo, R. R. d., & Sato, H. H. (2018). An overview of Bacillus proteases: from production to application. *Critical Reviews in Biotechnology*, 38(3), 321-334.
<https://doi.org/10.1080/07388551.2017.1354354>.
- Cu, T., Nguyen, T., Triolo, J. M., Pedersen, L., Le, V., Le, P., & Sommer, S. G. (2015). Biogas production from Vietnamese animal manure, plant residues and organic waste: influence of biomass composition on methane yield. *Asian-Australasian Journal of Animal Sciences*, 28(2), 280. <https://doi.org/10.5713%2Fajas.14.0312>.
- Cuetos, M. J., Martinez, E. J., Moreno, R., Gonzalez, R., Otero, M., & Gomez, X. (2017). Enhancing anaerobic digestion of poultry blood using activated carbon. *Journal of Advanced Research*, 8(3), 297-307. <https://doi.org/10.1016/j.jare.2016.12.004>.
- Czatkowska, M., Harnisz, M., Korzeniewska, E., & Koniuszewska, I. (2020). Inhibitors of the methane fermentation process with particular emphasis on the microbiological aspect: A

- review. *Energy Science & Engineering*, 8(5), 1880-1897.
<https://doi.org/10.1002/ese3.609>.
- Das, D., & Veziroglu, T. N. (2008). Advances in biological hydrogen production processes. *International Journal of Hydrogen Energy*, 33(21), 6046-6057.
<https://doi.org/10.1016/j.ijhydene.2008.07.098>.
- Dasgupta, C. N., Gilbert, J. J., Lindblad, P., Heidorn, T., Borgvang, S. A., Skjanes, K., & Das, D. (2010). Recent trends on the development of photobiological processes and photobioreactors for the improvement of hydrogen production. *International Journal of Hydrogen Energy*, 35(19), 10218-10238. <https://doi.org/10.1016/j.ijhydene.2010.06.029>.
- De Quadros, T. C. F., Sicchieri, I. M., Perin, J. K. H., Challiol, A. Z., Bortoloti, M. A., Fernandes, F., & Kuroda, E. K. (2022). Valorization of fruit and vegetable waste by anaerobic digestion: definition of co-substrates and inoculum. *Waste and Biomass Valorization*, 1-13. <https://doi.org/10.1007/s12649-022-01887-7>.
- Demirel, B., & Scherer, P. (2008). The roles of acetotrophic and hydrogenotrophic methanogens during anaerobic conversion of biomass to methane: a review. *Reviews in Environmental Science and Bio/Technology*, 7, 173-190. <https://doi.org/10.1007/s11157-008-9131-1>.
- Dennehy, C., Lawlor, P. G., Croize, T., Jiang, Y., Morrison, L., Gardiner, G. E., & Zhan, X. (2016). Synergism and effect of high initial volatile fatty acid concentrations during food waste and pig manure anaerobic co-digestion. *Waste Management*, 56, 173-180.
<https://doi.org/10.1016/j.wasman.2016.06.032>.
- Dhagat, S., & Jujjavarapu, S. E. (2022). Microbial Pathogenesis: Mechanism and Recent Updates on Microbial Diversity of Pathogens. *Antimicrobial Resistance: Underlying*

Mechanisms and Therapeutic Approaches, 71-111. https://doi.org/10.1007/978-981-16-3120-7_3.

- Dhiman, S. S., Shrestha, N., David, A., Basotra, N., Johnson, G. R., Chadha, B. S., Gadhamshetty, V., & Sani, R. K. (2018). Producing methane, methanol and electricity from organic waste of fermentation reaction using novel microbes. *Bioresource Technology*, 258, 270-278. <https://doi.org/10.1016/j.biortech.2018.02.128>.
- Dogan, T., Ince, O., Oz, N. A., & Ince, B. K. (2005). Inhibition of volatile fatty acid production in granular sludge from a UASB reactor. *Journal of Environmental Science and Health*, 40(3), 633-644. <https://doi.org/10.1081/ESE-200046616>.
- Dong, L., Zhenhong, Y., Yongming, S., Xiaoying, K., & Yu, Z. (2009). Hydrogen production characteristics of the organic fraction of municipal solid wastes by anaerobic mixed culture fermentation. *International Journal of Hydrogen Energy*, 34(2), 812-820. <https://doi.org/10.1016/j.ijhydene.2008.11.031>.
- Dooms, M., Benbelkacem, H., & Buffière, P. (2018). High solid temperature phased anaerobic digestion from agricultural wastes: Putting several reactors in sequence. *Biochemical Engineering Journal*, 130, 21-28. <https://doi.org/10.1016/j.bej.2017.11.011>.
- Dos Santos Aguilar, J. G., & Sato, H. H. (2018). Microbial proteases: Production and application in obtaining protein hydrolysates. *Food Research International*, 103, 253-262. <https://doi.org/10.1016/j.foodres.2017.10.044>.
- Dos Santos, L. A., Valenca, R. B., da Silva, L. C. S., de Barros Holanda, S. H., da Silva, A. F. V., Jucá, J. F. T., & Santos, A. F. M. S. (2020). Methane generation potential through anaerobic digestion of fruit waste. *Journal of Cleaner Production*, 256, 120389. <https://doi.org/10.1016/j.jclepro.2020.120389>.

- Duong, T. H., van Eekert, M., Grolle, K., Tran, T. V. N., Zeeman, G., & Temmink, H. (2021). Effect of solid retention time (SRT) on protein hydrolysis and acidogenesis at pH 5 and pH 7 using gelatine as a model protein. *Journal of Water Process Engineering*, *44*, 102398. <https://doi.org/10.1016/j.jwpe.2021.102398>.
- Elbeshbishy, E., Hafez, H., & Nakhla, G. (2011). Ultrasonication for biohydrogen production from food waste. *International Journal of Hydrogen Energy*, *36*(4), 2896-2903. <https://doi.org/10.1016/j.ijhydene.2010.12.009>.
- Elsamadony, M., Tawfik, A., Danial, A., & Suzuki, M. (2015). Use of Carica papaya enzymes for enhancement of H₂ production and degradation of glucose, protein, and lipids. *Energy Procedia*, *75*, 975-980. <https://doi.org/10.1016/j.egypro.2015.07.308>.
- Fagbohunge, M. O., Herbert, B. M., Hurst, L., Ibeto, C. N., Li, H., Usmani, S. Q., & Semple, K. T. (2017). The challenges of anaerobic digestion and the role of biochar in optimizing anaerobic digestion. *Waste Management*, *61*, 236-249. <https://doi.org/10.1016/j.wasman.2016.11.028>.
- Faisal, S., Thakur, N., Jalalah, M., Harraz, F. A., Al-Assiri, M. S., Saif, I., Ali, G., Zheng, Y., & Salama, E. S. (2021). Facilitated lignocellulosic biomass digestibility in anaerobic digestion for biomethane production: microbial communities' structure and interactions. *Journal of Chemical Technology & Biotechnology*, *96*(7), 1798-1817. <https://doi.org/10.1002/jctb.6747>.
- Feller, G., & Gerday, C. (2003). Psychrophilic enzymes: hot topics in cold adaptation. *Nature Reviews Microbiology*, *1*(3), 200-208. <https://doi.org/10.1038/nrmicro773>.

- Feng, L., Casas, M. E., Ottosen, L. D. M., Møller, H. B., & Bester, K. (2017). Removal of antibiotics during the anaerobic digestion of pig manure. *Science of the Total Environment*, *603*, 219-225. <https://doi.org/10.1016/j.scitotenv.2017.05.280>.
- Flotats, X., Palatsi, J., Ahring, B. K., & Angelidaki, I. (2006). Identifiability study of the proteins degradation model, based on ADM1, using simultaneous batch experiments. *Water Science and Technology*, *54*(4), 31-39. <https://doi.org/10.2166/wst.2006.523>.
- Fonknechten, N., Chaussonnerie, S., Tricot, S., Lajus, A., Andreesen, J. R., Perchat, N., Pelletier, E., Gouyvenoux, M., Barbe, V., & Salanoubat, M. (2010). *Clostridium sticklandii*, a specialist in amino acid degradation: revisiting its metabolism through its genome sequence. *BMC genomics*, *11*(1), 1-12. <https://doi.org/10.1186/1471-2164-11-555>.
- Fotidis, I. A., Karakashev, D., Kotsopoulos, T. A., Martzopoulos, G. G., & Angelidaki, I. (2013). Effect of ammonium and acetate on methanogenic pathway and methanogenic community composition. *FEMS Microbiology Ecology*, *83*(1), 38-48. <https://doi.org/10.1111/j.1574-6941.2012.01456.x>.
- Gagaoua, M., Dib, A. L., Lakhdara, N., Lamri, M., Botineștean, C., & Lorenzo, J. M. (2021). Artificial meat tenderization using plant cysteine proteases. *Current Opinion in Food Science*, *38*, 177-188. <https://doi.org/10.1016/j.cofs.2020.12.002>.
- Gaibor-Chávez, J., Niño-Ruiz, Z., Velázquez-Martí, B., & Lucio-Quintana, A. (2019). Viability of biogas production and determination of bacterial kinetics in anaerobic co-digestion of cabbage waste and livestock manure. *Waste and Biomass Valorization*, *10*, 2129-2137. <https://doi.org/10.1007/s12649-018-0228-7>.
- Gao, Y., Fang, Z., Liang, P., Zhang, X., Qiu, Y., Kimura, K., & Huang, X. (2019). Anaerobic digestion performance of concentrated municipal sewage by forward osmosis membrane:

- Focus on the impact of salt and ammonia nitrogen. *Bioresource Technology*, 276, 204-210. <https://doi.org/10.1016/j.biortech.2019.01.016>.
- Gavala, H. N., Angelidaki, I., & Ahring, B. K. (2003). Kinetics and modeling of anaerobic digestion process. *Biomethanation I*, Vol. 81 (57-93), Springer, Berlin, Heidelberg, Germany. https://doi.org/10.1007/3-540-45839-5_3.
- Gelegenis, J., Georgakakis, D., Angelidaki, I., & Mavris, V. (2007). Optimization of biogas production by co-digesting whey with diluted poultry manure. *Renewable Energy*, 32(13), 2147-2160. <https://doi.org/10.1016/j.renene.2006.11.015>.
- Gerardi, M. H. (2003). *The Microbiology of Anaerobic Digesters*. John Wiley & Sons, Inc.: Hoboken, New York, USA, 2003; ISBN 0471206938.
- Ghimire, A., Trably, E., Frunzo, L., Pirozzi, F., Lens, P. N., Esposito, G., Cazier, E. A., & Escudié, R. (2018). Effect of total solids content on biohydrogen production and lactic acid accumulation during dark fermentation of organic waste biomass. *Bioresource Technology*, 248, 180-186. <https://doi.org/10.1016/j.biortech.2017.07.062>.
- Ghosh, S., Gillis, A., Sheviriyov, J., Levkov, K., & Golberg, A. (2019). Towards waste meat biorefinery: Extraction of proteins from waste chicken meat with non-thermal pulsed electric fields and mechanical pressing. *Journal of Cleaner Production*, 208, 220-231. <https://doi.org/10.1016/j.jclepro.2018.10.037>.
- Gielen, D., Boshell, F., Saygin, D., Bazilian, M. D., Wagner, N., & Gorini, R. (2019). The role of renewable energy in the global energy transformation. *Energy Strategy Reviews*, 24, 38-50. <https://doi.org/10.1016/j.esr.2019.01.006>.

- Glyk, A., Solle, D., Scheper, T., & Beutel, S. (2015). Optimization of PEG–salt aqueous two-phase systems by design of experiments. *Chemometrics and Intelligent Laboratory Systems*, *149*, 12-21. <https://doi.org/10.1016/j.chemolab.2015.09.014>.
- Gomez-Romero, J., Gonzalez-Garcia, A., Chairez, I., Torres, L., & Garcia-Peña, E. I. (2014). Selective adaptation of an anaerobic microbial community: Biohydrogen production by co-digestion of cheese whey and vegetables fruit waste. *International Journal of Hydrogen Energy*, *39*(24), 12541-12550. <https://doi.org/10.1016/j.ijhydene.2014.06.050>.
- Gonzalez-Rabade, N., Badillo-Corona, J. A., Aranda-Barradas, J. S., & del Carmen Oliver-Salvador, M. (2011). Production of plant proteases in vivo and in vitro—a review. *Biotechnology Advances*, *29*(6), 983-996. <https://doi.org/10.1016/j.biotechadv.2011.08.017>.
- Goswami, R., Chattopadhyay, P., Shome, A., Banerjee, S. N., Chakraborty, A. K., Mathew, A. K., & Chaudhury, S. (2016). An overview of physico-chemical mechanisms of biogas production by microbial communities: a step towards sustainable waste management. *3 Biotech*, *6*, 1-12. <https://doi.org/10.1007/s13205-016-0395-9>.
- Gourdon, R., & Vermande, P. (1987). Effects of propionic acid concentration on anaerobic digestion of pig manure. *Biomass*, *13*(1), 1-12. [https://doi.org/10.1016/0144-4565\(87\)90067-9](https://doi.org/10.1016/0144-4565(87)90067-9).
- Gujer, W., & Zehnder, A. J. (1983). Conversion processes in anaerobic digestion. *Water Science and Technology*, *15*(8-9), 127-167. <https://doi.org/10.2166/wst.1983.0164>.
- Guo, L., Li, X.-M., Bo, X., Yang, Q., Zeng, G.-M., Liao, D.-x., & Liu, J.-J. (2008). Impacts of sterilization, microwave and ultrasonication pretreatment on hydrogen producing using

- waste sludge. *Bioresource Technology*, 99(9), 3651-3658.
<https://doi.org/10.1016/j.biortech.2007.07.026>.
- Guo, W.-Q., Ren, N.-Q., Wang, X.-J., Xiang, W.-S., Meng, Z.-H., Ding, J., Qu, Y.-Y., & Zhang, L.-S. (2008). Biohydrogen production from ethanol-type fermentation of molasses in an expanded granular sludge bed (EGSB) reactor. *International Journal of Hydrogen Energy*, 33(19), 4981-4988. <https://doi.org/10.1016/j.ijhydene.2008.05.033>.
- Gutiérrez, A. S., Eras, J. J. C., Hens, L., & Vandecasteele, C. (2020). The energy potential of agriculture, agroindustrial, livestock, and slaughterhouse biomass wastes through direct combustion and anaerobic digestion. The case of Colombia. *Journal of Cleaner Production*, 269, 122317. <https://doi.org/10.1016/j.jclepro.2020.122317>.
- Ha, M., Bekhit, A. E. D., Carne, A., & Hopkins, D. L. (2013). Comparison of the proteolytic activities of new commercially available bacterial and fungal proteases toward meat proteins. *Journal of Food Science*, 78(2), C170-C177. <https://doi.org/10.1111/1750-3841.12027>.
- Habib, M., ul Haq, I., Mustafa, P., Rehman, H., Khan, R., & Khan, A. U. (2015). Production of biofuels from micro ALGAE and green wastes through Anaerobic Digestion. 2015 Power Generation System and Renewable Energy Technologies (PGSRET), Islamabad, Pakistan, 2015, pp. 1-6, doi: 10.1109/PGSRET.2015.7312230.
- Hahnke, S., Langer, T., Koeck, D. E., & Klocke, M. (2016). Description of *Proteiniphilum saccharofermentans* sp. nov., *Petrimonas mucosa* sp. nov. and *Fermentimonas caenicola* gen. nov., sp. nov., isolated from mesophilic laboratory-scale biogas reactors, and emended description of the genus *Proteiniphilum*. *International Journal of Systematic and Evolutionary Microbiology*, 66(3), 1466-1475.

- Hajizadeh, A., Saady, N. M. C., Zendehboudi, S., Rajagopal, R., & Hung, Y.-T. (2021). Biohydrogen production through mixed culture dark anaerobic fermentation of industrial waste. In: Wang, L.K., Wang, M.H.S., Hung, Y.T., Shammass, N.K. (ED) *Integrated Natural Resources Management. Handbook of Environmental Engineering, vol 20. Springer, Switzerland. ISBN 978-3-030-55172-8*. https://doi.org/10.1007/978-3-030-55172-8_8.
- Halim, A., Lee, K., & Idris, M. (2017). Biogas production from goat and chicken manure in Malaysia. *Applied Ecology and Environmental Research*, 15(3), 529-535. http://dx.doi.org/10.15666/aecer/1503_529535.
- Hallaji, S. M., Kuroshkarim, M., & Moussavi, S. P. (2019). Enhancing methane production using anaerobic co-digestion of waste activated sludge with combined fruit waste and cheese whey. *BMC Biotechnology*, 19, 1-10. <https://doi.org/10.1186/s12896-019-0513-y>.
- Hamza, T. A. (2017). Bacterial protease enzyme: safe and good alternative for industrial and commercial use. *International Journal of Chemical Biomolecular Science*, 3(1), 1-0. <http://www.aiscience.org/journal/ijcbs>.
- Hamzah, A. F. A., Hamzah, M. H., Man, H. C., Jamali, N. S., Siajam, S. I., & Show, P. L. (2022). Biogas production through mono-and co-digestion of pineapple waste and cow dung at different substrate ratios. *BioEnergy Research*, 1-12. <https://doi.org/10.1007/s12155-022-10478-2>.
- Handous, N., Gannoun, H., Hamdi, M., & Bouallagui, H. (2019). Two-stage anaerobic digestion of meat processing solid wastes: methane potential improvement with wastewater addition and solid substrate fermentation. *Waste and Biomass Valorization*, 10, 131-142. <https://doi.org/10.1007/s12649-017-0055-2>.

- Harirchi, S., Wainaina, S., Sar, T., Nojoumi, S. A., Parchami, M., Parchami, M., Varjani, S., Khanal, S. K., Wong, J., & Awasthi, M. K. (2022). Microbiological insights into anaerobic digestion for biogas, hydrogen or volatile fatty acids (VFAs): a review. *Bioengineered*, *13*(3), 6521-6557. <https://doi.org/10.1080/21655979.2022.2035986>.
- Harrison, O., Rapheal, I. A., & Moki, E. C. (2020). Comparative Study of Biogas Production from Anaerobic Co-digestion of Donkey Dung and Swine Dung. *International Journal of Biochemistry, Biophysics & Molecular Biology*, *5*(2), 34. [10.11648/j.ijbbmb.20200502.13](https://doi.org/10.11648/j.ijbbmb.20200502.13).
- Hasan, M. J., Haque, P., & Rahman, M. M. (2022). Protease enzyme based cleaner leather processing: A review. *Journal of Cleaner Production*, 132826. <https://doi.org/10.1016/j.jclepro.2022.132826>.
- He, J., Sung, Y., Dollhopf, M. E., Fathepure, B. Z., Tiedje, J. M., & Löffler, F. E. (2002). Acetate versus hydrogen as direct electron donors to stimulate the microbial reductive dechlorination process at chloroethene-contaminated sites. *Environmental Science & Technology*, *36*(18), 3945-3952. <https://doi.org/10.1021/es025528d>.
- Hejnfelt, A., & Angelidaki, I. (2009). Anaerobic digestion of slaughterhouse by-products. *Biomass and Bioenergy*, *33*(8), 1046-1054. <https://doi.org/10.1016/j.biombioe.2009.03.004>.
- Hernández, M. A., Susa, M. R., & Andres, Y. (2014). Use of coffee mucilage as a new substrate for hydrogen production in anaerobic co-digestion with swine manure. *Bioresource Technology*, *168*, 112-118. <https://doi.org/10.1016/j.biortech.2014.02.101>.
- Ho, Q. T., Murphy, K. M., Drapala, K. P., Fenelon, M. A., O'Mahony, J. A., Tobin, J. T., & McCarthy, N. A. (2019). Modelling the changes in viscosity during thermal treatment of

- milk protein concentrate using kinetic data. *Journal of Food Engineering*, 246, 179-191.
<https://doi.org/10.1016/j.jfoodeng.2018.10.026>.
- Holechek, J. L., Geli, H. M., Sawalhah, M. N., & Valdez, R. (2022). A global assessment: can renewable energy replace fossil fuels by 2050? *Sustainability*, 14(8), 4792.
<https://doi.org/10.3390/su14084792>.
- Holm-Nielsen, J. B., Al Seadi, T., & Oleskowicz-Popiel, P. (2009). The future of anaerobic digestion and biogas utilization. *Bioresource Technology*, 100(22), 5478-5484.
<https://doi.org/10.1016/j.biortech.2008.12.046>.
- Hsiao, N.-W., Chen, Y., Kuan, Y.-C., Lee, Y.-C., Lee, S.-K., Chan, H.-H., & Kao, C.-H. (2014). Purification and characterization of an aspartic protease from the *Rhizopus oryzae* protease extract, Peptidase R. *Electronic Journal of Biotechnology*, 17(2), 89-94.
<https://doi.org/10.1016/j.ejbt.2014.02.002>.
- Huang, X., Yun, S., Zhu, J., Du, T., Zhang, C., & Li, X. (2016). Mesophilic anaerobic co-digestion of aloe peel waste with dairy manure in the batch digester: Focusing on mixing ratios and digestate stability. *Bioresource Technology*, 218, 62-68.
<https://doi.org/10.1016/j.biortech.2016.06.070>.
- Igarashi, K., & Kato, S. (2017). Extracellular electron transfer in acetogenic bacteria and its application for conversion of carbon dioxide into organic compounds. *Applied Microbiology and Biotechnology*, 101, 6301-6307. <https://doi.org/10.1007/s00253-017-8421-3>.
- Jabłoński, S. J., Biernacki, P., Steinigeweg, S., & Łukaszewicz, M. (2015). Continuous mesophilic anaerobic digestion of manure and rape oilcake—Experimental and modelling study. *Waste Management*, 35, 105-110. <https://doi.org/10.1016/j.wasman.2014.09.011>

- Jacob, S., & Banerjee, R. (2016). Modeling and optimization of anaerobic codigestion of potato waste and aquatic weed by response surface methodology and artificial neural network coupled genetic algorithm. *Bioresource Technology*, 214, 386-395.
<https://doi.org/10.1016/j.biortech.2016.04.068>.
- Jain, M., Singh, R., & Tauro, P. (1981). Anaerobic digestion of cattle and sheep wastes. *Agricultural Wastes*, 3(1), 65-73. [https://doi.org/10.1016/0141-4607\(81\)90007-X](https://doi.org/10.1016/0141-4607(81)90007-X).
- Jamdar, S. N., & Harikumar, P. (2005). Autolytic degradation of chicken intestinal proteins. *Bioresource Technology*, 96(11), 1276-1284.
<https://doi.org/10.1016/j.biortech.2004.10.014>.
- Jarunglumlert, T., Prommuak, C., Putmai, N., & Pavasant, P. (2018). Scaling-up bio-hydrogen production from food waste: Feasibilities and challenges. *International Journal of Hydrogen Energy*, 43(2), 634-648. <https://doi.org/10.1016/j.ijhydene.2017.10.013>.
- Jin, S., Jeon, Y., Jeon, M. S., Shin, J., Song, Y., Kang, S., Bae, J., Cho, S., Lee, J.-K., & Kim, D. R. (2021). Acetogenic bacteria utilize light-driven electrons as an energy source for autotrophic growth. *Proceedings of the National Academy of Sciences*, 118(9), e2020552118. <https://doi.org/10.1073/pnas.2020552118>.
- Jin, W., Xu, X., & Yang, F. (2018). Application of rumen microorganisms for enhancing biogas production of corn straw and livestock manure in a pilot-scale anaerobic digestion system: performance and microbial community analysis. *Energies*, 11(4), 920.
<https://doi.org/10.3390/en11040920>.
- Jovanović, J. R., Stefanović, A. B., Šekuljica, N. Ž., Tanasković, S. M. J., Dojčinović, M. B., Bugarski, B. M., & Knežević-Jugović, Z. D. (2016). Ultrasound pretreatment as an useful tool to enhance egg white protein hydrolysis: kinetics, reaction model, and

- thermodynamics. *Journal of Food Science*, 81(11), C2664-C2675.
<https://doi.org/10.1111/1750-3841.13503>.
- Kafle, G. K., & Chen, L. (2016). Comparison on batch anaerobic digestion of five different livestock manures and prediction of biochemical methane potential (BMP) using different statistical models. *Waste Management*, 48, 492-502.
<https://doi.org/10.1016/j.wasman.2015.10.021>.
- Kangle, K., Kore, S., Kore, V., & Kulkarni, G. (2012). Recent trends in anaerobic codigestion: a review. *Universal Journal of Environmental Research and Technology*, 2(4), 210-219.
<http://www.environmentaljournal.org/2-4/ujert-2-4-3.pdf>.
- Karasov, W. H., & Douglas, A. E. (2013). Comparative digestive physiology. *Comprehensive Physiology*, 3(2), 741. <https://doi.org/10.1002%2Fcphy.c110054>.
- Karikalan, S., & Mohankumar, A. (2016). Production, isolation and partially purification of alkaline protease from marine macro algae surface associated *Bacillus* spp. *International Journal of Biology Research*, 1(1), 63-66.
- Karlsson, A., Vallin, L., & Ejlertsson, J. (2008). Effects of temperature, hydraulic retention time and hydrogen extraction rate on hydrogen production from the fermentation of food industry residues and manure. *International Journal of Hydrogen Energy*, 33(3), 953-962.
<https://doi.org/10.1016/j.ijhydene.2007.10.055>.
- Kayhanian, M. (1994). Performance of a high-solids anaerobic digestion process under various ammonia concentrations. *Journal of Chemical Technology & Biotechnology: International Research in Process, Environmental and Clean Technology*, 59(4), 349-352.
<https://doi.org/10.1002/jctb.280590406>.

- Khamtib, S., Sittijunda, S., Imai, T., & Reungsang, A. (2021). Co-digestion of Oil Palm Trunk Hydrolysate and Slaughterhouse Wastewater for Biohydrogen Production in a Fixed Bed Reactor by Immobilized *Thermoanaerobacterium thermosaccharolyticum* KKU19 on Expanded Clay. *Frontiers in Energy Research*, 9, 683989.
<https://doi.org/10.3389/fenrg.2021.683989>.
- Khawer, M. U. B., Naqvi, S. R., Ali, I., Arshad, M., Juchelková, D., Anjum, M. W., & Naqvi, M. (2022). Anaerobic digestion of sewage sludge for biogas & biohydrogen production: State-of-the-art trends and prospects. *Fuel*, 329, 125416.
<https://doi.org/10.1016/j.fuel.2022.125416>.
- Khoobakht, G., Najafi, G., Karimi, M., & Akram, A. (2016). Optimization of operating factors and blended levels of diesel, biodiesel and ethanol fuels to minimize exhaust emissions of diesel engine using response surface methodology. *Applied Thermal Engineering*, 99, 1006-1017. <https://doi.org/10.1016/j.applthermaleng.2015.12.143>.
- Kim, D.-H., & Kim, M.-S. (2011). Hydrogenases for biological hydrogen production. *Bioresource Technology*, 102(18), 8423-8431.
<https://doi.org/10.1016/j.biortech.2011.02.113>.
- Kim, Y. K., Bae, J. H., Oh, B. K., Lee, W. H., & Choi, J. W. (2002). Enhancement of proteolytic enzyme activity excreted from *Bacillus stearothermophilus* for a thermophilic aerobic digestion process. *Bioresource Technology*, 82(2), 157-164.
[https://doi.org/10.1016/S0960-8524\(01\)00177-8](https://doi.org/10.1016/S0960-8524(01)00177-8).
- Kirli, B., & Karapinar, I. (2018). The effect of HRT on biohydrogen production from acid hydrolyzed waste wheat in a continuously operated packed bed reactor. *International*

- Journal of Hydrogen Energy*, 43(23), 10678-10685.
<https://doi.org/10.1016/j.ijhydene.2018.01.175>.
- Kobayashi, T., Xu, K.-Q., Li, Y.-Y., & Inamori, Y. (2012). Evaluation of hydrogen and methane production from municipal solid wastes with different compositions of fat, protein, cellulosic materials and the other carbohydrates. *International Journal of Hydrogen Energy*, 37(20), 15711-15718. <https://doi.org/10.1016/j.ijhydene.2012.05.044>.
- Konkol, I., Świerczek, L., & Cenian, A. (2023). Chicken Manure Pretreatment for Enhancing Biogas and Methane Production. *Energies*, 16(14), 5442.
<https://doi.org/10.3390/en16145442>.
- Kopasz, J., Dolan, C., Gangi, J., & Homann, Q. (2022). *Hydrogen and Fuel Cell Technologies Market Report 2020*. 10.2172/1859747.
- Kotay, S. M., & Das, D. (2008). Biohydrogen as a renewable energy resource—prospects and potentials. *International Journal of Hydrogen Energy*, 33(1), 258-263.
<https://doi.org/10.1016/j.ijhydene.2007.07.031>.
- Kovács, E., Wirth, R., Maróti, G., Bagi, Z., Nagy, K., Minárovits, J., Rákhely, G., & Kovács, K. L. (2015). Augmented biogas production from protein-rich substrates and associated metagenomic changes. *Bioresource Technology*, 178, 254-261.
<https://doi.org/10.1016/j.biortech.2014.08.111>.
- Kovács, E., Wirth, R., Maróti, G., Bagi, Z., Rákhely, G., & Kovács, K. L. (2013). Biogas production from protein-rich biomass: fed-batch anaerobic fermentation of casein and of pig blood and associated changes in microbial community composition. *Plos One*, 8(10), e77265. <https://doi.org/10.1371/journal.pone.0077265> .

- Kraemer, J. T., & Bagley, D. M. (2007). Improving the yield from fermentative hydrogen production. *Biotechnology letters*, 29(5), 685-695. <https://doi.org/10.1007/s10529-006-9299-9>.
- Krishna, K. V., Bhavana, S., Koujalagi, K., & Malaviya, A. (2023). Biofuels From Bio-Waste and Biomass, (pp. 75-118). IGI Global, Beijing, China . 10.4018/978-1-6684-5269-1.ch006.
- Kuhar, N., Sil, S., & Umapathy, S. (2021). Potential of Raman spectroscopic techniques to study proteins. *Spectrochimica Acta Part A: Molecular and Biomolecular Spectroscopy*, 258, 119712. <https://doi.org/10.1016/j.saa.2021.119712>.
- Kundu, K., Sharma, S., & Sreekrishnan, T. (2012). Effect of operating temperatures on the microbial community profiles in a high cell density hybrid anaerobic bioreactor. *Bioresource Technology*, 118, 502-511. <https://doi.org/10.1016/j.biortech.2012.05.047>.
- Langone, M., Ferrentino, R., Freddi, F., & Andreottola, G. (2019). Anaerobic digestion of blood serum water integrated in a valorization process of the bovine blood treatment. *Biomass and Bioenergy*, 120, 1-8. <https://doi.org/10.1016/j.biombioe.2018.10.015>.
- Lasekan, A., Bakar, F. A., & Hashim, D. (2013). Potential of chicken by-products as sources of useful biological resources. *Waste Management*, 33(3), 552-565. <https://doi.org/10.1016/j.wasman.2012.08.001>.
- Lauwers, J., Appels, L., Thompson, I. P., Degève, J., Van Impe, J. F., & Dewil, R. (2013). Mathematical modelling of anaerobic digestion of biomass and waste: Power and limitations. *Progress in Energy and Combustion Science*, 39(4), 383-402. <https://doi.org/10.1016/j.pecs.2013.03.003>.

- Lawrance, A., Haridas, A., Savithri, S., & Arunagiri, A. (2022). Development of mathematical model and experimental Validation for batch bio-drying of municipal solid waste: Mass balances. *Chemosphere*, 287 (3), 132272.
<https://doi.org/10.1016/j.chemosphere.2021.132272>.
- Laxman Pachapur, V., Jyoti Sarma, S., Kaur Brar, S., Le Bihan, Y., Ricardo Soccol, C., Buelna, G., & Verma, M. (2015). Co-culture strategies for increased biohydrogen production. *International Journal of Energy Research*, 39(11), 1479-1504.
<https://doi.org/10.1002/er.3364>.
- Lay, J.-J., Fan, K.-S., & Ku, C.-H. (2003). Influence of chemical nature of organic wastes on their conversion to hydrogen by heat-shock digested sludge. *International Journal of Hydrogen Energy*, 28(12), 1361-1367. [https://doi.org/10.1016/S0360-3199\(03\)00027-2](https://doi.org/10.1016/S0360-3199(03)00027-2).
- Levin, D. B., Zhu, H., Beland, M., Cicek, N., & Holbein, B. E. (2007). Potential for hydrogen and methane production from biomass residues in Canada. *Bioresource Technology*, 98(3), 654-660. <https://doi.org/10.1016/j.biortech.2006.02.027>.
- Li, D., Zhou, T., Chen, L., Jiang, W., Cheng, F., Li, B., & Kitamura, Y. (2009). Using porphyritic andesite as a new additive for improving hydrolysis and acidogenesis of solid organic wastes. *Bioresource Technology*, 100(23), 5594-5599.
<https://doi.org/10.1016/j.biortech.2009.06.005>.
- Li, K., Liu, R., & Sun, C. (2015). Comparison of anaerobic digestion characteristics and kinetics of four livestock manures with different substrate concentrations. *Bioresource Technology*, 198, 133-140. <https://doi.org/10.1016/j.biortech.2015.08.151>.

- Li, Y., Jin, Y., Borrion, A., & Li, J. (2018). Influence of feed/inoculum ratios and waste cooking oil content on the mesophilic anaerobic digestion of food waste. *Waste Management*, 73, 156-164. <https://doi.org/10.1016/j.wasman.2017.12.027>.
- Li, Y., Jin, Y., Li, H., Borrion, A., Yu, Z., & Li, J. (2018). Kinetic studies on organic degradation and its impacts on improving methane production during anaerobic digestion of food waste. *Applied Energy*, 213, 136-147. <https://doi.org/10.1016/j.wasman.2017.12.027>.
- Li, Y., Park, S. Y., & Zhu, J. (2011). Solid-state anaerobic digestion for methane production from organic waste. *Renewable and Sustainable Energy Reviews*, 15(1), 821-826. <https://doi.org/10.1016/j.rser.2010.07.042>.
- Li, Y., Zhang, R., Liu, X., Chen, C., Xiao, X., Feng, L., He, Y., & Liu, G. (2013). Evaluating methane production from anaerobic mono-and co-digestion of kitchen waste, corn stover, and chicken manure. *Energy & Fuels*, 27(4), 2085-2091. <https://doi.org/10.1021/ef400117f>.
- Lim, J. S., Manan, Z. A., Alwi, S. R. W., & Hashim, H. (2012). A review on utilisation of biomass from rice industry as a source of renewable energy. *Renewable and Sustainable Energy Reviews*, 16(5), 3084-3094. <https://doi.org/10.1016/j.rser.2012.02.051>.
- Lin, C.-Y., Chu, C.-Y., Lay, C.-H., & Leu, H.-J. (2016). Fermentative hydrogen and methane productions from organic wastes: a review. *Current Biochemical Engineering*, 3(1), 16-23.
- Lin, C., & Lay, C. (2004). Carbon/nitrogen-ratio effect on fermentative hydrogen production by mixed microflora. *International Journal of Hydrogen Energy*, 29(1), 41-45. [https://doi.org/10.1016/S0360-3199\(03\)00083-1](https://doi.org/10.1016/S0360-3199(03)00083-1).

- Ling, Z., Thakur, N., El-Dalatony, M. M., Salama, E.-S., & Li, X. (2022). Protein biomethanation: insight into the microbial nexus. *Trends in Microbiology*, *30*(1), 69-78. <https://doi.org/10.1016/j.tim.2021.06.004>.
- Litti, Y. V., Kovalev, A., Kovalev, D., Katraeva, I., Parshina, S., Zhuravleva, E., & Botchkova, E. (2021). Characteristics of the process of biohydrogen production from simple and complex substrates with different biopolymer composition. *International Journal of Hydrogen Energy*, *46*(52), 26289-26297. <https://doi.org/10.1016/j.ijhydene.2021.05.165>.
- Liu, C., Luo, G., Wang, W., He, Y., Zhang, R., & Liu, G. (2018). The effects of pH and temperature on the acetate production and microbial community compositions by syngas fermentation. *Fuel*, *224*, 537-544. <https://doi.org/10.1016/j.fuel.2018.03.125>.
- Liu, C., Ren, L., Yan, B., Luo, L., Zhang, J., & Awasthi, M. K. (2021). Electron transfer and mechanism of energy production among syntrophic bacteria during acidogenic fermentation: A review. *Bioresource Technology*, *323*, 124637. <https://doi.org/10.1016/j.biortech.2020.124637>.
- Liu, S., Li, W., Zheng, G., Yang, H., & Li, L. (2020). Optimization of cattle manure and food waste co-digestion for biohydrogen production in a mesophilic semi-continuous process. *Energies*, *13*(15), 3848. <https://doi.org/10.3390/en13153848>.
- Loganath, R., & Senophiyah-Mary, J. (2020). Critical review on the necessity of bioelectricity generation from slaughterhouse industry waste and wastewater using different anaerobic digestion reactors. *Renewable and Sustainable Energy Reviews*, *134*, 110360. <https://doi.org/10.1016/j.rser.2020.110360>.
- Lokshina, L. Y., Vavilin, V., Salminen, E., & Rintala, J. (2003). Modeling of anaerobic degradation of solid slaughterhouse waste: inhibition effects of long-chain fatty acids or

- ammonia. *Applied Biochemistry and Biotechnology*, 109, 15-32.
<https://doi.org/10.1385/ABAB:109:1-3:15>.
- López, I., Benzo, M., Passeggi, M., & Borzacconi, L. (2021). A simple kinetic model applied to anaerobic digestion of cow manure. *Environmental Technology*, 42(22), 3451-3462.
- López-Otín, C., & Bond, J. S. (2008). Proteases: multifunctional enzymes in life and disease. *Journal of Biological Chemistry*, 283(45), 30433-30437.
<https://doi.org/10.1080/09593330.2020.1732473>.
- Lory, J. A. (2019). What is the energy potential from manure produced by livestock? University of Missouri, USA.
- Lu, L., Ren, N., Zhao, X., Wang, H., Wu, D., & Xing, D. (2011). Hydrogen production, methanogen inhibition and microbial community structures in psychrophilic single-chamber microbial electrolysis cells. *Energy & Environmental Science*, 4(4), 1329-1336.
<https://doi.org/10.1039/C0EE00588F>.
- Lu, L., Xing, D., Ren, N., & Logan, B. E. (2012). Syntrophic interactions drive the hydrogen production from glucose at low temperature in microbial electrolysis cells. *Bioresource Technology*, 124, 68-76. <https://doi.org/10.1016/j.biortech.2012.08.040>.
- Łukajtis, R., Hołowacz, I., Kucharska, K., Glinka, M., Rybarczyk, P., Przyjazny, A., & Kamiński, M. (2018). Hydrogen production from biomass using dark fermentation. *Renewable and Sustainable Energy Reviews*, 91, 665-694. <https://doi.org/10.1016/j.rser.2018.04.043>.
- Ma, J., Carballa, M., Van De Caveye, P., & Verstraete, W. (2009). Enhanced propionic acid degradation (EPAD) system: Proof of principle and feasibility. *Water Research*, 43(13), 3239-3248. <https://doi.org/10.1016/j.watres.2009.04.046>.

- Ma, J., Yu, L., Frear, C., Zhao, Q., Li, X., & Chen, S. (2013). Kinetics of psychrophilic anaerobic sequencing batch reactor treating flushed dairy manure. *Bioresource Technology*, *131*, 6-12. <https://doi.org/10.1016/j.biortech.2012.11.147>.
- Madhusankha, G., & Thilakarathna, R. (2021). Meat tenderization mechanism and the impact of plant exogenous proteases: A review. *Arabian Journal of Chemistry*, *14*(2), 102967. <https://doi.org/10.1016/j.arabjc.2020.102967>.
- Margesin, R., & Schinner, F. (1994). Properties of cold-adapted microorganisms and their potential role in biotechnology. *Journal of Biotechnology*, *33*(1), 1-14. [https://doi.org/10.1016/0168-1656\(94\)90093-0](https://doi.org/10.1016/0168-1656(94)90093-0).
- Martín, M., Siles, J., Chica, A., & Martín, A. (2010). Biomethanization of orange peel waste. *Bioresource Technology*, *101*(23), 8993-8999. <https://doi.org/10.1016/j.biortech.2010.06.133>.
- Maruthiah, T., Somanath, B., Jasmin, J. V., Immanuel, G., & Palavesam, A. (2016). Production, purification and characterization of halophilic organic solvent tolerant protease from marine crustacean shell wastes and its efficacy on deproteinization. *3 Biotech*, *6*, 1-9. <https://doi.org/10.1007/s13205-016-0474-y>.
- McHugh, S., Collins, G., & O'Flaherty, V. (2006). Long-term, high-rate anaerobic biological treatment of whey wastewaters at psychrophilic temperatures. *Bioresource Technology*, *97*(14), 1669-1678. <https://doi.org/10.1016/j.biortech.2005.07.020>.
- Menon, A., Wang, J.-Y., & Giannis, A. (2017). Optimization of micronutrient supplement for enhancing biogas production from food waste in two-phase thermophilic anaerobic digestion. *Waste Management*, *59*, 465-475. <https://doi.org/10.1016/j.wasman.2016.10.017>.

- Mills, E. C., Jenkins, J. A., Alcocer, M. J., & Shewry, P. R. (2004). Structural, biological, and evolutionary relationships of plant food allergens sensitizing via the gastrointestinal tract. *Critical Reviews in Food Science and Nutrition*, 44(5), 379-407.
<https://doi.org/10.1080/10408690490489224>.
- Mitra, P., & Chakrabartty, P. K. (2005). An extracellular protease with depilation activity from *Streptomyces nogalator*. *Journal of Scientific and Industrial Research*, 64 (12), 978-983.
<http://nopr.niscpr.res.in/handle/123456789/5374>.
- Mizuno, O., Dinsdale, R., Hawkes, F. R., Hawkes, D. L., & Noike, T. (2000). Enhancement of hydrogen production from glucose by nitrogen gas sparging. *Bioresource Technology*, 73(1), 59-65. [https://doi.org/10.1016/S0960-8524\(99\)00130-3](https://doi.org/10.1016/S0960-8524(99)00130-3).
- Moeller, L., & Zehnsdorf, A. (2016). Process upsets in a full-scale anaerobic digestion bioreactor: over-acidification and foam formation during biogas production. *Energy, Sustainability and Society*, 6, 1-10. <https://doi.org/10.1186/s13705-016-0095-7>.
- Mohamed, M. A., & Hussein, M. (2007). Purification and characterization of an alkaline protease produced by the bacterium *Xenorhabdus nematophila* BA2, a symbiont of entomopathogenic nematode *Steinernema carpocapsae*. *Research Journal of Agriculture and Biological Sciences*, 3(5), 510-521.
- Mohan, S. V., Babu, V. L., & Sarma, P. (2008). Effect of various pretreatment methods on anaerobic mixed microflora to enhance biohydrogen production utilizing dairy wastewater as substrate. *Bioresource Technology*, 99(1), 59-67.
<https://doi.org/10.1016/j.biortech.2006.12.004>.

Mohd Azmi, S. I., Kumar, P., Sharma, N., Sazili, A. Q., Lee, S.-J., & Ismail-Fitry, M. R. (2023).

Application of Plant Proteases in Meat Tenderization: Recent Trends and Future

Prospects. *Foods*, 12(6), 1336. <https://doi.org/10.3390/foods12061336>.

Molaey, R., Bayrakdar, A., Sürmeli, R. Ö., & Çalli, B. (2019). Anaerobic digestion of chicken

manure: Influence of trace element supplementation. *Engineering in Life Sciences*, 19(2),

143-150. <https://doi.org/10.1002/elsc.201700201>.

Moletta, R., Finck, J., Goma, G., & Albagnac, G. (1985). Influence of hydrogen addition on the

potential of methanogenic ecosystems. W. Palz, J. Coombs, D.O. Hall (ED), Energy from

Biomass, Third EC Conference, Venice, Italy, Elsevier, Applied Science Publishers,

London, pp. 510-515.

Möller, K., & Müller, T. (2012). Effects of anaerobic digestion on digestate nutrient availability

and crop growth: A review. *Engineering in Life Sciences*, 12(3), 242-257.

<https://doi.org/10.1002/elsc.201100085>.

Momoh, Y. O., & Saroj, D. (2016). Development and testing of surface-based and water-based-

diffusion kinetic models for studying hydrolysis and biogas production from cow manure.

Renewable Energy, 86, 1113-1122. <https://doi.org/10.1016/j.renene.2015.09.036>.

Mönch-Tegeder, M., Lemmer, A., Oechsner, H., & Jungbluth, T. (2013). Investigation of the

methane potential of horse manure. *Agricultural Engineering International: CIGR*

Journal, 15(2), 161-172.

Morais, N. W. S., Coelho, M. M. H., e Silva, A. d. S., Silva, F. S. S., Ferreira, T. J. T., Pereira, E.

L., & Dos Santos, A. B. (2021). Biochemical potential evaluation and kinetic modeling of

methane production from six agro-industrial wastewaters in mixed culture.

Environmental Pollution, 280, 116876. <https://doi.org/10.1016/j.envpol.2021.116876>.

- Moscoviz, R., Trably, E., Bernet, N., & Carrère, H. (2018). The environmental biorefinery: state-of-the-art on the production of hydrogen and value-added biomolecules in mixed-culture fermentation. *Green Chemistry*, *20*(14), 3159-3179.
<https://doi.org/10.1039/C8GC00572A>.
- Mu, Y., Wang, G., & Yu, H.-Q. (2006). Response surface methodological analysis on biohydrogen production by enriched anaerobic cultures. *Enzyme and Microbial Technology*, *38*(7), 905-913. <https://doi.org/10.1016/j.enzmictec.2005.08.016>.
- Muske, A.N., Venkateswara Rao, P. (2019). Evaluation of Biogas Production Potential by Anaerobic Co-digestion with Substrate Mixture of Fruit Waste, Lawn Grass, and Manures. In: Rathinasamy, M., Chandramouli, S., Phanindra, K., Mahesh, U. (eds) *Water Resources and Environmental Engineering II*. Springer, Singapore.
https://doi.org/10.1007/978-981-13-2038-5_9.
- Mutezo, G., & Mulopo, J. (2021). A review of Africa's transition from fossil fuels to renewable energy using circular economy principles. *Renewable and Sustainable Energy Reviews*, *137*, 110609. <https://doi.org/10.1016/j.rser.2020.110609>.
- Mutungwazi, A., Ijoma, G. N., Ogola, H. J., & Matambo, T. S. (2022). Physico-Chemical and Metagenomic Profile Analyses of Animal Manures Routinely Used as Inocula in Anaerobic Digestion for Biogas Production. *Microorganisms*, *10*(4), 671.
<https://doi.org/10.3390/microorganisms10040671>.
- Nagase, M., & Matsuo, T. (1982). Interactions between amino-acid-degrading bacteria and methanogenic bacteria in anaerobic digestion. *Biotechnology and Bioengineering*, *24*(10), 2227-2239. <https://doi.org/10.1002/bit.260241009>.

- Nakakubo, R., Møller, H. B., Nielsen, A. M., & Matsuda, J. (2008). Ammonia inhibition of methanogenesis and identification of process indicators during anaerobic digestion. *Environmental Engineering Science*, 25(10), 1487-1496. <https://doi.org/10.1089/ees.2007.0282>.
- Naveena, B., Mendiratta, S., & Anjaneyulu, A. (2004). Tenderization of buffalo meat using plant proteases from *Cucumis trigonus* Roxb (Kachri) and *Zingiber officinale* roscoe (Ginger rhizome). *Meat Science*, 68(3), 363-369. <https://doi.org/10.1016/j.meatsci.2004.04.004>.
- Nazifa, T. H., Saady, N. M. C., Bazan, C., Zendehboudi, S., Aftab, A., & Albayati, T. M. (2021). Anaerobic digestion of blood from slaughtered livestock: A review. *Energies*, 14(18), 5666. <https://doi.org/10.3390/en14185666>.
- Ndubuisi-Nnaji, U. U., Ofon, U. A., Asamudo, N. U., & Ekong, V. M. (2020). Enhanced biogas and biofertilizer production from anaerobic codigestion of harvest residues and goat manure. *Journal of Scientific Research and Reports*, 26(3), 1-13. [10.9734/jsrr/2020/v26i330231](https://doi.org/10.9734/jsrr/2020/v26i330231).
- Nelson, A., Peter, A., & Saju, F. (2022). A review on chemistry, therapeutic applications, extraction & purification of bromelain. *International Journal of Pharmacognosy and Chemistry*, 25-33. <https://doi.org/10.46796/IJPC.V3I1.297>.
- Nelson, M., & Holder, A. (2009). A fundamental analysis of continuous flow bioreactor models governed by Contois kinetics. II. Reactor cascades. *Chemical Engineering Journal*, 149(1-3), 406-416. <https://doi.org/10.1016/j.cej.2009.01.028>.
- Neshat, S. A., Mohammadi, M., & Najafpour, G. D. (2017). Photosynthesis assisted anaerobic digestion of cattle manure leachate in a hybrid bioreactor: an integrated system for

- enhanced wastewater treatment and methane production. *Chemical Engineering Journal*, 330, 616-624. <https://doi.org/10.1016/j.cej.2017.08.001>.
- Neshat, S. A., Mohammadi, M., Najafpour, G. D., & Lahijani, P. (2017). Anaerobic co-digestion of animal manures and lignocellulosic residues as a potent approach for sustainable biogas production. *Renewable and Sustainable Energy Reviews*, 79, 308-322. <https://doi.org/10.1016/j.rser.2017.05.137>.
- Neves, L., Oliveira, R., & Alves, M. (2009). Co-digestion of cow manure, food waste and intermittent input of fat. *Bioresource Technology*, 100(6), 1957-1962. <https://doi.org/10.1016/j.biortech.2008.10.030>.
- Nguyen, T.-T., Chu, C.-Y., & Ou, C.-M. (2021). Pre-treatment study on two-stage biohydrogen and biomethane productions in a continuous co-digestion process from a mixture of swine manure and pineapple waste. *International Journal of Hydrogen Energy*, 46(20), 11325-11336. <https://doi.org/10.1016/j.ijhydene.2020.05.264>.
- Nguyen, T.-T., Ta, D.-T., Lin, C.-Y., & Chu, C.-Y. (2022). Biohythane production from swine manure and pineapple waste in a single-stage two-chamber digester using gel-entrapped anaerobic microorganisms. *International Journal of Hydrogen Energy*, 47(60), 25245-25255. <https://doi.org/10.1016/j.ijhydene.2022.05.259>.
- Nikolaeva, S., Sánchez, E., Borja, R., Raposo, F., Colmenarejo, M., Montalvo, S., & Jiménez-Rodríguez, A.-M. (2009). Kinetics of anaerobic degradation of screened dairy manure by upflow fixed bed digesters: effect of natural zeolite addition. *Journal of Environmental Science and Health Part A*, 44(2), 146-154. <https://doi.org/10.1080/10934520802539715>.

- Ning, Z., Ji, J., He, Y., Huang, Y., Liu, G., & Chen, C. (2016). Effect of lipase hydrolysis on biomethane production from swine slaughterhouse waste in China. *Energy & Fuels*, *30*(9), 7326-7330. <https://doi.org/10.1021/acs.energyfuels.6b01097>.
- Niu, Q., Kubota, K., Qiao, W., Jing, Z., Zhang, Y., & Yu-You, L. (2015). Effect of ammonia inhibition on microbial community dynamic and process functional resilience in mesophilic methane fermentation of chicken manure. *Journal of Chemical Technology & Biotechnology*, *90*(12), 2161-2169. <https://doi.org/10.1002/jctb.4527>.
- Noorollahi, Y., Kheirrouz, M., Asl, H. F., Yousefi, H., & Hajinezhad, A. (2015). Biogas production potential from livestock manure in Iran. *Renewable and Sustainable Energy Reviews*, *50*, 748-754. <https://doi.org/10.1016/j.rser.2015.04.190>.
- Obileke, K., Mamphweli, S., Meyer, E. L., Makaka, G., & Nwokolo, N. (2020). Design and fabrication of a plastic biogas digester for the production of biogas from cow dung. *Journal of Engineering*, *2020*, 1-11. <https://doi.org/10.1155/2020/1848714>.
- Oh, S.-E., Van Ginkel, S., & Logan, B. E. (2003). The relative effectiveness of pH control and heat treatment for enhancing biohydrogen gas production. *Environmental science & technology*, *37*(22), 5186-5190. <https://doi.org/10.1021/es034291y>.
- Okamoto, M., Miyahara, T., Mizuno, O., & Noike, T. (2000). Biological hydrogen potential of materials characteristic of the organic fraction of municipal solid wastes. *Water Science and Technology*, *41*(3), 25-32. <https://doi.org/10.2166/wst.2000.0052>.
- Ozbayram, E., Akyol, Ç., Ince, B., Karakoç, C., & Ince, O. (2018). Rumen bacteria at work: bioaugmentation strategies to enhance biogas production from cow manure. *Journal of Applied Microbiology*, *124*(2), 491-502. <https://doi.org/10.1111/jam.13668>.

- Özmiğçi, S., Hacıoğlu, İ., & Altındağ, E. E. (2022). Impacts of mycotoxin on biohydrogen production from waste dry fruits. *Journal of Material Cycles and Waste Management*, 24(5), 1736-1746. <https://doi.org/10.1007/s10163-022-01418-5>.
- Palatsi, J., Viñas, M., Guivernau, M., Fernandez, B., & Flotats, X. (2011). Anaerobic digestion of slaughterhouse waste: main process limitations and microbial community interactions. *Bioresource Technology*, 102(3), 2219-2227. <https://doi.org/10.1016/j.biortech.2010.09.121>.
- Park, H. J., Han, S. J., Yim, J. H., & Kim, D. (2018). Characterization of an Antarctic alkaline protease, a cold-active enzyme for laundry detergents. *Korean Journal of Microbiology*, 54(1), 60-68. <https://doi.org/10.7845/kjm.2018.7080>.
- Patel, S. K., Das, D., Kim, S. C., Cho, B.-K., Kalia, V. C., & Lee, J.-K. (2021). Integrating strategies for sustainable conversion of waste biomass into dark-fermentative hydrogen and value-added products. *Renewable and Sustainable Energy Reviews*, 150, 111491. <https://doi.org/10.1016/j.rser.2021.111491>.
- Pennington, B. O., Sears, D., & Clegg, D. O. (2014). Interactive Hangman teaches amino acid structures and abbreviations. *Biochemistry and Molecular Biology Education*, 42(6), 495-500. <https://doi.org/10.1002/bmb.20826>.
- Perman, E., Schnürer, A., Björn, A., & Moestedt, J. (2022). Serial anaerobic digestion improves protein degradation and biogas production from mixed food waste. *Biomass and Bioenergy*, 161, 106478. <https://doi.org/10.1016/j.biombioe.2022.106478>.
- Pilli, S., Yan, S., Tyagi, R. D., & Surampalli, R. Y. (2015). Thermal pretreatment of sewage sludge to enhance anaerobic digestion: a review. *Critical Reviews in Environmental Science and Technology*, 45(6), 669-702.

- Pramanik, S. K., Suja, F. B., Porhemmat, M., & Pramanik, B. K. (2019). Performance and kinetic model of a single-stage anaerobic digestion system operated at different successive operating stages for the treatment of food waste. *Processes*, 7(9), 600. <https://doi.org/10.3390/pr7090600>.
- Puig-Castellví, F., Cardona, L., Jouan-Rimbaud Bouveresse, D., Cordella, C. B., Mazéas, L., Rutledge, D. N., & Chapleur, O. (2020). Assessment of the microbial interplay during anaerobic co-digestion of wastewater sludge using common components analysis. *Plos One*, 15(5), e0232324. <https://doi.org/10.1371/journal.pone.0232324>.
- Qiao, W., Yan, X., Ye, J., Sun, Y., Wang, W., & Zhang, Z. (2011). Evaluation of biogas production from different biomass wastes with/without hydrothermal pretreatment. *Renewable Energy*, 36(12), 3313-3318. <https://doi.org/10.1016/j.renene.2011.05.002>.
- Rafieenia, R., Girotto, F., Peng, W., Cossu, R., Pivato, A., Raga, R., & Lavagnolo, M. C. (2017). Effect of aerobic pre-treatment on hydrogen and methane production in a two-stage anaerobic digestion process using food waste with different compositions. *Waste Management*, 59, 194-199. <https://doi.org/10.1016/j.wasman.2016.10.028>.
- Rai, P., Pandey, A., & Pandey, A. (2019). Optimization of sugar release from banana peel powder waste (BPPW) using box-behnken design (BBD): BPPW to biohydrogen conversion. *International Journal of Hydrogen Eenergy*, 44(47), 25505-25513. <https://doi.org/10.1016/j.ijhydene.2019.07.168>.
- Ramezani, R., Aminlari, M., & Fallahi, H. (2003). Effect of chemically modified soy proteins and ficin-tenderized meat on the quality attributes of sausage. *Journal of Food Science*, 68(1), 85-88. <https://doi.org/10.1111/j.1365-2621.2003.tb14119.x>.

- Ramírez Calderón, O. A. (2020). Modelling the anaerobic digestion of microalgae grown on wastewater: Impact of reactor configuration on methane production. IHE Delft Institute for Water Education.
- Ramos-Suárez, J., Ritter, A., González, J. M., & Pérez, A. C. (2019). Biogas from animal manure: A sustainable energy opportunity in the Canary Islands. *Renewable and Sustainable Energy Reviews*, *104*, 137-150. <https://doi.org/10.1016/j.rser.2019.01.025>.
- Ramsay, I. R., & Pullammanappallil, P. C. (2001). Protein degradation during anaerobic wastewater treatment: derivation of stoichiometry. *Biodegradation*, *12*(4), 247-256. <https://doi.org/10.1023/A:1013116728817>.
- Rawoof, S. A. A., Kumar, P. S., Vo, D.-V. N., Devaraj, T., & Subramanian, S. (2021). Biohythane as a high potential fuel from anaerobic digestion of organic waste: A review. *Renewable and Sustainable Energy Reviews*, *152*, 111700. <https://doi.org/10.1016/j.rser.2021.111700>.
- Razzaq, A., Shamsi, S., Ali, A., Ali, Q., Sajjad, M., Malik, A., & Ashraf, M. (2019). Microbial proteases applications. *Frontiers in Bioengineering and Biotechnology*, *7*, 110. <https://doi.org/10.3389/fbioe.2019.00110>.
- Ristow, N., Sötemann, S., Wentzel, M., Loewenthal, R., & Ekama, G. (2006). The effects of hydraulic retention time and feed COD concentration on the rate of hydrolysis of primary sewage sludge under methanogenic conditions. *Water Science and Technology*, *54*(5), 91-100. <https://doi.org/10.2166/wst.2006.551>.
- Robledo-Narváez, P. N., Muñoz-Páez, K. M., Poggi-Varaldo, H. M., Ríos-Leal, E., Calva-Calva, G., Ortega-Clemente, L. A., Rinderknecht-Seijas, N., Estrada-Vázquez, C., Ponce-Noyola, M. T., & Salazar-Montoya, J. A. (2013). The influence of total solids content and

- initial pH on batch biohydrogen production by solid substrate fermentation of agroindustrial wastes. *Journal of Environmental Management*, 128, 126-137.
<https://doi.org/10.1016/j.jenvman.2013.04.042>.
- Robert, J.D.; Caseiro, M.C (1965). Basic Principles of Organic Chemistry, 2nd ed.; W.A. Benjamin, Inc.: Menlo Park, CA, USA; Photochemistry.
- Ruiz, B., & Flotats, X. (2016). Effect of limonene on batch anaerobic digestion of citrus peel waste. *Biochemical Engineering Journal*, 109, 9-18.
<https://doi.org/10.1016/j.bej.2015.12.011>.
- Saady, N. M. C., Rezaeitavabe, F., & Ruiz Espinoza, J. E. (2021). Chemical Methods for Hydrolyzing Dairy Manure Fiber: A Concise Review. *Energies*, 14(19), 6159.
<https://doi.org/10.3390/en14196159>.
- Salem, A. H., Brunstermann, R., Mietzel, T., & Widmann, R. (2018). Effect of pre-treatment and hydraulic retention time on biohydrogen production from organic wastes. *International Journal of Hydrogen Energy*, 43(10), 4856-4865.
<https://doi.org/10.1016/j.ijhydene.2018.01.114>.
- Sambusiti, C., Bellucci, M., Zabaniotou, A., Beneduce, L., & Monlau, F. (2015). Algae as promising feedstocks for fermentative biohydrogen production according to a biorefinery approach: a comprehensive review. *Renewable and Sustainable Energy Reviews*, 44, 20-36. <https://doi.org/10.1016/j.rser.2014.12.013>.
- Sanders, W., Geerink, M., Zeeman, G., & Lettinga, G. (2000). Anaerobic hydrolysis kinetics of particulate substrates. *Water Science and Technology*, 41(3), 17-24.
<https://doi.org/10.2166/wst.2000.0051>.

- Sangavai, C., Bharathi, M., Ganesh, S. P., & Chellapandi, P. (2019). Kinetic modeling of Stickland reactions-coupled methanogenesis for a methanogenic culture. *AMB Express*, 9(1), 1-13. <https://doi.org/10.1186/s13568-019-0803-8>.
- Sanjaya, A. P., Cahyanto, M. N., & Millati, R. (2016). Mesophilic batch anaerobic digestion from fruit fragments. *Renewable Energy*, 98, 135-141. <https://doi.org/10.1016/j.renene.2016.02.059>.
- Sarkar, O., Butti, S. K., & Mohan, S. V. (2018). Acidogenic biorefinery: food waste valorization to biogas and platform chemicals. *Waste Biorefinery*, 203-218. <https://doi.org/10.1016/B978-0-444-63992-9.00006-9>.
- Sawatdeenarunat, C., Saipa, S., & Suaisom, P. (2021). Anaerobic digestion of elephant camp-derived wastes: methane potential, kinetic study, and biorefinery platform. *Biomass Conversion and Biorefinery*, 1-10, 6175–6184. <https://doi.org/10.1007/s13399-021-01576-w>.
- Scherer, S.; Neuhaus, K. Life at low temperatures. In *The Prokaryotes*; Dworkin, M., Falkow, S., Rosenberg, E., Schleifer, K.H., Stackebrandt, E., (ED); Springer: New York, NY, USA, 2006; pp. 210–262.
- Schnürer, A. Biogas Production: Microbiology and Technology. In *Anaerobes in Biotechnology. Advances in Biochemical Engineering/Biotechnology*; Hatti-Kaul, R., Mamo, G., Mattiasson, B., Eds.; Springer: Cham, Switzerland, 2016; Volume 156, pp. 195–234. ISBN 978-3-319-45651-5.
- Schuchmann, K., Chowdhury, N. P., & Müller, V. (2018). Complex multimeric [FeFe] hydrogenases: biochemistry, physiology and new opportunities for the hydrogen economy. *Frontiers in Microbiology*, 9, 2911. <https://doi.org/10.3389/fmicb.2018.02911>.

- Sellami-Kamoun, A., Ghorbel-Frikha, B., Haddar, A., & Nasri, M. (2011). Enhanced *Bacillus cereus* BG1 protease production by the use of sardinelle (*Sardinella aurita*) powder. *Annals of Microbiology*, *61*, 273-280. <https://doi.org/10.1007/s13213-010-0134->.
- Shang, T. (2007). Value added products from animal manure, Bioprocessing for value-added products from renewable resources, new technologies and applications. *Dublin (OH): Elsevier*, 641-651.
- Shanmugam, S., Mathimani, T., Rene, E. R., Geo, V. E., Arun, A., Brindhadevi, K., & Pugazhendhi, A. (2021). Biohythane production from organic waste: Recent advancements, technical bottlenecks and prospects. *International Journal of Hydrogen Energy*, *46*(20), 11201-11216. <https://doi.org/10.1016/j.ijhydene.2020.10.132>.
- Shanthi, G., Premalatha, M., & Anantharaman, N. (2021). Potential utilization of fish waste for the sustainable production of microalgae rich in renewable protein and phycocyanin-*Arthrospira platensis*/Spirulina. *Journal of Cleaner Production*, *294*, 126106. <https://doi.org/10.1016/j.jclepro.2021.126106>.
- Sharma, P., & Melkania, U. (2018). Enhancement effect of amino acids on hydrogen production from organic fraction of municipal solid waste using co-culture of *Escherichia coli* and *Enterobacter aerogenes*. *Energy Conversion and Management*, *163*, 260-267. <https://doi.org/10.1016/j.enconman.2018.02.072>.
- Shen, F., & Sergi, C. (2022). Biochemistry, Amino Acid Synthesis and Degradation. In StatPearls; StatPearls Publishing: Treasure Island, FL, USA.
- Shen, J., Zhao, C., Liu, Y., Zhang, R., Liu, G., & Chen, C. (2019). Biogas production from anaerobic co-digestion of durian shell with chicken, dairy, and pig manures. *Energy*

Conversion and Management, 198, 110535.

<https://doi.org/10.1016/j.enconman.2018.06.099>.

Shen, M.-Y., Torre, M., Chu, C.-Y., Tratzi, P., Carnevale, M., Gallucci, F., Paolini, V., & Petracchini, F. (2022). Green biohydrogen production in a Co-digestion process from mixture of high carbohydrate food waste and cattle/chicken manure digestate.

International Journal of Hydrogen Energy, 47, 40696–40703.

<https://doi.org/10.1016/j.ijhydene.2022.09.104>.

Siddique, M. N. I., & Wahid, Z. A. (2018). Achievements and perspectives of anaerobic co-digestion: A review. *Journal of Cleaner Production*, 194, 359-371.

<https://doi.org/10.1016/j.jclepro.2018.05.155>.

Siegert, I., & Banks, C. (2005). The effect of volatile fatty acid additions on the anaerobic digestion of cellulose and glucose in batch reactors. *Process Biochemistry*, 40(11), 3412-3418. <https://doi.org/10.1016/j.procbio.2005.01.025>.

Sillero, L., Solera, R., & Pérez, M. (2022). Effect of the hydraulic retention time on the acidogenic fermentation of sewage sludge, wine vinasse and poultry manure for biohydrogen production. *Biomass and Bioenergy*, 167, 106643.

<https://doi.org/10.1016/j.biombioe.2022.106643>.

Silva-López, R., & Gonçalves, R. (2019). Therapeutic proteases from plants: biopharmaceuticals with multiple applications. *Journal of Applied Biotechnology Bioengineering*, 6(2), 101-109. <https://doi.org/10.15406/jabb.2019.06.00180>.

Sindhu, R., Binod, P., Pandey, A., & Gnansounou, E. (2020). Agroresidue-based biorefineries,

- In Refining Biomass Residues for Sustainable Energy And Bioproducts; Kumar, R.P., Gnansounou, E., Raman, J.K., Baskar, G. (ED.), Academic Press, pp. 243-258, Elsevier. <https://doi.org/10.1016/B978-0-12-818996-2.00011-9>.
- Singh, P.K.; Shrivastava, N.; Ojha, B.K. Enzymes in the meat industry. In Enzymes in Food Biotechnology: Production, Applications, and Future Prospects; Academic Press: Cambridge, MA, USA, 2019; pp. 111–128. ISBN 9780128132807.
- Singh, R., Mittal, A., Kumar, M., & Mehta, P. K. (2016). Microbial proteases in commercial applications. *Journal of Pharmaceutical, Chemical and Biological Science*, 4(3), 365-374. <https://doi.org/10.3390/jof8020109>.
- Solanki, P., Putatunda, C., Kumar, A., Bhatia, R., & Walia, A. (2021). Microbial proteases: ubiquitous enzymes with innumerable uses. *3 Biotech*, 11(10), 428. <https://doi.org/10.1007/s13205-021-02928-z>.
- Solli, L., Håvelsrud, O. E., Horn, S. J., & Rike, A. G. (2014). A metagenomic study of the microbial communities in four parallel biogas reactors. *Biotechnology for Biofuels*, 7(1), 1-15. <https://doi.org/10.1186/s13068-014-0146-2>.
- Söllinger, A., & Urich, T. (2019). Methylotrophic methanogens everywhere—physiology and ecology of novel players in global methane cycling. *Biochemical Society Transactions*, 47(6), 1895-1907. <https://doi.org/10.1042/BST20180565>.
- Song, W., Cheng, J., Zhou, J., Xie, B., Su, H., & Cen, K. (2010). Cogeneration of hydrogen and methane from protein-mixed food waste by two-phase anaerobic process. *International Journal of Hydrogen Energy*, 35(7), 3141-3146. <https://doi.org/10.1016/j.ijhydene.2009.09.102>.

- Sorapukdee, S., Sumpavapol, P., Benjakul, S., & Tangwatcharin, P. (2020). Collagenolytic proteases from *Bacillus subtilis* B13 and *B. siamensis* S6 and their specificity toward collagen with low hydrolysis of myofibrils. *Lwt*, *126*, 109307. <https://doi.org/10.1016/j.lwt.2020.109307>.
- Sravan, J.S.; Tharak, A.; Mohan, S.V. Chapter 1-Status of biogas production and biogas upgrading: A global scenario. In *Emerging Technologies and Biological Systems for Biogas Upgrading*; Aryal, N., Mørck Ottosen, L.D., Wegener Kofoed, M.V., Pant, D., (ED); Academic Press: Cambridge, MA, USA; pp. 3–26. <https://doi.org/10.1016/B978-0-12-822808-1.00002-7>.
- Srinivasan, T., Das, S., Philip, V. B. R., & Kannan, N. (2009). Isolation and characterization of thermostable protease producing bacteria from tannery industry effluent. *Recent Research in Science and Technology*, *1*(2), 63-66.
- Srisowmeya, G., Chakravarthy, M., & Devi, G. N. (2020). Critical considerations in two-stage anaerobic digestion of food waste—A review. *Renewable and Sustainable Energy Reviews*, *119*, 109587. <https://doi.org/10.1016/j.rser.2019.109587>.
- Stamatelatou, K., G. Antonopoulou, and P. Michailides. 2014. 15 - Biomethane and Biohydrogen Production via Anaerobic Digestion/Fermentation. In *Advances in Biorefineries: Biomass and Waste Supply Chain Exploitation*, Waldron, K. (ED), 476–524. London: Woodhead Publishing, Amsterdam, Netherlands.
- Sun, C., Cao, W., Banks, C. J., Heaven, S., & Liu, R. (2016). Biogas production from undiluted chicken manure and maize silage: a study of ammonia inhibition in high solids anaerobic digestion. *Bioresource Technology*, *218*, 1215-1223. <https://doi.org/10.1016/j.biortech.2016.07.082>.

- Sundararajan, S., Kannan, C. N., & Chittibabu, S. (2011). Alkaline protease from *Bacillus cereus* VITSN04: potential application as a dehairing agent. *Journal of Bioscience and Bioengineering*, *111*(2), 128-133. <https://doi.org/10.1016/j.jbiosc.2010.09.009>.
- Sutaryo, S., Ward, A., & Moller, H. (2014). Ammonia inhibition in thermophilic anaerobic digestion of dairy cattle manure. *Journal of the Indonesian Tropical Animal Agriculture*, *39*(2), 83-90. [http://www.jppt.undip.ac.id/pdf/39\(2\)2014p83-90.pdf](http://www.jppt.undip.ac.id/pdf/39(2)2014p83-90.pdf).
- Taiganides, E. P., & Stroshine, R. L. (1971). Impacts of farm animal production and processing on the total environment. In: Proceedings of the international symposium on livestock wastes, livestock management and pollution abatement, April 19–22, p. ASAE: Columbus, Ohio, USA.
- Tangwe, S., Mukumba, P., & Makaka, G. (2022). Comparison of the Prediction Accuracy of Total Viable Bacteria Counts in a Batch Balloon Digester Charged with Cow Manure: Multiple Linear Regression and Non-Linear Regression Models. *Energies*, *15*(19), 7407. <https://doi.org/10.3390/en15197407>.
- Tantamacharik, T.; Carne, A.; Agyei, D.; Birch, J.; Bekhit, A.E.-D.A. Use of Plant Proteolytic Enzymes for Meat Processing. In *Biotechnological Applications of Plant Proteolytic Enzymes*; Springer International Publishing: Cham, Switzerland, 2018; pp. 43–67. https://doi.org/10.1007/978-3-319-97132-2_3.
- Tasaki, K. (2021). Chemical-free recovery of protein from cow manure digestate solid and antioxidant activity of recovered protein. *Environmental Challenges*, *4*, 100132. <https://doi.org/10.1016/j.envc.2021.100132>.

- Tavano, O. L. (2013). Protein hydrolysis using proteases: An important tool for food biotechnology. *Journal of Molecular Catalysis B: Enzymatic*, *90*, 1-11.
<https://doi.org/10.1016/j.molcatb.2013.01.011>.
- Tenca, A., Schievano, A., Perazzolo, F., Adani, F., & Oberti, R. (2011). Biohydrogen from thermophilic co-fermentation of swine manure with fruit and vegetable waste: maximizing stable production without pH control. *Bioresource Technology*, *102*(18), 8582-8588. <https://doi.org/10.1016/j.biortech.2011.03.102>.
- Theuerl, S., Klang, J., & Prochnow, A. (2019). Process disturbances in agricultural biogas production—Causes, mechanisms and effects on the biogas microbiome: A review. *Energies*, *12*(3), 365. <https://doi.org/10.3390/en12030365>.
- Tian, H., Duan, N., Lin, C., Li, X., & Zhong, M. (2015). Anaerobic co-digestion of kitchen waste and pig manure with different mixing ratios. *Journal of Bioscience and Bioengineering*, *120*(1), 51-57. <https://doi.org/10.1016/j.jbiosc.2014.11.017>.
- Treu, L., Tsapekos, P., Peprah, M., Campanaro, S., Giacomini, A., Corich, V., Kougias, P. G., & Angelidaki, I. (2019). Microbial profiling during anaerobic digestion of cheese whey in reactors operated at different conditions. *Bioresource Technology*, *275*, 375-385.
<https://doi.org/10.1016/j.biortech.2018.12.084>.
- Qaramaleki, S., Villamil, J. A., Mohedano, A. F., & Coronella, C. J. (2020). Factors affecting solubilization of phosphorus and nitrogen through hydrothermal carbonization of animal manure. *ACS Sustainable Chemistry & Engineering*, *8*(33), 12462-12470.
<https://doi.org/10.1021/acssuschemeng.0c03268>.
- Vasiliadou, I. A., Gioulounta, K., & Stamatelatou, K. (2023). Production of biogas via anaerobic digestion. In *Handbook of Biofuels Production*. Luque, R., Lin, C. S. K., Wilson, K., Du,

- C., (ED). Woodhead Publishing Series in Energy (253-311), Woodhead Publishing, UK., ISBN 9780323911931. <https://doi.org/10.1016/B978-0-323-91193-1.00010-X>.
- Vavilin, V., Fernandez, B., Palatsi, J., & Flotats, X. (2008). Hydrolysis kinetics in anaerobic degradation of particulate organic material: an overview. *Waste Management*, 28(6), 939-951. <https://doi.org/10.1016/j.wasman.2007.03.028>.
- Venugopal, M., & Saramma, A. (2007). An alkaline protease from *Bacillus circulans* BM15, newly isolated from a mangrove station: characterization and application in laundry detergent formulations. *Indian Journal of Microbiology*, 47(4), 298. <https://doi.org/10.1007/s12088-007-0055-1>.
- Vidal, G., Carvalho, A., Mendez, R., & Lema, J. (2000). Influence of the content in fats and proteins on the anaerobic biodegradability of dairy wastewaters. *Bioresource Technology*, 74(3), 231-239. [https://doi.org/10.1016/S0960-8524\(00\)00015-8](https://doi.org/10.1016/S0960-8524(00)00015-8).
- Vignais, P. M., Billoud, B., & Meyer, J. (2001). Classification and phylogeny of hydrogenases. *FEMS Microbiology Reviews*, 25(4), 455-501. <https://doi.org/10.1111/j.1574-6976.2001.tb00587.x>
- Wadjeam, P., Reungsang, A., Imai, T., & Plangklang, P. (2019). Co-digestion of cassava starch wastewater with buffalo dung for bio-hydrogen production. *International Journal of Hydrogen Energy*, 44(29), 14694-14706. <https://doi.org/10.1016/j.ijhydene.2019.04.138>.
- Wang, H., Fotidis, I. A., & Angelidaki, I. (2015). Ammonia effect on hydrogenotrophic methanogens and syntrophic acetate-oxidizing bacteria. *FEMS Microbiology Ecology*, 91(11). <https://doi.org/10.1093/femsec/fiv130>.

- Wang, S., Ping, Q., & Li, Y. (2022). Comprehensively understanding metabolic pathways of protein during the anaerobic digestion of waste activated sludge. *Chemosphere*, 297, 134117. <https://doi.org/10.1016/j.chemosphere.2022.134117>.
- Wang, H., Zhang, Y., & Angelidaki, I. (2016). Ammonia inhibition on hydrogen enriched anaerobic digestion of manure under mesophilic and thermophilic conditions. *Water Research*, 105, 314-319. <https://doi.org/10.1016/j.watres.2016.09.006>.
- Wang, K.-S., Chen, J.-H., Huang, Y.-H., & Huang, S.-L. (2013). Integrated Taguchi method and response surface methodology to confirm hydrogen production by anaerobic fermentation of cow manure. *International Journal of Hydrogen Energy*, 38(1), 45-53.
- Wang, K., Khoo, K. S., Chew, K. W., Selvarajoo, A., Chen, W.-H., Chang, J.-S., & Show, P. L. (2021). Microalgae: the future supply house of biohydrogen and biogas. *Frontiers in Energy Research*, 9, 660399. <https://doi.org/10.3389/fenrg.2021.660399>.
- Wang, L., Zhou, Q., & Zheng, G. (2006). Comprehensive analysis of the factors for propionic acid accumulation in acidogenic phase of anaerobic process. *Environmental Technology*, 27(3), 269-276. <https://doi.org/10.1080/09593332708618640>.
- Wang, S.-C., & Lee, C. T. (2006). Protein secondary structure controlled with light and photoresponsive surfactants. *The Journal of Physical Chemistry B*, 110(32), 16117-16123. <https://doi.org/10.1021/jp060981n>.
- Wang, S., Jena, U., & Das, K. C. (2018). Biomethane production potential of slaughterhouse waste in the United States. *Energy Conversion and Management*, 173, 143-157. <https://doi.org/10.1016/j.enconman.2018.07.059>.
- Wang, S., Ma, Z., Zhang, T., Bao, M., & Su, H. (2017). Optimization and modeling of biohydrogen production by mixed bacterial cultures from raw cassava starch. *Frontiers of*

- Chemical Science and Engineering*, 11, 100-106. <https://doi.org/10.1007/s11705-017-1617-3>.
- Wang, X., Li, Z., Bai, X., Zhou, X., Cheng, S., Gao, R., & Sun, J. (2018). Study on improving anaerobic co-digestion of cow manure and corn straw by fruit and vegetable waste: methane production and microbial community in CSTR process. *Bioresource Technology*, 249, 290-297. <https://doi.org/10.1016/j.biortech.2017.10.038>.
- Wang, Y., Zhang, Y., Wang, J., & Meng, L. (2009). Effects of volatile fatty acid concentrations on methane yield and methanogenic bacteria. *Biomass and Bioenergy*, 33(5), 848-853. <https://doi.org/10.1016/j.biombioe.2009.01.007>.
- Wen, Z., Liao, W., Liu, C., & Chen, S. (2007). Value-added products from animal manure. In *Bioprocessing for Value-Added Products from Renewable Resources*, Yang ST (ED), New Technologies and Applications, 629-651. ISBN 978-0-444-52114-9. <https://doi.org/10.1016/B978-0-444-52114-9.X5000-2>.
- Whalen, J. K., Thomas, B. W., & Sharifi, M. (2019). Novel practices and smart technologies to maximize the nitrogen fertilizer value of manure for crop production in cold humid temperate regions. *Advances in Agronomy*, 153, 1-85. <https://doi.org/10.1016/bs.agron.2018.09.002>.
- Wouters, A. G., Rombouts, I., Fierens, E., Brijs, K., & Delcour, J. A. (2016). Relevance of the functional properties of enzymatic plant protein hydrolysates in food systems. *Comprehensive Reviews in Food Science and Food Safety*, 15(4), 786-800. <https://doi.org/10.1111/1541-4337.12209>.
- Wu, S., Liu, G., Zhang, D., Li, C., & Sun, C. (2015). Purification and biochemical characterization of an alkaline protease from marine bacteria *Pseudoalteromonas* sp. 129-

1. *Journal of Basic Microbiology*, 55(12), 1427-1434.
<https://doi.org/10.1002/jobm.201500327>.
- Wu, S., Ni, P., Li, J., Sun, H., Wang, Y., Luo, H., Dach, J., & Dong, R. (2016). Integrated approach to sustain biogas production in anaerobic digestion of chicken manure under recycled utilization of liquid digestate: Dynamics of ammonium accumulation and mitigation control. *Bioresource Technology*, 205, 75-81.
<https://doi.org/10.1016/j.biortech.2016.01.021>.
- Wu, Y., & Song, K. (2021). Anaerobic co-digestion of waste activated sludge and fish waste: Methane production performance and mechanism analysis. *Journal of Cleaner Production*, 279, 123678. <https://doi.org/10.1016/j.jclepro.2020.123678>.
- Xia, Y., Massé, D. I., McAllister, T. A., Beaulieu, C., & Ungerfeld, E. (2012). Anaerobic digestion of chicken feather with swine manure or slaughterhouse sludge for biogas production. *Waste management*, 32(3), 404-409.
<https://doi.org/10.1016/j.wasman.2011.10.024>.
- Xiao, B., Han, Y., & Liu, J. (2010). Evaluation of biohydrogen production from glucose and protein at neutral initial pH. *International Journal of Hydrogen Energy*, 35(12), 6152-6160. <https://doi.org/10.1016/j.ijhydene.2010.03.084>.
- Xiao, B., Qin, Y., Wu, J., Chen, H., Yu, P., Liu, J., & Li, Y.-Y. (2018). Comparison of single-stage and two-stage thermophilic anaerobic digestion of food waste: Performance, energy balance and reaction process. *Energy Conversion and Management*, 156, 215-223.
<https://doi.org/10.1016/j.enconman.2017.10.092>.

- Xiao, N., Chen, Y., Chen, A., & Feng, L. (2014). Enhanced bio-hydrogen production from protein wastewater by altering protein structure and amino acids acidification type. *Scientific Reports*, 4(1), 1-9. <https://doi.org/10.1038/srep03992>.
- Xiao, Y., Yang, H., Yang, H., Wang, H., Zheng, D., Liu, Y., Pu, X., & Deng, L. (2019). Improved biogas production of dry anaerobic digestion of swine manure. *Bioresource Technology*, 294, 122188. <https://doi.org/10.1016/j.biortech.2019.122188>.
- Xu, F., Li, Y., Ge, X., Yang, L., & Li, Y. (2018). Anaerobic digestion of food waste—Challenges and opportunities. *Bioresource Technology*, 247, 1047-1058. <https://doi.org/10.1016/j.biortech.2017.09.020>.
- Xu, S. Y., Karthikeyan, O. P., Selvam, A., & Wong, J. W. (2012). Effect of inoculum to substrate ratio on the hydrolysis and acidification of food waste in leach bed reactor. *Bioresource Technology*, 126, 425-430. <https://doi.org/10.1016/j.biortech.2011.12.059>.
- Xu, Y., Lu, Y., Zheng, L., Wang, Z., & Dai, X. (2020). Perspective on enhancing the anaerobic digestion of waste activated sludge. *Journal of hazardous materials*, 389, 121847.
- Xue, Y., Liu, H., Chen, S., Dichtl, N., Dai, X., & Li, N. (2015). Effects of thermal hydrolysis on organic matter solubilization and anaerobic digestion of high solid sludge. *Chemical Engineering Journal*, 264, 174-180. <https://doi.org/10.1016/j.jhazmat.2019.121847>.
- Yaldız, O. (2015). Effects of mixture ratio of cow manure and greenhouse wastes on anaerobic co-digestion process. *Agricultural Engineering International: CIGR Journal*. 2015;2015:160–167.
- Yan, M., Fotidis, I. A., Tian, H., Khoshnevisan, B., Treu, L., Tsapekos, P., & Angelidaki, I. (2019). Acclimatization contributes to stable anaerobic digestion of organic fraction of municipal solid waste under extreme ammonia levels: focusing on microbial community

- dynamics. *Bioresource Technology*, 286, 121376.
<https://doi.org/10.1016/j.biortech.2019.121376>.
- Yang, G., & Wang, J. (2019). Enhancing biohydrogen production from waste activated sludge disintegrated by sodium citrate. *Fuel*, 258, 116177.
<https://doi.org/10.1016/j.fuel.2019.116177>.
- Yang, Z., Wang, W., He, Y., Zhang, R., & Liu, G. (2018). Effect of ammonia on methane production, methanogenesis pathway, microbial community and reactor performance under mesophilic and thermophilic conditions. *Renewable Energy*, 125, 915-925.
<https://doi.org/10.1016/j.fuel.2019.116177>.
- Yaqoob, H., Teoh, Y. H., Din, Z. U., Sabah, N. U., Jamil, M. A., Mujtaba, M., & Abid, A. (2021). The potential of sustainable biogas production from biomass waste for power generation in Pakistan. *Journal of Cleaner Production*, 307, 127250.
<https://doi.org/10.1016/j.jclepro.2021.127250>.
- Yenigün, O., & Demirel, B. (2013). Ammonia inhibition in anaerobic digestion: a review. *Process Biochemistry*, 48(5-6), 901-911. <https://doi.org/10.1016/j.procbio.2013.04.012>.
- Yılmaz, Ş., & Şahan, T. (2020). Utilization of pumice for improving biogas production from poultry manure by anaerobic digestion: a modeling and process optimization study using response surface methodology. *Biomass and Bioenergy*, 138, 105601.
<https://doi.org/10.1016/j.biombioe.2020.105601>.
- Yin, J., Yu, X., Wang, K., & Shen, D. (2016). Acidogenic fermentation of the main substrates of food waste to produce volatile fatty acids. *International Journal of Hydrogen Energy*, 41(46), 21713-21720. <https://doi.org/10.1016/j.ijhydene.2016.07.094>.

- Yokoyama, H., Waki, M., Ogino, A., Ohmori, H., & Tanaka, Y. (2007). Hydrogen fermentation properties of undiluted cow dung. *Journal of Bioscience and Bioengineering*, *104*(1), 82-85. <https://doi.org/10.1263/jbb.104.82>.
- Yong, B., Fei, X., Shao, H., Xu, P., Hu, Y., Ni, W., Xiao, Q., Tao, X., He, X., & Feng, H. (2020). Recombinant expression and biochemical characterization of a novel keratinase BsKER71 from feather degrading bacterium *Bacillus subtilis* S1-4. *AMB Express*, *10*, 1-10. <https://doi.org/10.1186/s13568-019-0939-6>.
- Yu, J., & Takahashi, P. (2007). Biophotolysis-based hydrogen production by cyanobacteria and green microalgae. In *Communicating Current Research and Educational Topics and Trends in Applied Microbiology*; Méndez-Vilas, A., (ED). FORMATEX: Badajoz, Spain, 2007; Volume 1, pp. 79–89.
- Yuan, H., & Zhu, N. (2016). Progress in inhibition mechanisms and process control of intermediates and by-products in sewage sludge anaerobic digestion. *Renewable and Sustainable Energy Reviews*, *58*, 429-438. <https://doi.org/10.1016/j.rser.2015.12.261>.
- Zarkadas, I., Dontis, G., Pilidis, G., & Sarigiannis, D. (2016). Exploring the potential of fur farming wastes and byproducts as substrates to anaerobic digestion process. *Renewable energy*, *96*, 1063-1070. <https://doi.org/10.1016/j.renene.2016.03.056>.
- Zhang, D., Zhu, W., Tang, C., Suo, Y., Gao, L., Yuan, X., Wang, X., & Cui, Z. (2012). Bioreactor performance and methanogenic population dynamics in a low-temperature (5–18 C) anaerobic fixed-bed reactor. *Bioresource Technology*, *104*, 136-143. <https://doi.org/10.1016/j.biortech.2011.10.086>.

- Zhang, S., Kim, T.-H., Lee, Y., & Hwang, S.-J. (2012). Effects of VFAs concentration on biohydrogen production with *Clostridium bifermentans* 3AT-ma. *Energy Procedia*, *14*, 518-523. <https://doi.org/10.1016/j.egypro.2011.12.968>.
- Zhang, W., Wei, Q., Wu, S., Qi, D., Li, W., Zuo, Z., & Dong, R. (2014). Batch anaerobic co-digestion of pig manure with dewatered sewage sludge under mesophilic conditions. *Applied Energy*, *128*, 175-183. <https://doi.org/10.1016/j.apenergy.2014.04.071>.
- Zhang, Z., Zhang, G., Li, W., Li, C., & Xu, G. (2016). Enhanced biogas production from sorghum stem by co-digestion with cow manure. *International Journal of Hydrogen Energy*, *41*(21), 9153-9158. <https://doi.org/10.1016/j.ijhydene.2016.02.042>.
- Zhao, C., Yan, H., Liu, Y., Huang, Y., Zhang, R., Chen, C., & Liu, G. (2016). Bio-energy conversion performance, biodegradability, and kinetic analysis of different fruit residues during discontinuous anaerobic digestion. *Waste Management*, *52*, 295-301. <https://doi.org/10.1016/j.wasman.2016.03.028>.
- Zheng, Z., Liu, J., Yuan, X., Wang, X., Zhu, W., Yang, F., & Cui, Z. (2015). Effect of dairy manure to switchgrass co-digestion ratio on methane production and the bacterial community in batch anaerobic digestion. *Applied Energy*, *151*, 249-257. <https://doi.org/10.1016/j.apenergy.2015.04.078>.
- Zhu, A., Qin, Y., Wu, J., Ye, M., & Li, Y.-Y. (2021). Characterization of biogas production and microbial community in thermophilic anaerobic co-digestion of sewage sludge and paper waste. *Bioresour Technol*, *337*, 125371. <https://doi.org/10.1016/j.biortech.2021.125371>.

Zieliński, M., Korzeniewska, E., Filipkowska, Z., Dębowski, M., Harnisz, M., & Kwiatkowski,

R. (2017). Biohydrogen production at low load of organic matter by psychrophilic bacteria. *Energy*, *134*, 1132-1139. <https://doi.org/10.1016/j.energy.2017.05.119>.

Zubair, M., Wang, S., Zhang, P., Ye, J., Liang, J., Nabi, M., Zhou, Z., Tao, X., Chen, N., & Sun,

K. (2020). Biological nutrient removal and recovery from solid and liquid livestock manure: Recent advance and perspective. *Bioresource Technology*, *301*, 122823. <https://doi.org/10.1007/s13762-021-03301-6>.

CHAPTER THREE

ENHANCING MANURE PROTEIN DEGRADATION BY KIWI PEEL WASTE: STATISTICAL OPTIMIZATION USING BOX-BEHNKEN DESIGN AND RESPONSE SURFACE METHODOLOGY

Abstract

Anaerobic digestion (AD) of protein-rich waste (PRW) is challenged by ammonia accumulation. This study explores the potential of Kiwi peel waste (KPW)-derived proteases (actinidin) to enhance manure protein degradation. It used Box–Behnken response surface design to optimize the protein quantity and ammonia reduction. It studied the individual and interactive effects of manure hydrolysis conditions (manure dosage, KPW dosage, and time). The experimental data were assessed through ANOVA analysis, and a highly predictive second-order polynomial model was established using multiple regression analysis. The optimal hydrolysis conditions for reducing manure protein quantity by $39\pm 0.54\%$ are $4 \text{ g VS}_{\text{manure}} \text{ L}^{-1}$, $7.5 \text{ g VS}_{\text{KPW}} \text{ L}^{-1}$, and 48 h hydrolysis time. However, the optimum hydrolysis conditions for reducing $\text{NH}_3\text{-N}$ by $64\pm 0.65\%$ are $9 \text{ g VS}_{\text{manure}} \text{ L}^{-1}$, $7.5 \text{ g VS}_{\text{KPW}} \text{ L}^{-1}$ and 48 h hydrolysis time. Predicted and experimentally observed reductions were consistent. The effects of the KPW on functional groups and morphological structure of manure were also investigated through Fourier Transform Infrared (FTIR) spectroscopy and Scanning Electron Microscopy (SEM). The disturbance of hydrogen bonds and the breaking of amide or N-H bonds within side chains in the hydrolyzed manure sample are confirmed through a change and decrease in peak intensity from 3200 to 3400 cm^{-1} . The tests characterizing the hydrolyzed substrate and the statistical model data affirm that employing KPW for manure hydrolysis is a feasible and economically viable strategy to tackle ammonia buildup.

This approach can potentially enhance protein degradation in manure, resulting in increased biohydrogen and biomethane production in dark fermentation. These results are based on lab-scale experiments. A scale-up study would be crucial to evaluate the feasibility and efficiency of the optimized conditions in industrial settings. Also, there is a new scope of research to explore the effects of using different types of manure (chicken, pig, etc.) or other slaughterhouse waste to understand the model's viability on different proteinous wastes. To find out the highest operating condition, there could be investigations on the stability of actinidin under different environmental conditions, such as temperature, pH, nutrients, etc.

Keywords: Actinidin enzyme, Response Surface Method, Manure protein, Ammonia, Hydrolysis, Proteases

3.1 Introduction

The meat processing industry produces diverse products, including fresh and frozen meat and processed products. The production of meat products generates roughly the same volume of waste from the slaughterhouses (Wang et al., 2018). These waste materials comprise manure, blood, feathers, and organ tissues rich in protein and lipids. Incorrect disposal of such waste harms air and water quality and raises concerns about human health due to pathogenic microorganisms (Tolera and Alemu, 2020). Furthermore, different categories of cattle produce varying quantities of manure, with dairy cows being the highest contributors, further exacerbating waste management issues. However, dairy cows are the highest manure producers, generating around 62 kg day⁻¹, about 10% of their body weight (Statistics Canada 2006). Traditional waste disposal methods are inadequate to address the growing concerns associated with slaughterhouse waste and the inherent

variations in manure production. Therefore, exploring innovative and sustainable solutions to manage these waste streams effectively and harness their potential for bioenergy production is imperative.

Research has shown that anaerobic digestion (AD) technology can substantially impact waste management and the production of biofuels and energy, including biogas, biomethane, and biohydrogen (Harris and McCabe, 2015). The methane or hydrogen generated can produce electricity or be refined into transportation fuels and renewable natural gas (Kabeyi and Olanrewaju, 2022). When examining the AD of slaughterhouse and poultry waste, it becomes apparent that such wastes have an imbalanced carbon-to-nitrogen ratio due to their elevated nitrogen content. The presence of excessive nitrogen compounds during the AD process leads to the accumulation of high levels of ammonia. This, in turn, can disrupt the intracellular pH and deactivate essential enzymes by permeating microbial cell walls, thereby impacting biochemical reactions during the AD of protein-rich substrates (Wang et al., 2019).

The biomethane potential of organic substrates, such as protein-rich substrates (manure or slaughterhouse waste), depends on their composition, particularly the proportions of proteins, carbohydrates, and lipids. These compounds degrade at different rates and yield varying amounts of biomethane or biohydrogen (Saady and Hung, 2015; Yang et al., 2015). Unfortunately, the AD of protein-rich waste has not been widely adopted due to challenges.

A significant challenge is the accumulation of elevated ammonia levels during protein-rich waste AD, leading to the buildup of volatile fatty acids (VFAs) and process instability. This results in low biogas production and low methane yield (Tian et al., 2019). Ammonia is toxic to methanogens at concentrations above $3 \text{ g NH}_4^+ \text{ N L}^{-1}$, especially in its gaseous form (NH_3), which

can penetrate cells. Some studies reported that even concentrations above $0.15 \text{ g NH}_3\text{-N L}^{-1}$ are inhibitory in AD (Massé et al., 2014).

Using a batch reactor is valuable in carrying out studies to understand and analyze the impact of various design and operational factors in AD. Batch reactors enable researchers to conduct characterization experiments and explore multiple parameters that can affect the results. The properties, such as nitrogen removal and substrate degradation, could be monitored and measured directly (Coelho et al., 2000). Furthermore, the batch reactor allows for the simultaneous execution of multiple experiments and replication (duplicate or triplicate) of experiments. Compared to continuous reactors, batch reactors eliminate the influence of certain parameters (reaction kinetics, enthalpy of reaction, heat and mass transfer, etc.) that may interfere with the experimental outcomes.

A metabolite that disturbs the stability of AD, reduces the abundance of microorganisms, and hampers their activity is referred to as inhibitory. The inhibition caused by a specific substrate is called substrate-induced inhibition, as elucidated by Fagbohunge et al. (2017). Another challenge is the unbalanced carbon-to-nitrogen (C/N) ratio due to the high nitrogen content of protein-rich wastes; for example, cow manure, poultry manure, slaughterhouse waste, and poultry blood have C/N of 18 to 20, 15, 2, and 2.8 (Nazifa et al. 2021). A low C/N ratio, resulting from protein degradation, further increases NH_3 concentration and hinders the steady-state AD process (Hao et al., 2022). Generally, efficient biogas and methane production occur when the C/N ratio is 20 to 30 (Zheng et al., 2021; Xue et al., 2020). However, the high nitrogen content in protein-rich waste limits achieving this optimal C/N ratio for efficient hydrogen and methane production. To overcome these challenges, this study explores the potential of plant-derived proteases, such as

actinidin, from green kiwifruit peel waste, in enhancing manure protein degradation in the hydrolysis stage of AD.

Proteins are composed of amino acids linked together by peptide bonds. The basic structure of an amino acid includes an amine group (NH_2), a carboxyl group (COOH), a hydrogen atom (H), and a variable R group (side chain). The R group gives each amino acid unique properties, and it can be any one of a variety of functional groups, such as hydroxyl (OH), amine (NH_2), carboxyl (COOH), sulfhydryl (SH), and more (Damodaran and Parkin, 2017). Enzymes, which are specialized proteins themselves, play a crucial role in degrading proteins. Proteolytic enzymes, also known as peptidases or proteases, are responsible for breaking down the peptide bonds between amino acids. They do this by utilizing their active sites, which have specific shapes that match the substrate (protein) structure they are targeting. The enzyme recognizes and binds to the target protein at specific sites where peptide bonds must be cleaved. The enzyme catalyzes a hydrolysis reaction, in which water molecules are utilized to breakdown the peptide bonds between amino acids. This process involves adding a water molecule (H_2O) to the peptide bond, causing it to split into two amino acids (Qiu et al., 2020).

Protein-rich waste are hydrolyzed in AD, where various proteolytic bacteria break down proteins into amino acids and ammonia. Ammonia generated during hydrolysis exists in two primary forms within the aqueous phase of AD reactors: the ionized (NH_4^+) and the free gaseous ammonia (NH_3). Hydrolytic bacteria release protease enzymes to facilitate the breakdown of protein-rich waste (Ariaenejad et al., 2022). However, microbial protease enzymes have limitations. Microbial protease enzymes are often substrate-specific; thus, they may not effectively break down all types of proteins (Gurumallesh et al., 2019). This limitation can result in incomplete degradation of protein-rich substrates, leading to the accumulation of organic matter and potential

process inefficiency. Also, the activity of microbial protease enzymes is sensitive to temperature and pH. Suboptimal temperature and pH ranges can significantly reduce microbial protease efficiency, potentially slowing down degradation (Thapa et al., 2019).

Plant proteases exhibit similar or sometimes superior efficiency compared to microbial or animal proteases in the hydrolysis of protein-based substrates for valorizing by-products, such as gelatin, collagen, bird feathers, cheese whey, keratinous materials, soy protein, and fish (David Troncoso et al., 2022). Plant proteases have been conventionally utilized for many years in the realm of biotechnology. Notably, bromelain (from pineapple) and papain (from papaya) have been emphasized. However, in recent years, other plants like kiwi and fig, yielding proteases such as actinidin and ficin, respectively, have emerged as valuable protease sources with promising commercial prospects. Table 3-2 provides plant proteases extracted from different plant parts, the optimum pH, temperature, molecular weight, and their applications in various protein substrate hydrolysis.

Plant-derived proteases are attracting interest because of their strong proteolytic capabilities and specificity towards particular substrates. They display excellent stability across broad operating conditions (temperatures up to 60 °C and pH 4 to 10); they are cost-effective due to the abundant and inexpensive raw materials (Arshad et al., 2016).

Protein extracts can be derived from various parts of plants, including root, fruit, flower, peel, or latex, as outlined in Table 3-1. Sun et al. (2016) conducted a thorough comparative analysis of proteolytic activity across 90 plant resources using casein as a substrate at different pH levels (pH 3.0 to 10.5). Notably, high proteolytic activity (1% casein substrate) was observed for kiwifruit extracts (28.8 U g^{-1}) > broccoli (16.9 U g^{-1}) > ginger (16.6 U g^{-1}) > red pepper (15.8 U g^{-1}).

Table 3- 1. Plant proteases with source and industrial uses.

Source	Protease enzyme	Optimum temperature (°C)	pH	Molecular weight (KDa)	Application	References
Kiwi fruit, peel (<i>Actinidia deliciosa</i>)	Actinidia deliciosa	40	6	24.5	i) Hydrolysis of chicken and fish proteins. ii) Solubilization of protein aggregates for alcohol production.	Homaei and Etemadipour (2015)
Fig fruit (<i>Ficus carica</i>)	Ficin	60	8	23.9	i) Tenderizing meat by hydrolyzing myofibrillar proteins. ii) Milk coagulation. iii) Producing bioactive peptides. iv) Hydrolyzing synthetic fibers. v) Biomedical applications: Generating active antibody fragments through proteolysis for hemostatic purposes. vi) Extracting proteins from barley and malt in the brewing industry. vii) Enhancing meat tenderness by myofibrillar protein hydrolysis.	Morellon-Sterling et al. (2020)
Papaya fruit, root and leaves (<i>Carica papaya</i>)	Papain	65	5-9	23.4	i) Tenderizing meat by hydrolyzing myofibrillar proteins and connective tissue. ii) In the dairy industry, the production of cream cheese, semisoft cheese, and protein hydrolysates. iii) Reducing allergenic protein levels in cereals for the baking industry. iv) Generating bioactive peptides for animal feed. v) Solubilizing protein aggregates in the brewing and wine industry.	Fernández-Lucas et al. (2017)
Pineapple fruit and stem (<i>Ananas comosus</i>)	Bromelain	70	5-10	28 to 32	i) Tenderizing meat by hydrolyzing myofibrillar proteins. ii) Producing biopeptide hydrolysates in the fish industry. iii) Enabling alcohol production through solubilizing protein aggregates. iv) Promoting protein degradation in ruminant feed for animal nutrition. v) Facilitating protein solubilization in the textile industry.	Arshad et al. (2014)

In an in vitro investigation, Kaur et al. (2010) discovered that actinidin protease, which is isolated from green kiwifruit, facilitates the digestion of gluten proteins in the small intestine. Additionally, Mostafaie et al. (2008) demonstrated that actinidin activity affected collagen hydrolysis. According to their research, actinidin may be a useful tool for hydrolyzing collagen types I and II.

Microbial enzymes such as *Aspergillus oryzae* and *Bacillus subtilis* elastase enzyme can also be used for softening of meat. Qihe et al. (2006) studied the action of *Bacillus spp* elastase and papain proteases, observing a significant degradation of meat protein myofibrils, myofibril fragmentation of 230% and 245% by elastase and papain, respectively. Ashie et al. (2002) showed that aspartic protease (AP) enzyme from *Aspergillus oryzae* is of interest in the softening process of beef than papain. Abril et al. (2023) investigated the degree of softening of the meat protein using several types of enzymes (*Aspergillus oryzae* 400 proteases (A400) and *Aspergillus oryzae* concentrate protease (ACONC) are two of the proteases from *Aspergillus oryzae*, along with, bromelain, zingibain, papain and ficin). The study showed that plant-extracted proteases led to a balanced degradation of collagen and myofibrillary proteins. In contrast, those of microbial origin degraded higher myofibrillar protein than collagen (Abril et al., 2023). Additionally, and somewhat successfully, attempts have been made to utilise microbial proteinases to assure controlled degradation of animal proteins (Singh et al., 2016; Verma et al, 2017). However, because of the possible toxicity of the enzyme source, these proteinases have not garnered much attention (Ikram et al., 2021). A unique sulfhydryl protease called actinidin (isolated from kiwi fruit), used commercially in the meat industry to tenderize meat and enhance the chemical process related to the breakdown of myofibrillar proteins to produce peptides (Mohd Azmi et al., 2023). Actinidin's benefits over other plant proteases like papain and ficin have led to a wide range of uses in the

food sector. Table 3-2 depicts the pH, optimum temperature, and enzymatic hydrolysis potency for myofibrillar proteins and collagen, as influenced by different protease enzymes originated from microorganisms and plants.

Table 3- 2. pH, Temperature, and strength of hydrolysis of myofibrillar proteins and collagen by various enzymes.

Protease	Optimum pH	Optimum Temperature (°C)	Collagen hydrolysis	Myofibrillar protein hydrolysis	Reference
Bacillus	< 6.5	55 - 60	Excellent	Poor	Sharma et al. (2017)
Aspergillus	7.0	55 - 60	Poor	Moderate	Sharma et al. (2017)
Ficin	7.0	60 - 70	Excellent	Moderate	Mazorra-Manzano et al. (2018)
Bromelain	5.0 - 6.0	65 - 75	Excellent	Moderate	Mazorra-Manzano et al. (2018)
Papain	4.0 - 6.0	65 - 75	Moderate	Excellent	Tacias-Pascacio et al. (2021)

Although the potential of plant proteases gains significance, their application, especially actinidin, in the degradation of protein-rich waste remains relatively unexplored. Most existing applications have focused on pure proteins, meat, or in-vitro studies, leaving a gap in understanding their potential in the complex matrix of manure, a significant protein-rich waste source. This study aims to bridge this gap by exploring, for the first time, the protein degradation capacity of actinidin from kiwi peel waste (KPW), focusing on dairy manure, an abundant complex protein-rich waste from dairy farms. The objective of this research is to screen the hydrolysis conditions using Box–Behnken Design and to optimize parameters including manure dosage, Kiwi peel waste (KPW) dosage, and hydrolysis time for manure protein and ammonia reduction using Response Surface Methodology (RSM).

Addressing ammonia accumulation in protein-rich waste (PRW) AD is crucial for sustainable waste management and energy production. The novel aspect of this study lies in employing Kiwi peel waste-derived proteases (actinidin) to enhance manure protein degradation. This offers an

economically viable strategy to tackle ammonia buildup and increases biohydrogen and biomethane production.

3.2 Materials and Methods

Several experimental methods were employed to assess the impact of blending various proportions of manure, kiwi peel waste (KPW), and duration on the efficient hydrolysis of manure protein. The reduction in protein, ammonia, ammonium, and volatile solids (VS) were analyzed in the conducted experiments. The following subsections detail the substrates, chemicals, and reagents utilized in the laboratory-based optimization of manure hydrolysis.

3.2.1 Chemicals and reagents

ACS reagent grade ($\geq 99.0\%$) ammonium chloride and sodium chloride were purchased from Sigma-Aldrich, USA. To prepare NH_3 and NH_4 , standard reagent-grade ammonium chloride (NH_4Cl) was used. 2 mL of Ionic Standard Adjuster (ISA) was added to every 100 mL of the sample or standard solution for a background ionic strength of 0.10M. Reagent-grade sodium chloride (NaCl) was used to prepare 10 M NaOH and 5 M NaOH as ISA for NH_3 and NH_4 measurements in the standards and samples. Pierce Coomassie (Bradford) Protein Assay Kit, a ready-to-use Bradford assay reagent purchased from Thermo Fisher Scientific, USA, measured total protein concentration compared to a protein standard (bovine serum albumin). De-ionized water is used for all the sample preparation.

3.2.2 Feedstock

Fresh manure (M) from dairy cows was collected from Lester’s Dairy Farm on the Avalon Peninsula in Newfoundland. The manure was collected from under the wet barn’s animal before reaching the floor. After collection, the manure was transferred to an air-tight plastic container and kept at a temperature of 4 °C until ready to be used in the digesters. The hydrolysis experiment used kiwi peel waste (KPW) as a proteinase enzyme source. The fruits were purchased from local groceries in St. John’s and stored refrigerated in plastic bags. The fresh fruits were washed with tap water to remove all the dirt, then peeled and cut into small pieces. Finally, small pieces of peels were blended using a magic bullet® with a 250-Watt motor and 2000 rpm (LLC Los Angeles, CA 90025, USA). A 500 mL capacity cup was set onto the motor blade for 60 sec at a constant speed. Before being fed to the reactors, these feedstocks (M and KPW) were subjected to physiochemical characterization (Table 3-3).

Table 3- 3. Physiochemical characteristics of the substrates

Parameter	Cow Manure (M)	Kiwi peel Waste (KPW)
pH	7.5	6.5
Total Solids, TS (%)	14.7	17.03
Volatile Solids, VS (%)	7	10.17
Chemical Oxygen Demand, COD (g L ⁻¹)	105.3	80.32
Protein (g L ⁻¹)	1.2	0.84
NH ₃ -N (g L ⁻¹)	2.2	-
NH ₄ -N (g L ⁻¹)	2.1	-

3.3 Hydrolysis Tests

A statistically designed experiment has been conducted with manure and KPW in batch digesters. Each experimental condition for optimization tests were tested in duplicate air-tight 0.5 L Wheaton glass bottles (digester) with a working volume of 0.3 L. Hydrolysis of cow manure

with KPW wastes was carried out in the batch reactors at 20 ± 1 °C. KPW were fed in mixing ratios of 5-10 g VS L⁻¹ with the manure (4-9 g VS L⁻¹).

3.4 Box-Behnken Design

Several batches of identical reactors were used to examine the effects of different dosages of KPW with different incubation times on dairy manure protein degradation, ammonia nitrogen (NH₃-N) and ammonium nitrogen (NH₄-N) removal, and volatile solids (VS) reduction. The Response Surface Methodology (RSM) and Box-Behnken Design (BBD) were employed at three levels (-1, 0, +1) to determine the optimum hydrolysis conditions for protein degradation and ammonia removal. Box-Behnken Design (BBD) is a symmetrical experimental design approach that facilitates the evaluation of the significant effects of various experimental parameters and their interactions (Gulcan et al., 2023). This methodology reduces the overall number of experiments required and is considered cost-effective while still providing an opportunity to optimize the experimental conditions (Mondal et al., 2017). The RSM and BBD have been applied using Minitab® 21.4 Statistical Software (LLC, Pennsylvania, USA). The experimental data were used to develop a predictive model for protein and ammonia removal. The model identifies interactional effects and optimizes the process parameters to maximize the removal of the applied parameters, providing a useful tool for predicting and optimizing the process. Equation 3-1 gives the number of experiments/runs for the three-levels in BBD.

$$N = 2k(k - 1) + C_p \quad (3-1)$$

where N represents the number of experimental runs, C_p is the number of central points, and k is the number of parameters such as substrate dosage, time, etc. The total number of experiments carried out in this study was 15 for manure and KPW, with 12 experiments for each factor (manure loading, KPW loading, and time) at three levels and three central experiments. The Box-Behnken Design (BBD) methodology employed in this study involved adjusting all factors at three evenly spaced levels (-1, 0, +1), as is typical for this approach. The Minitab® 21.4 Statistical Software was utilized to generate the experimental points according to the BBD methodology. Table 3-4 displays the hydrolysis process variables under investigation, which include the dosage of manure (g VS L⁻¹), KPW (g VS L⁻¹), and the incubation time (ranging from 3 to 48 h).

Table 3- 4. Levels of different variables for Box-Behnken Design for manure and kiwi peel waste.

Factors	Codes	Level		
		Low (-1)	Intermediate (0)	High (+1)
Manure proportion (g VS L ⁻¹)	A	4	6.5	9
Kiwi peel waste (KPW) proportion (g VS L ⁻¹)	B	5	7.5	10
Time (h)	C	3	25.5	48

The manure dosage was between 4 to 9 g VS L⁻¹, KPW dosage was between 5 to 10 g VS L⁻¹, and incubation time was varied from 3 to 48 h. The matrix transformation (Table 3-5) served as the basis for the experimentation. With these experimental combinations, four parameters were monitored, viz. reduction (%) of protein, NH₃-N, NH₄-N, and VS. The three process factors were the independent variables (parameter), and reduction (%) was the dependent variable (response). In Figure 3-1, the overall process diagram is displayed.

The BBD is utilized to analyze the quadratic response and produces a mathematical model of a second-degree polynomial equation (Equation (3-2)) that can predict the optimal conditions.

$$Y = \beta_0 + \beta_1\beta_1 + \beta_2\beta_2 + \beta_3\beta_3 + \beta_{11}\beta_{21} + \beta_{22}\beta_{22} + \beta_{33}\beta_{23} + \beta_{12}X_1X_2 + \beta_{23}X_2X_3 + \beta_{13}X_1X_3 \quad (3-2)$$

where, Y is the dependent or response variable (removal or reduction (%) of protein, NH₃-N, NH₄-N, and VS); The coefficients for linear expressions are β_0 , β_1 , β_2 , and β_3 . Quadratic coefficients are β_{11} , β_{22} , and β_{33} , and interaction coefficients are β_{12} , β_{23} , and β_{13} . The independent variables are represented by the variables X₁, X₂, and X₃.

Table 3- 5. Matrix transformation of Box-Behnken Design for manure and kiwi peel waste (KPW) hydrolysis.

Run	Manure (g VS L ⁻¹)	KPW (g VS L ⁻¹)	Time (h)
1	4	5	25.5
2	9	5	25.5
3	4	10	25.5
4	9	10	25.5
5	4	7.5	3
6	9	7.5	3
7	4	7.5	48
8	9	7.5	48
9	6.5	5	3
10	6.5	10	3
11	6.5	5	48
12	6.5	10	48
13	6.5	7.5	25.5
14	6.5	7.5	25.5
15	6.5	7.5	25.5

3.5 Analytical Methods

The substrates were meticulously characterized based on their TS, VS, pH, NH₃-N, and NH₄-N prior to experiment. The TS and VS were conducted following the standard methods for examining water and wastewater (Method no. 1684) (APHA, 1998). The pH of any sample was

recorded by pH meter (PH/ORP Temperature Control Monitor, PH-204, 110 V, USA). All the characterizations were conducted in duplicated. The measurements of protein quantity, $\text{NH}_3\text{-N}$, $\text{NH}_4\text{-N}$, and VS were conducted as explained in sections 3.5.1 to 3.5.3. Sample preparations for the characterization tests by Fourier transform infrared spectroscopy (FTIR) and Scanning electron microscope (SEM) are discussed in sections 3.5.4 and 3.5.5.

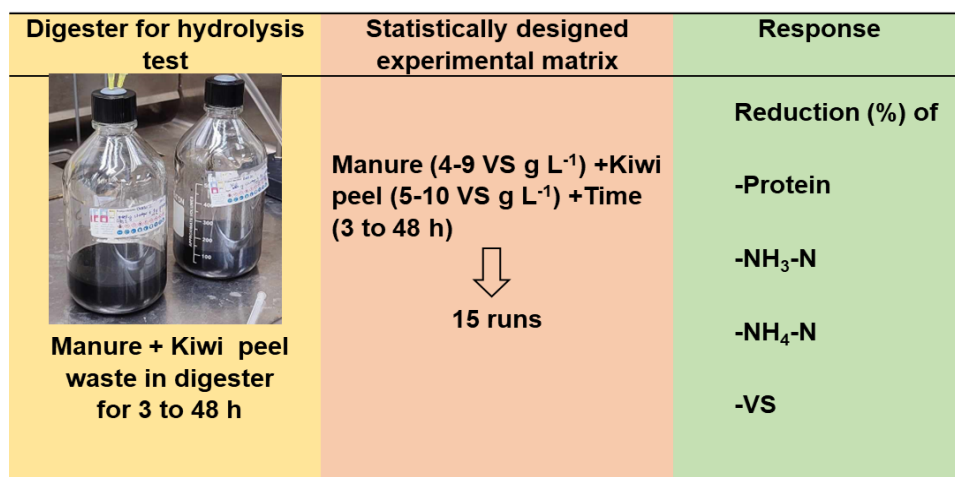


Figure 3- 1. Schematic of the experimental setup and responses of the hydrolysis process optimization test.

3.5.1 Protein quantity measurement

Protein quantity was measured using Bradford technique (Kielkopf et al., 2020). The Bradford technique is based on the absorbance shift that can be seen in an acidic Coomassie® Brilliant Blue G-250 dye solution (Bradford, 1976). The dye turns blue when introduced to a protein-containing solution because it attaches to the protein molecules, which are previously reddish brown in colour. It is believed that the dye binds to the protein through the sulfonic groups' electrostatic affinity. When the acidic dye solution binds to protein molecules, its peak absorbance shifts from 465 to 595 nm (Bonjoch and Tamayo, 2001). Therefore, all the samples were measured using a UV-

spectrophotometer (GENESYS 10S UV-VIS, Thermo Scientific, Madison, USA) at an absorbance of 595 nm mixed with Coomassie® Brilliant Blue, which allowed an accurate quantification of the protein content of a sample. With the integration of a protein solution, the acidic Coomassie dye reagent undergoes a chromatic transformation, transitioning from a brown hue to a blue shade. This alteration in color corresponds directly to the quantity of protein present in the specimen. Consequently, protein assessments are conducted by juxtaposing the color reaction against protein assay standards. Bovine Serum Albumin (BSA) was used as a protein standard to prepare a standard curve and a standard curve equation. Later, the standard curve equation was used to calculate the protein concentrations of unknown sample based on their respective absorbance values measured from a UV-spectrophotometer at an absorbance of 595 nm. The reduction (%) in protein quantity is calculated from the difference between the control and sample values following statistical matrix runs.

3.5.2 NH₃-N and NH₄-N measurement

The ammonia gas sensing electrode (Cole-Parmer model #K-27502-00) and ammonium glass electrode (Cole-Parmer #K-27502-03) were used to measure the NH₃-N and NH₄-N of the samples. By serial dilution, a three-point calibration curve (Appendix A) is prepared as per the Cole-Parmer model guideline manual delivered with the respective electrodes. The calibration has been performed using 1, 10, and 100 ppm of the standard ammonia and standard ammonium solutions. A 100 mL solution from each digester was withdrawn immediately after preparation (time = 0), serving as a control. After a specific time, the 100 mL samples were withdrawn from the digester bottles, and values were measured (Figure 3-2). The difference in the readings between the control and the samples provided the data on the reduction of NH₃-N or NH₄-N.

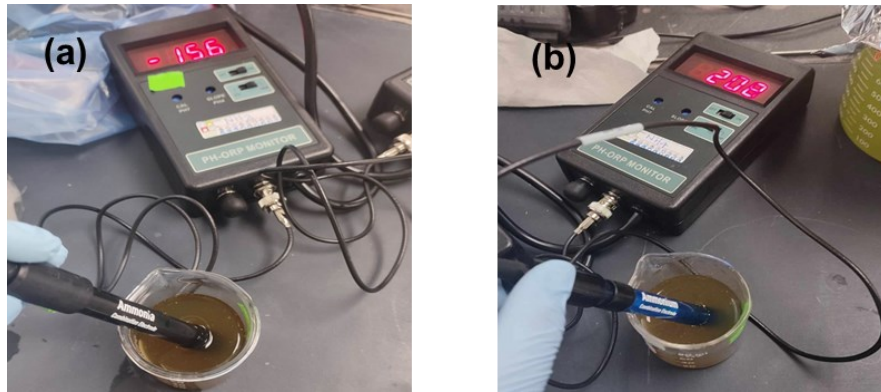


Figure 3- 2. Ammonia and ammonium measurement using (a) ammonia (b) and ammonium probes.

3.5.3 Volatile solids measurement

Volatile solids (VS) represent the amount of volatile (organic) matter present in the undissolved solid fraction of the measured solution that is lost on ignition of dry solids for 1 h at 550 °C. The first step in determining VS is to determine the total solids (TS). Total solids are the remaining dry solids present in a vessel after the evaporation and drying of a sample at 105 °C in an oven. A digital balance (Denver instrument model A-160, USA) was used to measure the samples' mass for TS and VS determination (Figure 3-3). Finally, the data on the removal of VS content is calculated from the VS of the control and that of the samples.

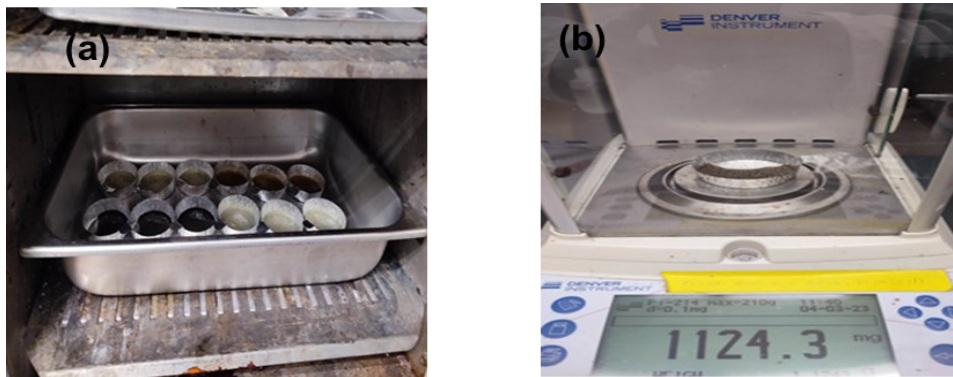


Figure 3- 3. (a) Samples for total solids (TS) or volatile solids (VS) determination in the oven and (b) measuring the weight of the aluminum pans for TS or VS reduction determination.

3.5.4 Fourier transform infrared spectroscopy (FTIR)

Fourier transform infrared spectroscopy (FTIR), the most widely used type of infrared spectroscopy, was used to identify the samples' functional groups. The basis for all infrared spectroscopies is the idea that the type of vibration (bending or stretching) that an infrared beam causes in a sample relies on the atoms that make up the bond. The transmittance pattern varies for distinct molecules due to the fact that different bonds and functional groups absorb different frequencies (Mohamed et al., 2017).

Prior to FTIR analysis, the liquid samples were dried for 24 hours at 70–80 °C. A little over 0.5 g of dehydrated materials were placed at a 45° angle in an FTIR spectroscopy machine (PerkinElmer Spectrum IR-C115599, USA). The range of the spectra was adjusted to 4000–650 cm^{-1} . Wavenumber (cm^{-1}) was shown on the x-axis of the graph, and transmittance was plotted on the y-axis, to record the spectrum.

3.5.5 Scanning electron microscope (SEM)

The surface morphology of the control and samples after 6, 12, 24, and 48 h were analyzed using a Scanning Electron Microscope (SEM) (Model JEOL JSM 7100F, USA). The samples underwent a sputtering technique to apply a gold covering. Carbon tape was used to affix each sample separately under a microscope holder. High vacuum conditions and a 20 kV accelerating voltage were used to capture the images with a different magnification range (400x to 4000x).

3.6 Statistical Analysis of Experimental Results

The maximum protein, ammonia, ammonium, and VS reduction were represented as a response, whereas the dosages of manure, KPW wastes, and time were represented as independent variables. The statistical significance of the regression model was tested using the Analysis of Variance (ANOVA) technique. ANOVA was performed to study the effect of the parameters on protein quantity, $\text{NH}_3\text{-N}$, $\text{NH}_4\text{-N}$, and VS reduction and to verify the derived model's variability. The strength or goodness of the model was explained by the coefficient of determination (regression coefficient, R^2) and adjusted regression coefficient R^2 -adjusted value. Three-dimensional (3D) interfaces, two-dimensional (2D) contour plots, and the experimental matrix were produced. It is required to minimize the dosages of manure, KPW, and time and maximize the reductions in optimizing the parameters employed in hydrolysis. Results of RSM optimisation could be utilised to determine optimal hydrolysis condition parameters of manure for anaerobic co-digestion, maximizing protein degradation or ammonia removal and minimizing reaction time, and substrate quantity. The RSM gave the optimal solution, and the highest desirability of the optimal set was selected. The effects of these three independent variables for the maximum protein, ammonia, ammonium and VS reduction were assessed statistically and described with MINITAB 21.1. (Minitab, LLC, USA).

3.7 Results and Discussion

This research conducted laboratory experiments to gather numerical data. Experiments were conducted to hydrolyze manure using various combinations of manure and kiwi peel waste as suggested by Box-Behnken Design matrix. The analysis focuses on determining the quantity of protein degradation and ammonia, ammonium, and VS reductions during manure hydrolysis. The

following subsections (3.8.1 to 3.8.5) will present and discuss the outcome obtained from each experiment.

3.7.1 Overall experiment

The fifteen combinations of manure dosage (g VS L⁻¹), kiwi peel waste (g VS L⁻¹), and time (h) were designed by BBD based on RSM and were run experimentally in duplicates, as summarized in Table 3-6. The experimental and predicted values as a response are given in the last four columns of Table 3-6.

Table 3- 6. Box-Behnken Design with predicted and experimental responses for manure and kiwi peel waste.

Run	Experimental response (reduction (%))				Predicted response (reduction (%))			
	Protein	NH ₃ -N	NH ₄ -N	VS	Protein	NH ₃ -N	NH ₄ -N	VS
1	20±0.71	41±1.1	74 ±0.7	26.7±0.51	18	41	72	26
2	21±0.95	44±0.98	73 ±0.21	33.7±0.57	23	40	75	25
3	22±0.15	39±1.05	69 ±0.6	27.0±0.45	21	39	67	21
4	21±1.5	43±0.56	70 ±0.25	28.5±0.11	22	42	72	31
5	6±0.85	13±0.7	25 ±0.43	15.7±0.8	6	12	29	11
6	9±1.05	16±0.9	30 ±0.32	29.3±0.7	11	16	32	30
7	39±0.61	62±0.25	55 ±0.65	29.6±0.23	39	61	73	29
8	37±1.5	64±0.65	83 ±0.32	28.7±0.19	32	64	81	27
9	7±0.95	15±0.56	26 ±0.45	26.6±0.65	8	14	39	26
10	9±0.55	12±0.75	27 ±1	22.7±0.11	6	15	21	21
11	37±1.05	63±1.05	83 ±0.95	29.2±0.21	35	62	83	31
12	39±0.54	61±0.91	73 ±0.87	28.6±0.32	33	61	75	29
13	22±0.35	42±0.77	75 ±0.13	38.1±0.33	21	42	73	33
14	20±0.25	43±0.65	67 ±0.19	41.4±0.29	21	42	73	38
15	20±0.51	43±0.23	72 ±0.29	35.4±0.49	21	42	73	35

The experimental reduction (%) of protein quantity, NH₃-N, NH₄-N, and VS ranged from 6 to 39%, 13 to 64%, 46 to 83%, and 16 to 41%, respectively. The highest protein reduction was observed in run 7 (manure 4 g VS L⁻¹, KPW 7.5 g VS L⁻¹, and time 48 h). In comparison, the

highest NH₃-N reduction was observed in run 8 (manure 9 g VS L⁻¹, KPW 7 g VS L⁻¹, and time 48 h). The highest NH₄-N (83%) was achieved in runs 7 and 11. The considerable variations in the reduction of protein, NH₃-N, NH₄-N, and VS indicate that the degradation pathways of feedstock in the co-digestion of manure and KPW were complex.

3.7.2 ANOVA and response model

Analysis of variance (ANOVA) was used to assess the statistical significance of the components and verify the suitability of the chosen quadratic model. The ANOVA of the results (Table 3-7) and (Table 3-8) illustrates the significance of the second-order polynomial for the protein quantity reduction and NH₃-N reduction after hydrolysis.

Table 3- 7. ANOVA table for a quadratic model of protein reduction with three-factor Box-Behnken Design for manure and kiwi peel waste (KPW).

Source	DF	Adj SS	Adj MS	F-Value	<i>p</i> -Value
Model	9	1854.77	206.09	818.15	0.000
Linear	3	1833.27	611.09	2425.98	0.000
A-Manure VS (g L ⁻¹)	1	0.33	0.33	1.29	0.307
B-KPW VS (g L ⁻¹)	1	4.22	4.22	16.77	0.009
C-Time (h)	1	1828.72	1828.72	7259.89	0.000
Square	3	15.56	5.19	20.59	0.003
A ² -Manure VS (g L ⁻¹)*Manure VS (g L ⁻¹)	1	0.17	0.17	0.67	0.449
B ² -KPW VS (g L ⁻¹)*KPW VS (g L ⁻¹)	1	0.31	0.31	1.23	0.318
C ² -Time (h)*Time (h)	1	15.49	15.49	61.49	0.001
2-Way Interaction	3	5.94	1.98	7.86	0.024
AB-Manure VS (g L ⁻¹)*KPW VS (g L ⁻¹)	1	0.65	0.65	2.59	0.168
AC-Manure VS (g L ⁻¹)*Time (h)	1	5.19	5.19	20.61	0.006
BC-KPW VS (g L ⁻¹)*Time (h)	1	0.09	0.09	0.36	0.572
Error	5	1.26	0.25		
Lack-of-Fit	3	0.28	0.09	0.19	0.898
Pure Error	2	0.98	0.49		
Total	14	1856.03			
<i>R</i> ²		<i>R</i> ² (adjusted)		<i>R</i> ² (predicted)	
0.9993		0.9981		0.9964	

KPW = Kiwi peel waste.

When the p -value is less than 0.05, it indicates significance (Guo et al., 2009), and a p -value lower than 0.01 indicates a high significance (Taherdanak et al., 2015). On the other hand, when the p -value is higher than 0.05, it suggests insignificance (Balat, 2008; Dolly et al., 2015). Accordingly, the model is statistically significant based on its p -value (< 0.0001) (Table 3-7 and 3-8).

Table 3- 8. ANOVA table for a quadratic model of $\text{NH}_3\text{-N}$ reduction with three factors Box-Behnken Design for manure and kiwi peel waste (KPW).

Source	DF	Adj SS	Adj MS	F-Value	p -Value
Model	9	4791.27	532.36	197.09	0.000
Linear	3	4730.50	1576.83	4730.50	0.000
A-Manure VS (g L^{-1})	1	18.00	18.00	54.00	0.001
B-KPW VS (g L^{-1})	1	8.00	8.00	24.00	0.004
C-Time (h)	1	4704.50	4704.50	14113.50	0.000
Square	3	60.02	20.01	60.02	0.000
A^2 -Manure VS (g L^{-1})*Manure VS (g L^{-1})	1	0.01	0.01	0.02	0.895
B^2 -KPW VS (g L^{-1})*KPW VS (g L^{-1})	1	3.39	3.39	10.17	0.024
C^2 -Time (h)*Time (h)	1	57.85	57.85	173.56	0.000
2-Way Interaction	3	0.75	0.25	0.75	0.187
AB-Manure VS (g L^{-1})*KPW VS (g L^{-1})	1	0.25	0.25	0.75	0.046
AC-Manure VS (g L^{-1})*Time (h)	1	0.25	0.25	0.75	0.325
BC-KPW VS (g L^{-1})*Time (h)	1	0.25	0.25	0.75	0.426
Error	5	1.67	0.33		
Lack-of-Fit	3	1.00	0.33	0.10	0.535
Pure Error	2	0.67	0.33		
Total	14	4792.93			
R^2			R^2 (adjusted)		R^2 (predicted)
0.9997			0.9990		0.9963

KPW = Kiwi peel waste.

The elevated F -value suggests that the regression model equation accounts for a significant portion of the response variation (Monte et al., 2011). The model F -value, 818 and 197 (Table 3-7 and 3-8), and p -value (< 0.001) suggests that the model is highly significant. From Table 3-7, the p -value (< 0.05) implies that the linear (B, C), square (C^2), and interaction (AC) were significant

terms for protein reduction in this study. At the same time, A, A², B², AB, and BC were insignificant (p -value > 0.05). Similarly, for NH₃-N reduction (Table 3-8), equivalent p -value and the associated coefficient estimates showed that, amongst the factors used in the study, A (manure), B (kiwi peel waste), C (time), the square effect of factors B² (kiwi peel waste), C² (time) and interactive effect of AB (manure * kiwi peel waste) had a significant effect on NH₃-N removal. At the same time, the rest of the interactions were insignificant.

The developed model for protein and NH₃-N reduction, which reduced ammonia accumulation in the reactor, had R^2 values of 0.9993 and 0.9997 and R^2 predicted values of 0.9981 and 0.9990. The high R^2 value obtained from the constructed statistical model indicates its successful alignment with the experimental data and its ability to account for the observed variations. Furthermore, the high R^2 values for both statistical models demonstrate that these models effectively elucidate the differences present among the independent factors. The result demonstrated that the models can explain 99% of the variability in the response variable. Moreover, the R^2 predicted (0.9981) and R^2 adjusted (0.9964) values for the protein reduction, and R^2 predicted (0.9990) and R^2 adjusted (0.9963) values for the NH₃-N reduction were close, which is favorable. This suggests that any potential block effect is minimal, and the developed models are the most suitable for optimization purposes. The predicted R^2 value of protein reduction (0.9964) and NH₃-N reduction (0.9963) exhibited a satisfactory level of concordance with the adjusted R^2 value of 0.9981 and 0.9990. The insignificance of the Lack-of-Fit (F -value) values, 0.19 (Table 3-7) and 0.10 (Table 3-8), indicate that a considerable portion (19% and 10%) of the lack of fit can be attributed to random noise (Casabar et al., 2020). The experimental test data underwent multiple regression analysis, leading to the derivation of the second-degree polynomial Eqs (3-3) and (3-4).

$$\begin{aligned} \text{Protein reduction (\%)} = & 1.53 + 0.636 * A - 0.053 * B + 0.05771 * C + 0.0343 A * A + \\ & 0.0464 B * B + 0.004046 C * C - 0.0647 A * B - 0.02026 A * C + \\ & 0.00269 B * C \end{aligned} \quad (3-3)$$

$$\begin{aligned} \text{NH}_3\text{-N reduction (\%)} = & 2.92 + 0.327 * A + 1.527 * B + 1.4721 * C + 0.0067 A * A - \\ & 0.1533 B * B - 0.007819 C * C + 0.0400 A * B - 0.00444 A * C + \\ & 0.00444 B * C \end{aligned} \quad (3-4)$$

where A, B, and C represent manure loading, kiwi peel waste loading, and reaction time, respectively.

3.7.3 Interactive effects of parameters

The present research comprehensively examined the three-dimensional (3D) representations and contour plots to understand how various parameters interact and impact protein and ammonia reduction. Figure 3-4 illustrates the interaction effects between two factors on protein reduction using 3D response surface plots constructed based on Eq. (3-3).

Variations of manure and KPW dosages markedly affect protein reduction (Figure 3-4 (a)). Increasing the KPW from 5 to 10 g VS L⁻¹ increased protein reduction (36% to 39%). However, protein reduction decreased from 38% to 36% with increasing the manure dosage from 4 to 9 g VS L⁻¹. The highest protein reduction (37-39%) is observed at a lower manure dosage (4-5 g VS L⁻¹) with a higher KPW dosage (8-10 g VS L⁻¹). Proteins in manure are derived from various sources, including animal feces, urine, and organic feed materials. This results in a mixture of proteins with different primary structures and compositions, making the overall protein structure complex and heterogeneous (Delve et al., 2001).

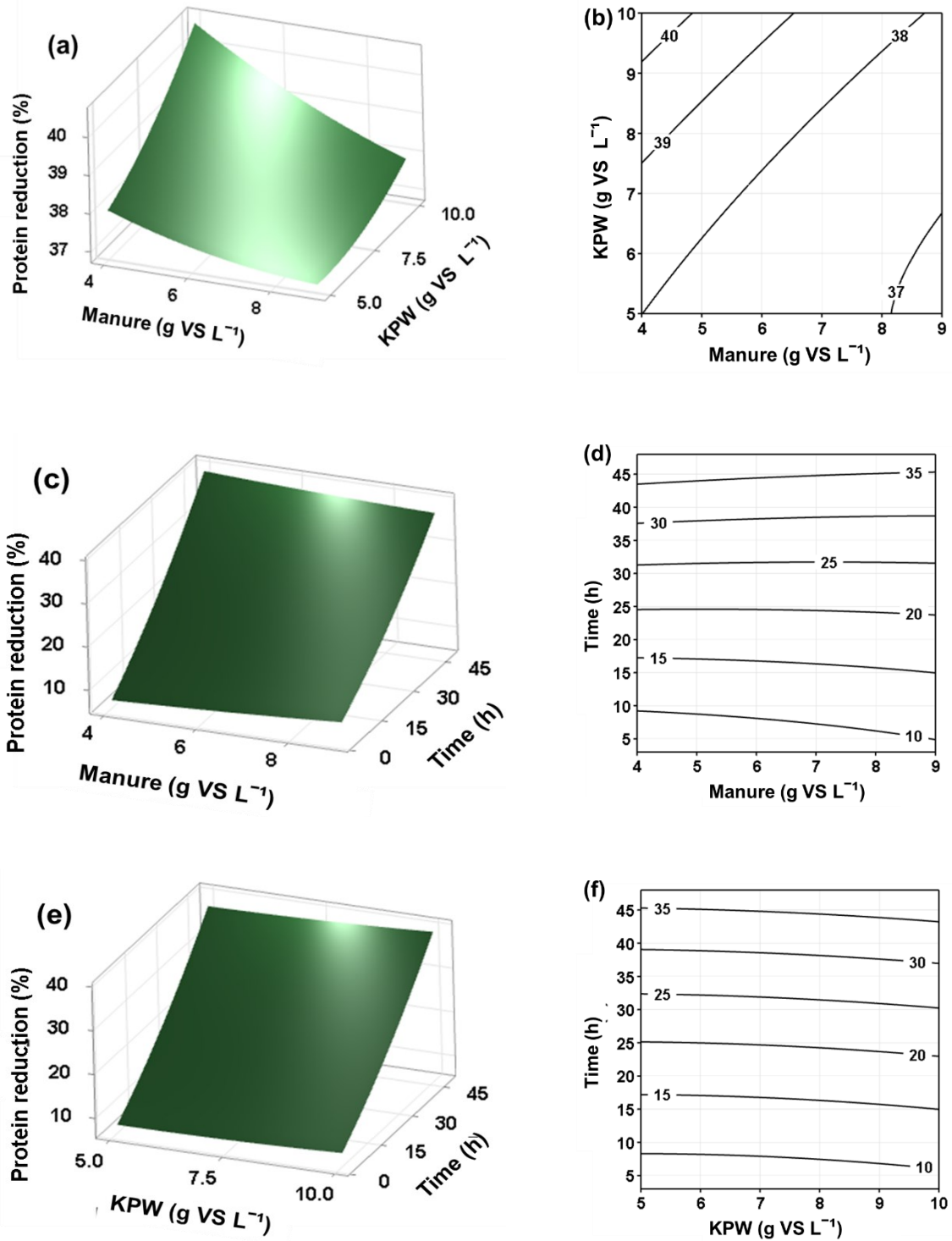


Figure 3- 4. Contour response surface and 3D plots of the interactive effect of (a) and (b) manure with kiwi peel waste (KPW) dosage, (c) and (d) manure dosage with hydrolysis time, and (e) and (f) KPW dosage with time on protein reduction.

Dairy manure and other nitrogen-rich lignocellulosic materials contain proteins that render a solution's total protein concentration inappropriate for fast degradation in a hydrolysis reaction. The higher the manure dosage, the more complex structures provide instability and resistance against protein degradation. Most of the proteins in manure exist in a form that can combine with other compounds, such as cellulose, lignocellulose, and hemicellulose (Liao et al., 2008). Figures 3-4 (b) and (c) show that reaction time favors protein reduction without being greatly affected by the manure or KPW dosage. The highest protein reduction (39%) is obtained at the end of the experiment (48 h). Chen et al. (2019) reported a high reaction time (10 days) to reduce pig manure nitrogen and carbon by 24% and 46%, respectively.

Manure is a rich potential supply of proteins and carbohydrates that can be processed to produce mono-sugars and amino acid intermediates that are useful. Figures 3-4 (b), (d), and (f) show the contour shape indicating the interaction between the factors. Circular contour shape demonstrates the interaction between any two factors is least significant (Shamsul et al., 2017). The partially elliptical contour plots that have been observed for manure and KPW interaction suggest the interaction between them is not entirely insignificant. However, the ANOVA study reported none of the manure * kiwi peel waste (0.168) and kiwi peel waste * time (0.572) interactions were significant (Table 3-7). On the other hand, ANOVA shows that the manure-time interaction is highly significant (p -value = 0.0006), showing linear plots in the contour graph. Similar disagreement between the ANOVA study and the contour plot has been observed in a previous study on co-digestion of pineapple waste and cow dung (Hamzah et al., 2022).

Figure 3-5 illustrates the impact of the interaction between two factors on the reduction of $\text{NH}_3\text{-N}$, as depicted by three-dimensional response surface plots derived from Equation (3-4).

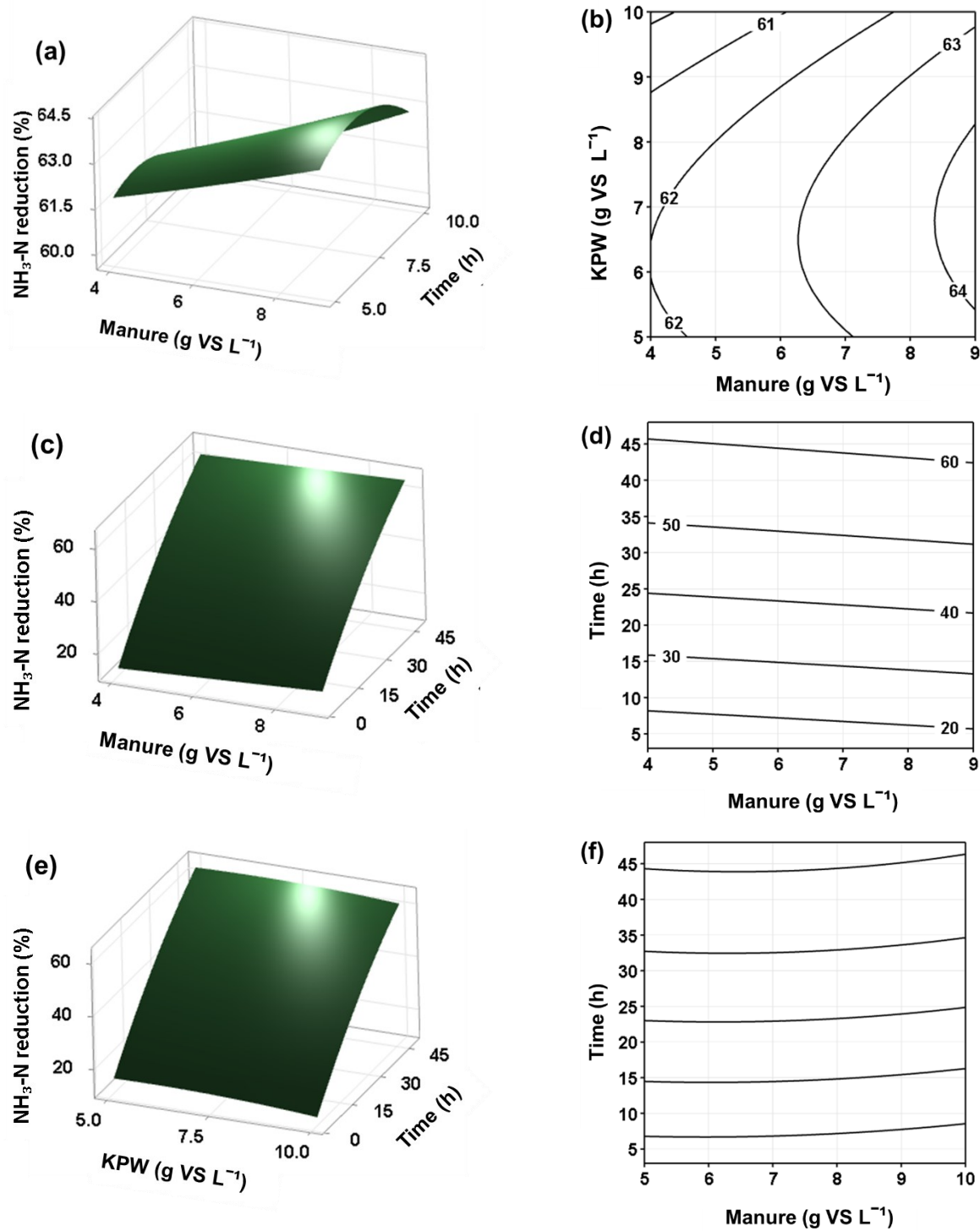


Figure 3- 5. 3D plots and contour response surface of the interactive effect of each variable on $\text{NH}_3\text{-N}$ reduction; (a) and (d) manure with kiwi peel waste (KPW) loading, (b) and (e) manure with hydrolysis time, and (c) and (f) KPW with time on $\text{NH}_3\text{-N}$ reduction.

Figure 3-5 (a) presents the response surface for $\text{NH}_3\text{-N}$ reduction with respect to manure and KPW loading. NH_3 reduction (%) increased from 61 to 62.5 as the manure increased from 4 to 9 g VS L^{-1} at the KPW dosage of 5 g VS L^{-1} . Also, ammonia reduction (%) increased from 61.5 to 64 with an increase of KPW dosage from 5 to 7.5 g VS L^{-1} . On the other hand, ammonia reduction increased significantly with the increase in KPW dosage from 5 to 7.5 g VS L^{-1} , then decreased with a further increase in KPW dosage at 10 g VS L^{-1} across all the manure dosage values monitored. This suggests that KPW present at 10 g VS L^{-1} is insufficient to degrade manure nitrogen molecules as free NH_3 .

At the KPW dosage of 7.5 g VS L^{-1} , hydrolysis might have reached an optimal condition where the enzyme concentration and other factors (pH and temperature) are conducive to efficient protein hydrolysis. This results in the maximum achievable ammonia reduction at this particular KPW dosage. Further increase of the KPW dosage to 10 g VS L^{-1} might be experiencing a decreasing trend. This means that adding more KPW beyond the optimal dosage does not lead to a proportionate increase in enzyme activity. Other factors, such as substrate availability or enzyme-substrate interactions, may start to limit the rate of ammonia reduction. Another reason is likely that at the higher KPW dosage, the substrate (manure) becomes saturated with enzymes. This means that more enzyme molecules are available than the substrate molecules to act upon. In this situation, adding extra KPW does not significantly increase ammonia reduction because the substrate is already saturated with enzymes.

A similar phenomenon was reported during the hydrolysis of cornstalk waste with the enzyme cellulase. When the enzyme concentration increased from 5 to 10 g L^{-1} , the average hydrogen (H_2) production rate increased from 8.0 to 11.5 $\text{mL g}^{-1} \text{h}^{-1}$, whereas a further increase of enzyme concentration to 15 g L^{-1} decreased the H_2 production rate to 7.9 $\text{mL g}^{-1} \text{h}^{-1}$ (Ma et al., 2011). A

higher dose of KPW (10 g VS L⁻¹) might lower the system pH, subsequently lowering the ammonia removal. Various phenolic compounds, including protocatechuic acid, chlorogenic acid, caffeic acid, rutin, p-hydroxybenzoic acid, and quercetin, are abundantly found in different components of kiwi fruit, with the highest concentrations observed in the peel (Wang et al., 2018). Sahu et al. (2017) found lower total ammonia nitrogen and free ammonia nitrogen removal under acidic conditions. A drastic increase in ammonia removal was obtained when the pH was increased, particularly at pH 6.5 to 8. Figure 3-5 (b) shows the response surface for ammonia reduction with respect to manure and time. Figures 3-5 (b) and (c) show that a high contact time favors the reduction of NH₃-N, without being greatly affected by the manure or KPW dosage. This implies that a longer contact between the reactants (manure and KPW) enhances the conversion of NH₃-N (ammonia nitrogen) into other forms. This suggests that the hydrolysis reaction is not instantaneous and requires sufficient time for the complete breakdown of the complex organic compound like manure.

The maximum ammonia reduction was found at a manure dosage of 9 g VS L⁻¹ (Figure 3-5 (c)) and KPW dosage of 5 g VS L⁻¹ at 48 h (Figure 3-5 (e)). This is also consistent with the results obtained from the protein reduction experiments. The contour plot of the manure-KPW interaction (Figure 3-5 (b)) shows that the contour plot was semi-elliptical, indicating a good interaction between the two factors (Liu et al., 2020). The interaction is also supported by a low *p*-value (0.046) (Table 3-7). However, the interaction between time and manure dosage and between time and KPW dosage were more constant than the interaction between manure and KPW, which seemed relatively flat near the optimal point.

3.7.4 Effect on ammonium reduction

Figure 3-6 shows the $\text{NH}_4\text{-N}$ concentrations in run 1 to run 15. During runs 2, 4, 6, and 8, the $\text{NH}_4\text{-N}$ concentration of the control digester is high (682, 991, 957, and 906 ppm), reflecting the high manure loading in each run, with a dosage of 9 g VS L^{-1} . In the rest of the sets, the control $\text{NH}_4\text{-N}$ concentration began to diverge, reflecting the effect of different proportions of manure in each digester. The most common inorganic type of nitrogen in manure is ammonium nitrogen ($\text{NH}_4\text{-N}$). The higher manure loading is the reason for the high $\text{NH}_4\text{-N}$ concentration in control sets 2, 4, 6, and 8 compared to other control test runs (Babae et al., 2013). Figure 3-6 also demonstrates the system's $\text{NH}_4\text{-N}$ removal efficiencies for the tested hydrolysis time (3 to 48 h). It shows that this bioreactor could reduce $\text{NH}_4\text{-N}$ quantity for the time being experimented. The $\text{NH}_4\text{-N}$ reduction (%) increased from $26 \pm 0.45\%$ to $83 \pm 0.95\%$, depending on the hydrolysis time 3 to 48 h. This $\text{NH}_4\text{-N}$ reduction efficiency is at the same level reported by other studies on the effect of long retention time in the hydrolysis of swine manure and pineapple waste, showing 78% and 85% $\text{NH}_4\text{-N}$ removal at 6 and 24 h, respectively (Nguyen et al., 2022).

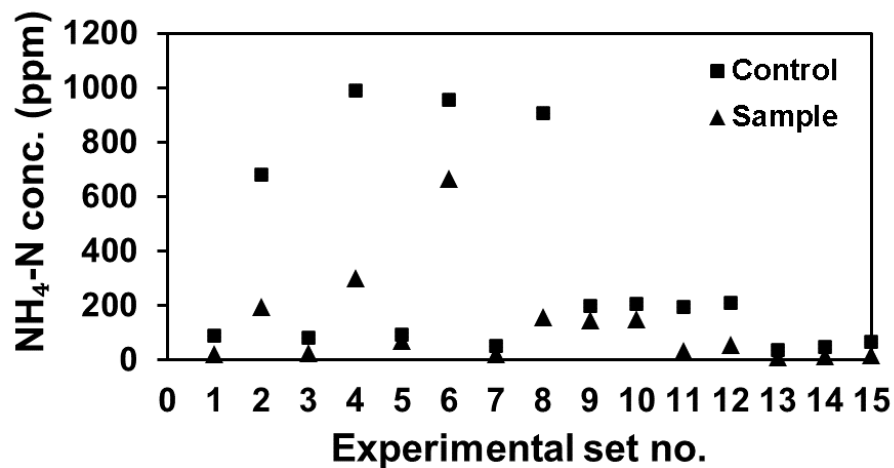


Figure 3- 6. $\text{NH}_4\text{-N}$ concentration of control and after 3 to 48 h in the test samples.

Nitrogen in the feedstock plays a crucial role in a bioprocess. When utilizing actual feedstock in a bioreactor, the effectiveness of removing ammonia and ammonium directly impacts the quality of the hydrolyzed substrate. As demonstrated in Figure 3-6, the system's ammonia and ammonium removal efficiencies provide a comprehensive overview of the results obtained from the conducted experiments. According to Figure 3-6, the system exhibited varying efficiency in removing ammonium, ranging from $25\pm 0.43\%$ to $83\pm 0.95\%$ with an average of $60.6\pm 0.69\%$ and from 12 ± 0.75 to $64\pm 0.65\%$ for ammonia reduction with an average of $40.1\pm 0.7\%$. In this case, lower $\text{NH}_4\text{-N}$ reduction ($55\pm 0.65\%$) was obtained where the KPW proportions were almost double than manure loading, such as in run 7 ($55 \pm 0.65\%$) compared to runs 8 ($83\pm 0.32\%$), 11 ($83\pm 0.95\%$), and 12 ($73\pm 0.87\%$) for 48 h. A considerably low ammonium reduction is observed where the KPW proportions are higher (acidic condition) than manure loading, similar to the ammonia reduction during the same study. Sahu et al. (2017) found lower total ammonia reductions at pH 5 (25%) compared to pH 6.6 (85%), which shows a similar trend to this study.

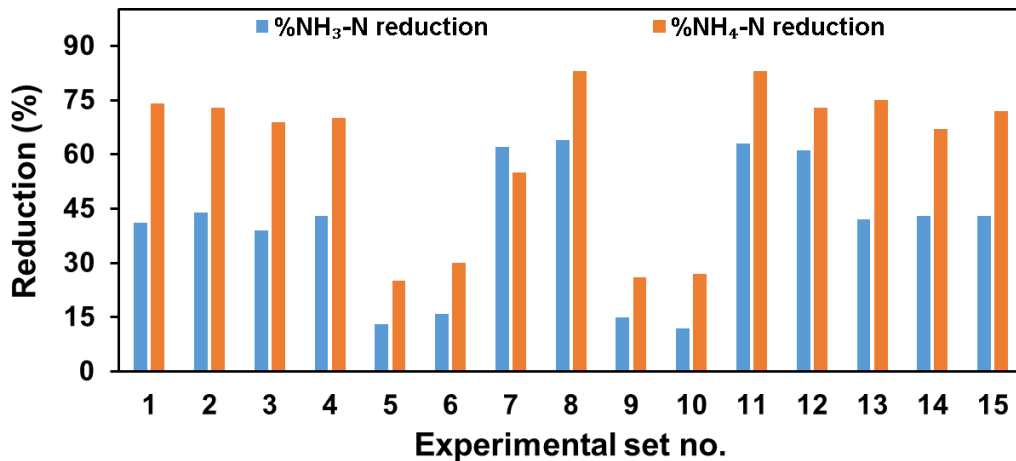


Figure 3- 7. NH_3 and $\text{NH}_4\text{-N}$ reduction efficiency of kiwi peel waste and manure hydrolysis as per statistical design.

Overall, the ammonium reductions were more prominent than ammonia reduction (Figure 3-7) in all runs except run 7, where NH_4 reductions ($55\pm 0.65\%$) were less than NH_3 reduction ($62\%\pm 0.25$). In the case of manure, which is rich in organic matter, hydrolysis leads to the breakdown of proteins, peptides, and other nitrogen-containing organic compounds into amino acids. These amino acids are further hydrolyzed into simpler forms, such as ammonium ions (NH_4^+), through the action of enzymes (Ma et al., 2020). To make the concept clearer, Eqs (3-5) and (3-6) present some typical examples of amino acid (glycine and alanine) hydrolysis reactions (Alexandrova and Jorgensen, 2011).

The most basic amino acid is glycine, which has a hydrogen atom as a side chain. When hydrolyzed, it undergoes the reaction in Eq. (3-5). This reaction breaks the peptide bond between the amino group (NH_2) and the carboxyl group (COOH), resulting in the formation of ammonium ions (H_3N^+) and the carboxylate ion (COO^-) along with hydroxide ions (OH^-). Schematic of hydrolysis of glycine showing three steps: before, during, and post hydrolysis by-products are presented in Figure 3-8.

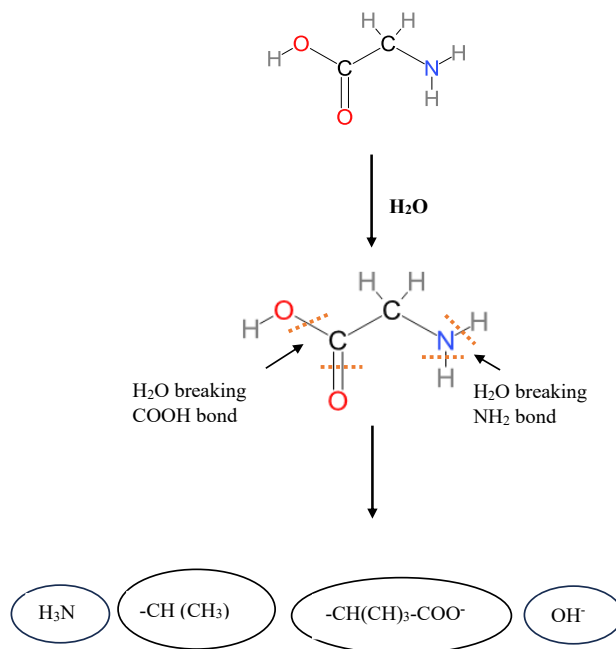
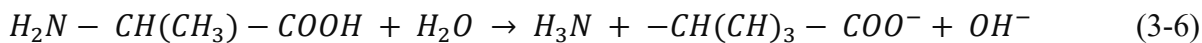
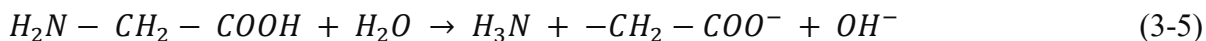


Figure 3- 8. Schematic drawing of hydrolysis of glycine.



Alanine is another common amino acid; its hydrolysis can be represented in Eq. (3-6). Again, the peptide bond is cleaved, leading to the formation of ammonium ions (H_3N^+), the alanine carboxylate ion (COO^-), and hydroxide ions (OH^-) (Taniguchi, 2010). These equations illustrate the general process of amino acid hydrolysis. In the context of manure decomposition, various enzymes facilitate the hydrolysis of complex proteins and peptides into these simpler nitrogen-containing compounds. This breakdown is essential for nutrient cycling and releasing valuable nitrogen sources like ammonium ions, which plants and microorganisms can utilize in the ecosystem. The hydrolysis of amino acids is a fundamental step in transforming organic nitrogen within manure and has significant implications for nutrient availability and soil fertility.

The ammonium ions have a higher solubility in water than ammonia gas; hence, ammonium is typically more readily dissolved (Franus and Wdowin, 2010; Vassileva and Voikova, 2009). In addition, this could be attributed to the function of KPW, which contains proteinase enzyme, which aid in the dissolution of ammonium nitrogen and inorganic ammonia in soluble components during hydrolysis or proteolysis reactions. (Li et al., 2016). Plant proteinase enzyme was shown to be effective in total ammonium nitrogen solubilization (Nguyen et al., 2022). In the present study, the dissolved $\text{NH}_4\text{-N}$ could also be used in the biological conversion of NH_4^+ into nitrogen gas (such as NH_3) and biomass. In the hydrolysis experiment of manure and KPW, the removed $\text{NH}_4\text{-N}$ and $\text{NH}_3\text{-N}$ may be processed by metabolism to produce biomass and nitrogen gas through an enzymatic reaction. Although biomass fluctuations in the liquid suspension were not measured in the current work, previous studies reported that 40 to 42% of $\text{NH}_4\text{-N}$ can be incorporated into biomass (Hoppensack et al., 2003; Sun et al., 2016; Sun et al., 2017). To gain a comprehensive understanding of the mechanisms involved in removing ammonium vs ammonia, additional information, such as changes in substrate concentration and measurements of enzyme kinetics, is essential. These factors need to be thoroughly investigated in order to achieve a clearer elucidation of the processes responsible for ammonium or ammonia removal. Table 3-9 provides an evaluation comparing the reduction of ammonia and/or protein in manure across different factors, emphasizing the study's results.

Table 3- 9. A comprehensive comparison of ammonia and/or protein reduction from manure across various variables.

Substrate	Ammonia / Ammonium removal (%)	Protein degradation (%)	Time (days)	Reacto r type	References
Manure and Kiwi peel waste	64%	39%	2	Batch	This study
Poultry manure, cheese factory, and coffee house waste	73% (NH ₃ -N)	-	0.25	Batch	Adghim et al. (2022)
Chicken manure	18% (NH ₄ ⁺ -N)	-	1	Batch	Yin et al. (2019)
Food waste	15.4 -16.4% per day (NH ₃ -N)	-	2-5	Batch	Serna-Maza et al. (2014)
Chicken manure	50% (for total NH ₄ -N 2000 mg/L) 30% (for total NH ₄ -N 2000 mg/L)	-	30	CSTR	Niu et al. (2013)
Livestock and poultry farm slurry	75.81% (NH ₃ -N)	-	3	Batch	Yang et al. (2017)
Chicken manure		45.8%	10	-	Chen et al. (2019)
Bovine manure from breeding farm		46.4%	10	-	Chen et al. (2019)
Waste-activated sludge and resin		21.8%	0.33	Batch	Pang et al. (2020)

3.7.5 Effect on volatile solids reduction

Volatile solids (VS) can serve as a valuable tool for evaluating the efficiency of AD, estimating the biogas production potential of various biomass materials, and determining the level of biomass decomposition (Orhororo et al., 2017). The inorganic fraction refers to the residual matter that remains after biomass combustion at 550 °C. VS represents the organic matter present in the substrate, including proteins, carbohydrates, and lipids. During biological treatment processes, such as AD or composting, organic matter degradation reduces the VS. Figure 3-9 presents the amount of VS reduction over the hydrolysis of manure and KPW as per statistical modeling.

Maximum VS destruction of about 41±0.29% was observed with manure and KPW in run 14, whereas the lowest VS reduction was 15.7±0.8% (run 5). However, within each run, VS reduction efficiency significantly increased with time. Overall, VS reductions amongst runs differed significantly; VS removal (calculated from control to sample VS) ranged from 15±0.89% to

29±0.89% in 3 h, 26-41±0.77% in 25.5 h, and 27-29±0.57% in 48 h with an increasing removal rate as time increased.

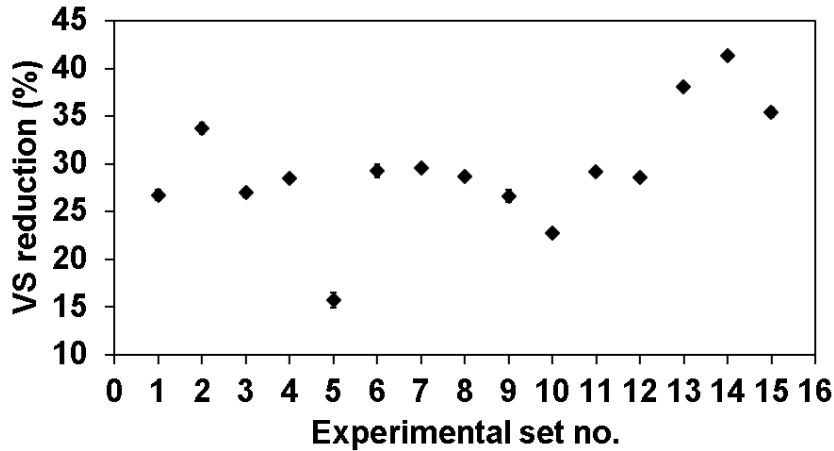


Figure 3- 9. Volatile solids (VS) reduction in 15 experimental sets for manure protein hydrolysis by KPW.

The efficiency of VS removal in this system was comparatively lower when compared to findings from long-term studies that involved the processing of pig manure (46.4±20%) (Gómez et al., 2019), fruit and vegetable waste (70.9%), pig manure (97.53%) (Yang et al., 2020), while a few other studies revealed similar values 38-51% VS reduction of waste activated sludge co-digested with food waste (Liu et al., 2019), 32-34% for citrus fruit waste (Lukitawesa et al., 2018), 23% for waste activated sludge (Wu et al., 2015), and 34-41% for pineapple peel and chicken manure (Kumar et al., 2017). The average VS reductions were 23±0.48% at 3 h, 33±0.53% at 25.5 h, and 28±0.26% at 48 h. This indicates that the VS reduction initially increased, reaching its peak at 25.5h. After this peak, there was a decline in the average VS reduction by 48h, although this reduction at 48h was still higher than the reduction observed at 3 h. Liu et al. (2019) also observed a similar result, 38% VS reduction at 8 h. In contrast, a further increase in time (25 h) caused a

51% reduction during the co-fermentation of food waste and waste-activated sludge. This could be due to increased non-disintegrated carbon and nitrogen residue, particularly cellulose, hemicellulose, lignin, and protein, which have comparatively lower biodegradability (Jabeen et al., 2015). During hydrolysis, enzymatic action breaks down complex organic compounds such as proteins, carbohydrates, and fats, converting them into simpler soluble compounds. This process increases VS reduction as the readily available organic matter is rapidly degraded by hydrolytic enzymes. However, as the hydrolysis proceeds and the readily accessible organic compounds are depleted, the process slows down. This can lower the VS reduction as the remaining substrate becomes more resistant to disintegration. These compounds may require a longer retention time or specialized treatment to be further broken down. Table 3-10 provide some previous studies corresponding different VS reduction amount.

Table 3- 10. Reported volatile solids reduction of various substrates in anaerobic digestion.

Substrate	VS reduction (%)	Time (day)	References
Cow manure	40±1.2	1	This study
Digester sludge	46-65	3	Kumar et al. (2006)
Swine manure and corn stover	7-33	15	Arias et al. (2021)
Cow manure and pineapple peel	41.72	80	Kumar et al. (2017)
Cow manure and pineapple leaf	30.86	80	Kumar et al. (2017)
Waste activated sludge	23	3	Wu et al. (2015)
Pig manure	46±20	18	Yang et al. (2020)
Pig manure	19.68 ± 4.66	6	Adghim et al. (2022)
Rumen waste	32	7	Issah & Kabera (2021)
Mixed food waste	64	1	Kiran et al. (2015)

3.8 Optimization and Model Validation

In hydrolysis reactors, protein degradation and ammonia removal should be maximized because high ammonia removal and high protein degradation can reduce ammonia accumulation problems, consequently supporting a high gas yield in the digesters. Different combinations were

responsible for different optimum outputs, such as run 8 (manure 9 g VS L⁻¹ and KPW 7.5 g VS L⁻¹ for 48 h) for maximum NH₃-N removal (64±0.65%), run 7 (manure 4 g VS L⁻¹ and KPW 7.5 g VS L⁻¹ for 48 h) for maximum protein reduction (39±0.61%) and run 14 (manure 6.5 g VS L⁻¹ and KPW 10 g VS L⁻¹ for 48 h) for maximum VS reduction (41±0.29%). The maximum NH₄-N removal (83±0.32%) was observed in run 8 (manure 9 g VS L⁻¹ and KPW 7.5 g VS L⁻¹ for 48 h) and 11 (manure 6.5 g VS L⁻¹ and KPW 5 g VS L⁻¹ for 48 h). However, average VS reduction was observed at 25.5 h; after that, VS reduction decreased over time for all combinations. At the beginning of hydrolysis (3 h), there might be a lag phase where the enzymes in the KPW establish their activity for the substrate (manure). The acceleration period (up to 25.5 h) represents a phase where the hydrolysis process becomes more efficient. Enzymes may have familiarized to the substrate, and their activity has increased, leading to a higher rate of VS reduction. Conditions during this phase may be favorable for enzyme activity, such as optimal pH, temperature, and substrate availability. Beyond 25.5 h, the system may enter a plateau phase where the available substrate (manure) starts to become limited. Enzymes may also experience a decline in activity over time due to factors such as depletion of essential cofactors, accumulation of inhibitory by-products, or changes in environmental conditions (Gonzalez and Aranda, 2023). Manure is a complex substrate with a variety of organic compounds. The initial rapid reduction may involve the breakdown of more easily degradable components, while the slower phase may involve the breakdown of more complex and recalcitrant materials (Dalby et al., 2021; Labatut, 2012).

Therefore, achieving optimal conditions for all responses simultaneously is challenging as their respective regions of interest vary. Hence, the responses were superimposed based on the defined constraints to determine the optimization region. The overlaying method employed constraints to set the NH₃-N removal (%), NH₄-N removal (%), and protein degradation within a specified range;

40%, 70% and 20% as maximum value, respectively. To validate the models, optimal parameters, 9 g VS L⁻¹ manure, 7.5 g VS L⁻¹ kiwi and time 24 h were chosen as presented in Table 3-11.

Table 3- 11. Ammonia nitrogen and protein reduction under optimum conditions.

Manure dosage (g VS L ⁻¹)	Kiwi waste dosage (g VS L ⁻¹)	Time (h)	Reduction (%)			
			NH ₃ -N	Protein	NH ₄ -N	VS
9	7.5	24	39	18.5	68	28.4
9	7.5	24	41	21.9	67	25.7
9	7.5	24	38	19.2	65	20.0

From Table 3-10, the experimental average optimal responses for the NH₃-N and protein reduction (%) were 39.3±0.9% and 19.87±0.55%, respectively. In addition, the NH₄-N and VS reduction (%) were 66.7±1.01% and 24.7±0.57%, respectively. The specified conditions were implemented in successive triplicate experiments, which indicated their effectiveness in achieving the desired removal of NH₃-N and protein reduction, along with a satisfactory NH₄-N and VS reduction.

3.9 Chemical and Morphological Analysis

Section 3.10 focuses on chemical and morphological Analysis. This section is divided into two parts. In the first part, 3.10.1, we will look at FTIR (Fourier Transform Infrared Spectroscopy), a method used to identify different functional groups involved. The second part, 3.10.2, discusses SEM (Scanning Electron Microscopy), which helps us see the small details and surface patterns of materials. Both these methods are important for understanding what our materials are made of and how they look up close upon hydrolysis.

3.9.1 FTIR

The impact of hydrolysis on the degradation of manure and KPW was examined by conducting thorough Fourier transform infrared spectroscopy (FTIR) analysis on samples for up to 48 h. The FTIR plots of manure and kiwi waste pre- and post-hydrolysis have differences, and the functional groups changed over hydrolysis time (Figure 3-10).

Significant peaks emerged at 3290, 2919, 2851, 1610, 1420, 1245 and 1034 cm^{-1} (Figure 3-9 (control)). In the FTIR analysis, a broad band around 3290 cm^{-1} correspond to amide A absorption characteristics (Zhou et al., 2016). This peak is typically observed in the region of 3300-3500 cm^{-1} . It corresponds to the stretching vibration of the N-H bonds involved in hydrogen bonding. The absorption band at 3290 cm^{-1} decreased over time and shifted to 3340 cm^{-1} during enzymatic hydrolysis (Figure 3-10 (48 h)).

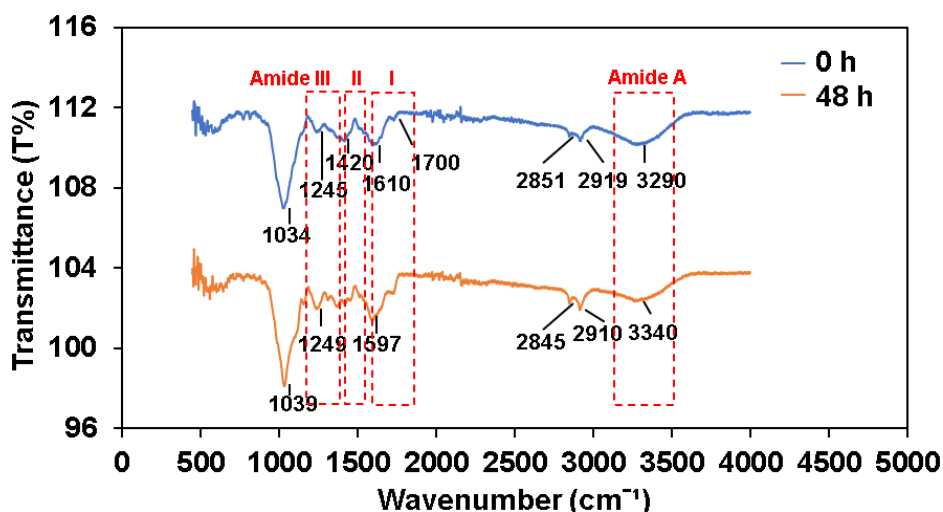


Figure 3- 10. FTIR spectrum of manure and kiwi peel waste at 0 h (control) and 48 h.

The observed shift and decreased peak in the spectrum is ascribed to the perturbation of hydrogen bonds and the breaking of amide bonds or N-H bonds within the side chains and might be indicating the cleavage of peptide bonds and the release of amino groups, which contributes to

the deformation of the sample protein structure (Rabotyagova et al., 2008). The bands at 2851 and 2919 cm^{-1} represent the CH_3 and CH_2 - asymmetric vibration mode, respectively. The band at 2851 and 2919 cm^{-1} shifted to a lower frequency (2845 and 2910 cm^{-1}), indicative of bond alteration (Sionkowska, 2006).

The wavenumber range of 1700-1600 cm^{-1} corresponds to the Amide I region, and it arises from the stretching vibration of C=O bonds within the amide group. On the other hand, the wavenumber range of 1580-1420 cm^{-1} is associated with the Amide II region. The presence of Amide II is attributed to the stretching vibrations of N-H and C-H bonds. Among these regions, Amide I exhibits the most pronounced transmission band and is highly responsive to variations in hydrogen-bonding environments, particularly in relation to secondary structures such as α -helix, β -sheet, turn, and unordered conformations (Miller et al., 2013). Amide III peak is usually found in the 1200-1350 cm^{-1} range, which signifies the N-H bending and C-N stretching coupled with C-C stretching (Prajapati et al., 2021). The regions of amide I (1600-1700 cm^{-1}) and amide II (1580-1420 cm^{-1}), which provide insights into protein's secondary and tertiary structure, have been examined extensively as they exhibit the most prominent spectral alterations resulting from digestion. Upon hydrolysis by KPW proteases, the amide I band centered around 1610 and 1700 cm^{-1} is shifted towards lower wavenumber 1597 and 1738 cm^{-1} , whereas a sharp peak around 1420 cm^{-1} (Amide II) disintegrated into small irregular peaks in the course of hydrolysis time which are explained by the free carboxylates COO^- 's antisymmetric stretching (Güler et al., 2016) and the distinct increase at 1597 cm^{-1} after hydrolysis (before hydrolysis at 1610 cm^{-1}), corresponding to the scissoring vibration of NH_3^+ (Böcker et al., 2017). Amide II arises from the combined vibrational modes of N-H bending and C-N stretching in the protein backbone. Changes in the Amide II peak during hydrolysis can indicate modifications in the protein's secondary structure

(Bai et al., 2023). The easily identified absorption peak at 1100-1000 cm^{-1} corresponding to crystalline cellulose and amorphous cellulose (Zhu et al., 2021), particularly a sharp peak at 1034 cm^{-1} shifted at 1039 cm^{-1} confirms hemicellulose distortion in both of the samples (Cheng et al., 2014).

3.9.2 SEM

Scanning electron microscope (SEM) analysis assesses the effectiveness of hydrolysis techniques by comparing the structural changes observed in samples subjected to different conditions or treatments. The morphology of manure and KPW before and after 6, 12, 24, and 48 h hydrolysis was observed by SEM at different magnifications (Figure 3-11).

In SEM images of the sample before hydrolysis (control sample), the surface typically appeared rough and heterogeneous (Figure 3-11 (a) and (b)). The image reveals a complex structure consisting of organic matter, fibrous materials, particulate components, and inorganic particles. The unhydrolyzed sample had dense and intact tissue with wrinkled planes, probably contributing to the fibrous part of the manure, similar to the SEM observations of chicken manure by Ormaechea et al. (2018) showing the substrate with heterogeneous size particles corresponding to the plant remnants that have not been broken down by an animal's digestive system. The enzymatic activity derived from KPW modulated the intracellular packing of nonfibrillar/ fibrillar protein and different ratios of biopolymers such cellulose, hemicellulose, and lignin in manure.

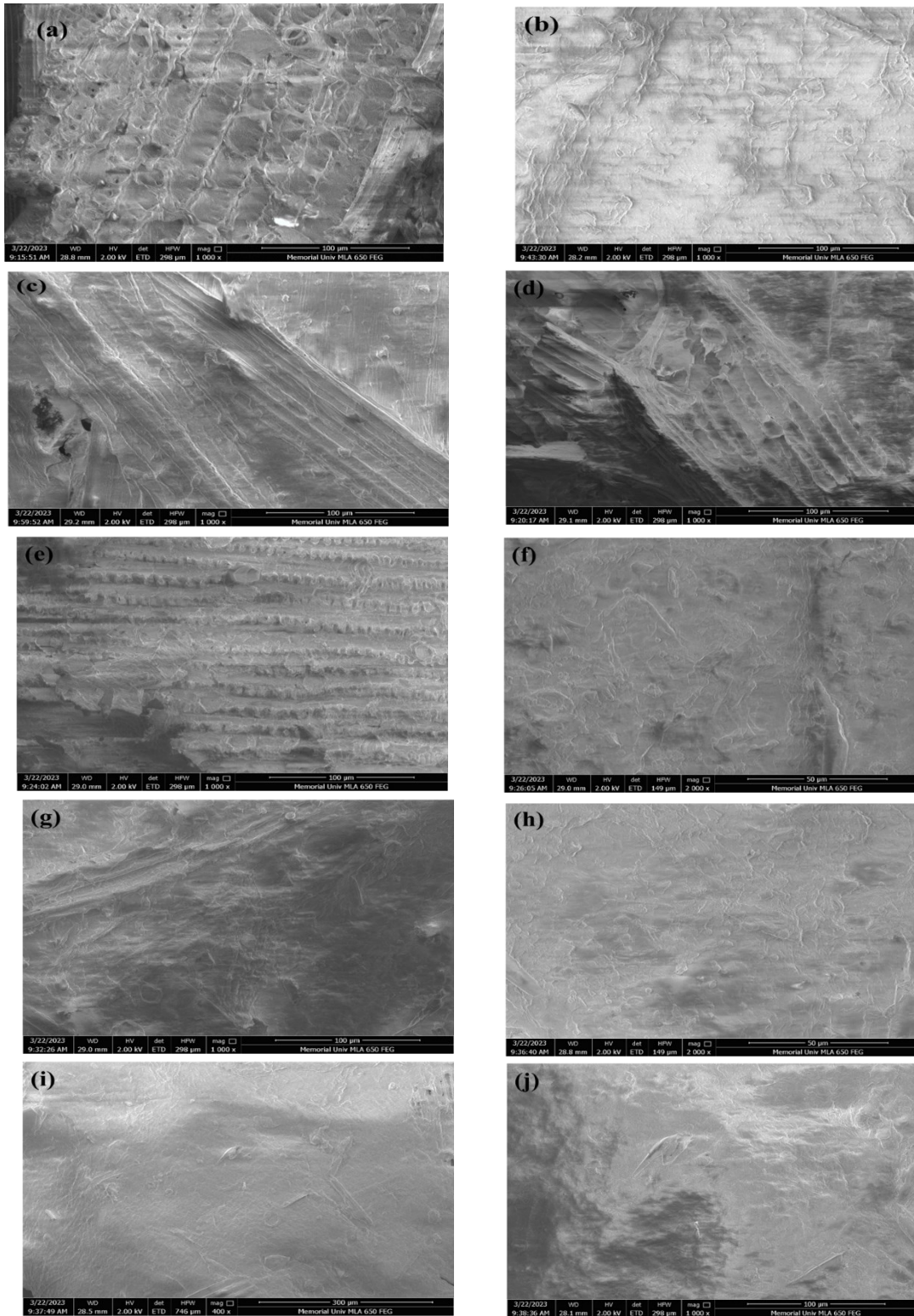


Figure 3- 11. Scanning electron microscope (SEM) images of (a) and (b) manure-kiwi peel waste (KPW) substrate control, and after hydrolysis at (c) and (d) 6 h, (e) and (f) 12 h, (g) and (h) 24 h, and (i) and (j) 48 h.

Hydrolysis is a process that breaks down complex organic compounds, such as proteins, carbohydrates, and lipids, into simpler forms. As a result, the complex manure-KPW structure undergoes significant alterations (Figure 3-11 (c) and (d) to (i) and (j)). The surface appeared smoother and more homogeneous compared to the pre-hydrolysis state. The distinct particles, fibers, or other structures observed before hydrolysis are less pronounced or completely absent after hydrolysis. In the hydrolyzed sample for 6 h (Figure 3-11 (c) and (d)), the fibrils demonstrate characteristic cross-striation patterns characterized by irregular intervals almost similar to the control sample, suggesting the protease enzyme took more than 6 h to fully function. This result also reinforces our previous statistical modeling result, showing higher protein degradation was achieved after 24 h (Figure 3-11 (g) and (h)) and highest at 48 h (Figure 3-11 (i) and (j)). The texture of the fibrous structure of the control manure-KPW sample was rougher than that of fiber in the sample at 24 and 48 h. This means that more substances were attached to the surface of the fiber's main structure in the control sample compared to the hydrolyzed sample (Molinuevo-Salces et al., 2012).

Liao et al. (2004) conducted chemical composition analysis and SEM of manure before hydrolysis, which provided evidence indicating that majority of such compounds mostly nitrogen-based component, such as proteins. Ganesh Kumar et al. (2008) findings from 72 h of hydrolysis of high protein content tannery solid waste align with and support the current study outcomes. The unhydrolyzed protein-rich solid waste was visualized with vertical and longitudinal fibrillar tissue fibers; however, 72 h hydrolysis altered the microstructural arrangements, and fibrillar tissue was completely damaged.

3.10 Conclusions

This study has successfully demonstrated the potential of Kiwi peel waste (KPW)-derived proteases to mitigate ammonia accumulation during anaerobic digestion of protein-rich waste. Through statistical experimental design and analysis, optimal hydrolysis conditions were established, leading to significant reductions in manure protein quantity and ammonia concentration. The results from the hydrolysis experiment revealed that the dosage of pineapple peel waste with manure had an impact on manure's protein quantity and ammonia reduction. As at 4 g VS L⁻¹ of manure mixed with 7.5 g VS L⁻¹ of KPW for 48 h, the maximum protein quantity reduction observed was 39±0.54%. However, 9 g VS L⁻¹ of manure mixed with 7.5 g VS L⁻¹ of KPW for 48h provided maximum NH₃-N reduction (64±0.65%). In addition, two more data were measured NH₄-N and VS reduction (%), a similar loading of manure, KPW, and hydrolysis time (9 g VS L⁻¹, 7.5 g VS L⁻¹, and 48 h) showed 83±0.32% NH₄-N reduction along with 41.4±0.29 % VS reduction at 6.5 g VS_{manure} L⁻¹ 7.5 VS_{KPW} 25.5 h. The response surface methodology's chosen experimental design turned out to be a reliable and affordable way for analysing, researching, and maximising the combined impacts of the three process factors: manure dosage, KPW, and time to reduce manure complex and NH₃-N accumulation. After the experimental data from the BBD matrix were examined, a very significant regression quadratic model equation ($R^2 = 0.99$; $p < 0.0001$) was produced for both protein reduction and NH₃-N reduction. The optimal value of NH₃-N (39.3±0.9%), protein (19.87±0.55%), NH₄-N (66.7±1.01%) and VS (24.7±0.57%) reduction were achieved when the dosages were loaded as 9 gVS_{manure} L⁻¹, 7.5 gVS_{KPW}L⁻¹ for 24h. Moreover, the integration of FTIR spectroscopy and SEM provided deeper insights into the structural changes induced by the treatment, reinforcing the effectiveness of the approach. Notably, the study offers an economically viable solution with the added benefit of enhancing biohydrogen

and biomethane yields by reducing ammonia accumulation and degrading protein quantity, which is essential for sustainable energy production by anaerobic digestion.

References

- Abril, B., Bou, R., García-Pérez, J. V., & Benedito, J. (2023). Role of Enzymatic Reactions in Meat Processing and Use of Emerging Technologies for Process Intensification. *Foods*, 12(10), 1940. <https://doi.org/10.3390/foods12101940>.
- Adghim, M., Sartaj, M., & Abdehagh, N. (2022). Post-hydrolysis ammonia stripping as a new approach to enhance the two-stage anaerobic digestion of poultry manure: Optimization and statistical modelling. *Journal of Environmental Management*, 319, 115717. <https://doi.org/10.1016/j.jenvman.2022.115717>.
- APHA (1998) Standard Methods for the Examination of Water and Wastewater. 20th Edition, American Public Health Association, American Water Works Association and Water Environmental Federation, Washington DC.
- Alexandrova, A. N., & Jorgensen, W. L. (2011). On the mechanism and rate of spontaneous decomposition of amino acids. *The Journal of Physical Chemistry B*, 115(46), 13624-13632. <https://doi.org/10.1021/jp2081808>.
- Ariaenejad, S., Kavousi, K., Mamaghani, A. S. A., Ghasemitabesh, R., & Salekdeh, G. H. (2022). Simultaneous hydrolysis of various protein-rich industrial wastes by a naturally evolved protease from tannery wastewater microbiota. *Science of the Total Environment*, 815, 152796. <https://doi.org/10.1016/j.scitotenv.2021.152796>.
- Arias, D. E., Veluchamy, C., Habash, M. B., & Gilroyed, B. H. (2021). Biogas production, waste stabilization efficiency, and hygienization potential of a mesophilic anaerobic plug flow reactor processing swine manure and corn stover. *Journal of Environmental Management*, 284, 112027. <https://doi.org/10.1016/j.jenvman.2021.112027>.

- Arshad, M. S., Kwon, J.-H., Imran, M., Sohaib, M., Aslam, A., Nawaz, I., Amjad, Z., Khan, U., & Javed, M. (2016). Plant and bacterial proteases: A key towards improving meat tenderization, a mini review. *Cogent Food & Agriculture*, 2(1), 1261780. <http://dx.doi.org/10.1080/23311932.2016.1261780>.
- Arshad, Z. I. M., Amid, A., Yusof, F., Jaswir, I., Ahmad, K., & Loke, S. P. (2014). Bromelain: an overview of industrial application and purification strategies. *Applied Microbiology and Biotechnology*, 98, 7283-7297. <https://doi.org/10.1007/s00253-014-5889-y>.
- Ashie, I. N. A., Sorensen, T. L., & Nielsen, P. M. (2002). Effects of papain and a microbial enzyme on meat proteins and beef tenderness. *Journal of Food Science*, 67(6), 2138-2142. <https://doi.org/10.1111/j.1365-2621.2002.tb09516.x>.
- Babae, A., Shayegan, J., & Roshani, A. (2013). Anaerobic slurry co-digestion of poultry manure and straw: effect of organic loading and temperature. *Journal of Environmental Health Science and Engineering*, 11, 1-6. <https://doi.org/10.1186/2052-336X-11-15>.
- Bai, X., Shi, S., Kong, B., Chen, Q., Liu, Q., Li, Z., Wu, K., & Xia, X. (2023). Analysis of the influencing mechanism of the freeze–thawing cycles on in vitro chicken meat digestion based on protein structural changes. *Food Chemistry*, 399, 134020. <https://doi.org/10.1016/j.foodchem.2022.134020>.
- Balat, M. (2008). Potential importance of hydrogen as a future solution to environmental and transportation problems. *International Journal of Hydrogen Energy*, 33(15), 4013-4029. <https://doi.org/10.1016/j.ijhydene.2008.05.047>.
- Böcker, U., Wubshet, S. G., Lindberg, D., & Afseth, N. K. (2017). Fourier-transform infrared spectroscopy for characterization of protein chain reductions in enzymatic reactions. *Analyst*, 142(15), 2812-2818. <https://doi.org/10.1039/C7AN00488E>.

- Bonjoch, N.P.; Tamayo, P.R. (2001). Protein content quantification by Bradford method. In Handbook of Plant Ecophysiology Techniques; Springer: Berlin/Heidelberg, Germany; pp. 283–295.
- Bradford, M. M. (1976). A rapid and sensitive method for the quantitation of microgram quantities of protein utilizing the principle of protein-dye binding. *Analytical Biochemistry*, 72(1-2), 248-254. [https://doi.org/10.1016/0003-2697\(76\)90527-3](https://doi.org/10.1016/0003-2697(76)90527-3).
- Casabar, J. T., Ramaraj, R., Tipnee, S., & Unpaprom, Y. (2020). Enhancement of hydrolysis with *Trichoderma harzianum* for bioethanol production of sonicated pineapple fruit peel. *Fuel*, 279, 118437. <https://doi.org/10.1016/j.fuel.2020.118437>.
- Chang, P., Zhao, Z., Xu, G., Ghosh, A., Huang, J., & Yang, T. (2020). Evaluation of the coal dust suppression efficiency of different surfactants: A factorial experiment. *Colloids and Surfaces A: Physicochemical and Engineering Aspects*, 595, 124686. <https://doi.org/10.1016/j.colsurfa.2020.124686>.
- Chen, X., Liu, R., Hao, J., Li, D., Wei, Z., Teng, R., & Sun, B. (2019). Protein and carbohydrate drive microbial responses in diverse ways during different animal manures composting. *Bioresource Technology*, 271, 482-486. <https://doi.org/10.1016/j.biortech.2018.09.096>.
- Chen, Z., Xu, Y., Cusack, D. F., Castellano, M. J., & Ding, W. (2019). Molecular insights into the inhibitory effect of nitrogen fertilization on manure decomposition. *Geoderma*, 353, 104-115. <https://doi.org/10.1016/j.geoderma.2019.06.034>.
- Cheng, J., Lin, R., Xia, A., Liu, Y., Zhou, J., & Cen, K. (2014). Sequential generation of fermentative hydrogen and methane from swine manure with physicochemical characterization. *Energy & Fuels*, 28(1), 563-570. <https://doi.org/10.1021/ef402388j>.

- Coelho, M., Russo, C., & Araujo, O. (2000). Optimization of a sequencing batch reactor for biological nitrogen removal. *Water Research*, 34(10), 2809-2817.
[https://doi.org/10.1016/S0043-1354\(00\)00010-5](https://doi.org/10.1016/S0043-1354(00)00010-5).
- Dalby, F. R., Hafner, S. D., Petersen, S. O., VanderZaag, A. C., Habtewold, J., Dunfield, K., & Sommer, S. G. (2021). Understanding methane emission from stored animal manure: A review to guide model development. *Journal of Environmental Quality*, 50(4), 817-835.
<https://doi.org/10.1002/jeq2.20252>.
- Damodaran, S. Amino acids, peptides, and proteins. In Fennema's Food Chemistry, 5th ed.; Damodaran, S., Parkin, K.L., (ED); CRC Press: Boca Raton, FL, USA, 2017; pp. 235–356.
- David Troncoso, F., Alberto Sánchez, D., & Luján Ferreira, M. (2022). Production of plant proteases and new biotechnological applications: an updated review. *Chemistry Open*, 11(3), e202200017. <https://doi.org/10.1002/open.202200017>.
- Delve, R. J., Cadisch, G., Tanner, J., Thorpe, W., Thorne, P. J., & Giller, K. E. (2001). Implications of livestock feeding management on soil fertility in the smallholder farming systems of sub-Saharan Africa. *Agriculture, Ecosystems & Environment*, 84(3), 227-243.
[https://doi.org/10.1016/S0167-8809\(00\)00244-9](https://doi.org/10.1016/S0167-8809(00)00244-9).
- Dhiman, V. K., Chauhan, V., Kanwar, S. S., Singh, D., & Pandey, H. (2021). Purification and characterization of actinidin from *Actinidia deliciosa* and its utilization in inactivation of α -amylase. *Bulletin of the National Research Centre*, 45, 1-9.
<https://doi.org/10.1186/s42269-021-00673-0>.
- Dolly, S., Pandey, A., Pandey, B. K., & Gopal, R. (2015). Process parameter optimization and enhancement of photo-biohydrogen production by mixed culture of *Rhodobacter*

sphaeroides NMBL-02 and Escherichia coli NMBL-04 using Fe-nanoparticle.

International Journal of Hydrogen Energy, 40(46), 16010-16020.

<https://doi.org/10.1016/j.ijhydene.2015.09.089>.

Fagbohunbe, M. O., Herbert, B. M., Hurst, L., Ibeto, C. N., Li, H., Usmani, S. Q., & Semple, K.

T. (2017). The challenges of anaerobic digestion and the role of biochar in optimizing anaerobic digestion. *Waste Management*, 61, 236-249.

<https://doi.org/10.1016/j.wasman.2016.11.028>.

Fernández-Lucas, J., Castañeda, D., & Hormigo, D. (2017). New trends for a classical enzyme:

Papain, a biotechnological success story in the food industry. *Trends in Food Science & Technology*, 68, 91-101. <https://doi.org/10.1016/j.tifs.2017.08.017>.

Franus, W., & Wdowin, M. (2010). Removal of ammonium ions by selected natural and

synthetic zeolites. *Mineral Resources Management*, 26, 133-148.

bwmeta1.element.baztech-article-BPZ1-0065-0009.

Ganesh Kumar, A., Venkatesan, R., Kirubakaran, R., Prabhakar, T., & Sekaran, G. (2008).

Effects of nonionic surfactant on hydrolysis and fermentation of protein rich tannery solid waste. *Biodegradation*, 19, 739-748. <https://doi.org/10.1007/s10532-008-9178-2>.

Gómez, D., Ramos-Suárez, J. L., Fernández, B., Muñoz, E., Tey, L., Romero-Güiza, M., &

Hansen, F. (2019). Development of a modified plug-flow anaerobic digester for biogas production from animal manures. *Energies*, 12(13), 2628.

<https://doi.org/10.3390/en12132628>.

Gonzalez, J. M., & Aranda, B. (2023). Microbial Growth under Limiting Conditions-Future

Perspectives. *Microorganisms*, 11(7), 1641.

<https://doi.org/10.3390/microorganisms11071641>.

- Gulcan, M. F., Karahan, B. D., & Keles, O. (2023). Application of the Box–Behnken design in the response surface methodology for the precipitation of Ni/Ni oxalate composite anodes. *Journal of Applied Electrochemistry*, 53, 1-13. <https://doi.org/10.1007/s10800-023-01846-7>.
- Güler, G., Vorob'ev, M. M., Vogel, V., & Mäntele, W. (2016). Proteolytically-induced changes of secondary structural protein conformation of bovine serum albumin monitored by Fourier transform infrared (FT-IR) and UV-circular dichroism spectroscopy. *Spectrochimica Acta Part A: Molecular and Biomolecular Spectroscopy*, 161, 8-18. <https://doi.org/10.1016/j.saa.2016.02.013>.
- Guo, W.-Q., Ren, N.-Q., Wang, X.-J., Xiang, W.-S., Ding, J., You, Y., & Liu, B.-F. (2009). Optimization of culture conditions for hydrogen production by *Ethanoligenens harbinense* B49 using response surface methodology. *Bioresource Technology*, 100(3), 1192-1196. <https://doi.org/10.1016/j.biortech.2008.07.070>.
- Gurumallesh, P.; Alagu, K.; Ramakrishnan, B.; Muthusamy, S. (2019). A systematic reconsideration on proteases. *International Journal of Biological Macromolecules*, 128, 254–267. <https://doi.org/10.1016/j.ijbiomac.2019.01.081>.
- Hamparian, V.V., Ottolenghi, A.C., Hughes, J.H. (1985). Enteroviruses in Sludge: Multiyear Experience with Four Wastewater Treatment Plants. *Applied and Environmental Microbiology*, 50, 280–286. <https://doi.org/10.1128/aem.50.2.280-286.1985>
- Hamzah, A. A., Hamzah, M., Mazlan, N., Man, H. C., Jamali, N., Siajam, S., & Show, P. (2022). Optimization of subcritical water pre-treatment for biogas enhancement on co-digestion of pineapple waste and cow dung using the response surface methodology. *Waste Management*, 150, 98-109. <https://doi.org/10.1016/j.wasman.2022.06.042>.

- Hao, T., Xiao, Y., & Varjani, S. (2022). Transiting from the inhibited steady-state to the steady-state through the ammonium bicarbonate mediation in the anaerobic digestion of low-C/N-ratio food wastes. *Bioresource Technology*, *351*, 127046. <https://doi.org/10.1016/j.biortech.2022.127046>.
- Harris, P. W., & McCabe, B. K. (2015). Review of pre-treatments used in anaerobic digestion and their potential application in high-fat cattle slaughterhouse wastewater. *Applied Energy*, *155*, 560-575. <https://doi.org/10.1016/j.apenergy.2015.06.026>.
- Homaei, A., & Etemadipour, R. (2015). Improving the activity and stability of actinidin by immobilization on gold nanorods. *International Journal of Biological Macromolecules*, *72*, 1176-1181. <https://doi.org/10.1016/j.ijbiomac.2014.10.029>.
- Hoppensack, A., Oppermann-Sanio, F. B., & Steinbüchel, A. (2003). Conversion of the nitrogen content in liquid manure into biomass and polyglutamic acid by a newly isolated strain of *Bacillus licheniformis*. *FEMS Microbiology Letters*, *218*(1), 39-45. <https://doi.org/10.1111/j.1574-6968.2003.tb11495.x>.
- Ikram, A., Ambreen, S., Tahseen, A., Azhar, A., Tariq, K., Liaqat, T., & Nasir, N. (2021). Meat tenderization through plant proteases: A mini review. *International Journal of Biosciences*, *18*(1), 102-112. <http://dx.doi.org/10.12692/ijb/18.1.102->.
- Issah, A.-A., & Kabera, T. (2021). Impact of volatile fatty acids to alkalinity ratio and volatile solids on biogas production under thermophilic conditions. *Waste Management & Research*, *39*(6), 871-878. <https://doi.org/10.1177/0734242X20957395>.
- Jabeen, M., Yousaf, S., Haider, M. R., & Malik, R. N. (2015). High-solids anaerobic co-digestion of food waste and rice husk at different organic loading rates. *International*

Biodeterioration & Biodegradation, 102, 149-153.

<https://doi.org/10.1016/j.ibiod.2015.03.023>.

Kabeyi, M. J. B., & Olanrewaju, O. A. (2022). Biogas production and applications in the sustainable energy transition. *Journal of Energy*, 2022, 1-43.

<https://doi.org/10.1155/2022/8750221>.

Kaur, L., Rutherford, S. M., Moughan, P. J., Drummond, L., & Boland, M. J. (2010). Actinidin enhances protein digestion in the small intestine as assessed using an in vitro digestion model. *Journal of Agricultural and Food Chemistry*, 58(8), 5074-5080.

<https://doi.org/10.1021/jf903835g>.

Kielkopf, C.L.; Bauer, W.; Urbatsch, I.L. (2020). Bradford Assay for Determining Protein Concentration. Cold Spring Harbour Protocol, 102269.

Kiran, E. U., Trzcinski, A. P., & Liu, Y. (2015). Enhancing the hydrolysis and methane production potential of mixed food waste by an effective enzymatic pretreatment.

Bioresource Technology, 183, 47-52. <https://doi.org/10.1016/j.biortech.2015.02.033>.

Kumar, M., Upadrasta, L., & Banerjee, R. (2017). Biomethanation of pineapple wastes using potent anaerobic consortia substituting cow manure. *Environmental Engineering & Management Journal*, 16(11). <http://omicron.ch.tuiasi.ro/EEMJ/>.

Kumar, N., Novak, J. T., & Water, D. (2006). Sequential anaerobic-aerobic digestion for enhanced volatile solids reduction and nitrogen removal. Proceedings of the Water Environmental Federation Residuals and Biosolids Management Conference, 12–14 March, 2006, Cincinnati, OH, USA.

- Labatut, R. (2012). Anaerobic biodegradability of complex substrates: performance and stability at mesophilic and thermophilic conditions. Doctoral thesis. Cornell University, Ithaca. <https://hdl.handle.net/1813/29168>.
- Li, X., Peng, Y., He, Y., Jia, F., Wang, S., & Guo, S. (2016). Applying low frequency ultrasound on different biological nitrogen activated sludge types: An analysis of particle size reduction, soluble chemical oxygen demand (SCOD) and ammonia release. *International Biodeterioration & Biodegradation*, *112*, 42-50. <https://doi.org/10.1016/j.ibiod.2016.04.025>.
- Liao, W., Liu, Y., Liu, C., & Chen, S. (2004). Optimizing dilute acid hydrolysis of hemicellulose in a nitrogen-rich cellulosic material—dairy manure. *Bioresource Technology*, *94*(1), 33-41. <https://doi.org/10.1016/j.biortech.2003.11.011>.
- Liao, W., Liu, Y., Wen, Z., Frear, C., & Chen, S. (2008). Kinetic modeling of enzymatic hydrolysis of cellulose in differently pretreated fibers from dairy manure. *Biotechnology and Bioengineering*, *101*(3), 441-451. <https://doi.org/10.1002/bit.21921>.
- Liu, S., Li, W., Zheng, G., Yang, H., & Li, L. (2020). Optimization of cattle manure and food waste co-digestion for biohydrogen production in a mesophilic semi-continuous process. *Energies*, *13*(15), 3848. <https://doi.org/10.3390/en13153848>.
- Liu, X., Li, R., & Ji, M. (2019). Effects of two-stage operation on stability and efficiency in co-digestion of food waste and waste activated sludge. *Energies*, *12*(14), 2748. <https://doi.org/10.3390/en12142748>.
- Lukitawesa, Wikandari, R., Millati, R., Taherzadeh, M. J., & Niklasson, C. (2018). Effect of effluent recirculation on biogas production using two-stage anaerobic digestion of citrus waste. *Molecules*, *23*(12), 3380. <https://doi.org/10.3390/molecules23123380>.

- Ma, Q., Wen, Y., Wang, D., Sun, X., Hill, P. W., Macdonald, A., Chadwick, D. R., Wu, L., & Jones, D. L. (2020). Farmyard manure applications stimulate soil carbon and nitrogen cycling by boosting microbial biomass rather than changing its community composition. *Soil Biology and Biochemistry*, *144*, 107760. <https://doi.org/10.1016/j.soilbio.2020.107760>.
- Madondo, N. I., & Chetty, M. (2022). Anaerobic co-digestion of sewage sludge and bio-based glycerol: Optimisation of process variables using one-factor-at-a-time (OFAT) and Box-Behnken Design (BBD) techniques. *South African Journal of Chemical Engineering*, *40*, 87-99. <https://doi.org/10.1016/j.sajce.2022.02.003>.
- Massé, D. I., Rajagopal, R., & Singh, G. (2014). Technical and operational feasibility of psychrophilic anaerobic digestion biotechnology for processing ammonia-rich waste. *Applied Energy*, *120*, 49-55. <https://doi.org/10.1016/j.apenergy.2014.01.034>.
- Mazorra-Manzano, M. A., Ramírez-Suarez, J. C., & Yada, R. Y. (2018). Plant proteases for bioactive peptides release: A review. *Critical reviews in food science and nutrition*, *58*(13), 2147-2163. <https://doi.org/10.1080/10408398.2017.1308312>.
- Miller, L. M., Bourassa, M. W., & Smith, R. J. (2013). FTIR spectroscopic imaging of protein aggregation in living cells. *Biochimica et Biophysica Acta (BBA)-Biomembranes*, *1828*(10), 2339-2346. <https://doi.org/10.1016/j.bbamem.2013.01.014>.
- Mohamed, M.A.; Jaafar, J.; Ismail, A.F.; Othman, M.H.D.; Rahman, M.A. (2017). Chapter 1—Fourier Transform Infrared (FTIR) Spectroscopy. In *Membrane Characterization*, 1st ed.; Hilal, N., Ismail, A.F., Matsuura, T., Oatley-Radcliffe, D., (ED); Elsevier: Amsterdam, The Netherlands, pp. 3–29.

- Mohd Azmi, S. I., Kumar, P., Sharma, N., Sazili, A. Q., Lee, S. J., & Ismail-Fitry, M. R. (2023). Application of Plant Proteases in Meat Tenderization: Recent Trends and Future Prospects. *Foods*, *12*(6), 1336. <https://doi.org/10.3390/foods12061336>.
- Molinuevo-Salces, B., González-Fernández, C., Gómez, X., García-González, M. C., & Morán, A. (2012). Vegetable processing wastes addition to improve swine manure anaerobic digestion: evaluation in terms of methane yield and SEM characterization. *Applied Energy*, *91*(1), 36-42. <https://doi.org/10.1016/j.apenergy.2011.09.010>.
- Mondal, N. K., Samanta, A., Dutta, S., & Chatteraj, S. (2017). Optimization of Cr (VI) biosorption onto *Aspergillus niger* using 3-level Box-Behnken design: equilibrium, kinetic, thermodynamic and regeneration studies. *Journal of Genetic Engineering and Biotechnology*, *15*(1), 151-160. <https://doi.org/10.1016/j.jgeb.2017.01.006>.
- Morellon-Sterling, R., El-Siar, H., Tavano, O. L., Berenguer-Murcia, Á., & Fernández-Lafuente, R. (2020). Ficin: A protease extract with relevance in biotechnology and biocatalysis. *International Journal of Biological Macromolecules*, *162*, 394-404. <https://doi.org/10.1016/j.ijbiomac.2020.06.144>.
- Mostafaie, A., Bidmeshkipour, A., Shirvani, Z., Mansouri, K., & Chalabi, M. (2008). Kiwifruit actinidin: a proper new collagenase for isolation of cells from different tissues. *Applied Biochemistry and Biotechnology*, *144*, 123-131. <https://doi.org/10.1007/s12010-007-8106-y>.
- Nazifa, T. H., Saady, N. M. C., Bazan, C., Zendehboudi, S., Aftab, A., & Albayati, T. M. (2021). Anaerobic digestion of blood from slaughtered livestock: A review. *Energies*, *14*(18), 5666. <https://doi.org/10.3390/en14185666>.

- Nguyen, T.-T., Ta, D.-T., Lin, C.-Y., & Chu, C.-Y. (2022). Biohythane production from swine manure and pineapple waste in a single-stage two-chamber digester using gel-entrapped anaerobic microorganisms. *International Journal of Hydrogen Energy*, 47(60), 25245-25255. <https://doi.org/10.1016/j.ijhydene.2022.05.259>.
- Niu, Q., Qiao, W., Qiang, H., Hojo, T., & Li, Y.-Y. (2013). Mesophilic methane fermentation of chicken manure at a wide range of ammonia concentration: stability, inhibition and recovery. *Bioresource Technology*, 137, 358-367. <https://doi.org/10.1016/j.biortech.2013.03.080>.
- Orhorhoro, E. K., Ebunilo, P. O., & Sadjere, G. E. (2017). Experimental determination of effect of total solid (TS) and volatile solid (VS) on biogas yield. *American Journal of Modern Energy*, 3(6), 131-135.
- Ormaechea, P., Castrillón, L., Suárez-Peña, B., Megido, L., Fernández-Nava, Y., Negral, L., Marañón, E., & Rodríguez-Iglesias, J. (2018). Enhancement of biogas production from cattle manure pretreated and/or co-digested at pilot-plant scale. Characterization by SEM. *Renewable Energy*, 126, 897-904. <https://doi.org/10.1016/j.renene.2018.04.022>.
- Pang, H., Chen, Y., He, J., Guo, D., Pan, X., Ma, Y., Qu, F., & Nan, J. (2020). Cation exchange resin-induced hydrolysis for improving biodegradability of waste activated sludge: characterization of dissolved organic matters and microbial community. *Bioresource Technology*, 302, 122870. <https://doi.org/10.1016/j.biortech.2020.122870>.
- Prajapati, S., Koirala, S., & Anal, A. K. (2021). Bioutilization of chicken feather waste by newly isolated keratinolytic bacteria and conversion into protein hydrolysates with improved functionalities. *Applied Biochemistry and Biotechnology*, 193, 2497-2515. <https://doi.org/10.1007/s12010-021-03554-4>.

- Qihe, C., Guoqing, H., Yingchun, J., & Hui, N. (2006). Effects of elastase from a *Bacillus* strain on the tenderization of beef meat. *Food Chemistry*, 98(4), 624-629.
<https://doi.org/10.1016/j.foodchem.2005.06.043>.
- Qiu, J., Wilkens, C., Barrett, K., & Meyer, A. S. (2020). Microbial enzymes catalyzing keratin degradation: Classification, structure, function. *Biotechnology Advances*, 44, 107607.
<https://doi.org/10.1016/j.biotechadv.2020.107607>.
- Rabotyagova, O. S., Cebe, P., & Kaplan, D. L. (2008). Collagen structural hierarchy and susceptibility to degradation by ultraviolet radiation. *Materials Science and Engineering: C*, 28(8), 1420-1429. <https://doi.org/10.1016/j.msec.2008.03.012>.
- Saady, N. M. C., & Hung, Y. T. (2015). Energy recovery through biohydrogen production for sustainable anaerobic waste treatment: an overview. *International Journal of Environment and Waste Management*, 15(2), 148-172.
<https://doi.org/10.1504/IJEW.2015.068939>.
- Sahu, N., Deshmukh, S., Chandrashekhar, B., Sharma, G., Kapley, A., & Pandey, R. (2017). Optimization of hydrolysis conditions for minimizing ammonia accumulation in two-stage biogas production process using kitchen waste for sustainable process development. *Journal of Environmental Chemical Engineering*, 5(3), 2378-2387.
<https://doi.org/10.1016/j.jece.2017.04.045>.
- Serna-Maza, A., Heaven, S., & Banks, C. J. (2014). Ammonia removal in food waste anaerobic digestion using a side-stream stripping process. *Bioresource Technology*, 152, 307-315.
<https://doi.org/10.1016/j.biortech.2013.10.093>.

- Shamsul, N., Kamarudin, S., Kofli, N., & Rahman, N. (2017). Optimization of bio-methanol production from goat manure in single stage bio-reactor. *International Journal of Hydrogen Energy*, 42(14), 9031-9043. <https://doi.org/10.1016/j.ijhydene.2016.05.228>.
- Sharma, K. M., Kumar, R., Panwar, S., & Kumar, A. (2017). Microbial alkaline proteases: Optimization of production parameters and their properties. *Journal of Genetic Engineering and Biotechnology*, 15(1), 115-126. <https://doi.org/10.1016/j.jgeb.2017.02.001>.
- Singh, R., Mittal, A., Kumar, M., & Mehta, P. K. (2016). Microbial proteases in commercial applications. *Journal Pharmaceutical, Chemical and Biological Sciences*, 4(3), 365-374. http://www.jpCBS.info/2016_4_3_06_Rajendra.pdf.
- Sionkowska, A. (2006). Effects of solar radiation on collagen and chitosan films. *Journal of Photochemistry and Photobiology B: Biology*, 82(1), 9-15. <https://doi.org/10.1016/j.jphotobiol.2005.08.003>.
- Sullivan, G. A., & Calkins, C. R. (2010). Application of exogenous enzymes to beef muscle of high and low-connective tissue. *Meat Science*, 85(4), 730-734. <https://doi.org/10.1016/j.meatsci.2010.03.033>.
- Sun, C., Cao, W., Banks, C. J., Heaven, S., & Liu, R. (2016). Biogas production from undiluted chicken manure and maize silage: a study of ammonia inhibition in high solids anaerobic digestion. *Bioresource Technology*, 218, 1215-1223. <https://doi.org/10.1016/j.biortech.2016.07.082>.

- Sun, Q., Zhang, B., Yan, Q.-J., & Jiang, Z.-Q. (2016). Comparative analysis on the distribution of protease activities among fruits and vegetable resources. *Food Chemistry*, *213*, 708-713. <https://doi.org/10.1016/j.foodchem.2016.07.029>.
- Sun, Y., Feng, L., Li, A., Zhang, X., Yang, J., & Ma, F. (2017). Ammonium assimilation: An important accessory during aerobic denitrification of *Pseudomonas stutzeri* T13. *Bioresource Technology*, *234*, 264-272. <https://doi.org/10.1016/j.biortech.2017.03.053>.
- Tacias-Pascacio, V. G., Castaneda-Valbuena, D., Morellon-Sterling, R., Tavano, O., Berenguer-Murcia, Á., Vela-Gutiérrez, G., ... & Fernandez-Lafuente, R. (2021). Bioactive peptides from fisheries residues: A review of use of papain in proteolysis reactions. *International Journal of Biological Macromolecules*, *184*, 415-428. <https://doi.org/10.1016/j.ijbiomac.2021.06.076>.
- Taherdanak, M., Zilouei, H., & Karimi, K. (2015). Investigating the effects of iron and nickel nanoparticles on dark hydrogen fermentation from starch using central composite design. *International Journal of Hydrogen Energy*, *40*(38), 12956-12963. <https://doi.org/10.1016/j.ijhydene.2015.08.004>.
- Taniguchi, N. (2010). Amino acids and proteins. In *Medical Biochemistry*; J.W Baynes, M.A. Dominiczak (ED); Elsevier, China, pp. 5-21.
- Thapa, S., Li, H., OHair, J., Bhatti, S., Chen, F.-C., Nasr, K. A., Johnson, T., & Zhou, S. (2019). Biochemical characteristics of microbial enzymes and their significance from industrial perspectives. *Molecular Biotechnology*, *61*, 579-601. <https://doi.org/10.1007/s12033-019-00187-1>.

- Tian, H., Mancini, E., Treu, L., Angelidaki, I., & Fotidis, I. A. (2019). Bioaugmentation strategy for overcoming ammonia inhibition during biomethanation of a protein-rich substrate. *Chemosphere*, 231, 415-422. <https://doi.org/10.1016/j.chemosphere.2019.05.140>.
- Tolera, S. T., & Alemu, F. K. (2020). Potential of abattoir waste for bioenergy as sustainable management, eastern Ethiopia, 2019. *Journal of Energy*, 2020, 1-9. <https://doi.org/10.1155/2020/6761328>.
- Verma, A., Singh, H., Anwar, S., Chattopadhyay, A., Tiwari, K. K., Kaur, S., & Dhillon, G. S. (2017). Microbial keratinases: industrial enzymes with waste management potential. *Critical Reviews in Biotechnology*, 37(4), 476-491. <https://doi.org/10.1080/07388551.2016.1185388>.
- Vassileva, P., & Voikova, D. (2009). Investigation on natural and pretreated Bulgarian clinoptilolite for ammonium ions removal from aqueous solutions. *Journal of Hazardous Materials*, 170(2-3), 948-953. <https://doi.org/10.1016/j.jhazmat.2009.05.062>.
- Vickers, N. J. (2017). Animal communication: when i'm calling you, will you answer too? *Current biology*, 27(14), R713-R715. <https://doi.org/10.1016/j.cub.2017.05.064>.
- Wang, F., Pei, M., Qiu, L., Yao, Y., Zhang, C., & Qiang, H. (2019). Performance of anaerobic digestion of chicken manure under gradually elevated organic loading rates. *International Journal of Environmental Research and Public Health*, 16(12), 2239. <https://doi.org/10.3390/ijerph16122239>.
- Wang, S., Jena, U., & Das, K. C. (2018). Biomethane production potential of slaughterhouse waste in the United States. *Energy Conversion and Management*, 173, 143-157. <https://doi.org/10.1016/j.enconman.2018.07.059>.

- Wang, Y., Li, L., Liu, H., Zhao, T., Meng, C., Liu, Z., & Liu, X. (2018). Bioactive compounds and in vitro antioxidant activities of peel, flesh and seed powder of kiwi fruit. *International Journal of Food Science & Technology*, 53(9), 2239-2245. <https://doi.org/10.1111/ijfs.13812>.
- Wu, L.-J., Qin, Y., Hojo, T., & Li, Y.-Y. (2015). Upgrading of anaerobic digestion of waste activated sludge by temperature-phased process with recycle. *Energy*, 87, 381-389. <https://doi.org/10.1016/j.energy.2015.04.110>.
- Xue, S., Wang, Y., Lyu, X., Zhao, N., Song, J., Wang, X., & Yang, G. (2020). Interactive effects of carbohydrate, lipid, protein composition and carbon/nitrogen ratio on biogas production of different food wastes. *Bioresource Technology*, 312, 123566. <https://doi.org/10.1016/j.biortech.2020.123566>.
- Yang, G., Zhang, P., Zhang, G., Wang, Y., & Yang, A. (2015). Degradation properties of protein and carbohydrate during sludge anaerobic digestion. *Bioresource technology*, 192, 126-130. <https://doi.org/10.1016/j.biortech.2015.05.076>.
- Yang, A., Zhang, G., Yang, G., Wang, H., Meng, F., Wang, H., & Peng, M. (2017). Denitrification of aging biogas slurry from livestock farm by photosynthetic bacteria. *Bioresource Technology*, 232, 408-411. <https://doi.org/10.1016/j.biortech.2017.01.073>.
- Yang, J., Wang, D., Luo, Z., Zeng, W., & Huang, H. (2020). The role of reflux time in a leach bed reactor coupled with a methanogenic reactor for anaerobic digestion of pig manure: Reactor performance and microbial community. *Journal of Cleaner Production*, 242, 118367. <https://doi.org/10.1016/j.jclepro.2019.118367>.

- Yin, D.-M., Qiao, W., Negri, C., Adani, F., Fan, R., & Dong, R.-J. (2019). Enhancing hyper-thermophilic hydrolysis pre-treatment of chicken manure for biogas production by in-situ gas phase ammonia stripping. *Bioresource Technology*, 287, 121470. <https://doi.org/10.1016/j.biortech.2019.121470>.
- Zhang, Y., Zhang, T., Zhang, Z., Tahir, N., & Zhang, Q. (2020). Biohydrogen production from *Humulus scandens* by dark fermentation: Potential evaluation and process optimization. *International Journal of Hydrogen Energy*, 45(6), 3760-3768. <https://doi.org/10.1016/j.ijhydene.2019.07.233>.
- Zheng, Z., Cai, Y., Zhang, Y., Zhao, Y., Gao, Y., Cui, Z., Hu, Y., & Wang, X. (2021). The effects of C/N (10–25) on the relationship of substrates, metabolites, and microorganisms in “inhibited steady-state” of anaerobic digestion. *Water Research*, 188, 116466. <https://doi.org/10.1016/j.watres.2020.116466>.
- Zhou, C., Li, Y., Yu, X., Yang, H., Ma, H., Yagoub, A. E. A., Cheng, Y., Hu, J., & Otu, P. N. Y. (2016). Extraction and characterization of chicken feet soluble collagen. *Lwt*, 74, 145-153. <https://doi.org/10.1016/j.lwt.2016.07.024>.
- Zhu, Y., Jin, Y., Liu, X., Miao, T., Guan, Q., Yang, R., & Qu, J. (2021). Insight into interactions of heavy metals with livestock manure compost-derived dissolved organic matter using EEM-PARAFAC and 2D-FTIR-COS analyses. *Journal of Hazardous Materials*, 420, 126532. <https://doi.org/10.1016/j.jhazmat.2021.126532>.

CHAPTER FOUR

ENHANCING MANURE PROTEIN DEGRADATION BY PINEAPPLE PEEL WASTE: STATISTICAL OPTIMIZATION USING BOX-BEHNKEN DESIGN AND RESPONSE SURFACE METHODOLOGY

Abstract

Animal farms generate large amounts of manure suitable as feedstock for producing biogas by anaerobic digestion (AD). However, AD encounters difficulties when manure contains excessive protein levels. This study investigates using pineapple peel waste (PPW)-derived protease enzyme (bromelain) to enhance manure's protein hydrolysis and improve biogas production. It aims to improve the degradation of manure protein and mitigate the inhibitory ammonia accumulation problem. The study applied a Box–Behnken design and analyzed the data using the Response Surface Methodology (RSM) to optimize protein reduction and diminishing ammonia levels. It examined the single and two-way impacts of parameters such as manure dosage, PPW dosage, and hydrolysis duration. The statistically derived optimal hydrolysis condition for $36\pm 0.25\%$ protein reduction was observed at $9 \text{ g VS}_{\text{manure}} \text{ L}^{-1}$, and $4 \text{ g VS}_{\text{PPW}} \text{ L}^{-1}$ at 48 h hydrolysis. However, the highest reduction of ammonia nitrogen ($\text{NH}_3\text{-N}$) by $72\pm 0.48\%$ was achieved under the optimal combinations of $6.5 \text{ g VS}_{\text{manure}} \text{ L}^{-1}$, and $7 \text{ g VS}_{\text{PPW}} \text{ L}^{-1}$ at 48 h hydrolysis. Fourier Transform Infrared (FTIR) spectroscopy and Scanning Electron Microscopy (SEM) analyses revealed changes, particularly weakening and cleavage of hydrogen and amide I, II and III bonds, confirming hydrolyzed manure's structural and morphological alterations. The hydrolyzed substrate characterization, paired with the rigorously developed statistical data, strongly supports using PPW as an effective agent to address the ammonia accumulation challenges. PPW significantly and

effectively enhances protein breakdown within manure, potentially increasing hydrogen and methane generation during AD.

Keywords: Manure, pineapple peel, nitrogen-rich feedstock, statistical optimization, FTIR, SEM.

4.1 Introduction

With energy consumption escalating sharply and provoking global concern, the energy shortage problem is intensifying. Projections suggest that by 2030, approximately 1.4 billion individuals may be at risk of lacking access to contemporary energy resources (Marie et al., 2021). In 2019, Canada generated 632.2 TWh of electricity, with hydro sources contributing 60% of this total. The rest came from diverse sources, such as biomass (1%), wind (5%), solar (0.3%), nuclear (15%), and natural gas (11%) (Tian et al., 2023; Giacosa & Walker, 2022). By 2021, Canada's energy use had risen by 2.8%, reaching 8,167 petajoules (Statistics Canada, 2022). Waste generation (such as animal manure and household, slaughterhouse, food, municipal, and agricultural waste) increased dramatically as a result of the growing population. Around 100 million tonnes of protein-rich waste (high in nitrogen content) are produced yearly, including slaughterhouse remnants, animal manure, and discarded meat products (Li et al., 2018). Each year, the livestock industry in Canada produces over 146 million tonnes of manure. This by-product of livestock farming, while often viewed as waste, is also a source of energy through biogas production (Wang et al., 2022). In recent years, the volume of waste directed towards anaerobic digestion (AD) within the European Union (EU) has seen an annual growth rate of 25%, driven by

substantial financial investments in both the biomass and Waste-to-Energy sectors (Ibarra et al., 2023).

This process uses four steps—hydrolysis, acidogenesis, acetogenesis, and methanogenesis—to transform protein-rich substrates into bioenergy, particularly biogas and biomethane, thus helping to manage the large amounts of such waste (Li et al., 2018). Protein-rich wastes, originating mainly from animal sources, such as slaughterhouse waste and livestock manure (from cows, pigs, cattle, chickens, etc.), have high protein content. These materials can cause ammonia build-up in digesters, which can impair performance unless a carbon source is added in AD to balance the carbon-to-nitrogen (C/N) ratio of the feedstock (González et al., 2022). The release of ammonium ions (NH_4^+) from protein breakdown can hinder AD when concentrations exceed $4.8 \text{ g NH}_4^+ \text{ N L}^{-1}$ (Astals et al., 2018). The inhibitory threshold for total ammonia concentration in biogas production varies with several factors, such as the nature of the substrate, acclimation, operational duration, pH, and temperature. Free ammonia (NH_3), which can cross cell membranes, is chiefly responsible for inhibition because it disrupts proton balance and potential to cause potassium deficiency. In contrast, the ammonium ion (NH_4^+) is comparatively less toxic. Anaerobic microbial communities that have adapted to ammonia were found to be inhibited at NH_3 concentrations ranging from 0.7 to $1.1 \text{ g NH}_3 \text{ N L}^{-1}$ (Kovács et al., 2013). The slow AD rates and inhibition issues from specific components in protein-rich wastes have been linked to limited biogas reactor performance. Industries like livestock farms, abattoirs, and those processing dairy products also generate protein-rich wastewater. If challenges in their AD are addressed, these protein-rich biomasses could become highly beneficial biogas sources. Additionally, the by-product of this AD process is an eco-friendly residue that serves as a high-quality agricultural fertilizer.

Mixing substrates with varying C/N ratios through co-digestion is an effective tactic to improve degradation efficiency and prevent the build-up of toxic levels of ammonia. Studies indicate that the ideal C/N ratio for efficient AD is between 20:1 to 30:1 (Banks and Heaven, 2013). However, the C/N ratios found in manure and various slaughterhouse wastes fall below this optimal range.

Amino acids are the building blocks of proteins, which are composed of amino acids joined by peptide bonds by enzyme proteases that follow various fermentation pathways depending on their types and concentrations (Tavano, 2013). Protease enzymes can be derived from plants, microbes, or fungi. For many years, plant proteases such as actinidin from kiwifruit (*Actinidia lindl*), ficin from fig (*Ficus carica*), papain from papaya (*Carica papaya*), and bromelain from pineapple (*Ananas comosus*) have been utilized traditionally (Mohd Azmi et al., 2023). Misran et al. (2019) noted that pineapple peels have a higher bromelain activity than the flesh. So far, only a few studies have explored the various applications of bromelain. Table 4-1 summarizes various applications of bromelain with different substrates in bioenergy and bioprocessing fields.

It shows that swine manure and pineapple waste can produce biohythane (a mixture of methane and hydrogen), with significant hydrogen and methane production rates and effective removal of COD and ammonium. The hydrolysis of aquaculture sludge with bromelain greatly enhances COD solubility (Syahirah & Nazaitulshila, 2018). Bromelain's application in meat processing results in extensive proteolysis, improving the breakdown of proteins in rejected meat from chicken, squid, and beef.

Additionally, the enzyme contributes to biogas generation, with a mix of cow dung and pineapple waste yielding high methane levels. These studies illustrate bromelain's potential in enhancing waste conversion to valuable bioproducts. Plant proteases can be extracted in vitro (using organs, tissues and cells) or in vivo (using a biological vector to express a particular

vegetable protein) or directly from vegetable biomass (roots, fruits, flowers and latex) through conventional agriculture. (David Troncoso et al., 2022).

Table 4- 1. Application of bromelain in various studies.

Application	Substrate	Results	References
Biohythane (H ₂ and CH ₄) generation	swine manure and pineapple waste	<ul style="list-style-type: none"> ▪ H₂ production rate is 1240 mL L⁻¹ d⁻¹ ▪ CH₄ production rate is 812 mL L⁻¹ d⁻¹ ▪ COD removal is 50-75.2 % ▪ Ammonium removal is 77.5-80.3 % 	(Nguyen et al., 2022)
Improvement of hydrolysis solubility	Aquaculture sludge	<ul style="list-style-type: none"> ▪ COD solubilizations with bromelain-treated sludge 84% 	(Syahirah & Nazaitulshila, 2018)
Hydrolysis of rejected meat in chicken, squid, and beef.	Meat myofibrillar protein	<ul style="list-style-type: none"> ▪ Extensive proteolysis and a reduction in the number and intensity of the protein bands in all of the treated samples. 	(Sunantha & Saroat, 2011)
Biogas generation	Cow dung	<ul style="list-style-type: none"> ▪ 1:1.5 ratio of cow dung and pineapple fruit waste resulted in 63.81% CH₄ and 34.47% CO₂ 	(Unnikrishnan & Ramasamy, 2022)
Biogas generation	Abattoir effluent (manure, blood, urine, fat, lumen and intestine)	<ul style="list-style-type: none"> ▪ Maximum biogas yield is 1.98 m³ 	(Otieno et al., 2023)

Every prior attempt at ammonia adaptation had the trait of mixing a significant amount of carbon-rich materials to the substrate with a high nitrogen content in order to get it closer to the suitable C/N/P ratio (Hernández Regalado et al., 2022). However, few studies have explored the potential of using protease enzymes derived from plant waste to break down proteins in protein-rich wastes. Pineapple waste is an excellent feedstock for co-digestion, given its high carbohydrate levels (about 40 g kg⁻¹), allowing for fast hydrolysis and organic matter acidification (Wijeratnam et al., 2005). It also contains bromelain enzyme that aids in the hydrolysis of soluble organic compounds into digestible forms for AD and can potentially reduce pollutant content and ammonia nitrogen levels (Syahirah and Nazaitulshila, 2018). Thus, pairing pineapple waste with manure

could optimize the C/N ratio, enhance the efficiency of biogas production, stabilize the process, and lower treatment costs for these organic wastes.

The information that is currently available indicates that the study's data are the first of their sort on the hydrolysis of manure using pineapple peel waste. Although few previous researchers had evaluated the mono digestion of pineapple waste (Rani & Nand, 2004) and mono digestion of protein-rich waste such as pig blood or casein (Kovács et al., 2013) and co-digestion of abattoir effluent with pineapple waste in AD, there is, however, no documentation on the optimal conditions for the protein and ammonia reduction when co-digesting pineapple peel waste and manure. This study is the first to elucidate the quantitative and morphological characteristics and show the morphological changes caused by pineapple peel waste to manure during hydrolysis over time. This study aims to identify optimal hydrolysis conditions using Box–Behnken Design and Response Surface Methodology (RSM), focusing on variables such as the amounts of manure (M), pineapple peel waste (PPW), and the duration of hydrolysis, to maximize the reduction of protein and ammonia in manure.

This research significantly enhances these waste streams' optimal and sustainable utilization as viable energy resources. The findings contribute to a deeper understanding and optimization of the hydrolysis stage of the AD process, paving the way for its establishment as an efficient treatment strategy for PPW and manure. Such advancements will bolster energy recovery from complex protein-rich wastes and promote environmental sustainability and resource conservation.

4.2 Materials and Method

The sub-sections below give an overview of the feedstocks, reagents, and chemicals used in the lab to improve the process of manure hydrolysis.

4.2.1 Chemicals and reagent

Ammonium chloride and sodium chloride of ACS reagent grade ($\geq 99.0\%$) were procured from Sigma-Aldrich, USA. Standard reagent-grade ammonium chloride (NH_4Cl) was employed to generate NH_3 and NH_4 . A 2 mL quantity of Ionic Standard Adjuster (ISA) was introduced to each 100 mL sample or standard solution to achieve a background ionic strength of 0.10M. Reagent-grade sodium chloride (NaCl) was utilized to prepare 10 M NaOH and 5 M NaOH as ISA for NH_3 and NH_4 measurements in both standards and samples. The Pierce Coomassie (Bradford) Protein Assay Kit, a pre-made Bradford assay reagent (Thermo Fisher Scientific, U.S.A.), was employed to determine the total protein concentration relative to a bovine serum albumin protein standard. De-ionized water was utilized for all aspects of sample preparation.

4.2.2 Feedstock

Dairy cow manure (M) in its fresh state was collected from a local dairy farm in St. John's, Newfoundland. The manure was obtained from beneath the animals in the wet barn before it reached the floor. After collection, the manure was transferred to an air-tight plastic container and stored at a temperature of 4 °C until it was fed to the digesters. Pineapple peel waste (PPW) served as the source of proteinase enzyme in the hydrolysis experiment. These fruits were procured from local groceries in St. John's and stored refrigerated in plastic bags. The fresh fruits were peeled, sliced into little pieces, and cleaned with tap water to get rid of any debris (Figure 4-1).



Figure 4- 1. Clean pineapple peel cuts ready for blending using a blender.

The peel pieces were blended using a magic bullet® with a 250-watt motor running at 2000 rpm (LLC Los Angeles, CA 90025, USA). A 500 mL capacity cup was affixed onto the motor blade and operated for 1 minute at a constant speed. Before feeding the reactors, both feedstocks (M and PPW) underwent physiochemical characterization (Table 4-2).

Table 4- 2. Physiochemical characteristics of the substrates.

Parameter	Cow Manure (M)	Pineapple peel waste (PPW)
pH	7.5	5.9
Total Solids, TS (%)	14.7	21
Volatile Solids, VS (%)	7	19
Chemical Oxygen Demand, COD (g L ⁻¹)	105.3	87
Protein (g L ⁻¹)	1.2	1.2
NH ₃ -N (g L ⁻¹)	2.2	-
NH ₄ -N (g L ⁻¹)	2.1	-

4.3 Hydrolysis Tests

A designed experiment incorporating statistical methods was executed using manure and PPW in batch digesters. Each set of conditions for optimization tests was evaluated in duplicate samples in air-tight 0.5 L Wheaton glass bottles (referred to as digesters), each having a working

volume of 0.3 L. The hydrolysis of cow manure with PPW wastes took place in the batch reactors at 20 ± 1 °C. PPW was introduced in mixing ratios ranging from 1 to 7 g VS L⁻¹ in conjunction with the manure (4 to 9 g VS L⁻¹).

4.4 Box-Behnken Design

Multiple batches of identical reactors were employed to investigate the impact of varying dosages of PPW over different incubation periods on the degradation of dairy manure protein, removal of ammonia nitrogen (NH₃-N) and ammonium nitrogen (NH₄-N), and volatile solids (VS) reduction. Response Surface Methodology (RSM) and Box-Behnken Design (BBD) were implemented, employing three levels (-1, 0, +1) to determine the optimal conditions for protein degradation and ammonia removal. BBD is an experimental design approach characterized by symmetry, facilitating the assessment of the significant effects of diverse experimental parameters and their interactions (Beg & Akhter, 2021). This method reduces the overall number of required experiments, providing a cost-effective means to optimize experimental conditions (Ince & Kaplan Ince, 2017). The application of RSM and BBD utilized Minitab® 21.4 Statistical Software (LLC, Pennsylvania, USA). The collected experimental data were used to construct a predictive model for removing protein and ammonia. By identifying interactional effects, this model seeks to optimize process parameters to maximize the removal of specified parameters. Equation (4-1) outlines the number of experiments or runs for the three levels in the Box-Behnken Design (BBD):

$$N = 2k(k - 1) + Cp \quad (4-1)$$

This study used the BBD methodology to investigate hydrolysis by conducting 17 experimental runs for manure and PPW. Each factor, manure loading, PPW loading, and time, was examined in 12 experiments at three levels and five central experiments. N denotes the number of experimental runs, C_p represents the central points number, and k indicates the number of parameters, such as substrate dosage and time.

Following the conventional approach, the BBD methodology was employed by adjusting all the factors at three evenly spaced levels (-1, 0, +1). The experimental points, generated according to the BBD methodology, were facilitated using Minitab® 21.4 Statistical Software. The hydrolysis process was examined based on the manure dosage (g VS L⁻¹), PPW (g VS L⁻¹), and the incubation time (from 4 to 48 h) (Table 4-3).

Table 4- 3. Variations in levels for different parameters in the Box-Behnken Design applied to manure and pineapple peel waste.

Factors	Codes	Low level (-1)	Intermediate level (0)	High level (+1)
Manure proportion (g VS L ⁻¹)	A	4	6.5	9
Pineapple peel proportion (g VS L ⁻¹)	B	1	4	7
Time (h)	C	4	26	48

The quantity of manure ranged from 4 to 9 g VS L⁻¹, the PPW dosage varied from 1 to 7 g VS L⁻¹, and the incubation time spanned 4 to 48 h. The experiments were executed following the matrix transformation detailed in Table 4-4. These experimental combinations involved monitoring four parameters: the reduction (%) of protein, NH₃-N, NH₄-N, and VS. The independent variables (parameters) were the three process factors, while the reduction (%) represented the dependent variable (response). The overall process diagram is depicted in Figure 4-2.

The BBD is employed to analyze quadratic responses, generating a mathematical model of a second-degree polynomial equation (Eq. (4-2)) that can predict optimal conditions.

$$Y = \beta_0 + \beta_1 X_1 + \beta_2 X_2 + \beta_3 X_3 + \beta_{11} X_1^2 + \beta_{22} X_2^2 + \beta_{33} X_3^2 + \beta_{12} X_1 X_2 + \beta_{23} X_2 X_3 + \beta_{13} X_1 X_3 \quad (4-2)$$

Where Y is the dependent or response variable (removal % or reduction %) of protein, NH₃-N, NH₄-N, and VS); $\beta_0, \beta_1, \beta_2, \beta_3$ are coefficients of linear expressions; $\beta_{11}, \beta_{22}, \beta_{33}$ are quadratic coefficients; $\beta_{12}, \beta_{23}, \beta_{13}$ are interaction coefficients; X_1, X_2, X_3 represents the independent variables.

Table 4- 4. Transformation of the matrix in the Box-Behnken Design applied to the hydrolysis of manure and pineapple peel waste (PPW).

Run	Manure VS (g L ⁻¹)	PPW VS (g L ⁻¹)	Time (h)
1	4.0	4	48
2	6.5	1	48
3	9.0	4	48
4	6.5	4	26
5	6.5	4	26
6	6.5	7	4
7	9.0	4	4
8	9.0	7	26
9	6.5	1	4
10	6.5	7	48
11	6.5	4	26
12	4.0	7	26
13	9.0	1	26
14	6.5	4	26
15	6.5	4	26
16	4.0	1	26
17	4.0	4	4

PPW = pineapple peel waste; VS = volatile solids

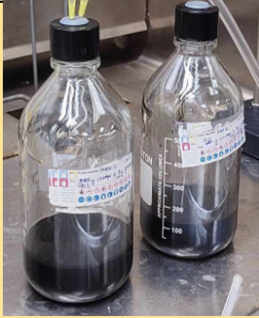
Digester for hydrolysis test	Statistically designed experimental matrix	Response
 <p data-bbox="367 678 599 827">Manure + Pineapple peel waste in digester for 4 to 48 h</p>	<p data-bbox="659 449 1003 562">Manure (4-9 VS g L⁻¹) +Pineapple peel (1-7 VS g L⁻¹) +Time (4 to 48 h)</p> <p data-bbox="813 569 857 636">↓</p> <p data-bbox="792 642 891 674">17 runs</p>	<p data-bbox="1101 384 1328 415">Reduction (%) of</p> <p data-bbox="1101 474 1211 506">-Protein</p> <p data-bbox="1101 569 1195 600">-NH₃-N</p> <p data-bbox="1101 663 1195 695">-NH₄-N</p> <p data-bbox="1101 758 1149 789">-VS</p>

Figure 4- 2. Illustration of the experimental arrangement and outcomes of the optimization tests for the manure and pineapple peel waste hydrolysis.

4.5 Analytical Methods

The substrates were characterized for total solids (TS), volatile solids (VS), pH, NH₃-N, and NH₄-N. pH values were measured with a pH meter (pH/ORP Temperature Control Monitor, pH-204, 110 V, USA), and all characterizations were performed in duplicate. Protein, NH₃-N, NH₄-N and VS were quantified according to the procedures explained in sections 4.5.1 to 4.5.3. The sample preparation for FTIR and SEM characterization is outlined in sections 4.5.4 and 4.5.5.

4.5.1 Protein quantity measurement

Protein concentration was assessed using the Bradford method (Kruger, 2009), which relies on the absorbance shift monitored in an acidic Coomassie® Brilliant Blue G-250 dye solution (Bradford, 1976). The dye binds to protein molecules in the presence of protein, inducing a color

change from reddish brown to blue (Figure 4-3). It is assumed that the dye's sulfonic groups attract the protein electrostatically to bond to it. The peak absorbance of the acidic dye solution shifts from 465 to 595 nm after it binds with protein molecules (Bonjoch & Tamayo, 2001). Consequently, all samples were analyzed using a UV-spectrophotometer (GENESYS 10S UV-VIS, Thermo Scientific, Madison, USA) at an absorbance of 595 nm, combined with Coomassie® Brilliant Blue. This approach ensured precise quantification of the protein content in each sample. Bovine Serum Albumin (BSA) served as the protein standard for creating a standard curve and its corresponding equation. Subsequently, this standard curve equation was applied to determine the protein concentrations of individual samples using their absorbance values measured at 595 nm with a UV-spectrophotometer. The reduction (%) in protein content was computed by comparing the sample and control values, as determined through statistical matrix runs.

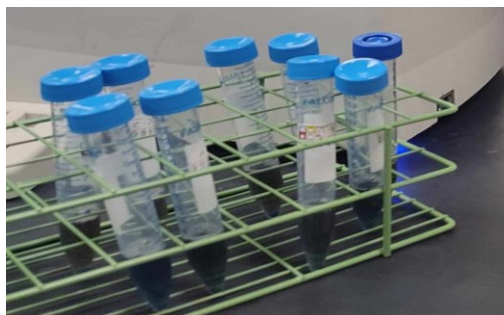


Figure 4- 3. A mixture of Coomassie dye and samples ready for protein quantity measurement.

4.5.2 $\text{NH}_3\text{-N}$ and $\text{NH}_4\text{-N}$ measurement

The ammonia gas sensing electrode (Cole-Parmer model #K-27502-00) and ammonium glass electrode (Cole-Parmer #K-27502-03) were employed to assess the $\text{NH}_3\text{-N}$ and $\text{NH}_4\text{-N}$ levels in the samples. A three-point calibration curve (Appendix A) was established through serial dilution,

adhering to the guidelines outlined in the Cole-Parmer model manual accompanying the respective electrodes. The calibration involved using standard ammonia and ammonium solutions at 1, 10, and 100 ppm concentrations. Control samples were obtained by withdrawing 100 mL from each digester immediately after preparation (time = 0). Subsequently, 100 mL samples were drawn from the digester bottles at specified intervals, mixed with 1 mL ISA, and the readings were recorded (Figure 4-4). The difference in readings between the control and the samples provided the reduction of $\text{NH}_3\text{-N}$ or $\text{NH}_4\text{-N}$.

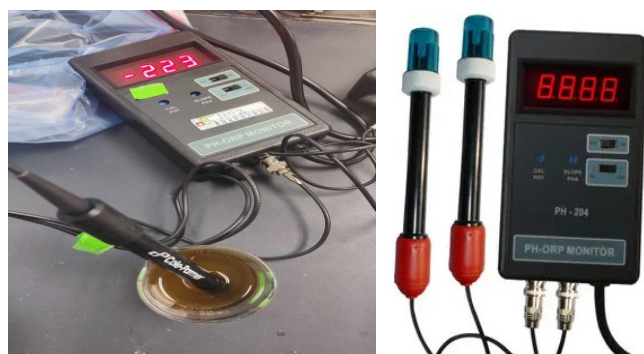


Figure 4- 4. Ammonium measurement using Cole Parmer ammonium probe meter connected with a pH-ORP monitor.

4.5.3 Volatile solids measurement

The removal of volatile solids (VS) is calculated using the measured VS of the control and that of the samples using the procedure of the standard methods (APHA-2540D). The first step involves determining the total solids (TS) (APHA-2540B), representing the remaining dry solids in a vessel after drying the sample at 105 °C in an oven. A digital balance (Denver instrument model A-160, USA) was employed to weigh the samples to measure TS and determine VS.

4.5.4 Fourier transform infrared spectroscopy (FTIR)

Understanding waste materials' state, stability, and reactivity is crucial for predicting their future behavior and degradability potential. Fourier transform infrared spectroscopy (FTIR) offers general insights into the chemistry of waste materials (Smidt & Meissl, 2007). For this purpose, liquid samples were withdrawn from the digesters at specific intervals (0 and 48 h) and oven-dried at 70-80 °C for 24 h before being subjected to FTIR. Approximately 0.5 g of the dried samples were analyzed using FTIR spectroscopy (PerkinElmer Spectrum IR-C115599, USA) with a spectral range of 650 to 4000 cm^{-1} and a resolution of 4 cm^{-1} . The resulting spectrum displayed wavenumber (cm^{-1}) on the X-axis and transmittance on the Y-axis.

4.5.5 Scanning electron microscope (SEM)

Analyzing the microstructural changes occurring in the samples during the hydrolysis period of 0 to 48 h using Scanning Electron Microscopy (SEM) (JEOL JSM 7100F, USA) facilitated the examination and validation of the results obtained in this study. The samples underwent a sputtering technique to apply a gold covering. Carbon tape was used to affix each sample separately under a microscope holder. High vacuum conditions and a 20 kV accelerating voltage were used to capture the images with a different magnification range (400x to 4000x).

4.6 Statistical Analysis of Experimental Data

Analysis of Variance (ANOVA) tests the statistical significance of the regression model, with coefficients of determination (R^2) assessing the model strength and goodness of fit. R^2 values range from 0 to 1, where a higher value indicates a better fit of the model to the data. Response Surface Methodology (RSM) optimization, aided by two-dimensional (contour) and three-dimensional

(surface) plots, aims to minimize manure dosage, PPW dosages, and time while maximizing parameter reductions. The optimal hydrolysis conditions are determined by RSM for anaerobic co-digestion, emphasizing maximal protein degradation or ammonia removal with minimal reaction time and substrate quantity. MINITAB 21.1 software (Minitab, LLC, Pennsylvania, USA) is used for statistical evaluation of the effects of independent variables and the relation between the variables.

4.7 Results and Discussion

This research employed laboratory experiments to collect numerical data, specifically focusing on various combinations of manure (M) and pineapple peel waste (PPW) hydrolysis as guided by the Box-Behnken Design matrix. The analysis aimed to determine the extent of protein degradation, ammonia, ammonium, and volatile solids (VS) reduction during manure hydrolysis. Section 4.8.1 presents the overall experimental result, and subsequent subsections (4.8.2 to 4.8.5) discuss the outcomes derived from each experiment along with relevant references.

4.7.1 Overall experiment

The experimental outcomes and the predicted values as responses are presented in the final four columns of Table 4-5. Seventeen combinations of manure dosage (g VS L^{-1}), PPW (g VS L^{-1}), and time (h) were systematically designed using the BBD within the framework of RSM; the details of these experimental combinations are provided in Table 4-3, and Table 4-4.

The observed reductions vary across different experimental runs, with protein quantity decreasing by 5% to 36%, $\text{NH}_3\text{-N}$ decreasing by 8% to 71%, $\text{NH}_4\text{-N}$ decreasing by 12% to 73%, and VS decreasing by 6% to 30%. Notably, the most significant reduction in protein occurred in

run 3 ($36\pm 0.25\%$ involving 9 g VS L⁻¹ manure, 4 g VS L⁻¹ PPW, and a 48-h duration) and 10 ($36\pm 0.53\%$ involving 6.5 g VS L⁻¹ manure, 7 g VS L⁻¹ PPW and 48 h). The highest NH₃-N reduction was noted in run 10 ($72\pm 0.48\%$ from 5 g VS L⁻¹ manure, 7 g VS L⁻¹ PPW and 48 h). Runs 1 (4 g VS L⁻¹ manure, 4 g VS L⁻¹ PPW and 48 h), 2 (6.5 g VS L⁻¹ manure, 1 g VS L⁻¹ PPW and 48h), and 3 (with 9 g VS L⁻¹ manure, 4 g VS L⁻¹ PPW and 48 h) stood out for achieving the highest NH₄-N reduction at 72%, 72%, and 73%, respectively.

Table 4- 5. Box-Behnken Design with predicted and experimental responses for manure and pineapple peel waste.

Run	Experimental response (reduction (%))				Predicted responses (reduction (%))			
	Protein	NH ₃ -N	NH ₄ -N	VS	Protein	NH ₃ -N	NH ₄ -N	VS
1	35±0.32	71±0.51	72±0.21	31±0.98	39	71	72	32
2	34±0.53	68±0.33	72±0.15	29±0.55	34	66	71	29
3	36±0.25	68±.55	73±0.54	32±0.35	39	69	74	32
4	24±0.55	49±0.24	43±0.22	19±0.11	28	51	43	22
5	24±0.65	41±0.71	40±0.35	21±0.87	27	43	41	22
6	7±0.12	9±0.43	12±0.21	6±0.75	5	13	9	7
7	5±0.60	8±0.32	12±0.55	6±0.12	6	7	11	8
8	25±0.26	41±0.55	43±0.32	19±0.21	25	40	42	21
9	5±0.56	8±0.5	12±0.58	7±0.55	6	8	12	8
10	36±0.53	72±0.48	69 ±0.09	30±0.12	39	75	75	32
11	24±0.25	38±0.21	41±0.92	19±0.19	25	36	40	19
12	24±0.44	41±0.54	41±0.84	20±0.23	25	43	39	22
13	22±0.15	39±0.25	40±0.23	19±0.43	25	40	38	23
14	24±0.65	40±0.51	41±0.39	20±0.55	24	40	42	25
15	24±0.32	42±0.33	43±0.36	21±0.51	23	42	41	21
16	23±0.21	41±0.46	42±0.23	20±0.32	21	41	40	20
17	8±0.32	10±0.67	12±0.65	7±0.29	7	11	12	8

4.7.2 ANOVA and response model

Once the design is chosen, subsequent experimental data will be presented through a surface plot and a second-order regression equation. Analysis of Variance (ANOVA) will further assess the model's quality. This involves comparing the variation attributed to treatment effects

(alterations in variable levels) with the inherent random errors in the measurements of the responses, providing a reliable means to evaluate the model fit (Chen et al., 2022). Through this comparison, assessing the significance of the regression employed for predicting responses becomes feasible, considering the various sources of experimental variance. The coefficient of determination, denoted as R^2 , represents the fraction of the overall variability in the response variable that can be accounted for by the independent variable. This metric serves as a means to assess the effectiveness and quality of the fit of the polynomial model. Overall, if the model is insignificant, the p -value will be greater than 0.05, while the p -value less than 0.05 proves the model is significant (Casabar et al., 2020). The ANOVA, conducted on the outcomes and presented in Tables 4-6 and 4-7, provides insights into the importance of the second-order polynomial concerning the reduction in protein quantity and $\text{NH}_3\text{-N}$ after hydrolysis.

In Tables 4-6 and 4-7, an ANOVA was conducted to determine how the variables and interactions among the variables affect the outcome. The ANOVA results consist of 17 cycles (Table 4-5). The calculated F -value for the model for protein reduction was 279.24, and 159.4 for $\text{NH}_3\text{-N}$ reduction, with a p -value of 0.0008 and 0.0009, respectively, indicating that the model terms are statistically significant. The coefficient of determination (R^2) was used to assess the model's accuracy. The R^2 values obtained for protein and $\text{NH}_3\text{-N}$ reduction were 0.9998 and 0.9660, respectively, suggesting that the model explains 99.98% and 96.6% of the total variation, respectively, leaving only 0.02% and 3.4% unaccounted for.

This indicates an excellent correlation between experimental and fitted values. This high R^2 value indicates a correlation between predicted data and experimental data. The elevated adjusted coefficient of determination, R^2 adjusted (0.9395 and 0.8968), supports the model's high significance.

Table 4- 6. ANOVA table for a quadratic model of protein reduction with three-factor Box-Behnken Design for manure and pineapple peel waste (PPW).

Source	DF	Adj SS	Adj MS	F-Value	p-Value
Model	9	1717.73	190.86	279.24	0.0008
Linear	3	1671.00	557.00	11029.28	0.000
A-Manure VS (g L ⁻¹)	1	0.23	0.23	4.51	0.071
B- Pineapple VS (g L ⁻¹)	1	8.60	8.60	170.34	0.000
C-Time (hrs)	1	1662.17	1662.17	32912.99	0.000
Square	3	42.13	14.04	278.09	0.000
A ² -Manure VS (g L ⁻¹)*Manure VS (g L ⁻¹)	1	0.15	0.15	2.92	0.131
B ² -Pineapple VS (g L ⁻¹)*Pineapple VS (g L ⁻¹)	1	1.28	1.28	25.36	0.002
C ² - Time (h)*Time (h)	1	39.35	39.35	779.25	0.000
2-Way Interaction	3	4.60	1.53	30.35	0.000
AB- Manure VS (g L ⁻¹)*Pineapple VS (g L ⁻¹)	1	1.62	1.62	32.09	0.001
AC-Manure VS (g L ⁻¹)*Time (h)	1	2.68	2.68	53.11	0.000
BC-Pineapple VS (g L ⁻¹)*Time (h)	1	0.30	0.30	5.85	0.046
Error	7	0.35	0.05		
Lack-of-Fit	3	0.20	0.07	1.79	0.288
Pure Error	4	0.15	0.04		
Total	16	1718.08			
R ²			R ² (adj.)		R ² (pred.)
0.9998			0.9395		0.9080

Table 4- 7. ANOVA table for a quadratic model of NH₃-N reduction with three-factor Box-Behnken Design for manure and pineapple peel waste (PPW).

Source	DF	Adj SS	Adj MS	F-Value	p-Value
Model	9	7459.07	828.79	159.40	0.0009
Linear	3	7450.07	2483.36	1676.18	0.000
A- Manure VS (g L ⁻¹)	1	6.19	6.19	4.18	0.080
B- Pineapple VS (g L ⁻¹)	1	4.39	4.39	2.96	0.129
C- Time (h)	1	7439.49	7439.49	5021.40	0.000
Square	3	4.84	1.61	1.09	0.414
AA- Manure VS (g L ⁻¹)*Manure VS (g L ⁻¹)	1	0.98	0.98	0.66	0.042
BB- Pineapple VS (g L ⁻¹)*Pineapple VS (g L ⁻¹)	1	0.74	0.74	0.50	0.052
CC-Time (h)*Time (h)	1	3.37	3.37	2.27	0.070
2-Way Interaction	3	4.15	1.38	0.93	0.073
AB-Manure VS (g L ⁻¹)*Pineapple VS (g L ⁻¹)	1	0.87	0.87	0.59	0.049
AC- Manure VS (g L ⁻¹)*Time (h)	1	0.41	0.41	0.28	0.091
BC-Pineapple VS (g L ⁻¹)*Time (h)	1	2.87	2.87	1.94	0.147
Error	7	10.37	1.48		
Lack-of-Fit	3	1.61	0.54	0.25	0.861
Pure Error	4	8.76	2.19		
Total	16	7469.44			
R ²			R ² (adj.)		R ² (pred.)
0.9660			0.8968		0.8170

Furthermore, the R^2 predicted (0.9080 and 0.8170) indicates favorable agreement between experimental and predicted values for protein and ammonia reduction, respectively. Notably, R^2 predicted aligns reasonably well with R^2 adjusted, affirming that the model effectively captures system response within the experimental range, providing reliable estimates. A lack-of-fit (LOF) test was conducted, and its results indicated insignificance, confirming the satisfactory fit of the developed model to the data. As depicted in Tables 4-6 and 4-7, the LOF test results for both responses were not statistically significant, providing 0.288 for protein reduction (Table 4-6) and 0.861 for NH₃-N reduction (Table 4-7). The obtained p -values for LOF have $p > 0.05$, proving that both responses were insignificant. Table 4-6 provides the p -values for each variable, indicating that manure (A), pineapple (B), and time (C) exert a significant ($p < 0.05$) influence on protein reduction. Additionally, BB, CC, AB, AC, and BC interactions significantly impact the reduction of manure protein. Similarly, the ANOVA table for NH₃-N (Table 4-7) indicates that C, AA, AC, and BC have a significant impact ($p < 0.05$). The data analysis for protein and NH₃-N reduction led to the derivation of the second-order polynomial model (Eqs 4-3 and 4-4).

$$\begin{aligned} \text{Protein reduction (\%)} = & 4.403 - 0.405 * A + 0.391 * B + 0.9034 * C - 0.0299 A * A - \\ & 0.0613 B * B - 0.006317 C * C + 0.0849 A * B + 0.01489 A * C - \\ & 0.00412 B * C \end{aligned} \quad (4-3)$$

$$\begin{aligned} \text{NH}_3\text{-N reduction (\%)} = & 10.15 - 1.45 * A - 0.864 * B + 1.469 * C + 0.0774 A * A + \\ & 0.0467 B * B - 0.00185 C * C + 0.0622 A * B - 0.0058 A * C + \\ & 0.01284 B * C \end{aligned} \quad (4-4)$$

Where A, B, and C represent manure loading, pineapple peel waste loading, and reaction time, respectively. In Eq. (4-3) and (4-4), the interactions (BC) and (AC) have negative coefficients, implying that the maximum protein reduction occurs at the center point. Additionally, if one variable increases while the others decrease beyond the center point, there is no significant impact on the protein or ammonia reduction. The negative regression coefficients for the square terms (AA, BB, CC) of Eq. (4-3) indicate that deviating from the center level reduces the optimal protein reduction, and (CC) of Eq. (4-4) indicates that deviating from the center level reduces the optimal ammonia reduction. This observation may be attributed to variations in parameter levels from the central points (Nashiruddin et al., 2022).

4.7.3 Interactive effects of parameters

The present investigation utilized three-dimensional (3D) and contour plots to assess the interactions among parameters such as manure, PPW, and time and their impact on protein and ammonia reduction. Figure 4-5 was generated by examining the relationships between two independent variables, with a third parameter held constant at optimal conditions.

This response surface plot, Figure 4-5 (a), depicts the combined effect of two independent variables, manure (x-axis) and PPW (y-axis) - on the response variable (protein reduction (%)), with the third factor (time) held constant at the midpoint level. The manure variable ranges from a low coded level of -1 to a high coded level of +1. Based on the axis labels, the corresponding manure's low amount is 4 g VS L⁻¹ and the high amount is 9 g VS L⁻¹. Similarly, the PPW variable ranges from a low coded level of -1 (1 g VS L⁻¹) to a high coded level of +1 (7 g VS L⁻¹). The response variable protein reduction (%) is represented vertically on the z-axis. Lower points indicate less reduction, while higher points indicate more reduction.

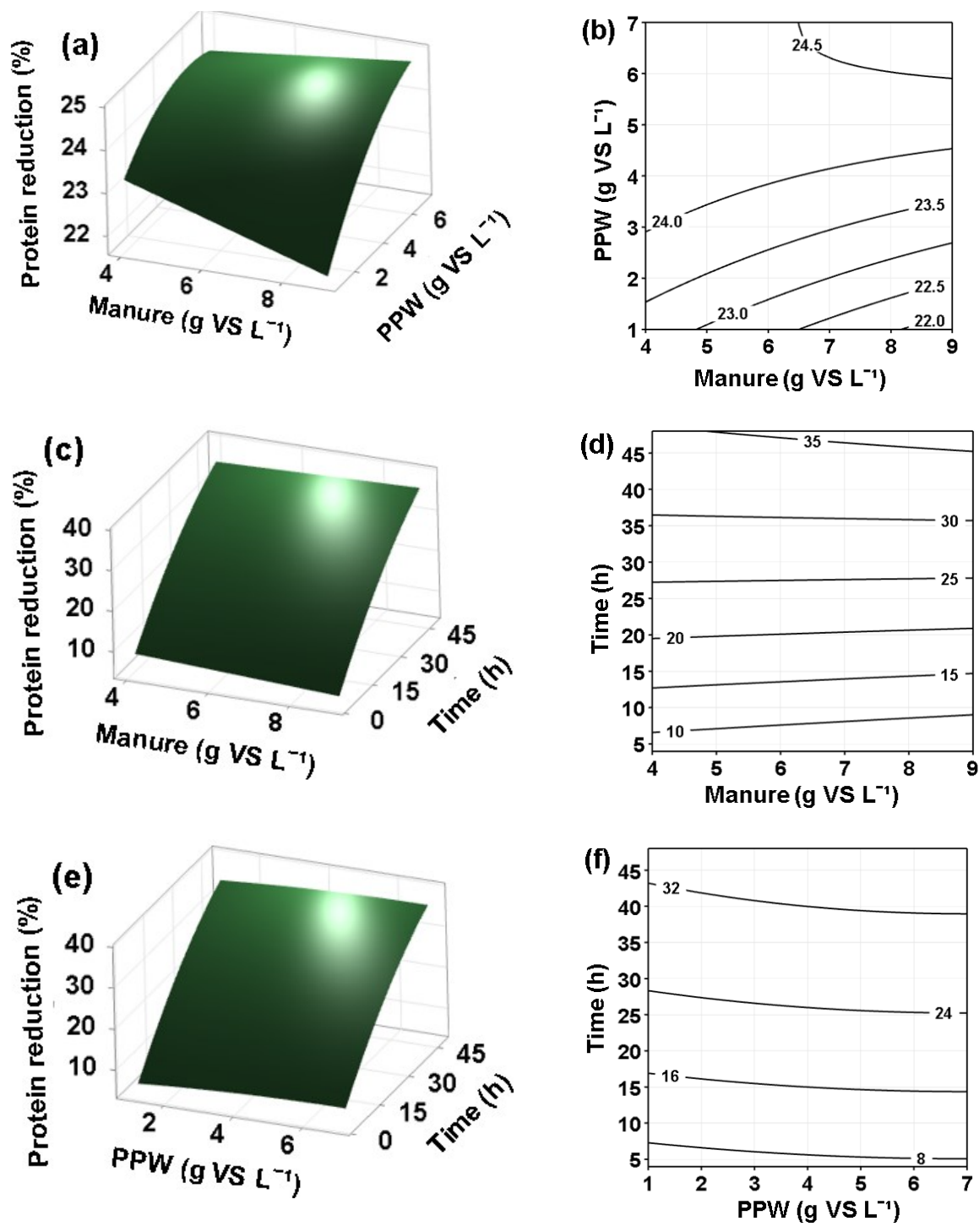


Figure 4- 5. 3D and contour response surface plots of the interactive effect of (a) and (b) manure with pineapple peel waste (PPW) dosage, (c) and (d) manure dosage with hydrolysis time, and (e) and (f) PPW dosage with time on protein reduction.

The plot shows that protein reduction increases by up to 25.2 % in a dose-dependent manner as manure increases from 4 to 9 g VS L⁻¹ and PPW amounts increase from 1 to 7 g VS L⁻¹.

The peak response (maximum protein reduction 25.2 %) occurs when both factors are at their high coded levels of +1, corresponding to 9 g VS L⁻¹ manure and 7 g VS L⁻¹ PPW. The positive correlation suggests that increased PPW amounts likely lead to higher concentrations of proteases, facilitating a more effective breakdown of proteins within a larger quantity of manure. Proteases can decompose proteins or peptides of manure by catalyzing hydrolysis of peptide bonds (Zhai et al., 2022). Figure 4-5 (c) This plot depicts the interaction of manure (x-axis) and time (y-axis) on protein reduction, with the PPW amount held constant at the midpoint.

The sharp upward slope along the y-axis indicates that reaction time favors protein reduction without being greatly affected by the manure dosage. The sharp upward slope along the y-axis from 5.3% to 32% at 4 g VS L⁻¹ manure loading indicates that time (h) has a pronounced positive effect on protein reduction.

This is likely because the extended hydrolysis duration, facilitated by the protease enzymes from KPW, enhances the breakdown of proteins in the manure. With higher protein reduction of 35.3% at 48 h compared to 8.1% at 4 h, the longer duration allows the reactions to proceed further. A similar study by Johny et al. (2021) reported 30 to 45 h for the highest enzymatic digestion of chicken egg white protein using protease from pineapple using Box-Behnken design. As the PPW dosage rises from 1 to 7 g VS L⁻¹, there is an evident increase in protein reduction, ranging from 5.3% to 7.9%. The most substantial protein reduction, reaching 36.3%, occurs when utilizing the highest PPW dosage of 7 g VS L⁻¹ coupled with the longest time (48 h). This finding indicates a synergistic effect of elevated PPW dosage and extended time on achieving the maximum reduction in protein content. Figure 4-5 (b) shows a contour plot exhibiting the effect of manure and PPW

on protein reduction (%). Figure 4-5 (b) shows the contour lines are evenly spaced, indicating a relatively linear increase in protein reduction when moving from lower to higher PPW and manure concentrations. A steep gradient or slope in the contour lines was observed moving from the x-axis (4 to 6 g VS L⁻¹ manure) to the y-axis (4 to 7 g VS L⁻¹ PPW). This visually indicates the strong positive effects of increasing both substrates. ANOVA table for protein reduction (Table 4-6) also proves a strong interaction between manure and PPW ($p < 0.05$) (Otieno et al., 2023). The concentric nature of the contour lines shows manure has a slightly stronger effect than PPW. The lines are more “stacked” vertically as manure increases. The evenly spaced, linear contour lines with manure on the y-axis and time on the x-axis indicate that the effect of one factor on the response variable is influenced by the level of the other factor (Choojit et al., 2018). The slope of the contours is steepest moving along time (y-axis), reflecting the dual positive effects of manure and time (Dahunsi et al., 2022). The evenly spaced horizontal contour lines indicate time's constant, linear impact in Figure 4-5 (f). As before, increasing either variable increases protein reduction. The effect of time is linear, while the effect of PPW is exponential.

Figure 4-6 presents a comprehensive graphical representation of the interactive effects of various treatment parameters on NH₃-N reduction. This figure is divided into three main parts, each illustrating different combinations of variables through both contour response surfaces and 3D plots. The interaction between manure and PPW dosage is presented in parts (a) and (b). Parts (c) and (d) focus on combining manure dosage and hydrolysis time. Lastly, parts (e) and (f) investigate the effects of varying PPW dosage with time.

Three-dimensional response surface plots based on Eq. (4-4) demonstrate the interaction effects of two factors on NH₃-N reduction (Figure 4-6).

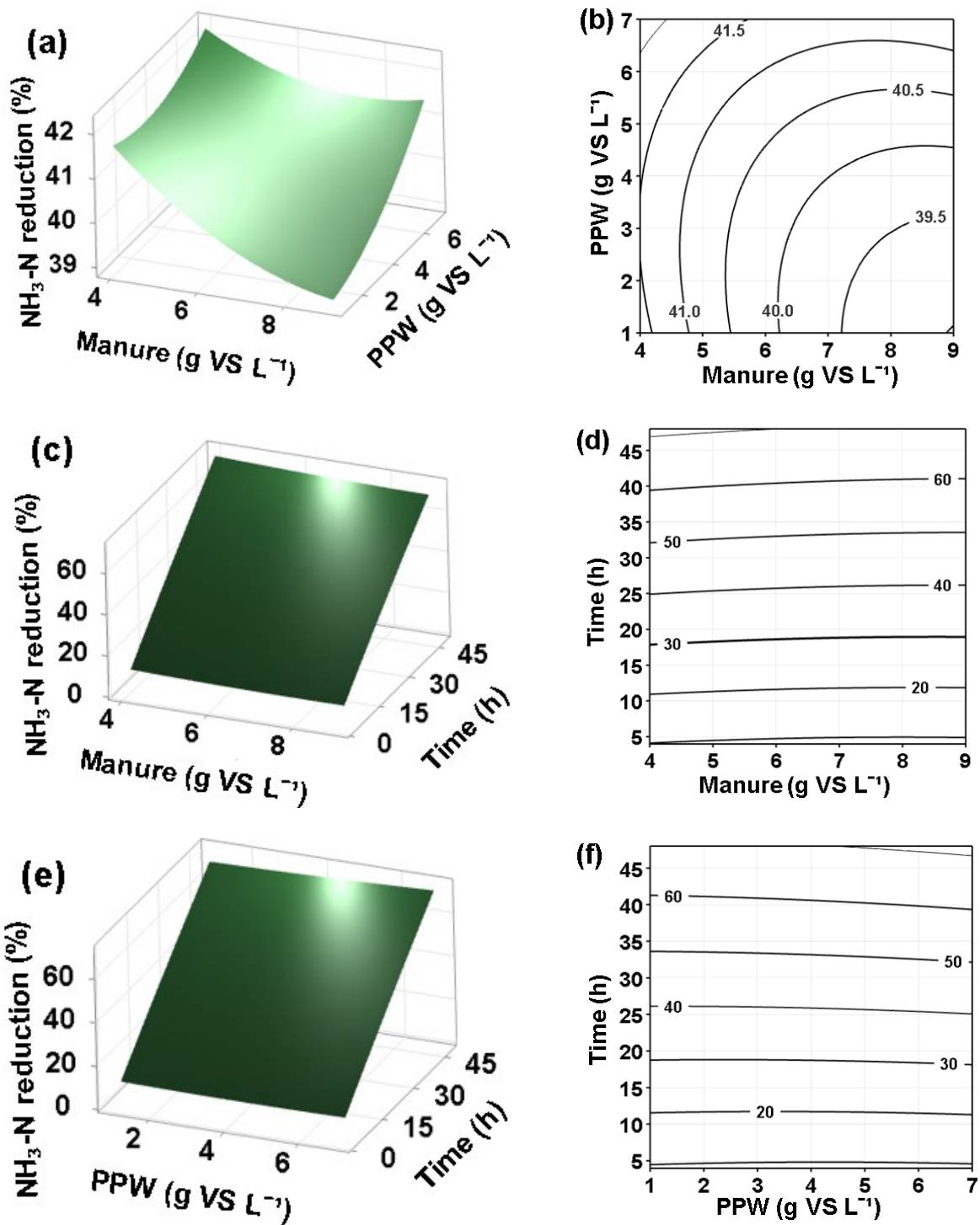


Figure 4- 6. 3D and contour response surface of the interactive effect of (a) and (b) manure with pineapple peel waste (PPW) dosage, (c) and (d) manure dosage with hydrolysis time, and (e) and (f) PPW dosage with time on $\text{NH}_3\text{-N}$ reduction.

Figure 4-6 (a) shows the interaction between PPW (g VS L^{-1}) and manure (g VS L^{-1}) on ammonia reduction (%). As PPW dosage increases, a greater $\text{NH}_3\text{-N}$ reduction is observed. At 9 g VS L^{-1} manure dosage, increasing the PPW dosage from 1 to 7 g VS L^{-1} increased $\text{NH}_3\text{-N}$ reduction from 39% to 41.4%. The combination of the lowest manure dosage (4 g VS L^{-1}) with the highest PPW dosage (7 g VS L^{-1}) provides the highest $\text{NH}_3\text{-N}$ reduction (42.2%). This suggests that PPW and manure work synergistically to reduce ammonia. The PPW likely provides enzymes like bromelain that help break down proteins and reduce ammonia (Agrawal et al., 2022). Meanwhile, the manure provides bacteria and other microorganisms that can metabolize and reduce ammonia (Kim et al., 2021). The C/N ratio is crucial in biological processes.

Manure typically has a high nitrogen content (Gong et al., 2020), and adding PPW, which likely has a higher carbon content (Zhu et al., 2019), may improve the C/N ratio. A balanced C/N ratio (20 to 30) is favorable for microbial activity involved in ammonia reduction (Wang et al., 2014). The interaction of manure (g VS L^{-1}) and time (h) on ammonia reduction (%) is presented in Figure 4-6 (c). Ammonia reduction increases over time for all manure concentrations from 4 to 9 g VS L^{-1} . At 48 h, a manure dosage of 4 and 9 g VS L^{-1} provided a maximum ammonia reduction of 70.2% and 68.9%, respectively. Lower manure concentrations lead to faster and more significant ammonia reduction. At higher manure concentrations, inhibitory substances, such as excessive ammonia, may accumulate, hindering microbial activity and creating a counterintuitive effect. On the other hand, a higher PPW dosage led to faster and greater ammonia reduction over time. Ammonia removal reached 69.1% after 48 h at a PPW dosage of 7 g VS L^{-1} , while a 65.3% reduction was observed at a PPW dosage of 1 g VS L^{-1} (Figure 4-6 (e)). Elevated enzyme activity in PPW, like bromelain, accelerates protein breakdown into ammonia (Paridhi et al., 2022).

Figure 4-6 (b) depicts the impact of the interaction between manure and PPW on ammonia reduction (%) at a constant 26 h hydrolysis time. The contour plot's shape can reveal the significance and interaction among variables. A larger gradient indicates a more substantial impact on the experiment. Elliptical contour lines indicate strong interaction, while circular contour lines suggest no interaction (Açikel et al., 2010). The contour plot (Figure 4-6 (b)), exhibiting an elliptical shape, signifies a substantial interaction between manure and PPW factors (Li et al., 2017), also aligns with the p-value ($p < 0.05$) presented in Table 4-7. The observed linear contours with parallel horizontal lines in the contour plot of manure (x-axis) and time (y-axis) (Figure 4-6 (d)) and PPW (x-axis) and time (y-axis) (Figure 4-6 (f)) suggest that changes in time have a consistent effect on the response variable (ammonia reduction) across different manure or PPW dosage. Likewise, changes in manure or PPW concentration have a consistent effect across different time points. This independence suggests that the impact of one variable does not depend on the level of the other, supporting the notion of their independence (Srinivasa et al., 2023). The ANOVA table (Table 4-7) also shows no significant two-way interaction between manure and time or PPW and time ($p > 0.05$).

4.7.4 Effects on ammonium reduction

Figure 4-7 allows us to easily compare and contrast the results between the control and the sample treated with PPW across all experimental sets. In all experimental sets, the $\text{NH}_4\text{-N}$ of the sample treated with PPW is lower than that in the control. This indicates that the treatment with PPW consistently reduces $\text{NH}_4\text{-N}$ concentration. The extent of reduction varies across experimental sets. For instance, set 1 shows a substantial reduction of $72 \pm 0.21\%$ (from 1028.90 ppm (control) to 279.83 ppm (treated)). Conversely, set 7 only shows a relatively minimal

reduction of $6\pm 0.12\%$ (from 1459.61 ppm (control) to 1272.34 ppm (treated)). The highest $\text{NH}_4\text{-N}$ concentration in the control is observed in set 7 at 1459.61 ppm (manure 9 g VS L^{-1}). In contrast, the lowest $\text{NH}_4\text{-N}$ concentration in the control is observed in set 12 at 897.81 ppm (manure 4 g VS L^{-1}), showing that higher manure loading causes higher $\text{NH}_4\text{-N}$. When manure is added to a digester, the organic nitrogen in the manure begins to break down in a process called mineralization. During mineralization, organic nitrogen is converted into inorganic forms, with ammonium (NH_4^+) being one of the primary products. This process increases the concentration of $\text{NH}_4\text{-N}$ in the system (Bhogal et al., 2016). The rate of $\text{NH}_4\text{-N}$ reduction is influenced by the time allowed for hydrolysis. The efficiency of decreasing $\text{NH}_4\text{-N}$ levels rose from $12\pm 0.21\%$ to $73\pm 0.54\%$, contingent on a hydrolysis duration ranging from 4 to 48 h. Allowing more time for the hydrolysis process can lead to an increased enzymatic action (Shahi et al., 2020). Arun and Sivashanmugam (2017) found that protease activity increased from 10.95 (U/ml) on day 1 to 76.53 (U/ml) on day 3. This performance in reducing $\text{NH}_4\text{-N}$ aligns with prior research by Nguyen et al. (2022) on prolonged hydrolysis in treating swine and pineapple wastes, which reported reductions of 78% and 85% over periods of 6 and 24 h, respectively.

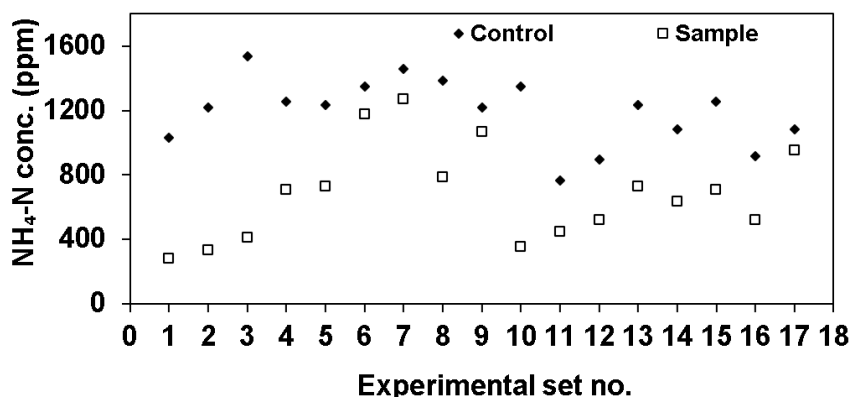


Figure 4- 7. Ammonium nitrogen ($\text{NH}_4\text{-N}$) concentration of control and in the test samples.

Figure 4-8 presents the reduction efficiency of ammonia nitrogen ($\text{NH}_3\text{-N}$) and ammonium nitrogen ($\text{NH}_4\text{-N}$) achieved through the hydrolysis of pineapple peel waste and manure, as outlined by the statistical design of the study.

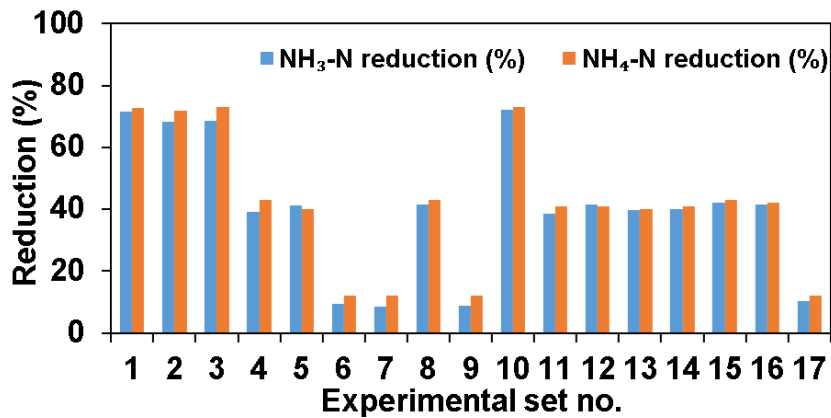


Figure 4- 8. Ammonia nitrogen ($\text{NH}_3\text{-N}$) and ammonium nitrogen ($\text{NH}_4\text{-N}$) reduction efficiency of pineapple peel waste and manure hydrolysis as per statistical design.

Overall, a noticeable trend emerges from the data, as represented in Figure 4-8. The reduction percentages for ammonium ($\text{NH}_4\text{-N}$) are predominantly higher than those for ammonia (NH_3) across most runs. Notable exceptions are run 1, 12, 13, 14, 15, and 16, where $\text{NH}_4\text{-N}$ reduction is recorded as the same or slightly higher at $72\pm 0.21\%$, $41\pm 0.84\%$, $40\pm 0.23\%$, $41\pm 0.39\%$, $43\pm 0.36\%$ and $42\pm 0.23\%$, respectively, while NH_3 reduction stands at $71\pm 0.51\%$, $41\pm 0.54\%$, $39\pm 0.25\%$, $40\pm 0.51\%$, $42\pm 0.33\%$ and $41\pm 0.46\%$, respectively. Runs 1, 2, 3, and 10 consistently show high reduction percentages for NH_3 and $\text{NH}_4\text{-N}$. This is especially pronounced for run 1, where NH_3 and $\text{NH}_4\text{-N}$ exhibit nearly identical reduction rates of $71\pm 0.51\%$ and $72\pm 0.21\%$, respectively. Such high efficiencies could indicate optimum substrate concentrations and treatment times, favoring maximum nitrogenous compound breakdown, as Fuchs et al. (2018) suggested. Runs 4, 5, 12, 15,

and 16 demonstrate a mid-tier reduction efficiency ranging from $40\pm 0.22\%$ to $43\pm 0.36\%$. The NH_3 and $\text{NH}_4\text{-N}$ reductions here are fairly close, suggesting a balanced enzymatic and metabolic activity under these conditions (Dai & Karring, 2014). Runs 7, 8, 9, and 17 display a pronounced disparity between NH_3 and $\text{NH}_4\text{-N}$ reduction rates. Specifically, run 7 stands out, with NH_3 was reduced by $8\pm 0.32\%$, while $\text{NH}_4\text{-N}$ was reduced by only $12\pm 0.55\%$. The divergence could be attributed to the inherent differences in pH, solubility, and enzymatic degradation rates between NH_3 and $\text{NH}_4\text{-N}$. NH_3 and $\text{NH}_4\text{-N}$ are interrelated, with the balance between them influenced by factors like pH (Park et al., 2015). Runs 11 ($38\pm 0.21\%$ and $41\pm 0.92\%$), 13 ($39\pm 0.25\%$ and $40\pm 0.23\%$), and 14 ($40\pm 0.51\%$ and $41\pm 0.39\%$) manifest slight variances in reduction percentages between NH_3 and $\text{NH}_4\text{-N}$. While not as pronounced as in the previous group, the differences still underscore the intricate balance of enzymatic processes and substrate availability.

4.7.5 Effects on volatile solids reduction

Figure 4-9 presents the VS reduction in the hydrolysis of manure by PPW as per the statistical modeling. The VS play a pivotal role in anaerobic digestion, serving as the primary substrate that undergoes microbial degradation. During the hydrolysis, these solids are broken down into smaller, soluble compounds, paving the way for subsequent biological processes. This step is crucial as it impacts the digestion process's efficiency and efficacy. VS are commonly perceived as an indicator of the organic component within the total solids (TS). However, a more precise characterization would regard it as the portion of the material in a sample that evaporates upon ignition. To ascertain the VS content, one ignites the residual solids from the TS determination at $500\text{-}550\text{ }^\circ\text{C}$, although some loss due to volatilization might have occurred during the total solids measurement (Telliard, 2001).

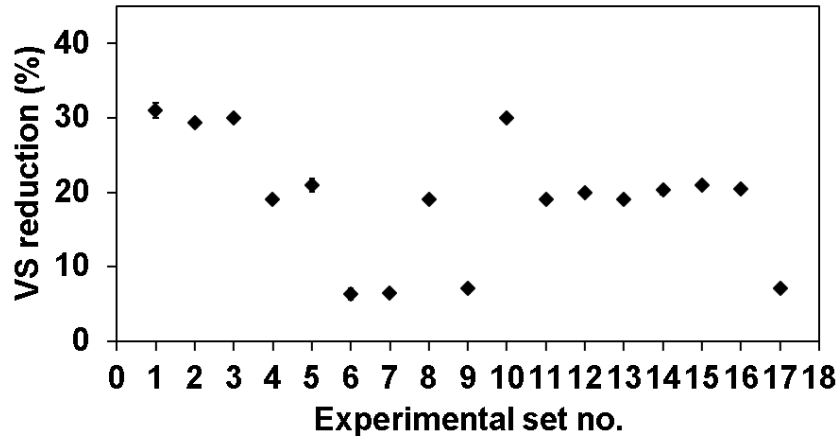


Figure 4- 9. Volatile solids (VS) reduction in the experimental sets for manure protein hydrolysis by pineapple peel waste.

In the assessment of VS reduction across 17 experimental sets, the maximum VS reduction observed was $32 \pm 0.35\%$ in run 3 (manure: 9 g VS L^{-1} , PPW: 4 g VS L^{-1} , time: 48 h), while the minimum reduction was $6 \pm 0.75\%$ in run 6 (manure: 6.5 g VS L^{-1} , PPW: 7 g VS L^{-1} , time: 4 h). Within individual runs, the VS reduction efficiency increased considerably over time, highlighting the temporal aspect of the hydrolysis process. When collated, the VS reductions amongst runs displayed significant differences. VS removal ranged from $6 \pm 0.75\%$ to $7 \pm 0.6\%$ at 4 h, $19 \pm 0.11\%$ to $21 \pm 0.87\%$ at 26 h, and $29 \pm 0.55\%$ to $31 \pm 0.98\%$ at 48 h. This data indicates an increasing removal rate as time progresses, with certain runs achieving peak reduction efficiencies at 48 h. Similarly, with the rise in time from 7 to 15 days, the VS reduction grew from 41.0% to 51.2% and further reached 63.4% at 25 days during municipal sludge hydrolysis (Wang et al., 2022). In another study, the co-digestion of cattle manure and corn stover pre-digested for 3 days yielded a VS reduction of 43.3%, while a 7-day pre-digestion resulted in an efficiency of 51.8% (Joseph et al., 2019). Ameen et al. (2021) observed analogous results, noting a $57 \pm 2\%$ reduction in VS after 48 h hydrolysis of animal manure combined with microbial biomass.

4.8 Optimization and Model Validation

Optimizing protein degradation and ammonia removal in hydrolysis reactors is crucial, as it minimizes ammonia accumulation, promoting higher gas yields in digesters. Different run combinations yielded optimal results: run 10 achieved the highest $\text{NH}_3\text{-N}$ removal ($72\pm 0.48\%$), run 3 provided maximum $\text{NH}_4\text{-N}$ removal ($73\pm 0.54\%$); and run 3 and 10 had maximum protein reduction ($36\pm 0.25\%$ and $36\pm 0.53\%$). Similarly, run 3 and 10 show the peak VS reduction ($30\pm 0.32\%$ and $30\pm 0.12\%$). Various mixtures led to distinct optimal results, such as manure 9 g VS L^{-1} , PPW 4 g VS L^{-1} and 48 h (run 3), and manure 6.5 g VS L^{-1} , PPW 7 g VS L^{-1} and 48 h (run 10). Thus, optimizing all four responses under identical conditions is challenging due to their distinct combination of substrate loading. The technique set constraints for $\text{NH}_3\text{-N}$ removal, $\text{NH}_4\text{-N}$ removal, and protein degradation at maximum values of 50%, 60%, and 30%, respectively. To confirm the models, optimal settings of 9 g VS L^{-1} manure, 6 g VS L^{-1} PPW, and a duration of 26 h were selected (Table 4-8).

The optimal settings for verifying the models were at manure dosage: 9 g VS L^{-1} , PPW dosage: 6 g VS L^{-1} , and 26 h hydrolysis time. The expected outputs were 40% and 42% $\text{NH}_3\text{-N}$ and $\text{NH}_4\text{-N}$ reduction, along with 25% protein reduction. The test under these conditions (manure dosage: 9 g VS L^{-1} , PPW dosage: 6 g VS L^{-1} , and 26 h hydrolysis time) reduced $\text{NH}_3\text{-N}$ by $39.5\pm 3.4\%$, protein by $23\pm 2.1\%$, $\text{NH}_4\text{-N}$ by $42\pm 1.8\%$, aligning with the predicted data. This suggests that the models effectively forecast the hydrolysis process. In consecutive quadruplicate tests using the defined conditions, desired reductions in $\text{NH}_3\text{-N}$, protein, $\text{NH}_4\text{-N}$, and VS were effectively achieved.

Table 4- 8. Ammonia nitrogen, ammonium nitrogen, and protein reduction under optimum conditions.

Dosage (g VS L ⁻¹)		Time (h)	Reduction (%)			
Manure	PPW		NH ₃ -N	Protein	NH ₄ -N	VS
9	6	26	43	25	39	22
9	6	26	41	25	44	22
9	6	26	35	20	42	19
9	6	26	39	22	43	21

4.9 Chemical and Morphological Analysis

Subsection 4.10.1 examines Fourier Transform Infrared Spectroscopy (FTIR), a technique used for detecting and identifying functional groups involved. Subsection 4.10.2 covers SEM (Scanning Electron Microscopy), which allows the examination of the minute structural details and surface textures of materials before and after hydrolysis. Both these techniques are crucial for thoroughly understanding the studied materials' composition and physical appearance.

4.9.1 Fourier Transform Infrared (FTIR) spectroscopy

The study assessed the influence of hydrolysis on the decomposition of manure and pineapple peel waste through an extensive analysis using Fourier Transform Infrared (FTIR) spectroscopy, spanning a duration of up to 48 h. Variations in the FTIR spectra within the sample mixture were identified by focusing on the wavenumber range of 4000 to 400 cm⁻¹. The FTIR graphs depicting the changes in manure and PPW characteristics before and after hydrolysis displayed discernible distinctions, with alterations observed in the functional groups as hydrolysis progressed (Figure 4-10).

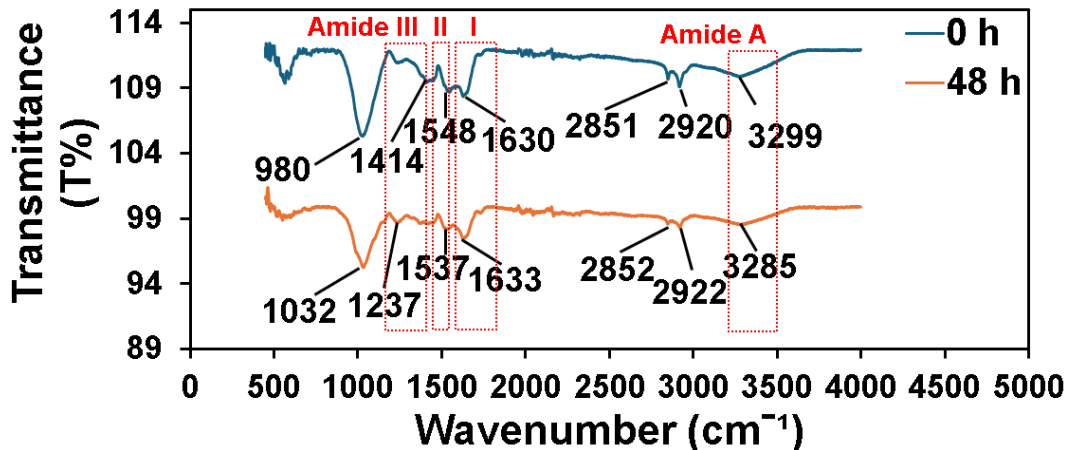


Figure 4- 10. FTIR spectrum of manure and pineapple peel waste at 0 h (control) and 48 h.

Prominent peaks were observed at 3299, 2920, 2851, 1630, 1548, 1414, 1244, and 980 cm^{-1} , as depicted in Figure 4-10 (control). Strong and broad peaks in 3550-3200 cm^{-1} belong to O-H stretching (Boukaoud et al., 2021). A peak at 3299 cm^{-1} indicates O-H stretching from alcohols, phenols, or N-H stretching from primary or secondary amines. In the 48-h sample, the peak's intensity became broader and shifted to 3285 cm^{-1} , suggesting an increase in the number of hydroxyl (alcohol or phenol) or amine groups as a result of the hydrolysis process. A shift to a lower wavenumber (3285 cm^{-1}) suggests the presence of more hydroxyl (alcohol) or amine groups in the sample. These groups are known for forming hydrogen bonds, which can cause this shift in IR spectra (Cheng et al., 2013). The peaks at 2920 cm^{-1} and 2851 cm^{-1} in control correspond to C-H stretching vibrations typical of alkanes. After 48 h hydrolysis, the peaks increased with slight shifting towards 2922 and 2852 cm^{-1} ; it could indicate the samples have not undergone significant changes or fewer alterations of alkane groups. However, shifting could suggest a change in the molecular environment, possibly due to the formation of new compounds or alteration of existing ones (Cheng et al., 2013). The spectral domain from 1700 to 1200 cm^{-1} encompasses a composite

assortment of vibrational bands attributed to the molecular constituents of fatty acids, proteins, and polysaccharides. The 1600 to 1800 cm^{-1} represents the Amide I peak, the Amide II peak at 1580 to 1400 cm^{-1} , and the Amide III peak at 1200 to 1350 cm^{-1} . Within the analyzed spectrum, three principal peaks are distinctly prominent in the control: the 1630 cm^{-1} , associated with C=O stretching and C-N stretching vibrations; the Amide II peak at 1548 cm^{-1} , corresponding to N-H bending and C-N stretching vibrations; and the Amide III 1244, which is characteristic of peptide bond vibrations (CO-NH). The prominence and intensity of these peaks are intricately connected to the protein content present in the samples (Fagbemi et al., 2020). The peak in the Amide I region has an intense or shifted position; it implies that the secondary structure of proteins has been disrupted. For example, a sharp peak and a shift towards 1633 cm^{-1} might suggest an increase in beta-sheet content, which is a sign of protein disintegration or unfolding (Furlan et al., 2007). The Amide II band is typically sharp and well-defined in spectra 1548 and 1414 cm^{-1} of 0 h sample, reflecting the combination of N-H bending and C-N stretching vibrations. A noticeable decrease in the intensity (loss of peak at 1414 cm^{-1}) or a shift of this band (at 1537 cm^{-1}) in the 48-h sample indicates a loss of native protein structure, potentially due to proteolysis. Since proteinase enzymes break peptide bonds, the N-H bending and C-N stretching vibrations would be affected, leading to a less defined Amide II region (Stani et al., 2020). The Amide III region can be complex due to the mixture of vibrations involved, but it generally provides additional confirmation of the protein's secondary structure. Changes in this region, such as a reduction in intensity or a shift in peaks (from 1244 cm^{-1} to 1237 cm^{-1}), would further corroborate the alteration or distortion of the protein structure (Lazarevska & Makreski, 2015). The region dominated by polysaccharide peaks is centered between 1150-900 cm^{-1} (El Darra et al., 2017), where the peak around 1032 cm^{-1} (48 h sample) is generally associated with OH stretch of carbohydrate. The carbohydrate region at 980

cm^{-1} in control (between 1150 and 900 cm^{-1}) transformed into spectra with a less sharpened peak (1032 cm^{-1}) in 48 h sample, proving the C-O peak (1032 cm^{-1}) decreased as hydrolysis proceeded (Andrade et al., 2019). A clear reduction in the intensity of the Amide bands and shift towards frequencies associated with unfolded proteins provide strong evidence of the proteolytic action of enzymes from the PPW.

4.9.2 Scanning Electron Microscopy

Evaluation through Scanning Electron Microscopy (SEM) is employed to determine the efficacy of hydrolysis methods by observing the morphological alterations in samples exposed to varying conditions or treatments. The structural transformation of manure and PPW at sequential hydrolysis intervals of 6, 12, 24, and 48 h was meticulously documented using SEM at various magnifications, as depicted in Figure 4.11.

The control sample (Figure 4-11 (a) and (b)) presents a relatively rough and fibrillar, intact morphological structure. The fibrous elements of manure are clearly visible, with distinct, unbroken strands that indicate their native, unaltered state. The surface is heterogeneous with areas of compaction and pockets of porosity, typical of organic waste material.

After 6 to 12 h (Figure 4-11 (c) to (f)), there appears a noticeable change in the morphology. The fibrous structures appear less defined, suggesting the initiation of protease activity. The protease enzymes begin to break down protein structures, leading to a more amorphous and fragmented appearance. The edges of the fibrous elements may appear frayed, indicative of enzymatic digestion at the surface.

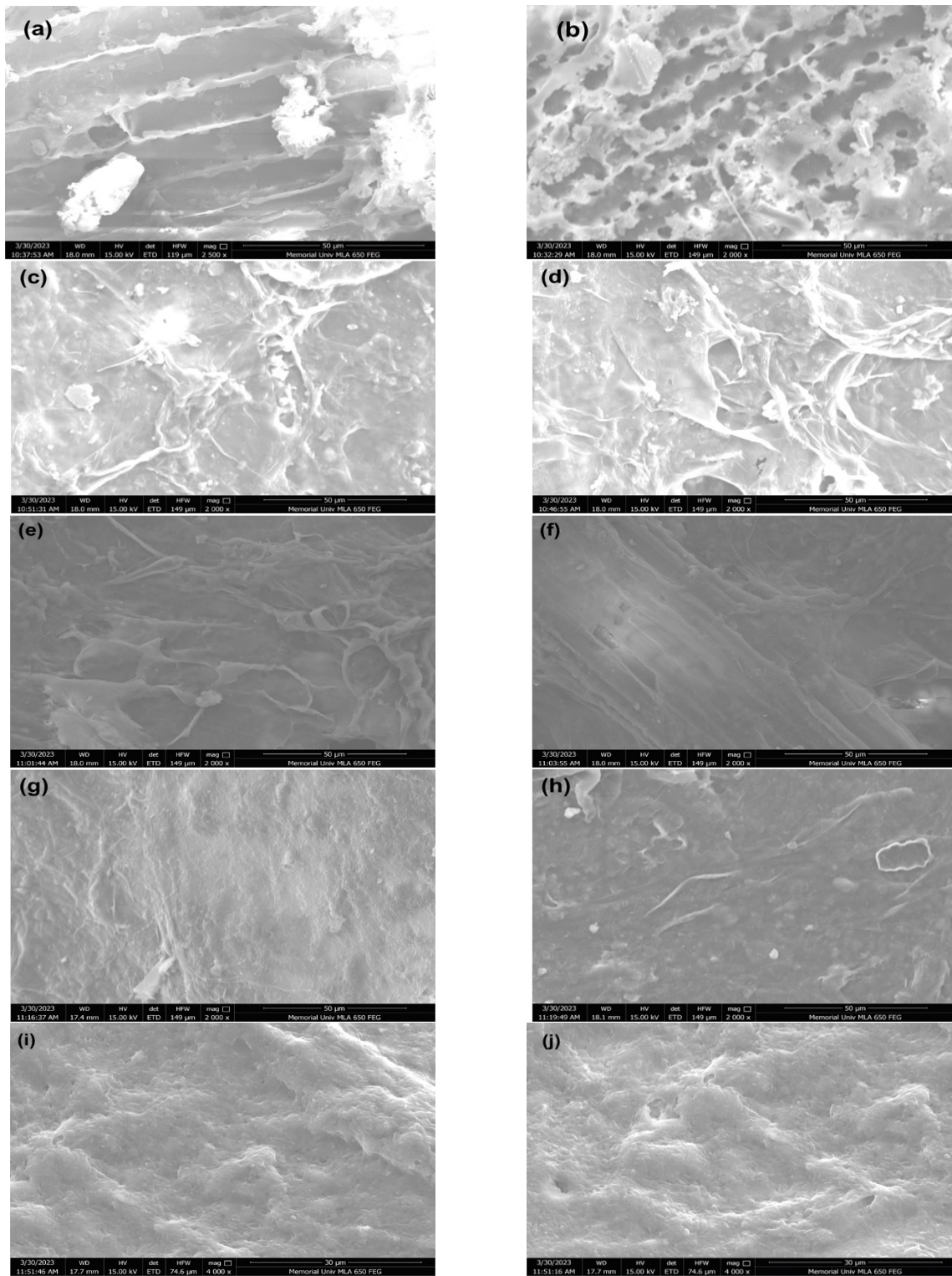


Figure 4- 11. Scanning electron microscope (SEM) images of (a) and (b) manure-pineapple peel waste (PPW) substrate control, and after hydrolysis at (c) and (d) 6 h, (e) and (f) 12 h, (g) and (h) 24 h, and (i) and (j) 48 h.

Shuai et al. (2022) observed similar findings; natural pea protein exhibits a tightly bound, non-uniform spherical shape. Following enzymatic treatment with agents such as flavourzyme, neutrase, alcalase, and trypsin, the spherical conformation of the protein is disrupted, resulting in fragmented structures.

At the 24-hour (Figure 4-11 (g) and (h)), the SEM images show an even greater degree of structural breakdown. The fibrous structures from the initial manure are becoming increasingly diffuse, and the porosity is more widespread. This indicates extensive proteolysis. After 48 h (Figure 4-11 (i) and (j)), the transformation is profound. The structural integrity of the original material is largely lost, replaced by a highly porous matrix that lacks a defined shape. This is characteristic of the final stages of protease action, where the resultant peptides and amino acids may be washed away or further degraded and fragmented, leaving behind a significantly altered microstructure. The results of this study agree closely with those reported by Islam et al. (2021), who observed that the protein in grass turtle muscle was broken down into smaller fragments with reduced particle size following the application of the papain enzyme during 8 h of hydrolysis. In addition, Ganesh Kumar et al. (2008) examined the 72 h hydrolysis of protein-laden tannery solid waste, and their results corroborate the results of the present study. The unhydrolyzed protein-rich solid waste initially displayed longitudinal and vertical fibrillar tissue fibers. Yet, after undergoing hydrolysis for 72 h, there was a significant alteration in the microstructural configuration, leading to the complete degradation of the fibrillar tissues.

4.10 Conclusions

This investigation has conclusively shown that proteases from pineapple peel waste (PPW) can effectively reduce protein content and ammonia build-up in the anaerobic digestion of protein-rich

waste. Using careful experimental design and statistical analysis, the study established the best conditions for manure protein hydrolysis, achieving notable decreases in protein levels and ammonia. The experiments indicated that varying the amounts of manure and PPW significantly impacted the reduction of manure proteins and ammonia. Specifically, a mixture 9 g VS_{manure} L⁻¹, and 4 g VS_{PPW} L⁻¹ over 48 h degraded protein by 36±0.25% and NH₄-N by 73±0.54%, while 6.5 g VS_{manure} L⁻¹, and 7 g VS_{PPW} L⁻¹ over 48 h reduced NH₃-N by 72±0.48% and volatile solids (VS) by 30±0.12%.

The resulting data produced a highly significant ($R^2 = 0.99$; $P < 0.0001$) quadratic regression model for both protein and NH₃-N reduction. Fourier Transform Infrared (FTIR) spectroscopy and Scanning Electron Microscopy (SEM) enabled an enhanced understanding of the structural modifications resulting from the treatment, thus affirming the proposed method's efficacy.

References

- Açikel, Ü., Erşan, M., & Açikel, Y. S. (2010). Optimization of critical medium components using response surface methodology for lipase production by *Rhizopus delemar*. *Food and Bioproducts Processing*, 88(1), 31-39. <https://doi.org/10.1016/j.fbp.2009.08.003>.
- Agrawal, P., Nikhade, P., Patel, A., Mankar, N., Sedani, S., & Nikhade, P. P. (2022). Bromelain: a potent phytomedicine. *Cureus*, 14(8), e2787610. [7759/cureus.27876](https://doi.org/10.7759/cureus.27876).
- Andrade, J., Pereira, C. G., de Almeida Junior, J. C., Viana, C. C. R., de Oliveira Neves, L. N., da Silva, P. H. F., Bell, M. J. V., & dos Anjos, V. d. C. (2019). FTIR-ATR determination of protein content to evaluate whey protein concentrate adulteration. *Lwt*, 99, 166-172. <https://doi.org/10.1016/j.lwt.2018.09.079>.
- Arun, C., & Sivashanmugam, P. (2017). Study on optimization of process parameters for enhancing the multi-hydrolytic enzyme activity in garbage enzyme produced from preconsumer organic waste. *Bioresource Technology*, 226, 200-210. <https://doi.org/10.1016/j.biortech.2016.12.029>.
- Astals, S., Peces, M., Batstone, D. J., Jensen, P. D., & Tait, S. (2018). Characterising and modelling free ammonia and ammonium inhibition in anaerobic systems. *Water Research*, 143, 127-135. <https://doi.org/10.1016/j.watres.2018.06.021>.
- Banks, C. J., & Heaven, S. (2013). Optimisation of biogas yields from anaerobic digestion by feedstock type. In *The Biogas Handbook: Science, Production and Applications*; Wellinger, A., Murphy, J., Baxter, D., (ED); Woodhead Publishing: Sawston, UK; pp. 131–165. <https://doi.org/10.1533/9780857097415.1.131>.

- Beg, S.; Akhter, S. Box–Behnken designs and their applications in pharmaceutical product development. In *Design of Experiments for Pharmaceutical Product Development: Volume: Basics and Fundamental Principles*; Beg, S., (ED); Springer: Singapore, 2021; pp. 77–85. https://doi.org/10.1007/978-981-33-4717-5_7.
- Bhogal, A., Williams, J., Nicholson, F., Chadwick, D., Chambers, K., & Chambers, B. (2016). Mineralization of organic nitrogen from farm manure applications. *Soil Use and Management*, 32, 32-43. <https://doi.org/10.1111/sum.12263>.
- Bonjoch, N.P.; Tamayo, P.R. (2001). Protein content quantification by Bradford method. In *Handbook of Plant Ecophysiology Techniques*; Springer: Berlin/Heidelberg, Germany; pp. 283–295. <https://doi.org/10.1111/sum.12263>.
- Boukaoud, A., Chiba, Y., & Sebbar, D. (2021). A periodic DFT study of IR spectra of amino acids: An approach toward a better understanding of the NH and OH stretching regions. *Vibrational Spectroscopy*, 116, 103280. <https://doi.org/10.1016/j.vibspec.2021.103280>.
- Bradford, M. M. (1976). A rapid and sensitive method for the quantitation of microgram quantities of protein utilizing the principle of protein-dye binding. *Analytical Biochemistry*, 72(1-2), 248-254. [https://doi.org/10.1016/0003-2697\(76\)90527-3](https://doi.org/10.1016/0003-2697(76)90527-3).
- Casabar, J. T., Ramaraj, R., Tipnee, S., & Unpaprom, Y. (2020). Enhancement of hydrolysis with *Trichoderma harzianum* for bioethanol production of sonicated pineapple fruit peel. *Fuel*, 279, 118437. <https://doi.org/10.1016/j.fuel.2020.118437>.
- Chen, W.-H., Uribe, M. C., Kwon, E. E., Lin, K.-Y. A., Park, Y.-K., Ding, L., & Saw, L. H. (2022). A comprehensive review of thermoelectric generation optimization by statistical

- approach: Taguchi method, analysis of variance (ANOVA), and response surface methodology (RSM). *Renewable and Sustainable Energy Reviews*, 169, 112917. <https://doi.org/10.1016/j.rser.2022.112917>.
- Cheng, F., Cao, Q., Guan, Y., Cheng, H., Wang, X., & Miller, J. D. (2013). FTIR analysis of water structure and its influence on the flotation of arcanite (K₂SO₄) and epsomite (MgSO₄· 7H₂O). *International Journal of Mineral Processing*, 122, 36-42. <https://doi.org/10.1016/j.minpro.2013.04.007>.
- Choojit, S., Ruengpeerakul, T., & Sangwichien, C. (2018). Optimization of acid hydrolysis of pineapple leaf residue and bioconversion to ethanol by *Saccharomyces cerevisiae*. *Cellulose Chemistry Technology*, 52, 247–257.
- Dahunsi, S. O., Ogunwole, J. O., Owoseni, A. A., Olutona, G. O., Nejo, Y. T., & Atobatele, O. E. (2022). Valorization of pineapple peel and poultry manure for clean energy generation. *Food and Energy Security*, 11(1), e228. <https://doi.org/10.1002/fes3.228>.
- Dai, X., & Karring, H. (2014). A determination and comparison of urease activity in feces and fresh manure from pig and cattle in relation to ammonia production and pH changes. *Plos One*, 9(11), e110402. <https://doi.org/10.1371/journal.pone.0110402>.
- David Troncoso, F., Alberto Sánchez, D., & Luján Ferreira, M. (2022). Production of plant proteases and new biotechnological applications: an updated review. *Chemistry Open*, 11(3), e202200017. <https://doi.org/10.1002/open.202200017>.
- El Darra, N., Rajha, H. N., Saleh, F., Al-Oweini, R., Maroun, R. G., & Louka, N. (2017). Food fraud detection in commercial pomegranate molasses syrups by UV–VIS spectroscopy,

- ATR-FTIR spectroscopy and HPLC methods. *Food Control*, 78, 132-137.
<https://doi.org/10.1016/j.foodcont.2017.02.043>.
- Fagbemi, O. D., Sithole, B., & Tesfaye, T. (2020). Optimization of keratin protein extraction from waste chicken feathers using hybrid pre-treatment techniques. *Sustainable Chemistry and Pharmacy*, 17, 100267. <https://doi.org/10.1016/j.scp.2020.100267>.
- Fuchs, W., Wang, X., Gabauer, W., Ortner, M., & Li, Z. (2018). Tackling ammonia inhibition for efficient biogas production from chicken manure: Status and technical trends in Europe and China. *Renewable and Sustainable Energy Reviews*, 97, 186-199.
<https://doi.org/10.1016/j.rser.2018.08.038>.
- Furlan, P. Y., Scott, S. A., & Peaslee, M. H. (2007). FTIR-ATR study of pH effects on egg albumin secondary structure. *Spectroscopy Letters*, 40(3), 475-482.
<https://doi.org/10.1080/00387010701295950>.
- Ganesh Kumar, A., Venkatesan, R., Kirubakaran, R., Prabhakar, T., & Sekaran, G. (2008). Effects of nonionic surfactant on hydrolysis and fermentation of protein rich tannery solid waste. *Biodegradation*, 19, 739-748. <https://doi.org/10.1007/s10532-008-9178-2>.
- Gong, X.-J., Qin, L., Liu, F., Liu, D.-N., Ma, W.-W., Zhang, T., Liu, X., & Luo, F. (2020). Effects of organic manure on soil nutrient content: A review. *The Journal of Applied Ecology*, 31(4), 1403-1416. <https://doi.org/10.13287/j.1001-9332.202004.025>.
- González, R., Peña, D. C., & Gómez, X. (2022). Anaerobic co-digestion of wastes: reviewing current status and approaches for enhancing biogas production. *Applied Sciences*, 12(17), 8884. <https://doi.org/10.3390/app12178884>.

- Giacosa, G., & Walker, T. R. (2022). A policy perspective on Nova Scotia's plans to reduce dependency on fossil fuels for electricity generation and improve air quality. *Cleaner Production Letters*, 100017. <https://doi.org/10.1016/j.clpl.2022.100017>.
- Hernández Regalado, R. E., Häner, J., Baumkötter, D., Wettwer, L., Brüggling, E., & Tränckner, J. (2022). Continuous Co-Digestion of Agro-Industrial Mixtures in Laboratory Scale Expanded Granular Sludge Bed Reactors. *Applied Sciences*, 12(5), 2295. <https://doi.org/10.3390/app12052295>.
- Ibarra-Esparza, F. E., González-López, M. E., Ibarra-Esparza, J., Lara-Topete, G. O., Senés-Guerrero, C., Cansdale, A., ... & Gradilla-Hernández, M. S. (2023). Implementation of anaerobic digestion for valorizing the organic fraction of municipal solid waste in developing countries: Technical insights from a systematic review. *Journal of Environmental Management*, 347, 118993. <https://doi.org/10.1016/j.jenvman.2023.118993>.
- Ince, M., & Kaplan Ince, O. (2017). Box–Behnken design approach for optimizing removal of copper from wastewater using a novel and green adsorbent. *Atomic Spectroscopy*, 38(6), 200-207. <https://doi.org/10.46770/AS.2017.06.005>.
- Islam, M. S., Hongxin, W., Admassu, H., Noman, A., Ma, C., & An Wei, F. (2021). Degree of hydrolysis, functional and antioxidant properties of protein hydrolysates from Grass Turtle (*Chinemys reevesii*) as influenced by enzymatic hydrolysis conditions. *Food Science & Nutrition*, 9(8), 4031-4047. <https://doi.org/10.1002/fsn3.1903>.

- Johny, L. C., Kudre, T. G., & Suresh, P. (2021). Production of egg white hydrolysate by digestion with pineapple bromelain: Optimization, evaluation and antioxidant activity study. *Journal of Food Science and Technology*, 59, 1769–1780. <https://doi.org/10.1007/s13197-021-05188-0>.
- Joseph, G., Zhang, B., Mahzabin Rahman, Q., Wang, L., & Shahbazi, A. (2019). Two-stage thermophilic anaerobic co-digestion of corn stover and cattle manure to enhance biomethane production. *Journal of Environmental Science and Health, Part A*, 54(5), 452-460. <https://doi.org/10.1080/10934529.2019.1567156>.
- Kim, S.-I., Heo, W., Lee, S.-J., & Kim, Y.-J. (2021). Isolation and characterization of effective bacteria that reduce ammonia emission from livestock manure. *Microorganisms*, 10(1), 77. <https://doi.org/10.3390/microorganisms10010077>.
- Kovács, E., Wirth, R., Maróti, G., Bagi, Z., Rákhely, G., & Kovács, K. L. (2013). Biogas production from protein-rich biomass: fed-batch anaerobic fermentation of casein and of pig blood and associated changes in microbial community composition. *Plos One*, 8(10), e77265. <https://doi.org/10.1371/journal.pone.0077265>.
- Kruger, N.J. (2019). The Bradford Method for protein quantitation. In *The Protein Protocols Handbook*; Walker, J.M., (ED); Springer Protocols Handbooks; Humana Press: Totowa, NJ, USA.
- Lazarevska, S., & Makreski, P. (2015). Insights into the infrared and Raman spectra of fresh and lyophilized royal jelly and protein degradation IR spectroscopy study during heating.

Macedonian Journal of Chemistry and Chemical Engineering, 34(1), 87-93.

<https://doi.org/10.20450/mjcce.2015.669>.

Li, K., Liu, R., Cui, S., Yu, Q., & Ma, R. (2018). Anaerobic co-digestion of animal manures with corn stover or apple pulp for enhanced biogas production. *Renewable Energy*, 118, 335-342. <https://doi.org/10.1016/j.renene.2017.11.023>.

Li, Y., Zhang, Z., Jing, Y., Ge, X., Wang, Y., Lu, C., Zhou, X., & Zhang, Q. (2017). Statistical optimization of simultaneous saccharification fermentative hydrogen production from *Platanus orientalis* leaves by photosynthetic bacteria HAU-M1. *International Journal of Hydrogen Energy*, 42(9), 5804-5811. <https://doi.org/10.1016/j.ijhydene.2016.11.182>.

Marie, M., Yirga, F., Alemu, G., & Azadi, H. (2021). Status of energy utilization and factors affecting rural households' adoption of biogas technology in north-western Ethiopia. *Heliyon*, 7(3), e06487. <https://doi.org/10.1016/j.heliyon.2021.e06487>.

Misran, E., Idris, A., Sarip, S. H. M., & Ya'akob, H. (2019). Properties of bromelain extract from different parts of the pineapple variety Morris. *Biocatalysis and Agricultural Biotechnology*, 18, 101095. <https://doi.org/10.1016/j.bcab.2019.101095>.

Mohd Azmi, S. I., Kumar, P., Sharma, N., Sazili, A. Q., Lee, S.-J., & Ismail-Fitry, M. R. (2023). Application of Plant Proteases in Meat Tenderization: Recent Trends and Future Prospects. *Foods*, 12(6), 1336. <https://doi.org/10.3390/foods12061336>.

Nashiruddin, N. I., Abd Rahman, N. H., A. Rahman, R., Md. Illias, R., Ghazali, N. F., Abomoelak, B., & El Enshasy, H. A. (2022). Improved Sugar Recovery of Alkaline Pre-

- Treated Pineapple Leaf Fibres via Enzymatic Hydrolysis and Its Enzymatic Kinetics. *Fermentation*, 8(11), 640. <https://doi.org/10.3390/fermentation8110640>.
- Nguyen, T.-T., Ta, D.-T., Lin, C.-Y., & Chu, C.-Y. (2022). Biohythane production from swine manure and pineapple waste in a single-stage two-chamber digester using gel-entrapped anaerobic microorganisms. *International Journal of Hydrogen Energy*, 47(60), 25245-25255. <https://doi.org/10.1016/j.ijhydene.2022.05.259>.
- Otieno, E. O., Kiplimo, R., & Mutwiwa, U. (2023). Optimization of anaerobic digestion parameters for biogas production from pineapple wastes co-digested with livestock wastes. *Heliyon*, 9 (3), e14041.
- Paridhi, A., Pradnya, N., Patel, A., Nikhil, M., & Shweta, S. (2022). Bromelain: A Potent Phytomedicine. *Cureus*, 14(8), e27876. [10.7759/cureus.27876](https://doi.org/10.7759/cureus.27876).
- Park, S.-H., Lee, B.-R., & Kim, T.-H. (2015). Effects of cattle manure and swine slurry acidification on ammonia emission as estimated by an acid trap system. *Journal of the Korean Society of Grassland and Forage Science*, 35(3), 212-216. <https://doi.org/10.5333/KGFS.2015.35.3.212>.
- Procházka, J., Dolejš, P., Máca, J., & Dohányos, M. (2012). Stability and inhibition of anaerobic processes caused by insufficiency or excess of ammonia nitrogen. *Applied Microbiology and Biotechnology*, 93, 439-447. <https://doi.org/10.1007/s00253-011-3625-4>.
- Rani, D. S., & Nand, K. (2004). Ensilage of pineapple processing waste for methane generation. *Waste Management*, 24(5), 523-528. <https://doi.org/10.1016/j.wasman.2003.10.010>.

- Shahi, Z., Sayyed-Alangi, S. Z., & Najafian, L. (2020). Effects of enzyme type and process time on hydrolysis degree, electrophoresis bands and antioxidant properties of hydrolyzed proteins derived from defatted *Bunium persicum* Bioss. press cake. *Heliyon*, 6(2), e03365. <https://doi.org/10.1016/j.heliyon.2020.e03365>.
- Shuai, X., Gao, L., Geng, Q., Li, T., He, X., Chen, J., Liu, C., & Dai, T. (2022). Effects of moderate enzymatic hydrolysis on structure and functional properties of pea protein. *Foods*, 11(15), 2368. <https://doi.org/10.3390/foods11152368>.
- Silva, T. H. L., dos Santos, L. A., de Melo Oliveira, C. R., Porto, T. S., Jucá, J. F. T., & Santos, A. F. d. M. S. (2021). Determination of methane generation potential and evaluation of kinetic models in poultry wastes. *Biocatalysis and Agricultural Biotechnology*, 32, 101936. <https://doi.org/10.1016/j.bcab.2021.101936>.
- Smidt, E., & Meissl, K. (2007). The applicability of Fourier transform infrared (FT-IR) spectroscopy in waste management. *Waste Management*, 27(2), 268-276. <https://doi.org/10.1016/j.wasman.2006.01.016>.
- Srinivasa, A. S., Swaminathan, K., & Yaragal, S. C. (2023). Microstructural and optimization studies on novel one-part geopolymer pastes by Box-Behnken response surface design method. *Case Studies in Construction Materials*, 18, e01946. <https://doi.org/10.1016/j.cscm.2023.e01946>.
- Stani, C., Vaccari, L., Mitri, E., & Birarda, G. (2020). FTIR investigation of the secondary structure of type I collagen: New insight into the amide III band. *Spectrochimica Acta*

- Part A: Molecular and Biomolecular Spectroscopy*, 229, 118006.
<https://doi.org/10.1016/j.saa.2019.118006>.
- Sunantha, K., & Saroat, R. (2011). Application of bromelain extract for muscle foods tenderization. *Food and Nutrition Sciences*, 2, 393-401 .
<https://doi.org/10.4236/fns.2011.25055>.
- Syahirah, M. F., & Nazaitulshila, R. (2018). The Utilization of Pineapples Waste Enzyme for the Improvement of Hydrolysis Solubility in Aquaculture Sludge. *Journal of Energy and Safety Technology*, 1, 35-41.
- Tavano, O. L. (2013). Protein hydrolysis using proteases: An important tool for food biotechnology. *Journal of Molecular Catalysis B: Enzymatic*, 90, 1-11.
<https://doi.org/10.1016/j.molcatb.2013.01.011>.
- Telliard, W. (2001). Method 1684: Total, Fixed, and Volatile Solids in Water, Solids, and Biosolids; U.S. Environmental Protection Agency: Columbia, Washington DC, USA.
- Tian, X., An, C., & Chen, Z. (2023). The role of clean energy in achieving decarbonization of electricity generation, transportation, and heating sectors by 2050: A meta-analysis review. *Renewable and Sustainable Energy Reviews*, 182, 113404.
<https://doi.org/10.1016/j.rser.2023.113404>.
- Unnikrishnan, G., & Ramasamy, V. (2022). Anaerobic digestion of pineapple waste for biogas production and application of slurry as liquid fertilizer carrier for phosphate solubilizers. *Indian Journal of Agricultural Research*, 56, 408-414.
<http://dx.doi.org/10.18805/IJARE.A-5777>.

- Wang, J., Sun, Y., Zhang, D., Broderick, T., Strawn, M., Santha, H., Pallansch, K., Deines, A., & Wang, Z. W. (2022). Unblocking the rate-limiting step of the municipal sludge anaerobic digestion. *Water Environment Research*, *94*(10), e10793.
<https://doi.org/10.1002/wer.10793>.
- Wang, X., Lu, X., Li, F., & Yang, G. (2014). Effects of temperature and carbon-nitrogen (C/N) ratio on the performance of anaerobic co-digestion of dairy manure, chicken manure and rice straw: focusing on ammonia inhibition. *Plos One*, *9*(5), e97265.
<https://doi.org/10.1371/journal.pone.0097265>.
- Wang, Y., Zhang, T., Akinremi, O., Bittman, S., Brown, C., Hao, X., Hunt, D., Li, S., Tan, C. S., & Ziadi, N. (2022). Phosphorus characteristics of Canada-wide animal manures and implications for sustainable manure management with a cleaner environment. *Science of the Total Environment*, *845*, 157200. <https://doi.org/10.1016/j.scitotenv.2022.157200>.
- Wijeratnam, R. W., Hewajulige, I., & Abeyratne, N. (2005). Postharvest hot water treatment for the control of *Thielaviopsis* black rot of pineapple. *Postharvest Biology and Technology*, *36*(3), 323-327. <https://doi.org/10.1016/j.postharvbio.2005.01.003>.
- Zhai, W., Li, X., Duan, X., Gou, C., Wang, L., & Gao, Y. (2022). Development of a microbial protease for composting swine carcasses, optimization of its production and elucidation of its catalytic hydrolysis mechanism. *BMC biotechnology*, *22*(1), 1-15.
<https://doi.org/10.1186/s12896-022-00768-0>.
- Zhu, M., Cai, W., Verpoort, F., & Zhou, J. (2019). Preparation of pineapple waste-derived porous carbons with enhanced CO₂ capture performance by hydrothermal carbonation-alkali

metal oxalates assisted thermal activation process. *Chemical Engineering Research and Design*, 146, 130-140. <https://doi.org/10.1016/j.cherd.2019.03.044>.

CHAPTER FIVE

ENHANCING BIOHYDROGEN PRODUCTION FROM MANURE AND KIWI PEEL WASTE: BOX-BEHNKEN DESIGN AND RESPONSE SURFACE METHODOLOGY OPTIMIZATION

Abstract

Energy needs are rising with growth and development, prompting a shift towards renewable energy to cut carbon emissions and mitigate climate change. In this aspect, reusing materials, including turning livestock waste into energy, is gaining attention. This study optimized manure and kiwi peel waste (KPW) anaerobic digestion (AD) under a fixed dose of oleic acid for biohydrogen production. Biohydrogen yield was optimized using manure (M) to kiwi peel waste (KPW) ratio (M:KPW; 0.5 to 1.5), pH (4 to 6), and inoculum dosage (4 to 7) through Box Behnken Response Surface Design. The results showed strong interaction between the factors ($p < 0.05$) and directly impacted biohydrogen production. Optimal conditions for the highest accumulative biohydrogen yield ($\text{mL g}^{-1} \text{VS}$) of 389 ± 11 on day 6 and 510 ± 7 on day 12 include M:KPW ratio of 0.5, pH 5, and inoculum 4 g VS L^{-1} . At these optimal conditions (substrate:KPW ratio of 0.5, pH 5, and inoculum 4 g VS L^{-1}), pure proteins, albumin and casein, produced biohydrogen yield ($\text{mL H}_2 \text{ g}^{-1} \text{VS}_{\text{substrate}}$) of 200 ± 3 on day 6 and 554 ± 3 at day 12 while casein produced 245 ± 3 on day 6 and 400 ± 4 at day 12. For manure:KPW, albumin, and casein, biohydrogen was mainly produced through the acetate pathway. This study's findings can help policymakers create strategies to promote biohydrogen from livestock waste as an essential green energy source for the economy.

Future studies may compare the efficiency of biohydrogen production from other livestock or slaughterhouse waste, such as blood, skin, etc., to determine the most effective substrates for AD.

Keywords: Manure, Biohydrogen, Response surface methodology, Kiwi peel waste.

5.1 Introduction

Modern economies' dependence on fossil fuels is unsustainable and harmful to the environment due to pollutant emissions and resource depletion. Hydrogen is a highly efficient alternative fuel, boasting a greater calorific value of 140 MJ kg^{-1} compared to methane's 50 MJ kg^{-1} and ethanol's 27 MJ kg^{-1} (Shanmugaratnam et al., 2021). Additionally, it is a clean energy source because its combustion generates heat and water only (Awasthi et al., 2022). However, the existing hydrogen production landscape is suboptimal, with more than 96% still generated from fossil fuels (Zhang et al., 2017). Industrial hydrogen production predominantly employs various reforming methods like steam methane reforming, partial oxidation, autothermal reforming, and steam iron processes. These techniques require operating at high temperatures, typically between 500 to 1000 °C (Kumar et al., 2021). In this regard, producing biohydrogen through biological and greenhouse gas-free techniques offers an eco-friendly and sustainable solution.

Key agro-industrial wastes include processed fruits, meats, vegetables, manure, and dairy products (Yaashikaa et al., 2022). High organic content and large volumes make the treatment of agro-industrial wastes essential before disposing of them in the environment. Current nonbiological treatment methods are costly and not environmentally friendly. A viable solution is to treat these effluents biologically, such as through anaerobic digestion (AD), which also allows for the generation of valuable by-products (methane, volatile fatty acids, fertilizer, and fibers), thereby reducing costs and addressing socio-environmental concerns (Awasthi et al., 2022).

AD is an eco-friendly approach for managing organic solid and liquid wastes. Its benefits include reduced chemical usage, minimal excess sludge production, and energy conservation by generating biofuels such as hydrogen and methane (Awasthi et al., 2022; Li et al., 2020). The typical AD process involves two stages: first, dark fermentation by bacteria, breaking down

complex organics into simpler compounds like volatile fatty acids (VFAs), ammonia, hydrogen, and carbon dioxide (CO₂). This is followed by methanogenesis, where archaea produce methane from acetate (as VFA) and/or hydrogen and CO₂. However, this sustainable process can be significantly hindered when fed with protein-rich substrates, posing a challenge for the anaerobes involved.

Ammonia, a by-product of the anaerobic decomposition of protein wastes (manure, cheese whey, slaughterhouse waste, etc.), can potentially inhibit the process. Specifically, free ammonia (NH₃) is the primary inhibitor, with its proportion in total ammonia-nitrogen increasing at high pH levels (≥ 7.0) and temperatures (Wang et al., 2016). Methanogenesis, particularly affected by ammonia, faces challenges as methanogenic archaea are highly sensitive to ammonia. Consequently, an alternative approach could be suppressing methanogenesis to increase hydrogen production from acetate, potentially addressing this inhibition issue. Enhancing H₂ yield (mL H₂ g⁻¹ VS_{substrate}) has been considered as the main aim for the efficiency of those alternative approaches.

Various inhibitors and stressing agents have been investigated, including heat shock for inhibiting H₂ consuming microorganisms (Yin et al., 2014), aeration to enrich H₂ producing bacteria and inhibit H₂ consumers (Zhu & Béland, 2006), irradiation (Elbeshbishy et al., 2010), 2-bromoethansulphonate (BES) or 2-bromoethansulphonate acid (BESA) (Kumar et al., 2016), chloroform (Chang et al., 2011), acetylene (Tiantao et al., 2009) and long chain fatty acids (LCFAs). However, long-term studies have shown that heat shock, aeration, irradiation, etc., are time-consuming and ineffective in the long term because of their limited scope and low yield (Rafieenia et al., 2018; Shanmugam et al., 2016). Chemical inhibition appears economically viable for full-scale applications due to its low energy needs and minimal capital expenses. However,

these methods have not received much attention in recent years due to several limitations, such as flammability issues with acetylene, significant cost concerns with BESA, and the inability of chloroform to inhibit all hydrogen consumers (Luo et al., 2010; Wong et al., 2014). On the other hand, the inhibitory effects of LCFAs on gram-positive bacteria have been established over the past decades. LCFAs can adhere to the cell walls of methanogens, which resemble those of gram-positive bacteria, thereby decreasing permeability and restricting the transport of soluble substrates (Elsamadony et al., 2021). LCFAs are affordable and eco-friendly alternatives to toxic chemical inhibitors. They have been effectively used to suppress methanogenesis and boost hydrogen production with linoleic (LA) (Saady et al., 2012), oleic (OA) (Shanmugam et al., 2014), palmitic, (PA) (Veeravalli et al., 2013) and lauric acids (LUA) (Shanmugam et al., 2014) showing notable inhibitory effects on methanogens.

Veeravalli et al. (2014) achieved a 99.86 mL H₂ g⁻¹ VS from switchgrass hydrolysate by pre-treating granular sludge with 1750 mg L⁻¹ LA. In another study, Shanmugam et al. (2016) informed a hydrogen yield of 2.58 mol mol⁻¹ glucose using LA in thermophilic dark fermentation, the highest among various pre-treatment methods like acid, heat shock, alkali and BES. Earlier, Shanmugam et al. (2014) found that combining LA and LUA to granular sludge cultures with glucose reduced hydrogen consumption by 65% and 86%, respectively. Furthermore, Chaganti et al. (2013) observed a hydrogen yield of 1.94 mol mol⁻¹ xylose after adding 2,000 mg L⁻¹ of LA to mixed anaerobic culture.

While there has been limited research on enhancing hydrogen yield using LCFAs, mostly with simple carbohydrate feedstocks like glucose, xylose, or carbohydrate-rich wastes, exploring their impact on hydrogen production from resistant, protein-rich wastes presents an intriguing study area. Using LCFAs to suppress methanogenic activity and enhance hydrogen production in the

anaerobic digestion of protein-rich wastes could be a cost-effective approach suitable for full-scale application due to its scalability and environmental benefits.

Kiwi peel waste (KPW), a by-product of *Actinidia deliciosa*, accounts for a substantial fraction of organic waste, with about 25% of kiwi production discarded. While often landfilled, leading to environmental problems, it is rich in carbohydrates and a promising candidate as a substrate in AD (Baumguertner et al., 2019). While Lee et al. (2021) have demonstrated the use of manure and food waste for ethanol production using BBD, its application in biohydrogen production from manure and kiwi peel waste (KPW) in a batch reactor with a mixed culture remains unexplored. Response Surface Methodology (RSM) optimizes various factors to achieve maximum response. It involves mathematical and statistical techniques for modeling and analysis when multiple variables influence a response. Among RSM methods, Box–Behnken Design (BBD) is widely used due to its simplicity and efficiency in fewer experiments. It effectively estimates first- and second-order coefficients, including interactions.

This study is designed to explore the synergistic effects of KPW and OA on biohydrogen and methane production during AD of manure. Specifically, this study aims to optimize the manure-to-KPW ratio, pH levels, and inoculum dosage to evaluate their collective impact on gas production using a statistical approach. KPW serves a dual role, being not only a complex substrate rich in carbohydrates but also a source of the protease enzyme actinidin, which is anticipated to enhance the breakdown of protein-rich substrates and, consequently, higher gas yields. In addition, the study will optimize the manure:KPW ratio of manure and kiwi peel waste, pH levels, and inoculum dosage to investigate their collective impact on gas production in the presence of OA. OA will be examined for its role as a metabolic modulator, potentially inhibiting methanogenic pathways and favoring hydrogen production. Another objective was to examine the impacts of

these three factors in the presence of OA on hydrogen and methane production using pure protein substrates (albumin and casein), as very little data exists in the literature.

5.2 Materials and Methods

5.2.1 Chemicals and reagents

The Pierce Coomassie (Bradford) Protein Assay Kit, a pre-prepared Bradford assay reagent obtained from Thermo Fisher Scientific, U.S.A., was utilized to determine the total protein concentration. This measurement was compared to a protein standard (bovine serum albumin) purchased from Thermo Fisher Scientific, U.S.A. Sodium Hydroxide Pellets form was purchased from MilliporeSigma™, U.S.A., ACS reagent grade, $\geq 97.0\%$ purity and technical grade (90%) oleic acid (OA) was purchased from Sigma-Aldrich, U.S.A. De-ionized water is used for all the standard and sample preparation. As a sample of model proteins, albumin in lyophilized powder form ($\geq 96\%$) (Sigma Aldrich, New Zealand) and casein (technical grade, Sigma Aldrich, U.S.A.) were used.

5.2.2 Inoculum

The Riverhead Wastewater Treatment Facility, a traditional treatment facility located in St. John's, Newfoundland and Labrador, Canada, provided the inoculum. The flocculent culture was collected in a 20-litre plastic bucket. The top layer of water was carefully decanted, and the remaining substance was stored at 4 °C in a glass jar for preservation and subsequent use. Before its use in batch studies, the inoculum's total solids (TS), volatile solids (VS), and pH were determined to be 5.1%, 3.9%, and 7.8, respectively.

5.2.3 Feedstock

Fresh dairy cow manure (M), collected from a local farm (Lester's Dairy Farm, Newfoundland) farm used in the hydrolysis experiment (described in Chapters 3 and 4), was used for biohydrogen production. Upon collection, manure was sealed in an airtight plastic container and stored at 4°C for use in biohydrogen digesters. Kiwi peel waste (KPW) was used as a co-substrate for the biohydrogen experiment. The kiwi fruits, bought from local groceries in St. John's, were washed, peeled, and the peels were cut into small pieces. These pieces were blended using a Magic Bullet® with a 250-watt motor at 2000 rpm for 60 s. The manure and KPW were analyzed physiochemically (Table 5-1) before being introduced to the anaerobic digesters.

Table 5- 1. Physiochemical characteristics of the substrates.

Parameter	Cow Manure (M)	Kiwi peel Waste (KPW)
pH	7.5	6.5
Total Solids, TS (%)	14.7	17.03
Volatile Solids, VS (%)	7	10.17
Chemical Oxygen Demand, COD (g L ⁻¹)	105.3	80.32
Protein (g L ⁻¹)	1.2	0.84
NH ₃ -N (g L ⁻¹)	2.2	-
NH ₄ -N (g L ⁻¹)	2.1	-

5.3 Batch Anaerobic Digestion Tests

A statistically designed experiment was conducted using different proportions of manure and kiwi peel waste (manure:KPW), pH, and inoculum dosage in batch digesters as per the combinations suggested by the statistical design. All experiments were conducted in batch reactors incubated with a fixed concentration of oleic acid and converted in anaerobic conditions by purging N₂ for 2 min. The digesters were injected with OA (4,000 mg L⁻¹) one day before the experiment started (day 0). For each set of conditions in the optimization tests, duplicate trials were conducted

in airtight 0.610 L Wheaton glass bottles (serving as digesters), each with a working volume of 0.2 L. The inoculum and substrates were added to the digester, which was then flushed with nitrogen gas and sealed to establish anaerobic conditions (Figure 5-1). These digesters were placed in dark containers to avoid light exposure. The digesters were kept inverted (upside down) to prevent gas leaks. The bioreactors were kept at a steady temperature of 20 ± 1 °C throughout the experiment. Headspace gas volumes were measured daily at a specific time. VFAs were monitored on days 2, 4, 6, 8, 10, and 12. Protein, VS, and COD were measured on days 6 and 12. The batch digesters were opened on day 6, then purged with N₂ for 2 min and re-sealed to maintain anaerobic conditions till day 12.



Figure 5- 1. Nitrogen gas is purged through the culture and substrate, ensuring the maintenance of anaerobic conditions in each digester.

5.4 Overall Experimental Design

The comprehensive experimental methodology of this research is strategically divided into two main parts (I and II). Figure 5-2 presents the overall experimental work conducted in Part I and II. Both parts are set to assess the biohydrogen and biomethane yield.

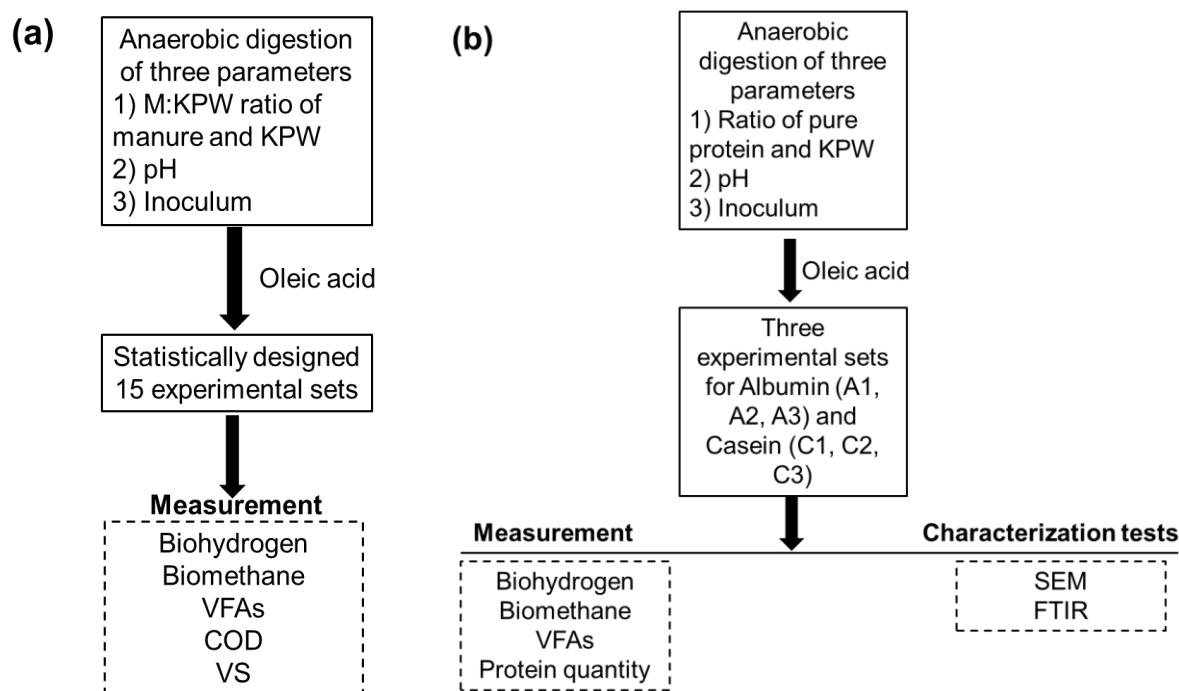


Figure 5- 2. Flowchart of the experimental works conducted in (a) Part I with manure and KPW and (b) Part II with pure proteins and KPW.

Part I investigated using manure as a substrate, and Part II used pure proteins (albumin and casein) as substrates. Part I investigated anaerobic digestion, focusing on three parameters: M:KPW ratio (manure:kiwi peel waste) (volatile solids based), pH, and inoculum amount, with a constant oleic acid concentration. Fifteen statistically designed experiments are conducted to assess biohydrogen and biomethane production, alongside measurement of VFAs, COD, and VS. In addition, characterization techniques like SEM and FTIR provided compositional and morphological changes in the substrates before and after digestion.

Part II investigated the anaerobic digestion of pure proteins (albumin and casein) using the optimal combination of three key parameters: i) manure:KPW ratio of manure and kiwi peel waste ii) pH, and iii) inoculum dosage identified in part I of the study. Three experimental sets are selected and designed for pure proteins such as albumin and casein in the presence of 4,000

mg L⁻¹ oleic acid (OA). Table 5-2 shows the experimental sets of pure proteins examined in Part II.

Sections 5.6 to 5.8 will provide a detailed exposition of the experimental approaches and their respective results as per the framework established in this section.

Table 5- 2. Three experimental sets of albumin and casein used in Part II of the study.

Substrate	Set	Substrate:KPW	pH	Inoculum dosage (g VS L ⁻¹)
Albumin (A)	A1	0.5	6	5.5
	A2	0.5	5	4
	A3	0.5	4	3.5
Casein (C)	C1	0.5	6	5.5
	C2	0.5	5	4
	C3	0.5	4	3.5

5.5 Box-Behnken Design

The study used the Response Surface Methodology (RSM) and Box-Behnken Design (BBD) to find the best conditions for biohydrogen yield. These methods were applied at three levels (low, medium, and high) to assess the impact of different experimental factors and their interactions. The Box-Behnken Design is a balanced experimental strategy that helps analyze the significant effects and interactions of various test parameters. The RSM and BBD were implemented using Minitab® 21.4, a statistical software from LLC, Pennsylvania, USA. In this study, a total of 15 experiments were conducted using manure and KPW. This included 12 experiments focusing on three factors: M:KPW, pH, and inoculum dosage, each tested at three levels, along with three central experiments. The BBD method used in his study involved setting each factor at three levels (-1, 0, +1), which is standard for this approach. Table 5-3 provides the variables of the anaerobic digestion process being studied, such as the amount of M: KPW ratio (0.5 to 1.5 g VS L⁻¹), pH (4 to 6), and inoculum (4 to 7 g VS L⁻¹).

The experiments followed the matrix transformation outlined in Table 5-4. In these experimental setups, the main aspects were tracked as biohydrogen and biomethane production, VS and COD reduction, and volatile fatty acid (VFA) production. The three process factors – the amounts of M:KPW, pH, and inoculum– were the independent variables, while biohydrogen production was the dependent variable or response. Figure 5-3 presents a diagram of the entire AD process.

Table 5- 3. Levels of different variables for Box-Behnken Design (BBD) for biohydrogen production using manure (M) and kiwi peel waste (KPW).

Factors	Codes	Level		
		Low (-1)	Intermediate (0)	High (+1)
M:KPW	A	0.5	1.0	1.5
pH	B	4	5	6
Inoculum (g VS L ⁻¹)	C	4	5.5	7

M = Manure; KPW = Kiwi peel waste.

Table 5- 4. Matrix transformation of Box-Behnken Design for manure (M) and kiwi peel waste (KPW) anaerobic digestion.

Std. Order	Run Order	Pt. Type	Blocks	M:KPW ratio	pH	Inoculum (g VS L ⁻¹)
13	1	0	1	1	5	5.5
7	2	2	1	0.5	5	7
15	3	0	1	1	5	5.5
10	4	2	1	1	6	4
14	5	0	1	1	5	5.5
3	6	2	1	0.5	6	5.5
5	7	2	1	0.5	5	4
2	8	2	1	1.5	4	5.5
9	9	2	1	1	4	4
4	10	2	1	1.5	6	5.5
8	11	2	1	1.5	5	7
11	12	2	1	1	4	7
1	13	2	1	0.5	4	5.5
6	14	2	1	1.5	5	4
12	15	2	1	1	6	7


Digester for anaerobic digestion test	Statistically designed experimental matrix	Responses
 <p data-bbox="332 569 625 758">Manure + Kiwi peel waste + inoculum in presence the of oleic acid in anaerobic digester</p>	<p data-bbox="667 411 1019 604">Manure:KPW ratio of manure and KPW (0.5 to 1.5) + pH (4 to 6) + Inoculum (4 to 7 g VS L⁻¹)</p> <p data-bbox="792 611 894 716">↓ 15 runs</p>	<p data-bbox="1101 323 1300 354">✓ Production</p> <p data-bbox="1101 375 1333 495">-Biohydrogen and biomethane -VFAs</p> <p data-bbox="1101 541 1344 573">✓ Reduction (%)</p> <p data-bbox="1101 604 1187 688">-COD -VS</p>

Figure 5- 3. Experimental design and the measured responses for optimizing the anaerobic digestion of manure using kiwi peel waste.

Building on the findings from Chapter 3, Chapter 5 applied the optimized conditions for manure and KPW interaction to enhance biohydrogen production through AD. The research aimed to investigate how the optimized protein degradation conditions could be leveraged to improve biohydrogen yields, with a focus on the manure ratio, pH, and inoculum dosage. In Chapter 3, the optimal KPW dosage for protein degradation was found to be $7.5 \text{ g VS}_{\text{KPW}} \text{ L}^{-1}$ with a manure dosage of $4 \text{ g VS}_{\text{manure}} \text{ L}^{-1}$. This ratio (M:KPW ratio of 0.53) and the understanding of KPW's proteolytic effects directly informed the experimental design in Chapter 5. In Chapter 5, the manure and KPW ratio (M:KPW) was further explored and optimized within a range (0.5 to 1.5) to enhance biohydrogen production. The findings from Chapter 3 about the effective ratio of manure and KPW provided a basis for these experiments.

5.6 Analytical Methods

The analytical parameters included headspace gases (H₂, CH₄, and CO₂), liquid components (protein and VFAs), and solid characterization (Fourier transform infrared spectroscopy and scanning electron microscopy analysis). The substrates, namely manure and kiwi peel waste, underwent initial characterization focusing on their total solids (TS), volatile solids (VS), pH levels, ammonia nitrogen (NH₃-N), and ammonium nitrogen (NH₄-N), as detailed in section 3.3.2. All these characterizations were performed in duplicate to ensure accuracy and reproducibility. Additionally, the procedures for measuring protein quantities and VS were carried out as described in sections 3.5.1 and 3.5.3 of the study. The remaining methods for measuring hydrogen, methane, VFAs, and substrates for characterization are elaborated in the following sections.

5.6.1 Biohydrogen and biomethane measurement

The volume of biogas produced was recorded each day using a pre-calibrated gas pressure meter (Dwyer Instruments Inc.; model: DPGA-10). The biohydrogen production (H₂) and biomethane (CH₄) presented were adjusted to standard temperature and pressure (STP), which is 273 K and 1 atmosphere using Eq. (5-1) (Ahmed et al., 2019).

$$V_{H_2 \text{ or } CH_4, STP} = \epsilon V_m \frac{T_s P_m}{T_m P_s} \quad (5-1)$$

In this context, V_m represents the volume of biohydrogen or biomethane measured; ϵ is the biohydrogen or methane content in the biogas as a percentage; T_m and P_m are the temperature and atmospheric pressure at the time of measurement, respectively; T_s and P_s denote the standard temperature and pressure. The term $V_{H_2 \text{ or } CH_4, STP}$ refers to the volume of biohydrogen or

biomethane adjusted to standard temperature and atmospheric pressure. The total biohydrogen or biomethane yield mentioned in this study is the cumulative specific H₂ or CH₄ yield. This specific H₂ or CH₄ yield was determined by dividing the produced H₂ or CH₄ (in mL) by the mass of the total volatile solids (VS) fed to the bioreactor at each experiment run.

5.6.2 Gas composition analysis

The composition of the biogas was analyzed using a gas chromatograph (Model 8610V, SRI Instruments, Torrance, CA), which was equipped with a thermal conductivity detector (TCD) and a molecular sieve column (Molecular sieve 5A, mesh 80/100, 6 ft × 1/8 in). The operational temperatures for the column and the TCD detector were set at 50°C and 95°C, respectively. A 500 µL of the sample was injected for analysis. Helium served as the carrier gas, maintained at a flow rate of 30 mL min⁻¹ throughout the analysis.

5.6.3 Volatile fatty acids (VFAs) measurement

A 0.5 mL sample was periodically withdrawn from each digester using a plastic disposable syringe (Thermo Scientific™, U.S.A.) and diluted in 4.5 mL de-ionized water in 12 mL culture tubes. These ten times diluted samples were centrifuged at 6,000 rpm for 8 min and kept at rest for 15 min. The centrifuged liquid was sequentially passed through two consecutive filters to remove suspended solids and heavy metals. Firstly, the centrifuged samples were filtered through a 0.45 µm polypropylene membrane and then passed through a 1 g ion exchange sodium resin (Chelex 100, Bio-Rad Laboratories, CA) encapsulated in a cartridge tube. The clarified filtrate was then stored in 2.0 mL vials (Millipore Sigma, USA) at 4 °C for subsequent VFA analysis.

The presence of volatile fatty acids (VFAs), such as acetic, propionic, butyric, isobutyric, valeric, and isovaleric acids, were determined using a gas chromatograph (GC) (Agilent, model 6890, U.S.A.). This GC was fitted with a Flame Ionization Detector (FID) and equipped with a J&W Scientific DB-FFAP high-resolution column (25 m × 0.32 mm × 0.50 μm). The instrument was calibrated using standard VFA solutions at 10, 20, 50, 100, and 200 mg/L concentrations. The inlet temperature of the GC was maintained at 260 °C, and it operated with a 20:1 split ratio for the carrier gas, helium, flowing at 2.4 mL min⁻¹. For each analysis, 0.5 μL of the sample was injected., To ensure accuracy, a vial containing a standard VFA solution was injected after every five unknown samples during the analytical process.

5.6.4 Fourier transform infrared (FTIR)

For FTIR analysis, a 5 mL liquid sample from each digester bottle was taken and oven-dried at 70-80 °C. About 0.5 g of dried samples were inserted into FTIR spectroscopy (PerkinElmer Spectrum IR-C115599, USA). The detailed procedure is provided in section 3.7.1.

5.6.5 Scanning electron microscope (SEM)

The surface morphology of the samples on days 0, 6, and 12 were analyzed using a Scanning Electron Microscope (SEM) (Model JEOL JSM 7100F, USA). The same sample used for FTIR is analyzed for SEM analysis. The detailed procedure is provided in section 3.7.2.

5.7 Results and Discussion

This experiment used a Box Behnken Design (BBD) matrix to explore different manure:kiwi peel waste (M:KPW) combinations, pH, and inoculum dosage. The analysis aimed to quantify biohydrogen yields through statistical design. The other parameters, such as biomethane yield, VS

reduction, and VFA production, were also monitored during manure-KPW anaerobic digestion. Subsequent sections (5.8.1 to 5.8.4) detail the experiment outcomes.

5.7.1 Hydrogen yield

In a comparative study of hydrogen production over 12 days, fifteen distinct sets were monitored for their hydrogen (Figure 5-4 and Table 5-5) and methane (Figure 5-5 and Table 5-6) yield measured in mL g⁻¹ VS. In Figure 5-5, set 7 (M:KPW ratio of 0.5, pH 5, and inoculum dosage 4 g VS L⁻¹) produced the highest H₂ yield, starting at 75±5 mL g⁻¹ VS (day 1) and steadily increasing to 509±12 mL g⁻¹ VS (day 12), without any plateau, suggesting optimal conditions for hydrogen production prevailed. In contrast, set 12 began with the lowest initial H₂ yield (14±18 g⁻¹ VS on day 1), yet it demonstrated resilience by ending at a moderate yield of 225±18 mL g⁻¹ VS (day 12).

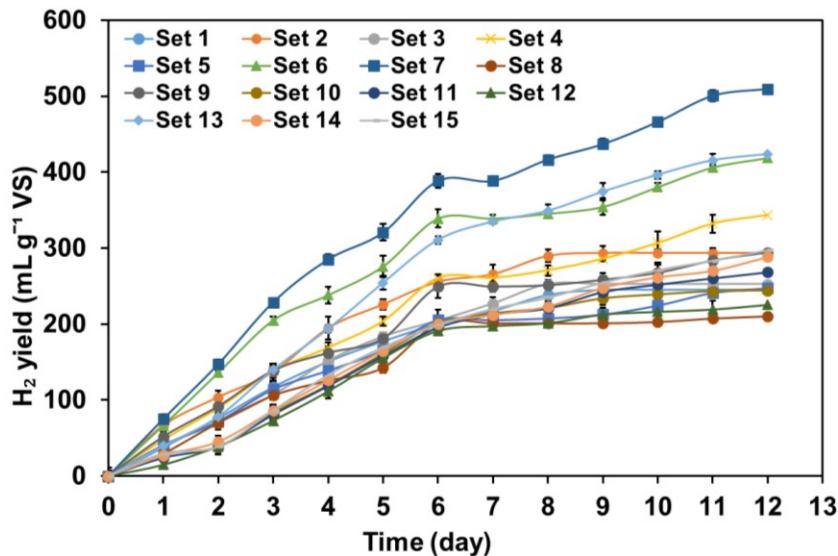


Figure 5- 4. Accumulative hydrogen yield during anaerobic digestion of manure and kiwi peel waste as per statistical design.

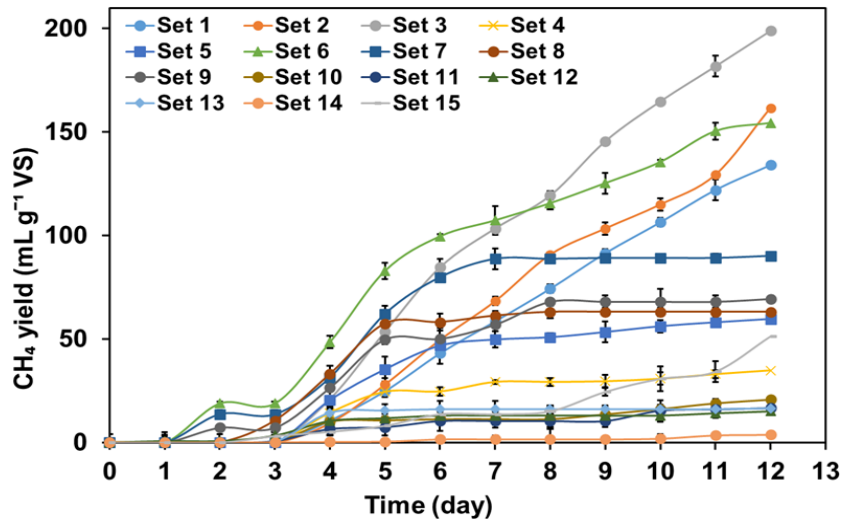


Figure 5- 5. Accumulative methane yield during anaerobic digestion of manure and kiwi peel waste as per statistical design.

A significant and uninterrupted increase in H_2 production in run 7 implies a favorable balance between the inoculum and substrate, allowing for a sustained bioconversion process over the entire duration of the experiment. This balance is critical as too high substrate concentration could lead to rapid depletion of nutrients or accumulation of inhibitory products, while too low a concentration may not provide sufficient nutrients for microbial growth and metabolism (Cappai et al., 2018; Florio et al., 2017). The variation in hydrogen production across the sets can likely be attributed to the differences in either or combinations of 'inoculum: substrate' ratios, pH, and inoculum dosage, affecting the microbial activity responsible for hydrogen generation. As seen in set 7, optimal ratios and concentrations facilitate sustained and efficient hydrogen production, whereas suboptimal conditions lead to lower yields and earlier production plateauing. Understanding the dynamics of these parameters is crucial for enhancing hydrogen yield in bioconversion processes.

Figure 5-5 shows the methane yield data across the 15 sets and highlights several notable observations for anaerobic digestion performance over 12 days. Set 3 (M:KPW ratio of 1, pH 5,

inoculum dosage 5.5 g VS L⁻¹) showed a robust initiation of methane production on day 4 and the highest final yield of 198±5 mL g⁻¹ VS, indicating a remarkably effective set of conditions for methanogenesis. Conversely, set 14 (M:KPW of 1.5, pH 5, and inoculum dosage 4 g VS L⁻¹) exhibits markedly different behavior, with methane production commencing on day 4 but achieving only a minimal yield of 4±1 mL g⁻¹ VS by day 12, suggesting less favorable conditions for methane-forming microbes or possibly indicative of low inoculum loading under a high inhibitory effect of oleic acid (OA) (Dasa et al., 2016). Set 6 (M:KPW of 0.5, pH 6, and inoculum dosage 5.5 g VS L⁻¹) suggests a successful adaptation or resistance to OA, with an early start on day 2 (19±3 mL g⁻¹ VS) and a substantial yield of 154±4 mL g⁻¹ VS by day 12.

Table 5- 5. Cumulative hydrogen yield during anaerobic digestion of manure and kiwi peel waste as per statistical design.

Days	Set number														
	1	2	3	4	5	6	7	8	9	10	11	12	13	14	15
0	0	0	0	0	0	0	0	0	0	0	0	0	0	0	0
1	38±1	67±5	40±3	48±1	41±5	67±5	75±3	30±6	52±7	29±7	24±11	15±5	40±1	27±11	29±5
2	76±1	104±7	70±5	89±1	72±6	136±8	147±6	70±1	92±5	38±2	39±6	39±5	78±5	45±5	39±5
3	117±2	137±8	107±2	138±2	114±11	205±3	229±6	106±2	139±7	83±10	81±5	73±2	140±2	86±8	86±9
4	151±5	195±11	152±6	169±5	139±9	238±5	285±2	126±6	162±9	120±8	119±9	112±6	194±6	126±5	133±8
5	178±6	226±15	184±8	204±7	166±5	276±11	321±7	143±12	181±9	161±10	158±8	156±9	254±5	165±6	170±5
6	201±5	256±7	205±5	261±6	205±15	339±14	389±11	201±7	249±1	201±12	195±9	191±6	311±9	200±6	199±7
7	217±3	266±9	227±3	261±5	205±14	339±12	389±9	201±4	249±15	214±9	213±5	198±3	335±5	212±3	220±5
8	239±11	290±12	253±8	271±6	208±9	345±5	417±5	201±7	251±7	221±5	221±12	201±6	349±3	223±3	235±8
9	245±5	294±8	253±6	286±7	213±5	354±3	437±6	201±6	258±5	234±12	242±8	213±5	374±8	248±6	255±4
10	245±8	294±9	253±11	307±3	224±7	380±11	466±7	203±5	268±9	239±9	252±11	216±9	397±11	262±9	271±6
11	245±12	294±5	253±6	332±15	241±11	406±5	501±2	207±2	284±11	243±6	260±9	219±12	416±5	270±10	284±10
12	245±9	294±5	253±9	343±12	247±6	419±4	510±7	210±1	295±16	244±5	268±5	226±11	424±8	288±5	298±6

Table 5- 6. Cumulative methane yield during anaerobic digestion of manure and kiwi peel waste as per statistical design.

Days	Set number														
	1	2	3	4	5	6	7	8	9	10	11	12	13	14	15
0	0	0	0	0	0	0	0	0	0	0	0	0	0	0	0
1	0	0	0	0	0	0	0	0	0	0	0	1±4	0	0	0
2	0	0	0	0	0	19±3	14±0	0	7±5	0	0	1±3	0	0	0
3	0	0	0	0	0	19±1	14±2	11±2	7±1	0	1±4	3±1	1±2	0	3±2
4	11±2	9±1	21±5	14±2	21±2	48±1	31±1	33±5	27±2	10±1	7±3	11±2	14±5	0	5±2
5	25±1	28±1	54±1	25±2	35±5	83±3	62±1	57±4	50±1	11±3	7±3	12±4	15±3	0	8±2
6	43±3	50±3	85±6	25±1	47±6	100±4	80±4	58±3	50±1	11±3	10±4	13±4	16±3	2±1	14±1
7	59±5	68±2	103±4	29±2	50±3	107±1	89±2	61±4	57±5	11±2	10±5	13±3	16±4	2±1	14±1
8	74±5	91±2	119±2	29±1	51±4	116±7	89±5	63±1	68±1	11±4	10±2	13±2	16±5	2±2	15±1
9	92±2	103±1	146±2	30±2	53±2	125±3	89±2	63±3	68±1	14±1	10±3	13±2	16±2	2±5	25±2
10	106±2	115±3	165±1	31±3	56±5	136±5	89±2	63±1	68±3	16±4	15±3	13±2	16±2	2±1	31±2
11	122±2	129±3	182±1	33±6	58±3	150±1	89±1	63±2	68±6	19±2	16±5	14±3	16±2	4±2	34±3
12	134±5	162±1	199±5	35±2	60±2	154±4	90±2	63±2	69±3	21±2	17±2	15±1	16±4	4±1	51±5

The Box-Behnken design with three distinct levels was employed to formulate mathematical models. These models specifically link the varying experimental factors to enhance biohydrogen production effectively throughout the AD process. In the AD process, hydrogen yield was observed as the primary response. The model equation (Eq. (5-2)) from the Box-Behnken 3-point design features highly significant terms in a coded format.

$$\text{Hydrogen yield (mL g}^{-1}\text{ VS)} = 1195.7 + 670.7 * A - 102.4 * B - 107.2 * C + 190 A * A + 12.5 B * B + 4.11 C * C - 14 A * B + 43 A * C - 0.5 B * C \quad (5-2)$$

where, A, B and C terms indicate manure:KPW ratio of manure and kiwi peel waste, pH and inoculum (g VS L⁻¹).

Equation (5-2) demonstrates the impact of individual (quadratic) and combined variable interactions on hydrogen generation. Coefficients with negative values in this equation suggest that these single or dual interactions among the independent variables diminish the outcome. Conversely, positive coefficient values signify an enhancement in the response within the experimental boundaries (Mahmoud & McConville, 2023). The appropriateness of the developed models has been confirmed through the analysis of variance (ANOVA), as detailed in Table 5-7. The polynomial models are deemed favorable due to their high coefficient of determination (R^2) values, which also improve the reliability of the model terms (Mosquera et al., 2020).

A key table in statistical analysis is the analysis of variance (ANOVA) table. It plays a crucial role in aiding researchers in examining the effects under consideration and the model coefficients (Deepanraj et al., 2021). The F -value serves as a statistical measure to ascertain whether the means across different variables have statistically significant differences.

Table 5- 7. Analysis of variance (ANOVA) for a quadratic model of hydrogen yield with three factors: BBD for manure and KPW for anaerobic digestion.

Source	DF	Adj SS	Adj MS	F-Value	P-Value
Model	9	44.7	38.3	27.71	0.000
Linear	3	72.7	57.6	63.93	0.000
A-Manure:KPW	1	76.1	76.1	261.99	0.000
B- pH	1	276.1	276.1	20.23	0.006
C-Inoculum (g VS L ⁻¹)	1	20.5	30.5	109.56	0.000
Square	3	13.4	34.5	112.78	0.000
A ² -Manure:KPW*Manure:KPW	1	30.8	32.8	110.31	0.000
B ² -pH*pH	1	576.9	576.9	42.27	0.001
C ² -Inoculum (g VS L ⁻¹)*Inoculum (g VS L ⁻¹)	1	315.9	315.9	23.14	0.005
2-Way Interaction	3	358.5	452.8	106.43	0.000
AB-Manure:KPW*pH	1	196.0	196.0	14.36	0.013
AC-Manure:KPW*Inoculum (g VS L ⁻¹)	1	160.2	160.2	304.78	0.000
BC-pH*Inoculum (g VS L ⁻¹)	1	2.3	2.3	0.16	0.702
Error	5	68.3	13.7		
Lack-of-Fit	3	60.3	20.1	5.02	0.171
Pure Error	2	8.0	4.0		
Total	14	612.9			
<i>R</i> ²		<i>R</i> ² (adjusted)		<i>R</i> ² (predicted)	
0.9987		0.9864		0.9613	

An *F*-value of 27.71 indicates a significant relevance of the regression model in predicting biohydrogen yield. Additionally, the *p*-value is another critical element that correlates strongly with the *F*-value. With the confidence interval set at 95%, a *p*-value less than 0.05 is deemed significant. Conversely, a *p*-value exceeding 0.1 falls into the category of being statistically insignificant. The constructed model demonstrates considerable significance, as evidenced by model *F*-values reaching up to 27.71 and the probability values (*p* model > *F*) being less than 0.0001. This implies that the likelihood of the model's results being a product of random noise is less than 0.01% (Abouelenien et al., 2021). In this scenario, the *p*-values associated with the coefficients A (manure:KPW), B (pH), C (inoculum), A² (manure:KPW*manure:KPW), B² (pH*pH), C² (inoculum*inoculum) and AB (manure: KPW*pH) are below 0.05. This indicates

that incorporating these coefficients into the model will enhance its fitting accuracy. The coefficient of determination (R^2) is utilized in statistical analysis to evaluate how effectively the proposed regression model aligns with the experimental data points. This coefficient's value can vary between 0 and 1, where a value approaching 1 signifies a high significance, indicating a strong fit of the model equation to the data points. Many researchers opt for the adjusted R^2 over the standard R^2 . This preference is because, unlike the basic R^2 , the adjusted R^2 does not automatically increase with the addition of a new variable. This model exhibits an exemplary alignment, as evidenced by an R^2 of 0.9987. This suggests that the model can explain 99% of the variance in the data. Additionally, the model boasts a predicted R^2 of 0.9864, showcasing its strong predictive power for responses to untested values within the parameters. Furthermore, with an adjusted R^2 of 0.9613, the model demonstrates that it could potentially account for approximately 96% of the variability if it were applied to different sample sets (Park et al., 2021).

The three-dimensional (3D) surface graphs, generated by varying two variables while keeping other elements fixed, offer valuable insights into the primary impacts and the interplay between these variables. Associated contour diagrams (2D) depict these response surfaces on the x-y axis to facilitate an assessment of how the independent factors influence the dependent factor (Liu et al., 2010). Figure 5-6 provides the generated 3D response surface graphs and associated contour diagrams.

The plots shown in Figures 5-6 (a and c) represent response surfaces, each forming a part of a parabolic sheet. They displayed the lowest and highest ridges within the explored area. For every response surface, the ideal levels of the varying elements, like the initial manure:KPW and pH, were discernible either through the saddle point or by pointing the peaks on the x- and y-axes.

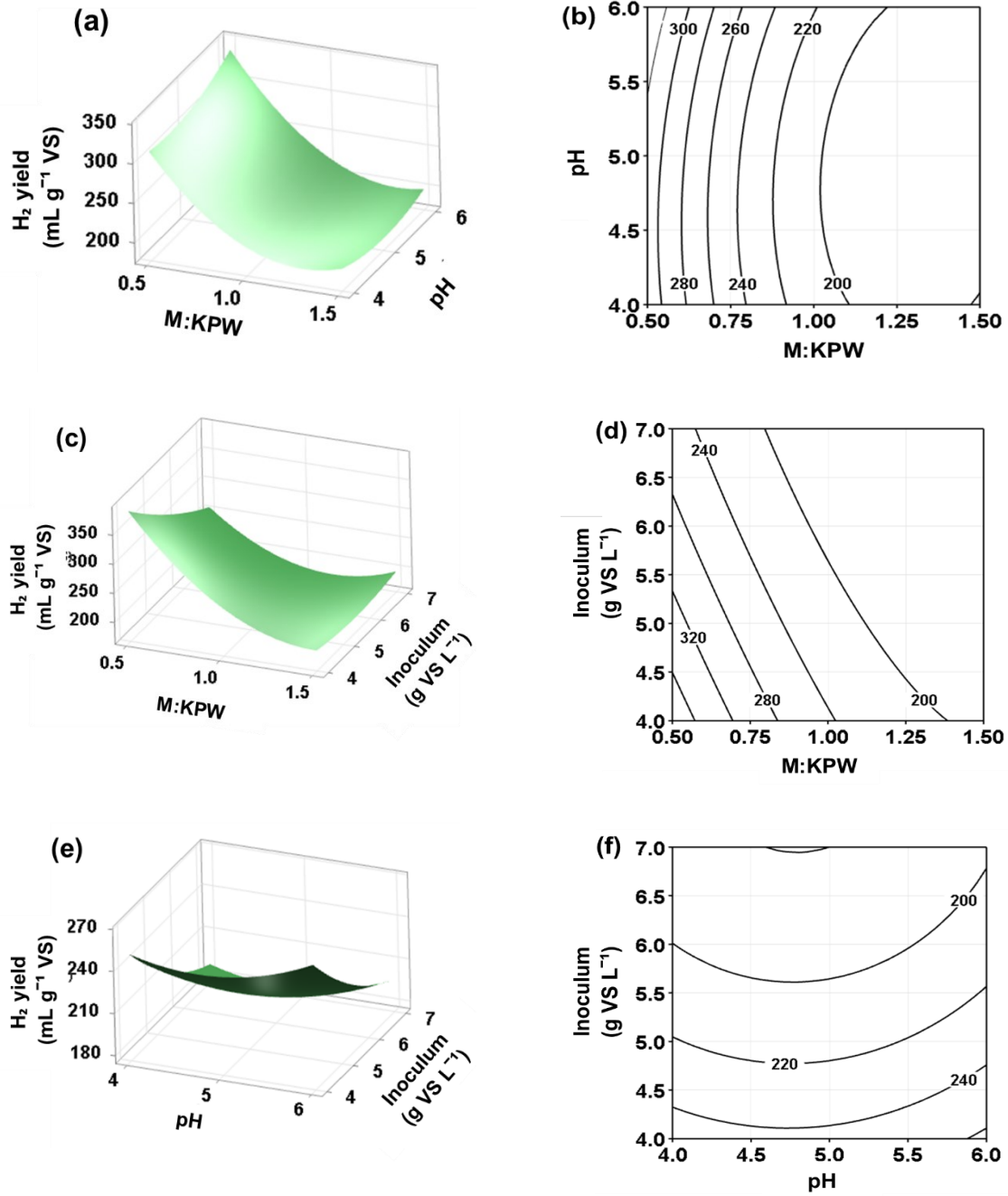


Figure 5- 6. 3D surface plots and contour response surface of the interactive effect of (a) and (b) manure:KPW ratio and pH, (c) and (d) manure:KPW ratio and inoculum, and (e) and (f) pH and inoculum on biohydrogen yield.

Figure 5-6 (a) reveals that the highest yield ($320 \text{ mL g}^{-1} \text{ VS}$) occurs at a pH near 6.0 and manure:KPW ratio of 0.5. The surface gently slopes downwards as the pH decreases or the manure:KPW ratio increases to 1.5, underscoring a non-linear response in the biohydrogen yield to these variables. The downward slope in the surface plot generating low hydrogen yield, observed as the pH moves towards the acidic range, can be attributed to the inhibitory effects on microbial consortia or the shift in metabolic pathways away from hydrogen production (Liu et al., 2011). A comparable outcome was observed by Dareioti et al. (2014); they identified a pH level of 6 as the most effective for maximizing biohydrogen production through the anaerobic digestion of agro-industrial wastewater composing olive mill wastewater, cheese whey, and liquid cow manure.

Notably, their investigation spanned a pH range from 4.5 to 7.5, providing a broad perspective on the impact of pH levels on biohydrogen production. In the contour plot (Figure 5-6 (b)), the contours are partly elliptical, which suggests a significant interaction between pH and the manure:KPW ratio of manure and kiwi peel waste (Liu et al., 2020). This interaction is further substantiated by the low *p*-value ($p < 0.05$) detailed in Table 5-7, underscoring the statistical significance of these findings.

Figure 5-6 (c and d) shows how biohydrogen yield varies with changes in the manure:KPW ratio of manure and kiwi peel waste and inoculum concentration. The plot exhibits a notable peak, with the highest yield around $368 \text{ mL g}^{-1} \text{ VS}$, suggesting an optimal combination of the two variables (manure:KPW ratio of 0.5 and 4 g VS L^{-1} inoculum) that favor biohydrogen production. The hydrogen yield decreases as inoculum dosage increases from 4 to 7 g VS L^{-1} , indicating less-than-ideal conditions. The subsequent decline of biohydrogen yield with the higher inoculum dosage suggests a possible decrease in microbial efficiency, potentially due to nutrient oversaturation or inhibitory effects at higher inoculum levels, consistent with the findings of

Nawaz et al. (2023). Nawaz et al. (2023) found that a continued increase in inoculum size from 10 to 15 mL led to a decline of biohydrogen from 13 to 10 mL g⁻¹ substrate. Figure 5-6 (d) shows that the contour lines are predominantly straight, suggesting that the relationship between the manure:KPW ratio and inoculum concentration is relatively linear within the tested range.

The relationship between pH levels and inoculum dosage on biohydrogen yield can be inferred by analyzing the 3D surface plot in Figure 5-6 (e). At the lowest inoculum dosage depicted on the plot, approximately 4 g VS L⁻¹, the biohydrogen yield varies with pH non-linearly. Specifically, at a pH of 4, the yield peaks at around 250 mL g⁻¹ VS. As the pH increases to 5, the yield decreases slightly, dropping to about 240 mL g⁻¹ VS. This reduction suggests that a pH of 4 is more favorable for biohydrogen production at this inoculum level. Interestingly, at pH 6, the yield slightly increases again to 245 mL g⁻¹ VS, indicating that the studied pH range (pH 4, 5, and 6) are well complemented with the inoculum used in the AD for biohydrogen production. Low pH (<4) or high pH (>12) hinder hydrogenase activity, a crucial enzyme in fermentative hydrogen production (Osman et al., 2020). At pH 4.0 to 6.0, the metabolic pathways for producing acetic and butyric acid are more active and preferred (Guo et al., 2010). Optimal pH values for various substrates in fermentation processes range widely from 4.0 to 6.5, but each specific case has a narrow ideal pH, typically within ±0.5 range. For example, a pH of 6.0 is optimal for cheese whey, food, and kitchen wastes, while a slightly lower pH of 5.5 is best for glucose. Conversely, a starting pH of 4.5 yields the highest hydrogen production with sucrose and starch as substrates (Dareioti et al., 2014). The shapes of the contour lines (Figure 5-6 (f)) are semi-elliptical, which suggests that the interaction between pH and inoculum concentration is not strictly linear and that there is an optimal combination of these two factors that maximizes yield. The interaction between pH levels and

inoculum concentration is significant, as observed by the formation of elliptical contours around stationary points (Sethupathy et al., 2018).

5.7.2 COD removal

Chemical Oxygen Demand (COD) gauges the oxygen required to oxidize the organics in the substrate, indicating the efficiency of anaerobic digestion. A decrease in COD reflects successful organic breakdown in the digester (Meegoda et al., 2018). Figure 5-7 presents a comparative analysis of the COD reduction percentages observed on days 6 and 12 of each experimental run.

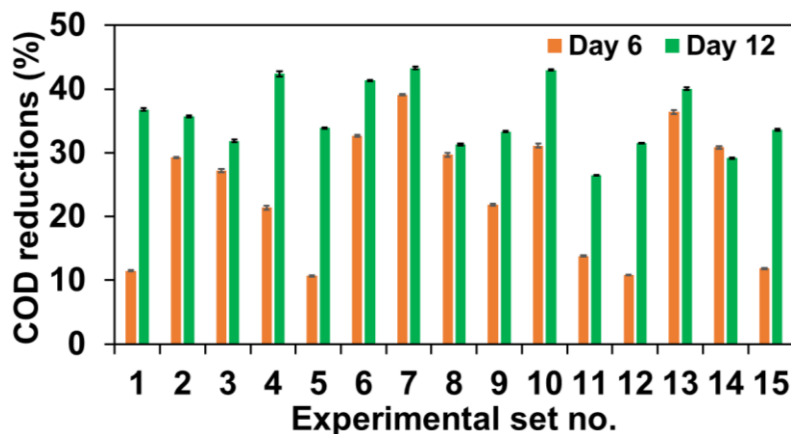


Figure 5- 7. Chemical Oxygen Demand (COD) reduction (%) in each run on days 6 and 12.

The data indicates a significant enhancement in COD reduction with increased treatment time. On day 6 of the treatment period, COD reduction ranged from $10.70 \pm 0.11\%$ (set 5) to $39.1 \pm 0.15\%$ (set 7), whereas day 12 reduced COD by $26.44 \pm 0.07\%$ (set 11) to $43.31 \pm 0.17\%$ (set 7). Notably, set 4 exhibited the most substantial increase in COD reduction from $21.4 \pm 0.31\%$ at day 6 to $42.4 \pm 0.42\%$ at day 12. The low COD removal efficiency initially observed, ranging between $10.7 \pm 0.1\%$ to $13.8 \pm 0.07\%$ (set 1, 5, 11, 12, and 15), can be attributed to the incomplete digestion

of organic compounds, particularly volatile fatty acids (VFAs) (Nguyen et al., 2021). This is consistent with some other studies; for example, 9.3% COD reduction was obtained by Zhou et al. (2013) during thermophilic acidogenic fermentation of food waste, COD removal efficiencies ranging from 10.7% to 23.0% from the hydrogen fermentation of microalgae (Sivagurunathan et al., 2017), and 5% to 16% COD removal from the co-digestion of manure, wine vinasse, and sewage sludge mixtures (Sillero et al., 2022). Analyzing day 12 data, most experimental sets exhibit an increase in COD removal efficiency compared to day 6, which aligns with some other previous studies shown in Table 5-8. On day 12, the COD removal (%) ranged from $26.44 \pm 0.07\%$ in set 11 to $43.31 \pm 0.17\%$ in set 7, indicating the progress of organic matter degradation over time. The increased time allows for a more prolonged microbial activity, leading to a greater breakdown of organic matter. Over time, the microbial consortia adapt and become more efficient at degrading complex organic compounds (Guieysse et al., 2001). Over time, conditions within the reactor could have changed, leading to an inhibitory environment for the microorganisms. The data for run 14 shows an anomaly compared to the general trend observed in the other experimental sets; it exhibits a decrease in COD removal from 30.9% on day 6 to 29.17% on day 12. Typically, one would expect a higher percentage of COD removal with an extended treatment period, as seen in the other runs, due to the prolonged degradation of organic material by microbial action or chemical processes. It is possible that in run 14, there was a high concentration of organic material that initially led to a higher rate of COD removal due to increased microbial activity. However, this can lead to substrate inhibition beyond a certain concentration, where the microbial process becomes inhibited, decreasing removal efficiency over time (Hou et al., 2018; Rajagopal et al., 2013). Anaerobic digestion typically proceeds through several phases, including hydrolysis, acidogenesis, acetogenesis, and methanogenesis. The latter stages can take longer to establish but

are crucial for significant COD reduction. Panichnumsin et al. (2010) observed that reducing ammonia levels from 100 to 10 mg NH₄-N L⁻¹ during AD of pig manure and cassava waste made methanogenesis unsuccessful, particularly in scenarios where the carbon to nitrogen (C:N) ratio ranged from 59 to 210.

Table 5- 8. Chemical Oxygen Demand (COD) removal efficiency of different substrates

Substrates	COD removal (%)	Inoculum type	Digester type	References
Manure and kiwi peel waste	43.31±0.32	Sewage sludge	Batch	This study
Microalgal biomass and swine manure	42 - 56	Anaerobic digester sludge	Batch	Kumar et al. (2018)
Pig manure, cocoa mucilage, and coffee mucilage	90	Anaerobic digester sludge	-	Rangel et al. (2021)
Poultry manure, wine vinasse	22 - 24	Sewage sludge	Batch	Meetiyyagoda et al. (2023)
Wine vinasse	< 24	Sewage sludge	Batch	Tena et al. (2020)
Swine manure and pineapple waste	90	Pig farm Biogas digester	CSTR	Nguyen et al. (2021)
Swine manure and corn silage	81	Digested slurry	Batch	Schievano et al. (2014)

CSTR = Continuous stirred tank reactor.

5.7.3 Volatile solids reduction

The measurement and analysis of volatile solids (VS) reduction is pivotal in AD. This parameter serves as an integral benchmark for assessing the efficiency of the digestion process. Volatile solids, essentially the organic fraction of the feedstock, undergo decomposition during digestion, leading to biogas production. The reduction of VS is widely regarded as the primary metric for evaluating the performance of anaerobic digestion processes (Kraemer & Bagley, 2005). A higher VS reduction percentage indicates more effective digestion and greater conversion of organic matter into biogas. Figure 5-8 presents the reduction (%) of volatile solids during 12-day AD.

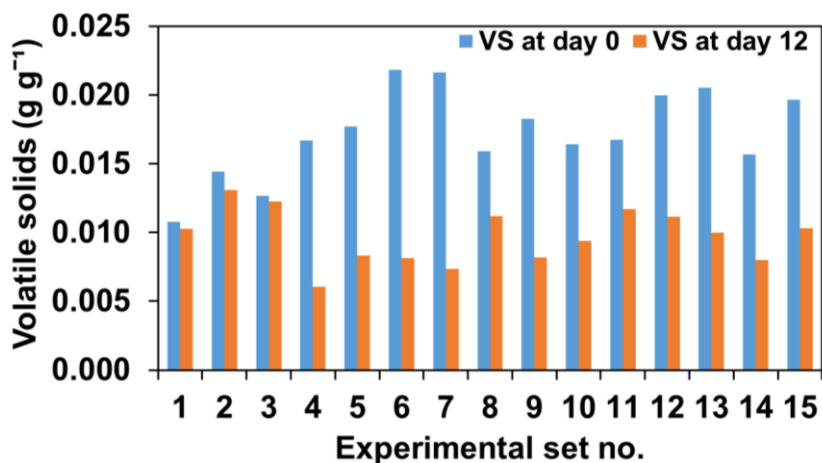


Figure 5- 8. Volatile solids (VS) profile of fifteen experimental sets.

The VS range at the start of the experiment (day 0) is from 0.007 (set 1) to 0.023 g g⁻¹ (set 7). This spread indicates the different initial conditions set for each experimental run, reflecting the variance in the concentration of VS due to the Box-Behnken design parameters. Similarly, total VS decreased (from 34.3±1.58 to 26.32±0.84 g L⁻¹) at all trials at the end of AD of manure, sewage sludge, and wine vinasses (Sillero et al., 2023). The VS range on day 12 spans from 0.006 to 0.013 g g⁻¹, showing a reduction across all sets. This reduction is indicative of AD process at work, where microorganisms break down organic matter and convert it into biogas components over time. Significant reductions, with set 6 having a 62.9% decrease (reduction of VS from 0.022 to 0.008 g g⁻¹) and 52.8% decrease in set 5 (from 0.018 to 0.008 g g⁻¹). Sets 4 and 7 have the most notable VS reductions. Set 4's VS reduction from 0.017 to 0.006 g g⁻¹ (63.8% decrease) and set 7's from 0.022 to 0.007 g g⁻¹ (66.0% decrease) likely represent the most optimized mixing conditions (manure:KPW ratio, pH, and inoculum dosage) among the experiments for producing biohydrogen and biomethane (Arelli et al., 2021). Figure 5-4 also coincides with the result, providing the highest biohydrogen yield observed at run 6 (419±4 mL H₂ g⁻¹ VS) and 7 (510±7 mL H₂ g⁻¹ VS) at day 12.

Set 1 and 3 show VS reduction of 4.9% (from 0.011 to 0.010 g g⁻¹) and 3% (from 0.013 to 0.012 g g⁻¹), respectively, which are the least reductions observed. The conditions here may have been suboptimal, potentially due to an imbalance in the substrate composition or less favorable environmental conditions for the microbes (Rabii et al., 2019; Rodríguez-Jiménez et al., 2022).

5.7.4 Volatile fatty acids

During the initial hydrolysis stage of anaerobic digestion AD, volatile fatty acids (VFAs) are generated during the acidogenic fermentation. These VFAs encompass a variety of soluble organic acids, with propionic, butyric, acetic, isovaleric, isobutyric, and valeric acid were detected in the AD when operated with manure and KPW as substrate in the presence of oleic acid (OA). The observed trend of total volatile fatty acids (TVFAs) produced is depicted in Figure 5-9.

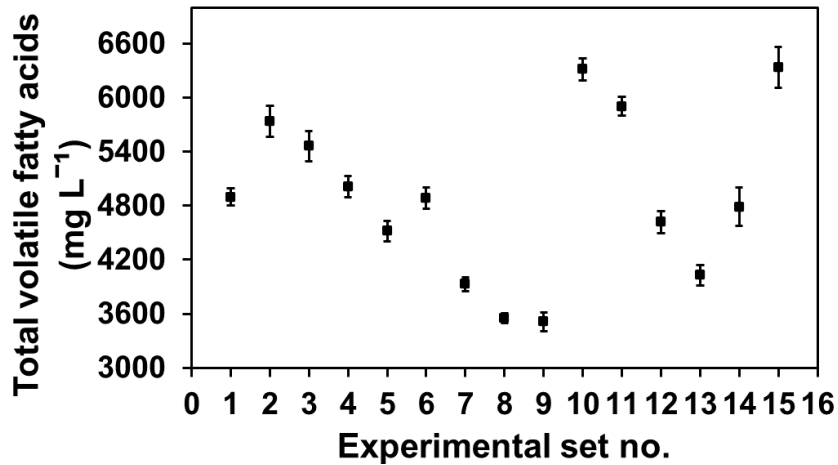


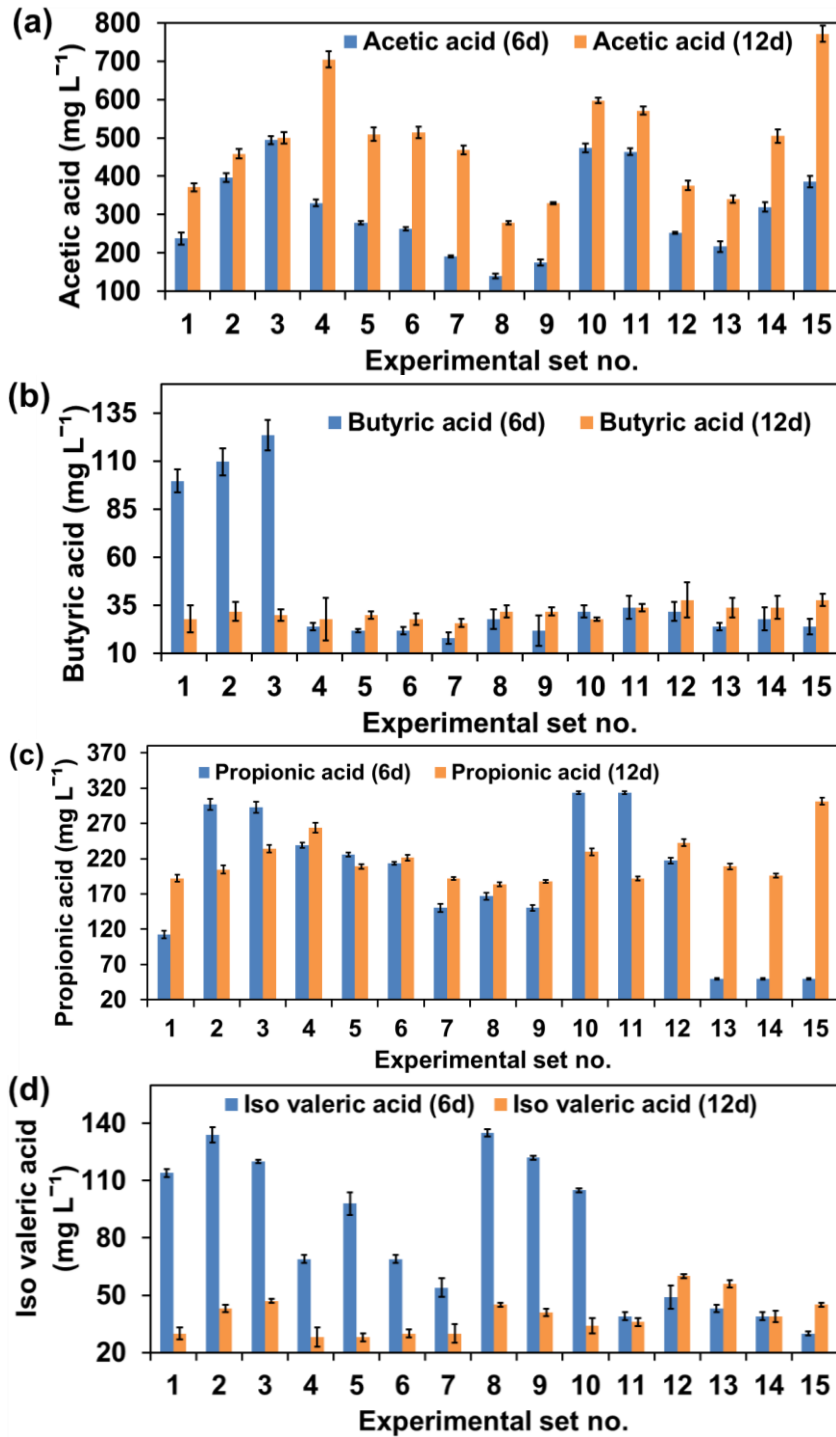
Figure 5- 9. Total volatile fatty acids (TVFAs) production over the digestion time.

The TVFAs values range from 3512±105 mg L⁻¹ to 6334±225 mg L⁻¹, indicating the variability in TVFAs production across the different experimental setups. The lowest average production was in set 8 (M:KPW ratio of 1.5, pH 4, inoculum 5.5) and the highest in set 15 (M:KPW ratio of 1.0,

pH 6, inoculum 7). Sets 2, 3, 4, 10, 11, and 15 have notably higher TVFA production than the other sets ($>5000 \text{ mg L}^{-1}$); this result agreed with Algapani et al. (2019), who found the concentration of TVFAs in the reactor $3500 \pm 700 \text{ mg L}^{-1}$ to $9600 \pm 1500 \text{ mg L}^{-1}$ during first-stage (biohydrogen reactor) AD of food waste. High TVFA production can be attributed to the presence of easily degradable organic matter, especially protein-rich substrates. Proteins are broken down into amino acids, which are further deaminated to produce ammonia and carbon skeletons. These skeletons are then converted into VFAs (Song et al., 2023). The substrate nature significantly influences the type and quantity of TVFAs produced. For instance, carbohydrates tend to produce more acetate and butyrate, while proteins and lipids form propionate, isobutyrate, valerate, and isovalerate, in addition to acetate and butyrate (Owusu-Agyeman et al., 2020). To comprehensively understand the biochemical pathways leading to biohydrogen and biomethane generation during anaerobic digestion, examining the production dynamics of the principal volatile fatty acids (VFAs) produced is essential. Figure 5-10 clearly shows how acetate, butyrate, propionate, isovaleric and valeric acid, which are the main volatile fatty acids produced in this experiment, contribute to the yield of biohydrogen and biomethane across 15 sets.

Figure 5-10 (a) shows a consistent increase in acetic acid levels from day 6 to 12 in all sets. Set 4 and 15 show a remarkable increase in acetic acid concentration from 330 ± 9 to $705 \pm 21 \text{ mg L}^{-1}$ and from 386 ± 15 to $772 \pm 15 \text{ mg L}^{-1}$. This is the largest absolute increase among all the sets, more than doubling the concentration over the period. Set 3 has the least change in acetic acid concentration, with a rise from 494 ± 10 to $500 \pm 12 \text{ mg L}^{-1}$. The small increase could indicate an already maximized acid production by day 6 or the onset of inhibitory conditions that prevent further acidogenesis. Set 8 starts with the lowest acetic acid concentration at $140 \pm 7 \text{ mg L}^{-1}$ on day 6 but doubles to $278 \pm 5 \text{ mg L}^{-1}$ by day 12. Similarly, set 7 shows a more than doubling of the

concentration from a lower initial value of 191 ± 3 to 469 ± 10 mg L^{-1} , which is one of the highest relative increases observed and may indicate a significant acidogenic potential that is realized over the period.



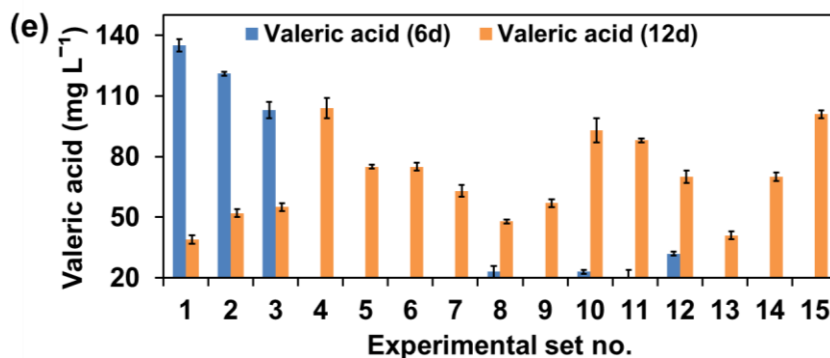
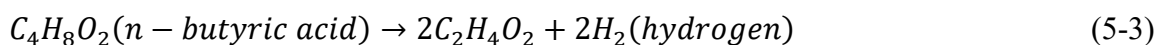


Figure 5- 10. Volatile fatty acid produced measured on days 6 and 12 (a) acetic acid (b) butyric acid (c) propionic acid (d) isovaleric acid and (e) valeric acid.

Figure 5-10 (b) provides data on the concentration of butyric acid on days 6 and 12 of anaerobic digestion across 15 different sets. For most sets, the concentration of butyric acid decreased from day 6 to 12, which is opposite to the trend observed with acetic acid in the previous dataset. This could suggest that butyric acid was consumed during the later stages of anaerobic digestion, possibly converted into other compounds such as acetic acid or directly utilized by methanogens to produce methane. According to Worm et al. (2014), the primary route for transforming butyrate into acetate and hydrogen in VFAs involves β -oxidation. Subsequently, hydrogen (H_2) and CO_2 , along with acetic acid, are utilized by methanogens to generate methane. One mole of n-butyric acid ultimately forms 2 moles of acetate and 2 moles of hydrogen through the β -oxidation process, as shown in Eq. (5-3) (Xu et al., 2023).



The first three sets showed the most substantial decrease in butyric acid levels, with set 1 dropping from 100 ± 6 to 28 ± 6 mg L⁻¹, set 2 from 110 ± 7 to 32 ± 5 mg L⁻¹, and set 3 from 124 ± 8 to 30 ± 3 mg L⁻¹. This indicates a more pronounced butyric acid consumption or conversion in these

sets. Interestingly, set 11 showed almost no difference in butyric acid concentration between days 6 and 12, remaining at 34 ± 6 to 34 ± 2 mg L⁻¹. This may indicate a balance between the production and consumption of butyric acid in this particular set.

The data on the concentrations of propionic acid measured on days 6 and 12 of anaerobic digestion across 15 sets is presented in Figure 5-10 (c). Sets 1, 4, 6, 7, 8, 9, 11, and 12 all show an increase in propionic acid concentration from day 6 to 12, indicating continued production or less consumption of propionic acid during this period. Sets 13, 14, and 15 show the most significant increase in propionic acid, with concentrations starting at 50 ± 1 mg L⁻¹ and increasing to 301 ± 5 mg L⁻¹. This suggests a high propionic acid production rate or buildup due to less efficient conversion to other compounds or gases in this set, yielding the lowest 3.8 to 51 ± 2 mL CH₄ g⁻¹ VS.

Several studies, particularly those focusing on treating protein-rich materials, have also documented the occurrence of valeric and isovaleric acids (Bevilacqua et al., 2021; Bolzonella et al., 2007; Yin et al., 2014). In this investigation, traces of isovaleric acid and valeric acid are also detected, though their levels are significantly lower than the other acids present. The production of isovaleric acid (Figure 5-10 (d)) varies significantly across the 15 experiments. On day 6, the concentration ranges from 30 ± 1 mg L⁻¹ to 135 ± 2 mg L⁻¹, while at day 12, it ranges from 28 ± 2 to 60 ± 1 mg L⁻¹. The highest concentration of isovaleric acid on day 6 is observed in set 8 (135 ± 2 mg L⁻¹), and on day 12 in set 12 (60 ± 1 mg L⁻¹). The lowest concentration on day 6 is found in experimental set 15 (30 ± 1 mg L⁻¹), while on day 12, it is 28 ± 2 mg L⁻¹ by set 5. In most experimental sets, isovaleric acid concentrations generally decreased significantly from day 6 to 12, indicating its consumption during the AD process. Yu et al. (2020) reported a similar finding; the concentration of isovaleric acid, acid for all experiments increased initially at day 10 (185 mg L⁻¹) and then decreased at day 20 (105 mg L⁻¹) over the whole process during AD of swine manure.

Valeric acid concentrations (Figure 5-10 (e)) exhibited significant increases and decreases over the 6 days. Set 7 showed the most considerable increase in valeric acid concentration, escalating from $3\pm 6 \text{ mg L}^{-1}$ (day 6) to $63\pm 3 \text{ mg L}^{-1}$ (day 12). Conversely, set 1 experienced the largest decrease, with valeric acid levels dropping from $135\pm 3 \text{ mg L}^{-1}$ (day 6) to $39\pm 2 \text{ mg L}^{-1}$ (day 12). The data suggest that the conditions of each experimental set-up influence valeric acid production significantly. An increase in valeric acid over time could indicate a successful adaptation or growth of acidogenic bacteria. Previous studies conducted by Owusu-Agyeman et al. (2020) and Esteban-Gutiérrez et al. (2018) have shown that with a rise in the protein content of the substrate, there is an increase in higher molecular weight volatile fatty acids, like valeric acid and caproic acid. On the other hand, a decrease might suggest inhibitory conditions or the consumption of valeric acid by methanogens or other microbial processes within the anaerobic digestion system (Bai et al., 2021).

The dominant single VFAs in each set are found to be different. The varying compositions observed for the VFA for sets 1 to 15 suggested that there were different pathways for hydrogen and methane production: the pathway of sets 1 to 15 mostly followed acetate-type fermentation during the first 6 and the second 6 days and also, sets 1, 2, 3, 10 and 11 followed butyrate pathways since a decreasing trend of the butyric acid production is observed from day 6 onwards. During the acidogenesis phase, acidogenic bacteria break down the products of hydrolysis into VFAs, hydrogen (H_2), and CO_2 , with trace amounts of hydrogen sulfide (H_2S), ethanol, and ammonia (NH_3). Following this, in the acetogenesis stage, acetogenic bacteria further process these VFAs into acetic acid, additional H_2 , CO_2 , and other minor by-products. The final phase, methanogenesis, involves methanogenic archaea converting acetic acid, H_2 , and CO_2 into methane (CH_4) and CO_2 . However, an observed increase in acetic acid concentration towards the end of the AD process,

particularly from day 6 to 12, implies a potential inhibition of methanogenic archaea by oleic acid and produced less methane (Figure 5-5) compared to hydrogen (Figure 5-4). Moreover, the observed VFA profile, which correlates with hydrogen (H₂) production, aligns with existing research on protein-based waste, indicating a preference for acetate-propionate type fermentation in H₂ generation (Capson-Tojo et al., 2017). High concentrations of propionic acid, known to potentially hinder hydrogen production, as suggested by Han et al. (2020), were observed in the study. However, according to Hans and Kumar (2019), the tolerance limit for propionic acid is around 900 mg L⁻¹. In this case, all experimental setups produced propionic acid concentrations below 350 mg L⁻¹, indicating they did not reach the inhibition threshold. This finding is consistent with those of relevant research. For example, Ma et al. (2017) noted that carbohydrate-rich waste primarily leads to butyrate formation, whereas lipids and proteins tend to yield valerate and propionate. Additionally, Zhang et al. (2022) identified acetic acid and propionic acid as the predominant VFAs during the fermentation of protein-rich biomass, further illustrating the variable impacts of different substrates on VFA production.

5.7.5 Model validation

The optimal operational conditions were determined through D-optimality analysis, which identified the best combination of factors: manure:KPW ratio of 0.5, a pH level of 6.0, and an inoculum dosage of 4 g VS L⁻¹. Under these conditions, the maximum hydrogen yield was predicted as 398 mL H₂ g⁻¹ VS. To validate this model prediction, an experiment was conducted in triplicate at the optimal settings. The results showed a peak hydrogen yield of 385±13 mL H₂ g⁻¹ VS, which was marginally lower (about 3.37%) than the predicted value. This slight discrepancy is likely due to variations in laboratory conditions. These experimental findings corroborate the

accuracy of the RSM based on BBD used in developing the model. Thus, the model demonstrated in this study is reliable and applicable within its defined operational range, offering valuable guidance for optimizing hydrogen production in similar setups.

5.8 Biohydrogen from Pure Proteins

In the context of the 15 statistically designed experiments outlined in section 5.6, three specific sets (6, 7, and 13 from Table 5-5) were identified as yielding the highest biohydrogen production. These sets were called A1, A2, and A3 for albumin sets and C1, C2, and C3 for casein sets following manure-KPW sets 6, 7, and 13. These sets were selected based on the optimal combination of three key parameters: i) manure:KPW ratio, ii) pH, and iii) inoculum dosage. Building on this framework, the same parameter combinations (Table 5-1), now adapted as i) albumin:KPW ratio, ii) pH, and iii) inoculum dosage, were applied to investigate the biohydrogen and biomethane yields, protein degradation, and VFA production using pure protein sources – albumin and casein in the presence of 4,000 mg L⁻¹ oleic acid (OA).

5.8.1 Biohydrogen and biomethane yield

This section illustrates the biohydrogen production from two protein-based substrates, albumin and casein, over 12 days (Figure 5-11). Each substrate was tested in three distinct experimental sets, with varying conditions. The data of the cumulative volume of biohydrogen gas produced allow for a comprehensive comparison between the different sets, showcasing the impact of the specific variables on the biohydrogen production process from these pure protein substrates.

The provided experimental data offers a compelling insight into the biohydrogen production capabilities of microbial cultures utilizing albumin and casein substrates over 12 days. Notably,

albumin set 2 demonstrated the most significant enhancement in hydrogen yield, escalating from 33 ± 3 mL H₂ g⁻¹ VS on day 1 to an impressive 554 ± 3 mL H₂ g⁻¹ VS by day 12, marking a substantial increase of 521 mL H₂ g⁻¹ VS.

This remarkable growth not only outstripped its own initial measurements but also surpassed the increases observed in all other albumin sets. For casein, set 3 showed the highest augmentation, starting from 45 ± 6 mL H₂ g⁻¹ VS and rising to 399 ± 5 mL H₂ g⁻¹ VS, totaling an increase of 354 ± 1 mL H₂ g⁻¹ VS.

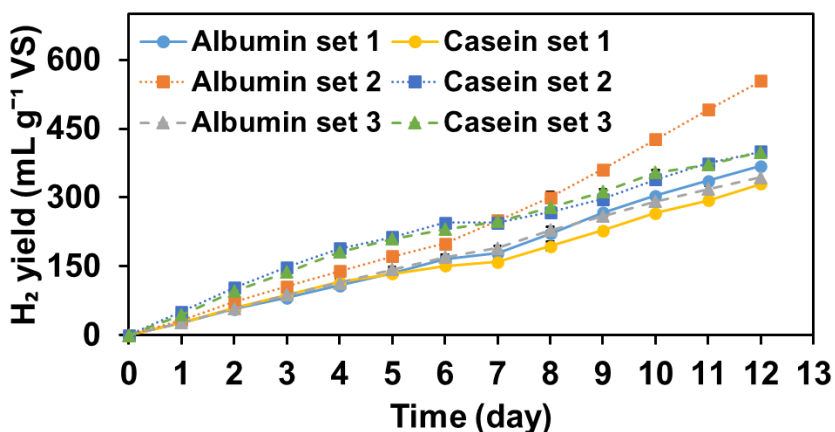


Figure 5- 11. Biohydrogen profile using albumin and casein as substrates for 12 days.

Interestingly, when examining the increments from day 1 to day 6, casein set 2 took the lead with an increase of 194 ± 2 mL H₂ g⁻¹ VS, indicating a robust early-stage hydrogen production. When comparing the highest yields of each type, albumin set 2 (555 ± 15) has a significantly higher yield than the best-performing casein set 2 (400 ± 3). By day 12, the difference between the highest-yielding albumin set (set 2) and the highest-yielding casein set (set 2) is 154 ± 1 mL H₂ g⁻¹ VS, a substantial difference indicating a more efficient process or better conditions for hydrogen production in the albumin set 2. Although albumin set 2 is particularly favorable for hydrogen production, the other albumin sets (1 and 3) have lower yields than casein sets 1 and 3, indicating

some variability in how these substrates are utilized for hydrogen production. These findings highlight the efficacy of albumin and casein as substrates for biohydrogen production and underscore the variance in productivity between different experimental conditions. Table 5-9 compares biohydrogen production from manure and pure protein sources under the same experimental settings. This straightforward comparison is designed to reveal the effectiveness of various substrates in producing hydrogen and assess how pure proteins perform compared to manure in a controlled environment.

Table 5- 9. Comparison of biohydrogen yield from manure and pure proteins under similar experimental conditions.

	Hydrogen yield (mL g ⁻¹ VS)									
	Manure			Albumin			Casein			
	Set 6	Set 7	Set 13	Set 1	Set 2	Set 3	Set 1	Set 2	Set 3	
Manure:KPW ratio	0.5	0.5	0.5	0.5	0.5	0.5	0.5	0.5	0.5	
pH	6	5	4	6	5	4	6	5	4	
Inoculum (g VS L ⁻¹)	5.5	4	5.5	5.5	4	5.5	5.5	4	5.5	
Day	1	67±5	75±3	40±1	27±1	33±3	27±2	27±3	51±5	45±6
	2	136±8	147±6	78±5	56±3	72±2	58±3	59±1	103±2	96±3
	3	205±3	229±6	140±2	82±4	106±3	88±1	89±2	148±3	138±2
	4	238±5	285±2	194±6	108±4	139±6	114±2	116±3	189±1	181±5
	5	276±11	321±7	254±5	136±2	172±6	143±6	134±4	213±5	210±3
	6	339±14	389±11	311±9	165±6	200±3	170±5	151±5	245±3	231±3
	7	339±12	389±9	335±5	179±5	250±8	190±5	159±7	245±7	248±4
	8	345±5	417±5	349±3	221±4	300±7	229±5	194±9	268±8	278±7
	9	354±3	437±6	374±8	267±5	361±11	260±7	228±7	296±9	313±9
	10	380±11	466±7	397±11	304±5	427±9	292±7	266±7	339±2	354±5
	11	406±5	501±2	416±5	336±2	492±7	318±12	293±4	374±5	371±5
	12	419±4	510±7	424±8	369±4	554±3	344±7	330±5	400±4	399±5

Set 6 (manure:KPW ratio of 0.5, pH 6 and 5.5 g VS L⁻¹) demonstrated a significant increase in yield from 67±5 mL H₂ g⁻¹ VS on day 1 to 419±4 mL H₂ g⁻¹ VS on day 12, culminating in a net

increase of 352 ± 1 mL H₂ g⁻¹ VS. When juxtaposed with the yields from albumin set 1 and casein Set 1, which showed increases of 341 mL H₂ g⁻¹ VS (from 27 ± 1 to 369 ± 1) and 302 mL H₂ g⁻¹ VS (from 27 ± 3 to 330 ± 5) respectively, set 6 not only surpasses the yield from casein set 1 but also outperforms the albumin set 1. Similarly, set 7 started with a yield of 75 ± 3 mL H₂ g⁻¹ VS and concluded with a substantial increase to 510 ± 7 mL H₂ g⁻¹ VS.

This remarkable growth, representing an overall increase of 435 ± 1 mL H₂ g⁻¹ VS, surpasses the yield from casein set 2 (from 51 ± 5 to 400 ± 4 mL H₂ g⁻¹ VS). Set 13 displays a significantly higher yield (311 ± 9 mL H₂ g⁻¹ VS) than both albumin set 3 (170 ± 5 mL H₂ g⁻¹ VS) and casein set 3 (231 ± 3 mL H₂ g⁻¹ VS) on day 6. This suggests that the manure with KPW substrate is substantially more effective for biohydrogen production by the sixth day than the pure protein substrates, albumin and casein, with KPW. By day 12, set 13 continues to outperform albumin set 3, yielding 424 ± 8 mL H₂ g⁻¹ VS against 344 ± 7 mL H₂ g⁻¹ VS, indicating a more sustained and higher hydrogen production rate. Compared to casein set 3, set 13 still maintains a higher yield, though with a smaller margin of 424 ± 8 mL H₂ g⁻¹ VS for set 13 versus 399 ± 5 mL H₂ g⁻¹ VS for casein set 3.

In the quest for sustainable biohydrogen production, set 6, 7, and 13's utilization of manure in conjunction with KPW has demonstrated a significant yield enhancement, showcasing the potential for agro-industrial by-products in renewable energy applications (Meiramkulova et al., 2018). The synergistic effect of the nutrient-rich manure, providing essential nitrogen and minerals, alongside the carbonaceous or low nitrogen content KPW, may optimize the carbon-to-nitrogen (C/N) ratio, which is critical for microbial metabolism (Ghinea et al., 2019). Furthermore, the physical structure of KPW could offer a larger surface area for microbial attachment, potentially facilitating higher rates of bioconversion (Miao et al., 2019). The comparative increase

in yield observed in sets 6, 7, and 13 underscores the effectiveness of manure-KPW substrate combination. It aligns with findings from relevant studies that highlight the benefits of mixed-substrate approaches to biohydrogen production. For example, with manure co-substrates such as wine vinasses, sewage sludge (Sillero et al., 2022), food waste (Liu et al., 2020), rice straw (Chen et al., 2021) and pineapple peel waste (Nguyen et al., 2021) are found to produce biohydrogen. Table 5-10 presents biohydrogen production from manure and other wastes.

Table 5- 10. An overview of biohydrogen production from manure and organic wastes.

Substrate	Co-substrate	Biohydrogen yield (mL g ⁻¹ VS)	References
Dairy manure	Kiwi peel waste	389±11	This study
Poultry manure	Sewage sludge and wine vinasse	40.41	Sillero et al. (2022)
Cattle manure	Food waste	30.00	Liu et al. (2020)
Cow manure	Waste milk	590.5	Lateef et al. (2012)
Cow dung	Fruit waste and tofu waste	231.02	Amekan et al. (2018)
Swine manure	Fruits and vegetable waste	126 ± 22	Tenca et al. (2011)
Cow manure	Cassava stillage	44	Wang et al. (2013)
Pig manure	Cassava stillage	51	Wang et al. (2013)

The successful application of such waste-derived co-substrates with manure could lead to a dual benefit of energy recovery and waste reduction, presenting an eco-friendly solution to energy demands (Jiang et al., 2021).

There were higher hydrogen yields in the sets utilizing KPW with manure (sets 6, 7, and 13) than KPW with pure protein albumin and casein (sets 1, 2, and 3). The manure is a complex mixture containing a wide range of organic compounds, including protein, lignocellulosic fibers, and carbohydrates (Wang et al., 2020), which can provide a more diverse and accessible range of nutrients for the microbial communities (Li et al., 2020). In the case of albumin and casein, these are pure protein substrates which, while rich in nitrogen (C:N is 8 and 3.68 for albumin and casein),

may not provide the same level of microbial accessibility or the balanced C:N ratio (approximately 20:1 to 30:1) that is crucial for optimal bacterial growth and metabolism (Jadhav et al., 2023; X. Li et al., 2020). The microbial consortia in manure may be more adapted or resilient to the fermentation process, possibly containing a higher proportion of hydrogen-producing bacteria when co-digested with KPW (Valdez-Vazquez & Poggi-Varaldo, 2009). The bacterial communities that develop in albumin and casein substrates might not be as efficient in hydrogen production due to a lack of necessary co-factors or inhibitors produced during protein breakdown. Batch experiments by Yokoyama et al. (2010) revealed that bacteria in cow manure produced significant hydrogen from sugars (glucose and sucrose) and wheat starch, with levels ranging from 863 to 1,331 mL H₂ Kg⁻¹ mixture. However, when manure was mixed with proteins such as casein, albumin, gelatin, and peptone, it did not lead to hydrogen generation but increased CO₂ output, indicating their decomposition without hydrogen release (Yokoyama et al., 2010). The fermentation of proteins like albumin and casein can produce inhibitory by-products such as ammonia and VFA, which can inhibit the activity of microbial community structure. Tang et al. (2005) studied a mesophilic anaerobic reactor to process synthetic wastewater with albumin as the sole nutrient source. This setup primarily yielded VFAs and ammonia as degradation products without producing methane. In the same experimental setup, sets 6, 7, and 13 yielded outputs of 154±4, 90±2, and 16±4 mL CH₄ g⁻¹ VS, respectively (Figure 5-5). However, it was noted that none of the three sets utilizing pure proteins, albumin and casein, produced any methane during the 12-day duration of the experiment. The sets containing pure proteins, such as albumin and casein, exhibited a pronounced inhibition in methane generation, which suggests that oleic acid (OA) had a more significant inhibitory effect on methanogenes in these pure protein sets compared

to those containing manure (set 6, 7, and 13). This finding underscores the sensitivity of methanogenic archaea to OA in environments with protein-rich substrates.

5.8.2 Protein quantity

Figure 5-12 (a and b) represents the concentration of albumin (A1, A2, A3 in mg L^{-1}) and casein (C1, C2, and C3 in mg L^{-1}) across three different experimental set 1, 2, and 3 under anaerobic conditions at different time points: initially (day 0), at days 6 and 12.

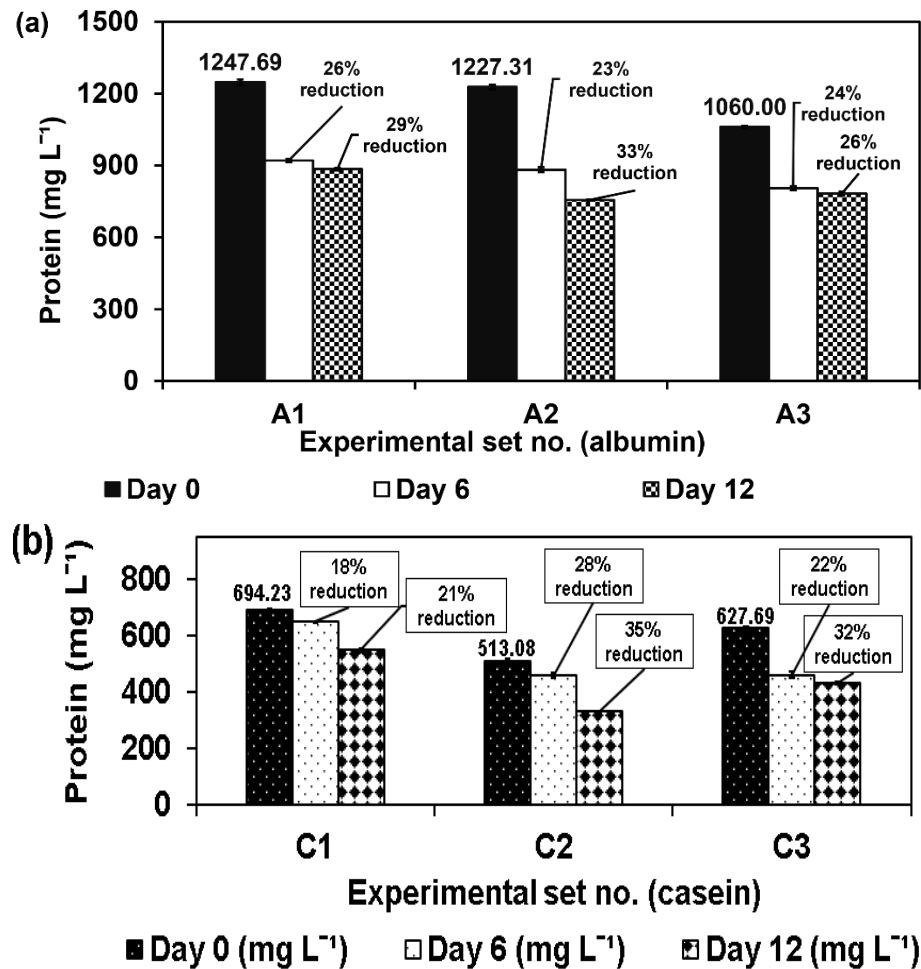


Figure 5- 12. Protein quantity of (a) albumin set A1 (albumin:KPW ratio of 0.5, pH 6, inoculum 5.5 g VS L^{-1}), set A2 (albumin:KPW ratio of 0.5, pH 5, inoculum 4 g VS L^{-1}), set A3 (albumin: KPW ratio of 0.5, pH 4, inoculum 5.5 g VS L^{-1}) on day 6 and day 12 (b) casein set C1 (casein:KPW ratio of 0.5, pH 6, inoculum 5.5 g VS L^{-1}), set C2 (casein:KPW ratio of 0.5, pH 5, inoculum 4 g VS L^{-1}), set C3 (casein:KPW ratio of 0.5, pH 4, inoculum 5.5 g VS L^{-1}) on day 6 and 12.

The percentages shown on the graph above each bar correspond to the reduction of albumin from the day 0 concentration for each set on days 6 and 12 (Figure 5-12 (a)). On day 0, albumin set A1 starts with $1247.69 \pm 11 \text{ mg L}^{-1}$, set A2 with $1227.31 \pm 9 \text{ mg L}^{-1}$, and set A3 with $1060 \pm 5 \text{ mg L}^{-1}$. At day 6, the albumin concentration decreases in all sets due to the digestion process. For set A1, the concentration drops to $920 \pm 7 \text{ mg L}^{-1}$, a $26.2 \pm 1\%$ reduction from day 0. Set A2 reduces to $882.31 \pm 11 \text{ mg L}^{-1}$, a $23.4 \pm 2\%$ reduction. Set A3 decreases to $805.38 \pm 9 \text{ mg L}^{-1}$, a $23.8 \pm 3\%$ reduction. On day 12, further reduction is observed. Set A1 decreases to $884.62 \pm 5 \text{ mg L}^{-1}$, a $29.1 \pm 2\%$ reduction from the initial concentration. Set A2 shows a more significant decrease to $756.15 \pm 3 \text{ mg L}^{-1}$, with a $33.2 \pm 1\%$ reduction, indicating the highest degradation rate among the three sets. Lastly, set A3 reaches $783.08 \pm 8 \text{ mg L}^{-1}$, a $26.3 \pm 1\%$ reduction. Despite a good start on day 6, it shows the least reduction by day 12 compared to the other sets.

Figure 5-12 (b) illustrates the degradation of casein protein in an anaerobic environment over 12 days, as evidenced by three sets of experimental data. The bars denote the initial day (0) concentrations of casein, concentrations on day 6, and the concentrations on day 12. Percentages above the bars indicate the reduction from the day 0 concentration. Casein set C1 begins with a day 0 concentration of 694.23 mg L^{-1} . After 6 days, the concentration drops to 649.62 mg L^{-1} , a reduction of 17.6% , and by day 12, it further reduces to 549.62 mg L^{-1} , totaling a 20.7% decrease from day 0. Set C2, despite starting with the lowest concentration of casein ($513.08 \pm 9 \text{ mg L}^{-1}$) it shows the greatest protein reduction at day 6 ($28.3 \pm 2\%$) and day 12 ($34.6 \pm 1\%$). Set C3 has a mid-range starting concentration ($627.69 \pm 7 \text{ mg L}^{-1}$), reduces to $462.69 \pm 11 \text{ mg L}^{-1}$ at day 6, a $22.4 \pm 1\%$ reduction, and ends at $432.31 \pm 4 \text{ mg L}^{-1}$ at day 12, marking a $32 \pm 1\%$ reduction. Set C2 shows the greatest reduction on day 6 and 12 despite starting with the lowest concentration of casein. Set C1

does not correspondingly show the highest reduction despite having the highest initial concentration.

Set 2 exhibits the highest protein reduction for albumin set A2 (33.2±1%) and casein set C2 (34.6±1%), a notable observation pointing towards the optimal conditions provided within this set for proteolytic activity. The pH of 5 in set 2 is crucial, likely aligning closely with the optimal activity range of proteases in the Kiwi Peel Waste (KPW). Proteases (actinidin) are known to have specific pH ranges (pH 4-10) where their catalytic activity is active (Kaur et al., 2023); however, at specific pH along with the substrate type form a favorable conformation of their active sites and substrate binding (David Troncoso et al., 2022). In a study by Chalabi et al. (2014), actinidin enzyme could disintegrate pure α -casein and major subunits of micellar casein, especially in acidic pH (4 to 6). Additionally, in sets A2 and C2, the microbial dynamics facilitated by an inoculum concentration of 4 mg L⁻¹ could have favored a microbial consortium adept at protein degradation. The slightly acidic conditions may inhibit non-proteolytic pathogens (Stringer et al., 1999), promoting a community structure centered around efficient protein-utilizing microorganisms. The combination of proteases from KPW and the microbial population from the inoculum might work synergistically to break down proteins more effectively in sets A2 and C2. The proteases could initiate the breakdown (Kaur & Boland, 2013), and the microbes could further metabolize the resulting peptides and amino acids (Bajić et al., 2022; Xiang et al., 2019). The protein reduction (%) discrepancies observed in sets 1 and 3 of albumin and casein could be due to different tertiary and quaternary structures of albumin and casein, which affect their susceptibility to enzyme-catalyzed hydrolysis. Albumin is a globular protein, generally more soluble, and may be more readily accessible to proteases. Casein, on the other hand, resembled a denatured globular protein

structure results in the hydrophobic portion of the amino acid building blocks being exposed, causing the entire protein water- insoluble (Huppertz et al., 2018; Sim et al., 2021).

5.8.3 Fourier transform infrared (FTIR)

This section investigates the impact of KPW on the anaerobic digestion process of two specific proteins: albumin and casein. The primary focus is on understanding how KPW facilitates or alters functional groups of the protein substrates during the hydrolysis stage of these proteins, offering insights into its role in enhancing digestion efficiency.

This analysis was carried out using in-depth Fourier Transform Infrared (FTIR) spectroscopy, with a wavenumber range of 4000 to 400 cm^{-1} , on samples collected at the start (day 0) and on day 12. The comparison of FTIR spectra of the day 0 sample with those obtained post-digestion revealed notable differences. These differences highlighted the shifting of the functional groups with time, as depicted in Figure 5-13 (a) and (b) for albumin and casein. The samples were extracted from albumin set A2 (albumin:KPW ratio of 0.5, pH 5, inoculum 4 g VS L^{-1}) and casein set C2 (casein:KPW ratio of 0.5, pH 5, inoculum 4 g VS L^{-1}).

In the FTIR spectrum of the albumin-KPW day 0 sample (Figure 5-13 (a)), which is a blend of albumin and KPW with oleic acid, several characteristic absorption peaks indicate molecular vibrations within the sample. The spectrum shows a broad peak around 3300 cm^{-1} , which can be attributed to the amide A band, typically found in the range of 3300 to 3500 cm^{-1} due to N-H and O-H stretching vibrations, often involved in hydrogen bonding (Webster & Kiemle, 2005). The amide I band is represented by a peak at 1709 cm^{-1} , falling within the expected range of 1600-1700 cm^{-1} , and is primarily associated with C=O stretching vibrations, a characteristic feature of protein secondary structures. The amide II band is usually observed between 1580-1410 cm^{-1} , and the

spectrum shows a peak at 1541 cm^{-1} , which is indicative of combined N-H bending and C-N stretching vibrations, further confirming the presence of proteins (Peltre et al., 2017).

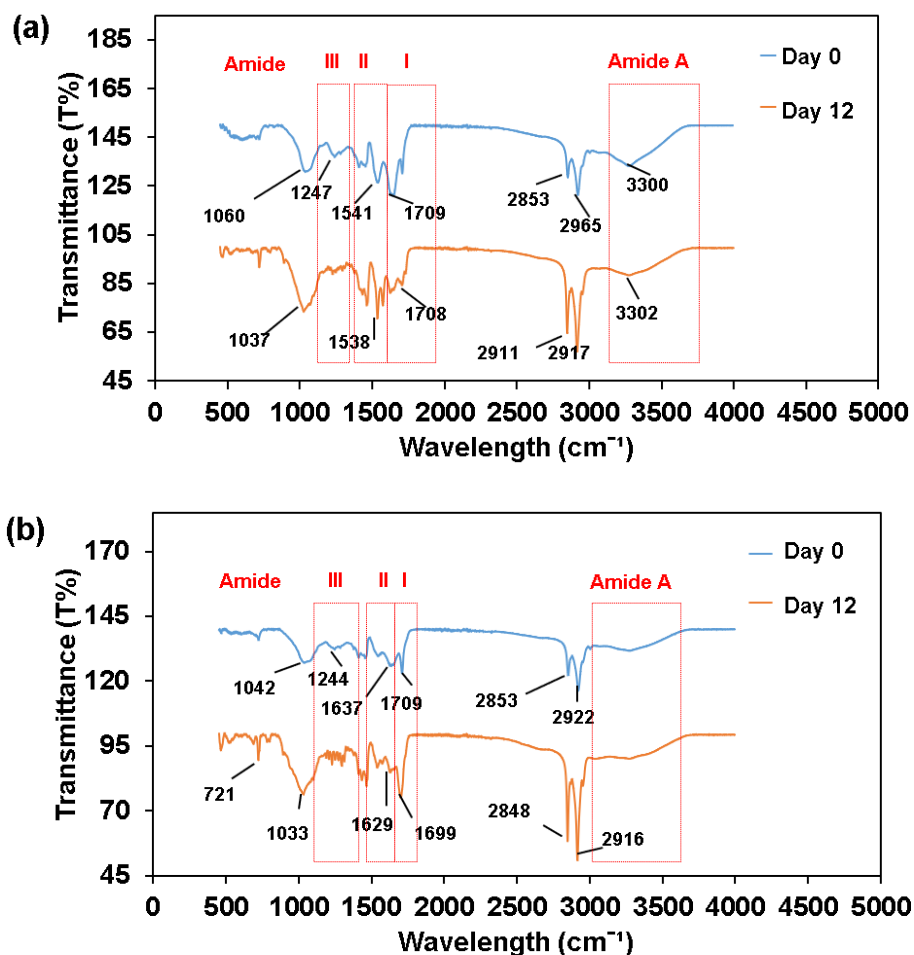


Figure 5- 13. Fourier Transform Infrared (FTIR) spectrum of (a) albumin and (b) casein on day 0 and day 12.

The amide III band ($1200\text{ to }1350\text{ cm}^{-1}$) arises from the combination of N-H bending and C-N stretching vibrations at 1247 cm^{-1} , which are associated with the protein's tertiary structure. The presence of this peak suggests the involvement of these molecular vibrations and confirms the integrity of protein structures within the sample (Stani et al., 2020). Additional sharp peaks are

noted at 2965 cm^{-1} and 2853 cm^{-1} , which are characteristic of C-H stretching vibrations commonly seen in organic compounds, suggesting the presence of oleic acid (Namazi et al., 2011).

The FTIR spectrum of the albumin-KPW sample on day 12 of anaerobic digestion (Figure 5-13 (a)) exhibits several changes when compared to the sample on day 0, indicating alterations in the protein structure due to the digestion process. Within the amide A region (3300 to 3500 cm^{-1}), there is a slight shift from the initial sharp peak at 3300 cm^{-1} to a diminished peak at 3302 cm^{-1} , suggesting a change in the hydrogen bonding pattern of the N-H groups. In the Amide I region (1600 - 1700 cm^{-1}), which is sensitive to protein secondary structure, there is a discernible shift from 1709 cm^{-1} in the day 0 sample to 1708 cm^{-1} after digestion, along with a decrease in peak intensity. This may reflect the breakdown of the protein's secondary structure, such as the disruption of α -helix or β -sheets (Huang et al., 2017). α -helix in the secondary structure of the protein wastewater was also found to be decreased by 46.3% during AD (Li et al., 2022). The Amide II region (1580 - 1410 cm^{-1}) shows a peak at 1538 cm^{-1} with a reduced intensity compared to the day 0 sample 1541 cm^{-1} , indicative of altered N-H bending and C-N stretching due to the digestion process (Zhang et al., 2020). Notably, the amide III band (1200 to 1350 cm^{-1}) is not clearly identified after AD, which might be due to significant distortion of the protein structure post-digestion (Ganesh Kumar et al., 2008). The peak at 2965 cm^{-1} on day 0 is now observed at 2917 cm^{-1} , with a reduced transmittance, suggesting possible oxidation of methylene groups or other modifications in the lipid components (Smidt & Schwanninger, 2005).

The comparative analysis of the FTIR spectra for the casein and KPW sample before and after 12 days of AD is presented in Figure 5-13 (b). The amide A band on day 0, typically between 3300 and 3500 cm^{-1} indicates of the N-H bend/ stretch vibration or hydroxyl H-O- bend/ stretch vibration. It shows a noticeable transformation or is possibly diminished after the digestion period. This could

signify a loss of secondary structures like alpha-helices or beta-sheets due to the breakdown of hydrogen bonds (Pavia et al., 2008). The peaks at 2922 cm^{-1} and 2853 cm^{-1} in the day 0 sample, typically attributed to the symmetric and asymmetric stretches of methylene groups ($-\text{CH}_2-$), respectively, have shifted to 2916 cm^{-1} and 2848 cm^{-1} . These shifts to lower wavenumbers could indicate a change in the chemical environment surrounding the methylene groups. The amide I band centered around 1709 cm^{-1} in the day 0 sample, which is sensitive to C=O stretching vibrations, is shifted to a lower wavenumber at 1699 cm^{-1} after digestion, with a reduced intensity. This shift is characteristic of alterations in the protein secondary structure, possibly indicating a loss of ordered protein structures (Chiang et al., 2023). In the amide II region, the peak initially at approximately 1637 cm^{-1} has shifted to 1629 cm^{-1} . The amide III band, which involves a mix of vibrations and is observed in the day 0 sample at 1244 cm^{-1} , shows a diminishing pattern at post-digestion, with a change in intensity. This alteration in the spectrum could represent a modification in the protein's tertiary structure or alterations in the side-chain interactions (Stuart, 2004). Other notable peaks in the spectrum show significant changes; for instance, new peaks emerge, or existing peaks become more prominent in the lower wavenumber region, such as at 721 cm^{-1} . This change can be attributed to new chemical structures or interactions that have developed during AD, affecting the skeletal vibrations of the molecules present in the sample.

5.8.4 Scanning Electron Microscopy (SEM)

This section delves into the detailed Scanning Electron Microscopy (SEM) analysis of albumin set A² (albumin:KPW ratio of 0.5, pH 5, inoculum 4 g VS L^{-1}) and casein set C2 (casein:KPW ratio of 0.5, pH 5, inoculum 4 g VS L^{-1}), providing a comparative insight into their microstructural

changes observed at the onset (day 0) and after a significant period (day 12). For clarity, the images of all the samples were taken at different magnifications.

The day 0 SEM images (Figure 5-14 (a, b)) of the albumin and KPW composite before AD displayed distinct morphological characteristics. Albumin, a globular protein, is presented as sizeable, irregular aggregates, reflecting its soluble yet aggregated nature in this context (Gülseren et al., 2007). The KPW showed heterogeneous fibrous structures with variable particulate sizes that indicate a relatively intact state before digestion. On day 6 of AD, the SEM images (Figure 5-13 (c, d)) suggested the beginning of structural alterations. The albumin-KPW aggregates appeared less defined, with signs of surface erosion possibly due to proteolytic activity. The KPW began to exhibit a breakdown of the fibrous matrix, with the increased presence of smaller fragments and less defined edges, indicative of partial degradation by microbial enzymes. After 12 days, the micrographs (Figure 5-14 (e, f)) depicted a substantial transformation. The albumin aggregates were visibly reduced and smoothed out, suggesting extensive microbial degradation facilitated by the inoculum's proteolytic and lipolytic enzymes (Molinuevo-Salces et al., 2012). Similarly, investigation through SEM studies indicated that protein-based waste leather showed uniform fluffiness after treatment in the experimental sample (Ma et al., 2014). The fibrous structure of KPW showed a near-complete loss of its original fibrous structure, indicating advanced cellulose breakdown (Weimer, 2022).

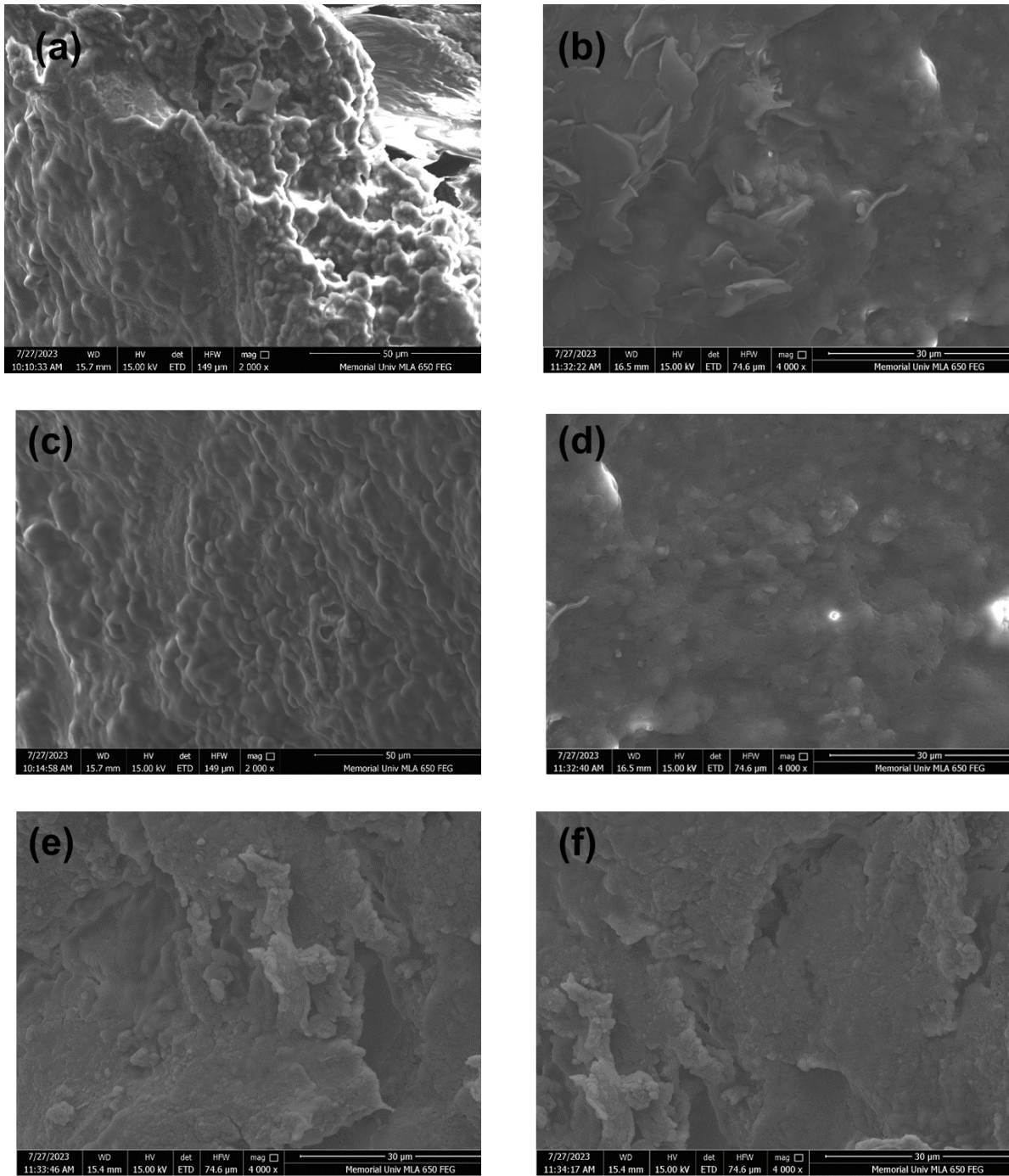


Figure 5- 14. Scanning Electron Microscopy (SEM) images of (a) and (b) albumin-KPW substrate on day 0, and after AD at (c) and (d) day 6, (e) and (f) day 12.

The SEM images in Figure 5-15 represent casein-KPW composite morphological features on days 0, 6, and 12 of AD. The day 0 sample's SEM images (Figure 5-15 (a, b)) likely depict casein protein's micellar structure, which is typical due to its colloidal nature in milk (De Kruif et al., 2012). The micelles appear as globular and somewhat clustered forms, which is characteristic of casein in its native state (De Kruif et al., 2012). The KPW adds to the complex matrix with its irregular, fibrous structures, often associated with plant cell wall components like cellulose and lignin (Weimer, 2022). The image presents a highly heterogeneous and rough landscape indicative of minimal prior degradation. On day 6 of AD, the SEM images (Figure 5-15 (c, d)) start showing minor transformation.

The casein micelles seem less distinct, suggesting the beginning of the digestion process. The surfaces look more eroded, and the fibrous structure starts to fragment, which could be attributed to the activity of cellulolytic and proteolytic enzymes from the KPW and microbial inoculum (Gang et al., 2020; Speda et al., 2017). As the process progresses to day 12 (Figure 5-15 (e, f)), the images suggest a thorough degradation of the casein-KPW complex, leaving behind a landscape lacking initial morphological features. The digestion of casein-KPW likely disrupted hydrogen bonds and Van der Waals forces in its polypeptide chains, leading to the breakdown of cross-links between protein molecules (Xu et al., 2020).

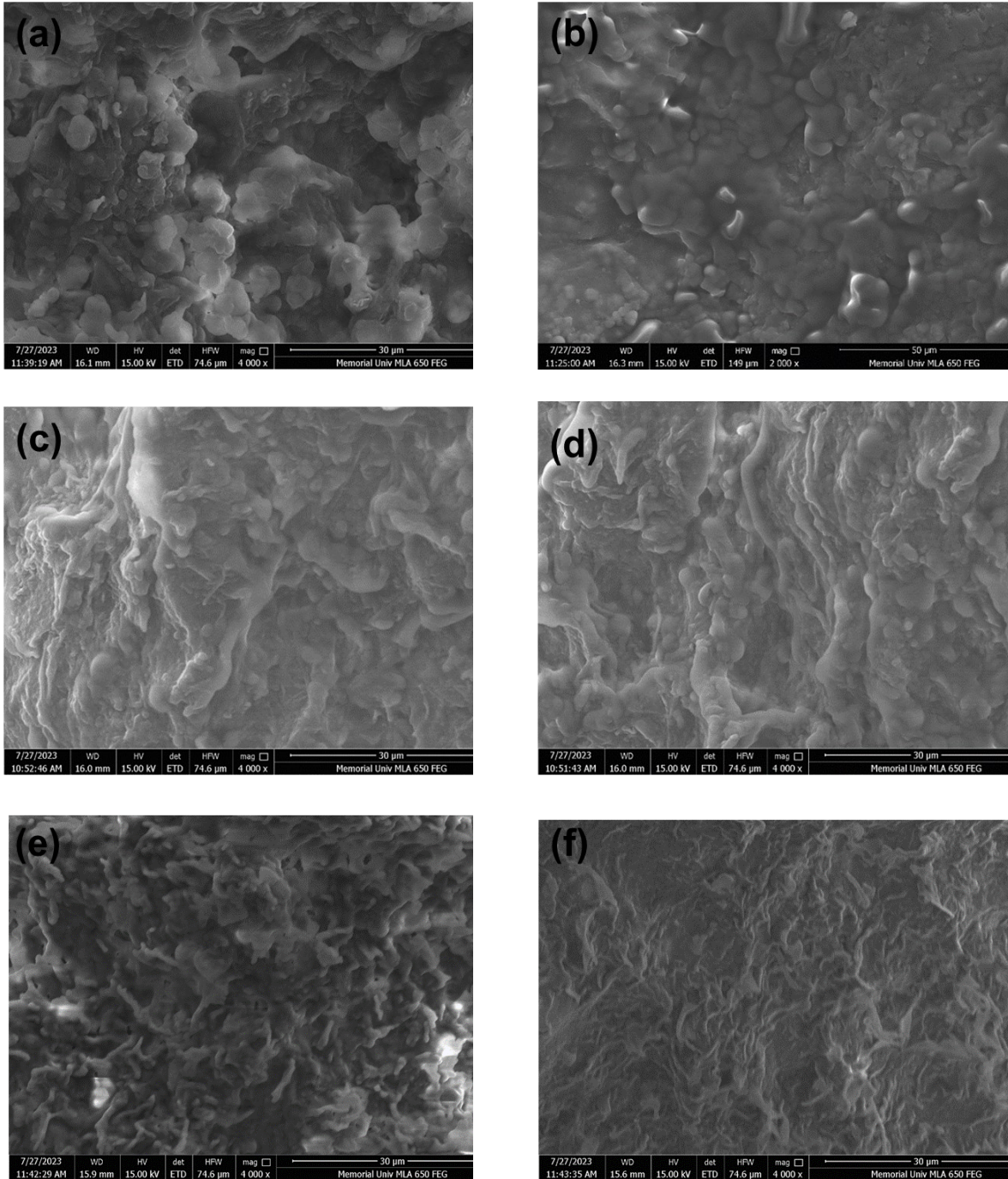


Figure 5- 15. SEM images of (a) and (b) casein -KPW substrate on day 0, and after AD at (c) and (d) day 6, (e) and (f) day 12.

5.8.5 Volatile fatty acids

In this section, the production of volatile fatty acids (VFAs) in the AD process using a mix of pure protein (albumin, casein) and KPW in the presence of oleic acid (OA) is observed. VFAs such as propionic, butyric, acetic, isovaleric, and valeric acids were measured throughout the experiment days. Figure 5-16 illustrates the overall trend in the production of these total volatile fatty acids (TVFAs) from albumin set 1 (albumin: KPW ratio of 0.5, pH 6, inoculum dose 5.5 mg L⁻¹), albumin set 2 (albumin: KPW ratio of 0.5, pH 5, inoculum dose 4 mg L⁻¹), albumin set 3 (albumin: KPW ratio of 0.5, pH 4, inoculum dose 5.5 mg L⁻¹), casein set 1 (casein: KPW ratio of 0.5, pH 6, inoculum dose 5.5 mg L⁻¹), casein set 2 (casein: KPW ratio of 0.5, pH 5, inoculum dose 4 mg L⁻¹) and casein set 3 (casein: KPW ratio of 0.5, pH 4, inoculum dose 5.5 mg L⁻¹).

For albumin sets 1, 2, and 3, the TVFA concentrations were recorded at 5864±95 mg L⁻¹, 4834±88 mgL⁻¹, and 5301±91 mgL⁻¹, respectively. Meanwhile, the TVFA concentrations for casein sets 1, 2, and 3 were notably higher, measured at 7811±69, 6539±65, and 7346±53 mg L⁻¹, respectively. This indicates a trend where casein substrates consistently yield higher TVFA outputs compared to albumin under the same experimental conditions.

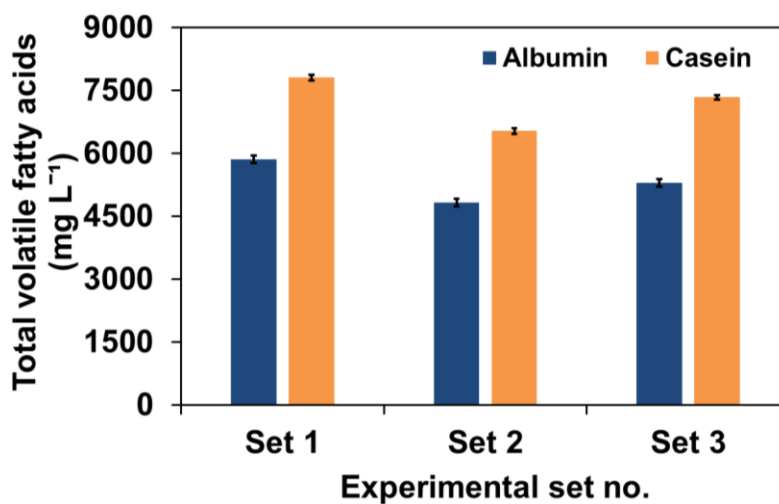


Figure 5- 16. Total volatile fatty acids (TVFAs) production by albumin and casein samples.

Casein, a more complex protein than albumin (Bhat et al., 2016), might offer a more varied nutrient profile or be more amenable to the microbial consortia within the anaerobic digester. These findings align with studies such as Deng et al. (2023), who noted that substrate complexity could significantly influence TVFA production in AD processes. Furthermore, the observed variations among the different sets within the same substrate type could be attributed to differences in sludge, digestion time, temperature, and substrate concentration (Feng et al., 2009; Tan et al., 2012; Yuan et al., 2009). High TVFA production was achieved in just one day with untreated, insoluble casein, indicating that seed culture microorganisms can efficiently convert insoluble proteins like casein into TVFAs. This suggests that protein solubility is not crucial for VFA production, but its biodegradability is (Bevilacqua et al., 2021). Tan et al. (2012) found that in fermentation with a solids retention time (SRT) of 12 days, the TVFA production from albumin and casein without any treatment reached up to 1200 and 1300 mg L⁻¹, respectively, lower than that obtained in the present study. Similar results were achieved from the AD of manure (4% TS), measured TVFAs of 7,210 mg L⁻¹ on day 7 and 9,400 on day 14 (Meng et al., 2018).

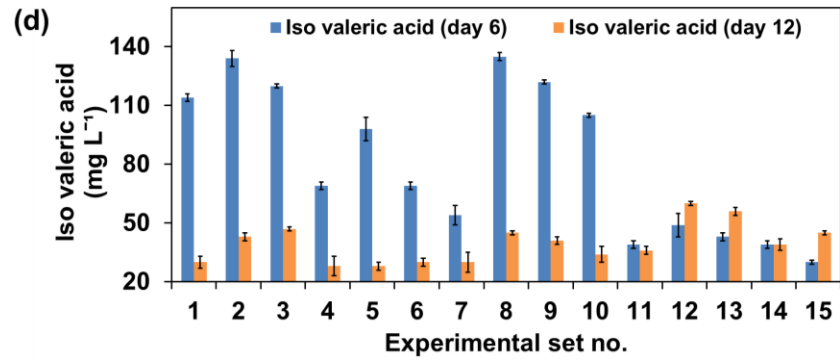
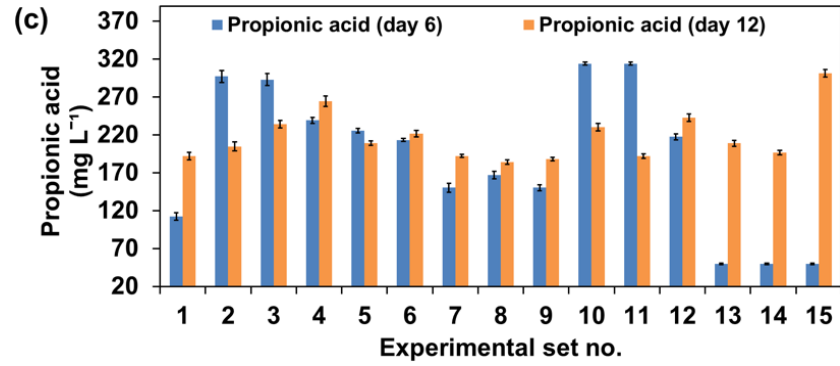
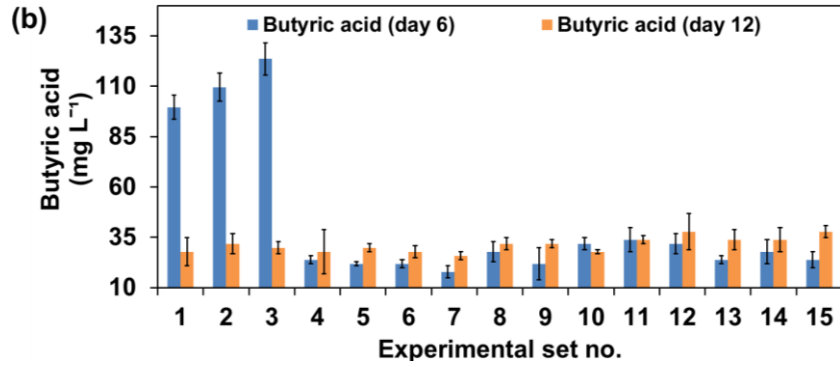
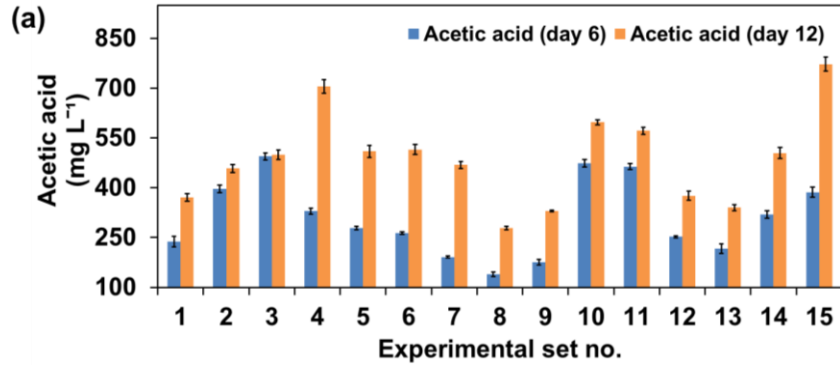
Figure 5-17 elucidates the production patterns of single VFAs at two distinct time intervals of the AD process. This figure provides a clear comparison of major VFAs produced, such as acetic, butyric, propionic, isovaleric, and valeric acids levels measured on days 6 and 12 on albumin set A1, A2, A3, and casein set C1, C2, and C3.

Figure 5-17 (a) shows that the acetic acid concentrations varied significantly across different sets and time intervals. For the albumin sets on day 6, acetic acid concentrations (mg L⁻¹) were measured at 695±7 for set 1 (A1), 499±5 for set 2 (A2), and 700±6 for set 3 (A3). By day 12, these figures had changed to 499±4 mg L⁻¹ for set A1, an increase to 674±8 mgL⁻¹ for set A2, and a

decrease to $504 \pm 5 \text{ mg L}^{-1}$ for set A3. On the other hand, the casein sets exhibited higher initial acetic acid concentrations (mg L^{-1}) on day 6, with set 1 (C1) at 931 ± 11 , set 2 (C2) at 808 ± 9 , and set 3 (C3) at 844 ± 12 . However, by day 12, the concentrations (mg L^{-1}) had decreased to 736 ± 11 , 633 ± 8 , and 818 ± 11 for sets C1, C2, and C3, respectively.

The decrease in acetic acid from day 6 to 12 could be because biohydrogen production occurred due to acetic acid and readily available residual substrate degradation (Capson-Tojo et al., 2017). Figure 5-11 proves the statement by showing increased hydrogen yield on day 12 compared to day 6 in all albumin and casein sets. Similarly, acetic acid was the dominant VFA, reaching 4100 and 1100 mg L^{-1} on days 6 and 12 of AD of food waste leachate (Khatami et al., 2021).

Unlike acetic acid, butyric acid production (Figure 5-17 (b)) does not follow a uniform decrease trend from day 6 to 12 across all sets. In particular, albumin sets A1 and A2 show an increase in butyric acid concentration by day 12, with set A2 showing a substantial rise from 30 ± 2 to $64 \pm 2 \text{ mg L}^{-1}$. Albumin set A3 remains consistent ($50 \pm 1 \text{ mg L}^{-1}$) on days 6 and 12. In contrast, the casein sets, which initially produce higher levels of butyric acid after day 6, experience a general decrease by day 12.



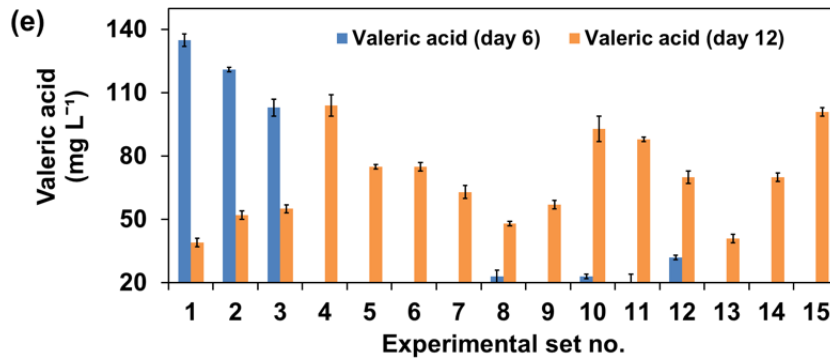


Figure 5- 17. Single volatile fatty acids (VFAs) measured on day 6 and 12 (a) acetic acid (b) butyric acid (c) propionic acid (d) isovaleric acid and (e) valeric acid.

For casein sets, set C1 displays a decrease from 80 ± 3 mg L⁻¹ on day 6 to 56 ± 1 mg L⁻¹ on day 12, set C2 decreases slightly from 60 ± 1 to 52 ± 3 mg L⁻¹, and set C3 shows a decrease, but to a lesser extent, from 80 ± 2 to 74 ± 1 mg L⁻¹.

Figure 5-17 (c) presents propionic acid concentrations in albumin and casein sets measured on days 6 and 12. Initially, on day 6, albumin set A1 and casein set C1 exhibited the highest propionic acid concentrations at 364 ± 9 and 420 ± 6 mg L⁻¹, suggesting a robust acidogenic phase. By day 12, these concentrations had declined to 234 ± 5 mg L⁻¹ for albumin set A1 and 192 ± 3 mg L⁻¹ for casein set C1, indicating a significant decrease in production. Albumin set A2 was an outlier, increasing from 150 ± 2 to 267 ± 2 mg L⁻¹. Conversely, both albumin set A3 and casein set C3 followed the general declining trend, with casein sets showing a more pronounced decrease.

Figure 5-17 (d) illustrates the concentrations of isovaleric acid. Albumin sets (A1-A3) exhibit isovaleric acid production at day 6 (ranging from 39 ± 2 to 52 ± 2 mg L⁻¹). By day 12, the concentration increases, indicating a continuous fermentation process, yet remains generally lower than the casein sets. Casein sets (C1-C3) show higher isovaleric acid production both at day 6 (ranging from 59 ± 3 to 71 ± 2 mg L⁻¹) and day 12 (ranging from 63 ± 3 to 85 ± 1 mg L⁻¹) compared to the albumin sets. Across all sets in Figure 5-17 (e), there is an increase in the concentration of

valeric acid from day 6 to day 12. Among all the sets, albumin set A3 shows the highest valeric acid concentration at both time intervals (89 ± 3 mg L⁻¹ on day 6 and 98 ± 1 mg L⁻¹ on day 12). Casein set C1 showed a considerable increase from 39 ± 2 mg L⁻¹ to 83 ± 2 mg L⁻¹. Casein sets C2 and C3 initially had no detectable valeric acid but showed production by day 12, reaching 55 ± 2 mgL⁻¹ and 37 ± 1 mg L⁻¹, respectively. The production of valeric acids is quite substantial, indicating active valeric acid production during the period. Owusu-Agyeman et al. (2020) reported similar results in their study on AD of sewage sludge and organic waste, noting valeric acid's increase from 0 to 11% in 20 days. High molecular weight VFAs, like isovaleric and valeric acids, can be produced from protein fermentation via the Stickland reaction, involving either the reductive deamination of amino acids or a redox process between amino acid pairs (Parawira et al., 2004). Additionally, shifts in VFA proportions, for example, decreased acetic acid (Figure 5-17 (a)) and increased valeric acids (Figure 5-17 (e)) throughout AD, are due to β -oxidation and isomerization processes (Parawira et al., 2004).

The concentrations (mg L⁻¹) of the top three VFAs for the albumin set A1 on day 6 are observed as acetic acid (695 ± 7) > propionic acid (364 ± 9) > butyric acid (52 ± 1). For albumin set A2 on day 6, the VFA concentrations (mg L⁻¹) followed acetic acid (495 ± 5) > propionic acid (150 ± 2) > butyric acid (30 ± 2). For albumin set A3 on day 6, the concentrations (mg L⁻¹) of single VFAs are acetic acid (700 ± 6) > propionic acid (188 ± 1) > butyric acid (50 ± 1) and acetic acid (504 ± 5) > propionic acid (146 ± 1) > butyric acid (50 ± 1) on day 12. In the case of the analysis of sets A1, A2, and A3, nearly identical trends in producing single VFAs were observed. In all three albumin or casein sets, acetic acid is the most abundant VFA after day 6, indicating that the microbial community within the anaerobic digester is efficiently converting substrates into acetate. This is expected since acetic acid is a direct precursor for methane generation in the methanogenesis phase

and is typically the most common VFA produced in AD (Luo et al., 2019). Yin et al. (2014) also indicated that in anaerobic digestion for methane production, one-third of the methane is produced from hydrogen, while two-thirds comes from acetic acid.

Although a mixture of albumin and starch in AD produced single VFAs as acetate > butyrate > propionate for biohydrogen production (Tepari Jr, 2019), this study showed single VFAs produced following acetate > propionate > butyrate order. A finding similar to the present study was reported by Jankowska et al. (2015), who obtained a reduction in butyrate and an increase in acetic and propionic acid production from primary and waste-activated sludge on day 15 compared to day 5 at pH 4. In the acidic fermentation of protein-based waste like cheese whey with mixed cultures, the VFAs distribution was consistent across varying retention times as acetate > propionate > butyrate > valerate, along with minor concentrations of iso-butyrate (Jankowska et al., 2017). Accumulation of propionic acid in the reactors was attributed to the buildup of formate and/or hydrogen, as its breakdown is thermodynamically efficient only within a narrow concentration range of these compounds (Capson-Tojo et al., 2017). When compared to carbohydrates, protein is more readily hydrolyzed by mixed flora, resulting in larger molecule acids like iso-butyric, n-butyric, isovaleric, and n-valproic acids. These can be transformed into acetic and propionic acids by hydrogen-producing acidogenic bacteria, as noted by Parawira et al. (2004). Consequently, the production of propionic acids and acetic acids are notably higher than other volatile fatty acids found in this experiment.

5.9 Conclusions

Biohydrogen production of manure and kiwi peel waste (KPW) during the anaerobic digestion was optimized using the Box–Behnken design (BBD). After analysing the experimental data from

the BBD matrix, a regression quadratic model equation was produced that was very significant ($R^2 = 0.99$; $p < 0.05$). The highest value of accumulative biohydrogen yield was $389 \pm 11 \text{ mL g}^{-1} \text{ VS}$ on day 6 and $510 \pm 7 \text{ mL g}^{-1} \text{ VS}$ on day 12 when the factors are set as M:KPW ratio of 0.5, pH 5.0, and inoculum 4 gVS L^{-1} . Under similar conditions, albumin:KPW ratio of 0.5, pH 5, and inoculum 4 gVS L^{-1} generated biohydrogen of $200 \pm 3 \text{ mL g}^{-1} \text{ VS}$ on day 6 and $554 \pm 3 \text{ mL g}^{-1} \text{ VS}$. Similarly, casein produced 245 ± 3 and $400 \pm 4 \text{ mL g}^{-1} \text{ VS}$ of biohydrogen on days 6 and 12. In the case of pure protein sources, protein quantity reductions were obtained at $33.2 \pm 1\%$ for albumin and $34.6 \pm 1\%$ for casein. Moreover, FTIR and SEM analysis on albumin-KPW and casein-KPW digestion provided an extensive overview of functional group alternation and morphological changes during AD. In summary, the findings of this study suggest that generating biohydrogen from both manure and KPW or pure protein and KPW presents viable alternatives. These results provide a basis for enhancing biohydrogen generation from protein-rich livestock waste.

References

- Abouelenien, F., Miura, T., Nakashimada, Y., Elleboudy, N. S., Al-Harbi, M. S., Ali, E. F., & Shukry, M. (2021). Optimization of biomethane production via fermentation of chicken manure using marine sediment: a modeling approach using response surface methodology. *International Journal of Environmental Research and Public Health*, *18*(22), 11988. <https://doi.org/10.3390/ijerph182211988>.
- Ahmed, A. M. S., Buezo, K. A., & Saady, N. M. C. (2019). Adapting anaerobic consortium to pure and complex lignocellulose substrates at low temperature: kinetics evaluation. *International Journal of Recycling of Organic Waste in Agriculture*, *8*, 99-110. <https://doi.org/10.1007/s40093-018-0238-2>.
- Algapani, D. E., Qiao, W., Ricci, M., Bianchi, D., Wandera, S. M., Adani, F., & Dong, R. (2019). Bio-hydrogen and bio-methane production from food waste in a two-stage anaerobic digestion process with digestate recirculation. *Renewable Energy*, *130*, 1108-1115. <https://doi.org/10.1016/j.renene.2018.08.079>.
- Amekan, Y., Wangi, D. S. A., Cahyanto, M. N., Sarto, S., & Widada, J. (2018). Effect of different inoculum combination on biohydrogen production from melon fruit waste. *International Journal of Renewable Energy Development*, *7*(2), 101-109. doi.org/10.14710/ijred.7.2.101-109.
- Arelli, V., Mamindlapelli, N. K., Begum, S., Juntupally, S., & Anupoju, G. R. (2021). Solid state anaerobic digestion of food waste and sewage sludge: Impact of mixing ratios and temperature on microbial diversity, reactor stability and methane yield. *Science of the Total Environment*, *793*, 148586. <https://doi.org/10.1016/j.scitotenv.2021.148586>.

- Awasthi, M. K., Paul, A., Kumar, V., Sar, T., Kumar, D., Sarsaiya, S., Liu, H., Zhang, Z., Binod, P., & Sindhu, R. (2022). Recent trends and developments on integrated biochemical conversion process for valorization of dairy waste to value added bioproducts: A review. *Bioresource Technology*, 344, 126193. <https://doi.org/10.1016/j.biortech.2021.126193>.
- Bai, S., Xi, B., Li, X., Wang, Y., Yang, J., Li, S., & Zhao, X. (2021). Anaerobic digestion of chicken manure: Sequences of chemical structures in dissolved organic matter and its effect on acetic acid production. *Journal of Environmental Management*, 296, 113245. <https://doi.org/10.1016/j.jenvman.2021.113245>.
- Bajić, B., Vučurović, D., Vasić, Đ., Jevtić-Mučibabić, R., & Dodić, S. (2022). Biotechnological production of sustainable microbial proteins from agro-industrial residues and by-products. *Foods*, 12(1), 107. <https://doi.org/10.3390/foods12010107>.
- Baumguertner, M., Kreutz, C., & Martins, R. (2019). Anaerobic digestion in the fruit waste disposal and valorization. In *Wastes: Solutions, Treatments and Opportunities III; 5th International Conference Wastes, September 4-6, 2019, Lisbon, Portugal*.
- Bevilacqua, R., Regueira, A., Mauricio-Iglesias, M., Lema, J. M., & Carballa, M. (2021). Steering the conversion of protein residues to volatile fatty acids by adjusting pH. *Bioresource Technology*, 320, 124315. <https://doi.org/10.1016/j.biortech.2020.124315>.
- Bhat, M. Y., Dar, T. A., & Singh, L. R. (2016). Casein proteins: Structural and functional aspects. In *Milk Proteins—From Structure to Biological Properties and Health Aspects; InTech: Rijeka, Croatia*. 10.5772/64187.
- Bolzonella, D., Pavan, P., Zanette, M., & Cecchi, F. (2007). Two-phase anaerobic digestion of waste activated sludge: effect of an extreme thermophilic prefermentation. *Industrial & Engineering Chemistry Research*, 46(21), 6650-6655. <https://doi.org/10.1021/ie061627e>.

- Cappai, G., De Gioannis, G., Muntoni, A., Spiga, D., Boni, M. R., Polettini, A., Pomi, R., & Rossi, A. (2018). Biohydrogen production from food waste: Influence of the inoculum-to-substrate ratio. *Sustainability*, *10*(12), 4506. <https://doi.org/10.3390/su10124506>.
- Capson-Tojo, G., Ruiz, D., Rouez, M., Crest, M., Steyer, J.-P., Bernet, N., Delgenès, J.-P., & Escudié, R. (2017). Accumulation of propionic acid during consecutive batch anaerobic digestion of commercial food waste. *Bioresource Technology*, *245*, 724-733. <https://doi.org/10.1016/j.biortech.2017.08.149>.
- Chaganti, S. R., Pendyala, B., Lalman, J. A., Veeravalli, S. S., & Heath, D. D. (2013). Influence of linoleic acid, pH and HRT on anaerobic microbial populations and metabolic shifts in ASBRs during dark hydrogen fermentation of lignocellulosic sugars. *International Journal of Hydrogen Energy*, *38*(5), 2212-2220. <https://doi.org/10.1016/j.ijhydene.2012.11.137>.
- Chalabi, M., Khademi, F., Yarani, R., & Mostafaie, A. (2014). Proteolytic activities of kiwifruit actinidin (*Actinidia deliciosa* cv. Hayward) on different fibrous and globular proteins: A comparative study of actinidin with papain. *Applied Biochemistry and Biotechnology*, *172*, 4025-4037. <https://doi.org/10.1007/s12010-014-0812-7>.
- Chang, S., Li, J.-Z., & Liu, F. (2011). Evaluation of different pretreatment methods for preparing hydrogen-producing seed inocula from waste activated sludge. *Renewable Energy*, *36*(5), 1517-1522. <https://doi.org/10.1016/j.renene.2010.11.023>.
- Chen, H., Wu, J., Wang, H., Zhou, Y., Xiao, B., Zhou, L., Yu, G., Yang, M., Xiong, Y., & Wu, S. (2021). Dark co-fermentation of rice straw and pig manure for biohydrogen production: effects of different inoculum pretreatments and substrate mixing ratio. *Environmental Technology*, *42*(28), 4539-4549. <https://doi.org/10.1080/09593330.2020.1770340>.

- Chiang, K.-Y., Matsumura, F., Yu, C.-C., Qi, D., Nagata, Y., Bonn, M., & Meister, K. (2023). True Origin of Amide I Shifts Observed in Protein Spectra Obtained with Sum Frequency Generation Spectroscopy. *The Journal of Physical Chemistry Letters*, *14*, 4949-4954. <https://doi.org/10.1021/acs.jpcclett.3c00391>.
- Dareioti, M. A., Vavouraki, A. I., & Kornaros, M. (2014). Effect of pH on the anaerobic acidogenesis of agroindustrial wastewaters for maximization of bio-hydrogen production: a lab-scale evaluation using batch tests. *Bioresource Technology*, *162*, 218-227. <https://doi.org/10.1016/j.biortech.2014.03.149>.
- Dasa, K. T., Westman, S. Y., Millati, R., Cahyanto, M. N., Taherzadeh, M. J., & Niklasson, C. (2016). Inhibitory effect of long-chain fatty acids on biogas production and the protective effect of membrane bioreactor. *BioMed Research International*, *2016*. <https://doi.org/10.1155/2016/7263974>.
- David Troncoso, F., Alberto Sánchez, D., & Luján Ferreira, M. (2022). Production of plant proteases and new biotechnological applications: an updated review. *Chemistry Open*, *11*(3), e202200017. <https://doi.org/10.1002/open.202200017>.
- De Kruijff, C. G., Huppertz, T., Urban, V. S., & Petukhov, A. V. (2012). Casein micelles and their internal structure. *Advances in Colloid and Interface Science*, *171*, 36-52. <https://doi.org/10.1016/j.cis.2012.01.002>.
- Deepanraj, B., Senthilkumar, N., Ranjitha, J., Jayaraj, S., & Ong, H. C. (2021). Biogas from food waste through anaerobic digestion: optimization with response surface methodology. *Biomass Conversion and Biorefinery*, *11*, 227-239. <https://doi.org/10.1007/s13399-020-00646-9>.

- Deng, Z., Ferreira, A. L. M., Spanjers, H., & van Lier, J. B. (2023). Anaerobic protein degradation: Effects of protein structural complexity, protein concentrations, carbohydrates, and volatile fatty acids. *Bioresource Technology Reports*, 101501. <https://doi.org/10.1016/j.biteb.2023.101501>.
- Elbeshbishy, E., Hafez, H., & Nakhla, G. (2010). Enhancement of biohydrogen producing using ultrasonication. *International Journal of Hydrogen Energy*, 35(12), 6184-6193. <https://doi.org/10.1016/j.ijhydene.2010.03.119>.
- Elsamadony, M., Mostafa, A., Fujii, M., Tawfik, A., & Pant, D. (2021). Advances towards understanding long chain fatty acids-induced inhibition and overcoming strategies for efficient anaerobic digestion process. *Water Research*, 190, 116732. <https://doi.org/10.1016/j.watres.2020.116732>.
- Esteban-Gutiérrez, M., Garcia-Aguirre, J., Irizar, I., & Aymerich, E. (2018). From sewage sludge and agri-food waste to VFA: Individual acid production potential and up-scaling. *Waste Management*, 77, 203-212. <https://doi.org/10.1016/j.wasman.2018.05.027>.
- Feng, L., Chen, Y., & Zheng, X. (2009). Enhancement of waste activated sludge protein conversion and volatile fatty acids accumulation during waste activated sludge anaerobic fermentation by carbohydrate substrate addition: the effect of pH. *Environmental Science & Technology*, 43(12), 4373-4380. <https://doi.org/10.1021/es8037142>.
- Florio, C., Pirozzi, D., Ausiello, A., Micoli, L., Pasquale, V., Toscano, G., Turco, M., & Dumontet, S. (2017). Effect of inoculum/substrate ratio on dark fermentation for biohydrogen production from organic fraction of municipal solid waste. *Chemical Engineering Transactions*, 57, 175-180. 10.3303/CET1757030.

- Ganesh Kumar, A., Kamatchi, P., Umashankari, J., Vidhya, S., Sriyutha Murthy, P., & Sekaran, G. (2008). Acidogenic fermentation of proteinaceous solid waste and characterization of different bioconversion stages and extracellular products. *Biodegradation*, *19*, 535-543. <https://doi.org/10.1007/s10532-007-9159-x>.
- Gang, G., Chen, S., Qiang, L., ZHANG, S.-l., Tao, S., Cong, W., WANG, Y.-x., XU, Q.-f., & HUO, W.-j. (2020). The effect of lactic acid bacteria inoculums on in vitro rumen fermentation, methane production, ruminal cellulolytic bacteria populations and cellulase activities of corn stover silage. *Journal of Integrative Agriculture*, *19*(3), 838-847. [https://doi.org/10.1016/S2095-3119\(19\)62707-3](https://doi.org/10.1016/S2095-3119(19)62707-3).
- Ghinea, C., Apostol, L. C., Prisacaru, A. E., & Leahu, A. (2019). Development of a model for food waste composting. *Environmental Science and Pollution Research*, *26*, 4056-4069. <https://doi.org/10.1007/s11356-018-3939-1>.
- Guieysse, B., Wikström, P., Forsman, M., & Mattiasson, B. (2001). Biomonitoring of continuous microbial community adaptation towards more efficient phenol-degradation in a fed-batch bioreactor. *Applied Microbiology and Biotechnology*, *56*, 780-787. <https://doi.org/10.1007/s002530100676>.
- Gülseren, İ., Güzey, D., Bruce, B. D., & Weiss, J. (2007). Structural and functional changes in ultrasonicated bovine serum albumin solutions. *Ultrasonics Sonochemistry*, *14*(2), 173-183. <https://doi.org/10.1016/j.ultsonch.2005.07.006>.
- Guo, X. M., Trably, E., Latrille, E., Carrère, H., & Steyer, J.-P. (2010). Hydrogen production from agricultural waste by dark fermentation: a review. *International Journal of Hydrogen Energy*, *35*(19), 10660-10673. <https://doi.org/10.1016/j.ijhydene.2010.03.008>.

- Han, Y., Green, H., & Tao, W. (2020). Reversibility of propionic acid inhibition to anaerobic digestion: Inhibition kinetics and microbial mechanism. *Chemosphere*, 255, 126840. <https://doi.org/10.1016/j.chemosphere.2020.126840>.
- Hans, M., & Kumar, S. (2019). Biohythane production in two-stage anaerobic digestion system. *International Journal of Hydrogen Energy*, 44(32), 17363-17380. <https://doi.org/10.1016/j.ijhydene.2018.10.022>.
- Hou, L., Ji, D., & Zang, L. (2018). Inhibition of anaerobic biological treatment: A review. IOP Conference Series Earth Environmental Science, 112, 012006. 10.1088/1755-1315/112/1/012006.
- Huang, W., Krishnaji, S., Tokareva, O. R., Kaplan, D., & Cebe, P. (2017). Tunable crystallization, degradation, and self-assembly of recombinant protein block copolymers. *Polymer*, 117, 107-116. <https://doi.org/10.1016/j.polymer.2017.04.029>.
- Huppertz, T., Fox, P., & Kelly, A. (2018). The caseins: Structure, stability, and functionality. In *Proteins in Food Processing*; Yada, R.Y., (ED); Elsevier: Amsterdam, The Netherlands, 2018; pp. 49–92. <https://doi.org/10.1016/B978-0-08-100722-8.00004-8>.
- Jadhav, D. A., Dutta, S., Sherpa, K. C., Jayaswal, K., Saravanabhupathy, S., Mohanty, K. T., Banerjee, R., Kumar, J., & Rajak, R. C. (2023). Co-digestion processes of waste: Status and perspective. In *Bio-Based Materials and Waste for Energy Generation and Resource Management* (pp. 207-241). Hussain C. M., Bharagava, R. N., (ED). Elsevier, WA, USA. ISBN 978-0-323-91149-8, <https://doi.org/10.1016/C2020-0-03950-2>.
- Jankowska, E., Chwialkowska, J., Stodolny, M., & Oleskiewicz-Popiel, P. (2017). Volatile fatty acids production during mixed culture fermentation–The impact of substrate complexity

- and pH. *Chemical Engineering Journal*, 326, 901-910.
<https://doi.org/10.1016/j.cej.2017.06.021>.
- Jankowska, E., Chwiałkowska, J., Stodolny, M., & Oleskiewicz-Popiel, P. (2015). Effect of pH and retention time on volatile fatty acids production during mixed culture fermentation. *Bioresource Technology*, 190, 274-280. <https://doi.org/10.1016/j.biortech.2015.04.096>.
- Jiang, Y., Zhang, Y., Wang, S., Wang, Z., Liu, Y., Hu, Z., & Zhan, X. (2021). Improved environmental sustainability and bioenergy recovery through pig manure and food waste on-farm co-digestion in Ireland. *Journal of Cleaner Production*, 280, 125034.
<https://doi.org/10.1016/j.jclepro.2020.125034>.
- Kaur, L., & Boland, M. (2013). Influence of kiwifruit on protein digestion. *Advances in Food and Nutrition Research*, 68, 149-167. <https://doi.org/10.1016/B978-0-12-394294-4.00008-0>.
- Kaur, S., Vasiljevic, T., & Huppertz, T. (2023). Milk Protein Hydrolysis by Actinidin—Kinetic and Thermodynamic Characterisation and Comparison to Bromelain and Papain. *Foods*, 12(23), 4248. <https://doi.org/10.3390/foods12234248>.
- Khatami, K., Atasoy, M., Ludtke, M., Baresel, C., Eyice, Ö., & Cetecioglu, Z. (2021). Bioconversion of food waste to volatile fatty acids: Impact of microbial community, pH and retention time. *Chemosphere*, 275, 129981.
<https://doi.org/10.1016/j.chemosphere.2021.129981>.
- Kraemer, J. T., & Bagley, D. M. (2005). Simulation of the impact of higher ammonia recycle loads caused by upgrading anaerobic sludge digesters. *Water Quality Research Journal*, 40(4), 491-499. <https://doi.org/10.2166/wqrj.2005.053>.

- Kumar, G., Nguyen, D. D., Sivagurunathan, P., Kobayashi, T., Xu, K., & Chang, S. W. (2018). Cultivation of microalgal biomass using swine manure for biohydrogen production: Impact of dilution ratio and pretreatment. *Bioresource Technology*, 260, 16-22. <https://doi.org/10.1016/j.biortech.2018.03.029>.
- Kumar, G., Zhen, G., Sivagurunathan, P., Bakonyi, P., Nemestóthy, N., Bélafi-Bakó, K., Kobayashi, T., & Xu, K.-Q. (2016). Biogenic H₂ production from mixed microalgae biomass: impact of pH control and methanogenic inhibitor (BESA) addition. *Biofuel Research Journal*, 3(3), 470-474. <https://doi.org/10.18331/BRJ2016.3.3.6>.
- Kumar, R., Kumar, A., & Pal, A. (2021). An overview of conventional and non-conventional hydrogen production methods. *Materials Today: Proceedings*, 46, 5353-5359. <https://doi.org/10.1016/j.matpr.2020.08.793>.
- Lateef, S. A., Beneragama, N., Yamashiro, T., Iwasaki, M., Ying, C., & Umetsu, K. (2012). Biohydrogen production from co-digestion of cow manure and waste milk under thermophilic temperature. *Bioresource Technology*, 110, 251-257. <https://doi.org/10.1016/j.biortech.2012.01.102>.
- Li, B., Yang, T., Li, R., & Kai, X. (2020). Co-generation of liquid biofuels from lignocellulose by integrated biochemical and hydrothermal liquefaction process. *Energy*, 200, 117524. <https://doi.org/10.1016/j.energy.2020.117524>.
- Li, J., Lu, S., Wu, S., Zhang, W., Hua, M., & Pan, B. (2022). The breakdown of protein hydrogen bonding networks facilitates biotransformation of protein wastewaters during anaerobic digestion methanogenesis: Focus on protein structure and conformation. *Environmental Research*, 208, 112735. <https://doi.org/10.1016/j.envres.2022.112735>.

- Li, X., Zhao, X., Yang, J., Li, S., Bai, S., & Zhao, X. (2020). Recognition of core microbial communities contributing to complex organic components degradation during dry anaerobic digestion of chicken manure. *Bioresource Technology*, *314*, 123765. <https://doi.org/10.1016/j.biortech.2020.123765>.
- Liu, I.-C., Whang, L.-M., Ren, W.-J., & Lin, P.-Y. (2011). The effect of pH on the production of biohydrogen by clostridia: thermodynamic and metabolic considerations. *International Journal of Hydrogen Energy*, *36*(1), 439-449. <https://doi.org/10.1016/j.ijhydene.2010.10.045>.
- Liu, S., Li, W., Zheng, G., Yang, H., & Li, L. (2020). Optimization of cattle manure and food waste co-digestion for biohydrogen production in a mesophilic semi-continuous process. *Energies*, *13*(15), 3848. <https://doi.org/10.3390/en13153848>.
- Liu, Y., Zheng, Y., & Wang, A. (2010). Response surface methodology for optimizing adsorption process parameters for methylene blue removal by a hydrogel composite. *Adsorption Science & Technology*, *28*(10), 913-922. <https://doi.org/10.1260/0263-6174.28.10.913>.
- Luo, G., Xie, L., Zou, Z., Wang, W., & Zhou, Q. (2010). Evaluation of pretreatment methods on mixed inoculum for both batch and continuous thermophilic biohydrogen production from cassava stillage. *Bioresource Technology*, *101*(3), 959-964. <https://doi.org/10.1016/j.biortech.2009.08.090>.
- Luo, K., Pang, Y., Yang, Q., Wang, D., Li, X., Lei, M., & Huang, Q. (2019). A critical review of volatile fatty acids produced from waste activated sludge: enhanced strategies and its applications. *Environmental Science and Pollution Research*, *26*, 13984-13998. <https://doi.org/10.1007/s11356-019-04798-8>.

- Ma, H., Liu, H., Zhang, L., Yang, M., Fu, B., & Liu, H. (2017). Novel insight into the relationship between organic substrate composition and volatile fatty acids distribution in acidogenic co-fermentation. *Biotechnology For Biofuels*, *10*(1), 1-15. <https://doi.org/10.1186/s13068-017-0821-1>.
- Ma, J., Lv, X., Gao, D., Li, Y., Lv, B., & Zhang, J. (2014). Nanocomposite-based green tanning process of suede leather to enhance chromium uptake. *Journal of Cleaner Production*, *72*, 120-126. <https://doi.org/10.1016/j.jclepro.2014.03.016>.
- Mahmoud, B. S., & McConville, C. (2023). Box–Behnken Design of Experiments of Polycaprolactone Nanoparticles Loaded with Irinotecan Hydrochloride. *Pharmaceutics*, *15*(4), 1271. <https://doi.org/10.3390/pharmaceutics15041271>.
- Meegoda, J. N., Li, B., Patel, K., & Wang, L. B. (2018). A review of the processes, parameters, and optimization of anaerobic digestion. *International Journal of Environmental Research and Public Health*, *15*(10), 2224. <https://doi.org/10.3390/ijerph15102224>.
- Meetiayagoda, T. A. O. K., Takahashi, T., & Fujino, T. (2023). Response surface optimization of chemical coagulation for solid–liquid separation of dairy manure slurry through Box–Behnken design with desirability function. *Heliyon*, *9* (2023), e17632. <https://doi.org/10.1016/j.heliyon.2023.e17632>
- Meiramkulova, K.; Bayanov, A.; Ivanova, T.; Havrland, B.; Kára, J.; Hanzlíková, I. Effect of different compositions on anaerobic co-digestion of cattle manure and agro-industrial by-products. *Agron. Res.* 2018, *16*, 176–187. <http://dx.doi.org/10.15159/ar.18.008>.
- Meng, X., Yu, D., Wei, Y., Zhang, Y., Zhang, Q., Wang, Z., Liu, J., & Wang, Y. (2018). Endogenous ternary pH buffer system with ammonia-carbonates-VFAs in high solid

- anaerobic digestion of swine manure: an alternative for alleviating ammonia inhibition?
Process Biochemistry, 69, 144-152. <https://doi.org/10.1016/j.procbio.2018.03.015>.
- Miao, L., Wang, P., Hou, J., Yao, Y., Liu, Z., Liu, S., & Li, T. (2019). Distinct community structure and microbial functions of biofilms colonizing microplastics. *Science of the Total Environment*, 650, 2395-2402. <https://doi.org/10.1016/j.scitotenv.2018.09.378>.
- Molinuevo-Salces, B., González-Fernández, C., Gómez, X., García-González, M. C., & Morán, A. (2012). Vegetable processing wastes addition to improve swine manure anaerobic digestion: Evaluation in terms of methane yield and SEM characterization. *Applied Energy*, 91(1), 36-42. <https://doi.org/10.1016/j.apenergy.2011.09.010>.
- Mosquera, J., Varela, L., Santis, A., Villamizar, S., Acevedo, P., & Cabeza, I. (2020). Improving anaerobic co-digestion of different residual biomass sources readily available in Colombia by process parameters optimization. *Biomass and Bioenergy*, 142, 105790. <https://doi.org/10.1016/j.biombioe.2020.105790>.
- Namazi, H., Fathi, F., & Dadkhah, A. (2011). Hydrophobically modified starch using long-chain fatty acids for preparation of nanosized starch particles. *Scientia Iranica*, 18(3), 439-445. <https://doi.org/10.1016/j.scient.2011.05.006>.
- Nawaz, A., Aamir, F., Huang, R., ul Haq, I., Wu, F., Munir, M., Chaudhary, R., Rafique, A., & Jiang, K. (2023). Co-production of biohydrogen and biomethane utilizing halophytic biomass *Atriplex crassifolia* by two-stage anaerobic fermentation process. *Frontiers in Chemistry*, 11. <https://doi.org/10.3389/fchem.2023.1233494>.
- Nguyen, T.-T., Chu, C.-Y., & Ou, C.-M. (2021). Pre-treatment study on two-stage biohydrogen and biomethane productions in a continuous co-digestion process from a mixture of

- swine manure and pineapple waste. *International Journal of Hydrogen Energy*, 46(20), 11325-11336. <https://doi.org/10.1016/j.ijhydene.2020.05.264>.
- Osman, A. I., Deka, T. J., Baruah, D. C., & Rooney, D. W. (2020). Critical challenges in biohydrogen production processes from the organic feedstocks. *Biomass Conversion and Biorefinery*, 1-19. <https://doi.org/10.1007/s13399-020-00965-x>.
- Owusu-Agyeman, I., Plaza, E., & Cetecioglu, Z. (2020). Production of volatile fatty acids through co-digestion of sewage sludge and external organic waste: Effect of substrate proportions and long-term operation. *Waste Management*, 112, 30-39. <https://doi.org/10.1016/j.wasman.2020.05.027>.
- Panichnumsin, P., Nopharatana, A., Ahring, B., & Chaiprasert, P. (2010). Production of methane by co-digestion of cassava pulp with various concentrations of pig manure. *Biomass and Bioenergy*, 34(8), 1117-1124. <https://doi.org/10.1016/j.biombioe.2010.02.018>.
- Parawira, W., Murto, M., Read, J. S., & Mattiasson, B. (2004). Volatile fatty acid production during anaerobic mesophilic digestion of solid potato waste. *Journal of Chemical Technology & Biotechnology: International Research in Process, Environmental & Clean Technology*, 79(7), 673-677.
- Park, M., Kim, N., Jung, S., Jeong, T.-Y., & Park, D. (2021). Optimization and comparison of methane production and residual characteristics in mesophilic anaerobic digestion of sewage sludge by hydrothermal treatment. *Chemosphere*, 264, 128516. <https://doi.org/10.1016/j.chemosphere.2020.128516>.
- Pavia, D., Lampman, G., Kriz, G., & Vyvyan, J. (2008). Introduction to Spectroscopy (4th edition), Cengage Learning, Mason, Ohio, USA.

- Peltre, C., Gregorich, E. G., Bruun, S., Jensen, L. S., & Magid, J. (2017). Repeated application of organic waste affects soil organic matter composition: evidence from thermal analysis, FTIR-PAS, amino sugars and lignin biomarkers. *Soil Biology and Biochemistry*, *104*, 117-127. <https://doi.org/10.1016/j.soilbio.2016.10.016>.
- Rabii, A., Aldin, S., Dahman, Y., & Elbeshbishy, E. (2019). A review on anaerobic co-digestion with a focus on the microbial populations and the effect of multi-stage digester configuration. *Energies*, *12*(6), 1106. <https://doi.org/10.3390/en12061106>.
- Rafieenia, R., Lavagnolo, M. C., & Pivato, A. (2018). Pre-treatment technologies for dark fermentative hydrogen production: current advances and future directions. *Waste Management*, *71*, 734-748. <https://doi.org/10.1016/j.wasman.2017.05.024>.
- Rajagopal, R., Massé, D. I., & Singh, G. (2013). A critical review on inhibition of anaerobic digestion process by excess ammonia. *Bioresource Technology*, *143*, 632-641. <https://doi.org/10.1016/j.biortech.2013.06.030>.
- Rangel, C. J., Hernández, M. A., Mosquera, J. D., Castro, Y., Cabeza, I. O., & Acevedo, P. A. (2021). Hydrogen production by dark fermentation process from pig manure, cocoa mucilage, and coffee mucilage. *Biomass Conversion and Biorefinery*, *11*, 241-250. <https://doi.org/10.1007/s13399-020-00618-z>.
- Rodríguez-Jiménez, L. M., Pérez-Vidal, A., & Torres-Lozada, P. (2022). Research trends and strategies for the improvement of anaerobic digestion of food waste in psychrophilic temperatures conditions. *Heliyon*, *8*, e11174. <https://doi.org/10.1016/j.heliyon.2022.e11174>.

- Schievano, A., Tenca, A., Lonati, S., Manzini, E., & Adani, F. (2014). Can two-stage instead of one-stage anaerobic digestion really increase energy recovery from biomass? *Applied Energy*, *124*, 335-342. <https://doi.org/10.1016/j.apenergy.2014.03.024>.
- Sethupathy, A., Ravi Teja, G., Arun, C., & Sivashanmugam, P. (2018). Study on optimization of co-digestion process parameters for enhancing biohydrogen production using response surface methodology. *Energy Sources, Part A: Recovery, Utilization, and Environmental Effects*, *40*(14), 1753-1764. <https://doi.org/10.1080/15567036.2018.1486909>.
- Shanmugam, S. R., Chaganti, S. R., Lalman, J. A., & Heath, D. D. (2014). Effect of inhibitors on hydrogen consumption and microbial population dynamics in mixed anaerobic cultures. *International Journal of Hydrogen Energy*, *39*(1), 249-257. <https://doi.org/10.1016/j.ijhydene.2013.10.084>.
- Shanmugam, S. R., Lalman, J. A., Chaganti, S. R., Heath, D. D., Lau, P. C., & Shewa, W. A. (2016). Long term impact of stressing agents on fermentative hydrogen production: Effect on the hydrogenase flux and population diversity. *Renewable Energy*, *88*, 483-493. <https://doi.org/10.1016/j.renene.2015.11.062>.
- Shanmugaratnam, S., Yogenthiran, E., Koodali, R., Ravirajan, P., Velauthapillai, D., & Shivatharsiny, Y. (2021). Recent progress and approaches on transition metal chalcogenides for hydrogen production. *Energies*, *14*(24), 8265. <https://doi.org/10.3390/en14248265>.
- Sillero, L., Solera, R., & Perez, M. (2022). Anaerobic co-digestion of sewage sludge, wine vinasse and poultry manure for bio-hydrogen production. *International Journal of Hydrogen Energy*, *47*(6), 3667-3678. <https://doi.org/10.1016/j.ijhydene.2021.11.032>.

- Sillero, L., Solera, R., & Perez, M. (2023). Effect of temperature on biohydrogen and biomethane production using a biochemical potential test with different mixtures of sewage sludge, vinasse and poultry manure. *Journal of Cleaner Production*, 382, 135237. <https://doi.org/10.1016/j.jclepro.2022.135237>.
- Sim, S. Y. J., Srv, A., Chiang, J. H., & Henry, C. J. (2021). Plant proteins for future foods: A roadmap. *Foods*, 10(8), 1967. <https://doi.org/10.3390/foods10081967>.
- Sivagurunathan, P., Kumar, G., Kobayashi, T., Xu, K., & Kim, S.-H. (2017). Effects of various dilute acid pretreatments on the biochemical hydrogen production potential of marine macroalgal biomass. *International Journal of Hydrogen Energy*, 42(45), 27600-27606. <https://doi.org/10.1016/j.ijhydene.2017.05.106>.
- Smidt, E., & Schwanninger, M. (2005). Characterization of waste materials using FTIR spectroscopy: process monitoring and quality assessment. *Spectroscopy Letters*, 38(3), 247-270. <https://doi.org/10.1081/SL-200042310>.
- Song, Y., Qiao, W., Xue, T., Zhou, Y., & Dong, R. (2023). Generation of High Concentration Free Volatile Fatty Acids from Continuous Anaerobic Digestion of Chicken Manure by Suppressing the Decomposition of Nitrogenous Components. *Molecular Biotechnology*, 1-9. <https://doi.org/10.1007/s12033-023-00905-w>.
- Speda, J., Johansson, M. A., Odnell, A., & Karlsson, M. (2017). Enhanced biomethane production rate and yield from lignocellulosic ensiled forage ley by in situ anaerobic digestion treatment with endogenous cellulolytic enzymes. *Biotechnology for Biofuels*, 10, 1-13. <https://doi.org/10.1186/s13068-017-0814-0>.
- Stani, C., Vaccari, L., Mitri, E., & Birarda, G. (2020). FTIR investigation of the secondary structure of type I collagen: New insight into the amide III band. *Spectrochimica Acta*

- Part A: Molecular and Biomolecular Spectroscopy*, 229, 118006.
<https://doi.org/10.1016/j.saa.2019.118006>.
- Stringer, S. C., Haque, N., & Peck, M. W. (1999). Growth from spores of nonproteolytic *Clostridium botulinum* in heat-treated vegetable juice. *Applied and Environmental Microbiology*, 65(5), 2136-2142. <https://doi.org/10.1128/AEM.65.5.2136-2142.1999>.
- Stuart, B. H. (2004). *Infrared Spectroscopy: Fundamentals and Applications*; Wiley: Hoboken, NJ, USA; Volume 8, ISBN 9780470011140.
- Tan, R., Miyanaga, K., Uy, D., & Tanji, Y. (2012). Effect of heat-alkaline treatment as a pretreatment method on volatile fatty acid production and protein degradation in excess sludge, pure proteins and pure cultures. *Bioresource Technology*, 118, 390-398.
<https://doi.org/10.1016/j.biortech.2012.05.064>.
- Tang, Y., Shigematsu, T., Morimura, S., & Kida, K. (2005). Microbial community analysis of mesophilic anaerobic protein degradation process using bovine serum albumin (BSA)-fed continuous cultivation. *Journal of Bioscience and Bioengineering*, 99(2), 150-164.
<https://doi.org/10.1263/jbb.99.150>.
- Tenca, A., Schievano, A., Perazzolo, F., Adani, F., & Oberti, R. (2011). Biohydrogen from thermophilic co-fermentation of swine manure with fruit and vegetable waste: maximizing stable production without pH control. *Bioresource Technology*, 102(18), 8582-8588. <https://doi.org/10.1016/j.biortech.2011.03.102>.
- Tepari Jr, E. A. (2019). Evaluation of Biohydrogen Production from Co-fermentation of Carbohydrates and Proteins. Masters Dissertation, University of Western Ontario, Canada. <https://ir.lib.uwo.ca/etd/6566>.

- Tiantao, Z., Zhang, L., Haoquan, C., & Youcai, Z. (2009). Co-inhibition of methanogens for methane mitigation in biodegradable wastes. *Journal of Environmental Sciences*, 21(6), 827-833. [https://doi.org/10.1016/S1001-0742\(08\)62348-7](https://doi.org/10.1016/S1001-0742(08)62348-7).
- Valdez-Vazquez, I., & Poggi-Varaldo, H. M. (2009). Hydrogen production by fermentative consortia. *Renewable and Sustainable Energy Reviews*, 13(5), 1000-1013. <https://doi.org/10.1016/j.rser.2008.03.003>.
- Veeravalli, S. S., Chaganti, S. R., Lalman, J. A., & Heath, D. D. (2014). Optimizing hydrogen production from a switchgrass steam exploded liquor using a mixed anaerobic culture in an upflow anaerobic sludge blanket reactor. *International Journal of Hydrogen Energy*, 39(7), 3160-3175. <https://doi.org/10.1016/j.ijhydene.2013.12.057>.
- Wang, W., Xie, L., Luo, G., & Zhou, Q. (2013). Enhanced fermentative hydrogen production from cassava stillage by co-digestion: the effects of different co-substrates. *International Journal of Hydrogen Energy*, 38(17), 6980-6988. <https://doi.org/10.1016/j.ijhydene.2013.04.004>.
- Wang, H., Zhang, Y., & Angelidaki, I. (2016). Ammonia inhibition on hydrogen enriched anaerobic digestion of manure under mesophilic and thermophilic conditions. *Water Research*, 105, 314-319. <https://doi.org/10.1016/j.watres.2016.09.006>.
- Wang, Q., Li, H., Feng, K., & Liu, J. (2020). Oriented fermentation of food waste towards high-value products: A review. *Energies*, 13(21), 5638. <https://doi.org/10.3390/en13215638>.
- Webster, F. X., & Kiemle, D. J. (2005). *Spectrometric identification of organic compounds (7th Edition)*. John Wiley & Sons, INC; Hoboken, New Jersey, USA. ISBN 978-0-471-75721-4.

- Weimer, P. J. (2022). Degradation of cellulose and hemicellulose by ruminal microorganisms. *Microorganisms*, 10(12), 2345. <https://doi.org/10.3390/microorganisms10122345>
- Wong, Y. M., Wu, T. Y., & Juan, J. C. (2014). A review of sustainable hydrogen production using seed sludge via dark fermentation. *Renewable and Sustainable Energy Reviews*, 34, 471-482. <https://doi.org/10.1016/j.rser.2014.03.008>.
- Worm, P., Koehorst, J. J., Visser, M., Sedano-Núñez, V. T., Schaap, P. J., Plugge, C. M., Sousa, D. Z., & Stams, A. J. (2014). A genomic view on syntrophic versus non-syntrophic lifestyle in anaerobic fatty acid degrading communities. *Biochimica et Biophysica Acta (BBA)-Bioenergetics*, 1837(12), 2004-2016. <https://doi.org/10.1016/j.bbabi.2014.06.005>.
- Xiang, H., Sun-Waterhouse, D., Waterhouse, G. I., Cui, C., & Ruan, Z. (2019). Fermentation-enabled wellness foods: A fresh perspective. *Food Science and Human Wellness*, 8(3), 203-243. <https://doi.org/10.1016/j.fshw.2019.08.003>.
- Xu, B., Yuan, J., Wang, L., Lu, F., Wei, B., Azam, R. S., Ren, X., Zhou, C., Ma, H., & Bhandari, B. (2020). Effect of multi-frequency power ultrasound (MFPU) treatment on enzyme hydrolysis of casein. *Ultrasonics Sonochemistry*, 63, 104930. <https://doi.org/10.1016/j.ultsonch.2019.104930>.
- Xu, Y., Meng, X., Song, Y., Lv, X., & Sun, Y. (2023). Effects of different concentrations of butyrate on microbial community construction and metabolic pathways in anaerobic digestion. *Bioresource Technology*, 377, 128845. <https://doi.org/10.1016/j.biortech.2023.128845>.
- Yaashikaa, P., Kumar, P. S., & Varjani, S. (2022). Valorization of agro-industrial wastes for biorefinery process and circular bioeconomy: A critical review. *Bioresource Technology*, 343, 126126. <https://doi.org/10.1016/j.biortech.2021.126126>.

- Yin, Y., Hu, J., & Wang, J. (2014). Enriching hydrogen-producing bacteria from digested sludge by different pretreatment methods. *International Journal of Hydrogen Energy*, 39(25), 13550-13556. <https://doi.org/10.1016/j.ijhydene.2014.01.145>.
- Yokoyama, H., Yamashita, T., Ogino, A., Ishida, M., & Tanaka, Y. (2010). Hydrogen fermentation of cow manure mixed with food waste. *Japan Agricultural Research Quarterly*, 44(4), 399-404. <https://doi.org/10.6090/jarq.44.399>.
- Yin, F., Zhang, W. D., Xu, L., Liu, J., Yang, H., & Zhao, X. L. (2014). Contribution of H₂ during the Two-phase Anaerobic Digestion. *Advanced Materials Research*, 908, 235-238. <https://doi.org/10.4028/www.scientific.net/AMR.908.235>.
- Yu, X., Zhang, C., Qiu, L., Yao, Y., Sun, G., & Guo, X. (2020). Anaerobic digestion of swine manure using aqueous pyrolysis liquid as an additive. *Renewable Energy*, 147, 2484-2493. <https://doi.org/10.1016/j.renene.2019.10.096>.
- Yuan, Q., Sparling, R., & Oleszkiewicz, J. (2009). Waste activated sludge fermentation: effect of solids retention time and biomass concentration. *Water Research*, 43(20), 5180-5186. <https://doi.org/10.1016/j.watres.2009.08.019>.
- Zhang, J., Fan, C., & Zang, L. (2017). Improvement of hydrogen production from glucose by ferrous iron and biochar. *Bioresource Technology*, 245, 98-105. <https://doi.org/10.1016/j.biortech.2017.08.198>.
- Zhang, W., Dai, X., Dong, B., & Dai, L. (2020). New insights into the effect of sludge proteins on the hydrophilic/hydrophobic properties that improve sludge dewaterability during anaerobic digestion. *Water Research*, 173, 115503. <https://doi.org/10.1016/j.watres.2020.115503>.

- Zhang, Z., Ping, Q., Guo, W., Cai, C., & Li, Y. (2022). A novel approach using protein-rich biomass as co-fermentation substrates to enhance phosphorus recovery from FePs-bearing sludge. *Water Research*, *218*, 118479. <https://doi.org/10.1016/j.watres.2022.118479>.
- Zhou, P., Elbeshbishy, E., & Nakhla, G. (2013). Optimization of biological hydrogen production for anaerobic co-digestion of food waste and wastewater biosolids. *Bioresource Technology*, *130*, 710-718. <https://doi.org/10.1016/j.biortech.2012.12.069>.
- Zhu, H., & Béland, M. (2006). Evaluation of alternative methods of preparing hydrogen producing seeds from digested wastewater sludge. *International Journal of Hydrogen Energy*, *31*(14), 1980-1988. <https://doi.org/10.1016/j.ijhydene.2006.01.019>.

CHAPTER SIX

ENHANCING BIOHYDROGEN PRODUCTION FROM MANURE AND PINEAPPLE PEEL WASTE: BOX-BEHNKEN DESIGN AND RESPONSE SURFACE METHODOLOGY

Abstract

Producing hydrogen (H_2) from renewable organic waste is attracting much attention. This research optimized H_2 production from dairy manure (M) and pineapple peel waste (PPW) through a psychrophilic batch dark fermentation using Box Behnken Design and Response Surface Methodology. The study examined the impact of varying the M:PPW ratio (0.9 to 2.0), pH levels (4 to 7 g VS L^{-1}), and inoculum concentrations (6 to 9 g VS L^{-1}) under a constant dose of a long-chain fatty acid (4,000 mg L^{-1} oleic acid) on H_2 yield. Significant interactions ($p < 0.05$) existed among the variables, directly influencing the H_2 yield. The highest cumulative H_2 yields (mL g^{-1} VS_{substrate}) obtained at optimal settings of M:PPW ratio of 0.9, pH 6, and an inoculum of 5.5 g VS L^{-1} were 345 ± 6 at day 6 and 385 ± 7 at day 12. At the same optimal settings, pure protein substrates yielded 213 ± 3 mL H_2 g^{-1} VS_{albumin} and 233 ± 3 mL g^{-1} VS_{casein} at day 6, with day 12 yields increasing to 247 ± 6 mL H_2 g^{-1} VS_{albumin} and 312 ± 3 mL g^{-1} VS_{casein}. The quadratic model showed a high R^2 of 0.9945, indicating strong predictive accuracy. Individual volatile fatty acids studies suggested H_2 was primarily produced via the acetate-producing pathway. Fourier transform infrared spectroscopy shows the diminish of Amide I and splitting of Amide II band peaks at the end of anaerobic digestion (AD), proving the alterations or breakdown of the protein structure of the substrate. Moreover, scanning electron microscope characterization reveals albumin and casein transformed from globular and micellar forms into a more uniform structure, highlighting

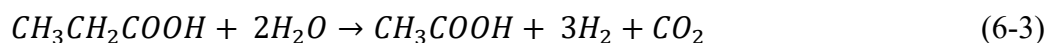
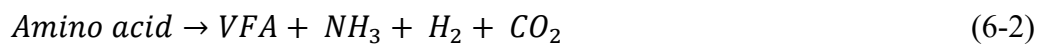
significant biodegradation during AD. This study demonstrates that PPW enhances H₂ production from dairy manure. Future studies may investigate combining dairy manure and other waste biomass that can be a source of hydrolytic enzymes.

Keywords: Manure, Pineapple peel waste, biohydrogen, Box Behnken design.

6.1 Introduction

The 21st century is undergoing a surge in investment and interest in renewable energy production due to the decline of fossil fuels and the impact of climate change (Dahunsi et al., 2022). This trend has prompted significant research into generating cleaner, sustainable gaseous and liquid biofuels from renewable sources such as agricultural waste, biomass, and plant or fruit residues (Ioelovich, 2015). Hydrogen is considered a viable alternative energy carrier, renowned as a clean fuel. Upon combusting, it only generates water and possesses an energy content 2.75 times greater than that of hydrocarbon fuels (Nasser et al., 2022). Hydrogen can be produced using chemical processes such as autothermal reforming, catalytic partial oxidation, water gas shift steam reforming, etc. (Chen et al., 2023). Most chemical processes for producing hydrogen consume substantial energy, typically from non-renewable resources, which can undermine its environmental advantages as a clean fuel. Processes like steam methane reforming are carbon-intensive, releasing CO₂ into the atmosphere and thus contributing to GHG emissions (Oni et al., 2022). Additionally, the infrastructure and materials needed for these chemical hydrogen production methods can be costly, affecting their cost-efficiency (Rasul et al., 2022). On the other hand, biological hydrogen production has attracted more attention than chemical methods due to its sustainability and lower energy consumption (Nikolaidis & Poullikkas, 2017).

Biological hydrogen production is categorized into phototrophic processes and dark fermentation or anaerobic digestion (AD). AD holds benefits over phototrophic methods by enabling continuous hydrogen generation from diverse feedstocks without the need for external energy sources like light (Bolatkhani et al., 2019; Sagir & Alipour, 2021). AD involves a series of redox reactions and biochemical transformations of organic matter into methane (CH₄) and carbon dioxide (CO₂) in an oxygen-free environment. This process is driven by the synergistic activity of a diverse consortium of microorganisms, including archaea and bacteria, which convert organic waste into valuable biogas through interconnected metabolic pathways (El Asri, 2022). Initially, complex organic polymers present in the feedstock, such as cellulose, lipids and proteins, are hydrolyzed into their constituent monomers, i.e., sugar, amino acid, and fatty acid, through enzymatic reactions. These reactions are facilitated by extracellular enzymes such as cellulases, proteases, and lipases. For instance, protein molecules in the organic waste are first hydrolyzed by proteolytic enzymes (Eq. 6-1), produced by hydrolytic bacteria, into their constituent amino acids. The amino acids produced during hydrolysis are then fermented by acidogenic bacteria, leading to the formation of volatile fatty acids (VFAs), carbon dioxide (CO₂), ammonia (NH₃), and hydrogen (H₂) (Eq. 6-2). In this stage, some VFAs produced during acidogenesis are converted into acetic acid, additional hydrogen, and CO₂ by acetogenic bacteria. For example, propionate (a three-carbon VFA) can be converted into acetic acid and CO₂ (Eq. 6-3). Finally, methanogens convert the products of acetogenesis (acetic acid, CO₂, and H₂) into methane (Eq. 6-4).





AD of protein-rich wastes, such as manure, slaughterhouse waste, and other similar organic materials, presents several challenges in biohydrogen production that can impact the efficiency and stability of the process. The high nitrogen content of these substrates can lead to ammonia inhibition, a major concern, which occurs when the concentration of total ammonia arising from the degradation of nitrogenous compounds such as proteins and urea exceeds a threshold level, typically around 1,500-3,000 mg L⁻¹ in the acidogenesis and acetogenesis stages (Lourinho et al., 2020). This inhibition can drastically reduce the microbial activity essential for hydrogen production. In addition, manure is rich in proteins (12-48 wt.%) that have complex, recalcitrant structures, making them difficult to break down (Vidmar & Vodovnik, 2018; Tasaki, 2021). The high nitrogen content associated with these proteins can also exacerbate ammonia production (Feng et al., 2023).

Employing inhibitors and stressing agents in AD to boost hydrogen production from manure while suppressing methanogenic archaeal growth involves strategies like adjusting pH (Dai et al., 2016), increasing temperature to 37-70 °C (Algapani et al., 2016; Khan et al., 2018), and using chemical inhibitors like 2-bromoethanesulfonate, acetylene, chloroform etc. (Saady, 2013). While low pH can reduce the formation of methanogenic archaea, slightly acidified circumstances (pH 5 to 6) may not be useful in treating methanogenesis when the intended gas is H₂ production (Baldi et al., 2019; Kumar et al., 2016). High-temperature operation increases operational costs in colder regions (Sudiartha et al., 2022) and poses operational challenges, such as increased viscosity and consistency, which can impact process efficiency (Fagbohunge et al., 2015). Chemical inhibitors,

while effective, can introduce toxicity issues, potentially affecting downstream uses of the digestate, and often do not drastically affect hydrogen production (Singh et al., 2022).

A promising solution to enhance hydrogen yield while suppressing methane production involves the application of long-chain fatty acids (LCFAs). LCFAs can selectively inhibit methanogenic archaea due to their specific metabolic pathways, favoring hydrogen-producing bacteria (Rodríguez-Méndez et al., 2017).

Palmitic acid (PA (C16:0)) (Deaver et al., 2020), stearic acid (SA (C18:0)) (Eftaxias et al., 2020), oleic acid (OA (C18:1)) (Eftaxias et al., 2020) and linoleic acid (LA (C18:2)) (Dasa et al., 2016) are commonly used LCFAs in AD for hydrogen production. A maximum hydrogen yield of 2.52 ± 0.2 mol mol^{-1} glucose was observed at mesophilic temperature with LA (750 mg L^{-1}) and MA (500 mg L^{-1}) in a flocculated culture (Saady et al., 2012). In another study, adding OA improved hydrogen production by limiting hydrogen-consuming microbes. Adjusting the glucose-to-xylose ratio also influenced hydrogen yield. Without OA, yields were low (1.6 ± 0.32 mol H_2 mol^{-1} glucose) due to electron flux towards non-hydrogen products like propionate and methane. With 2000 mg L^{-1} OA, electron flux shifted towards acetate and butyrate, boosting hydrogen yield to 2.84 ± 0.24 mol H_2 mol^{-1} glucose. This suggests OA effectively redirects electron flow toward hydrogen production in mixed cultures (Chaganti et al., 2012). Increasing OA concentration from 1.2 g L^{-1} to 2.4 g L^{-1} significantly enhanced hydrogen production from residual fermented solids, raising the yield from 50 to 238 ± 44 mL H_2 L^{-1} medium (dos Santos et al., 2021). Research on enhancing hydrogen and methane production with LCFAs at mesophilic temperatures using simple carbohydrates or carbohydrate-rich wastes has been abundant (Rafieenia, 2019; Duarte et al., 2021). However, examining their impact on hydrogen generation from protein-rich wastes at psychrophilic temperatures (20°C) opens up a novel area for investigation.

With that being the case, utilizing pineapple waste (PPW) with protein rich wastes feedstock is beneficial due to its high carbohydrate content (approximately 40 g L⁻¹), swift hydrolysis rate, and capability to acidify organic matter (Chu et al., 2020; Muenmee & Prasertboonyai, 2021). Additionally, PPW includes the protease enzyme bromelain, which facilitates the breakdown of organic matter into soluble forms readily usable in AD, serving as an effective biological treatment method for hydrolysis. This enzyme also helps to break recalcitrant protein structures and reduce ammonia nitrogen levels in protein-rich wastes (Cahyari et al., 2018; Syahirah & Nazaitulshila, 2018). Combining PPW with dairy manure presents a promising approach to increasing hydrogen production, optimizing the carbon-to-nitrogen (C/N) ratio for effective fermentation, ensuring process stability, and lowering the treatment costs of these organic wastes.

While adding LCFAs has been shown to initiate higher yields in biohydrogen production, their effectiveness in protein-rich wastes depends on various factors or parameters. A lack of balance among these factors could lead to digester failure or lower yields. Combining this understanding with the research focus on the synergistic effects of PPW and OA highlights the complexity of optimizing biohydrogen production from AD of dairy manure. The study aims to examine the impact of factors such as manure and PPW ratios, pH, and inoculum dosage, and their combination on biohydrogen production through response surface methodology (RSM) and Box Behnken design (BBD). This endeavor includes examining PPW's dual role as a complex substrate and a source of the protease enzyme bromelain, alongside OA's potential to introduce metabolic pathways towards enhanced hydrogen production. Lastly, the study investigates how these factors, combined with OA, affect hydrogen yield when using pure protein sources like albumin and casein, and compare the output with that of a manure-PPW study aiming to bridge a research gap.

Although the effect of adding LCFAs on biohydrogen production has been proven to initiate higher yield, the workability of LCFAs in protein-rich wastes depends on certain factors. Digester failure or low yield is possible without a balance of such factors.

6.2 Materials and Methods

6.2.1 Chemicals and reagents

To measure the total protein concentration, the study used the Pierce Coomassie (Bradford) Protein Assay Kit, a ready-to-use Bradford assay solution provided by Thermo Fisher Scientific, U.S.A. The results were then benchmarked against a standard protein solution, specifically bovine serum albumin (BSA), also acquired from Thermo Fisher Scientific, U.S.A. Sodium hydroxide in pellet form (ACS reagent standards, 97% purity) was acquired from MilliporeSigma™, U.S.A. Additionally, technical quality oleic acid (OA) (90% purity level) was sourced from Sigma-Aldrich, U.S.A. De-ionized water was utilized in the preparation of both standards and samples. As representative examples of model proteins, the experiment employed albumin in its freeze-dried powder state, with a purity exceeding 96% (obtained from Sigma Aldrich, New Zealand), and casein of technical grade, procured from Sigma Aldrich in the U.S.A.

6.2.2 Inoculum

The culture is obtained from the Riverhead Wastewater Treatment Plant, a standard facility in St. John's, Newfoundland and Labrador, Canada. After gently pouring off the top liquid layer of the collected culture, the leftover thick inoculum was kept in a glass jar at 4 °C to preserve it for

experimental purposes. Before the batch experiment, the inoculum was analyzed, revealing total solids (TS) at 5.1%, volatile solids (VS) at 3.9%, and a pH of 7.8.

6.2.3 Feedstock

Fresh cow manure (M) was gathered from Lester’s Dairy Farm on the Avalon Peninsula in Newfoundland. After collection, the manure was immediately sealed in an airtight plastic container and stored at 4°C, ready for use in anaerobic digesters. Pineapple peel waste (PPW), serving as a co-substrate, came from pineapple fruits purchased at local groceries in St. John's. These fruits were washed and peeled, and the peels were cut into small pieces for blending using a Magic Bullet® with a 250-watt motor at 2000 rpm for 60 sec. Before their introduction into the anaerobic digesters, the manure and PPW underwent physiochemical analysis, as outlined in Table 6-1.

Table 6- 1. Physiochemical characteristics of the substrates.

Parameter	Cow Manure (M)	Pineapple peel waste (PPW)
pH	7.5	5.9
Total Solids, TS (%)	14.7	21
Volatile Solids, VS (%)	7	19
Chemical Oxygen Demand, COD (g L ⁻¹)	105.3	87
Protein (g L ⁻¹)	1.2	1.2
NH ₃ -N (g L ⁻¹)	2.2	-
NH ₄ -N (g L ⁻¹)	2.1	-

6.3 Batch Anaerobic Digestion Tests

Following a statistical design, this experiment tested various manure and pineapple peel waste proportions (M:PPW), pH, and inoculum dosages in duplicate batch digesters. The experiments used 0.610 L Wheaton glass bottles as digesters, each with a 0.2 L working volume, and were conducted under anaerobic conditions established by a 2-minute nitrogen gas purge (Figure 6-1).

The digesters received an oleic acid (OA) dosage of 4,000 mg L⁻¹ one day before the commencement of the experiment (referred to as day 0). The digesters were stored in dark containers to prevent exposure to light and inverted to prevent gas leaks. The entire process was controlled at a constant 20±1 °C. Gas composition in the headspace was recorded daily, while volatile fatty acids (VFAs) were checked every other day (days 2, 4, 6, 8, 10, and 12). Protein, volatile solids (VS), and chemical oxygen demand (COD) were measured on days 6 and 12. To maintain anaerobic conditions, the digesters were opened and purged with nitrogen gas again on day 6 before being sealed until the end of the experiment on day 12.



Figure 6- 1. Nitrogen gas is flushed in each digester to sustain an anaerobic environment.

6.4 Overall Experimental Design

This study's experimental approach is methodically segmented into two distinct parts. Figure 6-2 outlines the experimental activities carried out in both parts. The objective across both parts (I and II) was to evaluate the yields of biohydrogen and biomethane. Part I explored the use of

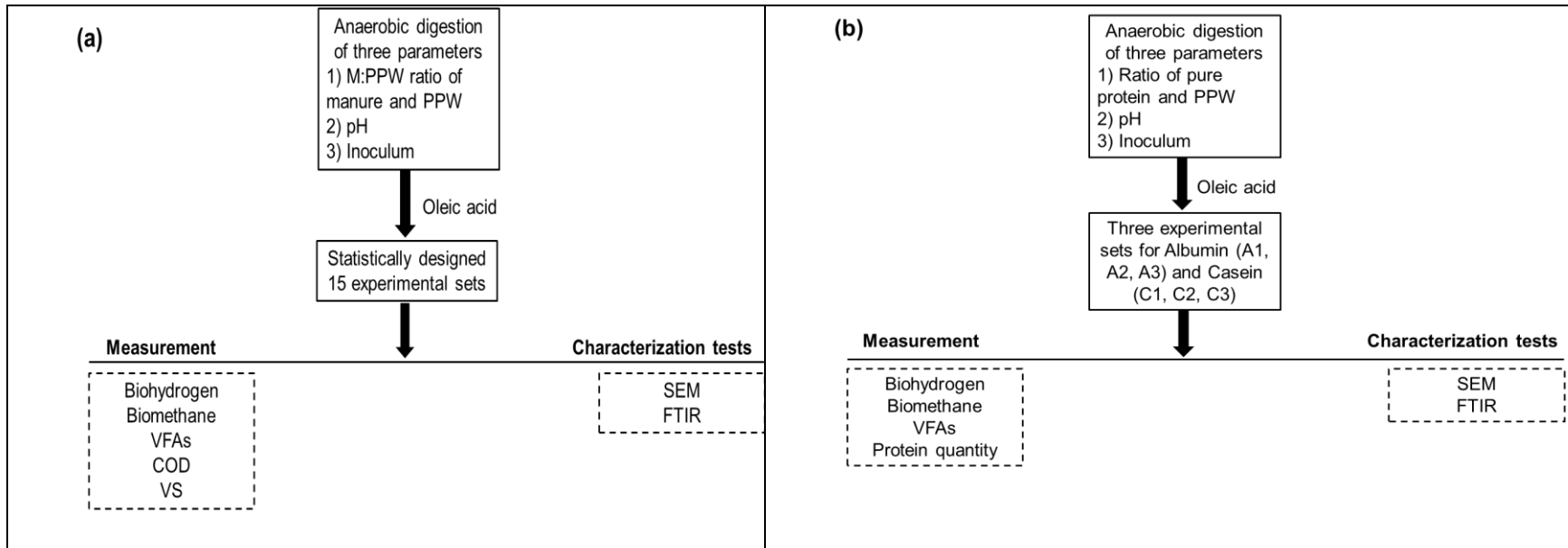
manure-PPW as a feedstock, focusing on anaerobic digestion by examining variables such as the M:PPW ratio (manure to pineapple peel waste, based on volatile solids (VS)), pH levels, and the quantity of inoculum, all under a fixed concentration of OA. A total of fifteen experiments, designed statistically, were performed to measure the outputs of biohydrogen and biomethane and monitor VFAs, COD, and VS.

Part II shifted focus to utilizing pure proteins-PPW (specifically albumin and casein) as substrates, employing optimal combinations of three critical factors: i) the ratio of manure to pineapple peel waste (M:PPW), ii) pH, and iii) the amount of inoculum. For this part, three experimental configurations tailored to the digestion of these specific proteins in conjunction with a 4,000 mg L⁻¹ concentration of OA were developed. Details of these experimental setups for the pure proteins are outlined in Table 6-2. Advanced characterization techniques like scanning electron microscope (SEM) and fourier transform infrared spectroscopy (FTIR) were employed to document the compositional and structural changes in the substrates pre- and post-digestion for parts I and II. The next sections (6.6 to 6.8) will present a comprehensive overview of the experimental procedures and their corresponding results based on the guidelines presented in this section.

Table 6- 2. Three distinct experimental sets of albumin and casein for part II of the research.

Substrate	Set	Substrate:PPW	pH	Inoculum dosage (g VS L ⁻¹)
Albumin (A)	A1	0.9	5	7
	A2	0.9	4	5.5
	A3	0.9	6	5.5
Casein (C)	C1	0.9	5	7
	C2	0.9	4	5.5
	C3	0.9	6	5.5

Figure 6- 2. Flowchart of the experiment's details of pineapple peel waste (PPW) with (a) Part I: manure and (b) Part II: pure proteins.



6.5 Box-Behnken Design

This research employed the Response Surface Methodology (RSM) and Box-Behnken Design (BBD) to optimize biohydrogen production. The study evaluated the influence of various factors and their interactions by applying these strategies across three levels (low, medium, and high). The RSM and BBD analyses were conducted through Minitab® 21.4 (LLC, Pennsylvania, USA). In this research, 15 experiments were carried out utilizing manure and pineapple peel waste (PPW), concentrating on three variables: the ratio of manure to pineapple peel waste (M:PPW), pH, and the amount of inoculum, with each being evaluated at three distinct levels (-1, 0, +1). Table 6-3 presents the factors of the anaerobic digestion study, including the M:PPW ratio (0.9 to 2 g VS L⁻¹), pH range (4 to 6), and inoculum (4 to 7 g VS L⁻¹).

Table 6- 3. Different variables for Box-Behnken Design (BBD) for biohydrogen yield using manure (M) and pineapple peel waste (PPW).

Factors	C odes	Level		
		Low (-1)	Interme diate (0)	High (+1)
M:PPW	A	0.9	1.45	2
pH	B	4	5	6
Inoculum (g VS L ⁻¹)	C	4	5.5	7

As described in Table 6-4, the experimental design adhered to a specific matrix involving three independent variables: the M:PPW ratios, pH levels, and inoculum amounts. Biohydrogen yield served as the primary outcome or dependent variable. The study also measured reductions in VS and the generation of VFA. A precise layout of the experimental setup and outcomes for the anaerobic digestion is presented in Figure 6-3.

Table 6- 4. Box-Behnken Design matrix for the anaerobic digestion using manure (M) and pineapple peel waste (PPW).

Std. Order	Run Order	Pt. Type	Blocks	M:PPW	pH	Inoculum (g VS L ⁻¹)
14	1	0	1	1.45	5	5.5
10	2	2	1	1.45	6	4
15	3	0	1	1.45	5	5.5
8	4	2	1	2	5	7
11	5	2	1	1.45	4	7
12	6	2	1	1.45	6	7
7	7	2	1	0.9	5	7
9	8	2	1	1.45	4	4
13	9	0	1	1.45	5	5.5
5	10	2	1	0.9	5	4
2	11	2	1	2	4	5.5
1	12	2	1	0.9	4	5.5
3	13	2	1	0.9	6	5.5
6	14	2	1	2	5	4
4	15	2	1	2	6	5.5

*M = Manure; PPW = Pineapple peel waste


Digester for anaerobic digestion test	Statistically designed experimental matrix	Responses
 <p>Manure + Pineapple peel waste + inoculum in presence the of oleic acid in anaerobic digester</p>	<p>Manure:PPW ratio of manure and PPW (0.9 to 2) + pH (4 to 6) + Inoculum (4 to 7 g VS L⁻¹)</p> <p style="text-align: center;">↓</p> <p>15 runs</p>	<p>✓ Production</p> <p>-Biohydrogen and biomethane</p> <p>-VFAs</p> <p>✓ Reduction (%)</p> <p>-COD</p> <p>-VS</p>

Figure 6- 3. Layout of the experimental setup and outcomes for the anaerobic digestion optimization.

In Chapter 6, the optimal conditions for biohydrogen production were aligned with the ammonia reduction conditions identified in Chapter 4. This alignment ensured that the benefits of reduced ammonia accumulation were fully realized in the biohydrogen production process. The manure and PPW dosage optimized in Chapter 4 (6.5 g VS_{manure} L⁻¹ and 7 g VS_{PPW} L⁻¹, i.e., M:PPW ratio of 0.93) for the highest NH₃-N reduction (72±0.48%) informed the experimental design basis in Chapter 6. By exploring a range of manure and PPW ratios of 0.9 to 2.0, the study in Chapter 6 aimed to identify the optimal combination that maximized biohydrogen yield while maintaining the ammonia reduction benefits.

6.6 Analytical Methods

The analysis involved evaluating gases in the headspace (H₂, CH₄, and CO₂), examining liquid constituents (proteins and VFAs), and characterizing solids through Fourier Transform Infrared (FTIR) spectroscopy and scanning electron microscopy (SEM). Initial tests on manure and pineapple peel waste measured the TS and VS, pH, ammonia, and ammonium nitrogen, as outlined in section 3.3.2. Protein and volatile solids quantification followed protocols in sections 3.5.1 and 3.5.3, respectively. The details on biohydrogen, biomethane, VFAs, and substrates for characterizations are presented in sections 5.7.1 to 5.7.5.

6.7 Results and Discussion

The study applied a BBD to test manure-PPW ratios, pH levels, and inoculum amounts, focusing on biohydrogen production. It also tracked biomethane output, VS reduction, and VFAs generation during the anaerobic digestion of the mix. Results are elaborated in sections 6.8.1 to 6.8.4.

6.7.1 Hydrogen yield

The experimental results reveal intricate details about biohydrogen (Figure 6-4 and Table 6-5) and biomethane (Figure 6-5 and Table 6-6) production across the 15 different setups. Each setup represents a distinct combination of parameters such as M:PPW ratio, pH level, and inoculum dosage, and their influence on respective yield are measured over 12 days.

In Figure 6-4, set 1 (M:PPW ratio of 1.45, pH 5, and inoculum dosage of 5.5 g VS L⁻¹) displays a gradual increase in hydrogen production from 26±2 mL g VS⁻¹ at day 1, showing steady growth to 202±1 mL g VS⁻¹ by day 6, and eventually reaching 304±5 mL g VS⁻¹ by day 12.

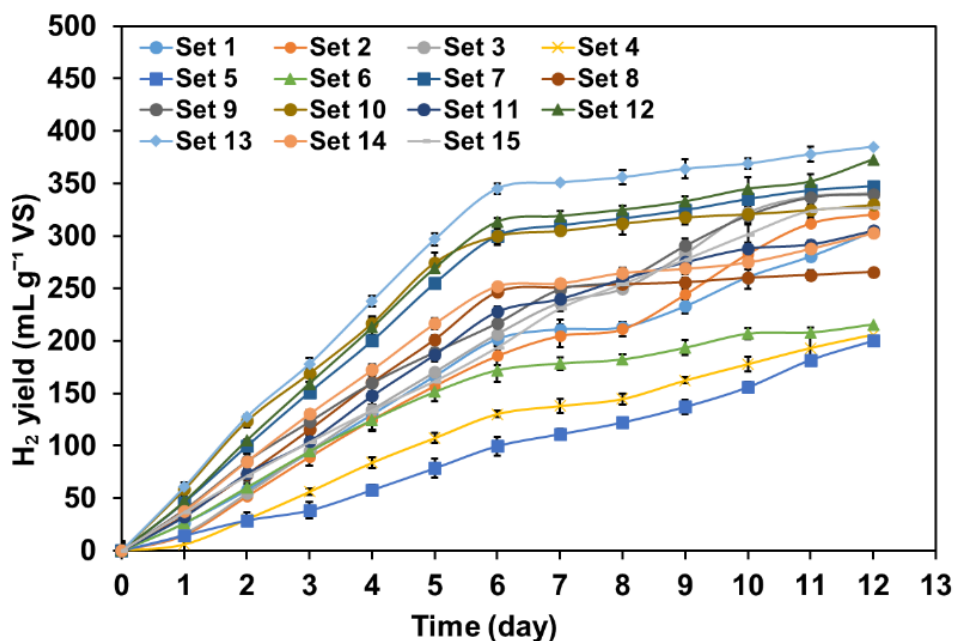


Figure 6- 4. Cumulative hydrogen yield in the anaerobic digestion of manure and pineapple peel waste.

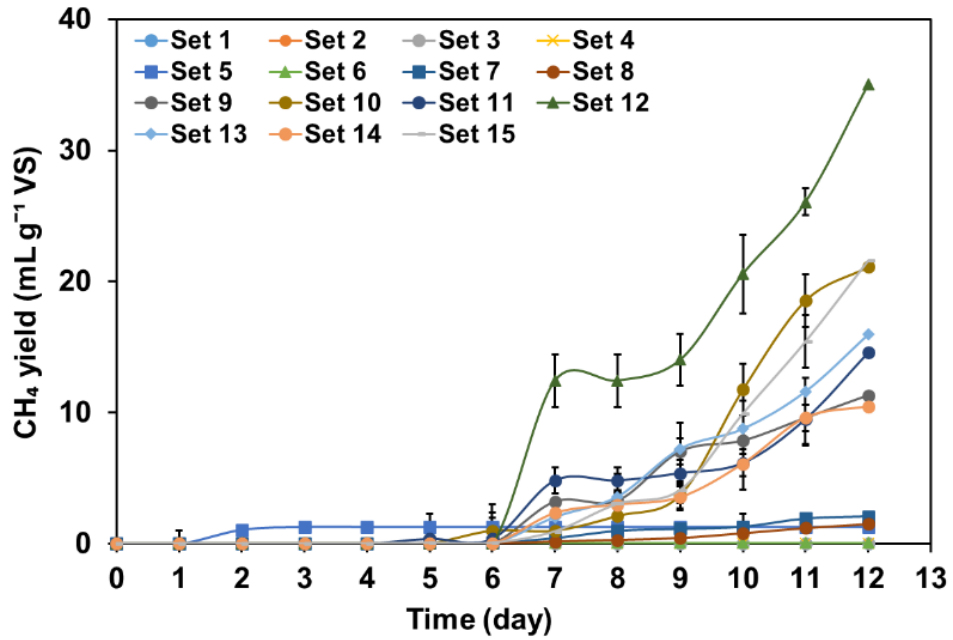


Figure 6- 5. Cumulative methane yield in the anaerobic digestion of manure and pineapple peel waste.

Table 6- 5. Cumulative hydrogen yield in the anaerobic digestion of manure and pineapple peel waste.

Days	Experimental set number														
	1	2	3	4	5	6	7	8	9	10	11	12	13	14	15
0	0	0	0	0	0	0	0	0	0	0	0	0	0	0	0
1	26±2	15±7	16±2	6±1	15±5	26±3	46±2	33±4	39±5	58±3	32±9	47±4	61±3	38±8	37±4
2	58±4	52±5	55±1	30±8	29±4	60±6	100±3	73±1	85±4	124±2	73±6	105±5	128±4	85±5	71±5
3	94±3	89±3	95±1	56±7	38±3	95±3	151±4	115±2	123±7	169±6	104±4	159±1	178±2	130±7	103±5
4	130±5	125±9	135±4	84±3	58±8	125±6	200±2	160±5	160±9	217±8	148±3	213±5	238±5	172±4	134±3
5	166±6	157±11	170±5	107±5	79±5	151±9	255±5	201±9	189±8	275±6	187±9	269±9	297±5	217±5	162±5
6	202±1	186±6	207±3	130±5	100±9	172±9	300±4	247±4	217±4	300±9	228±6	314±2	345±6	252±5	194±6
7	211±3	205±9	237±2	138±3	111±9	178±11	310±9	251±4	249±3	305±7	240±5	319±3	351±5	255±2	231±2
8	213±9	211±11	250±5	145±7	122±5	182±6	317±5	254±6	258±7	312±4	259±8	325±5	356±2	265±2	254±2
9	233±5	244±7	284±4	162±5	137±4	193±5	325±5	256±6	291±4	318±11	275±7	333±4	364±7	269±5	277±1
10	261±7	283±5	322±7	178±3	156±7	207±7	335±3	260±4	320±7	321±7	288±5	345±5	369±9	275±5	302±6
11	280±11	312±3	338±5	193±7	182±5	208±5	343±2	263±2	337±9	325±5	292±6	352±11	378±5	288±7	324±11
12	304±5	321±3	341±11	206±12	200±3	216±5	348±7	266±5	340±11	330±4	305±4	373±7	385±7	303±5	327±6

Table 6- 6. Cumulative methane yield in the anaerobic digestion of manure and pineapple peel waste.

Days	Experimental set number														
	1	2	3	4	5	6	7	8	9	10	11	12	13	14	15
0	0	0	0	0	0	0	0	0	0	0	0	0	0	0	0
1	0	0	0	0	0	0	0	0	0	0	0	0	0	0	0
2	0	0	0	0	1±1	0	0	0	0	0	0	0	0	0	0
3	0	0	0	0	1±0	0	0	0	0	0	0	0	0	0	0
4	0	0	0	0	1±0	0	0	0	0	0	0	0	0	0	0
5	0	0	0	0	1±0	0	0	0	0	0	0	0	0	0	0
6	0	0	0	0	1±1	0	0	0	0	1	0	0	0	0	0
7	0	0	0	0	1±0	0	0	0	3±0	1±1	5±2	12±3	2±0	2±0	1±1
8	0	0	0	0	1±0	0	1±0	0	3±0	2±0	5±1	12±2	4±1	3±0	3±0
9	0	0	0	0	1±0	0	1±0	0	7±2	4±1	5±1	14±2	7±1	4±1	4±1
10	0	0	0	0	1±0	0	1±0	1±0	8±1	12±1	6±1	21±2	9±2	6±1	10±1
11	0	0	0	0	1±0	0	2±1	1±0	10±1	19±2	10±1	26±3	12±3	10±2	15±1
12	0	0	0	0	1±0	0	2±0	2±0	11±1	21±2	15±2	35±1	16±1	10±2	22±2

This consistent rise indicates a stable fermentation process. Set 7 (M:PPW ratio of 0.9, pH 5, and inoculum dosage of 7 g VS L⁻¹), on the other hand, started strong with a yield of 46±2 mL g VS⁻¹ at day 1, higher than any other sets at this point, and continued to lead with the highest yields until day 6, reaching 310±4 mL g VS⁻¹. By day 12, the yield had only increased marginally to 348±7 mL g VS⁻¹, indicating a rapid approach to the plateau phase and possibly suggesting substrate availability or microbial activity limitations (Rasapoor et al., 2020). A distinct observation is made in set 8 (M:PPW ratio of 1.45, pH 4, and inoculum dosage of 4 g VS L⁻¹), which begins with a moderate yield of 33±4 mL g VS⁻¹ at day 1, then steadily increases to 247±4 mL g VS⁻¹ by day 6, and shows a notable increase, peaking at 266±5 mL g VS⁻¹ by day 12. The pattern suggests effective substrate utilization, although the growth rate diminishes slightly in the latter days, which could be due to the onset of substrate depletion or accumulation of inhibitory byproducts (Haq et al., 2023). On day 6, set 12 (M:PPW ratio of 0.9, pH 4, and inoculum dosage of 5.5 g VS L⁻¹) yielded a hydrogen production of 314±2 mL g VS⁻¹, which increased to 373±7 mL g VS⁻¹ by day 12. Set 13 (M:PPW ratio of 0.9, pH 6, and inoculum dosage of 5.5 g VS L⁻¹) showed a higher yield on day 6 with 345±6 mL g VS⁻¹ and continued to increase to 385±7 mL g VS⁻¹ by day 12. Despite having similar M:PPW ratio and inoculum, the differences between sets 12 and 13 can be rationalized as a slightly acidic pH can be beneficial for initial hydrogen production; an excessively low pH can lead to acidogenic bacteria outcompeting hydrogen producers in the digester, resulting in lower hydrogen yields (Moreno Cárdenas & Zapata Zapata, 2019).

Figure 6-5 indicates 15 experimental sets over 12 days with various responses to the applied anaerobic digestion conditions. Set 1 (M:PPW ratio of 1.45, pH 5, and inoculum dosage of 5.5 g VS L⁻¹), set 2 (M:PPW ratio of 1.45, pH 6, and inoculum dosage of 4 g VS L⁻¹), set 3 (M:PPW ratio of 1.45, pH 5, and inoculum dosage of 5.5 g VS L⁻¹) and set 4 (M:PPW ratio of 2, pH 5, and

inoculum dosage of 7 g VS L⁻¹) did not produce methane during the 12 days, which aligns with the inhibitory effects of oleic acid on methanogens.

Long-chain fatty acids (LCFAs), such as oleic acid (OA), are known to disrupt microbial cell membranes. This disruption leads to an accumulation of LCFAs within digesters, as the impaired microbial activity reduces the digestion process's efficiency in breaking down these fatty acids. Consequently, the accumulation of LCFAs results in long-term inhibition of methanogenesis (Zonta et al., 2013). Sets 6, 7, and 8 experienced a delayed start in methane production, with set 7 (M:PPW ratio of 0.9, pH 5, and inoculum dosage of 7 g VS L⁻¹) reaching 2 mL g⁻¹ VS by day 12. Set 8 (M:PPW ratio of 1.45, pH 4, and inoculum dosage of 4 g VS L⁻¹) demonstrated a similar pattern. This delayed and gradual increase could indicate a longer lag phase for methanogen growth. Set 12 (M:PPW ratio of 0.9, pH 4, and inoculum dosage of 5.5 g VS L⁻¹) stands out with a significantly higher methane yield, starting with 12±3 mL g⁻¹ VS on day 7 and rapidly increasing to 35±1 mL g⁻¹ VS by day 12. Set 13 (M:PPW ratio of 0.9, pH 6, and inoculum dosage of 5.5 g VS L⁻¹) also shows a notable increase from 2 to 16±1 mL g⁻¹ VS between days 7 and 12. This gradual increase, despite the presence of OA, suggests that some methanogenic populations might have developed resistance or adapted to the inhibitory conditions over time due to a suitable combination of other parameters such as pH and inoculum and substrate: inoculum ratio (Palatsi et al., 2010).

Models were developed to optimize biohydrogen yield in the AD process using a three-level Box-Behnken design, with Eq. 6-5 highlighting key significant factors.

$$\begin{aligned} \text{Hydrogen yield (mL g}^{-1} \text{ VS)} = & 559 - 380.7 * A - 39.5 * B + 58.8 * C + \\ & 216.7 A * A - 3.96 B * B - 12.76 C * C - 29.55 A * B - \\ & 36.97 A * C + 22.33 B * C \end{aligned} \quad (6-5)$$

Where, A, B and C terms indicate manure:PPW ratio of manure and pineapple peel waste, pH, and inoculum (g VS L⁻¹). The model (Eq. 6-5) derived from the three-level Box-Behnken design incorporates critical terms in a coded representation, showcasing its significant impact.

The effectiveness and suitability of the constructed models were validated through analysis of variance (ANOVA), with comprehensive details provided in Table 6-7. ANOVA is a statistical method used to examine the differences between the means of three or more groups to determine if at least one of the groups' means significantly differs from the others. ANOVA achieves this by comparing the variance (spread) of data points within each group to the variance between the groups (Kao & Green, 2008).

The ANOVA table summarizes the statistical analysis of a quadratic model used to assess hydrogen production from an experiment involving variables manure:PPW ratio, pH, and Inoculum dosage. The Model *F*-value (90.89) indicates the model is significant, and there is a 0.01% chance that such a large *F*-value could occur due to noise. Furthermore, the ANOVA for the quadratic regression model yielded significant results ($p < 0.05$). This *p*-value indicates the importance of the variables within the model, with lower *p*-values pointing to higher significance levels for every variable.

Table 6- 7. Analysis of variance (ANOVA) for the quadratic model assessing hydrogen production, comprising three variables: Box Behnken Design (BBD) applied to manure and pineapple peel waste (KPW).

Source	DF	Adj SS	Adj MS	F-Value	p-Value
Model	9	345	260.6	90.89	0.000
Linear	3	824	941.6	164.3	0.000
A-Manure:PPW	1	878.1	878.1	356.04	0.000
B- pH	1	6.1	6.1	0.08	0.783
C-Inoculum (g VS L ⁻¹)	1	940.5	940.5	136.76	0.000
Square	3	254	751.3	92.89	0.000
A ² -Manure:PPW*Manure:PPW	1	861.1	861.1	218.22	0.000
B ² -pH*pH	1	57.9	57.9	0.8	0.413
C ² -Inoculum (g VS L ⁻¹)*Inoculum (g VS L ⁻¹)	1	43.1	43.1	41.87	0.001
2-Way Interaction	3	266.3	88.8	42.5	0.001
AB-Manure:PPW*pH	1	156.3	56.3	14.53	0.012
AC-Manure:PPW*Inoculum (g VS L ⁻¹)	1	721	121.0	51.19	0.001
BC-pH*Inoculum (g VS L ⁻¹)	1	489	89	61.76	0.001
Error	5	63.4	52.7		
Lack-of-Fit	3	46.7	82.2	1.41	0.441
Pure Error	2	16.7	8.0		
Total	14	116.7			
R ²		R ² (adjusted)		R ² (predicted)	
0.9945		0.9845		0.9359	

The elevated *F*-value and a *p*-value below 0.05 led to rejecting the null hypothesis, demonstrating significant impacts from the obtained model (Jiménez et al., 2014). The regression analysis of the experimental design indicates that the linear factors A – Manure:PPW, and C - Inoculum (g VS L⁻¹), quadratic factors A² - (Manure:PPW * Manure:PPW) and C² (inoculum*inoculum), and the interaction factor AB - Manure:PPW*pH, AC- manure:PPW * inoculum and BC - pH * inoculum were significant (*p*-value less than 0.05). However, the linear and quadratic terms related to factor B - pH and B² - pH*pH did not show statistical significance (*p*-value greater than 0.05). The non-significant *p*-value (0.783) for B- pH indicates that pH alone does not significantly affect hydrogen production within the range tested. The R² value reflected

the extent to which independent variables could account for variability in the observed responses. The R^2 value of 0.9945 is very high, suggesting that the model explains 99.45% of the variability in hydrogen production, and merely 0.55% falls beyond the scope of what the model can not account for (Ruiz-Aguilar et al., 2023). The adjusted R^2 value was 0.9845, signaling the model's strong relevance. With a predicted R^2 of 0.9359, there was a notable consistency between the actual and predicted outcomes (Ruiz-Aguilar et al., 2023). The minor variation between adjusted and predicted R^2 suggests a strong alignment between the theoretical model and the experimental results, enabling precise forecasts of hydrogen production (Ahmad et al., 2024).

The three-dimensional response surface plots, created by varying two factors while holding others constant, are depicted as solid shapes in 3D space, aiding in the visualization of linear and interactive effects of these factors (Yetilmezsoy et al., 2009). These plots and their two-dimensional contour counterparts offer a clear method for assessing how experimental variables impact outcomes (Ahmad et al., 2024). In this study, with three independent variables in the regression model, one was kept constant at a midpoint. Figure 6-6 illustrate these 3D plots and their contour maps, showing the effects of two variables under the experimental condition.

It is observed from Figure 6-6 (a) that at manure:PPW ratio of 0.9 and a pH level of 4, the biohydrogen yield commenced at 301 mL g⁻¹ VS. As the pH was augmented to 5 and 6, the yield exhibited a substantial increase to 314 and 345 mL g⁻¹ VS, respectively. An increase in the manure:PPP ratio from 0.9 to 2.0 at any fixed pH decreases biohydrogen yield. For example, at pH 6, the yield decreased from 345 to 188 mL g⁻¹ VS, as the ratio increased further, suggesting that an imbalance in the carbon to nitrogen (C:N) ratio could negatively affect the microbial ecosystem responsible for biohydrogen production.

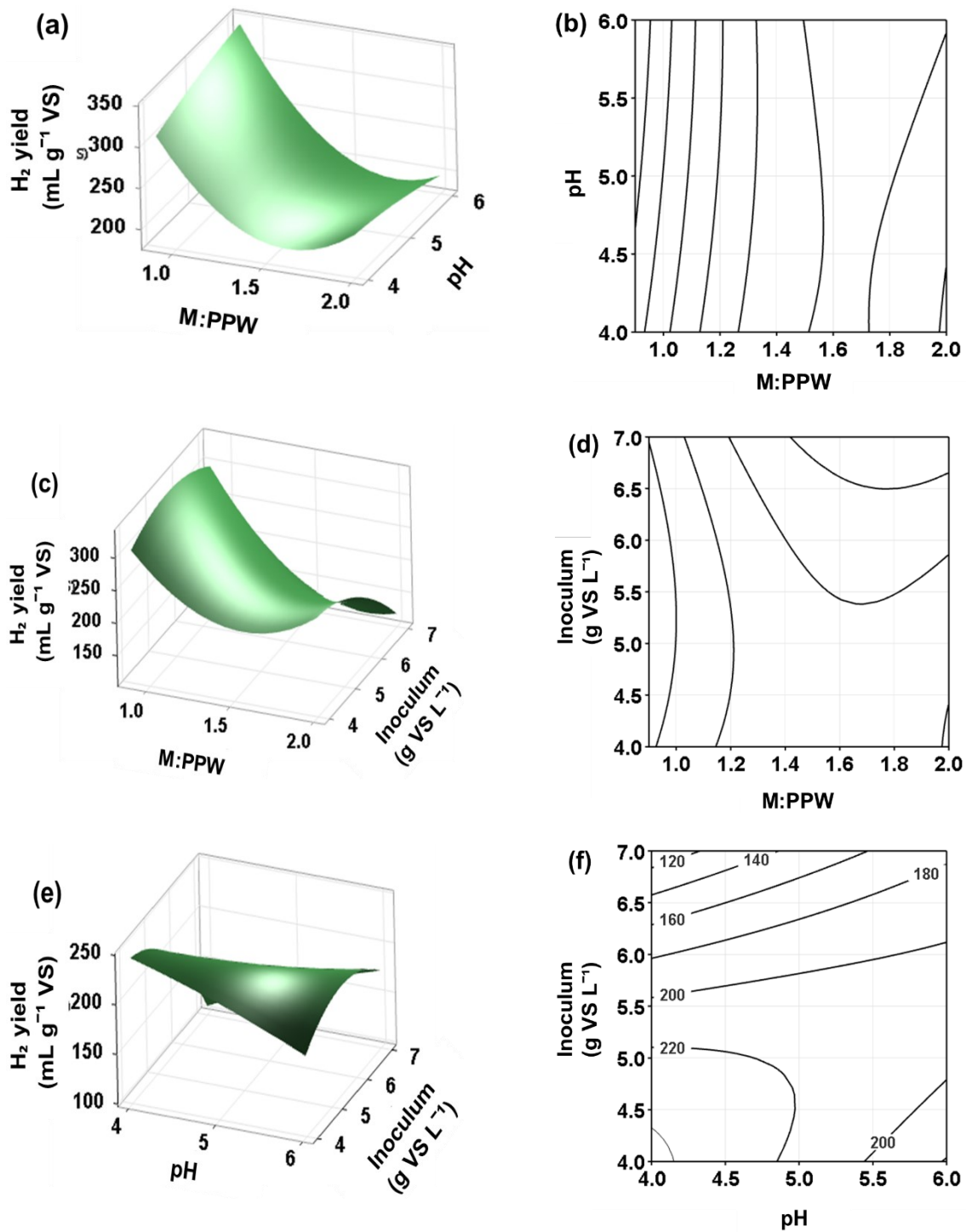


Figure 6- 6. 3D and contour plots illustrating the effects on biohydrogen yield from (a) and (b) manure:PPW ratio and pH, (c) and (d) manure:PPW ratio and inoculum, and (e) and (f) pH and inoculum.

The research by Arifan et al. (2021) supports this, indicating that an optimal mix of substrates is crucial for achieving peak biogas production, and deviations can lead to lower yields. In Figure 6-6 (b), the regions where the contour lines are straight and parallel, there is an indication that the biohydrogen yield is changing at a constant rate with respect to pH.

The curvature of the contour lines near the higher manure:PPW ratio indicates a nonlinear relationship and suggests that there are diminishing returns in biohydrogen yield as the ratio increases. For example, at a pH of around 5.0, increasing the manure:PPW ratio from 0.9 to 1.2 increases the yield from 250 to 300 mL g⁻¹ VS. However, further increasing the ratio to 1.5 does not lead to an increase in yield, which remains at 200 mL g⁻¹ VS.

Figure 6-6 (c and d) depicts the surface plot and contour plot among biohydrogen yield, manure:PPW ratio, inoculum, with the pH held constant at 5. At a low inoculum concentration of 4 g VS L⁻¹, the biohydrogen yield decreases with the increased manure:PPW ratio, starting from 298 mL g⁻¹ VS at a ratio of 0.9 and peaking at around 210 mL g⁻¹ VS at a ratio of 2. This suggests that increasing substrate availability at a lower inoculum concentration may decrease microbial activity and, thus, H₂ yield (Li et al., 2018). However, increasing the inoculum concentration from 6 to 7 g VS L⁻¹, regardless of the manure:PPW ratio, leads to a marked decrease in biohydrogen yield. The plot shows a decrease in yield down to 298 from 322 mL g⁻¹ VS across the range of manure:PPW ratios. This decline in yield at higher inoculum concentrations may be attributed to inoculum overloading, where an excess of microorganisms leads to a rapid depletion of available nutrients or accumulation of inhibitory products, thus hindering biohydrogen production (He et al., 2017). The shape of the contour lines (Figure 6-6 (d)) can be described as semi-elliptical, with the y-axis along the inoculum concentration. The semi-elliptical shape suggests a nonlinear relationship between biohydrogen yield, inoculum concentration, and manure:PPW ratio. The

semi-elliptical contours indicate an optimal range for these parameters and that deviating from this range either by increasing or decreasing the inoculum concentration or the manure:PPW ratio results in a lower yield of biohydrogen.

Figure 6-6 (e) shows that as the pH increases from 4 to 6 at a lower inoculum concentration of 4 g VS L^{-1} , the surface plot indicates a decrease in biohydrogen yield from 248 to $151 \text{ mL g}^{-1} \text{ VS}$. In Figure 6-6 (e), the optimal biohydrogen yield, given these parameters, appears to be at pH 4 and an inoculum concentration near 5 g VS L^{-1} . Operating outside these parameters, especially at higher inoculum concentrations (from 5 to 7 g VS L^{-1}), results in diminished yield, as indicated by the trough in the surface plot. The importance of balancing inoculum concentration to optimize anaerobic digestion performance is corroborated by Khadka et al. (2022), emphasizing the need to adjust inoculum levels to avoid process inhibition.

The shape of the contour lines in Figure 6-6 (f) is primarily straight over most of the pH range, suggesting that changes in pH have a less consistent effect on biohydrogen yield at each inoculum concentration level. This implies a direct relationship between pH and biohydrogen yield within the studied range, where the yield gradually increases with pH until reaching an optimal point, beyond which it starts to decline. The elliptical shape of the $220 \text{ mL g}^{-1} \text{ VS}$ contour line indicates a peak biohydrogen yield occurs at a pH around 4.5 to 5 with an inoculum concentration of approximately $5 \text{ mL g}^{-1} \text{ VS}$. The yield decreases symmetrically on either side of this peak along the pH axis.

6.7.2 Volatile solids reduction

In biohydrogen and biomethane generation through anaerobic digestion, the analysis of volatile solids (VS) reduction is crucial as it reflects the extent of biodegradation of organic matter. The

Box-Behnken design used for the 15 sets helps optimize the experimental conditions to determine the effects of different variables on VS reduction (Figure 6-7).

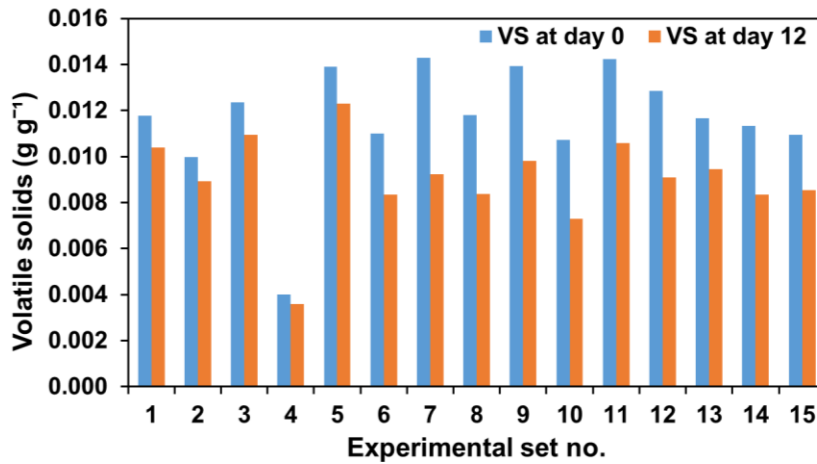


Figure 6- 7. Profile of volatile solids (VS) across fifteen experiments.

The VS data range at day 0 varies from 0.002 to 0.014 g g⁻¹, indicating the initial concentration of volatile solids present in the different sets. By day 12, the VS data range shifts to 0.004 to 0.012 g g⁻¹, demonstrating the degradation of volatile solids after digestion. Set 4 started with a low VS of 0.004 g g⁻¹ at day 0, slightly reducing to 0.0036 g g⁻¹ on day 12, resulting in a 10.0% reduction. Similarly, set 2 had a VS of 0.010 g g⁻¹ at day 0, reducing to 0.009 g g⁻¹ at day 12, with a 10.2% reduction. The slight reduction could be attributed to a less active microbial community under inadequate environmental conditions for digestion (Harirchi et al., 2022). Inappropriate conditions, such as a low pH or an imbalanced C/N ratio, can hinder microbial activity, reducing volatile solids reduction (Wang et al., 2023). Sets 1, 3, and 5 show moderate VS reductions. Set 1 had a VS of 0.012 g g⁻¹ reducing to 0.010 g g⁻¹ (11.7%), set 3 from 0.012 g g⁻¹ to 0.011 g g⁻¹ (11.9%), and set 5 from 0.014 g g⁻¹ to 0.012 g g⁻¹ (11.2%). These reductions suggest that the anaerobic digestion process was effective but not optimized. Set 7 demonstrated the most significant VS reduction,

decreasing from 0.014 g g^{-1} to 0.009 g g^{-1} , translating to a 35.4% reduction. Similarly, notable reductions were observed in set 10 and set 9; set 10 saw a reduction from 0.011 g g^{-1} to 0.007 g g^{-1} , marking a 31.9% decrease, while set 9's VS content was reduced from 0.014 g g^{-1} to 0.010 g g^{-1} , resulting in a 29.6% reduction. The highest reductions may be attributed to optimal conditions that promote robust microbial activity, such as adequate nutrient availability, favorable inoculum-to-substrate ratios, and suitable environmental conditions, which are essential for efficient organic matter breakdown (Filer et al., 2019; Moset et al., 2015; Oduor et al., 2022). Figure 6-7 also coincides with the result, providing the highest biohydrogen yield observed at run 7 ($348 \pm 7 \text{ mL H}_2 \text{ g}^{-1} \text{ VS}$) (Figure 6-4 and Table 6-4).

6.7.3 Volatile fatty acids

Volatile fatty acids (VFA) are excellent indicators for assessing the metabolic condition of anaerobic digestion processes (Habiba et al., 2009). Acetic (CH_3COOH), propionic ($\text{C}_2\text{H}_5\text{COOH}$), isobutyric, butyric ($(\text{CH}_3)_2\text{CHCOOH}$), isovaleric, valeric ($\text{CH}_3\text{CH}_2\text{CH}_2\text{COOH}$), and caproic ($(\text{CH}_3)_2\text{CHCH}_2\text{COOH}$) acids are among the most frequently encountered VFAs, (Wainaina et al., 2019). The variation in VFA production can be attributed to factors such as operational settings, the nature of the substrate, and the microbial consortium present in the AD process (Lukitawesa et al., 2020). Figure 6-8 illustrates the profile of total VFAs (TVFAs) production in 15 sets at the end of 12 days of the experiment.

The highest TVFAs production ($5848 \pm 71 \text{ mg L}^{-1}$) is observed in set 10 (M:PPW ratio of 0.9, pH 5, and inoculum dosage 4 g VS L^{-1}). On the other hand, the lowest production ($3323 \pm 78 \text{ mg L}^{-1}$) of TVFAs is observed in set 9 (M:PPW ratio of 1.45, pH 5, and inoculum dosage 5.5 g VS L^{-1}).

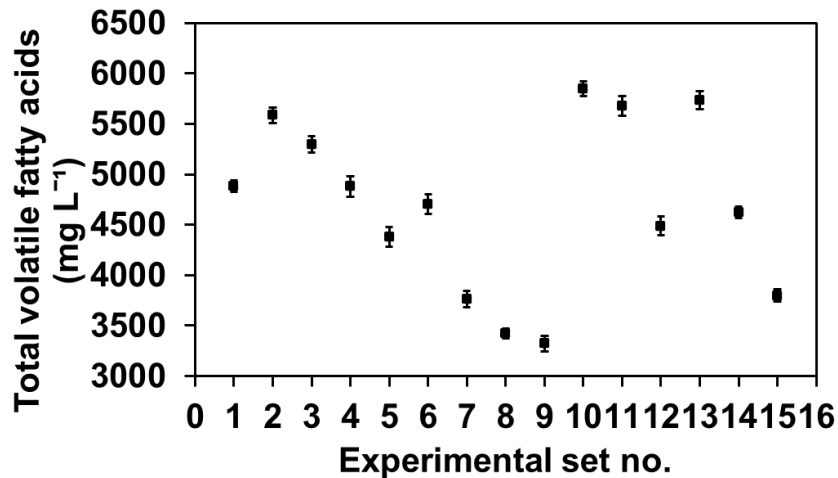
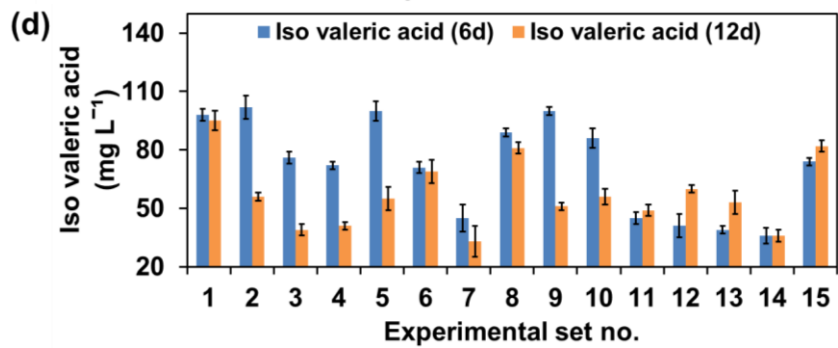
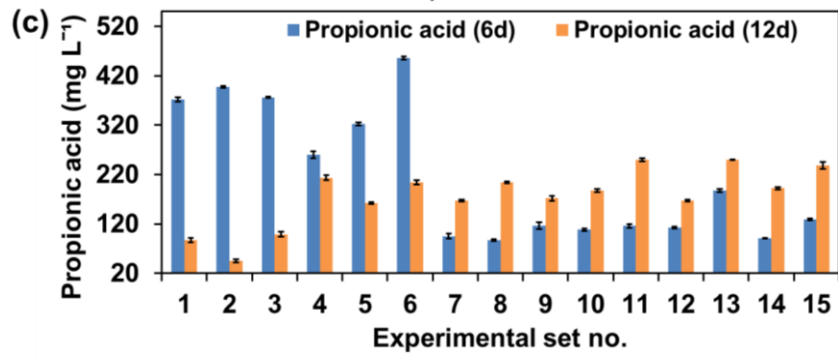
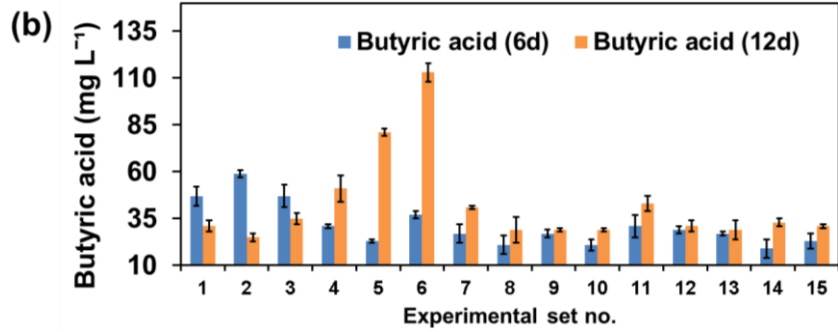
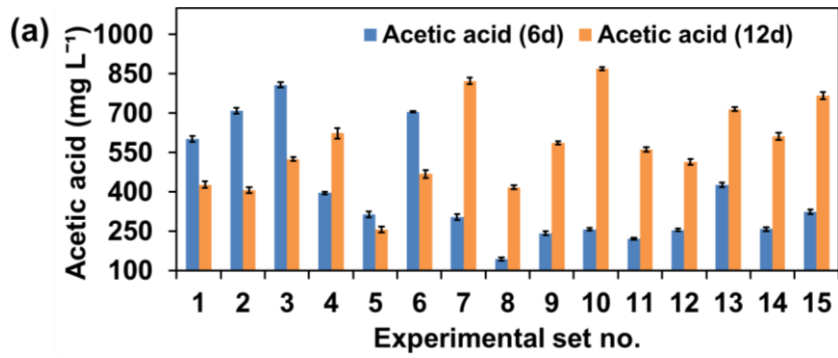


Figure 6- 8. Profile of total volatile acids (TVFAs) generated by 15 experimental sets measured on day 12.

Protein-rich wastes, such as manures, may contain high ammonia levels, which can inhibit microbial activity and suppress VFAs production (Mahato et al., 2020). Some other sets such as set 7 (M:PPW ratio of 0.9, pH 5, and inoculum dosage 7 g VS L⁻¹) yielded 3764±78 mg L⁻¹ of TVFAs, while set 12 (M:PPW ratio of 0.9, pH 4, and inoculum dosage 5.5 g VS L⁻¹) produced 4489±91 mg L⁻¹, and set 13 (M:PPW ratio of 0.9, pH 6, and inoculum dosage 5.5 g VS L⁻¹) exhibited a notably higher concentration of 5737±89 mg L⁻¹. Overall, the range of TVFAs produced across the 15 sets spans from 3323±78 mg L⁻¹ to 5848±71 mg L⁻¹. The reasons for the varied TVFAs profile could be an engagement of various parameters, such as the type of substrates, inoculum to substrate ratio, pH levels, digestion time, and organic loading rate, etc. For a thorough insight into the biochemical processes that facilitate biohydrogen and biomethane production in anaerobic digestion, analyzing the production trends of key VFAs is crucial. To get more information about the specific pathway of biohydrogen and biomethane, the production of principal VFAs (acetic acids, butyric acid, propionic acid, isovaleric acid, and valeric acid) are provided in Figure 6-9.



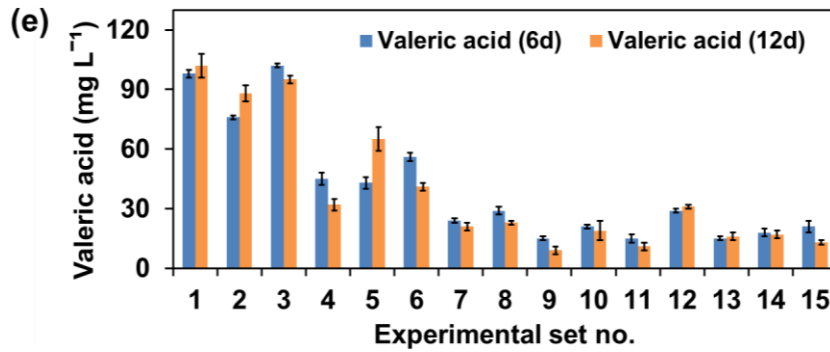


Figure 6- 9. Volatile fatty acid profile measured on days 6 and 12 (a) acetic acid, (b) butyric acid, (c) propionic acid, (d) isovaleric acid, and (e) valeric acid.

Figure 6-9 (a) shows the dynamics of acetic acid concentration across different sets over the digestion time provided. In set 1, the concentration of acetic acid was observed at $602 \pm 12 \text{ mg L}^{-1}$ at day 6, showing a reduction to $427 \pm 12 \text{ mg L}^{-1}$ by the end of day 12. Similarly, in set 2, acetic acid concentration decreased from 710 ± 11 to $406 \pm 12 \text{ mg L}^{-1}$ between days 6 and 12. Set 3 acetic acid level at day 6 was $808 \pm 10 \text{ mg L}^{-1}$ and decreased to $525 \pm 8 \text{ mg L}^{-1}$ at day 12, indicating a slower decrease compared to the first two sets. Contrasting these trends, set 7 to 15 has demonstrated an increased concentration of acetic acids at day 12 compared to day 6. For example, set 4 presented a concentration of $396 \pm 5 \text{ mg L}^{-1}$ on day 6, which increased to $623 \pm 19 \text{ mg L}^{-1}$ on day 12. A more pronounced increase was observed in set 7, where the acetic acid levels began at $304 \pm 11 \text{ mg L}^{-1}$ (day 6) and surged significantly to $823 \pm 12 \text{ mg L}^{-1}$ (day 12), marking the highest increase among the sets observed. The balance between acidogenic bacteria and methanogens can affect acetic acid levels. If methanogens are inhibited or have not yet reached their peak activity, acetic acid can accumulate (Jiang et al., 2022).

Figure 6-9 (b) shows the butyric acid profile generated over the digestion period. At day 6, the concentration of butyric acid ranges from $19 \pm 5 \text{ mg L}^{-1}$ in set 14 to $59 \pm 2 \text{ mg L}^{-1}$ in set 2. By day 12, the concentration spans from $25 \pm 2 \text{ mg L}^{-1}$ in set 2 to $113 \pm 5 \text{ mg L}^{-1}$ in set 6. A notable trend is

observed in the butyric acid generation between the two time points (days 6 and 12). While a few sets show a decrease in butyric acid concentration from day 6 to day 12, such as set 2, which decreases from 59 ± 2 to 25 ± 2 mg L⁻¹, almost all other sets (set 4 to 15) exhibit a significant increase, notably set 6, which rises from 37 ± 2 to 113 ± 5 mg L⁻¹, and set 5, which increases from 23 ± 1 to 81 ± 2 mg L⁻¹. The increase in butyric acid concentration from day 6 to 12 suggests that there might be a slowdown or inhibition in the microbial pathways that convert butyrate into methane (Gao et al., 2023).

Figure 6-9 (c) shows the propionic acid profile across the 15 sets at days 6 and 12 of anaerobic digestion. The day 6 concentrations of propionic acid are quite high, with set 6 displaying the highest concentration at 456 ± 3 and set 8 showing the lowest at 87 ± 2 mg L⁻¹. A notable observation is that for sets such as 1, 2, and 3, propionic acid concentration decreases from day 6 to 12. This trend suggests a transition in the anaerobic digestion process, where propionic acid is being consumed, possibly by acetogenic bacteria converting it to acetic acid, which methanogens can then use to produce methane (Annamalai et al., 2020). However, some sets experienced a notable increase in propionic acid concentrations, highlighting the dynamic nature of the process under study. Specifically, set 7 demonstrated a significant rise in concentration from 95 ± 5 to 167 ± 2 mg L⁻¹ between days 6 and 12. Similarly, set 11 followed this upward trajectory, with initial concentrations of 116 ± 4 mg L⁻¹ on day 6, escalating to 250 ± 3 mg L⁻¹ by day 12, indicating a substantial increase. Set 15 also followed this growth pattern, starting with a concentration of 129 ± 2 mg L⁻¹ on day 6 and experiencing a rise to $238 \text{ mg} \pm 7$ by day 12. This finding aligns with the research of Lee et al. (2015), which observed an elevation in propionic acid levels from 760 mg L⁻¹ on day 5 to 950 mg L⁻¹ by day 10.

Isovaleric acid (Figure 6-9 (d)) and valeric acid (Figure 6-9 (e)) are produced in low concentration during anaerobic digestion compared to acetic, butyric, and propionic acids. According to Strazzera et al. (2021), substrates rich in proteins can facilitate the generation of branched-chain VFAs, especially isovaleric and valeric acids. The isovaleric acid profile across 15 sets exhibits a general trend of decreasing concentration from day 6 to 12, with a few exceptions (sets 11, 12, and 15) where the concentration increases. For example, sets 2 and 5 show a substantial decrease in isovaleric acid concentration. Set 2 goes from 102 ± 6 to 56 ± 2 mg L⁻¹, and set 5 from 100 ± 5 to 55 ± 6 mg L⁻¹. Figure 6-9 (e) shows that by day 12, the valeric acid concentrations in most sets have either decreased or remained relatively constant. Sets 13 and 14 exhibit a relatively stable level of valeric acid, with set 13 slightly increasing from 15 ± 1 to 16 ± 2 mg L⁻¹, and set 14 showing a minor change from 18 ± 2 to 17 ± 2 mg L⁻¹. Sets 4, 6, 7, 9, and 10 show a decrease in valeric acid concentration by day 12. For example, set 4 goes from 45.0 ± 3 mg L⁻¹ on day 6 down to 32 ± 3 mg L⁻¹ on day 12, and set 9 from 15 ± 1 mg L⁻¹ to 9 ± 2 mg L⁻¹. A similar decreasing trend of valeric acid concentration is also reported by Mayer et al. (2010) on day 9 compared to day 5. This fact can be explained by the degradation of the longest VFAs (such as isovaleric valeric and valeric acids) into butyric and acetic acids (Magdalena et al., 2019).

The VFA profiles from the 15 experimental sets suggest that different hydrogen-producing pathways are active during anaerobic digestion. Typically, hydrogen production from protein-rich wastes through anaerobic systems is closely linked with forming and consuming VFAs like acetic, propionic, and butyric acids (Shen et al., 2017; Wainaina et al., 2019). The trend of overall VFAs production in all sets can be arranged as acetic acid > propionic acid > butyric acid > isovaleric acid > valeric acid. Sets 1 to 15 predominantly exhibited acetate-type fermentation in the entire fermentation period (12 days). A similar trend of VFA production was also observed by Sillero et

al. (2022). They observed $1817.62 \pm 32 \text{ mg L}^{-1}$ (acetic acid) $> 1377.34 \pm 29 \text{ mg L}^{-1}$ (propionic acid) $> 1275.02 \pm 12 \text{ mg L}^{-1}$ (butyric acid) during the anaerobic digestion of chicken manure and sewage sludge. The overall decreasing trend in VFA concentrations from day 6 to 12, with some exceptions, indicates that the acidogenic phase is active initially, producing these VFAs, which are then consumed during the later stages of digestion, potentially for hydrogen production. In particular, acetic acid is often associated with acetoclastic methanogenesis, which could also indicate acetoclastic pathways for hydrogen production (Aceves-Lara et al., 2008). Propionic acid is generally harder to degrade and can accumulate as an inhibitor in the anaerobic digestion process; however, the decrease in propionic acid concentrations in some sets suggests that the inhibitory effects are being overcome, possibly by syntrophic interactions between hydrogen-producing bacteria and propionate-degrading bacteria (Mu et al., 2023). Also, Hans & Kumar (2019) point out that propionic acid's tolerance threshold is approximately 900 mg L^{-1} . Observations from all experimental configurations revealed propionic acid levels remained under $397 \pm 2 \text{ mg L}^{-1}$, suggesting they stayed well below the critical limit for inhibition.

In summary, the hydrogen-producing pathways in these sets are likely driven by a combination of acidogenic bacteria that produce hydrogen from the fermentation of organic substrates, producing a variety of VFAs, followed by a syntrophic relationship with methanogenic archaea that further convert these VFAs into hydrogen (primarily) and methane, with the specific pathways being influenced by the abundance and activity of specific microbial populations within each experimental set.

6.7.4 Model validation

The optimal conditions for the digestion process were determined using the desirability function feature in Design-Expert software. The software's optimization tool allows for selecting inputs based on criteria like maximum, target, or minimum, aiming for an optimal response that meets specific requirements. For this study, the variables (Manure:PPW ratio, pH, and inoculum) were adjusted to fall within selected ranges, achieving a composite desirability of 1. The identified optimal settings were a manure:PPW ratio of 0.9, pH level of 6, and an inoculum concentration of 6.2 g VS L⁻¹. Optimization trials were conducted in triplicate under these ideal conditions to verify the precision of these optimal values and the model's validity. The predicted value provided a yield of 351 mL H₂ g⁻¹ VS. Experimental verification resulted in a yield of 355 mL H₂ g⁻¹ VS, indicating a 1.14% enhancement in performance with the optimized combination. The comparison of data from both experiments reveals negligible differences between the predicted outcomes and the actual experimental results. An earlier study has reported an improved predicted output (3.81%, yield 58.62 mL H₂ g⁻¹ TVS) (Sekoai & Kana, 2013) in anaerobic digestion of mixed agro municipal waste for biohydrogen production. Therefore, the experimental data closely aligns with the models optimized through RSM, indicating a strong correlation.

6.8 Biohydrogen from Albumin and Casein

Within the scope of 15 experiments detailed in section 6.6, sets 7, 12, and 13 (Table 6-4) emerged as the top producers of biohydrogen. The experimental combinations of sets 7, 12, and 13 were used, but the substrates were changed to albumin and casein and named A1, A2, and A3 for albumin sets and C1, C2, and C3 for casein sets. Introducing the new pure protein substrates,

further experiments assessed biohydrogen and biomethane output, protein breakdown, and VFA generation with albumin and casein, incorporating 4,000 mg L⁻¹ oleic acid.

6.8.1 Biohydrogen and biomethane yield

This section presents the biohydrogen and biomethane production data from albumin and casein substrates over 12 days (Figure 6-10). Three separate experimental setups with different conditions were applied to each substrate. An effective comparison across the sets is enabled by examining the biohydrogen and biomethane yields, highlighting how specific conditions influence biohydrogen and biomethane generation from these pure protein sources.

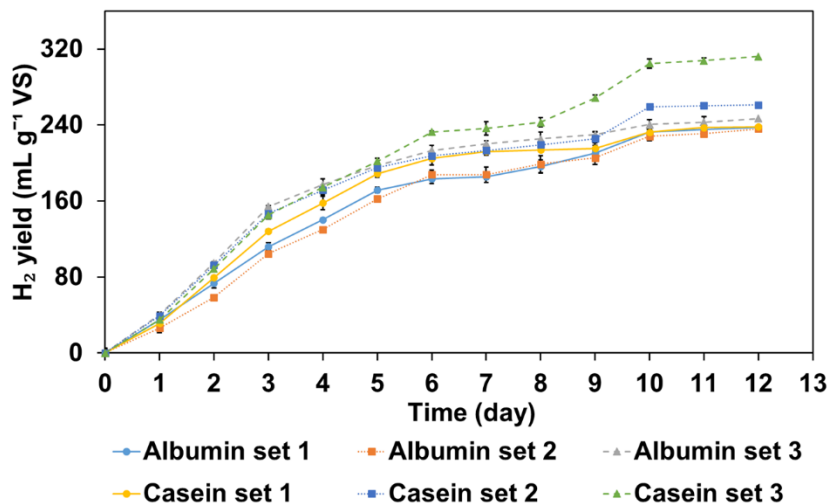


Figure 6- 10. Profile of biohydrogen yield using pineapple waste with albumin or casein as a substrate for 12 days.

The progress of biohydrogen production across three distinct sets over 12 days presents an intriguing pattern of growth (Figure 6-10). In albumin set 1, yield initially recorded at 35±2 mL g⁻¹ VS on day 1 experienced a robust increase, reaching 237±4 mL g⁻¹ VS by day 12. Conversely, albumin set 2 began at a slightly lower baseline yield of 26±4 mL H₂ g⁻¹ VS, and increased

gradually to 236 ± 3 mL H₂ g⁻¹ VS by day 12. The most notable performance was observed in albumin set 3, which started from a higher initial value of 40 ± 1 mL H₂ g⁻¹ VS (day 1), ultimately achieving the most substantial increase among the sets to culminate at 247 ± 6 mL H₂ g⁻¹ VS by day 12. Hence, albumin set 3 provided the most optimal environment for hydrogen production.

From Figure 6-10, casein set 1 starts at a hydrogen yield of 31 ± 4 mL g⁻¹ VS on day 1, gradually increasing over 12 days, ending at 238 ± 2 mL g⁻¹ VS. This shows a consistent upward trend in hydrogen production over time. Casein set 2 shows a slightly higher initial hydrogen yield of 39 ± 3 mL g⁻¹ VS on day 1, which suggests a more rapid onset of hydrogen production. By day 12, the yield has increased to 261 ± 1 mL g⁻¹ VS, indicating a robust production over the period. Casein set 3 begins with a hydrogen yield of 35 ± 5 mL g⁻¹ VS on day 1, and it experiences the most significant increase, finishing at 312 ± 3 mL g⁻¹ VS on day 12. This set demonstrates the highest final yield and the largest overall increase in hydrogen production over 12 days. In comparing these sets, it's evident that casein, when mixed with PPW under varying pH levels and inoculum sizes, has a strong potential for hydrogen production, and set 3 appears to be the most favorable, resulting in the highest hydrogen yield. The visual comparison shows that for set 1, the initial (day 1) production for albumin (35 ± 2 mL H₂ g⁻¹ VS) and casein (31 ± 4 mL H₂ g⁻¹ VS) are almost in a similar range. Similarly, by day 12, albumin and casein generated 236 ± 4 and 238 ± 2 mL H₂ g⁻¹ VS, respectively. Casein set 2 has a notably higher hydrogen yield than albumin set 2 from the start and maintains this lead, ending 25 ± 2 mL g⁻¹ VS higher on day 12. Casein set 3 outperforms the corresponding albumin set at every point. On day 6, casein set 3 has already achieved a higher yield (233 ± 3 mL g⁻¹ VS) compared to albumin set 3 (213 ± 6 mL g⁻¹ VS). This trend continues and is even more pronounced by day 12, where casein set 3 yields 312 ± 3 mL g⁻¹ VS, significantly outstripping albumin set 3's yield of 247 ± 6 mL g⁻¹ VS. The consistently higher performance of

casein set 3 at these intervals indicates that casein is a more efficient substrate for biohydrogen production in the given experimental setup, with its efficiency becoming increasingly apparent as the process progresses.

A direct comparison aims to uncover how well different substrates generate hydrogen and methane, focusing on comparing pure proteins and manure in a consistent setting. Hence, the outcomes of biohydrogen (Table 6-5) and biomethane (Table 6-6) production using PPW with manure and pure proteins (albumin and casein) under identical experimental conditions are presented (Table 6-8) and explained.

Table 6- 8. Evaluating hydrogen production from pineapple peel waste with manure and pure proteins under similar experimental settings.

		Hydrogen yield (mL g ⁻¹ VS)								
		Manure			Albumin			Casein		
		Set 7	Set 12	Set 13	Set 1	Set 2	Set 3	Set 1	Set 2	Set 3
Substrate:PPW ratio	0.9	0.9	0.9	0.9	0.9	0.9	0.9	0.9	0.9	
pH	5	4	6	5	4	6	5	4	6	
Inoculum (g VS L ⁻¹)	7	5.5	5.5	7	5.5	5.5	7	5.5	5.5	
Day	1	46±2	47±4	61±3	35±2	26±4	40±1	31±4	39±3	35±5
	2	100±3	105±5	128±4	73±1	58±5	95±3	79±2	92±2	89±3
	3	151±4	159±1	178±2	112±5	105±1	154±1	128±2	147±2	145±2
	4	200±2	213±5	238±5	140±4	130±1	177±1	158±2	172±2	174±4
	5	255±5	269±9	297±5	171±2	162±1	197±6	189±7	195±5	202±1
	6	300±4	314±2	345±6	183±3	188±2	231±3	205±4	207±2	233±3
	7	310±9	319±3	351±5	186±5	188±5	220±5	212±7	213±5	237±1
	8	317±5	325±5	356±2	196±3	199±8	225±3	214±4	219±5	243±7
	9	325±5	333±4	364±7	211±7	205±9	230±7	215±2	226±4	268±5
	10	335±3	345±5	369±9	232±3	228±7	240±3	232±6	259±7	305±3
	11	343±2	352±11	378±5	235±1	231±5	243±5	237±3	260±2	308±5
	12	348±7	373±7	385±7	236±4	236±3	247±6	238±2	261±1	312±3

Set 7 (manure:PPW ratio of 0.9, pH 5, and inoculum 7 g VS L⁻¹) starts with a higher yield on day 1 (46±2 mL H₂ g⁻¹ VS) compared to albumin set 1 (35±2 mL H₂ g⁻¹ VS) and shows a much greater yield by day 12 (set 7: 348±7 mL H₂ g⁻¹ VS, albumin set 1: 237±4 mL H₂ g⁻¹ VS). Similar to the albumin comparison, set 7 (manure:PPW ratio of 0.9, pH 5, and inoculum 7 g VS L⁻¹) exceeds casein set 1 in hydrogen production from the onset and maintains this lead, ending with a significantly higher yield (set 7: 348±7 mL H₂ g⁻¹ VS, casein set 1: 238±2 mL H₂ g⁻¹ VS). Set 12 (manure:PPW ratio of 0.9, pH 4, and inoculum 5.5 g VS L⁻¹) begins with a hydrogen yield of 47±4 mL H₂ g⁻¹ VS, outperforming albumin set 2's initial 26±4 mL H₂ g⁻¹ VS. This trend continues to day 12, with set 12 reaching 373±7 mL H₂ g⁻¹ VS, significantly higher than albumin set 2's yield of 236±3 mL H₂ g⁻¹ VS. The yield of set 12 on day 1 also surpasses that of casein set 2, which stands at 39±3 mL H₂ g⁻¹ VS. By the end of the digestion period, set 12 achieves a yield of 373±7 mL H₂ g⁻¹ VS, considerably outpacing casein set 2's 261±1 mL H₂ g⁻¹ VS. Lastly, starting with a hydrogen yield of 61±3 mL H₂ g⁻¹ VS on day 1, set 13 (manure:PPW ratio of 0.9, pH 6, and inoculum 5.5 g VS L⁻¹) significantly overtakes albumin set 3, which begins at 40±1 mL H₂ g⁻¹ VS. By day 12, set 13 reaches a yield of 385±7 mL H₂ g⁻¹ VS, which is notably higher than the 247±6 mL H₂ g⁻¹ VS achieved by albumin set 3. In the case of casein sets 3 and 13, set 13's initial hydrogen production is more than twice that of casein set 3, which is at 35±5 mL H₂ g⁻¹ VS on day 1. The final yield for set 13 stands at 385±7 mL H₂ g⁻¹ VS, surpassing casein set 3's yield of 312±3 mL H₂ g⁻¹ VS by a significant 18.96% on day 12.

The biohydrogen data highlight the robust performance of set 13 across the duration of the experiment, showcasing manure's capacity to act as a superior substrate for hydrogen production when compared to albumin and casein, particularly at a pH of 6. Table 6-8 indicates that the biological processes using manure as substrate are more conducive to the ongoing generation of

hydrogen, leveraging the alkaline environment to optimize the degradation of organic materials and release of biohydrogen. The considerable yield gap between corresponding sets of manure and pure proteins underlines the effectiveness of manure as a substrate, leading to superior hydrogen production, especially under slightly alkaline conditions. Manure is a rich source of diverse microbial consortia, including bacteria capable of breaking down complex organic compounds. The presence of various microbial species can lead to synergistic interactions that enhance the fermentation process and increase hydrogen yield (Greff et al., 2022). Manure contains a balanced mix of nutrients, including nitrogen, phosphorus, and various trace minerals essential for microbial growth and metabolism (Zhen et al., 2014). The presence of these nutrients in the right proportions can provide a more conducive environment for biohydrogen production than pure proteins' relatively narrow nutrient profile. Moreover, the breakdown of protein albumin and casein may lead to the creation of inhibitory substances like ammonia (Ying Li et al., 2017) and VFA (Siegert & Banks, 2005), potentially hindering the functionality of the microbial community.

In the experiment spanning 12 days, none of the sets using pure proteins, specifically albumin and casein, generated methane. This absence highlights a marked suppression of methane production in the presence of pure proteins, indicating that oleic acid (OA) exerted a similar stronger inhibitory effect on methanogenic activity in these sets than those of manure (sets 7, 12, and 13) (Figure 6-5 and Table 6-6). This observation aligns with Tang et al. (2005), who noted similar outcomes in a mesophilic anaerobic reactor treating synthetic wastewater with albumin as the primary nutrient, producing VFA and ammonia but no methane.

6.8.2 Protein quantity measurement

Measuring protein reduction is essential when anaerobic digestion involves pure protein substrates. This measurement indicates how effectively the digestion process converts protein molecules into smaller peptides and amino acids and subsequently into volatile fatty acids (VFAs). VFAs are crucial intermediates for biogas generation, directly indicating the process's efficiency in protein breakdown.

Figure 6-11 (a and b) displays the quantity of albumin (A1, A2, A3 in mg L^{-1}) and casein (C1, C2, C3 in mg L^{-1}) for three distinct experimental setups (1, 2, and 3) under anaerobic conditions at various intervals: at the start (day 0), on day 6, and day 12. The numbers above each bar on the graph represent the reduction percentage of albumin, calculated from its initial concentration on day 0 for each set, observed on days 6 and 12.

Figure 6-11 (a) shows that on day 0, the albumin quantities in sets A1, A2, and A3 were measured at 1507.69 ± 7 , 1425.00 ± 9 , and $1504.62 \pm 11 \text{ mg L}^{-1}$, respectively. By day 6, the albumin quantity (mg L^{-1}) decreased to 1150.38 ± 9 for A1 ($24 \pm 2\%$ reduction), 962.31 ± 3 for A2 ($32 \pm 2\%$ reduction), and 1125.00 ± 10 for A3 ($25 \pm 1\%$ reduction). Further reduction was observed by day 12, with protein levels (mg L^{-1}) dropping to 1062.31 ± 3 in A1 ($29 \pm 3\%$ reduction), 894.62 ± 2 in A2 ($37 \pm 2\%$ reduction), and 927.00 ± 1 in A3 ($38 \pm 1\%$ reduction). Set A2 had the most significant decrease in protein quantity by day 6, with a $32 \pm 2\%$ reduction, which was higher than the $24 \pm 2\%$ and $25 \pm 1\%$ reductions observed in sets A1 and A3, respectively.

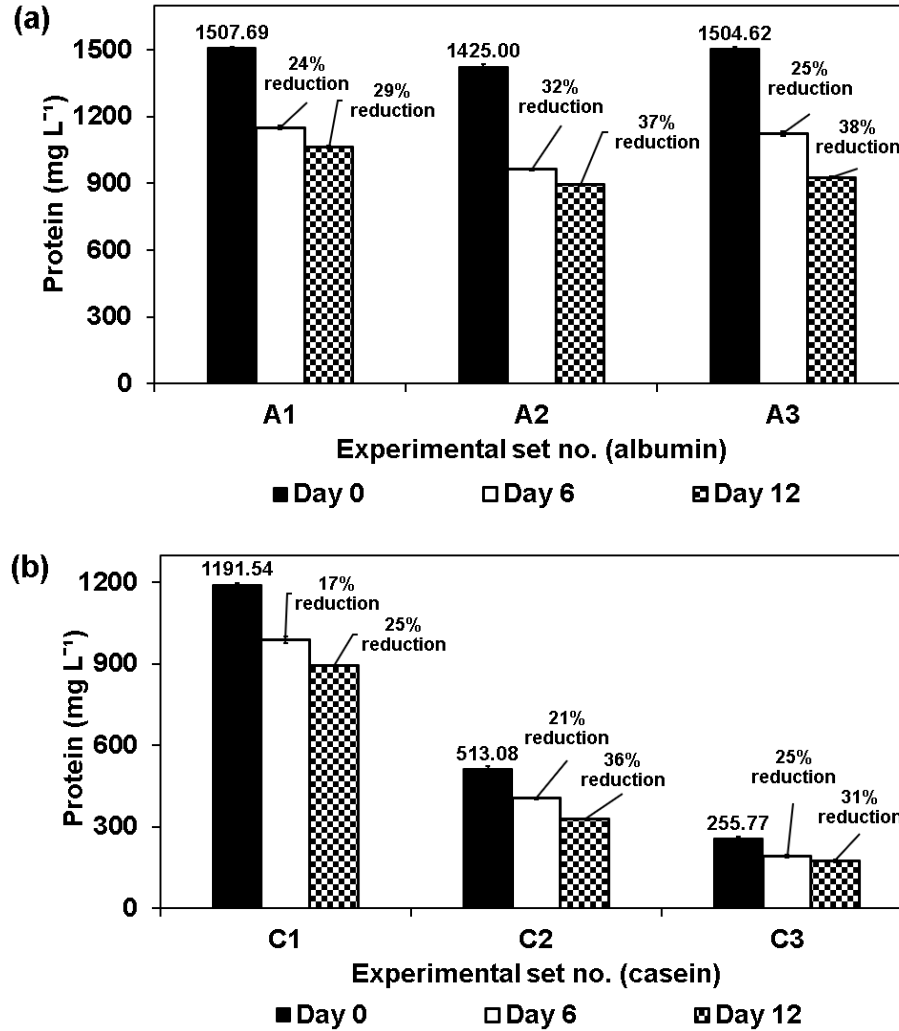


Figure 6- 11. Protein quantity of (a) albumin set A1 (albumin:PPW ratio of 0.9, pH 5, inoculum 7 g VS L⁻¹), set A2 (albumin:PPW ratio of 0.9, pH 4, inoculum 5.5 g VS L⁻¹), set A3 (albumin:PPW ratio of 0.9, pH 6, inoculum 5.5 g VS L⁻¹) on days 6 and 12 (b) casein set C1 (casein:PPW ratio of 0.9, pH 5, inoculum 7 g VS L⁻¹), set C2 (casein:PPW ratio of 0.9, pH 4, inoculum 5.5 g VS L⁻¹), set C3 (casein:PPW ratio of 0.9, pH 6, inoculum 5.5 g VS L⁻¹) on days 6 and 12.

At day 12, set A3 showed a slightly greater protein reduction at 38±1%, compared to A2's 37±2% reduction, while A1 had the lowest at 29±3%. Set A2 showed the highest protein reduction on day 6, and set A3 achieved the highest reduction on day 12. This indicates that the conditions in set A3, with a pH of 6 and an inoculum dosage of 5.5 mg L⁻¹, were most conducive for the

bromelain activity in PPW to facilitate the anaerobic digestion of albumin over the experiment duration.

Figure 6-11 (b) presents the protein reduction in three casein experimental sets (C1, C2, C3) over 12 days. Initially, at day 0, set C1 had a casein level of $1191.54 \pm 7 \text{ mg L}^{-1}$, which reduced to $989.00 \pm 12 \text{ mg L}^{-1}$ by day 6, a $17 \pm 2\%$ decrease, and further to $893.66 \pm 2 \text{ mg L}^{-1}$ by day 12, marking a $25 \pm 2\%$ overall decrease. Set C2 began with a lower day 0 casein concentration of $513.08 \pm 11 \text{ mg L}^{-1}$, which declined to $405.33 \pm 3 \text{ mg L}^{-1}$ by day 6 ($21 \pm 1\%$ reduction), and then to $328.37 \pm 2 \text{ mg L}^{-1}$ by day 12 ($36 \pm 1\%$ reduction). The initial casein level in set C3 was $255.77 \pm 7 \text{ mg L}^{-1}$, falling to $191.82 \pm 6 \text{ mg L}^{-1}$ after 6 days ($25 \pm 3\%$ reduction) and reaching $176.48 \pm 5 \text{ mg L}^{-1}$ by day 12 ($31 \pm 2\%$ reduction). Among three casein sets, C2 shows the greatest percentage reduction by day 12, indicating a higher rate of casein breakdown. Although C3 started with the lowest casein concentration, it showed a consistent reduction, surpassing C1 in percentage reduction by day 6 and maintaining a substantial reduction by day 12.

The albumin sets (A1, A2, A3) began with concentrations of 1507.69 ± 7 , 1425.00 ± 9 , and $1504.62 \pm 11 \text{ mg L}^{-1}$, respectively. By day 6, the albumin reductions observed were $24 \pm 2\%$, $32 \pm 2\%$, and $25 \pm 1\%$, and by day 12, they increased to $29 \pm 3\%$, $37 \pm 2\%$, and $38 \pm 1\%$ for A1, A2 and A3. The data suggests a gradual degradation process, with set A2 showing a substantial increase in degradation efficiency from day 6 to 12.

The initial concentrations of casein were lower compared to albumin, with C1, C2, and C3 starting at 1191.54 ± 7 , 513.08 ± 11 , and $255.77 \pm 7 \text{ mg L}^{-1}$. By day 6, the reductions were $17 \pm 2\%$, $21 \pm 1\%$, and $25 \pm 3\%$, and by day 12, they were $25 \pm 2\%$, $36 \pm 1\%$, and $31 \pm 2\%$. Although the reduction percentages for casein sets were lower than those for albumin on day 6, they showed a considerable increase by day 12, particularly for set C2. On average, albumin sets displayed a higher protein

reduction percentage than casein sets on days 6 and 12. The explanation behind this observation could be due to the inherent differences in the protein structures of albumin and casein. Albumin is a globular protein that may be more readily hydrolyzed by bromelain due to its conformation and the accessibility of cleavage sites (Maresca & Ferrari, 2017). Casein, which exists in micelle form in natural contexts (Holt et al., 2013), may present a more complex substrate for bromelain, leading to less efficient initial degradation. However, the increased percentage reduction in casein sets from days 6 to 12 suggests a possible time-dependent increase in enzyme-substrate interaction, potentially as the micellar structure is progressively broken down, making more cleavage sites accessible to the enzyme bromelain. Furthermore, bromelain is known to have an optimal pH range between 5.5 and 8, which may explain why certain sets (e.g., A2 and A3) showed higher degradation efficiencies (Chakraborty et al., 2021), as their experimental conditions might have been more closely aligned with this optimal pH range compared to some of the casein sets. Despite its slightly lower protein reduction (%) of set C3 ($31\pm 2\%$) compared to A3 ($38\pm 1\%$), casein produced a higher biohydrogen yield than albumin (Table 6-8). Casein is a complex protein composed of amino acids linked by peptide bonds. The enzymatic action of proteases, such as bromelain, hydrolyzes these peptide bonds during degradation, releasing amino acids and smaller peptides (Kovács et al., 2013). Specific microorganisms utilize these amino acids and peptides produced from casein hydrolysis as substrates for their metabolism. Peptide-fermentative bacteria can ferment these peptides, using them as both a carbon and an energy source (Gagliano et al., 2015). This process can lead to hydrogen production as a metabolic byproduct, contributing to a higher biohydrogen yield from casein sets despite the lower percentage of protein reduction compared to albumin sets.

6.8.3 Fourier Transform Infrared (FTIR)

The study utilized Fourier Transform Infrared (FTIR) spectroscopy to analyze the 4000 and 400 cm^{-1} spectral range. This was to examine samples from days 0 and 12. By comparing days 0 and 12 FTIR spectra, distinct shifts in functional groups were observed, indicating chemical changes over time. These alterations are documented in Figure 6-12 (a) and (b), focusing on albumin and casein samples from set A3 (albumin:PPW ratio of 0.9, pH 6, inoculum 5.5 g VS L^{-1}) and set C2 (casein:PPW ratio of 0.9, pH 4, inoculum 5.5 g VS L^{-1}), respectively.

The analysis of the peaks on day 0 (Figure 6-12 (a)) provides significant insights into the molecular composition of the albumin sample. The amide A band at 3274 cm^{-1} highlights strong N-H stretching, indicating hydrogen-bonded amine groups commonly found in proteins (Xu & Gowen, 2019). The peaks at 2923 cm^{-1} and 2853 cm^{-1} , both attributed to aliphatic C-H stretch, indicate the asymmetric and symmetric stretching vibrations of methylene groups, respectively (Tavanti et al., 2023). The amide I band observed at 1708 cm^{-1} is characterized by C=O stretching vibrations within the carbonyl group of amide linkages, further confirming proteins or peptides.

At 1626 cm^{-1} , the amide II band reflects N-H bending and C-N stretching, typical of protein amide structures, while the presence of another amide II band at 1536 cm^{-1} suggests additional amide structures or functional groups contributing to this peak's complexity (Belfer et al., 2000). The peaks at 1453 cm^{-1} and 1242 cm^{-1} (amide III) are associated with C-N stretching and N-H bending, with the latter also possibly indicating phospholipid vibrations (Hwang & Lyubovitsky, 2013). Lastly, the C-O Stretch at 1031 cm^{-1} likely indicates C-O stretching vibrations, which could be related to carbohydrates or ester groups in lipids (Lim & Wu, 2016), offering a comprehensive view of the sample's biochemical composition.

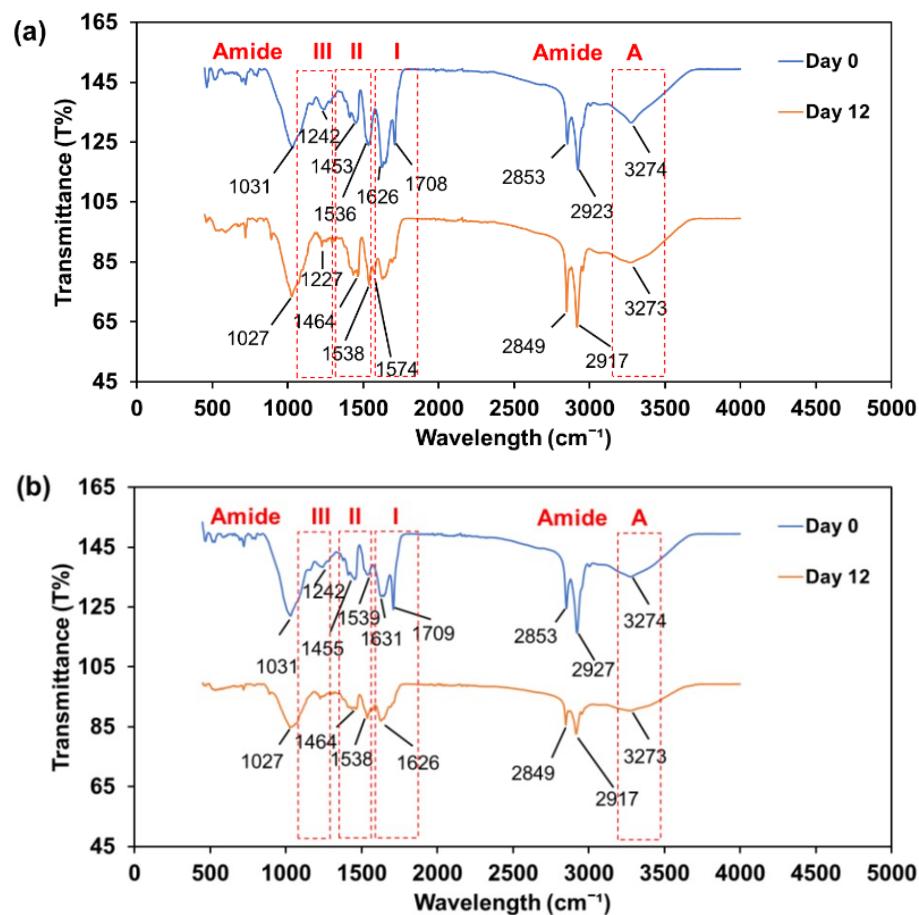


Figure 6- 12. Comparative FTIR Spectra for (a) albumin and (b) casein on days 0 and 12.

By day 12 (Figure 6-12 (a)), the FTIR spectral analysis revealed shifts and changes in peak positions compared to day 0, underscoring the dynamic nature of substrate transformation. The amide A band showed a negligible shift from its initial position (3274 cm^{-1}) to 3273 cm^{-1} , suggesting the N-H group's hydrogen bonding remained largely unaltered. Minor shifts in the aliphatic C-H Stretch bands, from 2923 to 2917 cm^{-1} and 2853 to 2849 cm^{-1} , prove a slight adjustment within the lipid matrix or its interactions. Notably, the absence of the amide I band peak, which was at 1708 cm^{-1} on day 0, disappeared in day 12 samples, suggesting considerable alterations or breakdown of amide carbonyl groups, possibly due to enzymatic breakdown (De Meutter & Goormaghtigh, 2021). The splitting of the amide II band into 1538 and 1574 cm^{-1} (1536

cm^{-1} at day 0) and the peak at 1453 cm^{-1} (day 0) band into 1435 and 1464 cm^{-1} could reflect changes in protein structures or their interactions (Cobb et al., 2020). A shift in the amide III peak to 1227 cm^{-1} from 1242 cm^{-1} and the C-O Stretch to 1027 cm^{-1} from 1031 cm^{-1} further indicates modifications in protein configurations or shifts in carbohydrate or ester components.

The FTIR analysis of the day 0 sample of casein-PPW substrates (Figure 6-12 (b)) highlighted several key peaks indicative of the sample's biochemical composition. At 3275 cm^{-1} , the amide A peak, characterized by N-H stretching vibrations, points to the presence of casein (Xu & Gowen, 2019). This peak's broadness suggests significant hydrogen bonding within the protein structures. The peak at 2927 cm^{-1} arises from the asymmetric stretching vibrations of CH_2 groups, a characteristic of fatty acids like OA found in lipids. Similarly, the 2853 cm^{-1} peak results from symmetric C-H stretching vibrations of CH_2 groups (Tavanti et al., 2023). The amide I band, observed at 1709 cm^{-1} , is identified by C=O stretching vibrations in amide groups, which is crucial for understanding protein secondary structures. Another peak at 1631 cm^{-1} , possibly part of the amide I band. The amide II band, peak at 1539 cm^{-1} , indicates N-H bending and C-N stretching vibration (Belfer et al., 2000). A peak at 1455 cm^{-1} , likely due to CH_2 and CH_3 bending vibrations, is found in lipids and proteins. The 1242 cm^{-1} peak may represent P=O stretching in phospholipids or C-O stretching in other organic molecules, including carbohydrates (Hwang & Lyubovitsky, 2013). Lastly, the 1031 cm^{-1} region, often linked with C-O stretching vibrations, suggests the presence of complex carbohydrates or polysaccharides (Lim & Wu, 2016).

By day 12 (Figure 6-12 (b)), the FTIR spectral analysis of the casein-PPW sample revealed several shifts and changes when compared to day 0. The amide A band at 3273 cm^{-1} shifted from 3275 cm^{-1} (day 1) and showed a subtle decrease, indicating slight modifications in the hydrogen bonding of protein N-H groups. The peak at 2917 cm^{-1} slightly moved from its day 1 position

(2927 cm^{-1}). The amide I peak at 1709 cm^{-1} at day 0 disappeared on day 12 sample, pointing to a notable protein structure transformation or loss, potentially from protease enzymatic breakdown of casein (De Meutter & Goormaghtigh, 2021). A slight alteration in the position of the peak at 1626 cm^{-1} on day 12 from 1631 cm^{-1} (day 1) could signify adjustments in the protein's secondary structure, while the sharper and slightly shifted peak at 1538 cm^{-1} (amide II) from 1539 cm^{-1} may reveal a more distinct protein configuration or interactions with other elements in the mix (Buhrke et al., 2022; Cobb et al., 2020). The change of peak to 1464 cm^{-1} (day 12) from 1455 cm^{-1} (day 1), with a less sharp peak, suggests modifications in CH group bending vibrations. Overall, the FTIR spectral changes from day 0 to day 12 provide a molecular fingerprint of the biochemical transformations occurring in the albumin-PPW and casein-PPW substrates, reflecting the dynamic nature of the fermentation process.

6.8.4 Scanning Electron Microscopy (SEM)

This section provides an in-depth examination through Scanning Electron Microscopy (SEM) of the microstructural transformations within albumin set A3 (albumin:PPW ratio of 0.9, pH 6, and 5.5 g VS L^{-1} inoculum) and casein set C2 (casein:PPW ratio of 0.9, pH 4, and 5.5 g VS L^{-1} inoculum).

Initially, the albumin-PPW complex appears as well-defined, spherical structures (Figure 6-13 (a,b)). These spheres are characteristic of albumin's natural, globular protein structure, which tends to form in aqueous solutions (Niknejad & Mahmoudzadeh, 2015). The surfaces appear smooth, and the structures are discrete, which indicates that the microbial activity or enzymatic process has not significantly altered the albumin.

On day 6 (Figure 6-13 (c,d)), there is a discernible change in the albumin-PPW structures. They no longer appear as uniform and spherical as on day 0. Some spheres seem to have merged, and the surfaces have become rougher, suggesting the onset of enzymatic degradation. By day 12 (Figure 6-13 (e)), the albumin's spherical morphology has significantly diminished, giving way to irregular, amorphous shapes (Molinuevo-Salces et al., 2012). This indicates extensive proteolysis, where the albumin protein structures are broken down into peptides and amino acids. Additionally, flakey structures observed in the micrographs (Figure 6-13 (f)) could be remnants of undigested pineapple peel waste. These flakey structures might be due to the fibrous nature of the peel, which resists complete degradation (Polanía et al., 2022). The overall appearance (Figure 6-13 (e, f)) is a more homogeneous mixture but with a less defined structure, indicative of a significant transformation of both the albumin protein and PPW complex.

The SEM micrographs (Figure 6-14) present the morphological characteristics of a casein-PPW substrate at different stages of biodegradation, taken on days 0, 6, and 12. The initial SEM micrographs (Figure 6-14 (a, b)) show casein in a configuration that is reflective of its colloidal micellar formation, commonly seen due to its properties in milk. The micelles are globular and tend to cluster, indicating casein's undisturbed state (Sadiq et al., 2021).

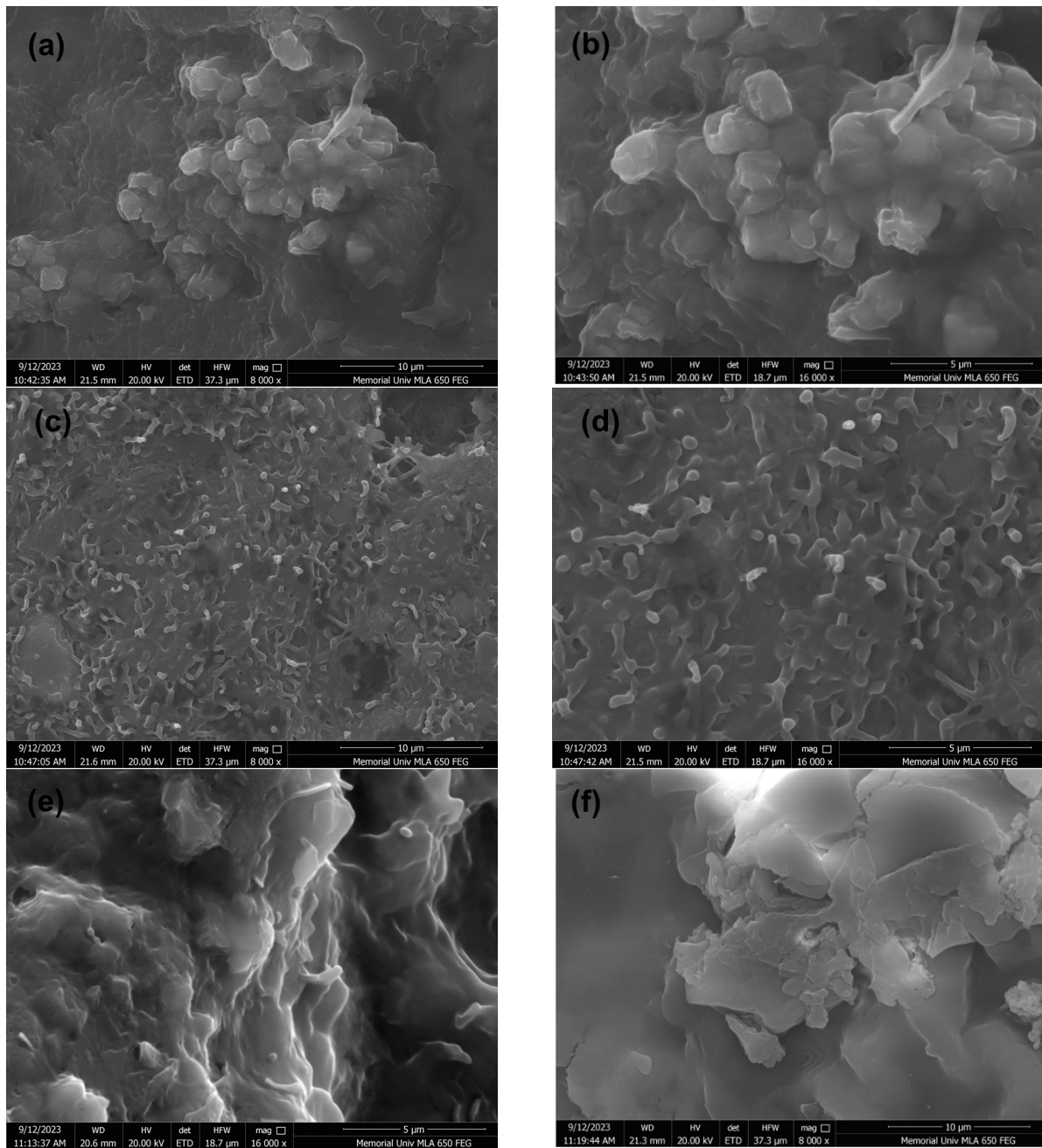


Figure 6- 13. Scanning Electron Microscopy (SEM) micrographs of albumin-PPW substrates on day 0 (a, b), on day 6 (c, d), and on day 12 (e, f) of anaerobic digestion.

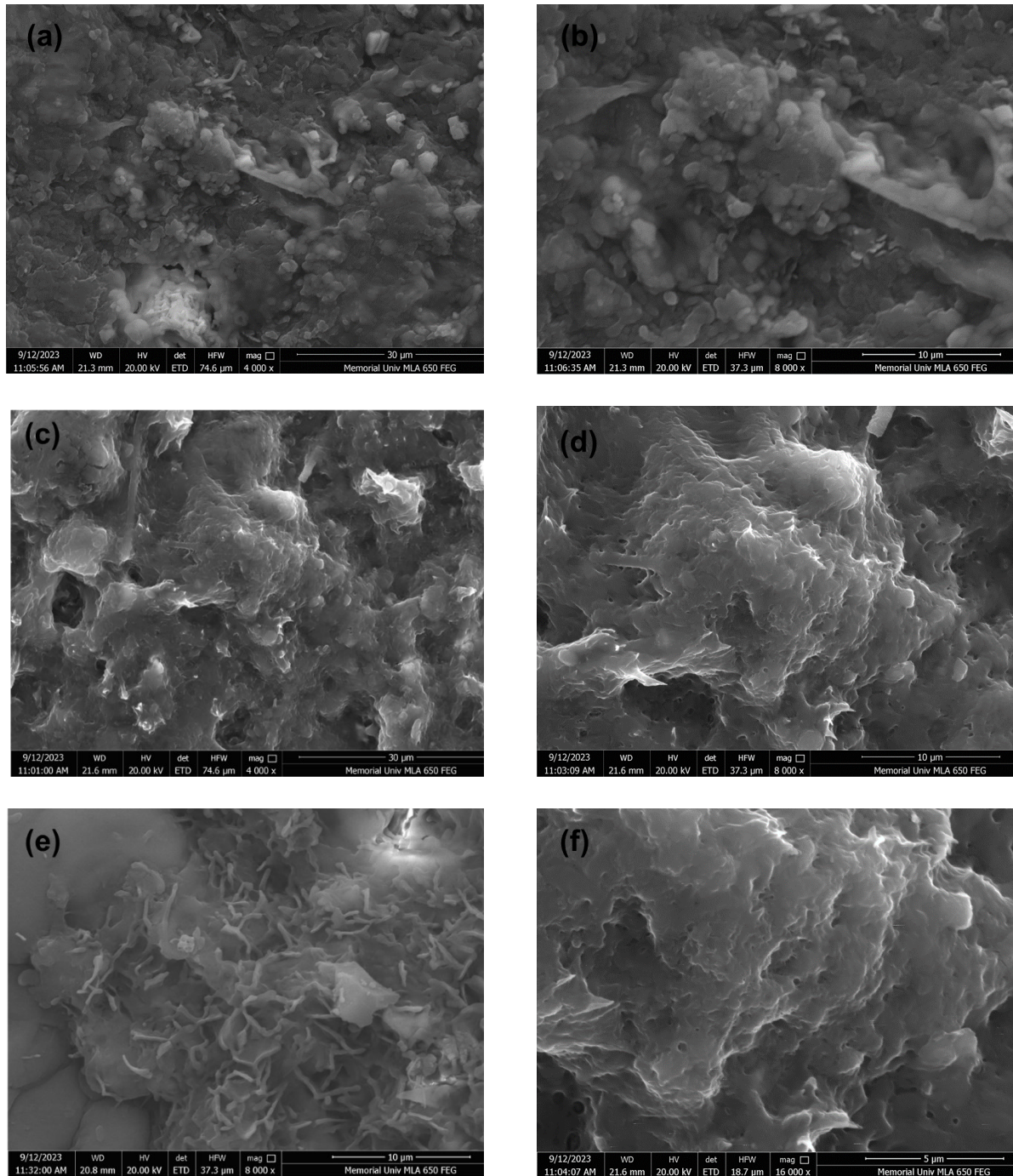


Figure 6- 14. Scanning Electron Microscopy (SEM) micrographs of casein-PPW substrates on day 0 (a, b), on day 6 (c, d), and on day 12 (e, f) of anaerobic digestion.

Accompanying the casein, the pineapple peel waste is identifiable by its more textured, fibrous appearance, providing a distinct structural contrast to the relatively smooth casein micelles (Polanía et al., 2022). In the micrographs from day 6 (Figure 6-14 (c, d)), the casein's globular structure has begun to alter, showing signs of deconstruction from the globular micelles to more irregular aggregates. This may be due to enzymatic action from the inoculum, which initiates proteolysis, breaking down the casein proteins and causing them to lose their distinct micellar structure.

By day 12 (Figure 6-14 (e, f)), the SEM micrographs reveal a marked departure from the initial well-ordered micellar arrangement of the casein. The once globular forms have been replaced by an assortment of irregular structures, signifying a profound degradation of the casein protein. No longer discernible as individual micelles, the casein-PPW complex now appears as an uneven, rough landscape with crevices and protrusions. This indicates the extensive proteolytic activity that has unfolded, likely facilitated by the microbial enzymes or protease enzyme present in the substrate complex (Poolman et al., 1996). The micrographs also show areas where the texture has a slightly flakey appearance. These residual fragments could be due to the resilient nature of the pineapple peel's fibrous matrix originating from cellulose (Aili Hamzah et al., 2021), which may degrade more slowly than the proteinaceous casein. The overall morphological changes in the substrate from day 0 to 12 illustrate the substantial transformation resulting from the biodegradation process.

6.8.5 Volatile fatty acids

This part of the study focuses on tracking volatile fatty acid (VFA) production during anaerobic digestion (AD) using combinations of pure proteins (albumin or casein) with PPW in oleic acid's

presence following three parameters combination such as albumin or casein to PPW ratios, pH levels, and inoculum doses mentioned in section 6.5. The experiment monitored the levels of various VFAs, including propionic, butyric, acetic, isovaleric, and valeric acids, over days 2, 4, 6, 8, 10, and 12. Figure 6-15 presents the trends in total VFA (TVFA) production across different setups: albumin sets 1 (albumin:PPW ratio of 0.9, pH 5, inoculum 7 g VS L⁻¹), albumin set 2 (albumin:PPW ratio of 0.9, pH 4, inoculum 5.5 g VS L⁻¹), albumin set 3 (albumin:PPW ratio of 0.9, pH 6, inoculum 5.5 g VS L⁻¹), and casein set 1 (casein:PPW ratio of 0.9, pH 5, inoculum 7 g VS L⁻¹), casein set 2 (casein:PPW ratio of 0.9, pH 4, inoculum 5.5 g VS L⁻¹) and casein set 3 (casein:PPW ratio of 0.9, pH 6, inoculum 5.5 g VS L⁻¹).

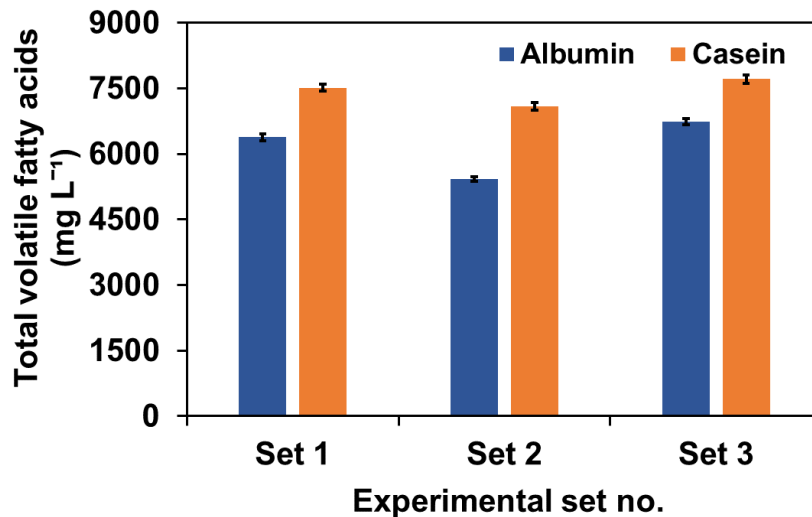


Figure 6- 15. Total volatile fatty acids (TVFAs) production by albumin-PPW and casein-PPW substrates.

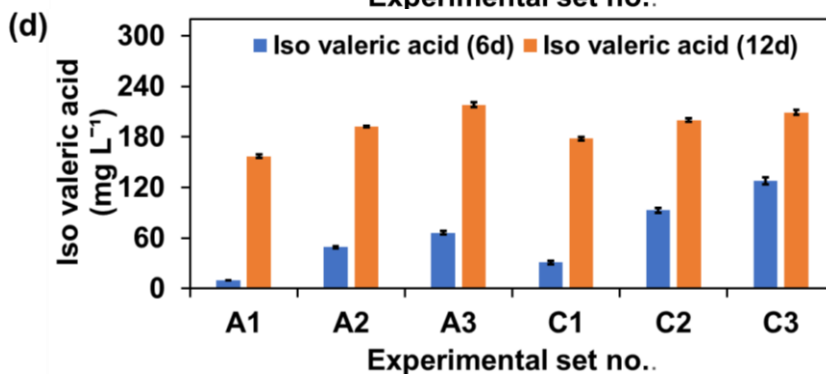
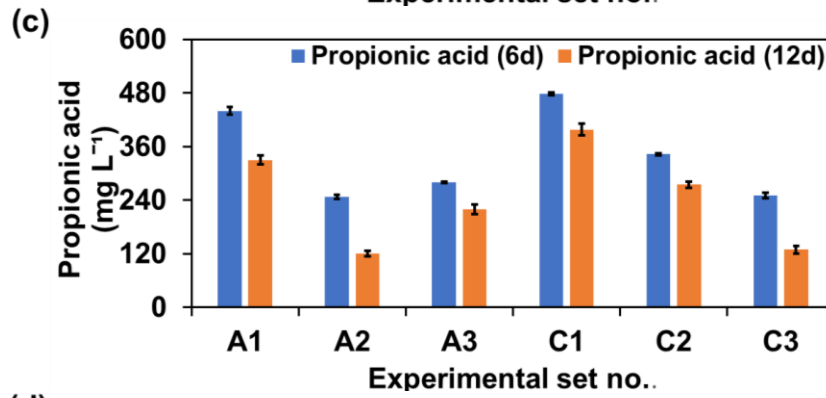
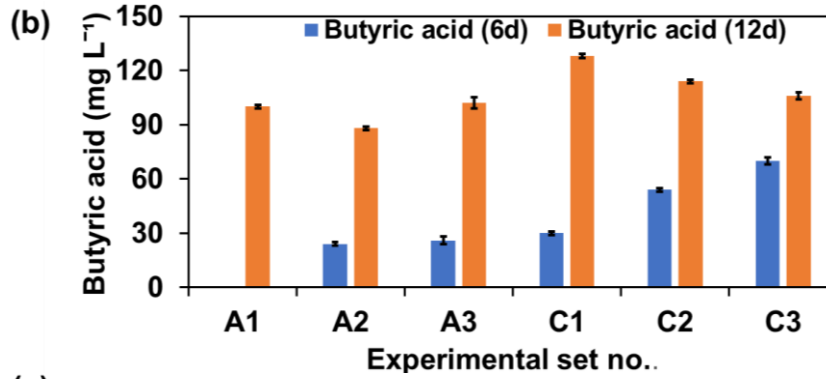
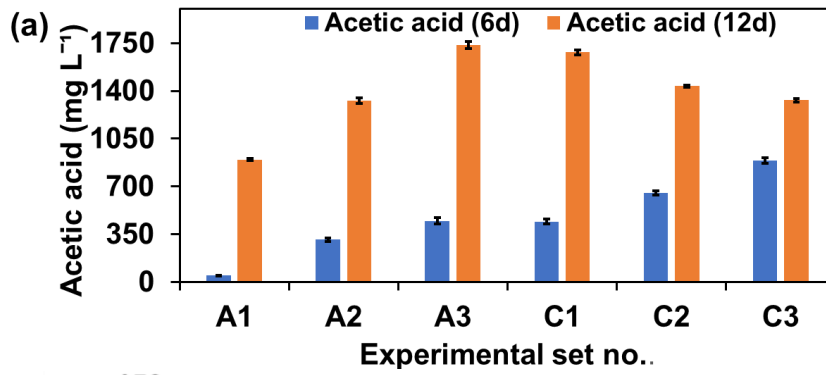
For albumin, the TVFA production showed variability across the three sets. Set 1 exhibited a TVFA concentration of 6383±81 mg L⁻¹. In set 2, there was a decrease in TVFA production, evidenced by a lower concentration of 5417±53 mg L⁻¹. However, in set 3, the TVFA production increased again, reaching a higher concentration of 6732±71 mg L⁻¹. In contrast, the casein sets

demonstrated a consistent trend of higher TVFA production than the albumin sets. Set 1 for casein showed a high TVFA concentration of $7513 \pm 77 \text{ mg L}^{-1}$. A slight decrease followed this in set 2, where the concentration was $7095 \pm 86 \text{ mg L}^{-1}$, but it was still higher than any of the albumin sets. Finally, set 3 for casein marked the highest TVFA production in the experiment with $7713 \pm 98 \text{ mg L}^{-1}$, indicating a clear increase from set 2 and substantially surpassing the TVFA production from albumin. These fluctuations in TVFA concentrations suggest that the conditions specific to each set influenced the microbial activity and the subsequent breakdown of albumin into volatile fatty acids. The differences across various sets using the same substrate may stem from factors like pH, inhibitors, digestion duration, temperature, and substrate concentrations (Lu et al., 2020).

Casein sets demonstrated consistently higher TVFA production compared to albumin sets (5417 ± 71 to $6732 \pm 71 \text{ mg L}^{-1}$), with values between 7095 ± 86 and $7713 \pm 98 \text{ mg L}^{-1}$. The combination of microbial specialization, casein's structural properties, and the microbes metabolic pathways contribute to the efficient breakdown of casein in AD (Bhat et al., 2016; Meegoda et al., 2018). Additionally, the microbial community's potential preference for casein is possibly due to its nutrient profile (Deng et al., 2022).

Figure 6-16 presents the production trends of VFAs, including acetic, butyric, propionic acid, isovaleric acid, and valeric acid, at two critical times (days 6 and 12) across albumin sets A1, A2, A3, and casein sets C1, C2, C3, within the AD process, offering insight into their varying levels.

Within the albumin sets observed in Figure 6-16 (a) on days 6 and 12, distinct trends in acetic acid production were noted. For set A1, the concentration began modestly at $47 \pm 2 \text{ mg L}^{-1}$ on day 6, experiencing a notable rise to $896 \pm 9 \text{ mg L}^{-1}$ by day 12. In set A2, the initial concentration was significantly higher at $309 \pm 11 \text{ mg L}^{-1}$ on day 6, with an impressive growth reaching $1328 \pm 22 \text{ mg L}^{-1}$ by day 12.



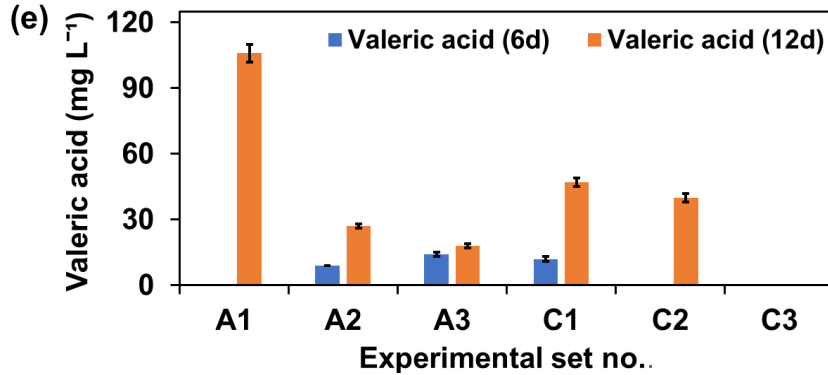


Figure 6- 16. Individual volatile fatty acids (VFAs) observed on days 6 and 12 (a) acetic acid (b) butyric acid (c) propionic acid (d) isovaleric acid and (e) valeric acid.

Set A3 showcased an initial concentration of $448 \pm 21 \text{ mg L}^{-1}$ on day 6, escalating to the highest recorded level among the albumin sets, $1734 \pm 25 \text{ mg L}^{-1}$, by day 12, highlighting the variable acetic acid production dynamics across the different albumin sets. On the other hand, comparing the acetic acid data, casein generally showed higher acetic acid concentrations than albumin on day 6. By day 12, while some albumin sets showed significant increases, casein sets maintained higher or comparable acetic acid levels. Set C1 mirrored the acetic acid production of set A3 on day 6, starting at $443 \pm 19 \text{ mg L}^{-1}$, and witnessed a significant increase to $1682 \pm 19 \text{ mg L}^{-1}$ by day 12. Set C2 began with an acetic acid level of $654 \pm 15 \text{ mg L}^{-1}$ on day 6, which then escalated to $1436 \pm 8 \text{ mg L}^{-1}$ by the end of day 12.

Meanwhile, set C3 displayed the highest initial acetic acid concentration among the casein sets at $891 \pm 21 \text{ mg L}^{-1}$ on day 6, culminating in a rise to $1333 \pm 13 \text{ mg L}^{-1}$ on day 12. The increase in acetic acid concentration from day 6 to 12 can be attributed to the microbial consortia's continued fermentation of albumin and casein. Over time, these microorganisms break down the proteins, accumulating acetic acid as a fermentation byproduct. Kovács et al. (2013) also documented comparable results, noting that by week 13, acetate levels had escalated to the critical point of 4 g L^{-1} in pig blood and 1.9 g L^{-1} in casein anaerobic digestion.

The butyric acid profile is shown in Figure 6-16 (b). Similar to the acetic acid profile, butyric acid also shows an overall increase in production on day 12 compared to day 6. Set A1 exhibited an interesting pattern, starting from a point where butyric acid was not detectable on day 6 (0 mg L^{-1}), yet showed a significant increase to $100 \pm 1 \text{ mg L}^{-1}$ by day 12. Conversely, set A2 began with a butyric acid level of $24 \pm 1 \text{ mg L}^{-1}$ on day 6, which then experienced a modest rise to $88 \pm 1 \text{ mg L}^{-1}$ by day 12. Set A3, starting with a butyric acid concentration close to that of set A2 at $26 \pm 2 \text{ mg L}^{-1}$ on day 6, experienced a slight increase, reaching $102 \pm 3 \text{ mg L}^{-1}$ on day 12, indicating a consistent pattern of growth in butyric acid concentration towards the end of the observed period. The increase in butyric acid concentration over time may be partially due to the initial accumulation of butyric acid as an intermediate product, which is subsequently utilized in the β -oxidation pathway to convert to acetate and hydrogen as the anaerobic digestion process matures (Worm et al., 2014). Similarly, butyric acid production increased at day 12 ($5100 \text{ mg COD L}^{-1}$) compared to day 8 ($3300 \text{ mg COD L}^{-1}$) during the anaerobic digestion of tuna waste at 5% TS (Bermúdez-Penabad et al., 2017).

Figure 6-16 (c) presents the propionic acid profile on days 6 and 12. The propionic acid concentrations in the sets showed a downward trend throughout the observation period. In set A1, the level began at $440 \pm 9 \text{ mg L}^{-1}$ on day 6 but decreased to $330 \pm 10 \text{ mg L}^{-1}$ by day 12, marking a notable decrease. Set A2 experienced a more pronounced drop, starting from $247 \pm 5 \text{ mg L}^{-1}$ on day 6 and falling sharply to $120 \pm 6 \text{ mg L}^{-1}$ by the end of the observation period. Similarly, set A3's propionic acid concentration reduced from $280 \pm 2 \text{ mg L}^{-1}$ on day 6 to $220 \pm 11 \text{ mg L}^{-1}$ on day 12. Across the casein sets, concentrations consistently decreased over the observed period. Set C1's levels dropped from 478 ± 3 to $398 \pm 13 \text{ mg L}^{-1}$, set C2 from 343 ± 2 to $275 \pm 7 \text{ mg L}^{-1}$, and set C3 underwent a notable decline from 251 ± 6 to $129 \pm 9 \text{ mg L}^{-1}$. Propionic acid, often identified as an

inhibitory compound in the anaerobic digestion process, has the potential to decrease the yield of biogas markedly (Han et al., 2020). This acid frequently emerges as a secondary product during the breakdown of organic waste and can build up to levels that hinder the digestion process (Capson-Tojo et al., 2017). Propionic acid, initially a dominant element of VFA on day 6, experienced a significant decline after that on day 12. This reduction might be attributed to the low introduction rates of organic material (Lin et al., 2011) coupled with the vigorous activity of the seed sludge (Yangyang Li et al., 2017). Moreover, on day 6, the concentration of acetic acid was at its lowest, whereas propionic acid levels were at their peak. Subsequently, acetic acid levels rose, in contrast to propionic acid concentrations, which followed a downward trajectory. A similar trend was reported by (Xu et al., 2023). Furthermore, a reduction in propionic acid levels was observed, alongside an increase in butyric acid concentrations during the anaerobic digestion of waste sewage sludge, as reported by (Roy et al., 2022). This pattern was similarly identified in the current experiment, as illustrated in Figure 6-16 (b) and (c).

Fatty acids with higher molecular weights, like isovaleric (Figure 6-16 (d)) and valeric (Figure 6-16 (e)), are predominantly linked to the breakdown of proteins during fermentation (Bermúdez-Penabad et al., 2017). All sets showed an increase in isovaleric acid from day 6 to 12. In albumin sets, concentrations of isovaleric acid started at lower levels (ranging from 10 to 66 ± 2 mg L⁻¹) and increased significantly by day 12 (reaching levels between 157 ± 2 and 218 ± 3 mg L⁻¹). Casein sets followed a similar pattern, starting from 31 ± 2 to 128 ± 4 mg L⁻¹ on day 6 and rising to between 178 ± 2 and 209 ± 3 mg L⁻¹ by day 12, with set 3 showing the highest initial and final concentrations. In contrast, valeric acid showed a different pattern. For albumin, set 1 started with no detectable valeric acid on day 6 and increased to 106 ± 4 mg L⁻¹ by day 12. Albumin sets 2 and 3 had small increases, from 9 ± 0 and 14 ± 1 mg L⁻¹ to 27 ± 1 and 18 ± 1 mg L⁻¹ valeric acid, respectively. Casein

sets showed a modest increase for sets 1 and 2, but set 3 had no detectable valeric acid at either time point.

Protein-rich waste anaerobic digestion doesn't necessarily mean generating the same VFA profile. For example, Shen et al. (2017) observed during the fermentation of tofu and egg white at 30 °C and pH 6.0, egg white yielded higher VFA levels than tofu and displayed a varied VFA composition. Tofu's VFA mix primarily consisted of acetic acid, whereas egg white showed a more balanced distribution of acetic, propionic, butyric, and valeric acids. Similarly, fermenting casein and gelatine at 25 °C with a neutral pH, Bevilacqua et al. (2020) noted distinct VFA outcomes based on the protein type, with casein generating higher yields than gelatine. While acetic acid was prevalent in both, casein fermentation produced increased butyric and propionic acids, and gelatine fermentation resulted in higher levels of propionic and valeric acids (Bevilacqua et al., 2020). In this present study of pure protein and PPW, sets A1, A2, and A3, similar patterns in the production of individual VFAs were noted. Across these sets, whether focusing on albumin or casein, acetic acid emerged as the predominant VFA. This suggests that the microbial populations in the AD system are effectively transforming the provided substrates into acetate. Among all the sets, acetic acid was the most produced acid, followed by propionic acid, isovaleric, butyric, and valeric acids. Acetic acid pathway has also been reported during the AD digestion of slaughterhouse blood (Plácido & Zhang, 2018). The accumulation of acetic acid was observed in the anaerobic digestion of waste sewage sludge in the presence of selenite, where methane generation was entirely suppressed (Roy et al., 2022). Similar to this study, valeric acid was reported to be the least VFA produced in some literature on the anaerobic digestion of protein wastewater (Duong et al., 2019) and gelatin (Flotats et al., 2006).

6.9 Conclusions

A mixture of dairy manure (M) and pineapple waste (PPW) produced biohydrogen and optimized using the Box–Behnken design (BBD) in a batch anaerobic fermentation system. PPW acts as a protease enzyme (bromelain) supplier to enhance the hydrolysis of dairy manure. Optimal conditions (M:PPW ratio of 0.9, pH 6.0, inoculum 5.5 g VS L⁻¹) led to maximum cumulative yields of 345±6 mL H₂ g⁻¹ VS_{substrate} by day 6 and 385±7 mL H₂ g⁻¹ VS_{substrate} by day 12. Under the optimal parameter, biohydrogen yields from albumin and casein were 213±3 mL H₂ g⁻¹ VS_{substrate} and 233±3 mL H₂ g⁻¹ VS_{substrate} on day 6, respectively, increasing to 247±6 mL H₂ g⁻¹ VS_{substrate} and 312±3 mL H₂ g⁻¹ VS_{substrate} by day 12. Protein reduction rates were 38±1% for albumin-PPW and 31±2% for casein-PPW composite. FTIR and SEM analyses also revealed significant changes in surface morphology and Amide (N-H) functional group changes during the digestion of albumin and casein with PPW. These results underscore the potential of using manure and PPW, as well as pure proteins with PPW, for efficient biohydrogen yield, offering a strategy to improve biohydrogen generation from recalcitrant protein-rich wastes.

References

- Aceves-Lara, C.-A., Latrille, E., Bernet, N., Buffière, P., & Steyer, J.-P. (2008). A pseudo-stoichiometric dynamic model of anaerobic hydrogen production from molasses. *Water Research*, 42(10-11), 2539-2550. <https://doi.org/10.1016/j.watres.2008.02.018>.
- Ahmad, A., Yadav, A. K., Singh, A., & Singh, D. K. (2024). A comprehensive machine learning-coupled response surface methodology approach for predictive modeling and optimization of biogas potential in anaerobic Co-digestion of organic waste. *Biomass and Bioenergy*, 180, 106995. <https://doi.org/10.1016/j.biombioe.2023.106995>.
- Aili Hamzah, A. F., Hamzah, M. H., Che Man, H., Jamali, N. S., Siajam, S. I., & Ismail, M. H. (2021). Recent updates on the conversion of pineapple waste (*Ananas comosus*) to value-added products, future perspectives and challenges. *Agronomy*, 11(11), 2221. <https://doi.org/10.3390/agronomy11112221>.
- Algapani, D. E., Qiao, W., Su, M., di Pumpo, F., Wandera, S. M., Adani, F., & Dong, R. (2016). Bio-hydrolysis and bio-hydrogen production from food waste by thermophilic and hyperthermophilic anaerobic process. *Bioresour. Technol.*, 216, 768-777. <https://doi.org/10.1016/j.biortech.2016.06.016>.
- Annamalai, N., Elayaraja, S., Oleskowicz-Popiel, P., Sivakumar, N., & Al Bahry, S. (2020). Volatile fatty acids production during anaerobic digestion of lignocellulosic biomass. In *Recent Developments in Bioenergy Research*; Elsevier: Amsterdam, The Netherlands; pp. 237–251. <https://doi.org/10.1016/B978-0-12-819597-0.00012-X>.
- Arifan, F., Abdullah, A., & Sumardiono, S. (2021). Effect of Organic Waste Addition into Animal Manure on Biogas Production Using Anaerobic Digestion Method. *International Journal*

of Renewable Energy Development, 10(3), 623-633.

<https://doi.org/10.14710/ijred.2021.36107>.

Baldi, F., Iannelli, R., Pecorini, I., Polettini, A., Pomi, R., & Rossi, A. (2019). Influence of the pH control strategy and reactor volume on batch fermentative hydrogen production from the organic fraction of municipal solid waste. *Waste Management & Research*, 37(5), 478-485. <https://doi.org/10.1177/0734242X19826371>.

Belfer, S., Fainchtain, R., Purinson, Y., & Kedem, O. (2000). Surface characterization by FTIR-ATR spectroscopy of polyethersulfone membranes-unmodified, modified and protein fouled. *Journal of Membrane Science*, 172(1-2), 113-124. [https://doi.org/10.1016/S0376-7388\(00\)00316-1](https://doi.org/10.1016/S0376-7388(00)00316-1).

Bermúdez-Penabad, N., Kennes, C., & Veiga, M. C. (2017). Anaerobic digestion of tuna waste for the production of volatile fatty acids. *Waste Management*, 68, 96-102. <https://doi.org/10.1016/j.wasman.2017.06.010>.

Bevilacqua, R., Regueira, A., Mauricio-Iglesias, M., Lema, J. M., & Carballa, M. (2020). Protein composition determines the preferential consumption of amino acids during anaerobic mixed-culture fermentation. *Water Research*, 183, 115958. <https://doi.org/10.1016/j.watres.2020.115958>.

Bhat, M. Y., Dar, T. A., & Singh, L. R. (2016). Casein Proteins: Structural and Functional Aspects. In *Milk Proteins—From Structure to Biological Properties and Health Aspects*; InTech: Rijeka, Croatia. <http://dx.doi.org/10.5772/64187>.

Bolatkhon, K., Kossalbayev, B. D., Zayadan, B. K., Tomo, T., Veziroglu, T. N., & Allakhverdiev, S. I. (2019). Hydrogen production from phototrophic microorganisms: reality and

- perspectives. *International Journal of Hydrogen Energy*, 44(12), 5799-5811.
<https://doi.org/10.1016/j.ijhydene.2019.01.092>.
- Buhrke, D., Michael, N., & Hamm, P. (2022). Vibrational couplings between protein and cofactor in bacterial phytochrome Agp1 revealed by 2D-IR spectroscopy. *Proceedings of the National Academy of Sciences*, 119(31), e2206400119.
<https://doi.org/10.1073/pnas.2206400119>.
- Cahyari, K., Putri, A., Oktaviani, E., Hidayat, M., & Norajsha, J. (2018). Biohydrogen production from pineapple waste: effect of substrate concentration and acid pretreatment. *IOP Conference Series: Materials Science and Engineering*, 358, 012001.10.1088/1757-899X/358/1/012001.
- Capson-Tojo, G., Ruiz, D., Rouez, M., Crest, M., Steyer, J.-P., Bernet, N., Delgenès, J.-P., & Escudié, R. (2017). Accumulation of propionic acid during consecutive batch anaerobic digestion of commercial food waste. *Bioresource Technology*, 245, 724-733.
<https://doi.org/10.1016/j.biortech.2017.08.149>.
- Chae, K.-J., Choi, M.-J., Kim, K.-Y., Ajayi, F., Park, W., Kim, C.-W., & Kim, I. S. (2010). Methanogenesis control by employing various environmental stress conditions in two-chambered microbial fuel cells. *Bioresource Technology*, 101(14), 5350-5357.
<https://doi.org/10.1016/j.biortech.2010.02.035>.
- Chaganti, S. R., Kim, D.-H., & Lalman, J. A. (2012). Impact of oleic acid on the fermentation of glucose and xylose mixtures to hydrogen and other byproducts. *Renewable Energy*, 42, 60-65. <https://doi.org/10.1016/j.renene.2011.09.015>.
- Chakraborty, A. J., Mitra, S., Tallei, T. E., Tareq, A. M., Nainu, F., Cicia, D., Dhama, K., Emran, T. B., Simal-Gandara, J., & Capasso, R. (2021). Bromelain a potential bioactive

- compound: a comprehensive overview from a pharmacological perspective. *Life*, 11(4), 317. <https://doi.org/10.3390/life11040317>.
- Chen, C.-Y., Saratale, G. D., Lee, C.-M., Chen, P.-C., & Chang, J.-S. (2008). Phototrophic hydrogen production in photobioreactors coupled with solar-energy-excited optical fibers. *International Journal of Hydrogen Energy*, 33(23), 6886-6895. <https://doi.org/10.1016/j.ijhydene.2008.09.014>.
- Chen, W. H., Biswas, P. P., Ong, H. C., Hoang, A. T., Nguyen, T. B., & Dong, C. D. (2023). A critical and systematic review of sustainable hydrogen production from ethanol/bioethanol: Steam reforming, partial oxidation, and autothermal reforming. *Fuel*, 333, 126526. <https://doi.org/10.1016/j.fuel.2022.126526>.
- Chen, W.-H., Lin, M.-R., Lu, J.-J., Chao, Y., & Leu, T.-S. (2010). Thermodynamic analysis of hydrogen production from methane via autothermal reforming and partial oxidation followed by water gas shift reaction. *International Journal of Hydrogen Energy*, 35(21), 11787-11797. <https://doi.org/10.1016/j.fuel.2022.126526>.
- Chowdhury, N., Lalman, J. A., Seth, R., & Ndegwa, P. (2007). Biohydrogen production by mesophilic anaerobic fermentation of glucose in the presence of linoleic acid. *Journal of Environmental Engineering*, 133(12), 1145-1152. [https://doi.org/10.1061/\(ASCE\)0733-9372\(2007\)133:12\(1145\)](https://doi.org/10.1061/(ASCE)0733-9372(2007)133:12(1145)).
- Chu, C. Y., Vo, T. P., & Chen, T. H. (2020). A novel of biohythane gaseous fuel production from pineapple peel waste juice in two-stage of continuously stirred anaerobic bioreactors. *Fuel*, 279, 118526. <https://doi.org/10.1016/j.fuel.2020.118526>.
- Cobb, J. S., Zai-Rose, V., Correia, J. J., & Janorkar, A. V. (2020). FT-IR spectroscopic analysis of the secondary structures present during the desiccation induced aggregation of elastin-

- like polypeptide on silica. *ACS Omega*, 5(14), 8403-8413.
<https://doi.org/10.1021/acsomega.0c00271>.
- Dahunsi, S. O., Ogunwole, J. O., Owoseni, A. A., Olutona, G. O., Nejo, Y. T., & Atobatele, O. E. (2022). Valorization of pineapple peel and poultry manure for clean energy generation. *Food and Energy Security*, 11(1), e228. <https://doi.org/10.1002/fes3.228>.
- Dahunsi, S. O., Oranusi, S., & Efevbokhan, V. E. (2017). Cleaner energy for cleaner production: Modeling and optimization of biogas generation from *Carica papayas* (Pawpaw) fruit peels. *Journal of Cleaner Production*, 156, 19-29.
<https://doi.org/10.1016/j.jclepro.2017.04.042>.
- Dai, X., Hu, C., Zhang, D., Dai, L., & Duan, N. (2017). Impact of a high ammonia-ammonium-pH system on methane-producing archaea and sulfate-reducing bacteria in mesophilic anaerobic digestion. *Bioresource Technology*, 245, 598-605.
<https://doi.org/10.1016/j.biortech.2017.08.208>.
- Dasa, K. T., Westman, S. Y., Millati, R., Cahyanto, M. N., Taherzadeh, M. J., & Niklasson, C. (2016). Inhibitory effect of long-chain fatty acids on biogas production and the protective effect of membrane bioreactor. *BioMed Research International*.
<https://doi.org/10.1155/2016/7263974>.
- Deaver, J. A., Diviesti, K. I., Soni, M. N., Campbell, B. J., Finneran, K. T., & Popat, S. C. (2020). Palmitic acid accumulation limits methane production in anaerobic co-digestion of fats, oils and grease with municipal wastewater sludge. *Chemical Engineering Journal*, 396, 125235. <https://doi.org/10.1016/j.cej.2020.125235>.

- De Meutter, J., & Goormaghtigh, E. (2021). Evaluation of protein secondary structure from FTIR spectra improved after partial deuteration. *European Biophysics Journal*, 50, 613-628. <https://doi.org/10.1007/s00249-021-01502-y>.
- Deng, Z., Ferreira, A. L. M., Spanjers, H., & van Lier, J. B. (2022). Characterization of microbial communities in anaerobic acidification reactors fed with casein and/or lactose. *Applied Microbiology and Biotechnology*, 106(18), 6301-6316. <https://doi.org/10.1007/s00253-022-12132-5>.
- Dos Santos, S. B., de Oliveira Faber, M., de Araujo Collaço, A. C., Aguiéiras, E. C. G., Freire, D. M. G., Langone, M. A., & Ferreira-Leitão, V. S. (2021). Sequential hydrogen and methane production using the residual biocatalyst of biodiesel synthesis as raw material. *International Journal of Hydrogen Energy*, 46(46), 23658-23669. <https://doi.org/10.1016/j.ijhydene.2021.04.172>.
- Duarte, M. S., Sinisgalli, E., Cavaleiro, A. J., Bertin, L., Alves, M. M., & Pereira, M. A. (2021). Intensification of methane production from waste frying oil in a biogas-lift bioreactor. *Renewable Energy*, 168, 1141-1148. <https://doi.org/10.1016/j.renene.2020.12.114>.
- Duong, T. H., Grolle, K., Nga, T. T. V., Zeeman, G., Temmink, H., & Van Eekert, M. (2019). Protein hydrolysis and fermentation under methanogenic and acidifying conditions. *Biotechnology for Biofuels*, 12(1), 1-10. <https://doi.org/10.1186/s13068-019-1592-7>.
- Eftaxias, A., Diamantis, V., Michailidis, C., Stamatelatou, K., & Aivasidis, A. (2020). Comparison of anaerobic digesters performance treating palmitic, stearic and oleic acid: determination of the LCFA kinetic constants using ADM1. *Bioprocess and Biosystems Engineering*, 43, 1329-1338. <https://doi.org/10.1007/s00449-020-02328-2>.

- El Asri, O. (2022). Anaerobic biodegradation: the anaerobic digestion process. In *Handbook of Biodegradable Materials* (pp. 1-26); Gam, A., and Ash, M., (ED); Springer International Publishing, Cham, pp 85–110. https://doi.org/10.1007/978-3-031-09710-2_4.
- Fagbohungebe, M. O., Dodd, I. C., Herbert, B. M., Li, H., Ricketts, L., & Semple, K. T. (2015). High solid anaerobic digestion: Operational challenges and possibilities. *Environmental Technology & Innovation*, 4, 268-284. <https://doi.org/10.1016/j.eti.2015.09.003>.
- Feng, K., Lian, S.-J., Zou, H., Guo, R.-B., Dai, X.-F., & Fu, S.-F. (2023). Ammonia Stress on Anaerobic Digestion: The More Sensitive Propionic/Butyric Acid-Degrading Bacteria over Methanogens. *ACS EST Engineering*, 4(3), 627–638. <https://doi.org/10.1021/acsestengg.3c00411>.
- Filer, J., Ding, H. H., & Chang, S. (2019). Biochemical methane potential (BMP) assay method for anaerobic digestion research. *Water*, 11(5), 921. <https://doi.org/10.3390/w11050921>.
- Flotats, X., Palatsi, J., Ahring, B. K., & Angelidaki, I. (2006). Identifiability study of the proteins degradation model, based on ADM1, using simultaneous batch experiments. *Water Science and Technology*, 54(4), 31-39. <https://doi.org/10.2166/wst.2006.523>.
- Gagliano, M., Braguglia, C., Petruccioli, M., & Rossetti, S. (2015). Ecology and biotechnological potential of the thermophilic fermentative *Coprothermobacter* spp. *FEMS Microbiology Ecology*, 91(5), fiv018. <https://doi.org/10.1093/femsec/fiv018>.
- Gao, X., Li, Z., Zhang, K., Kong, D., Gao, W., Liang, J., Liu, F., & Du, L. (2023). Layer Inoculation as a New Technology to Resist Volatile Fatty Acid Inhibition during Solid-State Anaerobic Digestion: Methane Yield Performance and Microbial Responses. *Fermentation*, 9(6), 535. <https://doi.org/10.3390/fermentation9060535>.

- Greff, B., Szigeti, J., Nagy, Á., Lakatos, E., & Varga, L. (2022). Influence of microbial inoculants on co-composting of lignocellulosic crop residues with farm animal manure: A review. *Journal of Environmental Management*, 302, 114088. <https://doi.org/10.1016/j.jenvman.2021.114088>.
- Habiba, L., Hassib, B., & Moktar, H. (2009). Improvement of activated sludge stabilisation and filterability during anaerobic digestion by fruit and vegetable waste addition. *Bioresource Technology*, 100(4), 1555-1560. <https://doi.org/10.1016/j.biortech.2008.09.019>.
- Han, Y., Green, H., & Tao, W. (2020). Reversibility of propionic acid inhibition to anaerobic digestion: Inhibition kinetics and microbial mechanism. *Chemosphere*, 255, 126840. <https://doi.org/10.1016/j.chemosphere.2020.126840>.
- Hans, M., & Kumar, S. (2019). Biohythane production in two-stage anaerobic digestion system. *International Journal of Hydrogen Energy*, 44(32), 17363-17380. <https://doi.org/10.1016/j.ijhydene.2018.10.022>.
- Haq, A., Malik, A., Khan, A., Weaver, J. E., Wang, L., Khan, H., Khan, S., Shah, A. A., Ahmed, S., & Jamal, A. (2023). Effect of removal of inhibitors on microbial communities and biogas yield of *Jatropha curcas* seeds during continuous anaerobic digestion. *Journal of Cleaner Production*, 426, 139154. <https://doi.org/10.1016/j.ijhydene.2018.10.022>.
- Harirchi, S., Wainaina, S., Sar, T., Nojourni, S. A., Parchami, M., Parchami, M., Varjani, S., Khanal, S. K., Wong, J., & Awasthi, M. K. (2022). Microbiological insights into anaerobic digestion for biogas, hydrogen or volatile fatty acids (VFAs): a review. *Bioengineered*, 13(3), 6521-6557. <https://doi.org/10.1080/21655979.2022.2035986>.
- He, Q., Li, L., & Peng, X. (2017). Early warning indicators and microbial mechanisms for process failure due to organic overloading in food waste digesters. *Journal of*

Environmental Engineering, 143(12), 04017077.

[https://doi.org/10.1061/\(ASCE\)EE.1943-7870.0001280](https://doi.org/10.1061/(ASCE)EE.1943-7870.0001280).

Holt, C., Carver, J., Ecroyd, H., & Thorn, D. (2013). Invited review: Caseins and the casein micelle: Their biological functions, structures, and behavior in foods. *Journal of Dairy Science*, 96(10), 6127-6146. <https://doi.org/10.3168/jds.2013-6831>.

Hu, H., Fan, Y., & Liu, H. (2008). Hydrogen production using single-chamber membrane-free microbial electrolysis cells. *Water Research*, 42(15), 4172-4178. <https://doi.org/10.1016/j.watres.2008.06.015>.

Hwang, Y. J., & Lyubovitsky, J. G. (2013). The structural analysis of three-dimensional fibrous collagen hydrogels by raman microspectroscopy. *Biopolymers: Original Research on Biomolecules*, 99(6), 349-356. <https://doi.org/10.1002/bip.22183>.

Ioelovich, M. (2015). Recent findings and the energetic potential of plant biomass as a renewable source of biofuels—a review. *Bioresources*, 10(1), 1879-1914. [10.15376/biores.10.1.1879-1914](https://doi.org/10.15376/biores.10.1.1879-1914).

Jiang, M., Qiao, W., Wang, Y., Zou, T., Lin, M., & Dong, R. (2022). Balancing acidogenesis and methanogenesis metabolism in thermophilic anaerobic digestion of food waste under a high loading rate. *Science of the Total Environment*, 824, 153867. <https://doi.org/10.1016/j.scitotenv.2022.153867>.

Jiménez, J., Guardia-Puebla, Y., Romero-Romero, O., Cisneros-Ortiz, M., Guerra, G., Morgan-Sagastume, J., & Noyola, A. (2014). Methanogenic activity optimization using the response surface methodology, during the anaerobic co-digestion of agriculture and industrial wastes. Microbial community diversity. *Biomass and Bioenergy*, 71, 84-97. <https://doi.org/10.1016/j.biombioe.2014.10.023>.

- Kao, L. S., & Green, C. E. (2008). Analysis of variance: is there a difference in means and what does it mean? *Journal of Surgical Research*, *144*(1), 158-170.
<https://doi.org/10.1016/j.jss.2007.02.053>.
- Khadka, A., Parajuli, A., Dangol, S., Thapa, B., Sapkota, L., Carmona-Martínez, A. A., & Ghimire, A. (2022). Effect of the substrate to inoculum ratios on the kinetics of biogas production during the mesophilic anaerobic digestion of food waste. *Energies*, *15*(3), 834.
<https://doi.org/10.3390/en15030834>.
- Khan, M. A., Ngo, H. H., Guo, W., Liu, Y., Zhang, X., Guo, J., Chang, S. W., Nguyen, D. D., & Wang, J. (2018). Biohydrogen production from anaerobic digestion and its potential as renewable energy. *Renewable Energy*, *129*, 754-768.
<https://doi.org/10.1016/j.renene.2017.04.029>.
- Kovács, E., Wirth, R., Maróti, G., Bagi, Z., Rákhely, G., & Kovács, K. L. (2013). Biogas production from protein-rich biomass: fed-batch anaerobic fermentation of casein and of pig blood and associated changes in microbial community composition. *Plos One*, *8*(10), e77265. <https://doi.org/10.1371/journal.pone.0077265>.
- Kumar, G., Zhen, G., Kobayashi, T., Sivagurunathan, P., Kim, S. H., & Xu, K. Q. (2016). Impact of pH control and heat pre-treatment of seed inoculum in dark H₂ fermentation: a feasibility report using mixed microalgae biomass as feedstock. *International Journal of Hydrogen Energy*, *41*(7), 4382-4392. <https://doi.org/10.1016/j.ijhydene.2015.08.069>.
- Lee, J., Koo, T., Han, G., Shin, S. G., & Hwang, S. (2015). Anaerobic digestion of cattle offal: protein and lipid-rich substrate degradation and population dynamics of acidogens and methanogens. *Bioprocess and Biosystems Engineering*, *38*, 2349-2360.
<https://doi.org/10.1007/s00449-015-1470-z>.

- Li, Y., Jin, Y., Borrion, A., Li, H., & Li, J. (2017). Effects of organic composition on mesophilic anaerobic digestion of food waste. *Bioresource Technology*, *244*, 213-224.
<https://doi.org/10.1016/j.biortech.2017.07.006>.
- Li, Y., Wang, Y., Yu, Z., Lu, J., Li, D., Wang, G., Li, Y., Wu, Y., Li, S., & Xu, F. (2018). Effect of inoculum and substrate/inoculum ratio on the performance and methanogenic archaeal community structure in solid state anaerobic co-digestion of tomato residues with dairy manure and corn stover. *Waste Management*, *81*, 117-127.
<https://doi.org/10.1016/j.wasman.2018.09.042>.
- Li, Y., Zhang, Y., Kong, X., Li, L., Yuan, Z., Dong, R., & Sun, Y. (2017). Effects of ammonia on propionate degradation and microbial community in digesters using propionate as a sole carbon source. *Journal of Chemical Technology & Biotechnology*, *92*(10), 2538-2545.
<https://doi.org/10.1002/jctb.5260>.
- Lim, S. L., & Wu, T. Y. (2016). Characterization of matured vermicompost derived from valorization of palm oil mill byproduct. *Journal of Agricultural and Food Chemistry*, *64*(8), 1761-1769. <https://doi.org/10.1021/acs.jafc.6b00531>.
- Lin, J., Zuo, J., Gan, L., Li, P., Liu, F., Wang, K., Chen, L., & Gan, H. (2011). Effects of mixture ratio on anaerobic co-digestion with fruit and vegetable waste and food waste of China. *Journal of Environmental Sciences*, *23*(8), 1403-1408. [https://doi.org/10.1016/S1001-0742\(10\)60572-4](https://doi.org/10.1016/S1001-0742(10)60572-4).
- Liu, H., Wang, J., Wang, A., & Chen, J. (2011). Chemical inhibitors of methanogenesis and putative applications. *Applied Microbiology and Biotechnology*, *89*, 1333-1340.
<https://doi.org/10.1007/s00253-010-3066-5>.

- Lourinho, G., Rodrigues, L., & Brito, P. (2020). Recent advances on anaerobic digestion of swine wastewater. *International Journal of Environmental Science and Technology*, 17(12), 4917-4938. <https://doi.org/10.1007/s13762-020-02793-y>.
- Lu, Y., Zhang, Q., Wang, X., Zhou, X., & Zhu, J. (2020). Effect of pH on volatile fatty acid production from anaerobic digestion of potato peel waste. *Bioresource Technology*, 316, 123851. <https://doi.org/10.1016/j.biortech.2020.123851>.
- Lukitawesa, Patinvoh, R. J., Millati, R., Sarvari-Horvath, I., & Taherzadeh, M. J. (2020). Factors influencing volatile fatty acids production from food wastes via anaerobic digestion. *Bioengineered*, 11(1), 39-52. <https://doi.org/10.1080/21655979.2019.1703544@kbie20.2019.11.issue-S11>.
- Magdalena, J. A., Greses, S., & González-Fernández, C. (2019). Impact of organic loading rate in volatile fatty acids production and population dynamics using microalgae biomass as substrate. *Scientific Reports*, 9(1), 18374. <https://doi.org/10.1038/s41598-019-54914-4>.
- Mahato, P., Goyette, B., Rahaman, M. S., & Rajagopal, R. (2020). Processing High-Solid and High-Ammonia Rich Manures in a Two-Stage (Liquid-Solid) Low-Temperature Anaerobic Digestion Process: Start-Up and Operating Strategies. *Bioengineering*, 7(3), 80. <https://doi.org/10.3390/bioengineering7030080>.
- Maresca, P., & Ferrari, G. (2017). Modelling of the kinetics of Bovine Serum Albumin enzymatic hydrolysis assisted by high hydrostatic pressure. *Food and Bioproducts Processing*, 105, 1-11. <https://doi.org/10.1016/j.fbp.2017.03.006>.
- Mayer, F., Adam, C., Noo, A., Guignard, C., Hoffmann, L., & Delfosse, P. (2010). Monitoring volatile fatty acid production during mesophilic anaerobic digestion exposed to

- increasing feeding rate. In Proceedings of the Third International Symposium on Energy from Biomass and Waste, Venice, Italy, 8–11 November 2010; pp. 1–9.
- Meegoda, J. N., Li, B., Patel, K., & Wang, L. B. (2018). A review of the processes, parameters, and optimization of anaerobic digestion. *International Journal of Environmental Research and Public Health*, *15*(10), 2224. <https://doi.org/10.3390/ijerph15102224>.
- Molinuevo-Salces, B., González-Fernández, C., Gómez, X., García-González, M. C., & Morán, A. (2012). Vegetable processing wastes addition to improve swine manure anaerobic digestion: Evaluation in terms of methane yield and SEM characterization. *Applied Energy*, *91*(1), 36-42. <https://doi.org/10.1016/j.apenergy.2011.09.010>.
- Moreno Cárdenas, E. L., & Zapata Zapata, A. D. (2019). Biohydrogen production by co-digestion of fruits and vegetable waste and coffee mucilage. *Revista Facultad Nacional de Agronomía Medellín*, *72*(3), 9007-9018. <https://doi.org/10.15446/rfnam.v72n3.73140>.
- Moset, V., Al-zohairi, N., & Møller, H. B. (2015). The impact of inoculum source, inoculum to substrate ratio and sample preservation on methane potential from different substrates. *Biomass and Bioenergy*, *83*, 474-482. <https://doi.org/10.1016/j.biombioe.2015.10.018>.
- Mu, L., Wang, Y., Xu, F., Li, J., Tao, J., Sun, Y., Song, Y., Duan, Z., Li, S., & Chen, G. (2023). Emerging Strategies for Enhancing Propionate Conversion in Anaerobic Digestion: A Review. *Molecules*, *28*(9), 3883. <https://doi.org/10.3390/molecules28093883>.
- Muenmee, S., & Prasertboonyai, K. (2021). Potential biogas production generated by mono-and co-digestion of food waste and fruit waste (Durian Shell, Dragon Fruit and Pineapple Peel) in different mixture ratio under anaerobic condition. *Environmental Research, Engineering and Management*, *77*(1), 25-35. <https://doi.org/10.5755/j01.ere.m.77.1.25234>.

- Nasser, M., Megahed, T. F., Ookawara, S., & Hassan, H. (2022). A review of water electrolysis–based systems for hydrogen production using hybrid/solar/wind energy systems. *Environmental Science and Pollution Research*, 29(58), 86994-87018. <https://doi.org/10.1007/s11356-022-23323-y>.
- Niknejad, H., & Mahmoudzadeh, R. (2015). Comparison of different crosslinking methods for preparation of docetaxel-loaded albumin nanoparticles. *Iranian Journal of Pharmaceutical Research*, 14, 385–394.
- Nikolaidis, P., & Poullikkas, A. (2017). A comparative overview of hydrogen production processes. *Renewable and Sustainable Energy Reviews*, 67, 597-611. <https://doi.org/10.1016/j.rser.2016.09.044>.
- Oduor, W. W., Wandera, S. M., Murunga, S. I., & Raude, J. M. (2022). Enhancement of anaerobic digestion by co-digesting food waste and water hyacinth in improving treatment of organic waste and bio-methane recovery. *Heliyon*, 8(9). <https://doi.org/10.1016/j.heliyon.2022.e10580>.
- Oni, A., Anaya, K., Giwa, T., Di Lullo, G., & Kumar, A. (2022). Comparative assessment of blue hydrogen from steam methane reforming, autothermal reforming, and natural gas decomposition technologies for natural gas-producing regions. *Energy Conversion and Management*, 254, 115245. <https://doi.org/10.1016/j.enconman.2022.115245>.
- Palatsi, J., Illa, J., Prenafeta-Boldú, F. X., Laureni, M., Fernandez, B., Angelidaki, I., & Flotats, X. (2010). Long-chain fatty acids inhibition and adaptation process in anaerobic thermophilic digestion: batch tests, microbial community structure and mathematical modelling. *Bioresource Technology*, 101(7), 2243-2251. <https://doi.org/10.1016/j.biortech.2009.11.069>.

- Plácido, J., & Zhang, Y. (2018). Production of volatile fatty acids from slaughterhouse blood by mixed-culture fermentation. *Biomass Conversion and Biorefinery*, 8(3), 621-634. <https://doi.org/10.1007/s13399-018-0313-y>.
- Polanía, A. M., Londoño, L., Ramírez, C., & Bolívar, G. (2022). Influence of ultrasound application in fermented pineapple peel on total phenolic content and antioxidant activity. *Fermentation*, 8(7), 314. <https://doi.org/10.3390/fermentation8070314>.
- Poolman, B., Juillard, V., Kunji, E.R.S., Hagting, A., Konings, W.N. (1996). Casein-breakdown by *Lactococcus lactis*. In *Lactic Acid Bacteria*; Bozoğlu, F, T., Ray, B. (ED). NATO ASI Series, vol 98, 303–326, Springer, Berlin, Heidelberg. https://doi.org/10.1007/978-3-642-61462-0_13.
- Rafieenia, R. (2019). Enhancement of hydrogen and methane production through anaerobic digestion using pre-treatments. PhD dissertation, Università Degli Studi Di Padova. <https://hdl.handle.net/11577/3425227>.
- Rasapoor, M., Young, B., Brar, R., Sarmah, A., Zhuang, W.-Q., & Baroutian, S. (2020). Recognizing the challenges of anaerobic digestion: Critical steps toward improving biogas generation. *Fuel*, 261, 116497.
- Rasul, M., Hazrat, M., Sattar, M., Jahirul, M., & Shearer, M. (2022). The future of hydrogen: Challenges on production, storage and applications. *Energy Conversion and Management*, 272, 116326. <https://doi.org/10.1016/j.fuel.2019.116497>.
- Ray, R., Cordova-Villegas, L., Sharma, M., Biswas, N. (2023). Hydrogen Production in Incubated Anaerobic Mesophilic Mixed Culture by Oleic Acid (OA) for Different Periods. In *Proceedings of the Canadian Society of Civil Engineering Annual Conference*

- 2021, Walbridge, S.(ED). Lecture Notes in Civil Engineering, vol 249. Springer, Singapore. https://doi.org/10.1007/978-981-19-1061-6_37.
- Reungsang, A., & Sreela-or, C. (2013). Bio-hydrogen production from pineapple waste extract by anaerobic mixed cultures. *Energies*, 6(4), 2175-2190. <https://doi.org/10.3390/en6042175>.
- Rodríguez-Méndez, R., Le Bihan, Y., Béline, F., & Lessard, P. (2017). Long chain fatty acids (LCFA) evolution for inhibition forecasting during anaerobic treatment of lipid-rich wastes: Case of milk-fed veal slaughterhouse waste. *Waste Management*, 67, 51-58. <https://doi.org/10.1016/j.wasman.2017.05.028>.
- Roy, C. K., Hoshiko, Y., Toya, S., & Maeda, T. (2022). Effect of different concentrations of sodium selenite on anaerobic digestion of waste sewage sludge. *Environmental Technology & Innovation*, 27, 102403. <https://doi.org/10.1016/j.eti.2022.102403>.
- Ruiz-Aguilar, G. M., Martínez-Martínez, J. H., Costilla-Salazar, R., & Camarena-Martínez, S. (2023). Using Central Composite Design to Improve Methane Production from Anaerobic Digestion of Tomato Plant Waste. *Energies*, 16(14), 5412. <https://doi.org/10.3390/en16145412>.
- Saady, N. M. C. (2013). Homoacetogenesis during hydrogen production by mixed cultures dark fermentation: unresolved challenge. *International Journal of Hydrogen Energy*, 38(30), 13172-13191. <https://doi.org/10.1016/j.ijhydene.2013.07.122>.
- Saady, N. M. C., Chaganti, S. R., Lalman, J. A., Veeravalli, S. S., Shanmugam, S. R., & Heath, D. D. (2012). Effects of linoleic acid and its degradation by-products on mesophilic hydrogen production using flocculated and granular mixed anaerobic cultures.

- International Journal of Hydrogen Energy, 37(24), 18747-18760.
<https://doi.org/10.1016/j.ijhydene.2012.09.065>.
- Sadiq, U., Gill, H., & Chandrapala, J. (2021). Casein micelles as an emerging delivery system for bioactive food components. *Foods*, 10(8), 1965. <https://doi.org/10.3390/foods10081965>.
- Sagir, E., & Alipour, S. (2021). Photofermentative hydrogen production by immobilized photosynthetic bacteria: Current perspectives and challenges. *Renewable and Sustainable Energy Reviews*, 141, 110796. <https://doi.org/10.1016/j.rser.2021.110796>.
- Sekoai, P., & Kana, E. G. (2013). A two-stage modelling and optimization of biohydrogen production from a mixture of agro-municipal waste. *International Journal of Hydrogen Energy*, 38(21), 8657-8663. <https://doi.org/10.1016/j.ijhydene.2013.04.130>.
- Shen, D., Yin, J., Yu, X., Wang, M., Long, Y., Shentu, J., & Chen, T. (2017). Acidogenic fermentation characteristics of different types of protein-rich substrates in food waste to produce volatile fatty acids. *Bioresource Technology*, 227, 125-132.
<https://doi.org/10.1016/j.biortech.2016.12.048>.
- Siegert, I., & Banks, C. (2005). The effect of volatile fatty acid additions on the anaerobic digestion of cellulose and glucose in batch reactors. *Process Biochemistry*, 40(11), 3412-3418. <https://doi.org/10.1016/j.procbio.2005.01.025>.
- Sillero, L., Solera, R., & Perez, M. (2022). Anaerobic co-digestion of sewage sludge, wine vinasse and poultry manure for bio-hydrogen production. *International Journal of Hydrogen Energy*, 47(6), 3667-3678. <https://doi.org/10.1016/j.ijhydene.2021.11.032>.
- Singh, H., Tomar, S., Qureshi, K. A., Jaremko, M., & Rai, P. K. (2022). Recent advances in biomass pretreatment technologies for biohydrogen production. *Energies*, 15(3), 999. <https://doi.org/10.3390/en15030999>.

- Strazzera, G., Battista, F., Andreolli, M., Menini, M., Bolzonella, D., & Lampis, S. (2021). Influence of different household Food Wastes Fractions on Volatile Fatty Acids production by anaerobic fermentation. *Bioresource Technology*, 335, 125289. <https://doi.org/10.1016/j.biortech.2021.125289>.
- Sudiarta, G. A. W., Imai, T., & Hung, Y.-T. (2022). Effects of stepwise temperature shifts in anaerobic digestion for treating municipal wastewater sludge: a genomic study. *International Journal of Environmental Research and Public Health*, 19(9), 5728. <https://doi.org/10.3390/ijerph19095728>.
- Syahirah, M. F., & Nazaitulshila, R. (2018). The Utilization of Pineapples Waste Enzyme for the Improvement of Hydrolysis Solubility in Aquaculture Sludge. *Journal of Energy and Safety Technology*, 1(2-2), 35-41.
- Tang, Y., Shigematsu, T., Morimura, S., & Kida, K. (2005). Microbial community analysis of mesophilic anaerobic protein degradation process using bovine serum albumin (BSA)-fed continuous cultivation. *Journal of Bioscience and Bioengineering*, 99(2), 150-164. <https://doi.org/10.1263/jbb.99.150>.
- Tasaki, K. (2021). Chemical-free recovery of protein from cow manure digestate solid and antioxidant activity of recovered protein. *Environmental Challenges*, 4, 100132. <https://doi.org/10.1016/j.envc.2021.100132>.
- Tavanti, R. F. R., Liñares, M. L., Soares, M. B., Trevisan, R. G., Tavanti, T. R., da Silva Freddi, O., Montanari, R., & González, A. P. (2023). Macro-scale spatial modeling reveals the role of soil organic matter quality in CO₂ emissions. *Geoderma Regional*, 34, e00690. <https://doi.org/10.1016/j.geodrs.2023.e00690>.

- Vidmar, B., & Vodovnik, M. (2018). Microbial keratinases: enzymes with promising biotechnological applications. *Food Technology and Biotechnology*, *56*(3), 312-328. <https://doi.org/10.17113/ftb.56.03.18.5658>.
- Wainaina, S., Lukitawesa, Kumar Awasthi, M., & Taherzadeh, M. J. (2019). Bioengineering of anaerobic digestion for volatile fatty acids, hydrogen or methane production: a critical review. *Bioengineered*, *10*(1), 437-458. <https://doi.org/10.1080/21655979.2019.1673937@kbie20.2019.11.issue-SI1>.
- Wang, Z., Hu, Y., Wang, S., Wu, G., & Zhan, X. (2023). A critical review on dry anaerobic digestion of organic waste: Characteristics, operational conditions, and improvement strategies. *Renewable and Sustainable Energy Reviews*, *176*, 113208. <https://doi.org/10.1016/j.rser.2023.113208>.
- Worm, P., Koehorst, J. J., Visser, M., Sedano-Núñez, V. T., Schaap, P. J., Plugge, C. M., Sousa, D. Z., & Stams, A. J. (2014). A genomic view on syntrophic versus non-syntrophic lifestyle in anaerobic fatty acid degrading communities. *Biochimica et Biophysica Acta (BBA)-Bioenergetics*, *1837*(12), 2004-2016. <https://doi.org/10.1016/j.bbabi.2014.06.005>.
- Xu, J.-L., & Gowen, A. A. (2019). Investigation of plasticizer aggregation problem in casein based biopolymer using chemical imaging. *Talanta*, *193*, 128-138. <https://doi.org/10.1016/j.talanta.2018.09.094>.
- Xu, Y., Meng, X., Song, Y., Lv, X., & Sun, Y. (2023). Effects of different concentrations of butyrate on microbial community construction and metabolic pathways in anaerobic digestion. *Bioresource Technology*, *377*, 128845. <https://doi.org/10.1016/j.biortech.2023.128845>.

- Yetilmezsoy, K., Demirel, S., & Vanderbei, R. J. (2009). Response surface modeling of Pb (II) removal from aqueous solution by *Pistacia vera* L.: Box–Behnken experimental design. *Journal of Hazardous Materials*, *171*(1-3), 551-562.
<https://doi.org/10.1016/j.jhazmat.2009.06.035>.
- Zhen, Z., Liu, H., Wang, N., Guo, L., Meng, J., Ding, N., Wu, G., & Jiang, G. (2014). Effects of manure compost application on soil microbial community diversity and soil microenvironments in a temperate cropland in China. *PLoS One*, *9*(10), e108555.
- Zonta, Ž., Alves, M., Flotats, X., & Palatsi, J. (2013). Modelling inhibitory effects of long chain fatty acids in the anaerobic digestion process. *Water Research*, *47*(3), 1369-1380.
<https://doi.org/10.1016/j.watres.2012.12.007>.

CHAPTER SEVEN

CONCLUSIONS AND RECOMMENDATION

7.1 Summary

The primary research problem addressed in this work revolves around the inefficiencies in anaerobic digestion (AD) of protein-rich livestock manure, specifically the rate-limiting step of protein hydrolysis and subsequent ammonia accumulation, which can severely inhibit the AD process. This challenge is significant due to the substantial contribution of livestock waste to organic waste worldwide, presenting both an environmental concern and an untapped opportunity for renewable energy production in the form of biohydrogen and biomethane. The importance of this research lies in its potential to enhance the conversion efficiency of high-protein organic wastes into valuable biohydrogen, thereby mitigating global greenhouse gas emissions from improper manure management and contributing to the sustainable production of renewable energy. Through a series of experiments designed by statistical optimization techniques (Box-Behnken Design (BBD) and Response Surface Methodology (RSM)), this thesis investigated the hydrolysis and digestion of complex protein-rich waste such as dairy manure using kiwi peel waste (KPW) and pineapple peel waste (PPW) as a source of protease enzyme actinidin and bromelain. Four experiments containing fifteen experimental sets were carried out in duplicate reactors across the hydrolysis and fermentation stages using manure as the substrate (Figure 7-1).

KPW- and PPW-derived protease enzymes achieved significant reductions in ammonia nitrogen (up to $64 \pm 0.65\%$ with KPW and $72 \pm 0.48\%$ with PPW) and enhanced protein degradation (up to $39 \pm 0.54\%$ with KPW and $36 \pm 0.25\%$ with PPW) in the hydrolysis stage with manure as substrate.

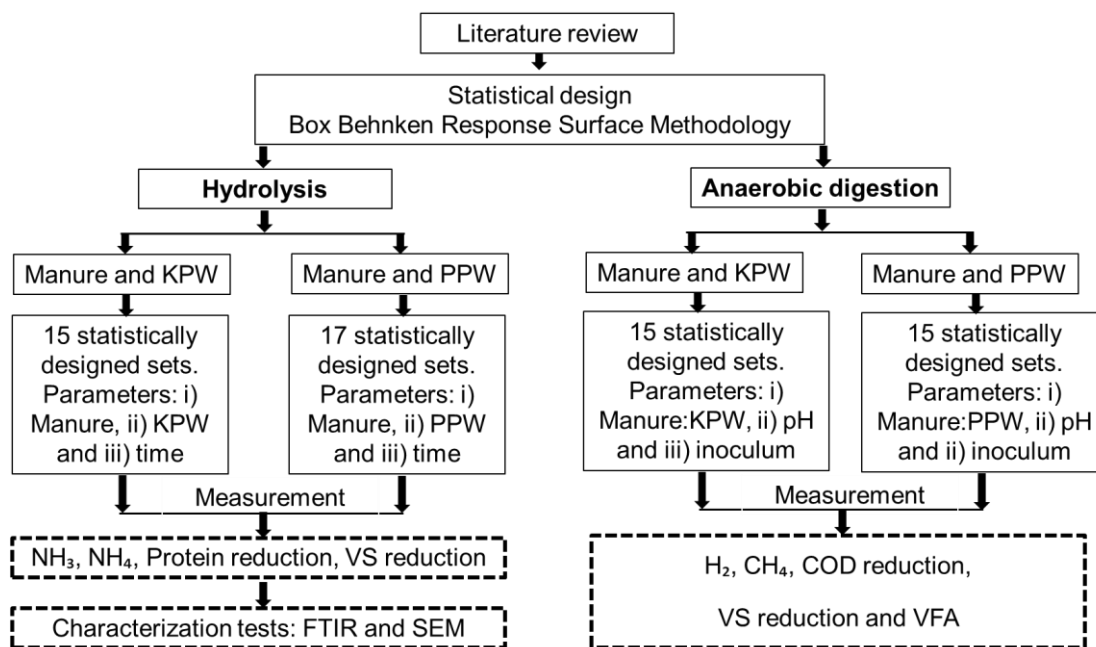


Figure 7- 1. Flowchart of the research conducted in this thesis using complex protein-rich (manure) as substrate with kiwi peel waste (KPW) and pineapple peel waste (PPW).

With the improvement of manure protein hydrolysis, this study analyzed biohydrogen production under inhibited methanogens using oleic acid concentration ($4,000 \text{ mg L}^{-1}$). It optimized the process parameters with manure-KPW (manure:KPW ratio, pH, inoculum) and manure-PPW substrates (manure:PPW ratio, pH, inoculum), leading to notable biohydrogen yields (up to $510 \pm 7 \text{ mL g}^{-1} \text{ VS}$ with KPW and $385 \pm 7 \text{ mL g}^{-1} \text{ VS}$ with PPW). For the first time, this research compared the biohydrogen production capabilities of these complex protein-rich substrates (manure-KPW and manure-PPW) to pure proteins such as albumin and casein (Figure 7-2), revealing optimized conditions that yielded substantial biohydrogen outputs (up to $554 \pm 3 \text{ mL H}_2 \text{ g}^{-1} \text{ VS}_{\text{albumin}}$, $400 \pm 4 \text{ mL H}_2 \text{ g}^{-1} \text{ VS}_{\text{casein}}$ with KPW and $247 \pm 6 \text{ mL H}_2 \text{ g}^{-1} \text{ VS}_{\text{albumin}}$, $312 \pm 3 \text{ mL H}_2 \text{ g}^{-1} \text{ VS}_{\text{casein}}$ with PPW). Data from the BBD generated a second-order polynomial equation, with

coefficients derived through multiple regression analysis. The model validity was checked using ANOVA, where each model was indicated by high F values (88 to 229) and low p values (< 0.05).

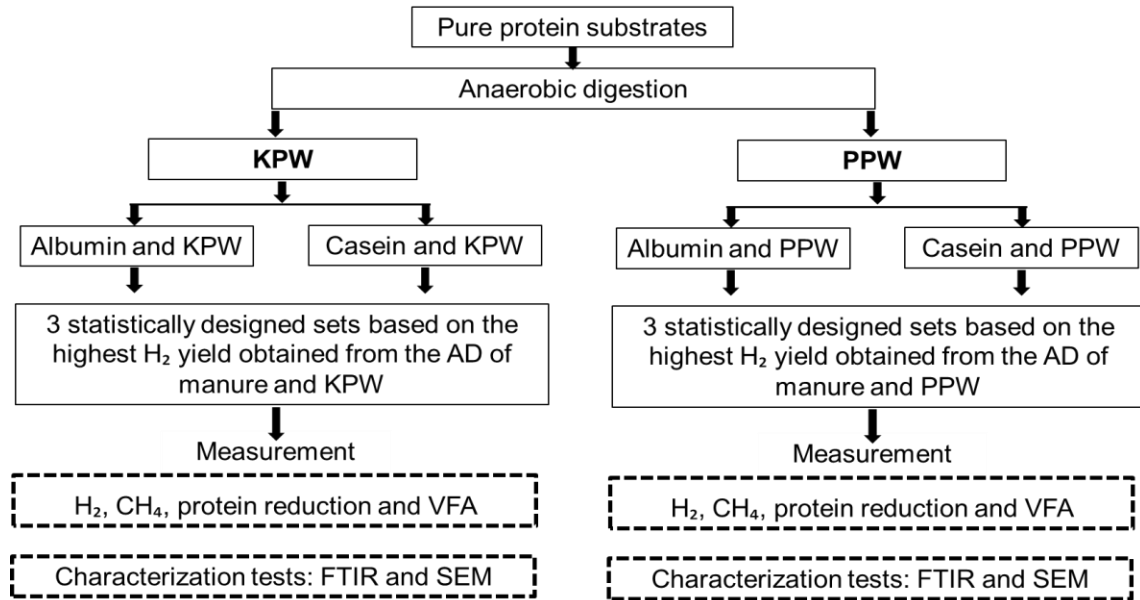


Figure 7- 2. Flowchart of the anaerobic digestion section of the thesis based on pure protein substrate (albumin and casein).

All the developed model's high R^2 values (0.97 to 0.99) suggest it explains 97% to 99% of data variability. Additionally, the comparison between experimental and predicted responses showed a negligible difference ($<5\%$), underscoring the model's accuracy. Upon successfully validating the models, this study proceeded with the substrate physicochemical characterization technique, such as Scanning Electron Microscope (SEM) and Fourier Transform Infrared Spectroscopy (FTIR) during hydrolysis and digestion stages at specific time intervals. The FTIR analysis of hydrolyzed and digested substrate samples revealed noticeable shifts in functional groups, highlighting chemical transformations across the hydrolysis and digestion period. In addition, SEM analysis

provided an in-depth examination of the microstructural transformations of substrates during pre and post-hydrolysis and digestion.

7.2 Conclusions

The main conclusions from this research are:

Hydrolysis studies:

- KPW-derived protease actinidin significantly enhanced manure protein degradation, with optimized conditions ($4 \text{ g VS}_{\text{manure}} \text{ L}^{-1}$, $7.5 \text{ g VS}_{\text{KPW}} \text{ L}^{-1}$, and a hydrolysis time of 48 h) leading to a protein degradation of up to $39 \pm 0.54\%$, and reductions of $64 \pm 0.65\%$ in $\text{NH}_3\text{-N}$ and $83 \pm 0.32\%$ in $\text{NH}_4\text{-N}$. However, the highest VS reduction ($41.4 \pm 0.29\%$) was achieved at $6.5 \text{ g VS}_{\text{manure}} \text{ L}^{-1}$ $7.5 \text{ VS}_{\text{KPW}}$ and a hydrolysis time of 25.5 h.
- Scanning electron microscope (SEM) images of the pre-hydrolysis stage of manure-KPW substrates show a rough, complex surface with organic, fibrous, and inorganic materials. The distinct particles, fibers, or other structures observed before hydrolysis are less pronounced or completely absent after 48 h hydrolysis.
- During enzymatic hydrolysis of manure-KPW, certain absorption bands shifted and weakened, suggesting hydrogen and amide bond (Amide A) disruption, peptide bond cleavage, and amino group release, altering the protein structure.
- Manure-PPW hydrolysis achieved a $36 \pm 0.25\%$ reduction in protein content and a $72 \pm 0.48\%$ decrease in $\text{NH}_3\text{-N}$ at optimal conditions ($9 \text{ g VS}_{\text{manure}} \text{ L}^{-1}$ and $4 \text{ g VS}_{\text{PPW}} \text{ L}^{-1}$, and 48 h hydrolysis). Adjusting the conditions ($6.5 \text{ g VS}_{\text{manure}} \text{ L}^{-1}$, $7 \text{ g VS}_{\text{PPW}} \text{ L}^{-1}$, and 48 h hydrolysis) reduced $\text{NH}_4\text{-N}$ by $73 \pm 0.54\%$ and VS by $30 \pm 0.12\%$.

- In the SEM analysis of manure-PPW hydrolysis, manure fibers initially appear distinct and unaltered, with a mix of compacted and porous areas. After 48 h of hydrolysis, protease enzymes fragment protein structures, leading to an amorphous appearance with frayed fiber edges, signifying enzymatic surface digestion.
- After 48 h hydrolysis of manure-PPW substrates, the N-H stretch peak shifted, indicating an increase in hydroxyl or amine groups. The Amide I peak in control shifted, suggesting altered protein structures, while the Amide II peak changed from a sharp to a less defined peak, reflecting proteolysis and structural disruption.
- The study highlighted that KPW and pineapple peel waste significantly improved manure hydrolysis, protein degradation, and ammonia reduction from 4 to 48 h under optimized conditions.
- The observations from SEM and FTIR analyses of manure-KPW and manure-PPW hydrolysis succinctly illustrate the structural and functional transformations of manure protein structure induced by KPW- and PPW-derived protease treatment.

Fermentation (anaerobic digestion) studies with Kiwi peel waste (KPW)

- In anaerobic digestion of manure-KPW substrates, optimal biohydrogen yield reached 389 ± 11 mL g^{-1} VS on day 6 and 510 ± 7 mL g^{-1} VS on day 12 with a M:KPW ratio of 0.5, pH 5, and 4 g VS L^{-1} inoculum. On the other hand, under similar conditions (albumin:KPW ratio of 0.5, pH 5, and 4 g VS L^{-1} inoculum and casein:KPW ratio of 0.5, pH 5, and 4 g VS L^{-1} inoculum), albumin yielded 200 ± 3 mL H_2 g^{-1} VS at day 6 and 554 ± 3 mL H_2 VS by day 12, respectively, while casein produced 245 ± 3 mL H_2 g^{-1} VS on day 6 and 400 ± 4 mL H_2 g^{-1} VS on day 12.

- The study identified optimal conditions (manure:KPW ratio of 0.5, pH 5, and 4 g VS L⁻¹ inoculum) that achieved a biomethane yield of up to 80±4 mL g⁻¹ VS on day 6 and 90±2 mL g⁻¹ VS on day 12 anaerobic digestion of manure-KPW. However, these optimal combinations for albumin (albumin:KPW ratio of 0.5, pH 5, and 4 g VS L⁻¹ inoculum) and casein (casein:KPW ratio of 0.5, pH 5, and 4 g VS L⁻¹ inoculum) did not produce any biomethane yield during the anaerobic digestion of albumin-PPW or casein-PPW.
- A combination of Manure:KPW of 0.5, pH 5, and inoculum 4 g VS L⁻¹ provided the highest COD and VS reduction of 43.31±0.17% and 66%.
- At day 0, average protein concentrations across the three sets of albumin-KPW were 1178 mg L⁻¹. By day 6, an average protein reduction of 24.5% indicated the effectiveness of the anaerobic digestion process. By day 12, this reduction deepened to an average of 29.5%, with the most significant decrease reaching 33.2%.
- At day 0, the average casein concentration across the three sets of casein-KPW was 611.67 mg L⁻¹. By day 6, the concentration had decreased to an average of 524.97 mg L⁻¹, reflecting an average protein reduction of 22.8%. By day 12, the average concentration further declined to 447.51 mg L⁻¹, marking an average reduction of 29.1%. This illustrates the progressive degradation of casein under different conditions.
- In the SEM micrograph of albumin-KPW anaerobic digestion, albumin's initial large, irregular aggregates and KPW heterogeneous, mostly intact fibrous structures underwent early structural changes by day 6. With surface erosion, albumin-KPW aggregates became less distinct, and KPW's fibrous matrix started breaking down into smaller, less defined fragments. By day 12, substantial degradation was evident: albumin aggregates smoothed

out, and KPW's fibrous structure was nearly lost, indicating microbial enzymes' effective proteolytic and lipolytic action.

- In SEM images of casein-KPW anaerobic digestion, initially (day 0), casein micelles showed typical globular structure, and KPW contributed irregular fibrous textures. By day 6, signs of digestion emerged, with less distinct micelles and eroded, fragmenting fibers, indicating enzyme activity. By day 12, extensive degradation erases the original morphological features, showcasing the disruptive effect on protein and fiber structures due to digestion.
- Fourier transform infrared (FTIR) analysis of albumin-KPW anaerobic digestion revealed changes and shifts between day 0 to day 12: amide I and amide II shifted their peaks, and amide III, initially initial peak became obscured, indicating significant protein structural changes.
- Significant shifts were observed in the FTIR analysis of casein-KPW anaerobic digestion at day 0 and day 12. After 12 days of AD, the amide I band in the casein-KPW sample shifted location with less intensity, suggesting changes in primary protein structures and alterations in secondary protein structures.
- Biohydrogen production from the anaerobic digestion of manure:KPW, albumin:KPW, and casein:KPW substrates predominantly followed the acetate pathway. The primary volatile fatty acids (VFAs) are produced in the following order of concentration: acetic acid > propionic acid > butyric acid > isovaleric acid > valeric acid.

Fermentation (anaerobic digestion) studies with Pineapple peel waste (PPW)

- Under optimal anaerobic digestion conditions (M:PPW ratio of 0.9, pH 6, inoculum 5.5 g VS L⁻¹), manure-PPW substrates produced biohydrogen yields of 345±6 and 385±7 mL g⁻¹ VS on day 6 and 12, respectively. Comparatively, albumin-PPW achieved 213±3 and 247±6 mL H₂ g⁻¹ VS on days 6 and 12, respectively. Casein-PPW yielded 233±3 and 312±3 mL H₂ g⁻¹ VS on days 6 and 12, respectively. These results highlight PPW's role in boosting biohydrogen production from protein-rich substrates.
- In the study of manure-PPW anaerobic digestion under optimal conditions (manure: PPW ratio of 0.9, pH 6, and inoculum 5.5 g VS L⁻¹), minimal methane production was observed by day 12 (6±1 mL_{methane} g⁻¹ VS). This contrasted with the results from similar conditions applied to albumin (albumin:PPW ratio of 0.9, pH 6, and inoculum 5.5 g VS L⁻¹) and casein (casein:PPW ratio of 0.9, pH 6, and inoculum 5.5 g VS L⁻¹), where no methane generation was observed on day 6 and 12.
- A combination of Manure:PPW of 0.9, pH 5 and inoculum 7 g VS L⁻¹ provided the highest VS reduction of 35.4% and highest COD reduction (64.8±0.99%) was obtained from manure: PPW of 1.45, pH 4 and inoculum 7 g VS L⁻¹.
- In albumin-PPW anaerobic digestion, at day 0, the average albumin concentration across three sets was 1479.10 mg L⁻¹. By day 6, this average dropped to 1079.23 mg L⁻¹, showing an average reduction of 27%. By day 12, the average reduction in albumin concentration further increased to 34.7%, likely due to optimal pH and inoculum levels for bromelain activity from PPW.
- Throughout the anaerobic digestion process using casein-PPW, the average initial (day 0) casein concentration for three sets was 653.46 mg L⁻¹. By day 12, it reduced to an average

of 466.17 mg L⁻¹, marking an average reduction of 30.7%. This highlights the process's capacity to degrade casein, with variations in degradation rates influenced by the initial pH levels and inoculum sizes.

- The albumin-PPW initially formed well-defined, spherical shapes, showing albumin's globular nature at day 0 of anaerobic digestion. By day 6, these spheres start merging, with surfaces roughening, signaling enzymatic breakdown. By day 12, the once spherical albumin transforms into irregular shapes, suggesting extensive proteolysis. Also, flaky structures, likely from undigested pineapple peel waste, indicate the peel's fibrous resistance to degradation. This results in a homogenized but structurally altered albumin-PPW mixture.
- Day 0 SEM images of casein-PPW digestion reveal casein's natural micellar formation alongside the textured, fibrous pineapple peel waste, highlighting casein's smooth micelles against the peel's rough texture. By day 6, enzymatic activity starts breaking down casein from globular micelles into irregular shapes, indicating the onset of proteolysis. By day 12, the transformation is profound; the casein's original micellar structure is replaced by a varied, rough texture, showcasing extensive protein degradation.
- FTIR analysis of albumin-PPW at day 0 and day 12 showed significant enzymatic changes in proteins, evidenced by shifts in amide A, disappearance of amide I, and alterations in amide II and III bands, indicating protein and lipid-carbohydrate structural transformations.
- By day 12, FTIR analysis of casein-PPW showed notable changes in amide bands, reflecting structural alterations in proteins due to enzymatic activity, with shifts in amide A, disappearance of amide I, and adjustments in amide II and III indicating significant protein transformation.

- In all experimental sets, acetic acid was the predominant acid produced, with propionic, isovaleric, butyric, and valeric acids following. Biohydrogen generation through anaerobic digestion of manure:PPW, albumin:PPW, and casein:PPW substrates mainly utilizes the acetate pathway.
- The suitability of the developed models for hydrolysis and digestion of manure-KPW and manure-PPW was verified by ANOVA, with polynomial models preferred for their high R^2 values of 0.99.

7.3 Recommendations for Future Studies

The current research has explored innovative strategies for enhancing manure protein degradation and biohydrogen production using kiwi and pineapple peel waste. Through a series of experiments and analysis by Box-Behnken Response Surface Methodology, this study has demonstrated the potential of kiwi peel and pineapple peel waste to improve the hydrolysis processes of manure. The research featured the role of kiwi peel waste and pineapple peel waste as a valuable source of protease enzymes, specifically actinidin and bromelain, further supporting biohydrogen production from protein-rich manure. The following recommendations are proposed to enhance the understanding of anaerobic digestion and biohydrogen production potential from manure using plant protease sources.

- Investigating the use of other agricultural or food waste sources rich in protease enzymes such as papain (from papaya), ficin (from fig), zingibain (from zinger) and compare their effectiveness in enhancing manure hydrolysis and biohydrogen production.
- Examining the applicability of the findings to different types of animal manure, such as poultry, cattle, and swine, to understand the broader potential of the proposed methods.

- Alkaline proteases from the genus *Bacillus* are widely distributed in sand soil, dried fish, and slaughterhouses. A comparison can be drawn by employing available microbial and plant proteases to enhance biohydrogen or biogas production from protein-rich wastes. In addition, fungal proteases from the *Aspergillus* genus can be studied for the same purpose. Plant, bacterial, and fungal proteases can be compared in biogas production from protein-rich wastes.
- Exploring biotechnological approaches to enhance the protease activity and stability of actinidin and bromelain under various operational conditions to improve hydrolysis efficiency further.
- Investigating the adaptation of microbial consortia specifically for the digestion of complex protein-rich wastes like manure under the effect of long-chain fatty acids (LCFAs) for biohydrogen production, aiming to improve process stability and efficiency.
- In the course of this research, it was observed that the usage of oleic acid in the digesters for albumin-KPW, albumin-PPW, casein-KPW, and casein-PPW did not result in methane production, highlighting a potential inhibitory effect of LCFAs on methane-generating pathways. Interestingly, a slight biomethane generation was noted in the later stages of anaerobic digestion for manure-KPW and manure-PPW substrates, suggesting a delayed onset of methanogenesis under these conditions. This discrepancy underscores the need for deeper exploration into the mechanisms of LCFAs-induced inhibition of methane production.
- Besides Box Behnken response surface methodology, biohydrogen or biogas yield can be analyzed using other advanced models, such as Artificial Neural Networks (ANN) and Multiple Linear Regression (MLR).

- Conducting comparative analyses of microbial communities in digesters processing manure alone versus those amended with kiwi and pineapple peel waste to identify enhanced digestion performance microbial indicators.
- Investigating the dynamics of microbial communities throughout the anaerobic digestion process to understand how adding kiwi and pineapple peel waste influences microbial population shifts, particularly those involved in hydrolysis, acidogenesis, acetogenesis, and methanogenesis stages.
- Examining how protease enzymes derived from kiwi and pineapple peel waste specifically affect the growth and activity of protein-degrading and methane-producing microorganisms to identify any potential synergies or inhibitions.
- Conduct long-term operational studies to assess the stability of the anaerobic digestion process under fluctuating conditions, such as mesophilic or thermophilic temperature, pH, and substrate composition.

List of Appendices

Appendix - A: Characterization Laboratory Report.....	427
Appendix - B: Analytical Method Procedures	428
Appendix - C: Copyright Permission.....	435

List of Figures

Figure B- 1. Calibration curve for ammonia measurement.	431
Figure B- 2. Calibration curve for ammonium measurement.	432
Figure B- 3. Procedure summary of Bradford protein quantity measurement.	433
Figure B- 4. Calibration curve for BSA using the standard test tube protocol of the Bradford method.....	434

Appendix - A:

Characterization Laboratory Report

Appendix A presents the characterization of raw dairy manure.



Soil, Plant and Feed Laboratory
Agriculture Production & Research Division
 204 Brookfield Road, PO Box 8700
 St. John's, NL A1B 4J6
 709.729.6738

MANURE ANALYTICAL REPORT

Submitted by:
 Name: Noori Saady
 Address: MUN, 240 Prince Philip Drive, St. John's, A1B 3X5
 Tel: 864.6087
 Email: nsaady@mun.ca

Date Received: January 19, 2023
Date Reported: February 1, 2023

Lab #: MC 54 **Type of Manure:** Dairy manure

Analysis Results (as received basis)		Nutrients Equivalency	kg/tonne	kg/1000 L
Dry Matter (%)	11.9	Nitrogen (N)		
pH	7.4	Phosphate (P ₂ O ₅)		
Total Nitrogen (%)	0.17	Potash (K ₂ O)		
Total Phosphorous (%)	0.044	Note: 1 kg/tonne = 2 pounds/ton 1 kg/1000 L = 10 pounds/1000 gallons		
Total Potassium (%)	0.11	Interpretation: Ten (10) thousand litres or tones of the manure would supply xx kg N, xx kg P ₂ O ₅ and xx kg K ₂ O for the 1 st year crop. Deduct fertilizer application rate accordingly.		
Total Calcium (%)	0.13	Application Time	Incorporation:	
Total Magnesium (%)	0.046	<input type="checkbox"/> Late Summer		
Total Iron (ppm)	140	<input type="checkbox"/> Early Fall		
Total Manganese (ppm)	19	<input type="checkbox"/> Late Fall/Winter		
Total Copper (ppm)	40	<input type="checkbox"/> Spring		
Total Zinc (ppm)	11	<input type="checkbox"/> Summer		
Total Boron (ppm)	2			
Total Sodium (ppm)	317			

Vlada Bogdanova/Time Strange
Soil & Feed Laboratory

You Jiao
Soil Fertility Specialist

For further information on manure nutrient availability and manure nutrient management, contact the Soil Fertility Specialist at 709.637.2685

Appendix - B:
Analytical Method Procedures

B. 1. Introduction

Appendix B outlines an in-depth methodology for the experimental analysis, detailing the procedures to measure total solids (TS), volatile solids (VS), chemical oxygen demand (COD), ammonia (NH₃), and ammonium (NH₄⁺) concentration.

B. 2. Total Solids (TS) Measurement (Method No 2540 B)

Total solids are defined as the residual material remaining in a container following the evaporation and subsequent oven-drying of a sample at a specified temperature (105±2°C). The procedure followed as-

- i) Record the weight of the evaporating dish (referred to as B).
- ii) Transfer 5 ml of a thoroughly mixed sample into the dish.
- iii) Place in an oven to dry at 105°C for one hour.
- iv) Allow to cool in a desiccator.
- v) Measure the weight of the dish after cooling.
- vi) Continue the cycle of drying, cooling, and weighing until achieving a weight difference of less than 4% (documented as A).

Calculations:

$$\text{mg total solids / L} = \frac{(A-B)*1000}{\text{Sample volume (mL)}}$$

Where: A = weight of solids + dish after drying in mg.

B = initial tare weight of dish in mg.

B. 3. Volatile Solids (VS) Measurement (Method No 2540 E)

- i) Heat the dish and its contents in a 550°C muffle furnace until a constant weight is reached (5-20 minutes).
- ii) Let the dish cool in air, then in a desiccator to room temperature, and weigh it.
- iii) Repeat the process of drying, cooling, and weighing until the weight stabilizes or the change is less than 4% or 0.5mg, whichever is smaller.

Calculations:

$$\text{mg volatile solids / L} = \frac{(A-B)*1000}{\text{Sample volume (mL)}}$$

Where:

A = weight of solids + dish before ignition in mg.

B = weight of solids + dish after ignition in mg.

B. 4. Chemical Oxygen Demand (COD) Measurement (EPA Method 410.4)

Chemical Oxygen Demand (COD) measures the amount of oxygen required to oxidize organic and inorganic compounds in water chemically. It's a critical parameter used to assess water quality, indicating the level of pollutants present. The following steps are followed-

- i) Clean all culture tubes and caps with 20% H₂SO₄ to avoid contamination.
- ii) Dispense 2.5 mL of the sample, blank, and standards into smaller tubes or 10 mL into larger tubes.
- iii) Introduce 1.5 mL of digestion solution into smaller tubes or 6.0 mL into larger tubes and stir.

- iv) Carefully add 3.5 mL of catalyst solution to smaller tubes or 14.0 mL to larger tubes.
- v) Securely cap tubes and shake to ensure thorough mixing. Be cautious of heat.
- vi) Heat tubes at 150°C for two hours in an oven.
- vii) After heating, mix, cool the tubes, and allow any sediment to settle. Use a spectrophotometer to measure the blank, standards, and sample at 600 nm.

B. 5. Ammonia (NH₃) Measurement

Ammonia (NH₃) in the sample was measured with an ammonia gas sensing electrode (#K-27502-00) inserted in a pH-204 Digital pH/ORP monitor following exactly the procedure shown in the manufacturer instructions that came with the instrument package. The steps are as follows-

- i) Connect the ammonia gas sensing electrode (#K-27502-00) to pH-ORP meter.
- ii) Prepare two standards close to the expected sample concentration.
- iii) Set the meter to concentration mode for 2 or 3-point calibration (Figure B-1).
- iv) Immerse the electrode in a less concentrated solution (500 ppm); stir with 2 mL of ionic strength adjuster (ISA).
- v) After 1 minute, fix the value per the manufacturer's instructions.
- vi) Rinse the electrode; dry with distilled water.
- vii) Place the electrode in a more concentrated solution (100 ppm); stir with 2 ml of ISA.
- viii) Add the sample and ISA to the beaker; immerse the electrode and stir it.
- ix) Read concentration from pH-ORP meter after 1 minute.
- x) Recalibrate pH-ORP meter every 2-3 hours; repeat steps ii to vii.

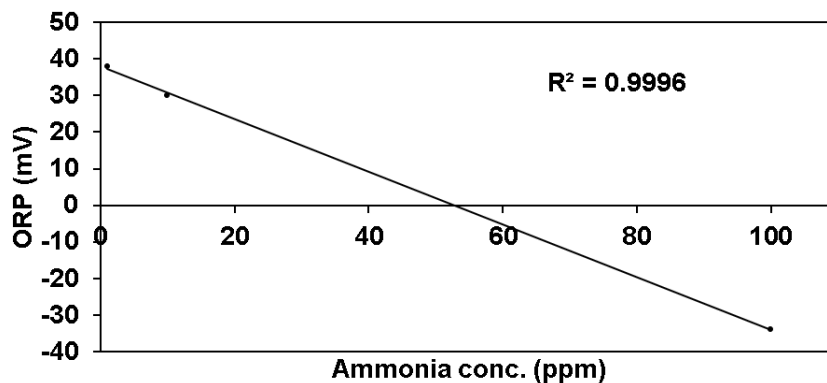


Figure B- 1. Calibration curve for ammonia measurement.

B. 6. Ammonium (NH₄⁺) Measurement

Ammonium (NH₄⁺) in the sample was measured with an ammonium gas sensing electrode (#K-27502-03) inserted in a pH-204 Digital pH/ORP monitor following exactly the procedure shown in the manufacturer instruction that came with the instrument package. The steps are as follows-

- i) Prepare three standard solutions by serial dilution of the 1000 ppm standard to match the expected sample concentration.
- ii) Immerse the electrode in a less concentrated solution (10 ppm); stir and add 2 ml of ISA.
- iii) After stirring for 1 minute, save the value in memory as per calibration instructions.
- iv) Rinse and dry the electrode with distilled water.
- v) Place the electrode in a more concentrated solution (1000 ppm); stir and add 2 ml of ISA.
- vi) After 1 minute, fix the value in the memory according to calibration instructions and prepare a calibration curve (Figure B-2).
- vii) Add 100 ml of sample and 2 ml of ISA to a beaker; start stirring.
- viii) After 1 minute, read the concentration from the meter display.

ix) Recalibrate the electrode every 1-2 hours, repeating steps ii to vii.

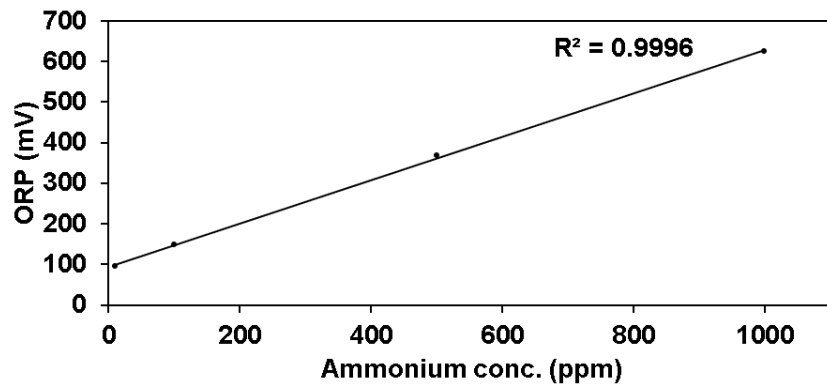


Figure B- 2. Calibration curve for ammonium measurement.

B. 7. Protein Quantity Measurement (Bradford method)

Pierce™ Bradford Plus Protein Assay Kit (Thermoscientific, Catalog # 23236) was used to measure the protein concentration of any sample. The kit came with Pierce™ Bradford Plus Protein Assay Reagent, 950 mL containing coomassie G-250 dye and Albumin Standard Ampules, 2 mg mL⁻¹, 10 X 1 mL ampules containing bovine serum albumin (BSA) at 2.0 mg mL⁻¹ in a solution of 0.9% saline and 0.05% sodium azide, methanol, phosphoric acid, and solubilizing agents in water. The experiment followed the following protocol (Figure B-3) to determine protein concentrations using the Bradford Plus assay method:

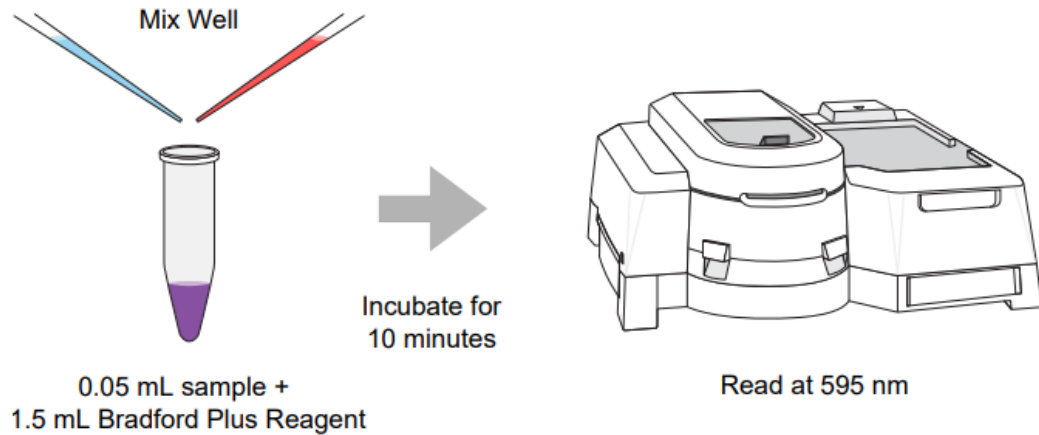


Figure B- 3. Procedure summary of Bradford protein quantity measurement.

- i) Transfer 0.05 mL of each sample into marked test tubes.
- ii) Combine 1.5 mL of Bradford Plus Protein Assay Reagent with the contents of each tube and thoroughly mix.
- iii) Allow the samples to stand for 10 minutes at room temperature.
- iv) Calibrate the spectrophotometer at 595 nm using a cuvette with water.
- v) Record the absorbance for each tube at 595 nm.
- vi) Calculate the net absorbance by deducting the average blank absorbance from each sample's absorbance.
- vii) Construct a standard curve (Figure B-4) with the corrected absorbance of the BSA standards against their concentrations and ascertain the protein concentration in the unknown samples.

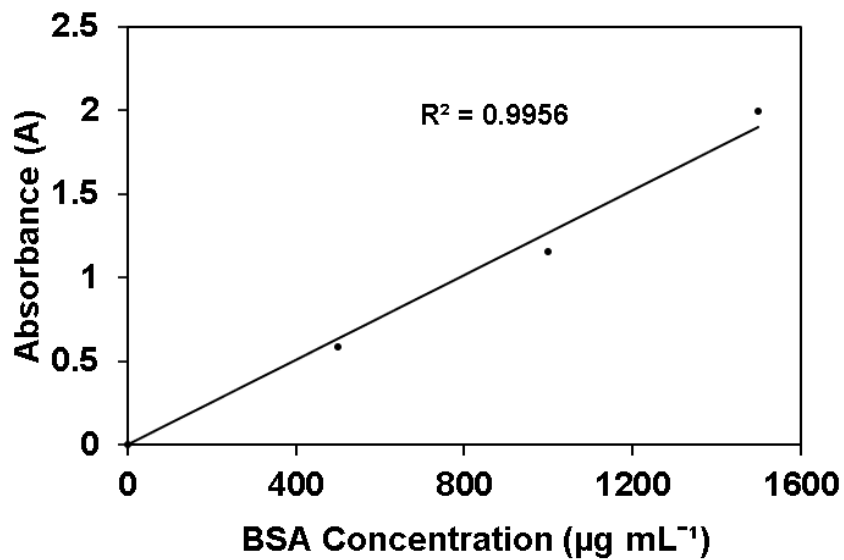


Figure B- 4. Calibration curve for BSA using the standard test tube protocol of the Bradford method.

Appendix - C:
Copyright Permission

3/8/24, 8:49 PM

RightsLink Printable License

**ELSEVIER LICENSE
TERMS AND CONDITIONS**

Mar 08, 2024

This Agreement between Memorial University of Newfoundland -- Tasnia nazifa ("You") and Elsevier ("Elsevier") consists of your license details and the terms and conditions provided by Elsevier and Copyright Clearance Center.

License Number	5744490624659
License date	Mar 08, 2024
Licensed Content Publisher	Elsevier
Licensed Content Publication	Trends in Microbiology
Licensed Content Title	Protein biometanation: insight into the microbial nexus
Licensed Content Author	Zhenmin Ling,Nandini Thakur,Marwa M. El-Dalatony,El-Sayed Salama,Xiangkai Li
Licensed Content Date	Jan 1, 2022
Licensed Content Volume	30
Licensed Content Issue	1
Licensed Content Pages	10
Start Page	69
End Page	78

<https://s100.copyright.com/AppDispatchServlet>

Type of Use	reuse in a thesis/dissertation
Portion	figures/tables/illustrations
Number of figures/tables/illustrations	1
Format	electronic
Are you the author of this Elsevier article?	No
Will you be translating?	No
Title of new work	Figure 2-6. Schematic representation of ammonia toxicity during anaerobic digestion (AD) of protein-rich biowastes. Modified from Ling et al. (2022).
Institution name	Memorial University of Newfoundland
Expected presentation date	Mar 2024
Portions	Figure 1. Schematic representation of ammonia toxicity during anaerobic digestion (AD) of protein-rich biowastes (PRBs). Page 3
Requestor Location	Memorial University of Newfoundland 240 Prince Phillip Drive St. John's, NL A1B 3X5 Canada Attn: Memorial University of Newfoundland
Publisher Tax ID	GB 494 6272 12
Total	0.00 CAD